Progress in Marine Science and Technology 2

Proceedings of the 20th International Ship and Offshore Structures Congress

Specialist Committee Reports

Edited by
Mirek Kaminski and Philippe Rigo

IOS Press

PROCEEDINGS OF THE 20TH INTERNATIONAL SHIP AND OFFSHORE STRUCTURES CONGRESS (ISSC 2018)
VOLUME 2

Progress in Marine Science and Technology

Progress in Marine Science and Technology (PMST) is a peer-reviewed book series concerned with the field of marine science and technology. It includes edited volumes, proceedings and monographs dealing with research in pure or applied science and work of a high international standard on subjects such as: conceptual design; structural design; hydromechanics and dynamics; maritime engineering; production of all types of ships; production of all other objects intended for marine use; shipping science and all directly related subjects; offshore engineering as related to the marine environment; oceanographic engineering subjects related to the marine environment.

Volume 2

Recently published in this series

Vol. 1. M.L. Kaminski and P. Rigo (Eds.), Proceedings of the 20th International Ship and Offshore Structures Congress (ISSC 2018) Volume 1

ISSN 2543-0955 (print)
ISSN 2543-0963 (online)

Proceedings of the 20th International Ship and Offshore Structures Congress (ISSC 2018)
Volume 2

Specialist Committee Reports

Edited by

Mirek L. Kaminski

Delft University of Technology, The Netherlands

and

Philippe Rigo

University of Liege, Belgium

IOS Press

Amsterdam • Berlin • Washington, DC

ISBN 978-1-61499-863-1 (print)
ISBN 978-1-61499-864-8 (online)
Library of Congress Control Number: 2018945814

Publisher
IOS Press BV
Nieuwe Hemweg 6B
1013 BG Amsterdam
Netherlands
fax: +31 20 687 0019
e-mail: order@iospress.nl

For book sales in the USA and Canada:
IOS Press, Inc.
6751 Tepper Drive
Clifton, VA 20124
USA
Tel.: +1 703 830 6300
Fax: +1 703 830 2300
sales@iospress.com

Preface

The first volume contains the eight Technical Committee reports presented and discussed at the 20th International Ship and Offshore Structures Congress (ISSC 2018) in Liege (Belgium) and Amsterdam (The Netherlands), 9–14 September 2018, and the second volume contains the reports of the eight Specialist Committees. The Official discusser's reports, all floor discussions together with the replies by the committees, will be published after the Congress in electronic form.

The Standing Committee of the 20th International Ship and Offshore Structures Congress comprises:

Chairman:	Mirek Kaminski	The Netherlands
Co-chairman:	Philippe Rigo	Belgium
	Segen Estefen	Brazil
	Neil Pegg	Canada
	Yingqiu Chen	China
	Jean-Yves Pradillon	France
	Patrick Kaeding	Germany
	Manolis Samuelides	Greece
	Stefano Ferraris	Italy
	Masahiko Fujikubo	Japan
	Rune Torhaug	Norway
	Carlos Guedes Soares	Portugal
	Yoo Sang Choo	Singapore
	Jeom Kee Paik	South Korea
	Ajit Shenoi	UK
	Xiaozhi Wang	USA

On behalf of the Standing Committee, we would like to thank the sponsors of ISSC 2018.

Mirek Kaminski
Chairman

Philippe Rigo
Co-chairman

Delft, 1st May 2018

This page intentionally left blank

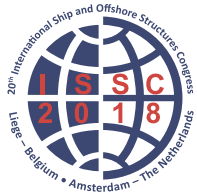

THANKS TO OUR SPONSORS FOR
THEIR FINANCIAL CONTRIBUTION

Move Forward with Confidence


MARIN


DN&T
Design Naval & Transports


SECO


Flanders
Hydraulics Research
Flanders
State of the Art

Contents

Preface v
Mirek Kaminski and Philippe Rigo

Committee V.1: Accidental Limit States 1
E. Rizzuto, L. Brubak, Z. Hu, G.S. Kim, M. Kõrgesaar, K. Nahshon, A. Nilva, I. Schipperen, G. Stadie-Frohboes, K. Suzuki, K. Tabri and J. Wægter

Committee V.2: Experimental Methods 73
D. Dessi, F. Brennan, M. Hoogeland, XB. Li, C. Michailides, D. Pearson, J. Romanoff, XH. Shi, T. Sugimura and G. Wang

Committee V.3: Materials and Fabrication Technology 143
Lennart Josefson, Stephen van Duin, Bianca de Carvalho Pinheiro, Nana Yang, Luo Yu, Albert Zamarin, Heikki Remes, Frank Roland, Marco Gaiotti, Naoki Osawa, Agnes Marie Horn, Myung Hyun Kim and Brajendra Mishra

Committee V.4: Offshore Renewable Energy 193
Zhen Gao, Harry B. Bingham, David Ingram, Athanasios Kolios, Debabrata Karmakar, Tomoaki Utsunomiya, Ivan Catipovic, Giuseppina Colicchio, José Miguel Rodrigues, Frank Adam, Dale G. Karr, Chuang Fang, Hyun-Kyoung Shin, Johan Slätte, Chunyan Ji, Wanan Sheng, Pengfei Liu and Lyudmil Stoev

Committee V.5: Special Craft 279
D. Truelock, Z. Czaban, H. Luo, X. Wang, M. Holtmann, E. Begovic, A. Yasuda, M. Ventura, R. Nicholls-Lee, E. Oterkus and P. Sensharma

Committee V.6: Arctic Technology 347
S. Ehlers, A. Polojärvi, A. Vredeveldt, B. Quinton, E. Kim, F. Ralph, J. Sirkar, P.O. Moslet, T. Fukui, W. Kuehnlein and Z. Wan

Committee V.7: Structural Longevity 391
P. Hess, S. Aksu, M. Vaz, G. Feng, L. Li, P. Jurisic, M.R. Andersen, P. Caridis, D. Boote, H. Murayama, N. Amila, B. Leira, M. Tammer, J. Blake, N. Chen and A. Egorov

Committee V.8: Report for Subsea Technology 461
Menglan Duan, Shuhong Chai, Ilson Paranhos Pasqualino, Liping Sun, Claus Myllerup, Spyros Mavrakos, Asokendu Samanta, Kieran Kavanagh, Masahiko Ozaki, Svein Sævik, Angelo Teixeira, Ying Min Low, Jung Kwan Seo, Sebastian Schreier, Pieter Swart and Hao Song

Subject Index 525

Author Index 527

This page intentionally left blank

Proceedings of the 20th International Ship and Offshore Structures Congress (ISSC 2018) Volume II – M.L. Kaminski and P. Rigo (Eds.)

doi:10.3233/978-1-61499-864-8-1

COMMITTEE V.1

ACCIDENTAL LIMIT STATES

COMMITTEE MANDATE

Concern for accidental scenarios for ships and offshore structures and for their structural components leading to limit states. Types of accidental scenarios shall include collision, grounding, dropped objects, explosion, and fire. Attention shall be given to hazard identification, accidental loads and nonlinear structural consequences including strength reduction, affecting the probability of failure and related risks. Uncertainties in the use of accidental scenarios for design and analysis shall be highlighted. Consideration shall be given to the practical application of methods and to the development of ISSC guidance for quantitative assessment and management of accidental risks.

AUTHORS/COMMITTEE MEMBERS

Chairman: E. Rizzuto, *Italy*
L. Brubak, *Norway*
Z. Hu, *China*
G.S. Kim, *Korea*
M. Kõrgesaar, *Finland*
K. Nahshon, *USA*
A. Nilva, *Ukraine*
I. Schipperen, *The Netherlands*
G. Stadie-Frohboes, *Germany*
K. Suzuki, *Japan*
K. Tabri, *Estonia*
J. Wægter, *Denmark*

KEYWORDS

Accidental situations Limit states; Abnormal environmental event; Collision; Grounding; Explosion Fires; Emergency Response Service; Benchmark on grounding simulation

CONTENTS

1. INTRODUCTION 4

2. SCENARIOS FOR THE DESIGN OF MARINE STRUCTURES 4
2.1 Probability of occurrence of a scenario 5
2.2 Consequences of exposure to a given scenario 5
2.3 Characteristics of scenarios for limit states design 6
2.3.1 Scenarios for verifications of ULSs 7
2.3.2 Wave loads scenarios for ULS 7
2.3.3 Scenarios for verifications of SLSs 9
2.3.4 Scenarios for verifications of FLSs 9
2.4 Accidental and abnormal environmental situations 9
2.5 Uncertainties in accidental scenarios 10
2.6 Design accidental/abnormal scenarios 10
2.7 Design Standards 11
2.8 Status of existing design standards for ships in relation to accidental scenarios 11

3. ABNORMAL ENVIRONMENTAL EVENTS 12
3.1 Abnormal waves 12
3.2 Abnormal wave design loads for offshore structures 13
3.3 Comments to offshore scenarios 14
3.4 Possible definition of abnormal wave scenarios for ships 15

4. METHODS AND PROCEDURES FOR THE ANALYSIS OF ALS 15
4.1 Introduction 15
4.2 Modelling details and response evaluation 17
4.2.1 Analytical methodology on response evaluation 17
4.2.2 Numerical simulation methodology 19
4.3 Present application and recent development in current standards 20
4.4 Material models to be used in FEM 21
4.4.1 Metallic Shipbuilding Materials 21
4.4.2 Composites 23
4.4.3 Foam 24
4.4.4 Rubber 26
4.4.5 Ice 26
4.4.6 Soil 27

5. COLLISION 28
5.1 Ship collision categories 28
5.1.1 Ship-ship collision 28
5.1.2 Ship-offshore collision 29
5.1.3 Ship-bridge collision 30
5.1.4 Ship-ice collision 31
5.2 Most critical/relevant condition and design/analysis methods 32
5.3 Acceptance criteria/consequence evaluation 33

6. GROUNDING 34
6.1 Introduction 34
6.2 Most critical/relevant condition 35
6.3 Analysis methods 37
6.3.1 Experiments 37
6.3.2 Statistical models 38

6.3.3 Numerical models 38
6.3.4 Empirical and regression models 39
6.3.5 Analytical models 40
6.4 Acceptance criteria/consequence evaluation 40

7. FIRE AND EXPLOSION 41
7.1 Introduction 41
7.2 Prescriptive vs performance based codes 41
7.3 Fire and explosion analysis: General 42
7.4 The Risk of Fire and Explosion accidents 43
7.4.1 Action effects and modelling 43
7.4.2 Accidental scenario and probability 44
7.5 Design Requirements of Fire and Explosion Accidents for LNG Ships 45
7.5.1 Fire and explosion design for LNG carriers and FSRU 45
7.5.2 Fire and explosion design for Gas fuelled ships 45
7.6 Fire and explosion analyses for LNG ships 46
7.6.1 Fire and explosion analyses for LNG carriers and FSRUs 46
7.6.2 Fire and explosion analyses for LNG fuelled ships 49

8. MARITIME SAFETY AND RESCUE SERVICES 49
8.1 Emergency Response Services - ERS 50
8.2 ERS Functionality 50
8.3 Basis for decisions making 51

9. BENCHMARK STUDY 52
9.1 Introduction 52
9.2 Experiment 52
9.3 Input data 53
9.4 Results 54
9.5 Sensitivity studies 55
9.5.1 Sensitivity for friction coefficients 55
9.5.2 Sensitivity to failure strain values 56
9.5.3 Sensitivity to mesh refinement 56
9.6 Summary 56

REFERENCES 58

ANNEX 70

1. INTRODUCTION

The term of Accidental Limit States design in technical language indicates a design procedure accounting for accidental situations in terms of specific initial states, actions and/or final states for the structure. The characteristic features of accidental situations in comparison to other scenarios considered in structural checks are discussed in chapter 2, where the motivations for the introduction of this class of scenarios are discussed, too.

Chapter3 reports a brief overview of the current and possible applications to ships and off shore structures design of the specific category of abnormal environmental situations, in which the event activating the scenario is represented by extraordinary wave events

The other typical accidental situations (collision, grounding, explosion and fire) are covered by chapters 5 to 7, where the various aspects of each specific scenario are analysed with the aim of providing a state of the art of the procedures available for investigations. When possible, reference is made in particular to ship structures.

Chapter 4 contains a discussion of tools available for the structural analysis of various of the following scenarios.

Chapter 8 touches upon a subject correlated to accidents, i.e. the Emergency Response Services, that are aimed at managing on the field accidental situations, thus limiting consequences.

Finally, the last chapter (n.9) includes a benchmark study carried out by some of the committee members and regarding a grounding event for which model scale experiments were available from literature. The force and the energy exchanged between an obstacle with a simple but realistic shape and a medium size specimen resembling the double bottom of a ship are derived by FEM simulation and compared to experimental surveys.

2. SCENARIOS FOR THE DESIGN OF MARINE STRUCTURES

Ships and offshore structures are subjected to various operational situations, from frequent and/or normal to extreme and/or accidental ones. In design, the main objective is to obtain a structure able to withstand these situations with an adequate probability of resisting them with limited unwanted effects. In other words, the target of design is to control the risk of operating the structure.

A key step for setting up a design procedure, therefore, is represented by the selection of a number of situations able to represent effectively the whole spectrum of hazards to which the structure is subjected during its life. In more details, this implies:

- to select the classes of scenarios that generate the largest contributions to risk of the structure,
- to identify examples of those scenarios in quantitative terms (selecting characteristic values for the elements of the scenario) and
- to use those scenarios to evaluate the implied risk and to control it.

Each relevant scenario allocates a certain risk contribution: the total lifetime risk, represented by the sum of all contributions, is to be kept within acceptable limits.

In this process, elements for the definition of the relevant scenarios are the probability of occurrence of the scenario itself, the initial state of the structure and the actions to which the structure is exposed. A further element for the evaluation of the risk inherent to the scenario is the final state of the structure, evaluated through the probability of exceeding specific limit states. Exceeding these limits has a direct influence on the consequences of the exposure.

In formal terms the risk allocated to a structure subjected to scenario S_i of exceeding the limit

state Lj thus generating consequences Cj can be expressed in terms of Eq. 1

$$R_{j,i} = \; C_j \, P(L_{j,i}) = C_j \, P(L_j \mid S_i) P(S_i) \tag{1}$$

Where

$P(S_i)$ = probability of occurrence of scenario Si
$P(L_j S_i)$ = conditional probability of exceeding the Limit State L_j given occurrence of scen. S_i
$P(L_{j,i})$ = probability of exceeding the Limit State L_j in scenario i
C_j = consequence of exceeding limit state j
$R_{j,i}$ = risk due exceeding limit state j in scenario i

Summation of the various contributions is carried out generally first within the single scenario and later among scenarios (Eq.2)

$$R = \sum_i R_i = \sum_i R \mid S_i \cdot P(S_i) = \sum_i \left[\sum_j C_j \, P(L_j \mid S_i) \right] P(S_i) \tag{2}$$

R = total risk
R_i = risk incurred in scenario i
$R \mid S_i$ = risk conditional to scenario i

In the following, a few general characteristics of the most typical scenarios adopted for structural verifications are recalled, with the aim of focusing later on accidental ones.

2.1 Probability of occurrence of a scenario

A key quantity of a scenario for design verification is represented by its probability of occurrence $P(S_i)$ in Eq. (1) and Eq. (2) and/or the expected number of times it will occur in the life of the structure. This is important because the risk evaluated in the scenario (i.e. conditional to the occurrence of the scenario) is to be weighted according to such probability (Eq.2). The probability of the scenario depends on the probability of the initial state featured by the system under consideration and on the probability of occurrence of the actions described in the scenario, which, in turn, may be conditional to that initial state. In the following, a quick review of how the concept is applied in various classes of scenarios is presented.

2.2 Consequences of exposure to a given scenario

When evaluating the effect of the exposure to a given scenario, the response of the structure (i.e. its final state) is to be modelled. In order to carry out an evaluation of consequences, the concept of limit state is widely used. A limit state defines the border of a region in the space of the possible states of the structure. Inside the region, the structure fulfils a given criterion, while, outside it, the state of the structure belongs to a different category of states, with significant differences in performances from the region inside the border.

The above border is expressed through the limit state equation, which, in turn, is formulated in terms of those state variables that are needed to identify the specific limit (or criterion). In structural design, these variables may refer to loads or other actions on the structure, to responses (stress, strain, displacement, etc.) or other variables, regarding the mechanical, thermal or any type of behaviour that may be of interest for checking the performance of the structure. Criteria may refer to performances like maintaining the structural integrity, the fitness for use, durability, fatigue resistance or other requirements. During the last two decades, the so called limit state design (LSD) has been increasingly applied in engineering, since a

rigorous design should be obtained evaluating directly all the various final states the structure can end up to, because of the different exposures experienced during its operational life.

Three types of limit states (LS) have been considered for a long time for steel structures (as already mentioned in Czujko et al. 2012): Ultimate Limit State (ULS), Serviceability Limit State (SLS) and Fatigue Limit State (FLS). The criteria at the basis of the formulation of the LSs characterize the reference scenario to such an extent, that, in common language, the type of analysis and the whole check situation is identified by the term indicating its (final) limit state. In the following, the characteristics of the three LSs (here intended in their narrower and more precise meaning) are summarized, while in the next paragraphs the corresponding scenarios are briefly recalled. A forth category (accidental scenarios), which is the main object of this report, is discussed from §2.4 onwards.

Serviceability Limit States (SLS): are used to check the adequacy of the structure during normal operation. SLS criteria in design may address for instance limits of deflection, vibration, motions, durability considerations, and similar.

Fatigue Limit States (FLS): refer to damages induced by repeated load cycles on the structure. Checks according to this criterion aim at ensuring that the structure has an adequate fatigue life for its anticipated operations. The predicted fatigue life can also be a basis for planning efficient inspection programs during operation of the structure. Formulations of this limit state may be based on two alternative models: Miner's Rule and Fracture Mechanics. The selection of the model reflects into different formulations and different choices of the relevant state variables.

Ultimate Limit States (ULS): refer to irreversible changes in the state in the system, associated with failure. Failure may be represented by structural collapse and, in this case, the limit state is often expressed in terms of those variables that characterise the stress-strain field in specific points of the structure or global loads and capacity of the whole structure. The loss of structural capacity may be related to collapse of individual strength members or collapse of the entire structure due to for instance buckling and plastic collapse of plating, stiffened panels and support members. On the other hand, failure can be represented by other criteria, very much dependent on the type of structure and on the scenario. For a floating structure, it could correspond to loss of water tightness or to exceedance of a given heeling angle (above which evacuation is impaired); for a structure subjected to thermal loads it could be represented by reaching a given surface temperature (above which an excessive decay of load carrying capacity is implied, etc.).

A structure designed by a LS is proportioned to sustain all actions likely to occur during its service life, and to keep on fulfilling the condition expressed by the LS, with an appropriate level of reliability for each limit state. The various types of limit states may be checked against different levels of probability of exceedance and such probability, not to be exceeded for a particular type of limit state, is in turn fixed in dependence of the foreseen consequences of going beyond the limit. The target is the control of the risk coming from that specific scenario. Limit states are therefore an important aspect in the characterisation of the situations foreseen for structural verifications.

2.3 Characteristics of scenarios for limit states design

As mentioned above, the probability for a structure to go beyond a specified limit state is to be computed with reference to the initial state and to the actions foreseen in the scenario under investigation. In the following, the characteristics of scenarios for ULS, SLS and FLS checks will be recalled, with the aim of introducing later those inherent to accidental situations.

2.3.1 Scenarios for verifications of ULSs

Typical strength verifications correspond to initially intact structures subjected to suitably chosen action levels. The final state is compared with an ULS resistance formulation.

The initial intact state is characterised by the absence of localised damages. Minor and diffused degradation effects, like corrosion, wearing or other material defects are sometimes included in the model. The probability associated with this initial state is very high (close to 1) because the structure will be intact (in the sense above mentioned) for most of its life.

For a structure subjected to a time variant load, the probability of exceeding a limit state in a given time period corresponds to the probability that the extreme load amplitude in that period exceeds the capacity of the structure. In general, therefore, the action level to be considered for reliability evaluations corresponds to the extreme value distribution of the action in the reference time for the analysis.

In a full reliability analysis, the extreme action as well as the resistance of the structure are treated as random variables.

The probability distribution of the extreme value of the action depends on the characteristics of the distribution of the action and on the reference time on which the extreme is evaluated (i.e. on the average number of times the action is occurring).

If the load is accounted for by the variable corresponding to the extreme value in the same reference time adopted for reliability evaluations, the probability that the structure will be exposed to such load in that time period is, by definition, 1 and this exposure will occur once. This means that the probability of exceeding the ULS computed with this load does not need to be weighted by the probability of occurrence of the load scenario (both initial state and loads feature a unit probability). The above probability of exceeding, therefore, can be directly multiplied by the consequences in order obtain the risk contribution by the scenario.

2.3.2 Wave loads scenarios for ULS

For wave loads, the average period of each single cycle is quite short, so the number of applications results to be quite large for any reference period chosen for the analysis. This is not the typical situation for other types of events, likes fires, explosions collisions or grounding, which are intrinsically rare and may not occur at all in the lifetime of a structure. Because of the high number of repetitions, for waves the distribution of single cycle amplitudes is well defined and described by continuous distributions un-limited to the right (see Figure 2). Accordingly, the distribution of extreme values is, too, un-limited to the right, showing progressively higher mean values for longer exposure periods. Again, this does not apply to the other types of hazards, for which probability distributions are in general not available and the procedure to find an extreme value among a multiple number of occurrences on the single structure does not apply.

In design checks at a lower level of analysis (e.g. in checks based on a LRF or Partial Safety Factor formats), single characteristic values, instead of probability distributions, are representative of each variable. This is presented in Figure 1 for the load and resistance variables sketched, and in Figure 1 for different choices of the characteristics values for wave loads. For ships, typical characteristic values for sea related actions are taken at levels with a 10^{-8} exceeding probability (referred to any single cycle). This is based on an average number of load cycles of 108 in the design life of ships, corresponding to 25 years. The same value corresponds to a probability of 1/25 (4%) of being exceeded by the annual extreme value (based on the corresponding number of 4 10^6 cycles/year). In 25 years, the same 10^{-8} value features an exceeding probability of 63% (coming from the application of basic hypotheses of the theory of extreme values).

In similar checks for offshore platforms, the characteristic value is defined with reference to the annual extreme distribution, with an exceeding probability of 10^{-2}. This value features in 100 years an exceeding probability again of 63%, while in 25 years (which could be a reasonable design lifetime also for an offshore installation) the exceeding probability is about 22%. The different ways of characterising wave actions are sketched in Figure 1 below.

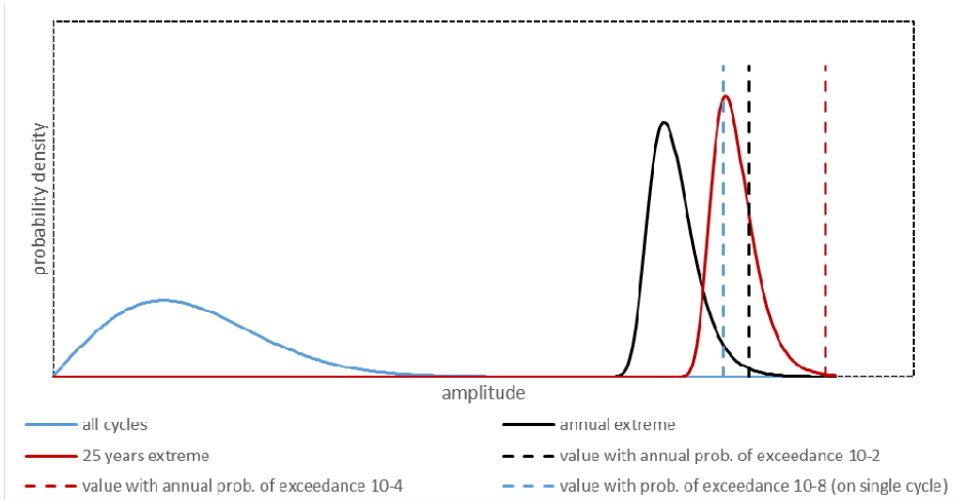

Figure 1: Different scenarios for wave actions

The above figure also indicates characteristic waves with a return period of 104 years (annual probability of exceedance of 10^{-4}). They are used in checks for abnormal environmental situations (see later). In this case the exceeding probability in 25 years is 2.5 10^{3}.

It is here marginally noted that, for a more precise comparison between characteristic values of loads for ships and for platforms (which is beyond the scope of the present report), other relevant aspects should actually be mentioned. Ships are not exposed for 365 days a year, but are considered to be sheltered from waves for about 15% of the time (in port or at dock), so the same design life corresponds anyway to a different number of exposure cycles (smaller for ships: about 85% of what is expected for platforms). Other differences are related to the fact that ships move and therefore experience in the same sea state a different wave encounter frequency than platforms.

In other types of checks for ships the concept of equivalent design waves is introduced. When checking the structural adequacy of the hull structure of ships, a set of load cases with different design waves is defined (see IACS 2017). In that case, the characteristics of design waves are selected in order to reproduce characteristic values of the wave effect (e.g. long term predictions of extreme values of the wave induced bending moment with exceeding probability of 10^{-8} during 25 years, see above).

When dealing with design waves for structural checks, a definition based on extreme values of the wave height (i.e. a characteristic value of the action, instead of the action effect) may also apply, based on the assumption that the effect is proportional to the wave height. This, however, should be checked carefully in those cases in which strong nonlinearities apply. In these cases, the average effect of a set of very high waves may be by far larger than the effect of a single wave with an average height computed on the same set.

2.3.3 Scenarios for verifications of SLSs

When the capability of maintaining a full operability of the structure is to be evaluated, the scenarios adopted are based in general on an initial intact state similar to that adopted for ULS checks, but on environmental loads corresponding to a shorter exposure time and on more restrictive criteria. The contribution to the risk is to be evaluated taking into account that these limits will be exceeded in the structure lifetime several times. The inherent consequences will therefore occur for the expected number of times (greater than 1) in which the limit is exceeded.

2.3.4 Scenarios for verifications of FLSs

Also in the case of fatigue verifications, the initial state is intact (an initial distribution of small defects may apply). When modelling the exposure by means of a long term prediction of the distribution of the load cycles amplitude, the reference time duration is the structure lifetime. Limits corresponding to fatigue collapse are set (different definitions may apply). The probability of this scenario is again 1, as the fatigue strength of the structure will definitely be put into trial by the lifetime distribution of the load cycles amplitude. Accordingly, the consequences of exceeding the limit do not need to be weighted.

In simplified checks, on the other hand, conservative load stress histories may be adopted. In this case, a lower probability of occurrence would apply.

2.4 Accidental and abnormal environmental situations

The situations to which the above three categories of LS are applied all are characterized by an initial intact condition of the structure and by a probability of occurrence of 1 of the scenario (Eq. 1 and 2), when a full reliability analysis is carried out. In addition to those situations, other scenarios have been recognized more recently to be relevant for design purposes. A further class is represented by those situations in which the structure, because of specific external actions, is in damaged conditions (with specific degradation effects concentrated in parts of the structure). These situations will not necessarily occur in the lifetime of all structures, but, as they imply large consequences, they need to be considered at the design stage. This class of low probability situations, corresponding to accidental and very rare (abnormal) events, is the object of the present report. Their distinctive features are therefore related to the presence of a localised damage (due to various types of hazards) and to the low probability of occurrence (typically a return period of a couple of orders of magnitude longer than the lifetime foreseen for the structure).

Accidental situations refer to hazards such as fire, explosion, collision, dropped objects or very rare environmental events. Checks are aimed at achieving that the main vital functions of the structure are not impaired (beyond a certain probability level) during any accidental event or within a certain time period after the accident. The analysis of these scenarios includes the evaluation of the immediate consequences of the event and/or the evaluation of the probability of occurrence of an escalation of events that, starting with the accident, may lead to a progressive collapse (exceeding various types of limit states). Such analyses have for several years been required for the design of offshore structures, where they are considered with reference to accidental limit states, ALSs. A quality of a structure relevant for such analyses is robustness, characteristics related to the ability of preventing progressive collapse of the structure following an initiating damage event.

This report is focused on accidental/abnormal situations and inherent characteristics. These scenarios imply in general an exceptional action, giving rise to an initial damage state, which needs to be characterized. The situation may imply further actions (e.g. environmental actions) on the damaged structure with specific characteristics in terms of amplitude, exposure times and resistance capabilities of the structure. The criterion for assessing the state of the

structure after damage is often related to ULS, even though the large variety of situations, different from each other, implies a variety in the definitions of the inherent LSs.

In accidental scenarios, loss of capacity of individual members and subassemblies may take place, but the focus is on maintaining main safety functions that prevent total collapse. This means that individual members can be subjected even to loads larger than from normal use (SLS and FLS) and extreme loads (ULS).

2.5 Uncertainties in accidental scenarios

In the assessment of the adequacy of a structure to accidental/abnormal scenarios, several uncertainties arise, due to the approximate nature of the methods for determining actions and action effects. Further uncertainties apply to the knowledge of the system characteristics (e.g. the material strength). The above uncertainties apply to any scenario for structural verification, but they are enhanced in the case of accidental scenarios, because of their characteristics. In particular: low probability of occurrence (i.e. difficulties in obtaining statistical data) and extreme variability in the types of situations (with particularly large complexity of the models involved in the performance prediction) and variety of limits states adopted for the assessment.

2.6 Design accidental/abnormal scenarios

Accidental scenarios for the design and assessment of structures and associated performance criteria should be set on the basis of risk assessment for a given type of structure. The first step is to perform a Quantitative Risk Assessment (QRA), which is a formalised specialist method for calculating individual, environmental, employee and public risk levels for comparison with regulatory risk criteria.

This should be done for all types of hazards/abnormal environmental events, identifying the probability of occurrence and the magnitude of actions, of action effects and of consequences. For each relevant category of scenarios, one or more specific scenarios or situations is to be defined for design purposes. For example, for a ship-ship collision scenario, a specific situation must be specified such as e.g a bow impact of a striking ship in the side of a struck ship. To proceed with the analysis, a further step is necessary, in which a quantification of the main variables is carried out (ex: impact angle, impact energy) in order to define a design situation. This is illustrated in Figure 2.

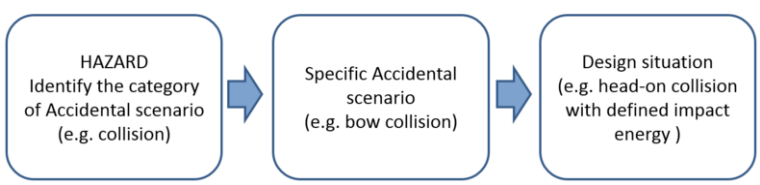

Figure 2: Flowchart for definition of design situation in ALS.

A design situation is meant to be representative of a wider class of real situations and should be chosen in such a way that the performance of the structure in that situation is as much as possible representative of the performances in the whole class of real situations. In the above example, the spectrum of possible ship-ship collisions is much wider, including impacts on different parts of the hull, with different angles and different relative velocities, but for design purposes, a discrete number of scenarios is considered.

In principle, the equivalence should be evaluated in terms of risk. In other words, the risk in the single design condition should be similar to the risk for the whole class of similar 'actual' situations. A way of ensuring such result is to select, as design case within a class, a specific scenario which allocates a major (or at least a large) part of the risk associated to the whole class and to attribute to that specific case the probability of occurrence of the whole class. A

similar procedure is suggested in (Rizzuto et al., 2010) for the case of a tanker in grounding conditions. The same concept was later refined in (Prestileo et al., 2013) with the use of a Bayesian Network to identify the damage case allocating the highest probability of failure for the hull girder of the ship.

2.7 Design Standards

Design standards, among other tasks, are meant to provide guidelines on how to determine the capacity of the structure to resist various types of scenarios, inclusive of accidental ones. In this context, they cover the definition of design scenarios, the evaluation of the response of the structure to the scenario and the assessment of such response. The latter is to be based in principle on a risk analysis including the classical three types of consequences: loss of life in the structure or the surrounding area, pollution of the environment and loss of property or financial exposure.

Guidelines may be provided on how to investigate a given scenario both using simplified solutions with explicit formulas or with more advanced numerical simulations. Since the computer resources are increasing continuously, it is more and more common to use advanced numerical simulations. The most usual tools and methods for advanced numerical simulations are Finite Element Method (FEM) for assessing the action effects and Computation Fluid Dynamic (CFD) analysis for assessing the external actions/loads. Advanced numerical simulations are very general and can be adopted for cases that are not properly covered by simplified solutions with explicit formulas. However, numerical simulations require experienced users and several factors must be accounted for in order to achieve reliable results. These factors can typically be material model, solution procedure, mesh refinement, etc. which are discussed in more detail in the following chapters with reference to accidental scenarios.

2.8 Status of existing design standards for ships in relation to accidental scenarios

All major standards for offshore structures offer a practical implementation of an explicit design approach against accidental and abnormal actions, even though the degree of details in characterizing actions and action effects may be different for the various situations. As stated in (Czujko et al. 2015) this approach has not yet been widely adopted by the shipbuilding industry, largely due to a conservative approach of this industry, which developed its know how by experience over hundreds of years. Another peculiarity is represented by the fact that accidental scenarios for ships are very case dependent on the ship design and type of operation. Also acceptance criteria can be formulated in quite different ways: safe return to port, safe evacuation, resistance to flooding, containment of oil spilling, etc.

A more traditional approach followed for ships is the development of prescriptive rules, derived from past experience and related studies and covering implicitly accidental criteria. Prescriptive provisions of this type are e.g. for all ships: the requirements about number and characteristics of watertight bulkheads (against flooding) and free board requirements against green water effects (when dealing with the encounter of extreme waves). For tankers, requirements are set about presence and dimensions of a double hull (against oil spilling caused by collision and grounding events).

A growing interest is shown, however, in the use of direct analysis to explore design solutions and this is also being pushed by IMO's long term target for Goal Based Standards. In this context, a few examples of requirements are present, where specific aspects related to accidental scenarios are considered (in particular for collision and grounding).

One example is the check for hull girder residual strength after a grounding or collision event that is incorporated into the Common Structural Rules for Bulk Carriers and Oil Tankers. In this check, a damage extent in the bottom and side is specified for grounding and collision, respectively.

In other cases, direct computations of accidental scenarios are applied for the assessment of alternative designs:

- Marpol collision and grounding equivalence: According to Marpol Annex I (IMO 2004a), comprehensive non-linear FE analyses can be used to demonstrate equivalence with regards to collision and grounding resistance of a combination carrier compared to a similar sized reference oil tanker. If strength equivalence or better can be shown, a less restrictive requirement to mean outflow parameter is accepted.
- Equivalent study for reduced minimum distance between outer skin to LNG tank: The safety against an impact of the tanks is dependent on the strength of the ship side, and FE analysis can be used to demonstrate that equivalent safety is kept for a strengthen ship side with reduced minimum distance between outer skin to LNG tank.
- FE analysis with dropped objects from crane operations that hit fender protections for LNG fuel tanks.

Another accidental scenario that can be relevant for ships is explosion, and not only related to the presence of hydrocarbon on board. In the recent years, there is more focus on the environment, and battery systems for electric propulsion ships (for instance on ferries, offshore vessels, etc.) is considered as an effective climate mitigation action. However, with battery systems there is a risk for fire and explosions, and for instance Norwegian Maritime Authority (NMA) now requires additional documentation such as fire extinguishing philosophy and explosion analysis.

In the following chapters, analysis procedures of what is presently available for the analysis of the main categories of accidental scenarios is presented, with particular focus, when possible, on ships.

3. ABNORMAL ENVIRONMENTAL EVENTS

In addition to the 'classical' accidental situations corresponding to collision, grounding, fire, explosion and similar, which are characterised by rare events with so large consequences that they cannot be neglected, it is also relevant to consider situations associated with rare environmental actions.

Actions due to environmental loads are included in other scenarios, like those to be checked against SLS, ULS and FLS (see chapter 2 above). The justification for introducing a new class of scenarios regarding environmental effects stands in the activation of a different risk generation mechanisms due to the presence in abnormal events of different phenomena in the actions themselves and/or of different effects in respect to those produced in the other scenarios.

For marine structures, abnormal environmental actions are mainly represented by extremely high waves. They feature, in comparison to the (relatively) lower waves relevant for ULS design, more severe kinematics near the free surface and also a different type of wave-structure interaction (for example: a wave hitting the deck has a different effect than one impacting only on the legs of a platform).

The models adopted for describing waves and their effects within ULS, FLS and SLS checks are not able to capture these different aspects, which need to be treated in a specific way with different models. The very low probability of occurrence of the abnormal wave events and their characteristics and effects justify the classification of these situations within the 'accidental' (in a broad sense) scenarios.

3.1 Abnormal waves

Rare events with long return periods are in principle included in the tails of the probability distributions of the extreme crest height used in ULS analysis. As Figure 1 shows, even a lim-

it corresponding to the height of a wave with return period of 10 000 year can be exceeded with a non-negligible probability in 25 years. However, the major contributions to the probability of exceeding the ULS come from waves with return periods of the order of magnitude of the design lifetime of the structure. For checks formulated in LRF or PSF formats, as mentioned above, characteristic values for wave and wave effects are set with typical return periods of 25 and 100 years for ships and platforms, respectively. Models of wave loads aimed at describing events with those return periods are unable to capture the wave in deck load and local pressures near the wave crest, typical of events with a much longer return period. Abnormal occurrences can also result in wave events that are steeper and higher than the surrounding waves.

The need for proper models of larger wave events has indeed focused the attention of the scientific and technical community, also because detailed experimental records were obtained for a number of very high single wave events in the last twenty years. These records shed a new light on previous reports of other extraordinary waves and of extraordinary damage events occurred to ship structures around the world. These data have prompted an intense research activity aimed at modelling in a proper way the mechanism of generation, the frequency and the characteristics of those events. The details of these discussions are quite complicated and fall outside the mandate of this committee. They have been documented extensively for instance in the last reports of the Committee I.1 of ISSC 'Loads' (see Bitner-Gregersen et al., 2012, 2015 and 2016).

3.2 Abnormal wave design loads for offshore structures

As reported in Czujko et al. (2015), in simplified checks for offshore platforms, based on characteristic values of wave height, abnormal environmental loads are defined with reference to events with a yearly probability of exceedance of 10^{-4} (as for other accidental scenarios), see ISO (2007) and NORSOK (2007). Slightly different approaches were originally used to determine the necessary design airgap in the above standards for the 10^{-4} wave event. More recently, a general concern for a worsening of sea conditions also due to climate changes has necessitated stricter design requirements. Thus, STATOIL introduced an internal conservative design requirement for the air gap of platforms accounting for the 10 000 year wave elevation increased by 10%. According to simple patterns like those of Figure 1, this 10% increase in the characteristic value corresponds to lowering the exceeding probability to about $1.5\ 10^{-5}$ in 25 years (if computed on the same base distribution of wave heights).

A recent formulation is contained in NORSOK (2017). Also in this case, to design the air gap between the sea surface and the deck of fixed platforms, it is strongly recommended to use a value of at least 1.1 times the 2nd order crest height (with probability 10^{-4}), plus the combined tide and storm surge. Another option to satisfy the same requirement of positive air gap, is to evaluate higher order wave effects and spatial statistics of wave elevation in detail. Alternatively, wave-in-deck scenarios are to be applied.

The effect of climate changes on permanent facilities with a planned service life of more than 50 years is considered, too. The motivation is that future wave, wind and sea level conditions are predicted with considerable uncertainty by the current models. In lack of more detailed information, the following increase in metocean characteristic values for predictions 50 years ahead is recommended in NORSOK (2017):

- extreme wave heights: +4% on characteristic values
- extreme wind speeds: +4% on characteristic values
- sea level: +0.25 m

The increase is to be applied for both the 100 years return period wave (design scenario for ULS verifications) and for the 10,000 years return period (design scenario for ALS verifications).

In the cases reported above, more restrictive requirements are set (in terms of a 10% increase in the height of the deck over the still water level) in order to improve, in respect to previous prescriptions, the safety of the structure as regards water on deck events. A question is raised, however, about the foreseen probability of exceeding the new limit. Currently, there is no definite answer to this (see later).

The increments in the platform height required by the most recent requirements are apparently justified as a consequence of new knowledge about actual wave events (now recognised to be higher than what before modelled, because of new effects included in wave models and/or of climate changes). No mention was found to a modification in exceeding probabilities. This can be interpreted as an indication that the new requirements are meant to re-establish the original probability of exceedance (10^{-4} in a year, 2.5 10^{-3} in 25 years) in the presence of a more severe distribution of wave heights. On the contrary, these requirements could have had in part also the implicit aim of reducing such probabilities.

3.3 Comments to offshore scenarios

The trend of research in the field of wave models is to obtain a comprehensive model for sea waves, able to capture effectively the whole spectrum of wave events, including the most rare ones, and to predict correctly their characteristics and frequency of occurrence. The improvement of wave models imply changes in the description not only of the crest elevation, but also of all the characteristics of the wave field (kinematics, steepness, etc.) that are essential to model the effects on the structure. A key point for a proper consideration of the scenario corresponding to an abnormal wave event remains however linked with the wave hitting or not the deck and the modelling of this situation.

It is to be noted that when designing the airgap of fixed platforms, the underlying idea is to move the event of a water impact on the platform deck in the region of 'negligible risk' by reducing so much the probability of occurrence that even a large consequence would not contribute significantly to risk. This way, a proper evaluation of the consequences of water on deck can be avoided. In principle, however, any platform, designed with any air gap, is subject to the possibility that a rogue wave reaches the deck and this would imply consequences, both for the global and local response of the structure. The probability for this to occur may be very low (and a good model is needed to evaluate it), but it will never be null. The risk associated with this situation is limited by the low probability of occurrence of the wave but, on the other hand, may be easily enhanced by large consequences. An exceeding probability of 10^{-4}, like that of the base event on which the present requirements on air gap seem still to be based, is low, but not low enough to consider negligible the corresponding risk (and to avoid a consequence evaluation of the exceedance). Consequences evaluation is actually carried out for other hazards at similar probability levels (fire, explosions, collision, dropped objects, grounding). The assumption that a proper consequences analysis can be avoided by compliance with the above airgap provisions appears therefore questionable in the context of a risk oriented design.

A consequence analysis of waves hitting the deck would provide the possibility of carrying out a cost benefit analysis on the design air-gap, and also the possibility of investigating the robustness of the structure to these events (and of increasing it, if applicable).

The possible introduction of an accidental scenario for waves hitting the deck of a fixed platform should include a wave actually reaching the deck. A possible way of formulating this scenario would be to take, as representative wave, one corresponding to a given height of water over the deck. The probability of occurrence of this scenario should of course be evaluated as an important characteristic, but also consequences and possible escalation of consequences should be quantified and can provide important information for design improvements.

3.4 Possible definition of abnormal wave scenarios for ships

A possible update of the currently used wave models (that are basically the same for ships and platforms) would imply an update also in the probability distributions of wave effects on ships. In particular, the increased frequency of occurrence (confirmed by theoretical analysis) of waves steeper than those provided by earlier models could suggest (in parallel with what already happened for the air gap of platforms) a revision of the present free board prescriptive requirements for ships. It is interesting to note that, due to the different response of floating structures, the worst situation refers to waves with a length similar to that of the vessel and not to longer waves (that are in general higher). Accordingly, free-board provisions do not contain explicitly parameters referred to waves, but only to the ship geometry.

In parallel with the situation of fixed platforms, a significant non-linearity in the structural response of ships to wave action is surely occurring both when the seawater floods the deck (green water event) and when the ship bottom hits the water surface (slamming event, possibly followed by a transient response of the hull girder: whipping). Both these events (which have a different probability of occurrence) have implications in terms of global and local response of the ship structure and may give rise to significant risk contributions.

Presently, these aspects are covered in an implicit way by design and operational prescriptive requirements issued by Class Societies. Minimum values are set and checked during the loading process for the free board (distance between the weather deck and the water plane in loaded conditions and for the draft of the ship). Bow and forward bottom impact loads are also considered since long time in Class Societies Rules in the context of ULS scenarios for local checks of the hull scantlings. Empirical values of green water pressures are set as well for the structural checks of exposed decks, bulkheads, hatchways and outfitting placed on the weather deck (see e.g. IACS 2017).

Explicit accidental scenarios dedicated to extreme weather events, however, have not been included so far in the design process of ships. They could be effectively adopted, and described in terms of actions, taking advantage of the recent progress achieved in wave model and above briefly mentioned. Also, as regards the models of effects, new possibilities of accounting for the non-linear effects of green water on deck in the context of hull girder loads have been reported, as well as the development of CFD techniques able to describe the dynamics of waves breaking on the deck. Some recent developments, referred to the EU funded EXTREME SEAS project are summarized in Bitner-Gregersen et al. (2016). Without going into more details on the development of these models, which is beyond the scope of the present text, it is here outlined that establishing accidental scenarios dedicated to extreme wave events seems to be possible in the near future. This would allow a more systematic exploration of innovative solutions aimed at risk reduction (possibly involving trade-offs between increases in free board and in deck scantling).

4. METHODS AND PROCEDURES FOR THE ANALYSIS OF ALS

4.1 Introduction

By definition, accidental limit state (ALS) and ALS design refer to structural integrity following an undesired situation, such as crash, impact, fire, collision or explosion. Due to the complexity of the situation and the physical size of the structures involved in such conditions, full-scale experiments are seldom performed. The usual approach for handling this is by performing numerical analysis and validation with scaled down experimental replications. This is showing that the correct Finite Element Method (FEM) analysis is crucial. Material models, definition of the loads and the boundary conditions require extra attention due to the nature of such accidental conditions with high strain rates or extreme conditions.

The analysis of extreme events on ship structure inherently involves plasticity and fracture. A key challenge is that both are inherently local material-scale or plate-scale phenomena and yet the analyses of interest typically have a length scale of tens of meters or more due to the large size of the structures of interest. Furthermore, planar shell elements are utilized for the vast majority of ALS analyses and these elements must be larger than the thickness of the plate structural member. Fortunately, since the typical analysis of an ALS seeks to capture gross structural behaviour, final deflections, and the gross extent of fracture and damage, only quantities that effect the overall structural response, i.e. material stress-strain and strain at failure, must be captured to address these disparate length scales. It is noted that for analysis cases where local structural details dominate the response modes, e.g. the analysis of connection details for internal explosions, a highly-refined FEM model of the relevant details is usually required. Such FEM's, due to the dramatic increase in computational power, have the potential to capture the details material response such as crack initiation and propagation.

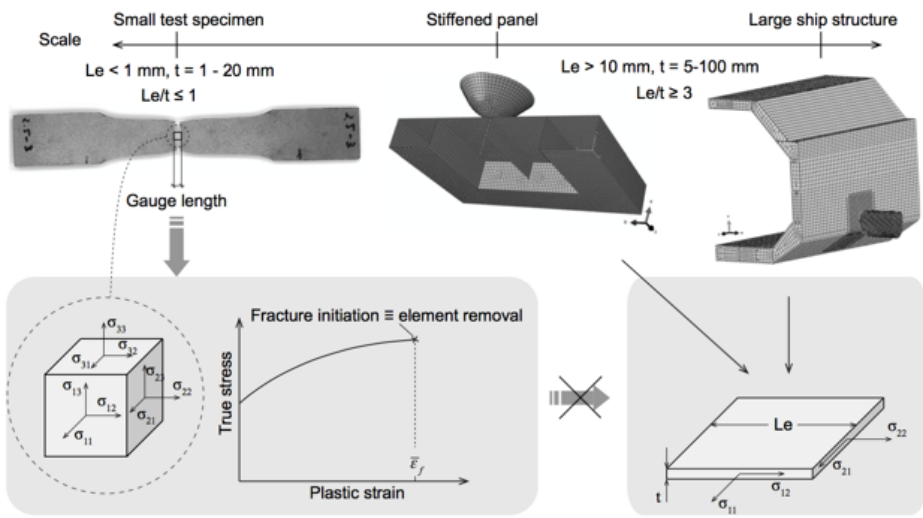

Figure 3: Illustration of the different scales in fracture analysis:
small test specimen, stiffened panel and large-scale ship structure.

When only the energy absorbing capacity of a ship during an impact event is needed, analyses can be limited to either FEM analyses up to failure or analytical or empirical solutions. For instance, the most well-known simplified empirical approach to collision analysis was made probably by Minorsky. In (Zhang and Pedersen, 2016) a simplified method for energy absorption is presented, based on plastic tension damage and crashing and folding damage. The rupture strain of the material is obtained from standard uniaxial tensile tests.

However, using the last couple of decades, the requirements related to the crashworthiness of ship structures were often broadened and involve hazards linked with pollution, stability in damaged condition and ultimate strength of a damaged ship. Further, there was a shift from deterministic methodologies to probabilistic methodologies, which are used both for the assessment of the crashworthiness of a structure as well as the effectiveness of risk control options.

These concepts also set different requirements to the methodologies that are used for the simulation of the impacts: it is, therefore, no longer appropriate to use a rupture criterion “uncoupled” with the simulation, but it is necessary to integrate the criterion in the FE software to simulate the propagation of rupture. This is now essential, because the required output, which is subsequently used for the calculation of oil outflow, the time to capsize and the ultimate

strength, is the description of the damage rather than the energy absorption capacity of the structure until rupture. For the determination of the extent of the rupture and damage in case of impact, it is not considered appropriate to use methodologies based on plastic collapse mechanisms, because such methodologies do not simulate the propagation of rupture other than the tearing of plate structures, when they are penetrated by an impactor moving parallel to the plate.

For all materials of interest, the analytical description of material behaviour consists of a constitutive model, which relates stress and strain, and a fracture model that describes the point of rupture. More advanced models couple the fracture and constitutive model to achieve a unified description of material behaviour. Since the fracture process has a length scale that is smaller than the resolution of the analysis, a mesh dependency of the fracture criteria is also required.

Within this chapter both developments and currently commercially available material models for several materials, such as steel, composites, foam, rubber, ice and soil, are discussed. First recent developments in modelling details and response evaluations are given. Furthermore, developments in standards are discussed. Looking at the applicability of material models for ALS, models of course include non-linear material behaviour and progressive failure.

4.2 Modelling details and response evaluation

Dynamic responses of a ship structure under the collision accidental scenario are related to many nonlinear effects, including load nonlinearity, geometry deformation nonlinearity and material nonlinearity et al. Modelling these nonlinear characteristics with proper methodology and analysis tool has been a challenge facing scholars and ship designers. In addition, the accuracy of response evaluation of ship structure under collision accidental scenario has to be relied on the qualities of analysis modelling details. Currently, analytical methodology, numerical simulation methodology and model testing methodology are the three tools used most frequently. The latest research outcomes of these three methodologies are summarized in this part.

4.2.1 Analytical methodology on response evaluation

Analytical method has always been granted as one of the most conveniently used methods to predict structural dynamic responses during ship collision and grounding scenarios, when interest is limited to energy absorbing capacity and failure initiation. The structural dynamic responses, including deformation resistance and energy dissipation, though much complicated due to their nonlinear characteristics, can be approximately estimated by analytical formulae within a short time. And the high efficiency and low cost on human labour and calculation time make analytical method much welcomed by ship designers. The analytical expressions for nonlinear structural deformation and responses are established based on internal elastic-plastic mechanisms, and external kinetic dynamics.

The prediction with analytical method for dynamic responses of ship shell, deck, girder and web-frame are mostly developed. The analytical method can be used separately to predict structural response of single structural component, and can also be integrated to predict global structural response of ship side or ship bottom during the ship collision and grounding scenarios.

Stretching of shell plating is playing a dominant role under ship collision scenario. Liu and Soares (2015a) proposed simplified evaluation methods to assess the energy dissipation for stiffened side shell plating under minor rigid bow striking scenario, and further (Liu, et al., 2015b) built a set of analytical methods to predict structural resistance and energy dissipation of stiffened-shell plate and that of damaged shell plate, under the striking of wedge-shape indenter during a quasi-static collision process. The initial minor collision damage is involved to evaluate the total damage of shell plating. The shell deformation mode they used is shown

in Figure 4. Similarly, Sun and Hu (2015) investigated the structural deformation resistance of side shell plate under raked bow collision scenario. The deformation of stiffeners attached on the side shell is taken into consideration, and an analytical method for the instant structural resistance of side shell under raked bow striking is proposed.

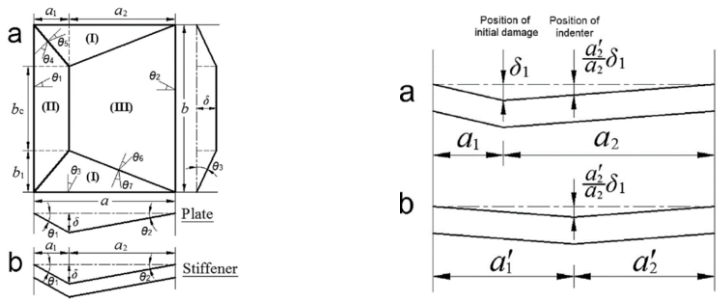

(a) Deformation mode of intact shell plating (b) Deformation mode of damaged shell plating

Figure 4: Deformation mode of shell plate under minor collision scenario

The in-plane deformation mode of the ship girders and webs is the one of the essentials to predict resistances and energy dissipations of these structures under collision scenario. Deformation models of girder and web have been proposed, including Gao and Hu (2014), and Liu and Soares (2015). Liu and Soares (2016a) further developed analytical method for estimating the crushing behaviour of web girder with stiffeners under collision scenario. Most of these models can be used to predict the deformation resistances with acceptable accuracy. Furthermore, the recent proposed analytical formulae are compared with those proposed in the past researches in Table 1.

Table 1 A summary of some existing simplified analytical methods for predicting the crushing resistance of web girders

Method	H	λ	F_m	F(δ)
Wang (1995)	$H=0.811b^{2/3}t^{1/3}$	0.67	$\frac{F_m}{M_0}=\frac{11.68}{\lambda}\left(\frac{b}{t}\right)^{1/3}$	-
Simonsen (1997)	$H=0.671b^{2/3}t^{1/3}$	1	$\frac{F_m}{M_0}=\frac{14.76}{\lambda}\left(\frac{b}{t}\right)^{1/3}$	$\frac{F(\delta)}{M_0}=\frac{4b}{H\sqrt{1-(1-\frac{\delta}{2H})^2}}+\frac{12H}{bt}\delta$
Zhang (1999)	$H=0.838b^{2/3}t^{1/3}$	0.75	$\frac{F_m}{M_0}=\frac{11.26}{\lambda}\left(\frac{b}{t}\right)^{1/3}$	$\frac{F(\delta)}{M_0}=4.37t^{-1/6}b^{2/3}\delta^{-1/2}+4.47b^{-1/3}t^{-2/3}\delta$
Simonsen and Ocakli (1999)	$H=0.377b^{2/3}t^{1/3}$	1	$\frac{F_m}{M_0}=\frac{18.72}{\lambda}\left(\frac{b}{t}\right)^{1/3}$	$\frac{F(\delta)}{M_0}=\frac{3b}{H\sqrt{1-(1-\frac{\delta}{4H})^2}}+\frac{22H}{bt}\delta$
Hong and Amdahl (2008)	$H=0.395b^{2/3}t^{1/3}$	-	$\frac{F_m}{M_0}=\frac{17.0}{\lambda}\left(\frac{b}{t}\right)^{1/3}$	$\frac{F(\delta)}{M_0}=\frac{1.2b}{H\sqrt{1-(1-0.3\frac{\delta}{H})^2}}\left(2+\frac{1-0.3\frac{\delta}{H}}{3+(1-0.3\frac{\delta}{H})^2}\right)+\frac{22.24H}{bt}\delta$
Liu and Soares (2015)	$H=\left(\frac{\pi}{36}b_1b_2t\right)^{\frac{1}{3}}=0$	-	$F_m=\frac{E}{3H}=\frac{\pi}{6}\sigma_0t^2(b_1$	$F(\delta)=\frac{\dot{E}}{\dot{\delta}}=\sigma_0t^2\frac{(b_1+b_2)}{3H\sqrt{1-\left(1-\frac{\delta}{3H}\right)^2}}+2\sigma_0tH\delta\left(\frac{1}{b_1}+\frac{1}{b_2}\right.$
Gao and Hu (2014)	$H=0.193(b_1b_2t)^{1/3}$	-	$F_m=\frac{0.75\pi M_0b}{H}+\frac{40}{}$	$F(\delta)=\frac{1.5M_0b}{H\sqrt{1-(1-\frac{\delta}{8H})^2}}+\frac{10.2N_0H\delta}{b}$

4.2.2 Numerical simulation methodology

Numerical simulation with nonlinear finite element method is one of the most powerful methodologies to estimate and evaluate structural responses during ship collision and grounding scenario and allows for the inclusion of progressive failure. These analyses can then be used in combined analyses including e.g. oil outflow or time to capsize. However, many uncertainties and challenges have not been overcome. And these are still obstructing the credibility of numerical simulation results to a further step. Many efforts have been made recently, gaining further insight in numerical simulation methodology. Among these challenges, the definition of structural failure criteria is of crucial importance. Proper definitions of element failure criteria will bring accurate simulation and analytical analysis results. Presently, there are several structural failure criterion existing that have been used and evaluated frequently. These structural failure criterions include equivalent strain criteria, FLD, BWH, RTCL et al.

Storheim and Amdahl (2017) carried out research on the sensitivity to work hardening and strain-rate effects in nonlinear FEM analysis of ship collisions. They investigate the effect of various features of the complete stress-strain curve on the predicted outcome of a collision simulation. The slope of stress-strain curve is strongly dependent on the yield ratio, yield plateau and the elongation to fracture. In addition, Martin Storheim et al. (2015) also presented a fast and reliable method for failure prediction of coarsely meshed shell structures. That method is especially relevant when investigating the impact performance of offshore structures and typically stiffened panel structures. The failure model was based on stress-based BWH local instability criterion and a coupled damage model, and the failure model was incorporated into LS-DYNA code.

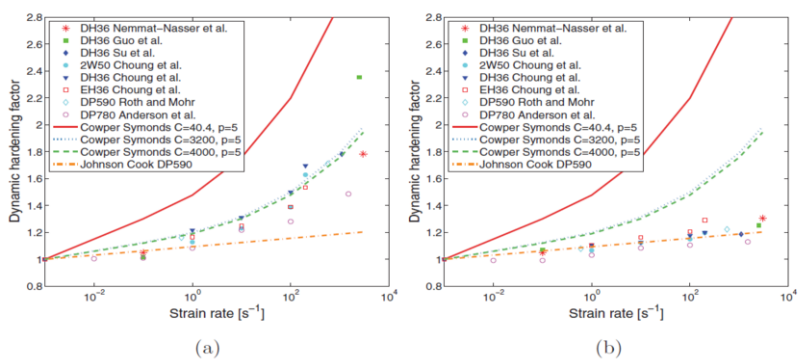

Figure 5: Comparison by Storheim (2017) on dynamic hardening factors for initial yield stress and average flow stress at different strain rates. (a) Yield-stress ratio. (b) Flow-stress ratio.

Yoshikawa et al. (2016) analysed the fracture considering the effect of stress tri-axiality, and they anticipated that the accuracy of fracture analysis can be improved by taking account of the tri-axial effect on fracture strain, due to the reason that the equivalent plastic strain at the ductile crack initiation will decrease with an increase of stress tri-axiality. A. Gilioli et al. (2015) made an analysis of plasticity and fracture test of different type of helicopter tail rotor transmission shaft specimens, to calibrate the phenomenological Modified Mohr-Coulomb model and the empirical Bao-Wierzbicki fracture models, through numerical simulations. A. Shaw et al. (2015) investigated the behaviour of cantilever beams subjected to projectile impact at its tip, through a kind of free-mesh method. A study on modelling of rate-dependent material behaviour in simulation of collision damage has been carried out by Burak Can Cerik (2016), and it is observed that Cowper-Symonds constitutive modelling with parameters based on lower yield stress does not always yield conservative results.

During recent years, Arctic sailing route has made the research on the collision between LNG ship and iceberg more popular than ever, but the challenge on simulation methodology for LNG ship structure in cold region has not been resolved. The influence of brittle fracture criteria on the crashworthiness of ships and offshore structures in arctic conditions is investigated by Woongshik Nam and Jørgen Amdahl (2016). The brittle property of steel exposed to low temperature and in range of ductile brittle transition temperature (DBTT) was considered, and RKR model was used for brittle fracture prediction in numerical simulation. It was concluded that failure criterion for building material used on LNG CCS (cargo containment system) might be quite different from those of normal steel material. The anti-collision capability of LNG carrier and FLNG depends much on the failure limit of the material used in LNG CCS system. Myung-Sung Kim et al. (2016) proposed a failure criteria for the primary barrier of a Mark III-type liquefied natural gas CCS, and the criteria was established based on the instability, ductility and shear failure. Chun-sik Shim et al. (2016) also carried out a study on material used in LNG carrier CCS system.

4.3 Present application and recent development in current standards

For accidental scenarios, the most important standards can be listed as ISO 19900 series, NORSOK standards, DNV-GL standards (DNVGL-RP-C204, 2010; DNVGL-RP-C208, 2016), API Recommended Practice, ABS standard and Lloyd's Register guidance notes on ALS. A more detailed overview of the standards can be found in Czujko et al. (2015).

In the design standards, an overview of approaches is presented that can be used to identify and assess the effects of accidental structural loads arising from accidental actions. It is required that damage from accidental actions with reasonable likelihood of occurrence shall not lead to complete loss of integrity of the structure, and the load-bearing function of the structures must be maintained. The design must be dimensioned such that critical parts for the overall strength are strong enough to withstand an accidental action, or alternatively, can be dimensioned in order to minimize the consequences with a certain redundancy without causing failure. There are different levels of complexity in the approaches ranging from simplified methods with explicit formulas using hand calculations to advanced state-of-the-art numerical methods (FEM, CFD, etc.). Since the computer resources are increasing continuously it is more and more common to use numerical simulations.

The design standards are continuously updated in order to be more accurate and suited for today's practice using numerical simulations. In the most recent version of DNVGL-RP-C208, more examples with details have been included in order to give guidance on how to perform non-linear FE analysis, since experienced users is usually required to obtain reliable results. These examples give a relatively detailed description on FE modelling (material, mesh, boundary conditions, calibration, etc.), analysis procedure and post-processing of the results. In addition, a detailed procedure on how to calibrate non-linear FE analysis against a known solution is included.

The most recent DNVGL-RP-C208 contains also a library with FE models to be used in collision analysis. These are FE models of the bow, side and the stern corner of offshore supply vessels (OSV) and the models are prepared both in Abaqus and LS-Dyna formats that can be downloaded. The library with the FE models will bring more consistency on how finite element analysis are performed. Moreover, this makes it easier with 3rd party verification of non-linear FE analysis.

The main reason for including FE models for collision analysis was because the previous acceptance criteria and analysis methodologies are specified in design standards written decades ago, and based on offshore supply vessel (OSV) design with raked bow and 5000 tons displacement. Today, the modern OSVs are larger and often designed with bulbous bow. Consequently, higher impact energy must be absorbed in the event of a collision, and the Petroleum

Safety Authority Norway recommended to increase the ship impact design energies (Kvitrud, 2013). Increased energy levels for collision scenarios are now implemented into todays practice in DNVGL-SI-0166, 2016 and NORSOK N-003, 2017.

4.4 Material models to be used in FEM

4.4.1 Metallic Shipbuilding Materials

The dynamic behaviour of steel, aluminum, and titanium at high strains reaching near the point of fracture are well described by classical plasticity theory with adjustments for high strain-rate and anisotropic behaviour. The combination of von Mises plasticity with Johnson-Cook (Johnson and Cook, 1983) or other similar hardening rules have proven to be the mainstay of dynamic analysis. For materials such as aluminum, the yield functions of Hill (1948), Hosford (1972) have shown to produce highly accurate results e.g. Yield surfaces for anisotropic materials are well established and have been used for decades in a wide variety of relevant applications.

The determination of fracture proves to be more difficult to capture since the process of ductile fracture is driven by the growth and coalescence of voids on a micron length scale. Although the capability of highly resolved 3D calculations of fracture specimens to provide a predictive capability is evident, such computations require a resolution that is entirely impractical for structural analyses. This can be observed by reviewing the results of the Sandia Fracture Challenge, a recently completed round-robin blind ductile fracture prediction study.

Thus, within the context of ALS analyses of large marine structures, fracture can only be included in a phenomenological manner by "encoding" the material description with a reasonably description of fracture in the relevant length scale of the element, usually as a failure strain that is a function of the stress state and loading rate. The simplest approach to achieving this has been to select a single uniform strain value at which the local element fails. Although this approach does not capture failure in a physically accurate manner, it is simple to use and implement and can be easily calibrated to experiments. An improved approach is to use a strain to failure value that is a function of the stress triaxiality (ratio of mean to effective stress) and J3, the third invariant of the stress deviator tensor. For shell elements, it was shown by [Wiez, AHSS] that due to the assumption of plane stress, J3 itself is not an independent function of the stress triaxiality thus greatly simplifying the problem. On that basis, one recent failure criteria includes the combined effect of mesh size and stress triaxiality on the failure strain, see (Kõrgesaar and Romanoff, 2014; Walters, 2014). The reasoning behind such scaling framework is that mesh size dependency of the FE solution depends on the amount of strain localization, which varies depending on the stress state (Kõrgesaar, et al., 2014). Kõrgesaar and Kujala (2016) showed that such an approach can reliably reproduce, based on comparison with available experimental data, the force-displacement curves of smaller panels as well as large-scale collision experiments. The drawbacks of the approach are that the set-up of the framework still requires user defined material modelling capabilities from the analyst and that the approach does not cover the full range of deformation modes, it being calibrated only for multi-axial tension, but excluding shear and bending. The effect of bending on mesh size sensitivity of the analysis is discussed in Storheim et al. (2015), while the solution to the bending problem was proposed recently by Pack and Mohr (2017). In particular, to differentiate necking initiation under membrane and bending loading they consider the damage accumulation in individual thickness integration points separately. Furthermore, it was shown in a simple manner that a direct relation exists between failure in the Forming Limit Diagram (FLD) space. The FLD space is the failure locus in terms of in-plane principal strains, and effective strain to failure-triaxiality space. Thus, a Fracture Forming Limit Diagram (FFLD) can be developed. This is a useful visualization tool that shows the locus of fracture relative to the limit of necking.

In (Marinatos and Samuelides, 2015) the authors investigate the effect of material modelling in simulation of several indentation and drop weight tests. It is claimed that in most of the examined cases triaxialities are above 1/3rd. Also Storheim et. al (2015) conclude in their paper, in which they study the results of FEM analyses of a collision scenario using different failure modes, that strain state dependent models show a better prediction than strain state independent models. Since failure analyses are also done in the design state, they aim to calibrate the material models based on known data at that state, e.g. uniaxial tensile tests. From the models tested it was concluded that the BWH (Bressan-Williams-Hill instability criterion) with damage and RTCL (Rice-Tracey Cockroft-Latham damage criterion) criterion performed best.

Table 2 The failure criteria compared by Storheim et al. (2015)

Name	Description
BWH w. dam	BWH criterion with damage and geometric mesh scaling
BWH no dam	BWH criterion without damage but with geometric mesh scaling
RTCL	RTCL criterion with geometric mesh scaling
GL	GL criterion on ε_1 and ε_{thin}
SHEAR	SHEAR criterion on ε_{eq}
RPC204	RP-C204 criterion on ε_{eq}
Peschmann	Peschmann's criteria on ε_{eq}
Damage	Ductile failure with coupled linear damage evolution

A more recent comparison study is performed by Calle et al. (2017). They performed several experiments using dogbone-shaped sample geometries to evaluate the constitute models for shipbuilding material SAE 1008 carbon sheet steel. They studied four different failure models also concluding that BWH and RTCL performed best. Furthermore, they studied the effect of mesh refinement. In areas of high strain gradients, independent of the used failure models, the coarser meshes show inaccuracies. Therefore, they recommend avoiding meshes with an aspect ratio > 8 for these situations. Below information on both the BWH and the RTCL criterion is given.

The BWH criterion developed in 2008 combines the shear stress criterion of Bressan and Williams with the local necking analysis in plates presented by Hill. The aim of this method is to define the onset of necking in plates. BWH uses a forming limit diagram (FLD) developed in stress space and limits the principal stresses according to the following formula (Eq.3):

$$\sigma_{1f} = \begin{cases} \dfrac{2K}{\sqrt{3}}\left(\dfrac{1+\frac{\beta}{2}}{\sqrt{\beta^2+\beta+1}}\right)\left(\dfrac{\varepsilon_{1c}\left(\frac{t}{L_e}+1\right)}{\sqrt{3}(1+\beta)}\sqrt{\beta^2+\beta+1}\right)^n & \beta \le 0 \\ \dfrac{2K}{\sqrt{3}}\dfrac{\left(\frac{1}{\sqrt{3}}\varepsilon_{1c}\left(\frac{t}{L_e}+1\right)\right)^n}{\sqrt{1-\left(\frac{\beta}{2+\beta}\right)^2}} & \beta > 0 \end{cases} \quad (3)$$

In this formula, β is defined as the relation between the minor and the major strain rates in the plane principal directions and can be approximated as $\beta = \dot{\varepsilon}_2/\dot{\varepsilon}_1$. K and n are the strength coefficient and strain hardening exponent of the power law respectively and the ε_{1c} is a material constant.

The RTCL criterion developed in 2003 combines Crockroft-Latham model and Rice-Tracy model that are respectively based on ductile shear fracture (low triaxilities range) and void growth (high triaxiliaties). The damage development is determined by Eq.4

$$D = \int_0^{\bar{\varepsilon}_f} f(\eta)_{RTCL}\, d\bar{\varepsilon} \tag{4}$$

Where

$$f(\eta)_{RTCL} = \begin{cases} 0 & \eta \le -\frac{1}{3} \\ \dfrac{2 + 2\eta\sqrt{12 - 27\eta^2}}{3\eta + \sqrt{12 - 27\eta^2}} & -\frac{1}{3} < \eta < \frac{1}{3}. \\ e^{\left(-\frac{1}{2}\right)} e^{\left(\frac{3}{2}\eta\right)} & \eta \ge \frac{1}{3} \end{cases}$$

An analytical approach applicable for shells exposed to multiaxial states of stress, including in-plane shear, is studied in (Walters, et al., 2017). This paper develops an analytical framework that enables the modeling of material wrinkle from their formation until material failure, accounting for triaxial stress effects. The analytical method results reasonably agree with finite element analysis especially for the folding behaviour of thin and moderately thick shells that have a single or a double curvature.

Usually the engineering stress-strain curve is not available at the design stage to determine the strain hardening of the material, and thus analytical expressions are required to estimate the flow stress curve. In (Liu et al., 2017) a new analytical expression is introduced to estimate the failure strain of coarse meshed ship structures struck by an indenter with hemispherical shape. This expression is derived by using finite element simulations of plate punching tests.

4.4.2 Composites

Composite material applications in the maritime field are mainly limited to novel navy ships, sport and leisure yachts and more recently energy harvesting and wind energy offshore structures. Composite materials are also used in the concept of sandwich plate (Notaro et al., 2013) to increase the collision resistance of ships and structures, such as polyurethane. Niklas and Kozak (2016) presented a concept of semi-elastic Steel–Concrete–Polymer structure which can absorb extra energy and protect water tightness of a compartment. Notaro et al. (2013) evaluated the rendering capabilities of a sandwich overlay consisting of a layer of elastomer. Kumar and Surendran (2013) used different kinds of fillers to develop cost-effective composites. Kim et al. (2003) and Rhymer et al. (2012) conducted experiments of carbon/epoxy composite laminates impacting with ice. Tiberkak et al. (2008) studied the fiber-reinforced composite plates subjected to low velocity. Mocanu et al. (2012), Gaiotti and Rizzo (2012) also performed investigations of fiberglass reinforced composite laminates.

Oterkus et al. (2015) reviewed the fracture modes, damage tolerances and fatigue mitigation in marine composites. And the techniques used in finite element modelling to determine the failure progress are listed: virtual crack closure technique; cohesive zone model (CZM); extended finite element (XFEM).

A recently developed continuum mechanics formulation called peridynamics is a tool for failure prediction based on mathematical formulations (Oterkus et al., 2015). Hu et al. (2017) studied the application of peridynamics to predict damage initiation and growth for composites under cyclic loading. Another recently proposed failure theory (Daniel, 2016) is North-

western (NU-Daniel) theory which predicts the yielding and failure of multi-directional laminates under static and dynamic loadings. Daniel compares the other commonly used failure theories for carbon/epoxy composite under matrix dominated states of stress with transverse compression, transverse tension and in-plane shear. The results of NU-Daniel model, as shown in Figure 6, are in good agreement with the experimental results.

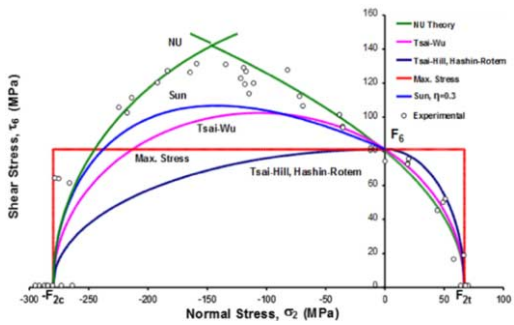

Figure 6: Comparison of failure theories and experimental results (Daniel, 2016)

Finite element modelling of nonlinear behaviour of composite structures at dynamic loading conditions are usually performed with Abaqus or LS-DYNA software. In 2017, Hassoon et al. (2017) showed the behaviour of two glass reinforced composite panels at different impact velocities. The model was developed in Abaqus and user defined VUMAT with Hashin criteria was applied for the 3D interlaminar damage model definition. Modelling of thick composites usually requires ply-by-ply simulation, which results in computationally expensive models. One alternative method is multi scale modelling approach. In 2016, Jia et al. (2016) studied the intra-laminar delamination failure of composites based on multi scale approach.

LS-DYNA has several material models available for composite structure modelling. The complete list of the material keywords that can be used for composite structures in LS-DYNA are provided in the LSTC website (LSTC) and have been summarized in the ANNEX, (Tables A1, A3).

4.4.3 Foam

Foam materials are often used within composite sandwich structures. The compressive behaviour of foam usually exhibit three regions; linear elastic, plateau and the final densification. Also for foam modelling, LS-DYNA has several keywords (see ANNEX, TableA2). Some of these models are mainly for compressive loading, others are capable of including strain rate dependent behaviour of foams. The strain rate dependent behaviour can be expressed as in Eq.5

$$\sigma(\varepsilon) = \sigma_o(\varepsilon)\left(\frac{\dot{\varepsilon}}{\dot{\varepsilon}_o}\right)^{n(\varepsilon)} \tag{5}$$

$$n(\varepsilon) = a + b\varepsilon \quad \text{for} \quad 10^{-3} \leq \dot{\varepsilon} \leq 10^{2} \tag{5a}$$

where σ_0 and $\dot{\varepsilon}_0$ are the quasi static values of stress and the strain rate, a and b are material constants that can be experimentally obtained.

One common issue with modelling foam under large deformations is the negative volumes of the elements which occur due to excessive distortion. In Ls Dyna, a negative volume calcula-

tion will cause the calculation to terminate unless ERODE in *control_timestep is set to 1 and DTMIN in *control_termination is set to any nonzero value in which case the element is deleted and the calculation continues (LSTC). Other recommendations to overcome the negative volume issue are listed here

- Stress vs strain curve can be stiffened up at large strains
- Tailor initial mesh
- Reduce timestep scale factor
- Avoid fully integrated solids which are usually less stable
- Increase DAMP parameter to 0.5 (LSTC)

In 2015, Chen et al. (2015) investigated the blast performance of insulated sandwich panels that consisted of extended polystyrene foam (EPS) and steel skin. They performed simulations using LS-Dyna and the *MAT_CRUSHABLE_FOAM. They compared the experimental results to the numerical ones and pointed out that the results were reasonably accurate. More detail on the comparison study can be found in their previous publication (Chen and Hao, 2014).

Perhaps one of the most comprehensive study on the foam modelling is done by Srivastava et al. (2014). On the performance of LS-DYNA for accurate modelling of foams, they mention that there is no model that can incorporate the different processing parameters, models usually capture limited loading types and usually unloading behaviour is not incorporated. They highlight that Mat 57 in LS-DYNA (Low Density Foam) is suitable for static loading, while Mat 83 (Fu Chang Foam) is suitable for rate sensitive dynamic loading. In ABAQUS, hyperfoam and Crushable Foam Plasticity Model are mentioned. Their review results highlighted that the researchers usually perform investigation using ABAQUS however, industry mostly prefers LS-DYNA, Pam-Crash or Radios. They report that in LS-DYNA, selection of Mat 57 and Mat 83 for modelling EPS resulted in ~28% difference in energy absorption values. Different theoretical models that were proposed throughout the years were schematically shown in the same paper (Srivastava and Srivastava, 2014) . This paper is certainly recommended to get a quick review of foam models.

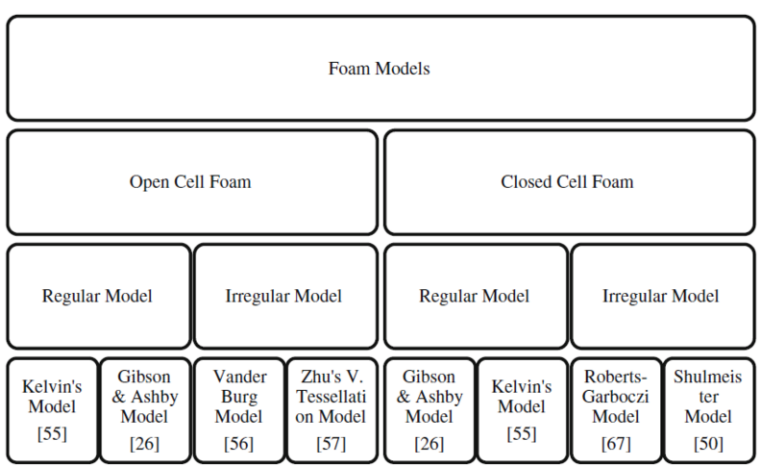

Figure 7: Theoretical models for foams (for the cited references see Jia et al., 2016)

Fang et al. (2015) developed a 3D mesoscopic model for closed-cell foams based on the behaviour of the entrapped air in the cells and the surrounding cell walls. They first randomly create a 3D model grid, then couple this with LS-DYNA. The ALE analysis is used to take into account the Fluid Structure Interaction (FSI). They compare the numerical results to ex-

perimental ones to validate the model. They use hydrocode in LS Dyna with ALE algorithm to model the static and dynamic behaviour of aluminum foam. The FSI is activated by using CONSTRAINED LAGRANGE IN SOLID card in LS-DYNA. Cell walls were modelled with Lagrangian elements (with SECTION SOLID keyword) and the air in cells with ALE elements (SECTION SOLID ALE). The material model is composed of two parts; the first part controls the yield strength and the second part is the equation of state the determine the hydrostatic pressure. In the model developed by Fang et al. PLASTIC KINEMATIC model, material type 3 was used for the cell walls without the strain rate effects. The maximum strain failure criterion was adopted in the Mat Add Erosion card; when the maximum tensile strain of cell-wall is larger than 0.37, the cell walls fail. Air in the cells were modelled with Mat Null (Mat type 9) card with the ideal gas state equation. Figure 8 shows the model, loading and the static compression results. In this model, CONTACT AUTOMATIC SURFACE TO SURFACE in LS-DYNA, was used to model the contact between the panels and the specimen and between all the cell-walls in the specimen. Similarly, dynamic simulations were also performed and compared to the experimental results. In the dynamic results, the entrapped air within the cells has greater effect at large deformations.

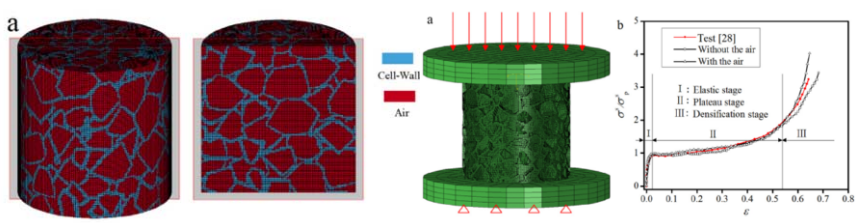

Figure 8: 3D mesoscopic model for closed-cell foams (LSTC).

4.4.4 Rubber

Xiao et al. (2015) published a comparative study on honeycomb rubber coatings that can be used as an energy absorber when applied on a ship structure. They considered three different cell geometry, and studied their behaviour and energy absorbing capacity in the event of underwater explosion. They first performed experiments, then numerical analysis of honeycomb coatings using ABAQUS. They modelled the geometry using CPE4R elements which are 4 node bilinear plane strain quadrilateral, reduced integration, hourglass control elements. The structure was compressed with a constant loading rate at the speed of 1, 10 and 30 m/s. Nonlinear stress vs strain behaviour of rubber was modelled with hyperelastic constitutive model based on assumption of isotropic behaviour. They compared five different models to the actual test data on the selected material, and decided to continue the analysis with the Arruda-Boyce model which captured the behaviour of neoprene, the rubber used in their study.

Rate dependency and hysteresis of neoprene rubber is also considered taking into account the viscoelastic model based on Prony series with the damping effect of the material. They conclude that the simulation results suggest that the compression speed and cell topology have a strong influence on the coating's dynamic compression performance.

4.4.5 Ice

Gao et al. (2015) simulated the impact of a ship with an iceberg. In their paper they proposed an isotropic elastic- perfectly plastic material model to represent ice and incorporated the material model in LS-DYNA via a user subroutine. The failure model depends on the effective

plastic strain and hydrostatic pressure. The properties assumed for the iceberg are given in the Table 3 below:

Table 3 (Gao et al., 2015).

Ice material parameters			
Element type	Solid	Density [kg/m^3]	900
Number of element nodes	8	Poisson's ratio	0.3
Number of element integration points	1	Young's modulus [MPa]	9500
Element length [mm]	50	Cut-off pressure; tension strength [MPa]	2
Strain rate	$>10^{-3}$	Strain hardening function	none
Limit of the elastic strain	10^{-3}	Limit of elastic stress [MPa]	9.5

Similarly, Kim (2014) has developed a user defined material model for ice to be incorporated in Ls Dyna. The material characteristics were taken from experiments. She assumed two different failure criteria; a generalized strain based and a triaxiality dependent criterion which produced similar results for ice crushing loads for scenario where ice impacts a steel panel at 2 m/s velocity. More recently, Shi et al. (2017) simulated a similar scenario where a spherical iceberg impacts a steel plate at 1 m/s velocity. The ice material model had two types of yield surface functions; Tsai-Wu and n-type. The failure criterion was based on the effective plastic strain and hydrostatic pressure. The implementation of this model is similar to the one performed by Gao et al. (2015). In contrast, Ince et al. (2016) presented a cohesive zone based ice material model that was validated with drop tests. The measured and simulated response showed good correspondence. However, it must be stressed that response includes the combined effect of ice (dropped cone) and steel response from deforming structure meaning that discrepancies between simulation and experiment cannot be explicitly singled out and assigned to the steel material model or the ice material model.

In Ferrari (2015) a material model describing the mechanical properties of ice is implemented in FORTRAN, for use during finite element analyses of the impact (performed using the software Abaqus CAE). The parameters affecting granular ice behaviour are reviewed in the paper, then, following (Liu et al. 2011) a numerical model describing the ice behaviour is formulated, based on a yield function and a failure criterion. The yield surface selected for the study was proposed by Liu et al. (2011), corresponding to the Tsai-Wu surface formulated for isotropic materials. In particular the considered case corresponds to a temperature of -11ºC, for which the surface parameters were derived empirically by Derradji-Aouat (2000). A failure criterion with a parabolic dependence on pressure was implemented following again Liu et al. (2011). The ice model is applied in a first case to a specific situation considering a spherical iceberg of given radius impacting the side of a specific ship (Ferrari et al. 2015). The problem is decoupled, following the NORSOK method, into the analysis of a deformable iceberg impacting a rigid ship side and the analysis of the 'mirror' situation (rigid iceberg against a deformable ship). For the latter case, reference is made to previous results (Addario et al. 2014). Outputs from the two analyses are coupled, assuming that the results, separately derived, can be jointly applied to the real case of an impact between two deformable bodies. The results obtained in this first application confirm that a significant part of the impact energy is actually dissipated by ice deformation, but they are still valid under the simplifying hypothesis of neglecting the contact interactions between the two deformable bodies. The implemented material model can be integrated in the FEM analysis to study the coupled problem.

4.4.6 Soil

Wang et al. (2017) performed a numerical study using a 2D LS-DYNA model to develop a simple and quick assessment of the ground deformation of granular soils due to dynamic

compaction which can successfully be implemented to moist and dry granular soils. The assuming loading was a drop of a 40 tons tamper from a height of 15 m. The developed model takes into account the physical phenomena in a compaction process with the dynamic equation of soil and the nonlinear material behaviour of soil as well as the soil-temper interaction. For the soil model they assumed a cap model which is the yield surface due to compression.

5. COLLISION

Collision is a major hazard to the safety of ships and other offshore installations and may result in severe economic loss, environmental pollution and fatalities. Scholars and researchers have strived for establishing a broadly acknowledged methodology, which can be used conveniently and with affordable cost and time to predict and evaluate the responses of the struck items and the striking ships. However, there are still many problems to be resolved before such a methodology can be accepted by the naval architecture and offshore engineering field. During the past years, many efforts have been made right in this direction. A summary of the latest research outputs according to the different ship collision categories is presented in this chapter. Then, the most critical and relevant conditions, including the analysis and design approaches and model test investigations are described. Finally, acceptance criteria for evaluation and corresponding consequences are discussed.

5.1 Ship collision categories

Nowadays, ship collision accidents can be approximately divided into four categories, which are: ship-ship, ship-offshore structure, ship-bridge and ship-iceberg collisions.

5.1.1 Ship-ship collision

Recent researches on ship-ship collision mainly focus on collision-avoidance and quantification of consequences after an accident. Collision-avoidance researches aim at proposing methods for safe manoeuvring. You and Rheeba (2016) made a prior study aimed at solving the intrinsic problem of the critical collision condition, including slower ship's dilemma by considering the manoeuvrability of the own ship and the International Regulations for Preventing Collisions at Sea (COLREGs). They developed a collision ratio that can be used to determine the time at which to begin the collision avoidance manoeuvre. Szlapczynski and Szlapczynska (2016) developed analytic formulas for domain-based collision risk parameters: degree of domain violation (DDV) and time to domain violation (TDV), with the purpose of overcoming the drawback of DCPA and TCPA, which lack efficient analytical solutions in real-time system where computational time is essential. Zhang et al. (2016) proposed a novel method detecting possible near miss ship–ship collisions from AIS data and then discussed how the near miss data can be used to gain further insight in safety of maritime transportation. Zhang et al. (2015) studied a multi-ship anti-collision decision support formulation in a distributed and real time way. It was proved that the formulation can avoid collisions when all ships have complied with COLREGs as well as when some of them do not take actions.

Researches on internal and external mechanism provide understanding of the responses under ship collision scenarios. Zhang et al. (2017) further analysed the validity and robustness of the closed-form analytical methods they proposed in 1998 and further improved the accuracy of some parameters, with 60 experimental results. A simple way of accounting for the effective mass of liquids with free surface carried on board of a ship was also introduced, and it was proved that the analytical procedure can be expanded to take into account the effect of ship roll on the energy released for crushing. By using the nonlinear finite element code LS-DYNA, Yu and Amdahl (2016a) firstly proposed a new coupled approach for a simultaneous calculation of the structural damage and of the 6DOF ship motions in ship collisions. The proposed method is particularly useful for design purposes because a detailed ship hull shape is not needed. The innovative procedure is shown in Figure 9. In addition, Yu et al. (2016b)

upgraded the approach taking into consideration the hydrodynamic loads, based on linear potential-flow theory in the LS-DYNA code. Thus, fully coupled six degrees of freedom (6DOF) dynamic simulation of ship collision and grounding accidents can be carried out, while ship motions and hydrodynamic loads have always been neglected in previous investigations.

B. Liu et al. (2015b) proposed a simplified analytical method to examine the energy absorbing mechanisms of small-scale stiffened plate specimens, quasi-statically punched at the midspan by a rigid indenter with a knife or a flat edge shape. Both experiments and numerical simulations were carried out to validate the analytical method. Calle (2017) summarised a series of experiments including scaled collision tests of a T cross-section beam, head-on collision of an oil tanker against a rigid wall, ship grounding and collision between two oil tankers, to validate their finite element analysis. They indicated that the mechanical properties of materials, slight misalignments in test arrangements, failure criteria, weld joints and sloshing effect of ship cargo all influence differences between numerical and experimental results.

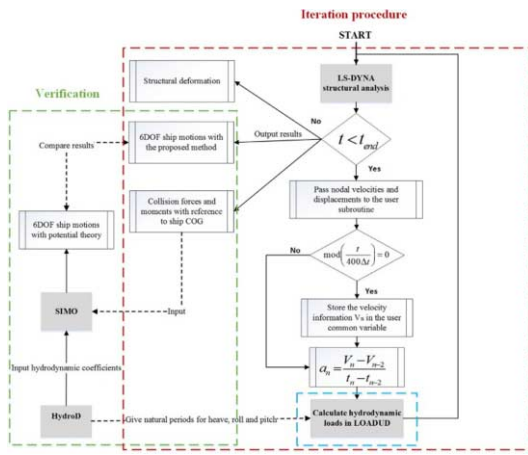

Figure 9: Illustration of the coupling algorithm

5.1.2 Ship-offshore collision

The public concern on ship collisions with offshore structures mainly focus on the consequences. Because the repairing cost for the offshore structure is higher than that of the striking ship, many researches are concentrated on the method to increase the crashworthiness of offshore structure during accidental collision scenarios. Furthermore, with the increasing number of offshore wind turbines along the coastlines, collisions between sailing ships and offshore wind turbines may become more frequent.

Zhang and Terndrup Pedersen (2015) conducted an analysis on collision energy and structural damage in ship - offshore platform collisions for various scenarios. They considered ship collision with offshore installations as one of the key concerns in the design and assessment of the performances and safety of platforms. An example of an ice-strengthened supply vessel colliding against a jack-up rig was analysed and the crushing resistance of the involved thin-walled structures was evaluated. Travanca and Hao (2015) analysed the energy dissipation in high-energy ship-offshore jacket collisions, with the aim of providing a clearer understanding on the strain-energy dissipation phenomenon, particularly as regards the ship-structure interaction. Vinnem et al. (2015) discussed the need for online decision support for FPSO–shuttle tanker collision risk reduction.

One of the most effective way to improve the crashworthiness of jacket platform is to analyse the anti-collision capability of the beam members. Pham and Hao (2017) investigated the

plastic hinges and inertia forces in RC beams under impact loads. Cerik et al. (2016) analysed the resistance of ring-stiffened steel cylinders subjected to low velocity mass impact. Furthermore, they also made a comparative study on the damage of tubular members subjected to mass impact. They studied the influence of the geometrical parameters and the interaction between the local shell denting and the global beam deformation modes. Zhang et al. (2016) carried out a theoretical study of low-velocity impact of geometrically asymmetric sandwich beams. Liu and Guedes Soares (2017) carried out model testing and numerical simulations on the influence of impact location on the plastic response and failure of rectangular cross section tubes struck transversely by a hemispherical indenter. Z.Wang et al. (2016) analysed the structural dynamic responses of T- joint of jack-up platform laterally punched by a knife edge indenter, through experimental and numerical simulation methods.

Although serious collision accidents between ships and offshore wind turbines have seldom been reported, the concern for this kind of accident has brought quite a number of related researches. Bela et al. (2017) carried out an analysis on ship collision with the monopile foundation for offshore wind turbines. They concluded that a slight variation of the impact velocity can lead to consequences ranging from minor damage of the OWT to total collapse. Hao and Liu (2017) made an evaluation and comparison for the impact-resistance performances of three typical types of foundations for offshore wind turbines: monopile, tripod and jacket. They found that the jacket solution features the minimum collision force, damage area and nacelle acceleration as well as a medium value of bending moment and steel consumption among the three types of foundations. In addition, C. Liu et al. (2015) proposed a crashworthy device for the monopile offshore wind turbine against ship impact, and completed the optimisation and application analysis.

5.1.3 Ship-bridge collision

Bridge structures across navigable waterways are vulnerable to barge collisions, and bridge pier can be struck by ships frequently. Bridge damage might lead to catastrophic consequences to life and economy. A few innovative bridges, such as the Norwegian floating bridge and tunnel concepts for the project “Ferry free coastal route E39” are also making a critical concern on the ship collision load. It is therefore of great importance to protect bridge structures, especially bridge piers, against impacts from vessels. As a typical engineering practice example, Sha and Amdahl (2017) analysed as case study the collision of a ship against the Bjørnafjorden floating bridge. The global response under ship collision loads was simulated, including the first vibration modes of the bridge. Sha and Hao (2013, 2014a, 2014b) conducted a series of investigations on the ship-bridge collision scenarios, through an analytical method, numerical simulations and model testing methodologies. Sha and Hao (2014a) also proposed a simplified approach for predicting bridge pier responses subjected to barge impact loading, considering material nonlinearity and structural damage. In addition, Sha and Hao, (2013) used numerical simulations to investigate the dynamic responses of continuous girder bridge and bridge damage detection after barge impact accidents. Bridge vibration responses before and after vessel impact were computed. Furthermore, laboratory tests (Sha and Hao, 2014b) and numerical simulations of CFRP strengthened RC pier were also carried out for analysing the dynamic responses due to barge impact load accidental scenario.

Further studies have been carried out on ship-bridge collision with different analysing methods. Fan and Yuan (2014) studied the failure modes and the dynamic interaction process of the pile-supported structures subjected to ship collisions. Their numerical simulations indicate that the platform and the connection of the protective system should be carefully designed to prevent brittle failure in addition to provide piles with enough ductility. Getter et al. (2015) pointed out that for numerical simulations of ship-bridge collision, constitutive relationships assigned to steel components in the vessel model must be capable of accounting for strain rate sensitivities and large-scale plastic deformations. Kang et al. (2017) proposed an effective

method to evaluate the cumulative response of steel bridge under earthquake and large drifting object impact due to tsunami flow, and an innovation on the ship-impact effect due to earthquake-induced tsunami directly into ductility demands, a phenomenon which was not previously studied. The impact force history during multicolumn barge flotilla collisions against bridge piers has been determined by Luperi and Pinto (2013). In order to evaluate the engineering standards employed in the United States on designing concrete waterway control structures for barge impact loading, Walters et al. (2017) used analytical techniques and numerical simulations to quantify barge impact loads over a wide range of conditions typically used in experimental testing. Their key finding is that flotilla impact loads are strongly correlated to the momentum of only the barges in the lead row of a flotilla, rather than the total momentum of the entire flotilla. Wang and Wang (2015) proposed a model to evaluate vessel-bridge collision probability. A general mathematical model for navigation channels was suggested for straight and meandering channels, and the effect of waterway obstacles and water levels were both taken into account in their model. The influence of ship-bridge collision on the running safety of moving rail train was investigated by W.Zhang et al. (2014) through numerical simulations. Cheng (2014) also analysed the integrity of the towers of the SuTong Bridge, a cable-stayed bridge in China, under ship impact scenario.

5.1.4 Ship-ice collision

Ship-ice interaction has attracted much more attention since it became possible for ships to sail across the Arctic Ocean. The main methods used for investigations on the interactions between ice and marine structures and on accidental scenarios including ship-iceberg collisions, can be divided into three categories: empirical methods, collision testing methods and numerical methods. With the improvement of computing capability and testing facility, the latter two methods are becoming more popular. These type of investigations are covered in the following.

Experimental methods have been used by researchers for a long time to investigate the fundamental properties of ice during the ice-marine structure interactions and collisions. Von bock and Ehlers (2014) made a qualitative assessment on selected topics to assess the differences between model-scale ice and sea ice and the influence of related experiments on determined mechanical properties is assessed. They concluded that the internal mechanics of Aalto model-scale ice and sea ice differ significantly. Kim et al. (2016) used an experimental method and nonlinear numerical simulations to examine the nonlinear impact response of steel-plated structures in an Arctic environment, and the effectiveness of nonlinear numerical simulation method was proved. The structural crashworthiness of steel-plated structures subject to low temperatures typical of the Arctic environment was investigated by crushing testing by Park et al. (2015b), and the testing results were compared with those from LS-DYNA computation. It was found that low temperatures have a significant effect on the crashworthiness of steel-plate structures in collision scenario in Arctic region.

Compared with collision testing method, numerical simulations can lower the research cost to a large extent, and make it possible for scholars from many countries far from Arctic Ocean to contribute to the research on interaction between ice-marine structures. Discrete Element Method and Finite Element Method are the two methodologies that have been most used world-wide.

Discrete Element Method has an outstanding ability in simulating brittle crush behaviour of ice. DEM can describe the meso-scale structure of ice and simulate the process from intact state to fractured state during ice-structure interaction. Ji, Di and Liu, (2015) investigated the interaction between ice cover and conical offshore structures and discrete element method (DEM) was introduced to determine the dynamic ice loads under different structure parameters and ice conditions. Robb, Gaskin and Marongiu, (2016) used a SPH-DEM model to simulate free-surface flows containing solids applied to river ice jams.

Finite element method (FEM) is a commonly used numerical method with a solid theoretical foundation and easy to implement. Developing effective ice constitutive models is crucial for FEM applications. Shi et al. (2017) proposed a temperature-gradient-dependent elastic-plastic material model of ice for a numerical study of the influence of temperature-gradient on impact force in ship-iceberg collisions. In addition, Shi et al. (2016) proposed a nonlinear viscoelastic iceberg material model and realised it within the LS-DYNA code. The strain-rate effect of ice material has been taken into consideration, too. Ortiz et al. (2015) took into account the well-known Mazars damage model, to simulate the dynamic behaviour of ice. The difference between the behaviour of ice in tension and compression and the influence of the strain-rate on the fragile ice material response were described. Delay effects were used to prevent numerical mesh sensitivity. The constant added mass (CAM) method and the fluid-structure interaction (FSI) method within LS-DYNA were used to simulate ship-ice collisions by Song et al. (2016). It was found that the FSI method yields better results for the motion of the floater, and CAM method was faster but predicted a higher peak contact force and more dissipated energy in the ice mass than in the FSI method. Addario et al. (2014) simulated a collision between the side of a double hull LNG carrier and an iceberg modelled as rigid by adopting ABAQUS, to investigate the influence of mass and shape of the iceberg on the damage of the structure. Based on the study above, Ferrari et al. (2015) adopted a complex material model (see § 4.4.3) to simulate the behaviour of ice. The collision between a spherical ice feature and the double hull of an LNG carrier was simulated to get an evaluation of the share of deformation energy between ice and structure.

Zhou et al. (2016) introduced a solution to the ship-ice interaction problem in the time domain by a combined method involving numerical simulations and semi-empirical formula. The breaking process of level ice is predicted by a 2D numerical method, and the simulation of ship manoeuvring in level ice is carried out by a 3-degree-of-freedom model. Kim et al. (2017) carried out laboratory experiments on shared-energy collisions between freshwater ice blocks and a floating steel structure, to study the physics of this event. A series of laboratory –scale impact tests of freshwater granular ice blocks against stiffened steel panels are described. Myland and Ehlers (2016) evaluated the contribution of the ice breaking force to the motion resistance in ice methodically for different bow shapes, through model tests method. Breaking patterns and geometric bow parameters were specially investigated, and the findings were compared with the selected-empirical method of Lindqvist. The frequency of ice loads of varying lengths and the occurrence probability of their magnitudes were studied in full-scale testing carried out on the Polar Supply and Research Vessel S.A. Agulhas II, by Suominen, Kujala, Romanoff et al. (2017). This statistical study showed that a Weibull distribution gives the best fit to the measured loads on a frame. Overload response of ship structures frames to ice loads were assessed by Daley et al. (2017) and Kõrgesaar et al. (2018).

5.2 Most critical/relevant condition and design/analysis methods

Researches on collision-related-design have not been as many as those on other fundamental aspects or as studies from engineering practices. ALS criteria are however introduced to limit the corresponding residual risk associated with accidental actions, i.e. to prevent progressive collapse failure of the whole structure. Moan (2017) summarized that to stop the escalation of an accident, one of the three following approaches should be taken (ISO, 2015; Moan et al., 2016)

- Designing the structure locally to sustain accidental actions and other relevant simultaneously occurring actions.
- Designing the structure by “accepting” local damage but requiring that the damaged structure survives the relevant accidental actions.
- Designing the structure to meet robustness requirements through (prescribed) minimum levels of ductility, continuity and tying.

Park et al. (2015a) carried out an accidental limit state-based ship collision analysis to identify the operability of aged non-ice class ships in the Arctic Ocean. An innovative relevant condition is that various Arctic ambient conditions, with temperatures down to -80˚C, were applied to the ambient exposed plating of the struck ship. Paboeuf et al. (2016) using a super-element method presented a work performed for the evaluation of an alternative construction within the scope of A.D.N. regulation, a European Agreement concerning the International Carriage of Dangerous Goods. A Bureau Veritas tool, SHARP, based on analytical formulations, permits to perform several quick ship collision analysis. In addition, Akhtar et al. (2016) discussed the methods for choosing collision scenarios and ship collision loads for bridge design. The design concept in DNV-RP-C204 (2010) was applied, as well as the concepts of ductile, strength and shared-energy design, applicable in bridge design, too.

Risk assessment method is a useful tool to evaluate crashworthiness and safety of ships and offshore structures under accidental limit state scenarios. Moan et al. (2017) made a review on the assessment of ship impact risk for offshore structures and pointed out that the new NORSOK N-003 guidelines for Norwegian Continental Shelf specify that ship impact actions and action effects should be determined by risk assessment.

Experiments in model scale have always played an important role in investigating the quasi-static and dynamic structural responses for steel and other materials used in building of ships and offshore structures. Test data have also always been used to validate analytical formulae and for comparison with numerical simulation results. Liu and Guedes Soares (2016b) carried out experiments and finite element simulations of small-scale stiffened web girders subjected to local in-plane loads, in order to examine their crushing deformations and energy absorbing mechanisms. Korgesaar and Kujala (2016) validated the failure criterion for large complex shell structures, through comparison with experimental results. The comparative simulations are performed with the GL failure criterion based on critical through thickness strain.

Model testing can also be used to analyse the resistance capacity of ship structures. J. Liu et al. (2016) conducted an experimental study on the resistance of hat-type stiffened plates struck by a bulbous bow indenter. Different X-core and Y-core sandwich plates were included in the test, and it was shown that significant improvement on energy dissipation capability can be achieved by hat-type stiffened plates, compared to those of conventional stiffened plates. Repeated mass impact model tests were conducted by Truong et.al (2016) at Ulsan University, to investigate the plastic response of steel grillages struck by a knife-edge striker. Holmen et al. (2015) carried out an experimental program investigating the behaviour of monolithic and multi-layered configurations of 0.8 mm and 1.8 mm medium-strength steel plates.

The influence of critical parameters relevant to ship collision can be analysed by model testing results. Antoine and Batra (2015) analysed the sensitivity to material parameters, layer thickness and impact speed of the plate deflection, the contact force between the impactor and the plate, the maximum length of a crack, and the energy dissipated during a low velocity impact at normal incidence of a clamped rectangular laminate by a rigid hemispherical-nosed cylinder. Xia et al. (2015) used various machines in material testing program covering quasi-static, intermediate and high strain-rates, which is referred to as a multiple-machine Program.

5.3 Acceptance criteria/consequence evaluation

Structural damage due to ship collision accidents can lead to serious consequences. For example, the reduction of ship longitudinal strength may induce global hull collapse. This makes the assessment of global strength after collision damage a necessary step in design. Furthermore, some other consequences, such as oil spill, flooding related salvage, and riser collision consequence have all attracted much attention by the scholars.

Global strength has always been a key concern for the damaged ship after collision accidents. Obisesan et al. (2016) proposed a framework for reliability assessment of ship hull damage

under ship bow impact. They used reliability computations to show that the probability of hull fracture increases as the hull deformation progresses, with maximum value occurring at the onset of outer hull fracture. Youssef, Faisal et al. (2016) proposed a method for assessing the risk of ship hull collapse following a collision. They used a probabilistic approach to establish the relationship between the exceedance probability of collision and the residual ultimate longitudinal strength index. Begovic (2017) carried out an experimental study on hull girder loads on an intact and damaged naval ship DTMB 5415 at zero speed. It was found that the moorings influence the hull girder loads at some wave frequencies. The global responses of struck ships in collision were investigated by Jia and Moan (2015), with emphasis on hydrodynamic effects. It was found that the equivalent added mass for sway motions depends not only on the duration of collision impact and on the impact force, but also on the collision position. Comparatively, the equivalent added mass for yaw motion could be assumed to be independent of collision position.

Flooding in damaged ships has also been a matter of concern. Lee (2015) proposed new models for vented compartments of damaged ships and an accumulator model, which can adjust the inner pressure in the calculation automatically. The dynamic–orifice equation was investigated in case of large openings. Manderbacka and Ruponen (2016) carried out research on the impact of inflow momentum on the transient roll response of a damaged ship. It was found that when the flooded compartment does not have significant obstructions, it is important to account for the inflooding moment flow. Acanfora and De Luca (2016) carried out an experimental investigation on the influence of the damage opening on ship response. The experimental results indicated that the roll behaviour of a damaged ship is affected not only by its size, but also by the position of damage opening. Rodrigues and Guedes Soares (2017) carried out a study on the transient still water vertical load during the flooding process for a damaged shuttle tanker in full load condition. The flooding progression is simulated by a quasi-static version of a generalized adaptive mesh pressure integration technique for progressive flooding of damage vessel. Total resistance of an intact and damaged tanker was predicted with flooded tanks in calm water scenario, by Basic et al. (2017). RANS equations with VOF technique were employed to solve the flow around the damaged ship in calm water. It was found that the total resistance due to the altered flow around the hole increased with 27%.

Furthermore, oil spills are one of the most crucial topics for investigation, due to the increasing public concern about the environmental protection. Afenyo et al. (2016) made a state-of-the-art review on the fate and transport of oil spills in open and ice-covered water. The review identifies the current knowledge gaps and future research directions. Kollo and Tabri (2017) proposed hydraulic models for one- and two-layer flows combined in different oil spill scenarios for tanker accidents. The discharge coefficients were determined from an experimental verification of the hydraulic models, and the head losses of a stratified flow through the double-hull tank hole was determined by an optimization algorithm.

Further, riser collision in offshore engineering is one of the accidents that generate a larger concern. Fu et al. (2017) carried out a reliability analysis for riser collision and presented an effective way for predicting the failure probability by considering various uncertain loads in the nature environment. They also studied the parameters which may result in riser collision.

6. GROUNDING

6.1 Introduction

Assessment of ship grounding is in many elements similar to that of collision assessment. In grounding, ship motions are mainly in the vertical plane (surge, heave and pitch), while in collision the focus in is on the motions in the horizontal plane (surge, sway and yaw). Similar to the collision assessment, one of the simplifications done in for the grounding assessment is to divide the analysis into external dynamics and internal mechanics. The external dynamics

evaluates the ship motions, resulting in the energy to be absorbed by structural deformations and the inner mechanics evaluates the deformations that the structures undergo while absorbing that energy. In addition to decoupled models, several coupled models have been developed, which successfully combine these two fields.

Any model development is related to simplifications and thus uncertainties with respect to the reality. The grounding process is a complex nonlinear process where highly coupled effects, such as large contact forces, large structural deformations and hydrodynamic loads, are coupled. The complexity of a grounding problem depends on whether the ship predominantly moves horizontally, vertically or is a combination of them with respect to the seabed obstruction. If a ship grounds over a sharp rock, then the grounding is termed as "bottom raking" and if over blunt "shoal"-type seabed, then the term of "bottom sliding" is used, see Figure 10: .

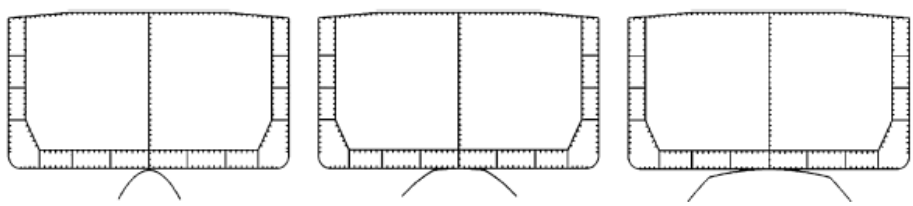

Figure 10: Sea-bed types (Alsos and Amdahl, 2007).

Furthermore, "hard" grounding refers to a grounding with undeformable seabed such as rocks, while the "soft" grounding takes place on deformable seabed. In between these two are the groundings on the reef-type rock. These different classifications correspond to different structural behaviours of a ship bottom, which yield to different failure models.

6.2 Most critical/relevant condition

Grounding assessment is required in sea regions, where the shipping lines are in the vicinity of shallow water or rocky areas. For example, the Gulf of Finland has a dense maritime transportation and it was shown by Brunila and Storgård (2012) that in the past two decades the oil transportation has quadrupled in the region. Due to shallow water areas, there are several grounding accidents and incidents in every year (Kujala et. al., 2009). The effectiveness of preventive measures in the region is obvious, since the number of accidents has not increased with the same rate as the amount of traffic. However, as the traffic continues to increase, it is necessary to further improve various measures to increase the safety at seas.

The definition of a relevant scenario, a crucial element in the development of the measures, is a demanding task. The scenario definition includes the quantification of the probability of occurrence of an accident and the definition of parameters such as the characteristics of the ship and the bottom topology.

Many methods have been applied for risk analysis the past few years, including Hazard and Operability Studies (HAZOP), Failure Mode and Effects Analysis (FMEA), Fault Tree Analysis (FTA), Event Tree Analysis (ETA) and Bayesian Network (BBN). Mazaheri, et al. (2014) reviewed existing risk models available in the literature for ship grounding events and proposed a methodological framework suitable for knowledge based risk modeling, in line with the recommendations issued by the IMO in the formulation of the Formal Safety Assessment procedures. The paper also highlights the models that are more appropriate for risk management and decision making. Amongst other investigation procedures, BBNs became more and more popular for maritime risk modeling during the last decade. They may use experts' knowledge to integrate scarce historical data and are particularly suited to model the causal relationship of shipping accidents which involve human and organizational factors.

Comprehensive literature review of using BBN models to model grounding accidents is provided by (Zhang and Liu, 2017). A detailed analysis of the benefits and challenges about Bayesian Networks for the study of prevention measures against maritime accident can be found in (Hänninen, 2014). Mazaheri (2017) proposed a BBN based framework for studying grounding scenarios. Traffic data from AIS combined with expert knowledge, ship grounding incident and accident reports are used in input. A region-specific semi-quantitative index, the Waterway Complexity Index is defined to take into account the dependency of ship grounding events on the navigational difficulty of a waterway. New versions of Human Factors Analysis and Classification System and new positive taxonomy as Safety Factors are also introduced. While experts' opinion still plays an important role in providing data for BBN models, data-driven BBNs are considered more objective since they work on objective data (Zhang and Liu, 2017).

Large efforts are therefore devoted to carry out statistical analyses of the available data. (Goerlandt et al., 2017) studied the accidents occurred during wintertime navigation in the Northern Baltic Sea in the period 2007–2013. The analysis is based on an integration of various data sources, aiming at reconstructing the accident conditions based on the best available data sources. Apart from basic accident information from the original accident databases, data from the Automatic Identification System is used to obtain insight in the operations during which the accident occurred, as well as into other dynamic aspects of the accident scenario. Finally, metocean and sea ice data are also integrated in the scenario description. Sormunen et al. (2016a) presented an overview of ship traffic volume and accidents in the Baltic Sea with a special focus on the Gulf of Finland. The annual number of accidents in the Baltic Sea reported to HELCOM varied in the range 34–54 for collisions and 30–60 for groundings. By analyzing two separate accident databases, an estimate for accident underreporting was also calculated. Different statistical methods yielded an underreporting rate in the range of 40–50%. The true number of accidents was estimated, based on the estimated underreporting percentage for the Baltic Sea. Eleftheria et al. (2016) presented a systematic analysis of ship accidents in the last decade as a way to evaluate the current level of safety for the majority of ship subtypes present in the world merchant fleet. The presented analysis also included a deeper investigation about possible relationships between accident rates and ship's age. The outcome of the present study indicated that in the last decade although the frequencies of ship accidents generally increased, the safety level of various ship types did not significantly change, as the consequences of accidents remained in average at about the same level.

Grounding consequences depend on the ship itself as well as on the bottom topology. (Sormunen et al., 2016b) investigated the relevancy of mathematical models to describe rock shape in grounding response analysis. Four different bottom topologies were studied, each described with four mathematical models and with one model following the real shape of the rock see Figure 11. Grounding response in terms of dissipated energy was evaluated for all the models. It was confirmed that the mathematical representation of the bottom topology is of great importance in the grounding response. The results showed that the ship damaged material volume is strongly linearly dependent on the rock area- and volume metrics. A similar linear dependency exists between the damaged volume and the energy dissipated in grounding, see Figure 12. Thus, one should be able to understand the bottom topology in the area under investigation.

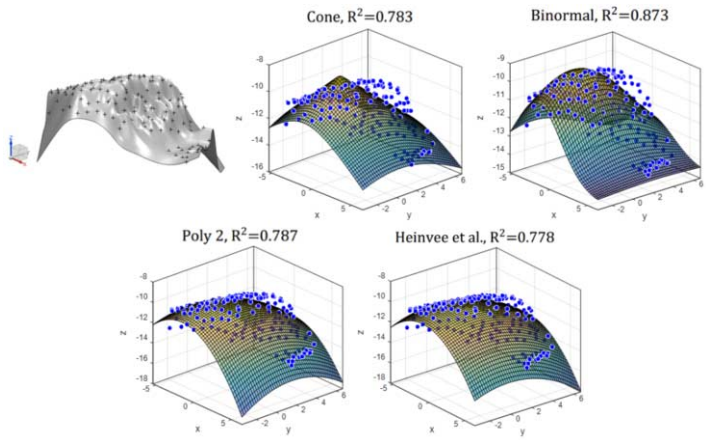

Figure 11: Approximated real rock surface and four fitted models (Sormunen *et al.*, 2016b).

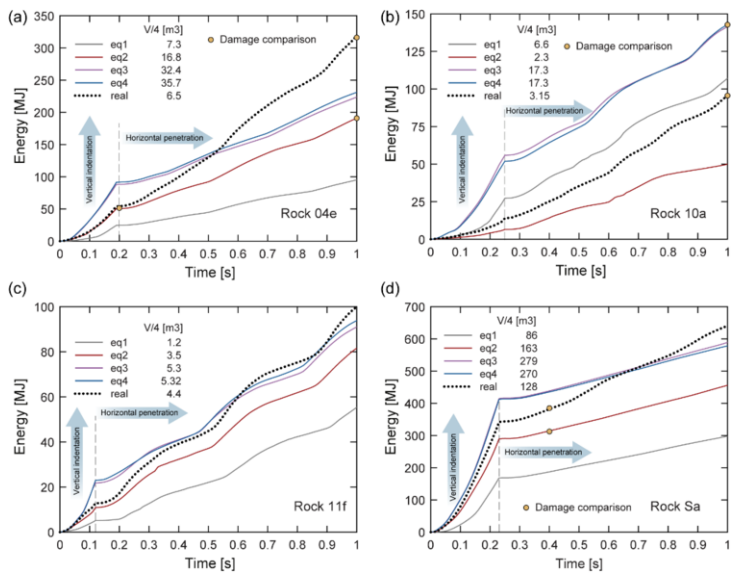

Figure 12: Deformation energy absorbed during grounding using different rock models (Sormunen *et al.*, 2016b).

6.3 Analysis methods

Once the accidental grounding scenario is defined, ship's response to grounding and the consequent damage is to be assessed. Assessment of ship grounding consequences has been the subject for a large number of research studies. Study methods include experimental, statistical, numerical simulations, empirical and regression models or simplified expressions for ship structural elements.

6.3.1 Experiments

Experiments are the most straightforward method to understand structural failure mechanisms. In the mid-1990s several large-scale grounding experiments with a scale of 1/4 were conducted, as reported by Rodd and Sikora (1995) and Vredeveldt and Wevers (1995). In both tests, double bottom structures for tanker models and cone shaped models for intruding

rocks were used to provoke the tearing failure modes. However, large scale experiments are expensive and rare. Accordingly, tests in smaller scales are carried out to observe the structural behaviour during the impact and to validate results of FE analysis. In Calle et al. (2017) miniature ship substructures (in particular bulbous bows and ship's mid-sections) were used for ships collision and grounding experiments. Structural resistance was measured and compared to the numerical simulations. Their study showed that it is possible to recognise the same structural behaviour as in case of structures of larger scale. Comparisons between FE simulations and experiments allowed to track and control the key aspects of FE modelling. On the side of the geometrical description, it was observed that slight misalignments could cause noticeable differences in the crushing modes, in the crushing force and in its peaks. As regards the material characterisation, results showed that appropriate failure criteria for base material should include a calibration of both crack initiation and propagation parameters. Liu and Guedes Soares (2016b) carried out experiments and finite element simulations of small-scale stiffened web girders subjected to local in-plane loads, in order to quantify crushing deformations and energy absorbing mechanisms. Three small-scale specimens were designed, one unstiffened web girder and two vertically stiffened web girders, in order to compare the influence of the vertical stiffeners on the structural deformation and response of stiffened web girders. The investigation provides practical information to study scenarios with local penetration of the ship bottom.

6.3.2 Statistical models

A practical framework for input data in risk analyses was adopted by the International Maritime Organization in IMO (1995) and, in revised a version, in IMO (2003). These guidelines present a probabilistic model for the damage extent of an oil tanker design in collision and grounding. The probability density distributions for the damage extent contained in the document were derived from the actual damage data of 63 grounding and 52 collision accidents of oil tankers, chemical tankers and Ore/Bulk/Oil carriers. The damage extent is given in non-dimensional form, as percentage of the length, beam and depth of the ship. It has been argued, see e.g. Sirkar et. al., (1997), Rawson et al. (1998), Pedersen and Zhang (2000) that the damage extension so identified does not reflect the actual dependency on the different structural arrangements and on ship size.

6.3.3 Numerical models

Due to the rapid evolution of computer capability, the numerical simulations of grounding and collision events are regarded as an investigation tool allowing an even better insight in the phenomena under study than the physical experiments. Information about the stress strain and damage spatial distributions are actually available everywhere in the simulated material domain, while transducers in experiments provide local information in a discrete number of locations. Main challenges of these simulations are however a proper representation of structural configuration and of material properties including constitutive equations and failure surface The selection of the size of elements is also important (see §4). Various publications present applications of nonlinear finite element (NLFE) techniques for grounding simulations: see among others Kitamura (2002), Naar et. al. (2002), Alsos and Amdahl (2007), Samuelides et. al (2007). AbuBakar & Dow (2013) focussed on the numerical prediction of the structural damage of ship's double bottom structure. Tests of stiffened panels penetration and double bottom damage, both carried out experimentally by Alsos et al. (2009a, 2009b) and Rodd (1996) were numerically simulated. Liu and Guedes Soares, (2016a) studied the behaviour of stiffened web girders subjected to local in-plane loads characteristic of grounding.

Liu et al (2017) carried out numerical stranding simulations of double hull tanker, studying the influence of different impact locations and failure criteria on the structural response of structural members. Locations showed a smaller impact than failure criteria on results in terms of resistance forces and deformation energies in the structural members. Marinatos and

Samuelides, (2015) carried out a systematic investigation on the main parameters of numerical simulations for the case of indentation of thin walled structures, deriving recommendations for the selection of parameters in ship collisions and groundings. Yu and Amdahl (2016a) presented full six degrees of freedom dynamic simulation of ship collision and grounding accidents, solving the coupled problem i.e. evaluating simultaneously external motions and structural response.

6.3.4 Empirical and regression models

Methods that combine numerical simulations or accidental data or experiments with the regression analysis allow developing formulas that consider main dependencies between the grounding response and the relevant parameters. One of the first empirical models in the field was created by Minorsky (1959) who studied actual collision accidents and found that the energy absorbed by ship structures is in linear correlation with the deformed steel volume. It was shown by Vaughan (1977) that a similar linear dependence is also valid for ship groundings. To determine the damage extent, both models require rather detailed information for ship scantlings. Simonsen et al. (2009) followed the same principles and developed an empirical damage prediction formula, based on a combination of full-scale testing and extensive non-linear finite element analyses. Curves expressing horizontal force as a function of the damage extent were obtained from 12 grounding FE simulations and then tuned to give a best possible fit (Figure 13). The formulation is intended only for grounding events over sharp rocks (raking) where the plate tearing is the dominant failure mode. The model in addition provides the damage size, which is not the same as the damage opening.

$$F_H = 0.77\sigma_0\varepsilon_f^{0.71}(t_{eq})^{1.17}(B_d)^{0.83}$$

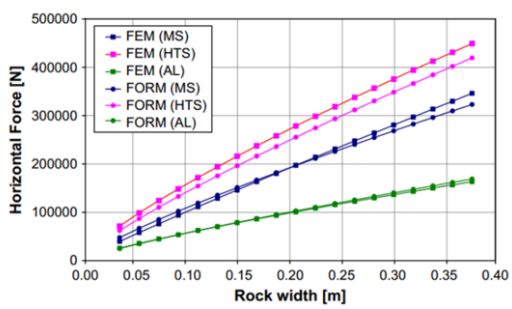

Figure 13: Simplified damage prediction formula and results compared with FEM dots: formula, squares: FEM, (Simonsen et. al. 2009).

However, it is often desired to predict also the size of the damage opening that can be used for flooding and oil spill simulations. Heinvee et al. (2013) presented a model for a rapid prediction of ship grounding damage. This regression model is developed based on a large number of numerical simulation with double-bottom tankers. The damage length and the opening width in outer and inner bottom of a double hull tanker are provided on the basis of a small number of input parameters describing ship size, the rock shape and size and penetration depth. Due to its simple structure and easy computation, the formulation can be effectively adopted when the consequences of a large number of grounding scenarios need to be evaluated. In Heinvee and Tabri (2015) the resistance formula was improved by introducing the ship structural resistance coefficient as a function of ship length. In Heinvee et al. (2016) the influence of transverse and longitudinal bulkheads on the grounding resistance was studied.

6.3.5 Analytical models

One alternative to the NLFEA grounding simulations is adoption of simplified analytical models where the total response of bottom structure is obtained through the summation of the responses of separate structural members. In grounding, the primary deformation modes for individual structural members are sliding deformation of longitudinal girders, denting and crushing of transverse members and indentation of plating. Simplified models for web girder crushing are proposed, for example, by Hong and Amdahl (2008), Yu et. al. (2015) and Gao and Hu (2015). Liu and Soares (2016) investigated the local (subjected local-static or dynamic load) crushing behaviour of transversally stiffened (large stiffeners) deep girders and derived analytical formulae able to estimate the relation between the crushing force and the indentation during the entire folding. This simplified method is only valid before the initiation of material rupture in the structure. Liu and Soares (2015) presented a new simplified analytical method to predict the crushing resistance of longitudinally stiffened deep web girders subjected to local load. The comparison among previously reported simplified methods demonstrates that the new approach can evaluate better the crushing behaviour of web girders during the entire deformation process. The present simplified approach can be combined with other simplified methods of stiffened plates to assess the resistance of the double- hull structures subjected to a wedge-shaped indenter. Yu et. al. (2015) presented a theoretical model for the calculation of grounding response of longitudinally stiffened girders. The model is formulated for shoal groundings. Yu claims that the resistance contribution of girders (longitudinal stiffeners) is underestimated. Therefore, a new girder model is proposed with an additional contribution from stiffeners. Sun et al. (2017) presented a simplified analytical method for predicting the resistance of ship bottom structures when a ship runs aground over rock-type seabed obstructions (raking grounding). The method shares similarities to the models reported earlier (Wang et al. (1997), Wang et al. (2000), Friis-Hansen & Simonsen (2002), where the total grounding resistance is expressed as the sum of resistances of individual structural members. The authors note that in case of powered groundings the contribution from bottom transverse floors to the grounding resistance is frequently underestimated and they claim that the novelty of the new simplified analytical model stands in the capability of accounting for the contribution of transverse floors in preliminary evaluations of the double bottom performances. The stiffeners attached to the plating are accounted through smeared thickness. This is justified with the small contact surface between the rock and the ship bottom.

6.4 Acceptance criteria/consequence evaluation

To evaluate the consequences of grounding, the focus is on the assessment of structural damage and following consequences such as flooding or, in the case of tankers, oil spill. Sergejeva et al. (2013) and Kollo et al. (2017) presented hydraulic models for one- and two-layer flows for different oil spill scenarios for tanker accidents. Five test cases were verified by comparison to the laboratory results of Tavakoli et al. (2011). The model provides the spill amount and duration. In (Sergejeva et al., 2017) the model was extended to account for wintertime conditions by taking into account the effects of emulsification and heat exchange occurring at the interface of fluids at different temperatures.

Tabri et al. (2015) combined the damage assessment model of Heinvee and Tabri (2015) and the oil spill model of (Sergejeva et al. 2013) with an oil spill propagation model (SMHI, 2012) and the environmental consequence models (Aps et al., 2009; Aps et al., 2014). Combining all these aspects together, the consequences can be evaluated not only in terms of structural damage or of amount of oil spill, but (using also meteorological info) as length of impacted shoreline.

7. FIRE AND EXPLOSION

7.1 Introduction

Fires and explosions account for 30% of ship losses records (Chen et al., 2017; Silva et al., 2015; Vairo et al., 2015). Most of the fires initiate in engine rooms. However, on board cruise vessels also fires initiating in cabins, restaurants or entertainment areas are to be taken into consideration, as well as fires starting in car decks on Ro-Ro vessel. A risk of fire or gas explosion accidents always exists in oil and gas facilities which are containing and processing flammable hydrocarbon mixtures. This is especially critical regarding the re-cent increase of LNG (Liquefied Natural Gas) shipping. LNG carriers, LNG-fuelled ships or LNG FSRUs (Floating Storage and Regasification Units) having gas processing units (re-liquefaction systems, fuel gas supply systems, re-gasification systems, etc.) have much more likelihood for fire and explosion accidents compared with the conventional gas carriers having just storage tanks for transportation. Potential accidents can result in serious impact on personnel, environmental or property. Therefore, the safety assessment against fire and explosion accidents should be performed during design phase to prevent loss of lives or catastrophic failure of structures. For offshore oil and gas industry, the design and operation procedures against fire and explosion accidents are well established with performance and risk based approach (Czujko et al. 2015).

Other ships having fire or explosion hazards are naval ships, passenger ships or electric powered vessels with battery systems, etc. Naval ships can be exposed to weapon explosions from above and below water that can affect the survivability of naval vessels, and one of the ISSC Committee has continuously reviewed the design of naval ship including weapon explosion (Ashe, G. et al., 2006; Dow, R. S. et al., 2015). Fire safety for passenger ships usually follows the FSS code (IMO, 2017a), FTP code (IMO, 2010) or SRtP (Safe Return to Port) regulations and Evacuation guidelines of SOLAS (IMO, 2017b). Alternative to these prescriptive requirements, the per-formance-based fire safety design was also suggested by MSC/Circ.1002 (IMO, 2001). Alt-hough the use of battery systems onboard ships is rather new area compared with land-based plants, guidelines have been already prepared (see e.g. DNVGL, 2014; LR, 2015).

7.2 Prescriptive vs performance based codes

With the ratification of IMO's resolution MSC.99 (73) on 1st July 2002, fire ship codes are shifted from prescriptive formats (rules in SOLAS) to performance-based (as long as an adequate level of safety is maintained) for technical, economic and social reasons. In prescriptive codes, most requirements indicate solutions without explicitly stating their aim. In performance-based codes, on the contrary, the desired objectives are presented and designers are given the possibility of choosing their solution, provided it meets the objectives. Generally, prescriptive codes are used as primary means to enforce fire safety in the ship design. They are based mainly on past experience (accidents or near-accidents history). As such, they may result to be either conservative (as a result of an over-reaction to a specific accident) or non-conservative (because they do not cover an accidental scenario not yet present in records). Moreover, the level of safety enforced is implicit and cannot be compared to requirements expressed in explicit levels. It is possible to synthesize the main advantages and disadvantages for the prescriptive and performance-based approaches.

Prescriptive codes:

- Advantages: simply evaluation of compliance with established requirements; no need for high level expertise.
- Disadvantages: requirements specified without a clearly statement of objectives; no promotion of cost-effective designs; very little flexibility for innovation.

Performance codes:

- Advantages: establishment of clear safety goals and leaving the means of achieving; permitting innovative design solutions that meet the performance requirements during first stages of application; facilitating use of new knowledge when available; allowance for cost- effectiveness and flexibility in design.
- Disadvantages: difficult to define quantitative levels of safety performance with those goals to the designer criteria; need for education because of lack of understanding especially; difficult to evaluate compliance with established requirements; need for validation of the tools used for quantification.

Areas where the application of performance codes is particularly promising are:

- large passengers (cruise) and ferry ships' passive fire protection (walls and ceilings) can be moved in order to create larger connected areas;
- in large ships higher passive resistance can substitute fixed installed fire suppression measure;
- in naval ships the expected extent of damage can be reduced through improved fire measures.

7.3 Fire and explosion analysis: General

Fire is a major threat to human life mainly due to toxic smoke. The important time dependent and location dependent factors to be determined during modelling are temperature, heat release rate, carbon monoxide, CO^2, and visibility. Two types of models are used to study the case: zone models and field models. Zone models divide the problem into a small number of zones, e.g. upper layer and lower layer. This kind of modelling is fast and a lot of different cases can be calculated in short time. Therefore, it is often used during design stage. More than 50 different zone models are available. Scenarios for the analyses are defined considering geometrical aspects, fire scenario, people, etc. Then the conversation laws for mass, energy, species (fuel, O^2, etc.) are applied.

The field models estimate the evolution of the fire in a space by mean of numerical tools, resolving the basic equations of mass, energy conservation, etc. The action characteristics of hydrocarbon fires can be modelled using the CFD method, which is recognized as one of the most powerful approaches and which makes it possible to model the fire phenomenon using first principles via solving the basic conservation equations of mass, energy and momentum (Paik et al., 2015; Novozhilov, 2001). In contrast, the action effects of fire on structures are characterized by the nonlinear finite element method (NLFEM) that can be solved with NLFEM codes such as LS-DYNA (LS-DYNA, 2013) or USFOS (USFOS, 2013).

The aim of fire CFD simulation is to characterize gas cloud dispersion, gas cloud temperatures and heat fluxes which are time- and space-dependent after the fire. Fire loads are elevated temperatures and heat fluxes in the ambient or gas cloud obtained by the fire CFD simulations. Radiation and convection associated with fire are key elements to characterize fire loads. One of the tools for fire CFD simulations well adopted for the offshore industry practices is KFX code (2013) which is a 3D transient finite volume CFD program. KFX is a cartesian, incompressible, three-dimensional transient finite volume CFD code that solves the discretized conservation equations for mass, energy and momentum adopting an iterative implicit pressure-correction method. Heat fluxes due to fire are transferred into structures with time, increasing the steel temperature which depends on the temperature of gas cloud, the area of steel exposed to the fire, and the characteristics of fire protection applied, among others. It is obvious that the gas cloud temperatures are not identical to the steel temperatures with time, and thus the heat transfer analysis should be performed to define the steel temperature with time. For practical purposes, the fire can be represented by temperature curve obtained from

rules or from CFD simulations. Another FE based simulation environment called VistaFire is provided as part of the VistaMat Suite. VistaFire is a thermomechanical analysis module for predicting fire effect on structures.

The explosion accident is a complex phenomenon derived by a number of random variables (e.g., leakage rate and direction; wind speed and direction; locations of ignition; gas clouds size, location and concentration, etc.), which have many uncertainties. The easiest way to get the explosion loads is to bring the prescriptive loads by referring to the relevant rules, standards or industrial guidance (API, 2006; DNV-OS-A101, 2014). However, it is often a conservative value and used in the early project phase. In the case of simplified calculation models for explosion loads, there are some empirical models such as TNT method for the high explosive and Multi-energy methods (Lees, 1996) or B-S-T model (Tang and Baker, 1999) for vapour cloud explosion. These are based on correlations with experimental data, and usually used to predict far field blast effects. However, these simplified models are gradually substituted by the numerical simulation. The numerical simulation model for explosion requires consideration of likely sources and magnitudes of leaks, ignition and consequent explosion development. These are presently well addressed by CFD which is the most fundamentally based method and has the best potential for accurate prediction of gas explosion phenomenon. These tools solve the conservation equations of mass, momentum and energy including turbulence and combustion. For instance, FLACS software is widely used for gas explosion simulations in oil and gas industries (Czujko et al. 2015).

7.4 The Risk of Fire and Explosion accidents

7.4.1 Action effects and modelling

The main parts of quantitative risk analysis are consequence calculation and probability estimation of selected design scenarios. Pitblado and Woodward (2011) performed comprehensive historical review on LNG risk, especially focused on the consequence route and modeling of LNG accidents, that is, discharge, evaporation, pool and jet fire, vapor cloud explosion, rollover, Rapid Phase Transitions (RPT), Boiling Liquid Evaporating Vapor Explosion (BLEVE). In (Woodward and Pitblado, 2010), predictions are compared of various LNG pool spread and pool fire models, and the possibility is discussed of a change in burning mechanism with large pool fires, fire engulfment of an LNG carrier causing cascading failures, the circumstances for a possible LNG BLEVE, and accelerated evaporation by LNG penetration into water.

LNG is highly flammable and explosive substance with ignition point of 650℃, rapid flame propagation, large mass burning rate about 2 times more than gasoline, high flame temperature, so the burning is of strong radiant heat, easy to form large area of fire. The LNG carrying ships have been designed, constructed and equipped to carry cryogenic liquefied natural gas stored at a temperature of -163℃. Breakage in the working piping or loading and unloading system, rupture in liquid hold, collision and other factors may lead to leakage of liquefied gas and create a liquid pool, which will result in fire accidents. Also, liquid cargo of ultra-low (cryogenic) temperature contacting with general hull, because local cooling produces excessive thermal stress, will make the hull brittle fractures spontaneously, and loses ductility, thereby endangering the entire ship's structure (Moon et al., 2009; Li and Huang, 2012).

The boiling point of LNG (taking methane into account) is 162℃, easy to be gasified. If LNG leaks or spills, initial flash vaporization of the leaking LNG occurs in the air, generating lots of steam instantaneously, mixing with surrounding air and forming cold steam fog and white smoke after condensation in the air, then diluted and heated to form flammable gas cloud with air (gas/air mixture), and reaching explosive concentrations (5 ~ 15 vol%), which will lead to Vapor Cloud Explosion (VCE) when encountering ignition sources.

When liquefied natural gas tanks on the ship are heated or exposed to external flame for a long time, the structural integrity of tanks will gradually decreases. When the structural capacity decreases to a certain extent, the tank will suddenly burst, resulting pressure suddenly reduces, and liquefied natural gas vaporizes and burn rapidly, resulting in Boiling Liquid Expanding Vapor Explosion (BLEVE) accidents. Sudden burst of tanks can release tremendous energy and produce shock waves and throw container pieces to the distant. Also, intense burning of liquefied petroleum gas can release enormous heat, resulting in a huge fireball and strong thermal radiation. Unlike the on-land LNG tank facilities, LNG marine shipping hazard studies have discounted BLEVE hazards associated with LNG vessels. Marine LNG vessels have differently designed tanks and it is demonstrated that the combination of physical barriers makes direct thermal input to the LNG inner tank more limited, but if it occurs these tanks cannot rise to a pressure sufficient to cause a large flash of liquid and consequent BLEVE event of a scale hypothesized in the literature (Pitblado, 2007).

7.4.2 Accidental scenario and probability

To establish accidental design scenarios used in risk assessment, not only the consequence models of the accidental scenarios, but also the possible accidental events and corresponding probabilities must be identified. The incident that follows a loss of containment event (such as the collapse of a tank, a hole in a pipe, etc.) can follow different sequences depending on the specific circumstances, which include the properties and condition of the released material, the presence of one or more safety barriers, and other factors. Each sequence will lead to a final accident scenario, the severity of which will range between "no outcome" (no consequences or negligible consequences for people and property) and a "major accident" such as an explosion or a large fire. As shown in Figure 14, Vílchez et al. (2011) presented a set of generic event tree analysis for the most common scenarios involving different types of hazardous materials and the corresponding intermediate probabilities based on the literature (BEVI, 2009).

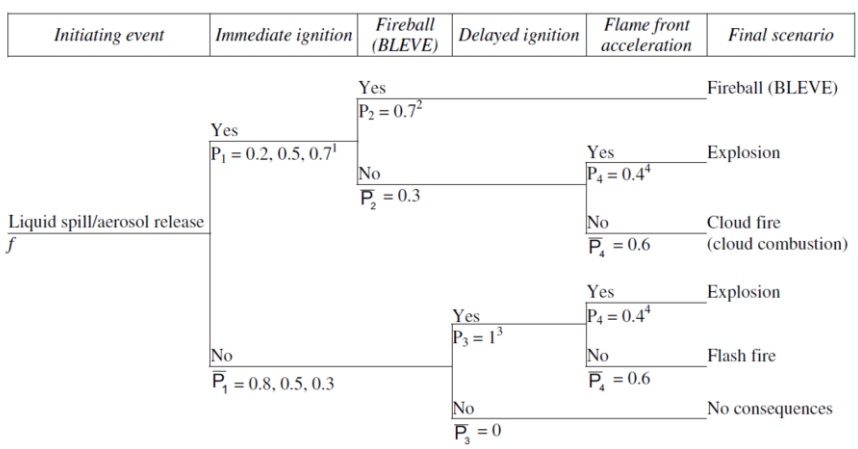

Figure 14: An example of Event Tree for instantaneous releases of extremely flammable pressurized liquefied gases (Vílchez, J. A. et al., 2011)

The probability is typically assessed by evaluation of historical data. Beside the statistical evaluation, Bayes networks are used to model the probability of fire for different locations. Independent variables and their conditional dependencies are used to determine probabilities.

Where conditional dependencies are unknown machine learning is considered. This dynamic Bayesian networks are gaining more popularity, especially in modelling fire risk modelling.

7.5 Design Requirements of Fire and Explosion Accidents for LNG Ships

7.5.1 Fire and explosion design for LNG carriers and FSRU

FSRU (Floating Storage and Regasification Unit) is a LNG Ship with large vaporizers to supply natural gas directly to clients and therefore ensuring that supply match demand at the right time and with the right supply conditions. It can be disconnected from the client at the location and is built under the traditional rules for ships as opposed to floating offshore installation. The uncontrolled leakage of the LNG from process equipment or cargo tanks during operation could result in fire or explosion accidents due to evaporation and dispersion of the product and, in some cases, could cause brittle fracture of the ship's hull due to low-temperature (cryogenic) exposure. Therefore, technical safety assurance, especially on regasification design integrity and operation in a whole ship, is required. International Code for the Construction and Equipment of Ships Carrying Liquefied Gases in Bulk or IGC code (IMO, 2016) is to provide design rules for the safe carriage by sea in bulk of liquefied gases. The revised IGC code, entered into force in 2016, indicates as potential risks for a ship equipped with a re-gasification system: fire and explosion; evacuation; extension of hazardous areas; pressurized gas discharge to shore; high-pressure gas venting; process upset conditions; storage and handling of flammable refrigerants; continuous presence of liquid and vapor cargo outside the cargo containment system; tank over-pressure and under-pressure; ship-to-ship transfer of liquid cargo; and collision risk during berthing maneuvers.

Compared with previous IGC code, the revised code suggests new requirements for the concept of re-gas vessels and possibility to use risk analyses to base design requirements. The risk assessment for fire and explosions specifically addresses areas or spaces containing piping, machinery, equipment and components. For example, cargo containment and handling space design refer to SOLAS for the purpose of fire protection and prevention of potential explosion. Furthermore, those areas shall be designed to retain their structural integrity in case of explosion or fire and this capability is to be substantiated on the basis of a risk analysis with due consideration of the characteristics of the safety measures like fire detection, suppression or pressure relieving devices. To address the collision risk and protect cargo tanks, the distance of cargo tanks from side shell has been increased as a function of the individual protected tank volume. Classification Societies have issued guidelines based on the IGC code (DNVGL, 2016 and 2017a; BV, 2017; LR, 2014). Fire and explosion safety assessment of FSRU, however, benefit from the experience gained in the similar field of offshore operation, where practices including the selection of design scenario or load from risk analyses and structural safety assessment are also widely used. For a detailed guidance on fire and explosion design for offshore structures see Czujko et al. (2015).

7.5.2 Fire and explosion design for Gas fuelled ships

The introduction of stricter local, national and international environmental legislations demands new fuel solutions within the maritime industry. One possible approach to meet the emission requirements is to use natural gas as fuel for propulsion. The typical systems for gas fuelled ships are containment and process systems. Even though the containment systems which store LNG on board ships follow the design principles known from gas carriers, LNG as a ship fuel has initiated new design concepts for containment systems. To use LNG as fuel it is necessary to extract it from the tank with pumps or pressure, and condition it by vaporization, pressurization and warming. Also, the natural gas has to be routed to the engine's gas

valve unit and into the engine itself. All these steps in the process must be accomplished without any gas leakage into the ship which can lead to fire or explosion accidents.

Until recently, there was a lack of international safety requirements for gas as fuel for non-LNG tankers, that is, ships other than gas tankers. However, the IGF Code (International Code of Safety for Ships using Gases or other Low-Flashpoint Fuels IGF code; IMO, 2017c) entered into force in 2017. The goal of the IGF Code is to provide an international standard for ships with natural gas-fuelled engine installations. Therefore, this code provides mandatory provisions for the arrangement and installation of low-flashpoint fuelled machinery. Similar to IGC code, IGF code also requires that risks affecting persons on board, the environment, the structural strength or the integrity of the ships are addressed by conducting risk assessments for the inherent hazards. The analysis shall ensure that risks are eliminated wherever possible. Risks which cannot be eliminated shall be mitigated as necessary. Especially, the code requires that explosion consequences shall not:

- cause damage to or disrupt the proper functioning of equipment/systems located in any space other than that in which the incident occurs;
- damage the ship in such a way that flooding of water below the main deck or any progressive flooding occur;
- damage work areas or accommodation in such a way that persons who stay in such areas under normal operating conditions are injured;
- disrupt the proper functioning of control stations and switchboard rooms necessary for power distribution;
- damage life-saving equipment or associated launching arrangements;
- disrupt the proper functioning of firefighting equipment located outside the explosion-damaged space;
- affect other areas of the ship in such a way that chain reactions involving, inter alia, cargo, gas and bunker oil may arise;
- prevent persons access to life-saving appliances or impede escape routes.

However, as this code also doesn't provide clear or prescriptive criteria of risk assessment or accidental limit state design for fire and explosion accidents, offshore practices of fire and explosion design (Czujko et al. 2015) are also widely used, together with classification society's rules and guidelines (DNVGL, 2017b; LR, 2016).

7.6 Fire and explosion analyses for LNG ships

7.6.1 Fire and explosion analyses for LNG carriers and FSRUs

Although in LNG shipping there has rarely been an event of cargo loss from accident, a relevant potential cause of leaks from LNG storage tanks is represented by collision or grounding accidents (Pitblado and Woodward, 2011). Therefore, the safety assessment of LNG carriers has been mainly focused on collision/grounding accidents and on following leakage events like dispersion or evaporation of LNG and heat radiation by pool fire. Luketa-Hanlin and Hightower (2008) have defined three categories of postulated LNG spills from carriers as shown in Fig. 15. The categories are basically Type I. above the water level; Type II. at the water level; Type III. below the water level. For each category, Pitblado and Woodward (2011) reviewed recent developments for collision/grounding calculation including leakage hole size and location, LNG pool size prediction, penetrations and hull pressure effects, etc. The theoretical models of dispersion, evaporation, pool fire and BLEVE from LNG spills are also reviewed.

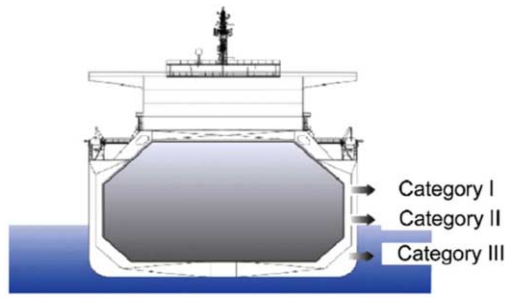

Figure. 15: Types of LNG leak location (Luketa-Hanlin and Hightower, 2008)

Fay (2003, 2007) proposed a comprehensive model for predicting the dynamics of spills from LNG tankers based on fluid mechanics principles and empirical properties of LNG spills on water, and Ray (2007) reviewed the integral and semi-empirical models (point source and solid flame) for LNG pool and vapor fire including thermal radiation hazard modelling. Recently, numerical simulations with CFD for LNG pool fire are widely used. Sun and Pareek (2015) analyzed the fire hazard and mitigation measures around an existing on-land LNG station using a computational fluid dynamics (CFD) model, and the results of CFD simulations were compared with the phenomenological models (Fig. 16). They also showed the CFD pool fire simulation of LNG spill on water for ship-to-ship bunkering between a LNG carrier and an FSRU as shown in Fig. 16(d). The significant hazards associated with LNG ship-to-ship bunkering could involve LNG vapor dispersion and LNG pool fires. The boil-off LNG vapor initially behaves as a denser-than-air vapor due to its cryogenic temperature and then is dissipated, as the vapor cloud heated up by surrounding environment. LNG pool fires occur due to either the source ignites immediately or a flash fire burns back to the source. It could cause thermal radiation damage to the surrounding properties or people. Due to different LNG discharge locations, three possibilities of lumped LNG vapor source planes (i.e. below waterline, at waterline and above waterline) were compared to investigate the vapor dispersion behaviour and fire radiation hazards in the different cases. in the study, thermal radiant heat flux and temperature were utilized to analyze the material effectiveness on both the LNG bunker and the cargo vessel. The water curtain, which is commonly used to prevent material stress cracking in case of LNG leakage, was also considered appropriately to mitigate the radiation hazard. Water curtain is often used as a physical barrier in the chemical and petrochemical industries which holds back the gas cloud and reduces the safety distance to a lower flammability limit (LFL) range. Detailed engineering criteria for designing an effective water curtain system are available from continuous research works in Mary Kay O'Connor Process Safety Center (Olewski et al., 2011, Kim et al., 2013).

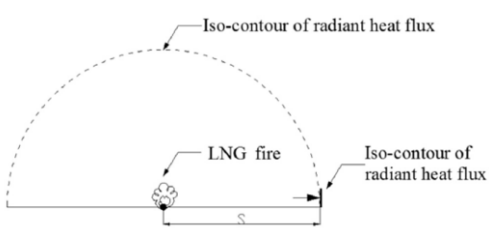

(a) Point source model

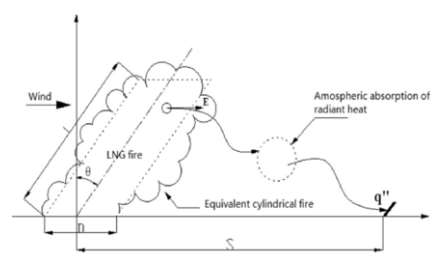

(b) Solid Flame model

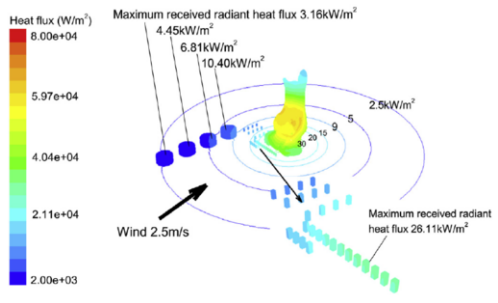

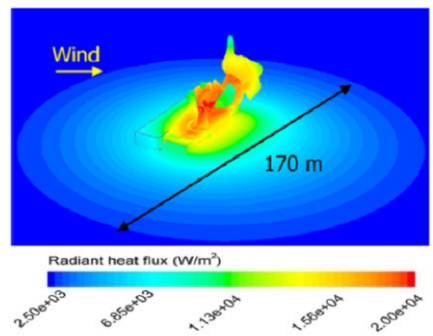

(c) CFD model on land tanks (d) CFD model of bunkering on sea water

Figure. 16: Radiant flux models (Sun and Pareek, 2015, 2017)

Martins et al. (2016) presented a complete quantitative risk analysis of undesired events (pool fire, jet fire, explosion, etc.) that may occur during the loading and unloading of LNG between a typical LNG carrier and an offshore terminal (FSRU). Initially, the potential hazardous events are categorized in some possible scenarios; the frequencies of occurrence of the undesired events are estimated; the weakness of each scenario is identified in the consequence analysis of a specified case; which is evaluated by providing the data to estimate the total risk of the installation. The risk was evaluated in terms of social and individual risk. Lastly, possible control measures able to reduce the frequency of occurrence, or mitigate the impacts associated with the analyzed scenarios, were proposed and new risks levels are estimated by considering those control measures.

Onboard ships, the most probable location of the fire is a machinery or engine room. Su and Wang (2013) used a CFD code to predict the developing processes of the fire in the design of engine room with multilayer structures, and Moon et al. (2009), CFD simulation for the arrangement of compressor room in LNG carriers. Kang (2017) also presented CFD simulations for the fire safety design of machinery room. In particular, he suggested a framework for using computational fire simulations during the early phases of ship design. This work is focused on how to arrange fire control options with minimal changes of existing design procedures. Currently, computational simulation tools are used to predict and mitigate fire propagation during the ship design process within the performance-based alternative design requirement.

Ignition of natural gas is generally not considered to pose explosion hazards in unconfined and low or medium congested areas. However, as the degrees of confinement and/or congestion increase, a potential exists for the ignition of a methane cloud to result in damaging overpressures. An area of potential interest for VCEs is the dock, while an LNG carrier is being offloaded: the vessel hull provides one degree of confinement and the shoreline may provide another; some degree of congestion is provided by the dock and associated equipment. Gavelli, et al. (2011), evaluated the consequences of the ignition of a flammable vapor cloud from an LNG spill during the LNG carrier offloading process. The CFD simulations show different approaches that can be followed to evaluate a vapor cloud explosion scenario in a partially confined and partially congested geometry

In addition to fire or explosions, another major safety concerns in LNG-related facilities is the reliability of a LNG Cargo containment system (CCS) for LNG carriers. Cryogenic LNG leakage due to CCS damage or failure can have dangerous effects on the ship structure. Lee et al. (2015) studied the LNG evaporation and heat diffusion through a membrane CCS with CFD simulations which considers liquid-to-gas phase changes and reactions in the porous insulation media and the accompanied rates of heat transfer. Choi et al. (2006) investigated,

further to LNG leakage, the consequent temperature change of the hull steel plate in a CCS. They used experimentally determined ductile-to-brittle transition temperature (DBTT) as the index of critical temperature for the hull plate, and a numerical simulation was performed to estimate the behaviour of cryogenic liquid in a porous structure in an LNG CCS and the resulting temperature change of the hull's plate due to LNG leakage. According to the study, the critical leakage hole size where temperature of hull plate did not reach a DBTT lies between 2 mm and 5 mm under the leakage conditions.

7.6.2 Fire and explosion analyses for LNG fuelled ships

For the use of natural gas as a fuel which should be stored in a liquefied form, a dedicated system, called the LNG fuel gas supply system (FGSS), should be installed on board. The system also needs subsystems for the storage and handling of pressurized LNG that surely present LNG-related risks. When the LNG-FGSS is above the deck, the fire risk is more detrimental than the explosion risk. An explosion in open space is unlikely to occur, and the overpressure even in the case of explosion is not considerable. In contrast, a fire due to cryogenic LNG and high-pressure natural gas after evaporation may lead to catastrophic consequences and should be addressed appropriately. A dedicated fire risk analysis was carried out by Chu and Chang (2017) with a structured procedure of quantitative risk analysis for fire accidents in FGSS. They performed primary tasks to estimate and manage the fire risks: the selection of representative scenarios, the estimation of frequency, the analysis of consequences and risk estimation for personnel. Lee et al. (2015) also conducted fire risk analysis for FGSS especially with CFD fire consequence analysis and estimation of design fire loads. A CFD explosion consequence analysis for LNG fuelled ships was carried out by Fu et al. (2016).

8. MARITIME SAFETY AND RESCUE SERVICES

Maritime Search and Rescue (SAR) services exist to assist people in distress or danger at sea, and involve activities such as assisting ships and vessels in difficulty, accident prevention, search and rescue, medical consultations and patient transport. An efficient response to maritime incidents and accidents is thus of vital importance. Apart from highlighting the need for research on and operational improvements for preventing accidents, the need for efficient response to maritime incidents and accidents is well acknowledged.

In (Nordström et al., 2016), a method is proposed for enhancing the communication between the SAR response operators and the crew of the distressed vessel. It aims at assessing and communicating whether a vessel can provide a safe environment for the people onboard. This method, named Vessel TRIAGE, borrowed the idea from the well-established working methods in emergency medicine, and it attempts to establish a shared understanding of the nature of the distress situation using a set of threat factors and a four-level ship safety categorization.

Especially in the Artic regions, due to the severe environmental conditions, there is a great concern about possible accidents, and their consequences for life and nature. Accordingly, a high level of preparedness for emergency cases is required. In Marchenko,et al. (2016) the rescue system resources of three northern regions of the Arctic are analyzed and compared, focusing on the need of international collaboration for safety on the sea in the border area.

Shipping accidents in northern Baltic sea areas are studied by (Goerlandt et al., 2017), providing insights in the operational types and environmental conditions under which the accidents occurred. According to the authors, the outcomes of their research could be useful for developing realistic training scenarios for oil spill response operations, although the results were primarily intended for improving risk analyses focusing on oil spill risks in winter conditions.

In Vettor & Guedes Soares (2015) the main features of the SAR intervention are described focusing on the existing components for an integrated information system in the Portuguese coasts. The subjects covered include the computation of the environmental conditions and the

adoption of dedicated graphical interface that provides all the necessary information to support and planning fast and efficient operations.

8.1 Emergency Response Services - ERS

On the 1st January of 2007 the Revised Annex I of MARPOL 73/78 entered into force. Regulation 37.4 of this Annex (IMO, 2004b) specifies that all oil tankers of 5000 tons deadweight or more shall have prompt access to computerized, shore-based damage stability and residual structural strength calculation programs. The same requirement was issued later in 2011 for passenger vessels (IMO, 2011). At a first sight, the specified Regulation regulates only nominating of the coastal organization which can assist vessel's crew in calculations, having provided carrying out emergency calculations for situations that are out of the crew's qualification. Emergency situations, however, set more stringent requirements. The vessel will not only need auxiliary calculations, but often a guide for carrying out fight for survivability or emergency salvage.

Purpose of the survivability or emergency salvage actions is the rescue action of emergency vessel by consecutive effective task prioritization on people rescue, preventing environmental pollution and eliminating the loss of property (vessel and/or cargo). Certainly, while specific experience and intuition is a necessary condition for successful res-cue operation, a key condition is the existence of operative and qualified forecast of conditions of the vessel in distress, and also the possibility to estimate the residual strength of the damaged hull as well as trim and stability changes with help of computation methods.

The corresponding problem includes a high degree of uncertainty and transient emergency situations. In combination with responsibility for people's life, survivability of a vessel and safety of cargo, this problem puts very rigid boundaries on the person in charge of decisions. This circumstance forced USA legislators first, and then IMO to create shore support for the vessel's Master in the form of ERS centres..

8.2 ERS Functionality

The adoption of the specified MARPOL Regulation initiated the creation of ERS centres. In the first place, ERS centres were organized Classification Societies, e.g. ABS (ABS, 2010), DNV (DNV-GL, 2016), BV. In addition, a number of other organizations claim to provide ERS for the marine industry, but the capability of the service provider is not addressed in the legislation. This has led to a situation where operators may even elect to provide this service internally without the assistance of external service providers. It is noted in OCIMF (2013) report that ERSs are rarely used, and accordingly may not attract appropriate priority by vessel management. Merely having a service agreement in place does not ensure that, when needed, the quality of service provided meets the need. Therefore, OCIMF (2013) report highlights a list of recommended minimum items for a prompt and reliable service.

The primary requirement of the ERS is to provide shore based damaged stability calculations. Further, it requires residual structural strength calculations as well as estimation of oil spill after groundings, collisions, breakage of construction, fires, explosions, etc. Regarding structural strength, an initial assessment should include a rapid assessment of the damage condition. This assessment should help to check that the vessel is in a condition to remain safely afloat and define the immediate corrective actions recommended to ensure the safety of the crew. There are two tiers in strength assessment, depending on the extent of the damage. First tier stipulates immediate (within 2h) longitudinal strength assessment in the damaged conditions. Second tier involves post initial response analysis either with 3D beam or FE analysis.

Such analyses require accurate calculation models on stable, pre-tested software. For instance, a ship stability calculation model should be prepared in advance and ready for use. This aspect should be part of the design approach, covering the entire lifecycle of the ship. As point-

ed out by Design Methods committee (ISSC, 2015a), this data sharing is certainly in the realms of present capabilities, but has some practical limitations such as intellectual property protection of the data within the systems. Shipyards are rightly concerned about exposing detailed production information to all downstream users.

According to the results of the calculation work by shore ERS centre, guidelines for the master are worked out. Guidelines include recommendations due to survivability fighting and decreasing of possible loss. Recommendations also include suggestions for emergency towing if needed.

The tasks set for ERS centres are quite similar for different organizations and can be derived by example from the Rapid Response Damage Assessment (RRDA) of ABS:

- development of a database of pertinent aspects of the vessel's structure, materials, machinery, and equipment;
- development of a computer model of the vessel that will allow for damage stability and residual strength analysis;
- evaluation of salvor's or owner's plans for off-loading, ballasting or cargo transfer sequences to improve residual stability and reduce hull girder loads and ground force reaction;
- calculation of bending and shear stresses caused by ground force;
- calculation of the residual hull girder strength based on the reported extent of damage;
- calculation of residual stability when the vessel's compartments are breached;
- calculation of hull girder strength in damaged condition with wave loading;
- calculation of hull girder ultimate strength;
- calculation of local strength in the damaged area;
- calculation of local buckling and ultimate strength;
- other calculations as appropriate for the vessel's condition.

ERS should be available round-the-clock without rest-days, but it is stressed that the success of the action is based on the predefined numerical models for the vessels managed by the centre.

8.3 Basis for decisions making

The general scheme for actions at the beginning of the emergency is given e.g. in Egorov et al. (2015). The actual formulation of rescue actions on board the vessel in distress starts after taking decisions about the object of rescue (people and/or vessel and/or cargo).

As pointed out by Egorov (1990), while preparing a plan for action one should take into consideration requirements about buoyancy, stability, maximum heeling angle, post damage global and local strength and restrictions in the capacity of compartments. While fixing limit values for trim and stability is quite straightforward, strength limits are not so obvious. In Egorov (2006), specific still water permissible bending moments are defined taking into consideration the missing part of the hull longitudinal members and a non axial bending load.

One of the most significant dangers is represented by water on deck that can imply a catastrophic decrease of vessel's stability leading in turn to capsize. Returning the vessel into the right floating position is a key for keeping it afloat. Therefore, an important phase of rescue actions is the righting of the vessel (Egorov et al. 2015), which means taking operational measures to control heel and trim after the accident.

9. BENCHMARK STUDY

9.1 Introduction

The objective of the benchmark study is to simulate a grounding scenario with finite element software and compare results with experimental tests. The ability to assess the strength of a ship against such incidents is crucial in the evaluation of this type of scenarios.

The following committee members have contributed to the benchmark study:

Table 4 Committee members contributed to the benchmark

Participation	Affiliation	Analysis software
L. Brubak	DNV GL, Norway	ABAQUS
Z. Hu	China	LS-DYNA
M. Kõrgesaar	Finland	ABAQUS
I. Schipperen	TNO, Netherland	LS-DYNA
K. Tabri	MEC, Estonia	LS-DYNA

A detailed FE model of one of the double bottom models tested in Rodd 1996 was created. The one chosen for the study was the conventional model most resembling the double bottom of a traditional tanker.

9.2 Experiment

The grounding model was created from the dimensions given in (Rodd, 1996) and (Simonsen, 1997), and shown here in Figure 17. The model includes the double bottom, the front, centre and aft bulkheads and the two sides. The double bottom features inner and outer plating with a thickness of 3mm, 7 transverse webs with a thickness of 1.9 mm between each bulkhead and one continuous longitudinal web in the centre of the model with a thickness of 2.28 mm. In addition to that, the inner and outer bottom is stiffened by folded plate continuous stiffeners and the transverse webs contain two manholes, one on each side of the longitudinal web. The manholes are reinforced by circumferential stiffeners along their edges. The bulkheads are vertically stiffened by L-stiffeners.

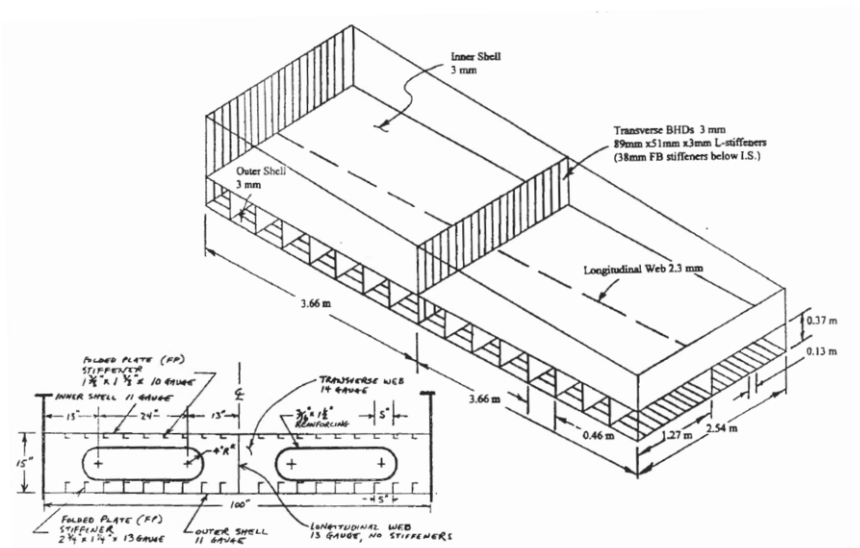

Figure 17 Model dimensions (Rodd 1996, Simonsen 1997).

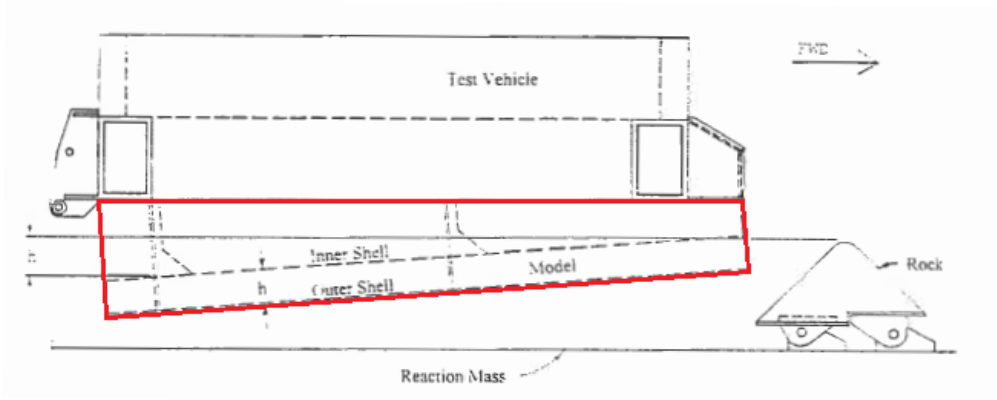

Figure 18 The grounding model mounted beneath the sled at an angle.

The grounding model is a 1:5 scale model of a ship double bottom and is meant to represent a conventional double bottom of a tanker in the 30,000-40,000 tones range. It was one of a total of four types of double bottom grounding models that were tested in the mid-1990s at the Naval Surface Warfare Centre in Virginia, USA. The methodology adopted for these tests and results obtained are presented in detail in (Rodd, 1996) and (Simonsen, 1997).

In the test, the scale model was fixed to a sled consisting of two railway bogies and dragged up an inclined slope to accumulate potential energy. The total mass of the grounding model and the sled was 223tons. At the end of the slope and centered between the two railway tracks was an artificial "rock" made of a steel cone with a semi-apex angle of 45° and a rounded tip with a radius of 0.17m. Details of the rock are shown in Figure 19.

The cone was fixed to a reinforced concrete pad with a mass of 1200tons. The test setup is shown in 18 reporting a cut view of the mounted model in way of the rock. The model was mounted with a longitudinal inclination (trim) angle so that when the model hits the tip of the rock, the tip is at the same level as the inner bottom plate. As the model moves over the rock, the rock tip is forced further up through the model and if the barge eventually clears the rock completely, the rock tip will be at a penetration height equal to twice the double bottom height. According to Simonsen (1997), this will ensure that the inner bottom is ruptured at some point during the test.

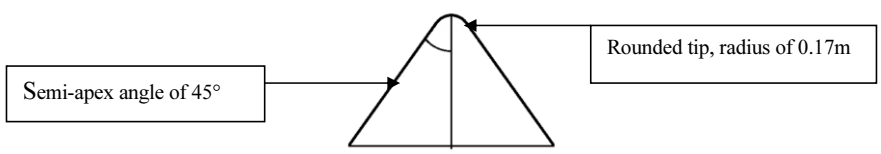

Figure 19 Artificial rock

9.3 Input data

The same geometry of the barge and the rock was used by all the contributors, with a friction coefficient equal to 0.35 (except in the sensitivity study reported in section 9.5). The material was ASTM A569 steel. Material characteristics are taken from the experiment description given in Simonsen (1997) and summarized in Table 5.

Other parameters relevant for the study (such as mesh size, failure strain, etc.) were assumed by each of the contributors. A summary is provided in Table 6.

Table 5 Material properties of ASTM A569

Material parameter	Value
Young's modulus	206 GPa
Poisson's ratio	0.3
Yield strength, σ_y	283 MPa
Ultimate strength, σ_u	345 MPa
Material flow stress, $\sigma_0=(\sigma_y+\sigma_u)/2$	314 MPa

Table 6 Assumptions in FE modelling by each contributor

parameter	Brubak	Hu	Kõrgesaar	Schipperen	Tabri
Strain hardening, n	0.22	0.22	0.2	n.a.	Full stress-strain curve
Mesh size	10 mm (3.3 times plate thickn.)	30mm	30 mm	30 mm	45 mm
Critical strain	Triaxiality depended; 22% for uniax. tension	0.17	Element thickness/ length/ triaxiality dep.	Element thickness/ length dependent	Through thickn. strain 0.087(3.4mm)/ 0.093 (3 mm)
Failure criterion	Damage evolution in Abaqus	plastic_ kinematic	Kõrgesaar & Romanoff (2014)	GL criterion, ADN-2015	Lehmann, et al. (2001)

9.4 Results

The results from the analyses are shown in Figure 20, where the energy and force curves are plotted against the horizontal position (grounding distance) of the barge. It can be seen that the agreement between experimental results and numerical simulations is relatively good.

From the force curve, several smaller spikes and two large spikes are observed, corresponding to the structure resisting deformations as the rock passes through the several smaller transverse frames and the two cargo hold bulkheads placed at mid-length and in the aft end. An overall increase in force is recorded, due to the trim angle. The absorbed energy can be found by integrating the reaction force over the grounding distance. Following the pattern of the force curve, the energy plot shows a slightly higher absorption rate (energy absorption per meter) around the two bulkheads than in the rest of the cargo hold.

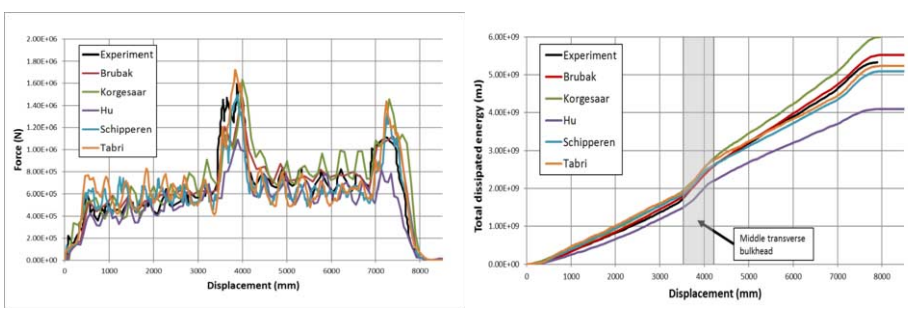

Figure 20 Results in terms of reaction force (left) and energy (right) versus grounding distance –base case, comparison among contributors.

The total dissipated energy can be broken down into several components such as friction, plastic deformation, elastic strain and energy gone into tearing elements apart. In the analyses that were run it is seen that most of the energy is dissipated by plastic deformation and friction while the other aforementioned contributions are relatively small. The ratio between the energy going into friction and plastic deformation varies depending on the coefficient of friction. A sensitivity study of the influence of the friction coefficient is presented in section 9.5.

Damages are shown in Figure 21, where deformations show to be very large. From what can be read from the pictures of the experimental test, the damages are very similar to what was found in the present finite element analysis. This illustrates that non-linear finite element computations can be used to estimate the damage extent with reasonable accuracy.

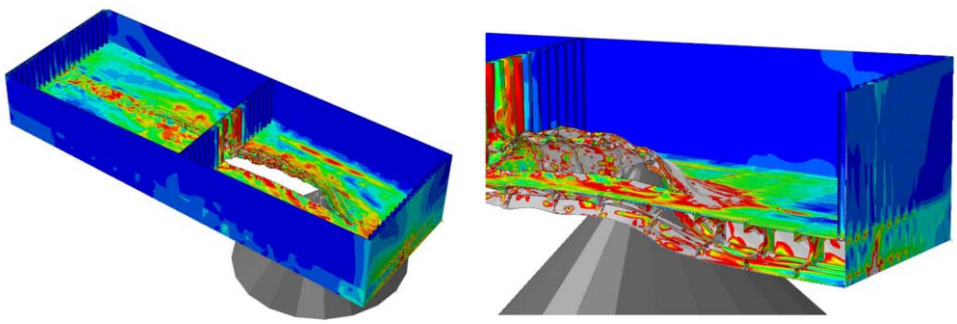

Figure 21 Damage extent of the barge (left) and close-up view of the damages (right).

9.5 Sensitivity studies

The results of the analyses are rather sensitive to different input parameters: a sensitivity study has been carried out to investigate to effect of: friction coefficients, failure strain values and mesh refinements. In order to isolate the effect of the different parameters, only one parameter per time is changed in respect to the model described in section 9.4.

9.5.1 Sensitivity for friction coefficients

The effect of the friction coefficient is studied for three different values: 0.3, 0.35 and 0.4. The other parameters are the same as in section 9.4. The average of results between the contributors is plotted in terms of force (left) and energy (right) in Figure 22

It can be noted that the failure mode may change slightly for different values of friction. This is the reason why the average result at the aft wall (about 8000 mm of displacement is higher for a friction coefficient equal to 0.35 compared to 0.4, since a higher friction caused a vertical rupture of the entire wall in the simulation by one of the contributors.

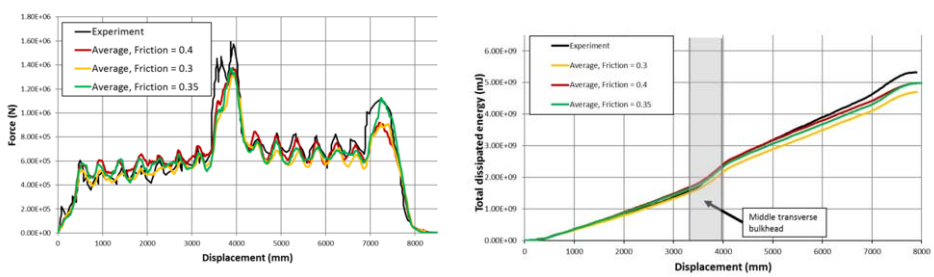

Figure 22 Sensitivity for friction coefficients (average values among contributors) Results in terms of force (left) and energy (right).

9.5.2 Sensitivity to failure strain values

The effect of different failure strain values is studied in the same manner as for the friction, by varying failure strain values and keeping all other parameters at the same value as in section 9.4. In total three different values of failure strain are used: the one from Table 6 and two more, corresponding to variations of +/- 20% (Figure 23). In the same manner as for friction, the failure mode may change for different values of failure strain.

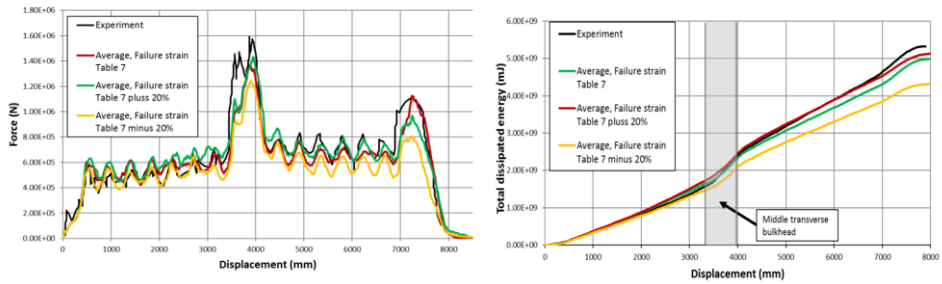

Figure 23: Sensitivity to failure strain (average values among contributors)
Results in terms of force (left) and energy (right)

9.5.3 Sensitivity to mesh refinement

The effect of mesh refinement is investigated with a fine and a coarse mesh by the various contributors. The size adopted as fine mesh is in the 10-15 mm range (i.e. 3-4 times the thickness of the outer plate) while for the coarse mesh is around 30 mm (about 10 times the outer plate thickness).

Mesh resolution has a relationship with material failure strain. The material models from each contributor are tuned for either a fine mesh (i.e. 3-5 times the thickness) or for a coarser mesh. In this section, the same material models are used for different mesh size in order to isolate the effect of mesh refinement. The effect of mesh refinement of using a coarser and a finer mesh is shown in Figure 24.

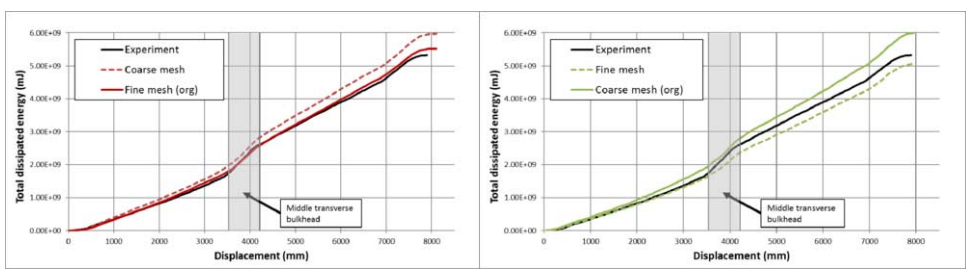

Figure 24 Sensitity study to mesh dimensions. Left: coarser right: finer

9.6 Summary

A benchmark study with five contributors has been performed with nonlinear finite element analyses of a grounding scenario and comparison with available results from an experimental test. The same geometry of the barge and the rock was used by all the contributors, and the adopted friction coefficient was equal to 0.35. The other input for the construction of the FEM models (such as mesh size, failure strain, etc.) were assumed freely by each of the contribu-

tors. The differences among the results reflect therefore the different choices made by the analysts. If this set of analyses is considered as representative of the typical dispersion in prediction results by experts in the field, the average value of predictions can be adopted to evaluate the bias between numerical results and experiments, while the standard deviation of numerical results can be assumed as an indication of the uncertainty in predictions. Figure 26 reports for force and energy the average curve and the confidence interval corresponding to +/- a standard deviation. The corrected standard deviation is used which gives an unbiased estimate of the variation and is more representative for small data sets. The figures show a small underestimation of force and energy in comparison to experiments. Most of the experimental values fall within the confidence interval corresponding to standard deviation for a given displacement. The standard deviation among the predicted forces and energies, expressed as percentage of the corresponding average value, features a mean value (computed on the whole test i.e. averaged over the barge length) of 16% and 11%, respectively. The maximum value of the same quantity is 28% for the force (at 7.2 meter displacement in Figure 25 left) and 13% for the energy (at 8 meter displacement in Figure 25 right).

In Figure 26, the ratio between the computed average value and the experimental result is plotted versus the displacements for energy and force. It can be seen that the average computed force deviates more from the corresponding experimental value (variations of the order of +/-40%) than the average energy (+/-10% in respect to experiments). This is expected, since the energy is an integral value of force. If the same ratios are averaged over the whole test, a value of 96% is obtained both for the force and the energy (same number since the energy is an integrated value of the force). This means that computed forces and energies are on the average 4% lower than the experimental results (this number quantifies the above mentioned underestimation).

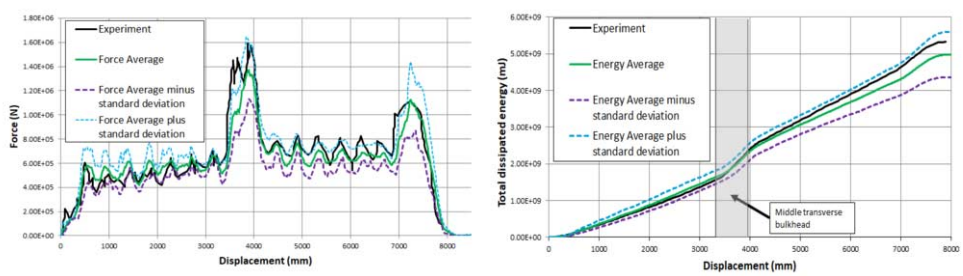

Figure 25 Average and standard deviation of results for base case in section 9.4.
On the left: force, on the right: energy

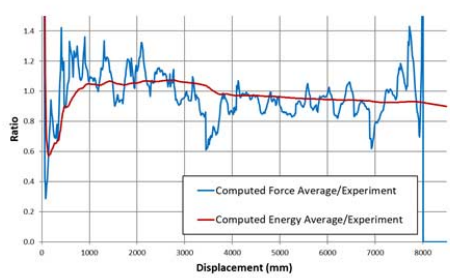

Figure 26 Ratio between average of computed values and experimental result for the energy

It is to be noted that the benchmark was not 'blind' (i.e. participants knew the experimental results) and this is always considered to improve the quality of predictions. However, it can be concluded that the fairly good agreement between experimental values and numerical predictions coming from this exercise demonstrates that a complex grounding scenario can be effectively simulated with nonlinear finite element analysis.

REFERENCES

ABS (2010) Guide for rapid response damage assessment, American Bureau of Shipping.

AbuBakar, A. & Dow, R. S. (2013) 'Simulation of ship grounding damage using the finite element method', International Journal of Solids and Structures. Elsevier Ltd, 50(5), pp. 623–636.

Acanfora, M. and De Luca, F. (2016) 'An experimental investigation into the influence of the damage openings on ship response', Applied Ocean Research, 58, pp. 62–70.

Addario, N., Rizzuto, E. and Prestileo, A. (2014)'Ship side damage due to collision with icebergs', Proceed. IMAM 2013, 15th Congress of the International Maritime Association of the Mediterranean, La Coruna ES.

Afenyo, M., Veitch, B. and Khan, F. (2016) 'A state-of-the-art review of fate and transport of oil spills in open and ice-covered water', Ocean Engineering, 119, pp. 233–248.

Akhtar, M. J. et al. (2016) 'The choice of multiple design ships for calculation of bridge collision design loads', Proceedings of 7th International Conference Collision and Grounding of Ships and Offshore Structures, Ulsan, Korea.

Alsos, H. S. and Amdahl, J. (2007) 'On the resistance of tanker bottom structures during stranding', Marine Structures, 20(4), pp. 218–237.

Alsos, H. S. and Amdahl, J. (2009a) 'On the resistance to penetration of stiffened plates, Part I - Experiments', International Journal of Impact Engineering, 36(6), pp. 799–807.

Alsos, H. S., Amdahl, J. and Hopperstad, O. S. (2009b) 'On the resistance to penetration of stiffened plates, Part II: Numerical analysis', International Journal of Impact Engineering, 36(7), pp. 875–887.

Antoine, G. O. and Batra, R. C. (2015) 'Sensitivity analysis of low-velocity impact response of laminated plates', International Journal of Impact Engineering, 78, pp. 64–80.

API, R., 2FB, Recommended Practice for the Design of Offshore Facilities against Fire and Blast Loading. 2006. Washington, DC: API.

Aps, R. et al. (2009) 'Bayesian inference for predicting potential oil spill related ecological risk', in WIT Transactions on the Built Environment, pp. 149–159.

Aps, R. et al. (2014) 'Incorporating dynamics factor to the Environmental Sensitivity Index (ESI) shoreline classification – Estonian and Spanish example', Journal of Coastal Research, 70, pp. 372–377.

Ashe G, et al. (2006) 'Committee V.5 Naval Vessel Design', Proceedings of the 16th Int. Ship and Offshore Structures Congress, Vol.2. August 2006. Southampton, UK.

Bašić, J., Degiuli, N. and Dejhalla, R. (2017) 'Total resistance prediction of an intact and damaged tanker with flooded tanks in calm water', Ocean Engineering, 130, pp. 83–91.

Begovic, E., Day, A. H. and Incecik, A. (2017) 'An experimental study of hull girder loads on an intact and damaged naval ship', Ocean Engineering, 133, pp. 47–65.

Bela, A. et al. (2017) 'Ship collision analysis on offshore wind turbine monopile foundations', Marine Structures, 51, pp. 220–241.

BEVI (2009) 'Reference Manual Bevi Risk Assessments', Ver.3.2, National Institute of Public Health and the Environment (RIVM), Netherlands.

Bitner-Gregersen E.M. and Gramstad O. (2016) 'Rogue Waves: Impact on ships and offshore structures' DNV-GL Position Paper 05–2015.

Bitner-Gregersen E.M. et al. (2012) 'Reply to discussers of the report of ISSC 2012 Committee I.1 Environment', Proceedings of the ISSC 2012, September 2012 Rostock, Germany.

Bitner-Gregersen, E.M., et al. (2015) 'Report of Committee I.1 Environment', Proceedings of the ISSC 2015, September 2015, Cascais, Portugal.
Brunila, O. P. and Storgård, J. (2012) 'Oil Transportation in the Gulf of Finland in 2020 and 2030', Publications from the Centre for Maritime Studies. Turku.
BV (2017) ' Rules for the Classification of Floating Storage Regasification Units', NR 645 DT R00 E, Bureau Veritas.
Calle, M. A. G., Oshiro, R. E. and Alves, M. (2017) 'Benchmark study of failure criteria for ship collision modeling using purpose-designed tensile specimen geometries', Marine Structures, 53, pp. 68–85.
Calle, M. A. G., Verleysen, P. and Alves, M. (2017) 'Ship collision and grounding: Scaled experiments and numerical analysis', International Journal of Impact Engineering, 103, pp. 195–210.
Cerik, B. C. (2016) 'A study on modelling of rate-dependent material behaviour in simulation of collision damage', Proceedings of 7th International Conference Collision and Grounding of Ships and Offshore Structures, Ulsan, Korea.
Cerik, B. C., Shin, H. K. and Cho, S. R. (2016) 'A comparative study on damage assessment of tubular members subjected to mass impact', Marine Structures, 46, pp. 1–29.
Chen, Q., Qi, X. and Sun, Q. (2017), 'Analysis of Causes of Maritime Accidents', 3rd International Conference on Applied Mechanics and Mechanical Automation (AMMA 2017).
Chen, W. and Hao, H. (2014) 'Experimental and numerical study of composite lightweight structural insulated panel with expanded polystyrene core against windborne debris impacts', Materials and Design, 60, pp. 409–423.
Chen, W. et al. (2015) 'Performance of composite structural insulated panel with metal skin subjected to blast loading', Materials & Design, 84, pp. 194–203.
Cheng, J. (2014) 'Reliability analysis of the Sutong Bridge Tower under ship impact loading', Structure and Infrastructure Engineering. Taylor & Francis, 10(10), pp. 1320–1329.
Chu, B., & Chang, D. (2017) 'Effect of full-bore natural gas release on fire and individual risks: A case study for an LNG-Fuelled ship', Journal of Natural Gas Science and Engineering, 37, 234–247.
Czujko, J. et al. (2012) 'Report of Committee V.1 Damage assessment following accidents', Proceedings of the ISSC 2012, September 2012 Rostock, Germany.
Czujko, J. et al. (2015) 'Committee V.1 Accidental limit states', Proceedings of 19th International ship and offshore structures congress, Sep. 2015, Cascais, Portugal.
D3view, 'Best Practices for Modeling Recoverable Low Density Foams – By Example', 12 10 2006. [Online]. Available: http://www.d3view.com/best-practices-for-modeling-recoverable-low-density-foams-by-example/. [Accessed 10 3 2017].
Daley, C. G. et al. (2017). 'Overload response of flatbar frames to ice loads', Ships and Offshore Structures, 12(sup1), pp. S68-S81.
Daniel, I. M. (2016) 'Yield and failure criteria for composite materials under static and dynamic loading', Progress in Aerospace Sciences, pp. 18–25.
Derradji-Aouat, A. (2000) 'A unified failure envelope for isotropic fresh water ice and iceberg ice', Proceeding of the ETCE/OMAE-2000 Joint Conference, Energy for the New Millennium, New Orleans, USA,
DNV GL (2014) 'Guideline for Large Maritime Battery Systems', No.2013-1632, Rev.1.0, Det Norske Veritas, Norway.
DNV GL (2016) 'Rules for Classification Ships – Part 5 Ship types – Chap. 7 Liquefied gas tankers', Det Norske Veritas, Norway.
DNV GL (2017a) 'Rules for Classification Ships – Part 6 Additional class notations – Chap. 2 Propulsion, power generation and auxiliary systems – Sec. 5 Gas fuelled ship installations – Gas Fuelled', Det Norske Veritas, Norway.

DNV GL (2017b) 'Rules for Classification Ships – Part 6 Additional class notations – Chap. 4 Cargo operations – Sec. 8 Regasification plant - REGAS', Det Norske Veritas, Norway.
DNV GL-RP-C204 (2010) 'Design against accidental loads', Recommended Practice C204, Det Norske Veritas Oct. 2010, Norway, pp.7-52.
DNV GL-RP-C208 (2016) 'Determination of structural capacity by non-linear FE analysis methods', Recommended Practice C208, Sep. 2010, Norway.
DNV-OS-A101 (2014) 'Safety Principles and Arrangements', Det Norske Veritas Apr. 2014, Norway.
Dow, R. S. et al. (2015) 'Committee V.5 Naval Vessel Design', Proceedings of the 19th Int. Ship and Offshore Structures Congress, Sep. 2015, Cascais, Portugal.
Egorov, G. V. (1990) 'Automated calculation of damaged vessel straightening with help of onboard personal computer // Present-day problems of shipbuilding and ship-repairing', Transactions of OIIMF. M., V/O "Mortekhinformreklama", pp. 26-30.
Egorov, G. V. (2006) 'Hull's residual strength in the damage stability calculations and providing of survivability fighting', Criteria and examples // Visnyk ONMU. Odessa: ONMU, Vol. 19. pp. 49-63.
Egorov, G. V., Vorona O.A. & Chernii V.A. (2015) '"Grigoriy Bugrov" tanker salvage operation execution with integrated approach to damage control with account of strength requirements' // Proc. of the 29th Asian Technical Exchange and Advisory Meeting on Marine Structures (TEAM'2015). – Vladivostok, Russia, pp. 35-42.
Eleftheria, E., Apostolos, P. and Markos, V. (2016) 'Statistical analysis of ship accidents and review of safety level', Safety Science. Elsevier Ltd, 85, pp. 282–292.
Fan, W. and Yuan, W. C. (2014) 'Numerical simulation and analytical modeling of pile-supported structures subjected to ship collisions including soil-structure interaction', Ocean Engineering, 91, pp. 11–27.
Fang, Q. et al. (2015) 'A 3D mesoscopic model for the closed-cell metallic foams subjected to static and dynamic loadings', International Journal of Impact Engineering, 82, pp. 103–112.
Fay, J. A. (2003) 'Model of spills and fires from LNG and oil tankers', Journal of Hazardous Materials, 96(2), pp. 171–188.
Fay, J. A. (2007) 'Spread of large LNG pools on the sea', Journal of Hazardous Materials, 140(3), pp. 541–551.
Ferrari, N., Rizzuto, E. and Prestileo, A. (2015) 'Modelling ice characteristics in iceberg-ship collision analyses', in 16th International Congress of the International Maritime Association of the Mediterranean, IMAM 2015, pp. 305–316..
Friis-Hansen, P. and Simonsen, B. C. (2002) 'GRACAT: Software for grounding and collision risk analysis', Marine Structures, 15(4–5), pp. 383–401.
Fu P., Leira B.J. & Myrhaug, D. (2016). 'Parametric Study Related to the Collision Probability Between Two Risers', In ASME 2016 35th International Conference on Ocean, Offshore and Arctic Engineering, American Society of Mechanical Engineers. Pusan, Korea.
Fu, P., Leira, B. J. and Myrhaug, D. (2017) 'Reliability analysis of wake-induced collision of flexible risers', Applied Ocean Research. Elsevier B.V., 62, pp. 49–56.
Fu, S. et al. (2016) Framework for the quantitative assessment of the risk of leakage from LNG-fuelled vessels by an event tree-CFD, Journ.of Loss Prevention in the Process Industries, 43, pp. 42–52.
Gaiotti M. and Rizzo C. M. (2012) 'An analytical/numerical study on buckling behaviour of typical composite top hat stiffened panels', Ships and Offshore Structures. Taylor & Francis, 7(2), pp. 151–164.
Gao, Y. et al. (2015) 'An elastic-plastic ice material model for ship-iceberg collision simulations', Ocean Engineering, 102, pp. 27–39.
Gao, Z., Yang, S. and Hu, Z. (2014) 'The resistance of ship web girders in collision and grounding', Mathematical Problems in Engineering, 2014.

Gao, Z. and Hu, Z. (2015) 'Structural response of ship bottom floor plating during shoal grounding', pp. 685–692.
Gavelli, F. et al. (2011) 'Evaluating the potential for overpressures from the ignition of an LNG vapour cloud during offloading', Journal of Loss Prevention in the Process Industries. Elsevier Ltd, 24(6), pp. 908–915.
Getter, D. J. et al. (2015) 'Strain rate sensitive steel constitutive models for finite element analysis of vessel-structure impacts', Marine Structures, 44, pp. 171–202.
Gilioli, A. et al. (2015) 'Predicting ballistic impact failure of aluminium 6061-T6 with the rate-independent Bao-Wierzbicki fracture model', International Journal of Impact Engineering, 76, pp. 207–220.
Goerlandt, F. et al. (2017) 'An analysis of wintertime navigational accidents in the Northern Baltic Sea', Safety Science, 92, pp. 66–84.
Hänninen, M. (2014) 'Bayesian networks for maritime traffic accident prevention: Benefits and challenges', Accident Analysis and Prevention. Elsevier Ltd, 73, pp. 305–312.
Hao, E. and Liu, C. (2017) 'Evaluation and comparison of anti-impact performance to offshore wind turbine foundations: Monopile, tripod, and jacket', Ocean Engineering, 130, pp. 218–227.
Hassoon, O. H., Tarfaoui, M. and El Moumen, A. (2017) 'Progressive damage modeling in laminate composites under slamming impact water for naval applications', Composite Structures, 167, pp. 178–190.
Heinvee, M. (2016) 'The Rapid Prediction of Grounding Behaviour of Double Bottom Tankers', Doctoral thesis, Tallinn University of Technology.
Heinvee, M. and Tabri, K. (2015) 'A simplified method to predict grounding damage of double bottom tankers', Marine Structures, 43, pp. 22–43.
Heinvee, M. et al. (2013) 'A simplified approach to predict the bottom damage in tanker grounding', in Collision and Grounding of Ships and Offshore Structures - Proceedings of the 6th International Conference on Collision and Grounding of Ships and Offshore Structures, ICCGS 2013.
Heinvee, M. et al. (2016) 'Influence of longitudinal and transverse bulkheads on ship grounding resistance and damage size', Proceedings of 7th International Conference Collision and Grounding of Ships and Offshore Structures, Ulsan, Korea.
Hill, R. (1948) 'A Theory of the Yielding and Plastic Flow of Anisotropic Metals', Proceedings of the Royal Society of London A: Mathematical, Physical and Engineering Sciences, 193(1033), pp. 281–297.
Holmen, J. K., Hopperstad, O. S. and Børvik, T. (2015) 'Low-velocity impact on multi-layered dual-phase steel plates', International Journal of Impact Engineering, 78, pp. 161–177.
Hong, L. and Amdahl, J. (2008) 'Crushing resistance of web girders in ship collision and grounding', Marine Structures, 21(4), pp. 374–401.
Hosford, W. F. (1972) 'A Generalized Isotropic Yield Criterion', Journal of Applied Mechanics, p. 607.
IACS (2017) 'Common Structural Rules for Bulk Carriers and Oil Tankers', Part 1 Chapter 4 Section 2- Dynamic load cases.
IMO (1995) Interim guidelines for approval of alternative methods of design and construction of oil tankers under regulation 13F(5) of Annex I of MARPOL 73/78, Resolution MEPC 66(37).
IMO (2001) 'Guidelines on Alternative Design and Arrangements for Fire Safety', MSC/Circ.1002, International Maritime Organization (IMO).
IMO (2003) Revised Interim Guidelines for the Approval of Alternative Methods of Design and Construction of Oil Tankers under Regulation 13F(5) of Annex I of MARPOL 3/78, Resolution MEPC 110(49).
IMO (2004a). Revised Annex I of MARPOL 73/78. Resolution MEPC.117(52).

IMO (2004b) 'Explanatory notes on matters related to the accidental oil outflow performance under regulation 23 of the revised MARPOL Annex I', RESOLUCIÓN MEPC.122(52), MEPC/52/24/Add.1
IMO (2010) 'The International Code Application of Fire Test Procedures (FTP Code)', International Maritime Organization (IMO).
IMO (2011) 'Guidelines on operational information for masters of passenger ships for safe return to port by own power or under tow', IMO, MSC.1/Circ.1400.
IMO (2016) 'International Code for the Construction and Equipment of Ships Carrying Liquefied Gases in Bulk (IGC Code)', International Maritime Organization (IMO).
IMO (2017a) 'The International Code for Fire Safety Systems (FSS Code)', International Maritime Organization (IMO).
IMO (2017b) 'International Convention for the Safety of Life at Sea (SOLAS)', International Maritime Organization (IMO).
IMO (2017c) 'International Code of Safety for Ships using Gases or other Low-Flashpoint Fuels (IGF code)', International Maritime Organization (IMO).
Ince, S. T. et al. (2016) 'An advanced technology for structural crashworthiness analysis of a ship colliding with an ice-ridge: Numerical modelling and experiments', International Journal of Impact Engineering.
ISO (2007) 'Fixed steel offshore structures', Standard ISO-19902 International Organization for Standardization.
ISO (2015) 'General principles on reliability for structures', International Organization for Standardization, London.
Ji, S., Di, S. and Liu, S. (2015) 'Analysis of ice load on conical structure with discrete element method', Engineering Computations, 32(4), pp. 1121–1134.
Jia, H. and Moan, T. (2015) 'Global Responses of Struck Ships in Collision With Emphasis on Hydrodynamic Effects', Journal of Offshore Mechanics and Arctic Engineering, 137(4), p. 41601.
Jia, L. et al. (2016) 'Combined modelling and experimental studies of failure in thick laminates under out-of-plane shear', Composites Part B: Engineering, 105, pp. 8–22.
Johnson, G. R. and Cook, W. H. (1983) 'A constitutive model and data for metals subjected to large strains, high strain rates and high temperatures', 7th International Symposium on Ballistics, pp. 541–547.
Kang, H. J. et al. (2017) 'A framework for using computational fire simulations in the early phases of ship design', Ocean Engineering, 129(September 2016), pp. 335–342.
Kang, L. et al. (2017) 'Accumulative response of large offshore steel bridge under severe earthquake and ship impact due to earthquake-induced tsunami flow', Engineering Structures, 134, pp. 190–204.
KFX (2013) 'User's manual for Kameleon FireEx', Computational Industry Technologies AS, Stavanger, Norway.
Kim, B. K. et al. (2013) 'Key parametric analysis on designing an effective forced mitigation system for LNG spill emergency', Journal of Loss Prevention in the Process Industries, 26(6), pp. 1670–1678.
Kim, E. (2014) 'Experimental and numerical studies related to the coupled behaviour ofice mass and steel structures during accidental collisions'. Skipnes kommunikasjon as.
Kim, E. et al. (2017) 'Laboratory experiments on shared-energy collisions between freshwater ice blocks and a floating steel structure', Ships and Offshore Structures. Taylor & Francis, 12(4), pp. 530–544.
Kim, H., Welch, D. A. and Kedward, K. T. (2003) 'Experimental investigation of high velocity ice impacts on woven carbon/epoxy composite panels', Composites Part A: applied science and manufacturing. Elsevier, 34(1), pp. 25–41.

Kim, K. J. et al. (2016) 'An experimental and numerical study on nonlinear impact responses of steel-plated structures in an Arctic environment', International Journal of Impact Engineering, 93, pp. 99–115.
Kim, M. et al. (2016) 'Dynamic failure analysis of mark III type LNG CCS primary barrier using instability, ductile and shear failure criteria', Proceedings of 7th International Conference Collision and Grounding of Ships and Offshore Structures, Ulsan, Korea
Kitamura, O. (2002) 'FEM approach to the simulation of collision and grounding damage', Marine Structures, 15, pp. 403–428.
Kollo, M., Laanearu, J. and Tabri, K. (2017) 'Hydraulic modelling of oil spill through submerged orifices in damaged ship hulls', Ocean Engineering. Elsevier, 130(December 2016), pp. 385–397.
Kõrgesaar, M. and Kujala, P. (2016) 'Experimental validation of failure criterion for large complex shell structures', in Proceedings of the International Conference on Collision and Grounding of Ships and Offshore Structures, pp. 47–53.
Kõrgesaar, M. and Romanoff, J. (2014) 'Influence of mesh size, stress triaxiality and damage induced softening on ductile fracture of large-scale shell structures', Marine Structures, 38, pp. 1–17.
Kõrgesaar, M., Kujala, P. & Romanoff, J. (2018). Load carrying capacity of ice-strengthened frames under idealized ice load and boundary conditions. Marine Structures, 58, pp.18-30.
Kõrgesaar, M., Remes, H. and Romanoff, J. (2014) 'Size dependent response of large shell elements under in-plane tensile loading', International Journal of Solids and Structures, 51(21–22), pp. 3752–3761.
Kujala, P. et al. (2009) 'Analysis of the marine traffic safety in the Gulf of Finland', Reliability Engineering & System Safety, 94(8), pp. 1349–1357.
Kumar, K. and Surendran, S. (2013) 'Design and analysis of composite panel for impact loads in marine environment', Ships and Offshore Structures, 8(5), pp. 597–606.
Lee, G. J. (2015) 'Dynamic orifice flow model and compartment models for flooding simulation of a damaged ship', Ocean Engineering, 109, pp. 635–653.
Lee, S., Seo, S., & Chang, D. (2015) 'Fire risk comparison of fuel gas supply systems for LNG fuelled ships', Journal of Natural Gas Science and Engineering, 27, pp. 1788–1795.
Lees, F. P. (1996) 'Loss prevention in the process industries', Butterworth Heinemann.
Li, J. and Huang, Z. (2012) 'Fire and explosion risk analysis and evaluation for LNG ships', Procedia Engineering, 45(Supplement C), pp. 70–76.
Liu, B. and Guedes Soares, C. (2015) 'Simplified analytical method for evaluating web girder crushing during ship collision and grounding', Marine Structures. Elsevier Ltd, 42, pp. 71–94.
Liu, B. and Guedes Soares, C. (2016a) 'Analytical method to determine the crushing behaviour of girders with stiffened web', International Journal of Impact Engineering, 93, pp. 49–61.
Liu, B. and Guedes Soares, C. (2016b) 'Experimental and numerical analysis of the crushing behaviour of stiffened web girders', International Journal of Impact Engineering, 88, pp. 22–38.
Liu, B. and Guedes Soares, C. (2017) 'Influence of Impact Location on the Plastic Response and Failure of Rectangular Cross Section Tubes Struck Transversely by a Hemispherical Indenter1', Journal of Offshore Mechanics and Arctic Engineering. ASME, 139(2), pp. 21603–21612.
Liu, B. et al. (2017) 'A simple criterion to evaluate the rupture of materials in ship collision simulations', Marine Structures, 54, pp. 92–111.
Liu, B., Villavicencio, R. and Guedes Soares, C. (2015a) 'Simplified method for quasi-static collision assessment of a damaged tanker side panel', Marine Structures, 40, pp. 267–288.
Liu, B., Villavicencio, R. and Guedes Soares, C. (2015b) 'Simplified analytical method to evaluate tanker side panels during minor collision incidents', International Journal of Impact Engineering, 78, pp. 20–33.

Liu, B., Zhu, L. and Chen, L. (2017) 'Numerical assessment of the resistance of ship double-hull structures in stranding', Proceeding of 6th International Conference on Marine Structures, pp. 469–475. May, Lisbon, Portugal.

Liu, C., Hao, E. and Zhang, S. (2015) 'Optimization and application of a crashworthy device for the monopile offshore wind turbine against ship impact', Applied Ocean Research, 51, pp. 129–137.

Liu, J., Cui, M., Zhang M. (2016) 'An experimental study on the resistance to penetration of hat-type stiffened plates', Proceedings of 7th International Conference Collision and Grounding of Ships and Offshore Structures, Ulsan, Korea.

Liu, Z. et al. (2011) 'Plasticity based material modelling of ice and its application to ship-iceberg impacts', Cold Regions Science and Technology, 65(3), pp. 326–334.

LR (2014) 'Provisional Rules for LNG Ships and Barges Equipped with Regasification Systems', Lloyd's Register.

LR (2015) 'Large Battery Installations – a Lloyd's Register Guidance Note', Lloyd's Register.

LR (2016) 'Rules and Regulations for the Classification of Natural Gas Fuelled Ships', Lloyd's Register.

LS-DYNA (2013) 'User's manual', version 14.0, ANSYS Inc., USA.

LSTC (2014) LS-DYNA Keyword User's Manual Volume II R7.1, Materials & Design.

LSTC, [Online]. Available: http://ftp.lstc.com/anonymous/outgoing/support/FAQ/composite.models. [Accessed 10 3 2017].

LSTC, [Online]. Available: http://ftp.lstc.com/anonymous/outgoing/support/FAQ/negative_volume_in_brick_element.tips. [Accessed 10 3 2017].

LSTC, [Online]. Available: http://www.lstc.com/dynamat/. [Accessed 10 3 2017].

Luketa-Hanlin, A., and Hightower, H. (2008) 'On the evaluation of models for hazard prediction for liquefied natural gas (LNG) spills on water', Sandia National Laboratories.

Luperi, F. J., & Pinto, F. (2013). 'Determination of Impact Force History during Multicolumn Barge Flotilla Collisions against Bridge Piers', Journal of Bridge Engineering, 19(3), p. 04013011.

Manderbacka, T. and Ruponen, P. (2016) 'The impact of the inflow momentum on the transient roll response of a damaged ship', Ocean Engineering, 120, pp. 346–352.

Marchenko, N. A. et al. (2016) 'Maritime safety in the high north - Risk and preparedness', Proceedings of the International Offshore and Polar Engineering Conference, 2016, Janua, p. 880653.

Marinatos, J. N. and Samuelides, M. S. (2015) 'Towards a unified methodology for the simulation of rupture in collision and grounding of ships', Marine Structures. Elsevier Ltd, 42, pp. 1–32.

Mazaheri, A. (2017) A framework for evidence - based risk modeling of ship grounding. Aalto University.

Mazaheri, A., Montewka, J. and Kujala, P. (2014) 'Modeling the risk of ship grounding—a literature review from a risk management perspective', WMU Journal of Maritime Affairs, 13(2), pp. 269–297.

Minorsky, V. U. (1959) 'An Analysis of Ship Collisions with Reference to Protection of Nuclear Power Plants', Journal of Ship Research, pp. 1–4.

Moan, T. (2016) 'Damage tolerance requirements to structures', Proceeding of 3rd offshore structural reliability conference, Stavanger, p.14

Moan, T., Amdahl, J. and Ersdal, G. (2017) 'Assessment of ship impact risk to offshore structures - New NORSOK N-003 guidelines', Marine Structures.

Mocanu, C. I., Tocu, F., Dobrot, O. M., & Teodor, F. (2012), 'The impact behaviour of plane and curved composite material plates with or without reinforcements', in

12th International Multidisciplinary Scientific GeoConference: SGEM: Surveying Geology & mining Ecology Management, 3, pp. 245-252.
Moon, K. et al. (2009) 'Fire risk assessment of gas turbine propulsion system for LNG carriers', Journal of Loss Prevention in the Process Industries, 22(6), pp. 908–914.
Myland, D. and Ehlers, S. (2016) 'Influence of bow design on ice breaking resistance', Ocean Engineering, 119, pp. 217–232.
Naar, H. et al. (2002) 'Comparison of the crashworthiness of various bottom and side structures', Marine Structures, 15, pp. 443–460.
Nam, W., Amdahl, J., Hopperstad, O. S. (2016) 'Influence of brittle fracture on the crashworthiness of ship and offshore structures in arctic conditions', Proceedings of 7th International Conference Collision and Grounding of Ships and Offshore Structures, Ulsan, Korea.
Niklas, K. and Kozak, J. (2016) 'Experimental investigation of Steel-Concrete-Polymer composite barrier for the ship internal tank construction', Ocean Engineering, 111, pp. 449–460.
Nordström, J. et al. (2016) 'Vessel TRIAGE: A method for assessing and communicating the safety status of vessels in maritime distress situations', Safety Science, 85, pp. 117–129.
NORSOK (2007) 'Action and action effects', Standard N-003, Norway Sept. 2007.
NORSOK (2017) 'Action and action effects', Standard N-003, Norway Jan. 2017.
Notaro, G. et al. (2013) 'Evaluation of the fendering capabilities of the sps for an offshore application', in 6th International Conference on Collision and Grounding of Ships and Offshore Structures, ICCGS, pp. 85–92.
Novozhilov, V. (2001) 'Computational fluid dynamics modeling of compartment fires', Progress in Energy and Combustion Science, Vol. 27, pp. 611–666
Obisesan, A., Sriramula, S. and Harrigan, J. (2016) 'A framework for reliability assessment of ship hull damage under ship bow impact', Ships and Offshore Structures. Taylor & Francis, 11(7), pp. 700–719.
OCIMF (2013). Oil Companies International Marine Forum (OCIMF). Guidelines on Capabilities of Emergency Response Services. Available in http://www.intertanko.com/Global/admin_WeeklyNews/Guidelines%20on%20Capabilities%20of%20Emergency%20Response%20Services%20.pdf
Ohtsubo, H. and Wang, G. (1995) 'An upper-bound solution to the problem of plate tearing', Journal of Marine Science and Technology, 1(1), pp. 46–51.
Olewski, T. et al. (2011) 'Medium scale LNG-related experiments and CFD simulation of water curtain', Journal of Loss Prevention in the Process Industries, 24(6), pp. 798–804.
Ortiz, R., Deletombe, E. and Chuzel-Marmot, Y. (2015) 'Assessment of damage model and strain rate effects on the fragile stress/strain response of ice material', International Journal of Impact Engineering, 76, pp. 126–138.
Oterkus, E. et al. (2015) 'Fracture modes, damage tolerance and failure mitigation in marine composites', in Marine Applications of Advanced Fibre-Reinforced Composites, pp. 79–102.
Paboeuf, S. et al. (2016) 'Crashworthiness of an alternative construction within the scope of A.D.N. regulations using super-elements method', Proceedings of 7th International Conference Collision and Grounding of Ships and Offshore Structures, Ulsan, Korea.
Pack, K. and Mohr, D. (2017) Combined Necking & Fracture Model to Predict Ductile Failure with Shell Finite Elements, Engineering Fracture Mechanics.
Paik, J. K. et al. (2015) 'A new procedure for the nonlinear structural response analysis of offshore installations in fires'. Transactions - Society of Naval Architects and Marine Engineers. 121, pp. 224-250.
Park, D. K. et al. (2015a) 'Operability of non-ice class aged ships in the Arctic Ocean-part II: Accidental limit state approach', Ocean Engineering. Elsevier, 102, pp. 206–215.

Park, D. K. et al. (2015b) 'On the Crashworthiness of Steel-Plated Structures in an Arctic Environment: An Experimental and Numerical Study', Journal of Offshore Mechanics and Arctic Engineering, 137(5), p. 51501.
Pedersen, P. T. and Zhang, S. (2000) 'Effect of ship structure and size on grounding and collision damage distributions', Ocean Engineering, 27, pp. 1161–1179.
Pham, T. M. and Hao, H. (2017) 'Plastic hinges and inertia forces in RC beams under impact loads', International Journal of Impact Engineering, 103, pp. 1–11.
Pitblado, R. (2007) 'Potential for BLEVE associated with marine LNG vessel fires', Journal of Hazardous Materials, 140(3), pp. 527–534.
Pitblado, R. M. and Woodward, J. L. (2011) 'Highlights of LNG risk technology', Journal of Loss Prevention in the Process Industries, 24(6), pp. 827–836.
Prestileo, A. et al. (2013) 'Bottom damage scenarios for the hull girder structural assessment', Marine Structures, 33, pp. 33–55.
Rawson, C., Crake, K. and Brown, A. (1998) Assessing the Environmental Performance of Tankers in Accidental Grounding and Collision, SNAME Transactions.
Rhymer, J., Kim, H. and Roach, D. (2012) 'The damage resistance of quasi-isotropic carbon/epoxy composite tape laminates impacted by high velocity ice', Composites Part A: Applied Science and Manufacturing. Elsevier, 43(7), pp. 1134–1144.
Rizzuto, E., Teixeira, A. and Soares, C. G. (2010) 'Reliability assessment of a tanker in grounding conditions', 11th International Symposium on Practical Design of Ships and Other Floating Structures, PRADS 2010, 2, pp. 1446–1458.
Robb, D. M., Gaskin, S. J. and Marongiu, J.-C. (2016) 'SPH-DEM model for free-surface flows containing solids applied to river ice jams', Journal of Hydraulic Research, 54(1), pp. 27–40.
Rodd, J. L. (1996) 'Observations on conventional and advanced double hull grounding experiments', in Int. Conf. on Designs and Methodologies for Collision and Grounding Protection of Ships, pp. 11–13.
Rodd, J. L. and Sikora, J. P. (1995) 'Double Hull Grounding Experiments', in Proceedings of the Fifth (1995) International Offshore and Polar Engineering Conference. The Hague, pp. 446–456.
Rodrigues, J. M. and Guedes Soares, C. (2017) 'Still water vertical loads during transient flooding of a tanker in full load condition with a probabilistic damage distribution', Ocean Engineering, 129, pp. 480–494.
Samuelides, M. (2015) 'Recent advances and future trends in structural crashworthiness of ship structures subjected to impact loads', Ships and Offshore Structures. Taylor & Francis, 10(5), pp. 1–10.
Samuelides, M. et al. (2007) 'Simulation of the behaviour of double bottoms subjected to grounding actions', in 4th International Conference on Collision and Grounding of Ships. Hamburg, pp. 93–102.
Sergejeva, M., Laanearu, J. and Tabri, K. (2013) 'Hydraulic modelling of submerged oil spill including tanker hydrostatic overpressure', in Analysis and Design of Marine Structures - Proceedings of the 4th International Conference on Marine Structures, MARSTRUCT 2013.
Sergejeva, M., Laanearu, J. and Tabri, K. (2017) 'On parameterization of emulsification and heat exchange in the hydraulic modelling of oil spill from a damaged tanker in winter conditions', pp. 43–50.
Sha, Y. and Hao, H. (2013) 'Numerical Simulation of Barge Impact on a Continuous Girder Bridge and Bridge Damage Detection', International Journal of Protective Structures, 4(1), pp. 79–96.
Sha, Y. and Hao, H. (2014a) 'A Simplified Approach for Predicting Bridge Pier Responses Subjected to Barge Impact Loading', Advances in Structural Engineering, 17(1), pp. 11–23.

Sha, Y. and Hao, H. (2014b) 'Laboratory Tests and Numerical Simulations of CFRP Strengthened RC Pier Subjected to Barge Impact Load', International Journal of Structural Stability and Dynamics. World Scientific Publishing Co., 15(2), p. 1450037.
Sha, Y., Amdahl, J. (2017) 'Ship collision analysis of a floating bridge in ferry-free E39 project', OMAE 2017-62720 Proceedings of 36th International Conference on Ocean, Offshore and Arctic Engineering. Trondheim, Norway.
Shaw, A. et al. (2015) 'Beyond classical dynamic structural plasticity using mesh-free modelling techniques', International Journal of Impact Engineering, 75, pp. 268–278.
Shi, C. et al. (2016) 'A nonlinear viscoelastic iceberg material model and its numerical validation', Proceedings of the Institution of Mechanical Engineers, Part M: Journal of Engineering for the Maritime Environment. SAGE Publications, 231(2), pp. 675–689.
Shi, C. et al. (2017) 'Validation of a temperature-gradient-dependent elastic-plastic material model of ice with finite element simulations', Cold Regions Science and Technology, 133, pp. 15–25.
Shim, C. et al. (2016) 'A study on materials used in LNGC cargo containment system', Proceedings of 7th International Conference Collision and Grounding of Ships and Offshore Structures, Ulsan, Korea.
Silva, F. and Raquel. S (2015), 'Analysis of Maritime Fire and Explosion Accidents', Universidade de Lisboa, Instituto Superior Técnico, Portugal.
Simonsen, B. C. (1997) 'Ship grounding on rock - I. Theory', Marine Structures, 10, pp. 519–562.
Simonsen, B. C. et al. (2009) 'A simplified grounding damage prediction method and its application in modern damage stability requirements', Marine Structures, 22, pp. 62–83.
Simonsen, B. C., & Ocakli, H. (1999). Experiments and theory on deck and girder crushing. Thin-walled structures, 34(3), 195-216.
Sirkar, J. et al. (1997) A Framework for Assessing the Environmental Performance of Tankers in Accidental Groundings and Collisions, SNAME Transactions.
SMHI (2012) 'SMHI. (2012). Manual Seatrack Web — a user-friendly system for forecasts and backtracking of drift and spreading of oil, chemicals and substances in water. https://stw-helcom.smhi.se/.', p. 2012.
Song M., Kim E., Amdahl J., Ma J. & Huang Y. (2016) 'A comparative analysis of the fluid-structure interaction method and the constant added mass method for ice-structure collisions', Marine Structures, 49, pp. 58–75.
Sormunen, O. V. E. et al. (2016a) 'Marine traffic, accidents, and underreporting in the Baltic Sea', Scientific Journals of the Maritime University of Szczecin, 46(118), pp. 163–177.
Sormunen, O. V. E. et al. (2016b) 'Comparing rock shape models in grounding damage modelling', Marine Structures, 50, pp. 205–223.
Srivastava, V. and Srivastava, R. (2014) 'On the polymeric foams: modeling and properties', Journal of Materials Science, 49(7), pp. 2681–2692.
Storheim, M. and Amdahl, J. (2017) 'On the sensitivity to work hardening and strain-rate effects in nonlinear FEM analysis of ship collisions', Ships and Offshore Structures. Taylor & Francis, 12(1), pp. 100–115.
Storheim, M. et al. (2015) 'A damage-based failure model for coarsely meshed shell structures', International Journal of Impact Engineering, 83, pp. 59–75.
Storheim, M., Amdahl, J. and Martens, I. (2015) 'On the accuracy of fracture estimation in collision analysis of ship and offshore structures', Marine Structures. Elsevier Ltd, 44, pp. 254–287.
Su, S., & Wang, L. (2013) 'Three dimensional reconstruction of the fire in a ship engine room with multilayer structures', Ocean Engineering, 70, pp. 201–207.
Sun, B., Guo, K., & Pareek, V. K. (2015) 'Dynamic simulation of hazard analysis of radiations from LNG pool fire', Journal of Loss Prevention in the Process Industries, 35, pp. 200–210.

Sun, B., Guo, K., & Pareek, V. K. (2017) 'Hazardous consequence dynamic simulation of LNG spill on water for ship-to-ship bunkering', Process Safety and Environmental Protection, 107, pp. 402–413.
Sun, B., Hu, Z. and Wang, G. (2015) 'An analytical method for predicting the ship side structure response in raked bow collisions', Marine Structures, 41, pp. 288–311.
Sun, B., Hu, Z. and Wang, J. (2017) 'Bottom structural response prediction for ship-powered grounding over rock-type seabed obstructions', Marine Structures, 54, pp. 127–143.
Suominen, M. et al. (2017) 'Influence of load length on short-term ice load statistics in full-scale', Marine Structures, 52, pp. 153–172.
Szlapczynski, R. and Szlapczynska, J. (2016) 'An analysis of domain-based ship collision risk parameters', Ocean Engineering, 126, pp. 47–56.
Tabri, K. et al. (2015) 'Modelling of structural damage and environmental consequences of tanker grounding', in Analysis and Design of Marine Structures - Proceedings of the 5th International Conference on Marine Structures V, pp. 703-710.
Tang, M. J. & Baker, Q. A. (1999), 'A new set of blast curves from vapor cloud explosion', Process Safety Progress, 18, pp. 235-240.
Tavakoli, M. T., Amdahl, J. and Leira, B. J. (2011) 'Experimental investigation of oil leakage from damaged ships due to collision and grounding', Ocean Engineering. Elsevier, 38(17–18), pp. 1894–1907.
Tiberkak, R. et al. (2008) 'Damage prediction in composite plates subjected to low velocity impact', Composite Structures, 83(1), pp. 73–82.
Travanca, J. and Hao, H. (2015) 'Energy dissipation in high-energy ship-offshore jacket platform collisions', Marine Structures, 40, pp. 1–37.
Truong, D. D. et al. (2016) 'Plastic response of steel grillages subjected to repeated mass impacts', Proceedings of 7th International Conference Collision and Grounding of Ships and Offshore Structures, Ulsan, Korea.
USFOS (2013) 'User's manual for USFOS', version 86a, USFOS A/S, Sandsli, Norway.
Vairo, T. et al. (2015), 'An Approach to Risk Evaluation in Connection with Fire Scenarios from a Cruise Ship', Chemical Engineering Transactions, 43, pp. 1939-1944.
Vaughan, H. (1977) Vaughan H. Damage to ships due to collision and grounding. DnV Technical Report No. 77-345. Oslo.
Vettor, R. and Soares, C. G. (2015) 'Computational System for Planning Search and Rescue Operations at Sea', Procedia Computer Science, 51, pp. 2848–2853.
Vílchez, J. A. et al. (2011) 'Generic event trees and probabilities for the release of different types of hazardous materials', Journal of Loss Prevention in the Process Industries. 24(3), pp. 281–287.
Vinnem, J. E., Utne, I. B. and Schjølberg, I. (2015) 'On the need for online decision support in FPSO-shuttle tanker collision risk reduction', Ocean Engineering, 101, pp. 109–117.
von Bock und Polach, R. and Ehlers, S. (2014, June). On the Scalability of Model-Scale Ice Experiments. In ASME 2014 33rd International Conference on Ocean, Offshore and Arctic Engineering (pp. V010T07A010-V010T07A010). American Society of Mechanical Engineers.
Vredeveldt, A.W & Wevers, L, T. (1995) 'Full scale grounding experiments', in Conference on Prediction Methodology of Tanker Structural Failure &: Consequential Oil Spill. Tokyo.
Walters, C. L. (2014) 'Framework for adjusting for both stress triaxiality and mesh size effect for failure of metals in shell structures', International Journal of Crashworthiness, 19(1), pp. 1–12.
Walters, R. A. et al. (2017) 'Characterization of multi-barge flotilla impact forces on wall structures', Marine Structures, 51, pp. 21–39.

Wang, G. (1995) 'Structural analysis of ships' collision and grounding', Ph.D. dissertation, Department of Naval Architecture and Ocean Engineering, University of Tokyo.
Wang, G., Arita, K. and Liu, D. (2000) 'Behaviour of a double hull in a variety of stranding or collision scenarios', Marine Structures, 13, pp. 147–187.
Wang, G., Ohtsubo, H. and Liu, D. (1997) 'A Simple Method for Predicting the Grounding Strength of Ships', 41(3), pp. 241–247.
Wang, J. and Wang, W. (2015) 'Estimation of Vessel-Bridge Collision Probability for Complex Navigation Channels', Journal of Bridge Engineering, 20(7), p. 4014091.
Wang, W., Chen, J. J. and Wang, J. H. (2017) 'Estimation method for ground deformation of granular soils caused by dynamic compaction', Soil Dynamics and Earthquake Engineering, 92, pp. 266–278.
Wang, Z. et al. (2016) 'Experimental and numerical investigations on the T joint of jack-up platform laterally punched by a knife edge indenter', Ocean Engineering, 127, pp. 212–225.
Woodward, J. L., Pitblado, R. M. (2010) 'LNG risk-based safety; modeling and consequence analysis', John Wiley and Sons, Inc.
Xia, Y., Zhu, J. and Zhou, Q. (2015) 'Verification of a multiple-machine program for material testing from quasi-static to high strain-rate', International Journal of Impact Engineering, 86, pp. 284–294.
Xiao, F. et al. (2015) 'Experimental and numerical investigation on the shock resistance of honeycomb rubber coatings subjected to underwater explosion', Proceedings of the Institution of Mechanical Engineers, Part M: Journal of Engineering for the Maritime Environment, 229(1), pp. 77–94.
Yoshikawa, T. et al. (2016) 'Fracture analysis considering the effect of stress tri-axiality', Proceedings of 7th International Conference Collision and Grounding of Ships and Offshore Structures, Ulsan, Korea.
You, Y. and Rhee, K. (2016) 'Development of the collision ratio to infer the time at which to begin a collision avoidance of a ship', Applied Ocean Research, 60, pp. 164–175.
Youssef, S. A. M. et al. (2016) 'Assessing the risk of ship hull collapse due to collision', Ships and Offshore Structures. Taylor & Francis, 11(4), pp. 335–350.
Yu, Z. and Amdahl, J. (2016a) 'Full six degrees of freedom coupled dynamic simulation of ship collision and grounding accidents', Marine Structures, 47, pp. 1–22.
Yu, Z. and Amdahl, J. (2016b) 'Influence of 6DOF ship motions in the damage prediction of ship collision and grounding accidents', 7th International Conference on Collision and Grounding of Ships and Offshore StructuresShips and Offshore Structures, (2010), pp. 199–205.
Yu, Z. et al. (2016) 'Implementation of Linear Potential-Flow Theory in the 6DOF Coupled Simulation of Ship Collision and Grounding Accidents', Journal of Ship Research, 60(3).
Yu, Z., Hu, Z. and Wang, G. (2015) 'Plastic mechanism analysis of structural performances for stiffeners on bottom longitudinal web girders during a shoal grounding accident', Marine Structures. Elsevier Ltd, 40, pp. 134–158.
Zhang, J. et al. (2015) 'A distributed anti-collision decision support formulation in multi-ship encounter situations under COLREGs', Ocean Engineering, 105, pp. 336–348.
Zhang, J. et al. (2016) 'A theoretical study of low-velocity impact of geometrically asymmetric sandwich beams', International Journal of Impact Engineering, 96, pp. 35–49.
Zhang, M. and Liu, J. X. (2017) 'Experimental and numerical analysis of tanker double-hull structures punched by a wedge indenter', (2009), pp. 549–556.
Zhang, S. (2002) 'Plate tearing and bottom damage in ship grounding', Marine Structures, 15, pp. 101–117.
Zhang, S. and Pedersen, P. T. (2016) 'A method for ship collision damage and energy absorption analysis and its validation', Ships and Offshore Structures. Taylor & Francis, 5302(May), pp. 1–10.

Zhang, S. et al. (2017) 'Impact mechanics of ship collisions and validations with experimental results', Marine Structures, 52, pp. 69–81.
Zhang, S., Pedersen, P. T. and Ocakli, H. (2015) 'Collisions damage assessment of ships and jack-up rigs', Ships and Offshore Structures. Taylor & Francis, 10(5), pp. 1–9.
Zhang, W. et al. (2016) 'A method for detecting possible near-miss ship collision from AIS data', Ocean Engineering, 107, pp. 60–69.
Zhang, W., Jin, X. and Wang, J. (2014) 'Numerical analysis of ship–bridge collision's influences on the running safety of moving rail train', Ships and Offshore Structures. Taylor & Francis, 9(5), pp. 498–513.
Zhou, Q., Peng, H. and Qiu, W. (2016) 'Numerical investigations of ship-ice interaction and maneuvering performance in level ice', Cold Regions Science and Technology, 122, pp. 36–49.

ANNEX

As described in Chapter 4, LS_DYNA provides several material models for composite structure modelling. Out of the complete set, the following material models are provided in the following tables with additional notes on their use.

Table A-1 Composite material model in LS_DYNA

	Material keywords	**Additional notes**
22	*MAT_COMPOSITE_DAMAGE	An orthotropic material with optional brittle failure for composites can be defined. Lamination theory is supported.
32	*MAT_LAMINATED_GLASS	A layered glass including polymeric layers can be modeled.
54/55	*MAT_ENHANCED_COMPOSITE_DAMAGE	Enhanced versions of the composite model material type 22. Arbitrary orthotropic materials can be defined.
58	*MAT_LAMINATED_COMPOSITE_FABRIC	This model may be used to model composite materials with unidirectional layers, complete laminates, and woven fabrics. Only for shell elements.
59	*MAT_COMPOSITE_FAILURE_OPTION_MODEL	For shell, solid and SPH.
114	*MAT_LAYERED_LINEAR_PLASTICITY	This model defined a layered elastoplastic material with an arbitrary stress versus strain curve and an arbitrary strain rate dependency.
116	*MAT_COMPOSITE_LAYUP	For the modelling of elastic responses of composite layups that have an arbitrary number of layers through the shell thickness. No stresses calculated. This model does not use laminated shell theory, which is not good for foam core/sandwich composites.
117/118	*MAT_COMPOSITE_MATRIX/DIRECT	This material is used for modeling the elastic responses of composites. No stresses calculated.
158	*MAT_RATE_SENSITIVE_COMPOSITE_FABRIC	Like 58 but with rate effects via viscoelastic stress term.

161/ 162	*MAT_COMPOSITE_MSC	Used to model the progressive failure analysis for composite materials consisting of unidirectional and woven fabric layers. Only for solid elements. Suitable for delamination studies.
219	*MAT_CODAM2	This model is a sub-laminate-based continuum damage mechanics model for fiber reinforced composite laminates made up of transversely isotropic layers.
221	*MAT_ORTHOTROPIC_SIMPLIFIED_DAMAGE	An orthotropic material with optional simplified damage and optional failure for composites. Only for 3D solid elements.
235	*MAT_MICROMECHANICS_DRY_FABRIC	The material model derivation utilizes the micro-mechanical approach and the homogenization technique. Accounting for reorientation of the yarns and fabric architecture.
249	*MAT_REINFORCED_THERMOPLASTIC	A reinforced thermoplastic composite material.
261/ 262	*MAT_LAMINATED_FRACTURE_DAIMLER_PINHO/ CAMANHO	Orthotropic continuum damage models for laminated fiber-reinforced composites. For shell, thick shell and solid elements.

Table A-2 Foam models in LS_DYNA

	Material keywords	**Additional note**
57	Mat Low Density Foam	An example can be found in (d3view, 2006)
61	MAT_KELVIN-MAXWELL_VISCOELASTIC	This material is a classical Kelvin-Maxwell model for modeling viscoelastic bodies, e.g., foams. This model is valid for solid elements only
62	*MAT_VISCOUS_FOAM	It is only valid for solid elements, mainly under compressive loading.
63	Mat Crushable Foam	
75	MAT_BILKHU/DUBOIS_FOAM	This model is for the simulation of isotropic crushable foams. Uniaxial and triaxial test data have to be used. For the elastic response, the Poisson ratio is set to zero.
83	Mat Fu Chang	
126	MAT_MODIFIED_HONEYCOMB	try ELFORM = 0 to avoid negative volume elements (d3view, 2006)
142	*MAT_TRANSVERSELY_ANISOTROPIC_CRUSHABLE_FOAM	This model is for an extruded foam material that is transversely anisotropic, crushable, and of low density with no significant Poisson effect. This material is used in energy-absorbing structures to enhance automotive safety in low velocity (bumper impact) and medium high velocity (interior head impact and pedestrian safety) applications.

144	*MAT_PITZER_CRUSHABLE_ FOAM	This model is for the simulation of isotropic crushable forms with strain rate effects. Uniaxial and triaxial test data have to be used. For the elastic response, the Poisson ratio is set to zero.
163	*MAT MODIFIED CRUSHABLE FOAM	

Proceedings of the 20th International Ship and Offshore Structures Congress (ISSC 2018) Volume II – M.L. Kaminski and P. Rigo (Eds.)

doi:10.3233/978-1-61499-864-8-73

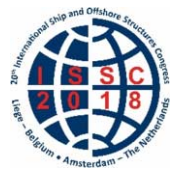

COMMITTEE V.2

EXPERIMENTAL METHODS

COMMITTEE MANDATE

Concern for advances in structural model testing and full-scale experimentation and in-service monitoring and their role in the design, construction, inspection and maintenance of ship and offshore structures. This shall include new developments in:
1. Best practice and uncertainty analysis
2. Experimental techniques;
3. Full field imaging and sensor systems;
4. Big data applications for ship and offshore structures
5. Correlation between model, full-scale and numerical datasets

AUTHORS/COMMITTEE MEMBERS

Chairman: D. Dessi, *Italy*
F. Brennan, *UK*
M. Hoogeland, *The Netherlands*
XB. Li, *China*
C. Michailides, *Cyprus*
D. Pearson, *Canada*
J. Romanoff, *Finland*
XH. Shi, *China*
T. Sugimura, *Japan*
G. Wang, *USA*

KEYWORDS

Experimentation, Structural Testing, Laboratory Testing, Small and Large scale, Full-scale Test, Similarity Laws, Correlation, Big-Data, Sensors.

CONTENTS

1. INTRODUCTION 76

2. ACRONYMS & ABBREVIATIONS 76

3. LABORATORY EXPERIMENTATION 77
3.1 Scaled and small size 77
3.1.1 Ultimate strength 77
3.1.2 Fatigue 78
3.1.3 Cracking and fracture 79
3.1.4 Corrosion 83
3.1.5 Friction 83
3.2 Large scale experiment 84
3.2.1 Ultimate strength 84
3.2.2 Large scale fatigue testing 85
3.3 Impact & impulsive loading and response assessment 86
3.3.1 Ship Collisions and Grounding 86
3.3.2 Underwater explosion 89
3.3.3 Vibration 90
3.4 Fluid-structure interaction 92
3.4.1 Hydroelastic scaled tests 92
3.4.2 Slamming and water impact tests 94

4. FULL SCALE TESTS 95
4.1 Ships and offshore structures 95
4.1.1 Monitoring of loads and responses 95
4.1.2 Structural identification 97
4.2 Application of experimentation, inspection and monitoring 99
4.2.1 Design 99
4.2.2 Construction 99
4.2.3 Operation, Inspection, Monitoring and Maintenance 100

5. CORRELATION ISSUES BETWEEN SCALED (PHYSICAL) MODELS, FULL-SCALE STRUCTURES (SHIP AND OFFSHORE) AND NUMERICAL SIMULATIONS 101
5.1 Scaling laws 101
5.2 Model to full-scale investigation 102
5.3 Integration of experiments and numerical simulations 103

6. BEST PRACTICE AND GUIDELINES 105
6.1 Data uncertainty 105
6.2 Design of experiments 106
6.3 Quality standards 107

7. CONTEMPORARY AND EMERGING TECHNIQUES 107
7.1 Overview of current techniques 108
7.1.1 Displacement measurement 108
7.1.2 Strain/stress measurement 108
7.1.3 Force measurement 110
7.1.4 Pressure measurement 110
7.1.5 Acceleration measurement 111
7.1.6 Multi-variable measurements 111
7.2 Novel measurement Techniques 112

7.2.1 MEMS 112
7.2.2 WSN 115
7.2.3 Energy Harvesting Devices 118
7.3 Big-data analysis 119
7.3.1 Values of Big Data as a Technology 119
7.3.2 Recent Activities in the Maritime Industry 120
7.3.3 Status of Maritime Application of Big Data 121
7.3.4 Future Potentials of R&D 122
7.3.5 Conclusions 122

8. CONCLUSIONS AND RECOMMENDATIONS FOR FUTURE WORK 122

REFERENCES 123

1. INTRODUCTION

Experimental research has a long tradition in naval architecture and marine engineering, as the early establishment of the International Towing Tank Conference (ITTC) gives evidence. Due to its focus on hydrodynamics, structure-related experimentation has received little or no attention within ITTC. Until the present ISSC, experimental investigations have been considered by different committees depending on their specific mandate. Thus, for the first time in the history of ISSC activity, a committee has been established to perform a systematic review of experimental methods focusing on their use in the structural design and operation of ships and offshore structures.

The need to delimit the vast field of experimental methods was clear from the beginning of the committee's work. The following criteria have been initially set to select the topics: (i) specific consideration of experimental methods concerning structural testing, or aimed to improve the reliability of structural design in a broader sense; (ii) priority to experimental topics related to Technical Committees; (iii) available expertise among the committee members.

The report can be divided into two parts; the first is dedicated to a general review of methods and techniques, further sorted based on the distinction between laboratory experimentation (Section 3) and full-scale tests (Section 4); the second is focused on some cross-cutting themes, as detailed in the following. The fundamental issue of the correlation and synergic use of model-scale, full-scale and numerical data is considered in Section 5, also accounting for approaches in structural scaling. Best practice and guidelines, involving uncertainty analysis, optimal test design and quality standards, are reviewed in Sections 6. Finally, Section 7 is dedicated to the review of contemporary and emerging techniques, with a special attention to the Big Data problem and its implications in ocean engineering.

2. ACRONYMS & ABBREVIATIONS

Some general acronyms and abbreviations frequently used in the report:

ABS	American Bureau of Shipping
AE	Acoustic Emission
API	American Petroleum Institute
ASME	American Society of Mechanical Engineers
ASTM	American Society for Testing Materials
BV	Bureau Veritas
BS	The British Standard Institution
CCS	China Classification Society
Class NK	Nippon Kaiji Kyokai (Japanese Classification Society)
CFD	Computer Fluid Dynamics
DIC	Digital Image Correlation
DNV	Det Norske Veritas
DNV-GL	Det Norske Veritas - Germanischer Lloyd
FBG	Fiber Bragg Grating
FDS	Fatigue Damage Sensor
FE(A)	Finite Element (Analysis)
FSI	Fluid Structure Interaction
IEC	International Electrochimical Commission
IEEE	Institute of Electrical and Electronics Engineers
IMO	International Maritime Organization
IMU	Inertial Motion Unit
ISA	International Society of Automation
ISO	International Organization for Standardization
ITTC	International Towing Tank Conference

LR	Lloyd's Register
MEMS	Micro-Electro Mechanical Systems
RBI	Risk Based Inspection
RMS	Root Mean Square
SHM	Structural Health Monitoring
UKAS	United Kingdom Accreditation Services
WES	The Japan Welding Society
WSN	Wireless Sensor Network

3. LABORATORY EXPERIMENTATION

With respect to laboratory tests, one can make a rough distinction between tests to determine fundamental mechanical properties and the dynamic structural response in dry or wet conditions. Fundamental mechanical properties include; strength/stiffness (ultimate strength, fracture and blast for example), resistance to deterioration mechanisms (fatigue, corrosion, and wear) and other properties such as friction and damping. Structural dynamic responses in dry conditions refer to vibration / noise, grounding and collision. Examples of dynamic response to wet conditions, involve fluid-structure interaction (underwater explosion, slamming, etc.).

Experimental methods used to determine mechanical properties are linked with laboratory scale tests of materials and small components (Section 3.1). Information concerning the material or components can generally be acquired at relatively low cost and short lead time. Either for novel solutions or for verification of analysis methods, laboratory-scale tests can provide useful information. Large scale experiments (Section 3.2) utilize full-scale structures to determine proof loading and handling qualities. In this case, complete structures, sometimes scaled, or full-scale sections are exposed to experimental validation. Some response tests require the load development and loading process to be accounted for. The setup complexity of these response tests involves reproducing the interaction (*e.g.*, solid/solid as in collision and grounding) or the excitation (underwater explosion) (Section 3.3), as well as consistent scaling (hydroelastically scaled tests in water and ice) (Section 3.4).

3.1 Scaled and small size

3.1.1 Ultimate strength

For steel in particular and metals in general, ultimate strength at the coupon scale level is related to fracture. This section is concerned about fracture when no pre-existing notch or fatigue crack is assumed. Within this group, the stress intensities and levels of stress triaxiality are relatively modest, and the material typically fails in a ductile way. This group is best characterized by strains. Collision and grounding are some key examples. Historically, tensile tests have been used for deriving the strain limits; forming large databases of test data as the one provided by Paik *et al.* (2017) for metallic materials at different temperatures and strain rates.

As multi-axiality has a large influence on the strain criteria, including multi-axiality in the test set-up is a challenge. For this purpose, tests devised in the metal forming industry can be used. Banabic (2000) provides a good summary of experiments developed for the sheet metal industry; focusing on methods that involve deforming the material out of plane until it fails by membrane stretching. Hoogeland and Vredeveldt (2017) recently performed similar tests in dynamic conditions on full-thickness steel plates similar to those used in the maritime and offshore industries. Mohr and Marcadet (2015) provide a small series of tests intended for sheet metal application that may be scalable to plates. These experiments feature specimens that have different cutouts and are pulled in either tension or combined tension/shear. Although the techniques of Banabic (2000) and Mohr and Marcadet (2015) have indicated that multiple specimens are needed to obtain full multi-axiality, Voormeeren *et al.* (2014) provides theoretical evidence that only one specimen may be necessary under certain conditions. Haag *et al.* (2017)

give an example of a structural surrogate test with a drop experiment that simulates raking a pinnacle or iceberg.

3.1.2 Fatigue

Understanding of the fatigue phenomenon has been advanced through data accumulation during cyclic testing. S-N curves are used for the fatigue life evaluation by the Minor damage accumulation approach and are fundamentally obtained by cyclic testing until material failure. Regarding welded-structure such as ship and offshore structures, two sets of limit S-N curves are used. In the first set, joints are classified and grouped according to their geometry. The second set consists of S-N curves for straight material, either base, welded and/or exposed to corrosive environments, and the actual fatigue driving stresses are derived from stress concentration factors. The undisturbed, far field stress is the basis of the stress cycles ("S"). The S-N curves for fatigue design are provided, for instance, by Class society guidelines such as DNV-GL guideline (2015). Fatigue testing in sea water is mainly carried out in a corrosive atmosphere to capture the environmental effects. "Dry" fatigue testing can be done at frequencies up to 70 Hz and "wet" fatigue testing shall be limited to about 1 Hz to allow corrosion products to develop inside the crack. Fatigue tests are also particularly important to evaluate the effect of material coatings on fatigue performance.

Test specimen / Thickness effect

The welded joint specimen is of special interest for the fatigue performance of ship and offshore structures. There is no clear standard defining the size of the fatigue test specimen of welded joints. Usually, specimens representing hull structural details are of the same thickness and welded condition. Base material testing has led to a clear understanding of the thickness effect: increase in plate thickness causes a decrease in fatigue strength. For this reason, a correction coefficient is proposed by Class guidelines, *e.g.*, DNV-GL guideline (2015) and ABS guideline for offshore structures (2014). Yamamoto *et al.* (2012) investigated the dominating factors of the thickness effect considering different structural joint types or different loading patterns by fundamental experiment and FEA. It is confirmed that the thickness effect on fatigue strength is dominated by the stress concentration and the stress gradient at the weld toe that changes according to the shape of the joint. Moreover, the effect is clearly apparent for a variation of primary plate thickness when the thickness of the attached plate is proportionally increased, while the thickness variation effect is less obvious when the thickness of the attached plate is kept constant.

Load history / Variable loading

The fatigue life of ship and offshore structures is generally estimated by using S-N curves with constant amplitude loading. The fatigue crack propagation behavior, however, is especially influenced by variable loading related to the acceleration and delay phenomenon of a fatigue crack (a result of to over- and underload). This means that the experiment shall apply a variable load and record the crack growth simultaneously. The crack growth can be measured in several ways. Maljaars *et al.* (2015) describe the use of special crack gauges consisting of many equally spaced wires. The advancement of the crack is determined by the number of broken wires. Potential drop (either Alternating Current or Direct Current) allows the operator to measure the position of the crack front.

Fatigue test machine

Fatigue testing is usually carried out under tensile or bending loading conditions to get S-N curves. Many fatigue tests are suited for welded joints in ship and offshore structures. Alternatively, S-N curve development of exotic-materials may be acquired by the rotating bending fatigue test. As ISSC2015 III.2 (2015) indicates, many fatigue tests under multiaxial loading have been recently carried out. Moreover, Osawa *et al.* (2013) developed a low-cost fatigue test machine which allows for imposing variable loads according to given time-histories. Fatigue strength of out-of-plane gusset welded joints subject to springing and whipping superimposed

loads is examined by using Plate-Bending-Vibration type fatigue testing machines. The wave load is applied by using motors with eccentric mass. Springing vibration is superimposed by attaching an additional vibrator to the test specimen, and whipping vibration is superimposed by an intermittent hammering.

Measurement techniques for fatigue damage

There are some measurement techniques used to experimentally estimate the fatigue life. Acoustic emission (AE) is a method to record the fatigue crack growth characteristics of structural steel and welded connections. AE is the phenomena in which transient elastic waves are generated by the rapid release of energy from localized sources within a material as it undergoes deformation. Barsoum *et al.* (2009) showed AE graphs of cumulative absolute energy versus fatigue cycles capable of capturing the fatigue process. These characteristic curves track the fatigue crack growth with respect to time and can be used to see the severity of the AE activity associated with the crack growth process. Aggelis *et al.* (2011) investigated the AE behaviour of aluminium with V-notch and showed that certain characteristics undergo clearly measurable changes much earlier than final fatigue fracture. Additionally, this work demonstrated that the crack growth rate can be effectively monitored by using lock-in thermography under cyclic loading. The results obtained using this method were in agreement with the conventional compliance method. Kobayashi *et al.* (2016) developed the fatigue damage sensor with a notched test piece. Characteristics of Fatigue Damage Sensors (FDS) that are in use for fatigue life estimation of monitoring structural welding members in ship structures are discussed to improve the prediction accuracy of estimated fatigue life exposed to random wave loads such as storms under various loading conditions. Akai *et al.* (2015) developed dissipated energy measurement to estimate the crack initiation point. Fatigue limit estimation based on dissipated energy has been getting considerable attention. In this method, temperature change due to irreversible energy dissipation is measured by infrared thermography for various levels of stress amplitude. The dissipated energy measurement was also used to estimate the crack initiation point.

3.1.3 Cracking and fracture

In Section 3.1.1, the fracture of specimens without pre-existing notch or fatigue crack was discussed. This section is concerned with conditions in which a notch or fatigue crack is present at the onset of material failure. In this group, the notch or fatigue pre-crack increases the stress intensity and localized levels of stress triaxiality. This makes the failure mode much more localized. While the high local stress triaxialities can facilitate brittle fracture due to cleavage, this type of testing is also frequently done to determine ductile failure. It is assumed here that a fatigue crack or small welding/production defects can exist prior to the onset of fracture. Several basic material characteristics may be measured in this case, which are outlined below:

- Crack initiation: extension of a pre-existing notch or fatigue crack,
- Ductile tearing: continued stable extension of a crack once it has already initiated from a pre-existing notch of fatigue crack,
- Ductile crack arrestability: ability of a material to arrest a crack once it has started to propagate in an unstable, ductile failure mode,
- Brittle crack arrestability: ability of a material to arrest a crack once it has started to propagate in an unstable brittle failure mode, and
- Measuring the temperature at which the ductile to brittle transition temperature occurs.

The last parameter has many different forms, one common form is the temperature at which a J-integral test produces a critical stress intensity factor (K_{Jc}) equal to 100 MPa$\sqrt{m}$ when adjusted to an equivalent 25 mm thickness under quasi-static conditions.

Most testing methods fall into one or more of the above categories. The tests used to measure the main material characteristics fall into two major categories. The first category is quality control; summarized in Table 1. Quality control tests are generally designed to be extremely

low cost so that they can be performed routinely. Their main result is intended to give a qualitative idea of the safety of the material. The second category of tests are primarily designed to measure material characteristics used for quantitative analyses such as; structural design (container ship hatch coaming) or material development (high ductility high yield strength steels).

Charpy V notch testing is a quality control test that is intended to check whether or not the material fails in a brittle way at a given temperature. This test captures information about crack initiation, ductile tearing, and crack arrest. Because all the information is mixed together into a single measured value (the total impact energy), it can be difficult to extract the data on any one of the parameters specifically. However, many other uses have been found for Charpy tests, including the use of empirical correlations to estimate the fracture toughness in ductile, brittle, and transition conditions, depending on the failure mode the test featured. The Charpy V test has also been used to estimate the ductile to brittle transition temperature. These empirical relationships are outlined in BS 7910:2013+A1 (2015).

Instrumented Charpy V testing can be seen as a separate test from the standard "dumb" Charpy V testing. Instrumented Charpy V testing records the force time history of the impact. Together with the parameters of the test setup, the force time history can be translated to a force versus displacement signal. This method is standardized in ISO 14556:2015 (2015). Good results have been found correlating aspects of force versus displacement curves from instrumented Charpy V tests to various aspects of fracture initiation, tearing, propagation, and arrest. For example, Wallin *et al.* (2016) (amongst others) has shown that there is good correlation between the stress intensity of brittle crack arrest and T4kN, which can be measured from an instrumented Charpy V test.

Unlike Charpy-V testing (with or without instrumentation), most tests are designed to test one specific material parameter. There is a class of tests that are designed to measure the crack initiation of a material. These experiments are more sophisticated (and expensive) than Charpy V testing; however, they also produce values that can be used in design. Linear-elastic fracture toughness can be measured by the K_{Ic} of the material. This is standardized in ASTM E399, among other standards. However, most metallic materials are tough enough that satisfactory conditions for K_{Ic} testing is generally not possible. For those materials, elastic-plastic fracture parameters such as CTOD (Crack Tip Opening Displacement) or *J*-integral testing is recommended. Some standards that describe the measurement of CTOD or *J*-integral is, amongst others, ISO 12135 (2016). In most standards, the typical way of measuring CTOD or *J*-integral has been through either Single Edge Notched Bending (SENB) or Compact Tension (CT) tests. It has been shown that Single Edge Notched Tension (SENT) tests have a state of stress at the crack tip that is more representative of structures in which the primary stress is tension, especially in girth welds of pipes. SENT tests can be less conservative than the typically bending-dominated SENB and CT tests. Therefore, there has been a lot of effort to standardize a SENT test (Crintea and Moore, 2016; Moore and Hutchison, 2016; Hutchison *et al.*, 2015; Sarzosa *et al.*, 2015; Xue *et al.*, 2009), which has come to fruition in BS 8571:2014.

Some other developments in crack initiation testing, include; the reduction of cost of testing, transferring results between specimen geometries, and non-destructive fracture testing. For example, Walters and Van der Weijde (2013) proposed a method to reduce the cost of standard CTOD testing for steels that are at brittle or lower transitional temperatures. Coppejans and Walters (2017) have proposed a method of using damage mechanics to transfer results from a single ductile CTOD test to other specimen sizes. Finally, it is currently being investigated whether or not very small specimens (0.5 mm thick by 8 mm in diameter, which can presumably be sampled non-destructively from large structures) can be used to estimate brittle CTOD values (Walters *et al.*, 2017).

For ductile materials, the resistance to tearing increases after failure initiation. Therefore, taking only the "critical" fracture toughness of a ductile material is considered to be conservative. For

less conservative analyses, the benefit of the increased resistance to tearing is taken into account. The measurement of resistance curves (ASTM E1820 and BS 7448) requires the knowledge of the crack length at any given point in the force versus deflection curve, by multiple or single specimens. The study by Pussegoda *et al.* (2013) compared a multi specimen SENT (Single Edge Notched Tension) technique for finding resistance curves with a single-specimen technique.

In some situations, a ductile crack can arise and propagate for long distances. For instance, in the case of on-shore an off-shore pipelines, there is a lot of energy stored in the compressed gas and the propagating crack can advance faster than the gas decompression wave. In those situations, it is important to measure the ductile crack arrestability of the material. This is typically done with the Drop Weight Tear Test (DWTT) (ASTM E436). Hara and Fujishiro (2010) have correlated the Drop Weight Tear Test and Charpy V with full scale burst test.

Brittle crack arrest is another concern. Several tests are known to address the brittle crack arrest properties of steel. They share that a crack shall be initiated in colder and/or embrittled material which needs to halt at a certain point in the material and conditions of interest.

Table 1 Overview of fracture tests

Name of test	Typical specimen size	Remarks/ reference
Charpy V	10x10x55 mm	ISO 148, ASTM E23 (amongst others)
Instrumented Charpy V	10x10x55 mm	ISO 14556:2015
CTOD, *J*-integral	Full-thickness, proportional	ASTM E1820, BS 7448, ISO 12135
Drop weight tear test	250x77 mm by full thickness	ASTM E436
Pellini (Nil Ductility Transition Temperature)	Three sizes, not exceeding 100x100 mm	Puzak and Babecki, (1959), ASTM E208 (2012)
Double tension test	Not clear from reference, could be up to 1000 mm wide	WES 2815:2014
ESSO test	Large specimens, 1000 m wide and total 7 m long	WES 2815:2014
Transition temperature	Variable	ASTM E1921

Arrestability is an especially important parameter for the high yield, large thickness steel in hatch coamings of container ships. ESSO and Double-tension tests (WES 2815) are expensive tests that can be used to find crack arrest parameters for design analysis. The Compact Crack Arrest (CCA) (ASTM E1221) is another standardized test that also aims at finding crack arrestability analysis parameters. Otani *et al.* (2011), Sugimoto *et al.* (2012) described the use of ESSO tests to indicate crack arrest properties. Kubo *et al.* (2012) compared large scale crack arrest tests with full scale components of a container ship and found good agreement. Extensive efforts have been done to relate crack initiation with crack arrest. Ishikawa *et al.* (2012) investigated the applicability of small scale crack arrest tests with the large ESSO (wide plate) tests. Because of the very high cost of quantitative brittle crack arrestability testing, there is a special interest in establishing a quality control test that can be used to assure brittle crack arrestability without resorting to routine expensive testing. For this role, the Pellini test, standardized in ASTM E208 (2012), is proposed. However, the Pellini test does not have the same ductile to brittle transition temperature as larger-scale crack arrest testing so the test temperature would need to be adjusted from the service temperature. Hauge *et al.* (2015) have suggested the use

of Pellini testing with an offset temperature for verification of brittle crack arrestability of structures in the Arctic.

A final consideration is the Ductile to Brittle Transition Temperature (DBTT). This temperature is the temperature at which the failure mode changes from ductile to brittle, and it is worth noting that it is defined in several ways depending on the testing technique. For example, one parameter is the T_{27J}, which is the temperature at which the Charpy V impact energy is equal to 27 J, and similar definition applies also to T_{40J}. Another parameter, the Fracture Appearance Transition Temperature (FATT), is determined as the temperature at which 50% of the Charpy fracture surface failed in a cleavage mode, with the other half presumably failed in a ductile mode. A parameter that makes use of more rigorous fracture mechanics principles is the T_0 value; which is the temperature at which the fracture toughness K_{Jc} is equal to 100 MPa√m for a specimen thickness of 25 mm in quasi-static testing (ASTM E1921).

A common way of reducing conservatism is accounting for the effect of crack tip constraint. This concept is based on the observation that the state of stress in a typical laboratory fracture specimen is different than found in the actual ship structure. Perhaps the most straightforward way to account for this would be to choose a fracture specimen that has a similar level of constraint as the structure; which has motivated the aforementioned interest in developing the SENT specimen. Alternative methods for reducing conservatism are based on post-processing test data; however, additional information is often required, such as the Weibull shape parameter *m* required by ISO 27306 for unwelded structures. The advice of ISO 27306 is to find this parameter by the procedure of Gao *et al.* (1998); requiring ten repetitions of two different fracture toughness specimen types, for a total of 20 tests. Other, less expensive ways of experimentally determining *m* have been proposed in the literature, *e.g.*, Andrieu *et al.* (2012), Cao *et al.* (2011), and Qian *et al.* (2015), the latter based on the T_0 value. Coppejans and Walters (2018) are currently comparing between the most recent test methods and the widely recognized approach of Gao *et al.* (1998). To avoid limitations of ISO 27306, recent research has dealt with extending its achievements to welded structures (Minami *et al.*, 2013); however, that work is still under development. Likewise, BS 7910 Annex N offers methods of adjusting for constraints depending on whether ductile or brittle failure is considered. Not all the methods presented in BS 7910 Annex N require further testing; however, many do. Best results would likely be achieved with some combination of using multiple specimen geometries and multiple crack depths, though this would clearly be the most expensive.

Figure 1: Raking damage tests: Mild Steel specimen is subjected to a lateral impact load. Deformation is recorded with DIC (Haag *et al.*, 2017).

3.1.4 Corrosion

Corrosion comes in many forms. It is the intention of this section to discuss the testing methods and measurement techniques that exist to capture the phenomenon. Corrosion tests are performed in laboratory conditions and exposure sites; either offshore or in sea wind and sun battered locations. Experimentation can be concerned with uniform corrosion. Corrosion rate (based on mass loss) as well as microscopic evaluation was performed; both typical methods for exposure test evaluations. For uniform corrosion tests and analyses, several methods are generally accepted:

- Open circuit potential (OCP)
- Linearized Polarization Resistance (LPR)
- Electrochemical Impedance Spectroscopy (EIS)

The first system defines the potential of a material with respect to a given reference electrode; most often Silver-Silverchloride (Ag-AgCl). A material with a higher potential value is commonly called more noble and may be less prone to corrosive degradation. The second method measures the resistance of a specimen when exposed to a variation of potentials around the OCP. Lower resistance normally indicates higher corrosion rates. Corrosion layers may also exhibit capacitive, protective capabilities. The protective capabilities can be found by EIS. The resistance of a specimen is measured along a long range of frequencies. The measured response can be modelled by a system of resistance and capacitive elements; the associated values provide information on uniform corrosion rate. It is important to note that these methods are based on the assumption of uniform corrosion. When local corrosion takes place, local electrochemical circuits (cathode-anode combinations) develop and may not be picked up by the measurement system.

Corrosion is a deterioration mechanism that requires long exposure periods; especially for general or uniform corrosion. Accelerating corrosion is limitedly possible. Raising the temperature is the best-known option to accelerate corrosion. The other challenge is consistency; feasible by controlling the test conditions. Localized corrosion poses specific challenges to experimental validation. For instance, the effect of microbial induced corrosion (MIC) is a trending topic. The variety of bacteria is large and the combination of the various species also influences the behavior of a single species. For example, Sulphur reducing bacteria in combination with Sulphur producing bacteria, will develop a lively, corrosive culture. Several works have addressed MIC in general; however, addressing the specific combination of electrochemical and MIC corrosion is less frequent. Zhang *et al.* (2016) describe a methodology used to combine clean working conditions with electrochemical measurements, described the effect of MIC activities on the electrochemical measurements, and recorded surface morphology as well as the material structure. Hence, the material constitution could be related to the corrosion behavior; which is influenced by local electrochemical corrosion and MIC.

3.1.5 Friction

Friction is a marginally understood phenomenon when it comes to steel-steel interaction during collision. Several publications underline the importance of friction, while none give the proper way to model and experimentally measure friction. Haag *et al.* (2017) has addressed the issue of friction by performing tests to measure the friction coefficient and show the influence on mechanical behavior. The friction was tested in a dedicated set-up. Further, two series of drop tests were performed: with and without friction. The contribution of friction on energy dissipation was estimated.

Dragt *et al.* (2015) have reported Full-scale bearing tests. A sliding bearing was tested for wear under operational conditions. The axle was pushed in the bearing (radial loading), whilst being rotated oscillatory between two defined points. This combination of loads makes it a complex test to perform. Measurement of small wear was performed with DIC.

3.2 Large scale experiment

3.2.1 Ultimate strength

Ultimate strength is a traditional topic of ISSC; which is related to the limit state of the ship and offshore structures. During the past few decades, the research was focused on plate, stiffened panels or box shaped specimens during the design stage without damages or deterioration. Due to the increased attention to life-cycle management in maritime industry, damaged and aged structures have been recently studied. Several experiments concerning the ultimate strength of plates or stiffened panels with cracks or pit corrosion were performed to investigate the collapse of the structural components and are considered in the following.

Specimens

Specimens are taking the form of plates, stiffened plates, box type specimens or part of ship structures. Normally they are large scale (¼ or more). Typically, the ultimate strength, post buckling strength or strength after initial deformation are considered. In the latter, the imposed deformation is the result of construction or aging processes, or other kinds of damage. In Shi *et al.* (2017) a series of stiffened plates with initial distortions and artificial cracks along the transverse, longitudinal and inclined directions were subjected to in-plane compression until achieving their ultimate strength. A plate cut from an aged ship was tested to obtain the ultimate strength including corrosion damage (Zhang *et al.,*2017d). Other types of damaged plate structures include severely corroded stiffened plates (Gorbatov *et al.*, 2017), thin steel plates with a central elongated circular opening (Saad-Eldeen *et al.*, 2016a), stiffened panels with a large lightening opening (Saad-Eldeen *et al.*, 2017) and steel plates with a large circular opening accounting for corrosion degradation and cracks (Saad-Eldeen *et al.*, 2016b).

Loading process

Loading is generally applied progressively on the short edge of the tested plates. Axial compression was applied using displacement control at the velocity of 0.5 mm/s by Chen *et al.* (1997) and recently by Shi *et al.* (2017) to capture the post-ultimate strength response. An alternative way is to apply the compression load at a specified rate, as reported by Zhang *et al.* (2017d), with a load rate of 1 kN/s up to a compression load of 50 kN, and beyond this value with a decreased rate of 0.5 kN/s.

Experiment set-up

Large scale ultimate load testing requires dedicated experimental set-ups. The Tubular Testing System (TTS) was first introduced by Chen *et al.* (1997). The TTS has the capability of applying both axial (tensile and compressive) and lateral loads to the specimens and can be used for fatigue testing as well. The set-up consists of a universal testing frame and electro-hydraulic servo controlled actuators with end supports designed to provide “pinned” connections as shown in Fig. 2 (see also Shi *et al.* (2017) for further comments about end supports). In the past decades, test set-ups have been continuously upgraded and the so-called Universal Testing Machine (UTM) can afford for testing in Arctic, cryogenic and elevated temperatures conditions; an example is the UTM recently installed at Korean Ship and Offshore Research Institute (KOSORI).

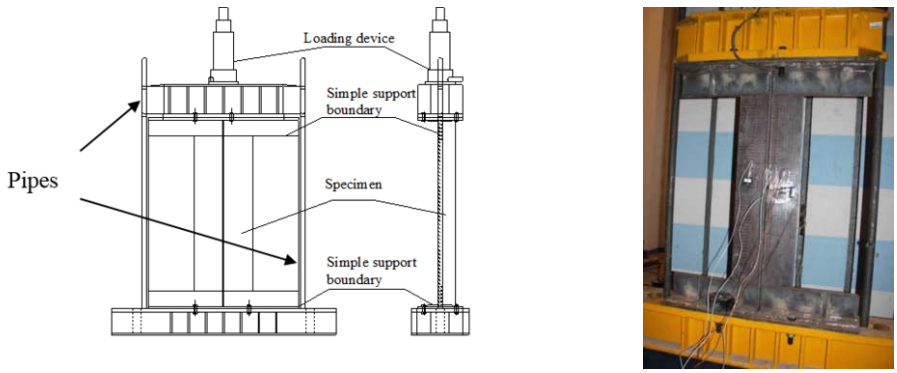

Figure 2: Test set-up (Shi *et al.*).

Boundary condition simulation

The boundary condition for an experiment is an idealization of the reality with the requirement to also be effective. One can choose pinned and/or fixed, and normally the cross section at the boundary remains unchanged during the experiment. Chen *et al.* (1997) described the end supports of TTS which were designed to provide "pinned" connections (see also Shi *et al.* (2017) for further comments). The design of the end supports allows the lateral displacement of the structure after ultimate point to simulate the post-buckling characteristics as well as rotations at the end. Instead of using a clamped support design, Zhang *et al.* (2017d) designed jigs to achieve a simple support boundary condition. Three types of the plate lateral edge support were also present in TTS, namely, (*i*) continuously supported edges, (*ii*) discretely support edges, (*iii*) free edges without any restraints. Finite element analyses showed that models with discretely supported edges have similar failure modes as the ones with continuously supported edges. The free edge boundary condition will have an effect on the failure mode of plate buckling. Models with discretely supported edges predicted multiple waves while the free edged model buckled in a single wave. These plate edge boundary conditions were also used in Shi *et al.* (2017) and the free edge in Zhang *et al.* (2017b) as the continuously supported edges.

Ship structures are normally exposed to a combination of loads; which, is difficult to simulate in a testing environment. Tanaka *et al.* (2015) described how the ultimate strength test of a hull girder with an open cross section could be analyzed regarding the ultimate strength under bending, warping and shear.

3.2.2 Large scale fatigue testing

To evaluate the fatigue strength of ship and offshore structures, large-scale model tests need to be performed under complex load and boundary conditions; consequently, different solutions have been adopted. Fricke and Paetzold (2010) carried out two types of full-scale tests: the first evaluated three models of web frame corners typical of ro/ro ships under constant amplitude loading and the second type tested five models representing the intersection between longitudinal and transverse web frames under constant and variable amplitude loading. All tests showed a relatively long crack propagation phase after crack initiation; calling for a reasonable failure criterion. The investigations provided good insight into the strength behaviour of complex welded structures and valuable information for validation of numerical codes.

Full scale fatigue tests of an aluminium ship structural detail were carried out by Tveiten *et al.* (2007) to obtain a design S-N curve. The test specimen consisted of a longitudinal stiffener and a transverse web plate. The fatigue test rig was designed to simulate the effect of lateral load transfer from a longitudinal stiffener into a transverse web. A total number of nine models were

tested at a constant load amplitude at a frequency of 2.5 Hz. Comparisons with the finite element method and recommendations on the procedure for fatigue assessment of aluminium ships (including S-N curve to be used) are provided.

Jang *et al.* (2010) investigated the fatigue crack propagation at the connection between a flat stiffener on a transverse web frame and the flange of a longitudinal stiffener on a bottom plate or inner bottom plate. Two typical types of web stiffeners were adopted; a straight end type and a softening end type. A test jig was designed to transfer the load from the actuator to the specimen along the line load at the centre of the specimen. Three different load levels and two types of specimens with load frequency of 5 Hz were tested. Two rolling supports were used to realize simple support boundary conditions. This paper proposes a set of formulas that are the most suitable for predicting a crack which starts from a welded joint of a top stiffener upon a longitudinal one and then grows into the bottom/side shell plate.

Yue *et al.* (2012) attempted to predict the fatigue life of a multi-planer tubular KK joint based on scaled model test and FEA. The specimen is welded by five hollow circular steel pipes. Although tubular KK joints among truss framed legs suffer a complex load combination, the axial load is usually predominant; it was also assumed dominant for the fatigue tests. A test rig was set up to fix the tubular joints subjected to axial loading and prescribed load application via the actuator. The FEA on both the real structure and the scaled model were performed to obtain their hot spot stress distributions. From the comparison and analysis of their hot spot stresses, the fatigue life of the real structure was provided based on the scaled model test result by use of the hot spot stress approach.

3.3 Impact & impulsive loading and response assessment

3.3.1 Ship Collisions and Grounding

Collisions and grounding are a major risk for maritime transport. Therefore, collision and grounding experiments have been carried out in full and model scales in order to investigate the collision mechanics of accidental events. In these experiments several effects can be included; however, simplifications are often required to narrow down the number of effects. Early experimental research dates back to the development of nuclear vessels (*e.g.*, Minorsky, 1959) and has been reviewed by Woisin (1979) with respect to internal mechanics with dry external mechanics. The heavily coupled internal and external mechanics are typically investigated separately to focus on some of the non-linear effects. Only a few actual collision or grounding event experiments were carried out in full scale (Vredeveldt and Wevers, 1992; Wevers and Vredeveldt, 1999; Lehmann and Peschmann, 2002; Wolf, 2003). Full scale experiments are expensive, difficult to perform and have provided limited validation data to give full understanding of the physics and uncertainties involved. As the data storage and the instrumentation capabilities increase, experiments based on extensive measurement techniques like Digital Image Correlation (DIC) are likely to improve our understanding of the coupled non-linear phenomena at full-scale. The following is a review of the different steps of the collision and grounding problem when experimental methods are utilised. Scaling issues are discussed in the following as well as in Section 5.1.

Collision and Grounding Event

Even if ship data in terms of production drawings, material certificates and surveying are well known, the collision or grounding event is often far less well-known. Sormunen *et al.* (2016a) investigated the influence of sea bottom shape idealisation with blunt cones in relation to the bathymetric big data (cloud of discrete points) measured from the Baltic Sea around the Finnish coast. It was shown that there are compensating effects when grounding damage is estimated with simplified models; for example, some errors can be made in the creation of "equivalent cones" for simulations or testing while the structural damage forms compensating effects. Further developments to form analytical models for simplified rock shapes are provided in Sormunen *et al.* (2016b) and Sormunen (2017). The analytical models can be used to simulate

true damages based on measured sea bottom shapes. Similarly, Roubos *et al.* (2017) investigated the berthing velocities at the port of Rotterdam with a portable laser system. Several measurements of relatively large seagoing container vessels were recorded and used as input for collision analysis; however, this kind of data generally allows for setting up more realistic grounding simulations as well. Numerical simulations involving internal and external mechanics are an increasingly accepted tool for design analysis (Moan *et al.*, 2017) of collision and grounding events. However, due to the strong non-linearities of the coupled problem, numerous challenges remain.

Experimental validation of analytical methods is of utmost importance due to their extensive use at the design stage. Zhang *et al.* (2017c) analysed 60 experimental results using analytical tools. A similar benchmark investigation was performed by Ehlers *et al.* (2008, 2012b) on full-scale experiments from the Netherlands. These benchmarks clearly demonstrated the gaps in modelling within the sub-problems of the coupled events. On the other hand, the experimental investigations at model scale by Tabri *et al.* (2008) focused on the coupled physics of ship motions, structural damage and sloshing in partial filled tanks. The scale ratio used by Tabri *et al.* (2008) was 35 and concluded that even though the similitude cannot be satisfied at the same time for all the influencing factors, the agreement between full- and model-scale experiments can be very good when proper values can be set. The study was later extended to include sloshing effects (Tabri *et al.,* 2009) and non-symmetric ship collisions in Tabri *et al.* (2010). Based on the above mentioned research, the full-scale results could be explained as well when all these phenomena were considered. Furthermore, the Froude-number based scaling is only partially effective as the different physical phenomena that affect the energy distribution in collision events do not scale in accordance with the same rules. In these experiments the structural response was simulated by homogenous foam to create the "equivalent" structural deformation in model and full-scale. This restriction was removed in the works of Calle *et al.* (2017b) who investigated the energy absorption of T cross-section beams and true ship structural topology in forced path on rigid wall as well as grounding and collision between two oil-tankers at 1:100 scale (scaled laser-welded metal structure). This work highlighted that as structures experience major non-linear deformations, the structural failure is difficult to predict. The difficulty is due to inapplicability of the usual material scaling as a result of necking formation and material characteristic microstructure (Calle and Alves, 2015). Thus, the scaling laws always neglect some aspects. The uncoupled approach remains a worthwhile simplification to gain insight into the physics of collision problem in addition to performing full and scaled tests as shown in the work of Cho *et al.* (2017). The coupling and scale effects remain unclear. On this side, Qiu *et al.* (2017) investigated the structural response and energy absorption of the simplified ship side under the impact of rigid indenters with different shapes and model scales.

Internal Mechanics

The key question relating to internal mechanics is the marine structure failure process and scaling of. Consequently, dynamic and quasi-static full-scale experiments are often employed to get new insights. Full and model-scale experiments of buffer bows are important for the validation of theoretical models as shown by Endo *et al.* (2002), Yamada and Endo (2005, 2007) and Yamada (2006). Quasi-static experiments were carried out to determine the interaction between the deformed colliding and collided ship structures (buffer-bow and double hull side structure) by Schöttelndreyer *et al.* (2011, 2013) and Tautz *et al.* (2013) who showed that the failure modes can be captured with theoretical models. Because of the complexity in modelling the complete scenario, further simplifications are frequently introduced in the experimental analysis by performing rigid indenter tests for the structural components. The panel experiments, complemented by material tests, by Rodd, (1996) Alsos (2008), Alsos and Amdahl (2009), Paik and Thambayalli (2003), Ehlers *et al.* (2012a), Liu *et al.* (2015b) indicate that the key question in the experiments is the failure process; which includes folding, buckling and fracture within the complex 3-dimensional shapes and welds. If the structure is designed ac-

cording to reliable design standards, it should not fail from the connections. The failure prediction then narrows down to the modelling of the failure strain of the base material; which requires proper material testing (*e.g.*, dog-bone specimen as prescribed by classification societies in their material certificates are often employed). The likeness of this test with respect to the failure mechanisms of 3D structures is limited because the strain path does not change as it does in real cases as shown by Benzerga and Leblond (2010) and Körgesaar *et al.* (2014). The problem becomes more complicated when temperature and strain-rate effects are included (Ehlers and Ostby, 2012; Park *et al.*, 2015).

Motivated by the full-scale experiments in The Netherlands, a sequence of structural strength tests on scaled structures have been carried out with Y and corrugated cores (Kitamura, 1997; Pedersen *et al.*, 2006; Rubino *et al.*, 2008a,b, 2009, 2010; St-Pierre *et al.*, 2015; Cao *et al.* 2017) as well as concrete structures (Niklas and Kozak, 2016; Woo *et al.*, 2015) reporting the experimental damage mechanisms of these crashworthy structures. More traditional marine structures have been investigated by Quinton *et al.* (2017) who showed that quasi-static assumptions of pressure patch for ice-induced load lead to unrealistic results due to neglected trailing edge effect by rigid rolling contact tests on plastically deforming steel plates. Gong *et al.* (2015) experimentally investigated the steel plate response and associated failure modes for different impactor shapes ranging from spheres to bulbs and rectangular sections. Liu *et al.* (2015a) investigated the dynamic response of impacted stiffened plates using traditional experimental techniques. Offshore structures response was investigated by Wang *et al.* (2016c) who performed experimental and numerical investigations on the T-joint of jack-up platform laterally punched by a knife edge indenter. A similar study was performed by Cerik *et al.* (2016).

The effects of cold environments on the physics of structural failures behind collision and grounding events have been experimentally investigated by many authors. Kim *et al.* (2016a) evaluated the effect of cold temperatures on the structural resistance of Arctic steel grades in terms of plates and stiffened plates. It was shown that during the room temperature tests the material remains ductile, however, the failure mode changes from ductile to brittle as a function of cold temperature. The investigations were extended in Ince *et al.* (2017) who performed impact experiments between steel plated structures and conical indenters made from steel and KOSORI fresh water ice, showing the possibility to numerically model the dynamic ice-structure-interaction.

Modern experimental techniques such as Digital Image Correlation (DIC) improves our understanding by measuring the strain fields on the specimen surface. One of the challenges in using DIC for collision and grounding tests is related to the adhesion of the speckle pattern used to identify the measurement facets when the fracture initiation and propagation is of concern. Gruben *et al.* (2017) and Körgesaar *et al.* (2017) applied DIC for the investigation of the fracture of stiffened panels under quasi-static and dynamic loading. Their study and the works of Hoogeland and Vredeveldt (2017) showed strain field data without adhesion issues; clearly demonstrating the potential of DIC in these highly challenging conditions. Another direction for future use of experimental investigations is provided by hybrid numerical-experimental methods (Getter *et al.*, 2015).

Consequences

Once collision or grounding has occurred, the consequence assessment becomes a coupled problem involving dynamic stability, progressive flooding and slowly varying loading on the ship (Bennet and Phillips, 2017). Jalonen *et al.* (2017) investigated the leakage and failure of non-watertight structures found in cruise ships in full scale. It was observed that the failure process is non-linear in terms of leakage as the structures start to collapse with large pressure heads increasing the gaps between frames and doors/classes. In Ruponen *et al.* (2013) the air compression effects inside a flooded tank of a damaged ship was studied through systematic full-scale tests with a decommissioned ship where the ventilation level of a flooded tank could be altered. Based on these ideas, Lee (2015b) predicted the capsize process of MV Sewol in

South Korea. Storheim *et al.* (2015) compared different state-of-the art failure criteria to predict the collision damage of the vessel Nils Holgersson collision.

3.3.2 Underwater explosion

Impact loading response of structures by underwater explosion has been investigated for many years. Experimentation has played an important role in understanding the underlying phenomena since the material characterization, loading description and associated responses are remarkably complex.

Test for material characterization

In order to understand the failure mechanisms under impact loading and perform numerical studies, a thorough understanding of the material properties is required. It is well known that the damage model under impact loading on metallic structures is related to the stress status. Some experiments were specifically carried out to test the dynamic mechanical behavior of materials for high-strength or high-temperature applications. Zhang and Suo (2017b) proposed a new experimental method for measuring the dynamic behavior of materials at high temperatures. The experimental set-up includes a classical split Hopkinson pressure bar and a MoSi2 heating source for achieving high temperatures. Experiments were successfully conducted on TC4 alloy with temperatures ranging from 20° to 1400° at the strain rate of 2000 s^{-1}, and on SiC at temperatures in the range 20°-1600° at the strain-rate of 250 s^{-1}. Fracture experiments of some high-strength steel were carried out by Fras *et al.* (2017), Li *et al.* (2014) and Li *et al.* (2015a). Fracture testing of sheet metal was investigated by Roth *et al.* (2015, 2016).

Loading

The pressure load produced by underwater explosion consists of a shock wave and bubble pulsation. After the detonation, there will be a shock wave propagating radially outwards, followed by a large oscillating bubble. The shock wave has the first damaging effect followed by successive bubble collapse and a high-speed jet.

Lee (2017) performed underwater explosion experiments using a small amount of shell-free Pentolite to observe the behavior of the generated gas bubble as well as measure the shock wave. Moon *et al.* (2017) measured the maximum pressure of the shock wave of an underwater explosion relying on underwater pressure sensors. To assess the measured signals, experiments were repeated five times under the same conditions. Small-scale underwater explosion experiments were carried out with two types of media at the bottom and different water depths in quasi-shallow water by Wang *et al.* (2015b). An analysis of measured data from different media at the bottom revealed that the peak pressure of shock waves in a water basin with a bottom of soft mud and rocks is about 1.33 times that of the case where the bottom material is only soft mud. Yanuka *et al.* (2015) conducted underwater experiments with wall boundaries having a parabolic cross section. This study showed that shock waves converge faster and the pressure near the line of convergence is larger. Zhang *et al.* (2015c) proposed a minus error approaching method to get the position of the explosion source using 4 effective pressure measurement points. Xie *et al.* (2015, 2016) have studied the time-frequency shock wave characteristics with underwater explosions in the free-field and near a ship hull. It revealed that more than 90% of the energy of the shock wave pressure signals condenses in the band lower than 8 kHz in the free-field and more than 80% of the hull pressure signals are mainly concentrated in a range of 20 kHz. Kostenko and Kryukov (2016) developed a technique to identify the explosion pulse based on the calculation and normalization of the mirror derivative of the received signal. In this way, the weak direct signals are amplified while the reflected ones can be suppressed.

The dynamics of underwater explosion bubbles has also received considerable attention with a particular focus on its dependence on the physical properties of boundaries adjacent to the bubble. Several experiments of a spark-generated bubble oscillating near a free surface and a rigid plate with a circular opening were conducted by Liu *et al.* (2017). Li *et al.* (2015b, 2017) studied the interaction between a violently oscillating bubble and a movable sphere with comparable size

near a rigid wall. Zhang *et al.* (2017a) investigated the interaction between an underwater explosion bubble and an elastic-plastic structure using small-scale experiments. Similar experiments were performed by Cui *et al.* (2016) to investigate bubbles subjected to gravity and various boundary conditions, including; single boundary, combined boundaries of free surface and solid wall, solid wall boundaries with a circular opening, and resilient wall boundaries. Ouyang *et al.* (2016) revealed that with an increase in charge density of each 100kg/m^3, the volume of the bubbles, acceleration and sound pressure level average increased by 1.78 times, 2.28 times and 1.15 times respectively. Zhang *et al.* (2015a) investigated the dynamics of large bubbles subject to various strengths of buoyancy effects.

Response

Underwater explosion is a severe threat to nearby ocean structures such as underwater construction, commercial and naval vessels. The latter requiring an assessment of their capability to withstand shock through expensive and lengthy tests. Scaled model experiments provide an opportunity to quantify the response associated with impact loading. Heshmati *et al.* (2017) designed a conical shock tube to investigate the underwater explosion phenomenon and its effects on nearby structures. Similar tests were conducted on a steel-plate (Park *et al.*, 2016) and clamped thin panel (Ren *et al.*, 2017). The influence of solid rubber coating on the transient response of floating structure to underwater shock wave was experimentally studied by Chen *et al.* (2016). It was shown that solid rubber coating can change the incident pressure on the wet surface as well as the dynamic characteristics of the coated structure. The high density and viscosity coating reduces the local deformation and global response when compared to high-stiffness low-compressibility coatings. A similar study was also carried out by Zhang *et al.* (2017a). Ming *et al.* (2016) experimentally recorded the damage process of ship structures subjected to underwater contact explosions. Zhang *et al.* (2015d) and Cheng *et al.* (2016) tested both a hull-girder model and a scaled ship model for dynamic response assessment to underwater explosion. The results show that the acceleration response and damage grade increase with shock factor and the local response is related to the vibration mode.

3.3.3 Vibration

Vibration and on-board noise measurements are related to distinct and often physically correlated phenomena for which sensors and experimental procedures are well consolidated for basic applications. For vibration and internal noise problems which depend strongly on the excitation and geometry of the structure, concerns at component level are limited to the estimation of structural damping or noise transmission coefficients. In the case of realistic configurations, the focus is on the response level related to comfort or fatigue and on the analysis of vibration and noise sources, transmission paths and influencing modal parameters (see Section 4.1.2).

Dry vibration testing

Vibration measurements require different levels of accuracy, bandwidth, spatial resolution and tolerance of insertion effects depending on the application. Vibration testing is used to estimate damping of structural components like a stiffened panel or more complicate configurations to improve the modeling of response at resonance. The structural damping is typically determined by evaluating the frequency response function with experimental modal analysis techniques during laboratory tests. The input force is applied and measured with instrumented hammers (impulsive force) or shakers (harmonic, sweep or stochastic load) and the vibratory response is recorded with modal accelerometers or strain gages. Soft-spring suspension is preferred when no specific boundary conditions are prescribed to facilitate FE model updating. When avoiding contact or insertion effect is desired, the laser Doppler vibrometry provides precise non-contact displacement measurements as required, for instance, to record the shaft vibrations induced by the propeller through the trust bearing (Pan *et al.*, 2002). Fiber Brag Grating (FBG) has also

been used for dynamic strain measurements (Jensen *et al.* 2000); who conducted wet-deck slamming tests with FRP sandwich panel using a network of 16 fiber optic Bragg grating strain sensors including comparison with the strain gage data.

Wet vibration testing

Dedicated experimental setups are required when the measurement of realistic vibration levels is the objective; as was done by Halswell *et al.* (2016) who dealt with the daily exposure limits to vibrations for the crew of high speed crafts. The core of the experimental campaign was based on 3D drop tests of rafts where three triaxial accelerometers were installed in place of the crew members. The measured acceleration time-histories provided peak values, RMS and weighted values from which the vibration dosage in the frequency range of 2-20Hz was obtained to verify the acceptance of regulations. The test matrix comprised of different drop heights and pitch angles to investigate the vibration exposure dependency on these factors. An important issue in complex set-ups is the cabling of sensor arrays. A solution was proposed by Bennet *et al.* (2014) who tested a wireless measurement system mounted on a floating elastic model excited by waves. The system consisted of three Shimmer 9DOFs wireless sensor nodes (triaxial accelerometer, gyroscope and magnetometer) equipped with SD card logger and Bluetooth connection. The triggering of the node acquisition and the post-test data downloading was obtained with an in-house MATLAB code. Good comparison was obtained in terms of heave and pitch response amplitudes (after proper processing of the node outputs) with the tethered system potentiometers. There is no direct comparison at the wireless nodes for elastic deformations, however, the node outputs are mixed with strain-gage information to provide the elastic line deformation. Among the few example of contactless measurements, Carrol (2006) estimated the radiated acoustic power of an underwater vibrating surface by measuring the response with a laser vibrometer and then compared the propagated noise inside the reverberant tank with hydrophone measurements. Kwon *et al.* (2013) applied digital image correlation to investigate the vibrational characteristics of composite beams immersed in water by collecting information about the added mass without the need to embed sensors potentially altering the structural properties or the interface with the surrounding fluid. Recently, the use of FBG for dynamic strain measurements in oscillating water intake risers is considered in the complex laboratory testing conducted by Wang *et al.* (2016d). The large deformations as well as the requirement of providing multiple measurement points along the entire riser length (up to 40 m, almost entirely and vertically immersed in the water pool) were driving factors for the choice of FBGs. There are 16 measuring stations in total along the riser. At each measuring station, there are four sensors around the circumference of the section: two for the in-plane responses, and the other two for the out-of-plane responses. The collected data allows for the determination of RMS of in-plane motion, out-of-plane motion and the separation of mode contributions to the overall deformation characterized by frequencies below 1 Hz.

Vibroacoustics

One of the main issues related to vibration and structure-borne noise onboard ships (this concept may be extended to offshore structures as well) mainly concerns the definition and fulfillment of (non-mandatory) habitability criteria, however, some mandatory rules apply to critical mechanical components like the propeller shaft. The ISO standards 6954-1984/2000 and 2631-1/2, as well as the optional class notations from classifications societies prescribe the significant physical parameters, acceptable exposure limits depending on ship areas, and experimental procedures for vibration level assessments (ISO 8041). The assessment of noise levels follows similar standards (IMO resolution MSC.337(91) for example) that indicate the procedures for the measurement of structure-borne noise. Therefore, the vibration and noise measurement sensor (accelerometers, velocity gauges, proximity probes, strain-gages and sound level meters) filter set, calibration and other requirements (sensor collocation, etc.) are prescribed to some extent. For this reason, relatively few accounts of experimental measurements appear in scientific literature while experimental procedures are periodically updated in technical papers issued by classification societies.

One of the most extensive experimental campaigns related to vibrations and noise has been carried out within the EU-FP7 project SILENV (2012). The main project objective involved the revision of the noise and vibration exposure requirements for crew and passengers of different ship categories; for which present and previously collected data were processed. New experimental procedures for vibration and noise measurements were defined and implemented by Turan *et al.* (2011) and Badino *et al.* (2012). Borelli *et al.* (2015) carried out full-scale noise level measurements in various compartments (living and working spaces) of a Ro-Pax ferry during navigation and maneuvers. The instrumentation was composed by two IEC 61672 Class 1 compliant sound level meters equipped with random incidence microphones and calibrated with IEC 60942 Class 1 compliant calibrators. When taking measurements in outdoor spaces, a windscreen was used along with proper correction factors. The measured levels were compared with recommended exposure limits to verify the compliance of the acoustic climate with regulations extensively reviewed in the paper.

3.4 Fluid-structure interaction

3.4.1 Hydroelastic scaled tests

Fluid-structure interaction (FSI) concerns all physical problems where rigid or elastic motion depends on, or are two-way coupled with, the nearby flow. The interaction between a rigid-body and the surrounding fluid is typically considered by ITTC (*e.g.*, seakeeping or propeller revolution). Here, the extent of FSI is restricted to the case of bodies subjected to deformations. Structural scaling allows for fitting the test setup into the laboratory space and preserving the basic features of the investigated phenomena in terms of elastic (and rigid) motions and fluid loads. To be effective, especially if getting new physical insights is the main objective, structural scaling requires consistent similarity laws as well as reducing in most cases the structural complexity of the full-scale problem. If the test purpose is extended or limited to the validation of FSI numerical codes, the reduction of uncertainties on the structural model can be attained by assessing the experimental setup through dedicated structural tests.

Ships

Segmented and elastically scaled models of ships have been used since the fifties (Mc Goldrick and Russo, 1956) for different aims (hydrodynamic load or vibratory response measurement) with their applications increasing in the last few decades. Apart from a few unsuccessful attempts with the so-called “continuous” models (Tasai, 1974; Hashimoto *et al*. 1978), elastic scaling has always implied a segmented hull layout achieved by an elastic backbone (Achtarides, 1979) or local springs (Jullumstrø and Aarsnes, 1993). The proper design of the metallic backbone (aluminum or steel) is a key factor in correctly accounting for the ship global deformations. The slenderness of backbones with hollow sections limits the correct frequency spacing of the bending modes due to lack of shear flexibility, however, the rotary inertia of the hull segments may partially recover shear flexibility up to the 3-node mode (Dessi *et al.*, 2008). Large open beam sections best fit the shear stiffness distribution while targeting torsional modes required for testing of containerships in oblique waves. To investigate the springing and whipping of ULCSs, Hong *et al.* used H-sections (2011,2012) and U-sections (2014). U-Section were capable of correctly replicating the first bending and torsional modes of a 10,000 TEU containership with a 6-segment model. To scale the stiffness of a 9000 TEU containership, Maron and Kapsenberg (2014) designed a box shaped backbone with openings on the top of the beam and a variation of the beam slope at the bow. Generally, the connection between the segments and the backbone must avoid relative rotations between the connecting parts especially for hull segments undergoing slamming; single bottom leg or double-side legs are exploited in most cases, however, more complicated arrangements can also be found as in Maron and Kapsenberg (2014). A special design of the structural layout allowed Jiao *et al.* (2015) to equip the segmented model with a self-propulsion system. The variable cross sections of the backbone matched the structural stiffness distribution while different solutions were adopted to link the backbone to the fiber-glass segments. Pressure was recorded at several points in the

bow along with vertical bending moments from calibrated strain measurements, thus accounting for the slamming loads and induced whipping response.

Scaled experiments with catamarans require a different arrangement of the backspline connecting the demihulls and supporting the deck. The first example was given by Hermundstad *et al.* (1994) who built a self-propelled flexible catamaran by using longitudinal and transversal connections (elastic hinges) between the demihull segments. The shear forces along the vertical axis and bending moments along the hinge axis were measured at each hinge by force transducers. The deck was divided into three parts and instrumented with small slamming panels to measure the impact forces which in turn provide the mean hydrodynamic pressure. The backbone layout was first exploited by Kyyro and Hakala (1997) for model tests in the towing tank and by Cheng (1997) in open water towing tests. The most systematic series of experiments has been carried out since 2006 with respect to fast catamarans exhibiting a centre-bow (Lavroff *et al.*, 2007; Thomas *et al.*, 2011). The segmented model is a hinge-type model with flexible connections between the 3 segments of each demihull and stiff bars connecting the segments from side to side; which also support the fore deck part with four load cells. Several pressure transducers were also installed on the centre-bow to map the slamming pressure field. The stiffness of the elastic links was adjusted to scale the vertical bending modes. The link deformations were measured with calibrated strain-gages to directly provide the bending moments. A different approach for the design of a flexible catamaran with a flat wetdeck (Figure 3) was followed by Dessi *et al.* (2016, 2017a). To reproduce the frequencies of the split and 2-node bending modes, a structural optimization procedure was employed for the design of the aluminum backspline connecting the hull portions (4+4 demihull segments and 2 wetdeck portions). The optimization procedure was also utilized to determine the distribution of structural mass and ballast required to match the rigid-body mass properties. The fore section of the flat wetdeck was suspended on two hinged bars affixed with piezo load cells and pressure caps to measure the global and local slamming load. The strains were measured on the aluminum truss at 36 points to provide bending moment and shear force distributions as well as the demihull segment forces.

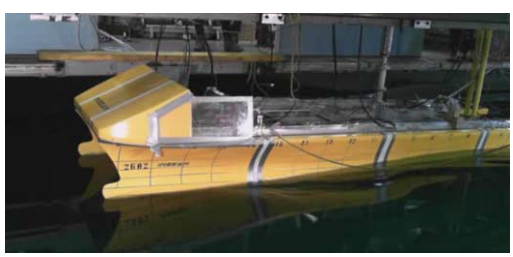

Figure 3: Flexible catamaran with elastic backspline (Dessi *et al.*, 2016)

Figure 4: Scaled test of the float-over concept with flexible topside (Dessi *et al.*, 2017b)

Offshore structures

FSI testing involving offshore structures have exhibited a wide range of study cases without a systematic classification over time. Thus, only some novel experimental applications are herein reported, and the reader has to refer to the reports of other Specialist Committees for a more extensive coverage. FSI testing on risers provides the ultimate step for verifying the effectiveness of vortex induced vibration (VIV) suppression devices as numerical modelling presents some issues for complex configurations. Gao *et al.* (2016) conducted experimental investigations on a flexible riser with and without helical strakes to assess the fatigue damage. The VIV were induced by towing a pretensioned riser model at constant speed. Up to 88 strain gages were applied on different riser sections to record the elastic response of in-line and cross-flow

vibration. The strain gauges provided sufficient data to compare the fatigue damage along the two directions with and without the suppression devices. Another example of unusual setups is the testing of float-over systems for the transportation and deployment of offshore structures. In Dessi *et al.* (2017b) the transported topside used to link two barges in a catamaran arrangement (Figure 4) was elastically scaled to investigate the relative rotations between the barges as well as the torsional and bending loads acting on the topside connections recorded with an optical system and a strain-gage array, respectively. A series of model tests with a realistic configuration of the vessel, carried topside and jacket were also performed by Kwon *et al.* (2017) and Kim *et al.* (2017) to investigate the performance of docking and mating operations in float-over installations. During the tests, the vessel motion, line tensions, fender forces and loads on LMUs (Leg Mating Unit) and DSUs (Deck Support Unit) were measured under various wave heading and amplitudes using special measuring devices.

Sloshing

Sloshing is another example of FSI for which the structural scaling of the tank elasticity affects the results. In Lugni *et al.* (2014) tank structural scaling was pursued by elastically scaling the first natural mode of a structural panel of Mark-III tank. The scaled instrumented elastic panel is clamped on the opposite top and bottom edges and sealed with silicon on the vertical sides. A static calibration of the strain gages applied on the plate was carried out under a uniform pressure load and their dynamical responses were verified by comparison with acceleration signals. The estimated structural damping was used in the plate FE model loaded with the measured pressures in a hybrid approach. The comparison of rigid and elastic (not-scaled) plate response for assessing the mitigation of the impulsive sloshing loads was carried out by Jiang *et al.* (2014), whereas Wei *et al.* (2015) considered inner structural details of the full-scale sloshing tank to experimentally identify the optimal value of the slat-screen solidity ratio to reduce the slamming loads. A challenging FSI investigation has been carried out by Lee *et al.* (2015a) who carried out a hydroelastic analysis of three elastic barges partially filled with water to validate numerical simulations. Using four cameras pointing to onboard infrared markers, they detected the relative torsional motion between the opposite sections of the flexible barges (made with Plexiglas) indicative of the hydroelastic response excited by oblique waves.

Ice

Testing in ice basins has received growing attention as long as artic routes become more affordable as a result of climate change. Dynamic ice-structure interaction has been subject to extensive research during the last decades to determine the ice-induced vibration fatigue. The goal of this research to consider ice-induced vibration fatigue at the design stage. Ziemer and Evers (2014) tested a compliant cylindrical structure (a lighthouse scaled by a factor of 8.7) under different ice conditions to investigate ice induced vibrations under laboratory conditions. Ice drift speed and thickness were varied to study the dependence of occurring vibrations on ice properties. The structural response was monitored by lasers as well as an inertia measurement unit to measure the acceleration and inclination of the structure. Ice loads were registered by two 6-component scales connecting the cylindrical structure to the mounting carriage. An open issue for ice tests is about the physical scaling of the ice sheet. These aspects were addressed by von Bock und Polach (2013, 2015) who presented a novel experimental technique to measure the model-scale ice property including grain size, elastic strain-modulus, compressive and tensile specimen tests. The model-scale ice thickness and the bending strength were also determined to classify the ice properties.

3.4.2 Slamming and water impact tests

Stenius *et al.* (2013) designed a new setup to experimentally investigate the consequences of slamming loads on impacting structures. Some representative high-speed craft hull bottom panels including; a glass-fiber reinforced single skin panel, foam-cored sandwich panel with glass fiber reinforced face sheets, and very stiff carbon-fiber sandwich panel were tested. Suàrez *et*

al. (2016) employed an experimental apparatus able to reproduce a cyclic slamming-like load in pre-impregnated and cured glass-fiber reinforced polymer panels. With respect to more realistic tests, the controlled environment allows for a precise correlation between the applied load and the damage propagation. High-speed velocity impact experiments were performed using the SHPB (split Hopkinson pressure bar) by Zhang *et al.* (2017b) to study the material properties under water impulsive loads. The specimen can be tested at high or low temperatures. A large impact facility to test metallic panels for ship and aeronautical applications has been recently developed for the EU project SARA (Figure 5). SARA enables the investigation of both elastic and plastic deformations at full-scale impacting speeds (Iafrati *et al.*, 2015, 2016). The specimen can be a panel or a portion of a real structure (Figure 6).

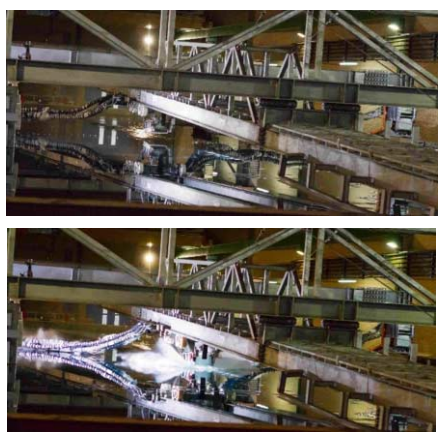

Figure 5: Large facility for high-speed impact testing.

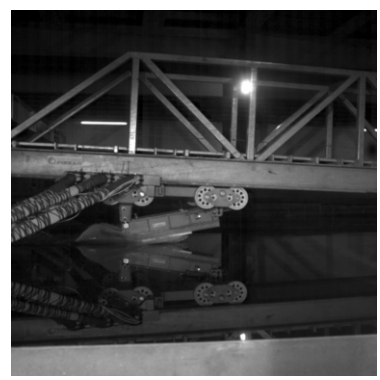

Figure 6: Detail of the carriage carrying the specimen.

4. FULL SCALE TESTS

4.1 Ships and offshore structures

4.1.1 Monitoring of loads and responses

This section reviews technologies for monitoring, environments, loads and responses of ships and offshore structures at sea.

(1) *Wave Measurement*
The WAMOS project (Hessner *et al.*, 2014) used the X-band radar for measuring waves from a sailing ship. The system gives the wave statistics values, such as the significant wave height and the directional spectrum, in real time. Koo *et al.* (2011) applied an onboard wave monitoring system (Wave Finder) to a large container ship. Using a marine X-band radar wave, parameters such as direction, period and height were acquired as done in the WAMOS project.

(2) *Load Measurement*
Schiere *et al.* (2017) developed a novel approach, or mode-based method, to derive load effects along the length of a vessel. In comparison, traditional approaches derive the sectional loads by processing strain gauge data in the section itself. The authors compared full scale trials and model tests along with numerical simulations and concluded that their mode-based method provide better results with less scatter than the traditional approach. Suominen *et al.* (2017a,b) discussed extensively the uncertainty related to measuring techniques related to ice loads. Historically, ice loads measurements onboard a ship were based on shear gauges placed side frames which are assumed to not deform plastically. This type of measuring system is very good for actual

operations as it is simple, robust and can be used both in short and long term. However, a major issue of this approach is that the ice load distribution was assumed beforehand. If this assumption is not accurate, the results will be too. If the strain measurement points in an instrumented panel can be increased significantly (by an order of magnitude or even more), the extension of the contact shape gets known far better. Digital Image Correlation (DIC) systems with computational inverse methods are potential future methods for this type of measurements.

Table 2: Notations for vessels with hull stress monitoring systems from major classification societies

Classification Society	HSMS Classification Notation Rules
DNV GL	HMON(A): where within the brackets is a better of A,C,D,E,G,H,L,M,N,O,P,S,T,W which denotes different sensors and data communications.
Bureau Veritas (BV)	MON-HULL
American Bureau of Shipping (ABS)	HM1:Motion Monitoring HM2:Stress Monitoring HM3:Voyage Data Recording for later evaluation
Lloyd's Register of Shipping (LRS)	ShipRight-SEA(Hss-n,optional extension) The extension –n signifies the number of strain gauges connected to the system. VDR An interface with the ship's voyage data recorder system to enable the recording of hull stress, ship motion and hull pressure information.
Korean Register of Shipping (KR)	Rules for Classification of Steel Ships(2008), Pt.9:Additional Installations, Ch.6:Hull Monitoring Systems
Nippon Kaiji Kyokai (NK)	Rules for Hull Monitoring Systems (valid at the date 07/2008)

Table 3: Sensors for monitoring ship hull structure of FPSO unit

Sensor Type	Monitoring Type	Maturity in Maritime
Strain Gauges (short and long baseline strain gauge)	Strain	Proven
Accelerometers	Acceleration	Proven
3D Laser Scannig	Optical	Proven
Photogrammetry	Optical	Proven
Fibre Optic	Optical	Proven
Pressure Sensors	Pressure	Proven
Conventional Ultrasonic Testing(UT)	Sound	Proven
Acoustic Resonance Testing(ART)	Sound	Un-Proven
Acoustic Emission Testing(AET)	Sound	Un-Proven
Guided Wave Testing(GWT)	Sound	Un-Proven
Remotely Operated Vehicle	Optical,Electrical, Sound	Un-Proven
Thermography	Temperature	Un-Proven
Sensor Networks (including Wireless Sensor Network)	Varies	Un-Proven
MEMS Accelerometers	Acceleration	State-of-the-art
MEMS Pressure Sensors	Pressure	State-of-the-art
Ice Accretion Sensor	Sound,Capacitance	State-of-the-art
Smart Coating	Color	State-of-the-art
Smart Dust	Electrical	State-of-the-art

(3) *Ship/Vessel Monitoring*

Fatigue damage assessment based on full scale monitoring of a large container carrier was reported by Koo *et al.* (2011). The full-scale monitoring system consists of a hull stress monitoring system (HSMS) and an onboard wave monitoring system (Wave Finder). The number of sensors in the midship region is four at each section. The HSMS provides an interactive user interface to display the bending moment, torsional moment, bottom slam occurrence, cumulative fatigue cycle count and real-time sensor display. The fatigue damage due to the high frequency components like springing/whipping was identified and found to be greater than what was expected. Guan (2015) reviewed commercially available HSMS and summarized notations for equipped vessels from major classification societies (see Tables 2 and 3). The author recommended that, for every FPSO vessel, at least one HSMS should be installed in compliance with regulation from the IMO. Additionally, he reviewed sixteen types of sensing technologies and categorized them into three groups: Proven, Un-Proven and State-of–the-art, according to the matureness and readiness for application in marine structures. He concluded that multiple sensing technologies should be systematically combined to provide more accurate information, and proposed the integration of proper wireless sensor network technology and Bayesian Network modelling as the future direction of FPSO hull monitoring system. Structural integrity

during operation is often ensured via monitoring the difference in loads in comparison with design loads. For example, in JIP MONITAS (Tammer *et al.*, 2014), prediction of soundness is tackled through monitoring of hull load.

(4) *Offshore structure monitoring*
Regarding riser structures, many real-time monitoring systems were proposed. Frazer *et al.* (2011) investigated the phenomenon known as Wake Induced Oscillation (WIO) of top tension risers (TTR) by monitoring the system in real time. To determine the riser motion amplitude, 3-DoF acceleration and 2-axis angular rate sensors are secured in a corrosion resistant Remotely Operated Vehicle (ROV) deployable canister. The selection of motion sensors is based on results from FEA conducted on the production TTRs. The strain sensors are mounted over critical welds above and below the upper centralizer to capture the strain response of fatigue critical areas on the TTR. Through the combination of motion and strain sensors a better understanding of WIO and its effects on fatigue can be gained. Using environmental data gathered from the vessel monitoring system and comparing it to the measured riser response future analytical models can be developed. Fibre optic sensors have gained increasing use in monitoring offshore structures, such as risers flowlines, umbilicals, wells, Tension Leg Platform (TLP) tendons, production and drilling risers, and mooring lines. Fiber optic sensors are capable of monitoring strain, temperature, pressure, and vibration. Eaton *et al.* (2015) details the plausibility of using pressure measurements from post-installed fiber Bragg grating (FBG) sensors with Model Predictive Control (MPC) to suppress severe slugging in subsea risers. Prior control schemes demonstrate that slugging is mitigated using a topside choke valve. The most effective methods use a pressure measurement immediately upstream of the touchdown zone of the riser; however, the majority of production risers do not have pressure sensing at that location. With advances in subsea clamp design and bonding it is now possible to install a non-penetrating FBG sensor to monitor pressure near the touchdown zone without shutting down production. Stabilizing the two-phase flow both reduces vibration-induced fatigue and has the potential to allow for increased throughput with relaxed topside processing constraints. The performance of the controller in reducing disturbances is influenced by sensor location, choke valve response time, and riser geometry. This study demonstrates that severe riser slugging is effectively controlled with MPC and a post-installed, non-penetrating FBG sensor.

In the subsea field, the efficiency of IRM (inspection, repair and maintenance) systems is progressing by development of communication technology with the sensor. The non-insertion type inspection of pipelines based on X-rays has been developed by Ledezma *et al.* (2015) as alternative of the pipeline inspection pig (a device inserted in the pipeline to perform various maintenance operations). In project 'Cage' (Kellner, 2015) General Electric (GE) exploits a smart platform for connecting a large e number of British Petroleum (BP) subsea wells to get information about vibrations, temperature, pressure. The implemented monitoring system is aimed to detect real-time abnormalities and to provide big data for improving performances and production.

4.1.2 Structural identification

Structural identification aims to validate or update mathematical models of structures using measurement results obtained from tests or full-scale trials. In daily practice structural identification involves also the assessment of test rigs and typically identification techniques are first verified at model-scale before being applied at full-scale. A related topic is structural health monitoring (SHM), which is also covered in the report of Committee V.7 (Structural Longevity).

Material properties
A FEM analysis of collision or grounding requires proper modelling of the material behaviour. The metal exhibits complex behaviour during a collision or grounding, involving triaxiality and "elemental" volume changes. Because there are very few studies on the influences of triaxiality

as traditionally, the strain-stress relationship of a metal is often defined based on uni-axial tensile tests. Many authors believe that strain rate, temperature and triaxiality have major influences on the simulation of collision or grounding events. Tests were conducted to steels (2W50, EH36, DH36) to various strain rates (0.001/s-200/s), at different temperatures (-40°C to +180°C) (Choung *et al.*, 2013), or at different triaxialities (Choung *et al.*, 2012). Recommendations were then made to change the Cowper-Symonds parameters. Kubiczek *et al.* (2017) used a high-speed camera to "measure" the strain field in the metal. They converted the measured load-end shortening curve into the stress-strain relationship with the assistance of a FEM analysis. Calle *et al.* (2017a) also adopted this hybrid experimental-numerical method in obtaining the stress-strain curves from experimentally obtained strain data. They tested different shell elements with a premise that the best element types would have the minimal differences between the calculated stress-strain curves and the measured force displacement curves.
Many FEM analyses treat ice as a unique material whose characteristics are defined based on either model tests or field measurements. Von Bock und Pollach and Ehlers (2017) developed an experimental technique to assess the material properties of the ice sheet in an ice basin. It is well acknowledged that scaling ice made in an ice basin to reproduce winter sea ice (see Section 3.4 for further details) remains a major technical challenge.

Dynamical structural properties
Structural identification of dynamical systems in engineering practice narrows the broader scope of system identification which aims to build mathematical models based on measured data. First attempts to use Fourier analysis, Auto-regressive Moving Average (ARMA), Maximum Entrophy Method (MEM) and Random Decrement Technique (RDT) for system identification of offshore platforms dated back to the seventies and eighties, in parallel to similar applications in civil engineering. From the nineties onwards, the system identification of ship and offshore structures benefited of the development of output-only methods for modal analysis which avoid the measurement of excitation.

Coppotelli *et al.* (2008) carried out a systematic identification of `wet' mode shapes and related modal parameters (frequency and damping) of a scaled ship model. They analysed the acceleration data using Frequency Domain Decomposition. Later, Mariani and Dessi (2012) used a tailored version of the Proper Orthogonal Decomposition on both acceleration and strain data. In both cases the required broadband excitation in the frequency range of interest was provided by the continuous wave loads. In Kim *et al.* (2016c) the identification of mode shapes is extended from bending to torsional modes using rosette type strain-gage measurements in five sections along the backbone of a 6-segments scaled model of a 10,000 TEU containership. The implemented POD technique for mode extraction follows that developed by Mariani and Dessi (2012) whilst the damping estimation is based on the linear decrement technique applied on a decay curve obtained from the random decrement technique. It is worth to recall that for a floating structure the concept of linear damping is an abstraction hard to verify in real-life, structural damping coexists with hydrodynamic damping, and relevant uncertainties on the results are present as shown also in Dessi *et al.* (2016, 2017a) for floating structures. The use of turbulent boundary layer excitation for extracting the modal parameters on plates wetted on one side was considered in Dessi and Faiella (2015) where specific attention was devoted to the possible change of the modal properties (frequency, damping and consequently added mass) with respect to the flow velocity. The plate was mounted on the bottom of a rigid ship model that underwent captive tests in the towing-tank. The adequate numerical representation of the real boundary conditions was one key issue in profitably comparing with theory and interpreting the experimental data, as also shown in the case of a similar full-scale application for the SILENV project. A method specifically developed for the identification of less excited modes in high-level, noisy, measured data from offshore structures is presented in Liu *et al.* (2016) and its effectiveness is compared with similar approaches like the Eigensystem Realization Algo-

rithm (ERA) and the Stochastic Subspace Identification (SSI) methods with respect to numerical cases. Its application to real cases has concerned two distinct offshore platforms under different excitations provided by ice and waves, respectively. At full-scale, using the FDD technique, Swartz *et al.* (2012) identified the low-frequency wet modes (along with the relative frequency and damping) of the Sea-Fighter catamaran with acceleration measurements collected from wireless sensor nodes. These mode shapes were used as reference for the design of the hydroelastically scaled model of the same catamaran in Dessi *et al.* (2017a), who applied input/output and output-only modal identification techniques along with DIC measurements to verify the effectiveness of the structural scaling of the catamaran.

4.2 Application of experimentation, inspection and monitoring

4.2.1 Design

An effective design is required to ensure the structural integrity of marine structures. Continuous monitoring and periodic inspections may contribute to improve the design accuracy by reducing the uncertainties on the expected loads and on the structural strength of the real structure. Storhaug and Haraide (2013) showed the results relative to hull monitoring measurements for a large containership. The owner/operator observed wave-induced vibrations (whipping/springing) via the hull monitoring system installed on-board. After a few years of measurements, the data was sent to DNV for assessment of the effect of vibrations and then to learn lessons about the design. The collected data show that the vessel was trading in more demanding areas than those (North Atlantic) assumed in design. The measured fatigue life based on a stress concentration factor of 2.0 was estimated to be well above the design life, implying that special attention to cracks should be seriously considered for future vessel operations even if no cracks had been identified so far during inspection. The vessel experienced two severe storms exceeding the rule of thumb value of 20% increase of loading level due to whipping. The measured wave bending moment (excluding whipping) also exceeded the long-term value specified by IACS URS11. The ultimate hull girder strength was calculated and compared with the combination of measured wave-induced bending moment and allowable (maximum) still water bending moment. If the maximum whipping moment is assumed, the safety margin of the hull girder bending strength is found to be below 1.0 for the original design, but keeps above for the strengthened vessel.
Drummen *et al.* (2008) carried out an experimental and numerical study of wave-induced fatigue damage in a containership which advances at a constant forward speed in irregular head waves. The model tests showed that the damage due to wave-induced vibrations made up approximately 40% of the total damage, and that this percentage slightly increased from bow to stern. The high-frequency contribution could be slightly smaller at full scale due to a larger damping. The main contribution to the high-frequency damage came from the two-node mode of hull vibration, while the other modes contributed less than 5% of the damage. The damage in the fore hull sections was negligible compared with the damage in the midships sections, while the damage in the aft sections was about 25% of this value. The largest contribution to the fatigue damage occurred in sea states with a peak period of around 14 s and a significant wave height of 5 m or above. Relatively to the investigated sea states, the experimental results indicated that the nonlinear effects on the wave frequency stress were mainly important in the forward cut, while they affected the high-frequency stress in all three cuts.

4.2.2 Construction

Since ship and offshore structures are huge welded structures, quality control of the assembling process under construction is very important. In recent years, 3D measurement technology has been applied to verify the final accuracy of the welded structures under construction and is more specifically introduced in Section 7.1. In this section some applications of 3D measurement are illustrated. The first one concerns the measurement method of welding deformation/strain to calculate the weld-induced residual stress. Shibahara (2012) used DIC technique developed

measuring both in-plane and out-of-plane deformations induced by weld. The stereo imaging method using two digital cameras has a high measurement accuracy and does not require calibration of the errors caused by the out-of-plane displacement. He demonstrated the measurement accuracy through a bead-on-plate welding test. The proposed method can measure transverse shrinkage and angular distortion with a high accuracy. This inherent strain data was then used as input for the simulation of welding deformation of large structure. The second application is aimed to assist the plate bending process. Sun and Hiekata (2014a,b) evaluated the accuracy of laser scanners in measuring the plate bending work. The evaluation process of the construction accuracy for curved shells and plates suffers from the lack of quantitative criteria, and heavily depends on implicit knowledge, that is, the skill and expertise of the workers. The shape of the objects is represented as cloud data points. In this system, cloud data points and design data are registered and displacement errors and evaluated and visualized by colour maps and histograms. In addition, Hiekata *et al.* (2016) visualized the result of evaluation by using the projection mapping. The output of the system was collectively projected on the curved shell and the difference with CAD shape was visualized. Matsuo *et al.* (2015) developed AR (Augmented Reality) application system to support shell metal forming by pressing or heating. The former AR application guide workers where and how to perform press work or gas heating work for getting the intended shape.

4.2.3 Operation, Inspection, Monitoring and Maintenance

The offshore oil and gas industry has accepted Risk-Based Inspection (RBI) as a rational way to carry out inspection, maintenance and repair for hull, topside, morning systems. Guidance on best practice of RBI has been published by API (2016a,b), ABS (2003), DNV (2010), LR (2010), and is covered by other ISSC committees.

Most of RBI programs relies on traditional means of inspection, mostly via human eyes. Some progressive operators/owners apply structural health monitoring techniques in some areas. Monitoring is considered viable especially for areas difficult or costly to access. The FPSO Joint Industrial Project (JIP) on Life Cycle Management Hull attempted to layout a framework for incorporating health monitoring into a FPSO's RBI scheme. This JIP (LMS, 2015) has a focus on monitoring corrosion and fatigue cracking, assessing their risks to the life-time structural integrity of FPSO, and planning and implementing inspection, repair, and maintenance accordingly. There is an apparent technological shift in industry, leveraging real-time monitoring to help owners and operators better understand the health of their assets and guide their maintenance and repair decisions.

A notable industrial project on health monitoring is MONITAS (Aalberts *et al.*, 2010), which has been extensively covered by ISSC over time. Tammer and Kaminski (2013) reviewed the methodology of the Risk Based Inspection (RBI) scheme and its application for safeguarding hull integrity of offshore floating structures, with fatigue as a primary degradation mechanism. The work has a distinct focus on the opportunities that RBI offers in combination with Structural Health Monitoring. To provide a clear picture of the state of the art knowledge, the current practices and regulations are briefly discussed after which the RBI methodology is introduced, the differences in guidelines and applications discussed and an 8-step approach is proposed. Subsequently, the methodology is outlined as an instrument for determining the residual fatigue life with the alternative inspection scope and schedule was discussed and within a framework specified in an Advisory Hull Monitoring System.

Increasingly, industrial guidance has become available to guide applying monitoring technologies. An example is the recently published *ABS Guidance Notes on Structural Monitoring Using Acoustic Emissions* (ABS, 2016). This guidance presents best practices for planning and executing Acoustic Emission Testing (AET), and has been built upon a series of at-sea tests on board tankers and containerships. Another example is the CCS Rules on Autonomous ship guidance (CCS (2015)). These Rules clearly include structural health monitoring a crucial part

of the future smart/intelligent shipping, and has specified in great details about how to plan hull monitoring, what frequency must be used for sensors, and how to interact with regulatory bodies. Generally, it is believed that we will see increased interest in R&D and application of health monitoring together with the supporting technologies such as sensoring, communication, data processing and decision-making (smart functions).

5. CORRELATION ISSUES BETWEEN SCALED (PHYSICAL) MODELS, FULL-SCALE STRUCTURES (SHIP AND OFFSHORE) AND NUMERICAL SIMULATIONS

5.1 Scaling laws

Scaling laws have been used in naval architecture since the foundation of dedicated experimental facilities like towing-tanks. Reynolds and Froude similarities have typically allowed for predicting the resistance and seakeeping behaviour of ships at full-scale. Later on hydroelastic scaling for ship structures have been based on an extended application of the Froude similarity; the ratio between the ship and the model scale values of several physical parameters (frequency, bending stiffness, shear area...) is expressed in terms of powers or fractional powers of the scale factor. A more cumbersome hydroelastic scaling with respect to vortex-induced vibration (VIV) tests where the investigation of the lock-in phenomenon implies that the structural frequency of the bluff-body oscillations falls close to the Strouhal frequency, which in turn depends also on the Reynolds number.

Recently, new advancements in the definition of scaling laws with respect to some specific structural problems, including; fatigue, collision and grounding, already mentioned in the specific sections. Kong *et al.* (2017) investigated the strain-rate effect of blast loaded plates by using dimensional analysis and analytical equations with emphasis on engineering calculations which need to be fast and robust. In addition, an empirical formula was developed to assess the equivalent stand-off distance, mass of TNT and impulse per unit area. A fundamental contribution concerning the scaling issues of ship collision and grounding, an extremely nonlinear phenomenon, is given by Pedersen and Zhang (2000) who reviewed the ship-size effect in relation to resulting damages. Although the focus in this research was on the ships with similar order of magnitude in size, the equations derived in the paper serve as background information for the scaling rules in ship grounding and collisions. However, when the level of fidelity is increased to account structural details, strain rate and plate thickness effects, the scaling issues become very complex; as discussed separately under the collision and grounding section. In this respect, the work of Oshiro *et al.* (2017) shows that traditionally used LMT-scaling (length, mass, time) should be replaced by VSG-m-scaling (velocity, stress, impact mass) when dynamic problems of ship collisions are concerned. This recommendation was based on tests on dry models where effects of moving cargo and hydrodynamics are neglected, and the focus is purely on structural responses. It is also highlighted that even though geometrical similitude could be kept, the nominally identical materials do not give the same results when the scale is changed. This is due to processing of the steel sheets and the fact that the similar microstructure through the thickness is very difficult to keep as it is within distortion tolerances after manufacturing. The recent review on structural testing by Coutinho *et al.* (2016) gives a comprehensive overview of needed viewpoints when new similarities are to be formed. The review covers dimensional analysis, differential equations and their combinations as well as the use of energetic methods. It also reviews the major areas of current research in the structural mechanics community including impacting structures, rapid prototyping and size effects on brittle, quasi-brittle and ductile materials.

In terms of motions and related loads, the paper by Lupton and Langley (2017) discusses the importance of the platform size on slow drift motion. It is claimed that the fact that in some

cases the second-order slow drift response is smaller than the first order motion; while in another case this is larger due to scale effects of the floating structures. An expression is derived which approximates the scaling of slow drift motion, platform size and wave conditions. The investigation by Lau and Kelso (2016) presented a scaling law for the time-averaged thrust on submerged heaving and pitching fish-inspired hydrofoils. The Strouhal number *St* was used as a scaling parameter and successfully validated the scaling law by varying several experimental parameters, including; the non-dimensional heave amplitude (0.1,1), the pitch amplitude (0°, 45°), the Strouhal number (0.1, 0.95) and the Reynolds number in the range 1500-12500. In cases where the non-dimensional heave amplitude is large in relation to the pitch amplitude, the experimental results deviate from the scaling law.

5.2 Model to full-scale investigation

The scaling laws considered in Section 5.1 address the problem of correlating model and full-scale tests. For instance, the full-scale correlation of the ship resistance measured over a physical model in the towing-tank has been traditionally one of the main problems addressed and continuously revised by ITTC to set precisely the required onboard power for a target speed. When more complex measurements like those related to structural variables are considered, the correlation between model and full-scale is not only a matter of similitude because of the physical objects, the test conditions and the measuring techniques may significantly differ. Here some illustrative examples of correlation efforts are reported.

The problem of extrapolating model-test data to full-scale for new ship designs (which lacks proven procedures) was considered in the Ship Structure Committee report in 1972 in relation to the S.S. Volverine State and S.S. California Bears. The main objective was the prediction of the bending moment long-term distribution based on model-test data and ocean wave spectra. A detailed analysis of acceptable comparison factors to be checked was carried out and a procedure for estimating the full-scale trends from model test was successfully established. In general, it appeared that predictions of long-term trends are satisfactory when adequate ocean wave data in spectral form are available for model tests. In Dessi *et al*. (2009) the correlation of the vertical bending moment (VBM) between full-scale trials and scaled-model tests was carried out in terms of the response amplitude operator (RAO) at approximately one quarter length from the ship bow. If the ship response is almost in the linear regime (up to a certain wave elevation), the comparison in terms of the RAO allows for accepting similar but not identical encountered wave spectra with the same relative wave direction. An analysis of possible error sources was carried out to explain differences in some frequency ranges. The correlation between model and full-scale measurements becomes elaborate when nonlinear phenomena such as springing and whipping occur. In Storhaug *et al.* (2009) the focus was on estimating the effect of whipping on extreme loading to verify the IACS UR S11 rule which turned out in revising the rule and increasing the requirements.

An interesting correlation study concerning cargo sloshing of LNG tanker tanks was carried out in the frame of a Joint Industry Project (JIP) with BW Gas, Teekay, DSME, Lloyd's Register, DNV, Light Structures and GTT (Pasquier and Berthon, 2012). A first comparison of sloshing impact recordings at full-scale and at model-scale was performed. For the model tests, the actual ship motions recorded at sea have been used as inputs for the simulation platform. This allows a direct comparison of full scale and model tests results without the bias induced by the use of numerical sea-keeping analysis to produce tank motions. The results of the model tests at 1:40 scale have shown a good correlation with full-scale measurements. The trend in terms of impact frequency over several days of navigation has been found fairly consistent. A comparison between the measurements in both instrumented tank corners was also found to be fairly consistent. This tends to confirm that experimental simulations of LNG sloshing at the small scale provides a correct representation of the global flow inside tanks; as expected according to theory.

5.3 Integration of experiments and numerical simulations

Individual research advances in the last decade such as high-fidelity numerical models utilizing high-performance computing, large-scale laboratory experimentation, field testing and real-time monitoring have undoubtedly increased our level of understanding of the behaviour of ships and offshore structures. In some cases, these advances are effectively harnessed in a manner that leverages all relevant developments and translates them into predictive tools that can be directly used by stakeholders that mean to improve the performance of ships and offshore structures.

Three main categories of analysis methods of ships and offshore structures exist, namely, (a) computational models (numerical simulations) based on a specific method (*e.g.,* Finite Element Method, Computational Fluid Dynamics, Smoothed-Particles Hydrodynamics, analytical, mathematical), (b) physical models that are built in a specific scale and are tested in basins, flumes or real sea, and (c) measured data analysis for the estimation of the 'health' of a structure as well as for the prediction of the future status of it. The combined use and integration of the three main categories can result in cost-effective design and construction of modern ships and offshore structures, improvement of existing ships and offshore structures as well as proactive management during their life-cycle. The required integration should focus on emphasizing the strengths and balancing their individual drawbacks. Different approach types (*e.g.*, straightforward or in-loop) for the integration are met for ships and offshore structures.

Regarding methods for prediction of future responses based on a structural health monitoring (SHM) system, Kvåle and Øiseth (2017) present a monitoring system that is designed and installed on the Ber gsøysund Bridge; measurements are used for the numerical estimation of extreme response of the offshore structure. Mondoro *et al.* (2016) present a methodology for using the Structural Health Monitoring (SHM) data recorded in observed operational cells to predict the structural response of ship hulls in unobserved cells. The approach integrates SHM data from sea keeping trials and numerical simulation in order to quantify and reduce uncertainties in the prediction of structural response. The proposed methodology fits SHM data with generalized fitting functions and then estimates the response in unobserved cells (*i.e.*, different operating conditions). The approach predicts the power spectral density (PSD) and the time domain response in unobserved cells and is capable of developing a full set of data to enable spectral and time-based fatigue life estimation approaches. Wang *et al.* (2014) propose a novel method of sub structural identification and genetic algorithms that can be applied to jack-up platforms. With this method, system identification of offshore structures with unknown wave loading, initial conditions and foundation conditions, is achieved. The proposed method is validated with numerical simulations and experimental data. Decò and Frangopol (2015) develop a risk-informed approach for ship structures that integrates SHM information for estimating real-time optimal short-range routing of ships. Risk is based on the reliability analysis of the midship section of a hull and on its associated failure consequences. Based on monitored time series, a numerical approach named Modified Endurance Wave Analysis (MEWA) is presented by Diznab *et al.* (2014) for accurate estimation of the structural performance of an offshore jacket considering the random and probabilistic nature of wave loading and utilizing optimal time duration. With regard to damage identification, Hosseinlou and Mojtahedi (2016) develop a robust simplified method for structural integrity monitoring of offshore platform structures. They provide a useful damage diagnosis process by introducing the pseudo simplified (PS) model technique and successfully acquired damage indicators by using PS baseline FE model based on monitored data. Moreover, the sensitivity of the damage diagnosis algorithm resulting from the removal of some available sensors is examined.

With regard to structural model updating based on SHM data, Wang *et al.* (2015) summarize a new approach and experimentally validate this approach on a small-scale platform model when only a few lower-order spatially incomplete modes are measured. To handle the spatially incomplete mode shapes, an interpolation mode expansion technique based on the optimal fitting

method is used. With this mode expansion method, the number of sensors, the measurement of degrees of freedom, has no distinct effect on the structural model updating of the deck mass. For the completion of missing measured monitored data (both of structural responses of a floating structure and environmental data) of a SHM system, Panapakidis *et al.* (2016, 2017) integrated clustering techniques and data analysis to establish a system identification scheme. With regards to control methods Kandasamy *et al.* (2016) provide information about hybrid vibration control methods that use monitored data and numerical analysis methods. They emphasize that hybrid vibration control methods provide more practical approaches for implementation.

SHM systems can be used for the uncertainty assessment integrated with numerical models. Aldous *et al.* (2015) propose and describe the development of a rigorous and robust method for assessing the uncertainty in ship performance quantifications. The method has been employed to understand the uncertainty in estimated trends of ship performance resulting in the use of different types of data (continuous monitoring) and different ways in which that data is collected and processed. Wu *et al.* (2016) presented an integrated monitoring system of FPSOs with soft yoke mooring systems capable for a safety assessment of the offshore structure.

A complete integration between numerical simulations, physical model tests and monitored data is presented by Yi (2016); a local damage detection approach for jacket-type offshore structures by principal component analysis (PCA) and linear adaptive filter (LAF) techniques using FBG sensors is proposed based on a statistical approach. In addition, environmental effects due to variations in temperature and external loading were investigated. The technical feasibility of the proposed method for damage detection and localization is experimentally validated against physical model tests. Apart from the integration of the analysis methods, integration can be applied for the numerical simulation of wave transformation in the nearshore. Integration between real measurements and numerical analysis may lead to decrease of scale effects.

It is common that new design tools are validated against experimental data with some recent examples mentioned in the following. Azcona *et al.* (2017) developed a code for the analysis of mooring lines that was validated against experimental data for static and dynamic conditions. Lugni *et al.* (2015) developed a combined experimental and numerical investigation on the occurrence of parametric roll and water on deck in bow-sea regular waves close to head sea for an FPSO ship, with a focus on the roll instability phenomenon. Very common linear and nonlinear damping coefficients of different rigid body motions are calculated with the use of experiments and used in integrated numerical analysis models (Irkal *et al.*, (2016); Nematbakhsh *et al.*, 2015). Zhao *et al.* (2014) proposed an integrated simulation model of a side-by-side moored Floating Liquefied Natural Gas and Liquefied Natural Gas carrier system that is calibrated with physical model tests for offloading operation.

Wave tank testing of scaled models is standard practice mainly for the validation of the dynamics of conceptual designs. For some types of offshore structures and ships, Froude-Reynolds scaling laws conflict when they are applied simultaneously (*e.g.* for the testing of offshore wind turbines). Also, for some types of structures or ships, the effect and the induced loads of mechanical mechanisms (*e.g.*, rotor nacelle assembly) that are part of the overall structure should be accounted for during the implementation of the tests. Sauder *et al.* (2016) presented a method for performing Real-Time Hybrid Model testing (ReaTHM testing) of a floating wind turbine. In ReaTHM testing, one part of the system is modelled physically, while the other part, whose behaviour is assumed to be well described theoretically, is modelled numerically. Both physical and numerical substructures interact in real-time through a network of sensors and actuators. As a result, the testing of the floating wind turbine is permitted in a basin without a real wind generation system. Azcona *et al.* (2014) proposed a new methodology for the scaling of aerodynamic loading during combined wave and wind scaled tests at a wave tank with the use of a

ducted fan governed by a real-time computation of the full rotor coupled with the platform motions during the test. The methodology has been applied to the test of a 6MW semisubmersible floating wind turbine. Bracco *et al.* (2015) developed a test rig for dry testing on the ISWEC to reproduce the rated conditions of the 1:8 ISWEC prototype. The test rig was designed to reproduce the pitching angle given a time history recorded in the wave tank tests (Feed-Through mode). A Hardware-In-the-Loop simulation is achieved since the configuration of the Power Take-Off of the ISWEC has been manufactured and mounted on a test rig that is able to simulate the wave actions on the hull of ISWEC.

6. BEST PRACTICE AND GUIDELINES

Engineering stress and structural analysis is fundamentally based on material and other structural parameters (*e.g.* stiffness) which are measured either in a laboratory or in the field *e.g.,* structural health monitoring. Clearly, there is no such thing as a one hundred percent accurate measurement as every measurement is subject to some uncertainty. Measurement uncertainties associated with material and structural test results account for the material safety factors applied in structural analysis and design (Bristow and Irving (2007)). Material test uncertainties complicate both the analysis of experimental data and their subsequent use for structural applications. Materials and structural data are imperative for all structural calculations meaning that structural design and integrity assessment of ships and offshore structures are founded upon empirical science. Contemporary structural design methods involve probabilistic risk- / reliability-based methods which in themselves are extremely powerful but also present certain concerns (UK HSE, 2001). These are identified as *"confusion which arises from vague language, ill-defined and inconsistent terminology, and misinterpretation often present in published material on the topic. This is perhaps the main reason for misuse in some applications of the methods."* Therefore, the aim of this section is to address uncertainty in mechanical test measurements and those taken in the field so that materials and structural data can be appropriately reported. An excellent starting point for understanding uncertainty in mechanical testing can be found in Kandil (2000a), Kandil (2000b) and Bell (2001). This begins with the fundamental principal that *"in general no measurement or test is perfect and the imperfections give rise to an error of measurement in the result. Consequently, the result of a measurement is only an approximation to the value of the measurand and is only complete when accompanied by a statement of the uncertainty of that approximation. Indeed, because of measurement uncertainty, a 'true value' can never be known*." The UNCERT series of publications referred to by Kandil (2000a) is an invaluable and detailed resource for this subject area and recommended for further reading. The following sections address developments in Data Uncertainty, Design of Experiments and Quality Standards as relevant to the ship and offshore structures community.

6.1 Data uncertainty

Data can be acquired from a variety of sources but for the purposes here, we will consider data produced from laboratory tests and from measurements/monitored structures and components in the field. The latter is an extremely active area for research with Structural Health Monitoring (SHM) becoming prominent for ships and in particular for new offshore wind structures and the challenge here often can be managing extremely large amounts of data generated (Brennan and de Leeuw, 2008). This study sought to provide a Structural Integrity Monitoring Index or SIMDex which related the "accuracy" or acceptable uncertainty to the manner in which the data would be used, *e.g.*, for low- or high-cycle fatigue.

With respect to uncertainty of measurement, the object of measurement is to determine the value of the measurand, *i.e.*, the specific quantity subject to measurement. A measurement begins with an appropriate specification of the measurand, the generic method of measurement and the specific detailed measurement procedure. The result of a measurement is only an

estimate of the value of the measurand and is only complete when accompanied by a statement of the uncertainty of that estimation. Uncertainty is a quantification of the doubt about the measurement results and it is a good practice in any measurement to evaluate and report the uncertainty associated with test results. There are two categories of uncertainty evaluations (UKAS, 2016):

I. Type A evaluation is made by calculation from a series of repeated observations using statistical methods;

II. Type B evaluation is done using data from calibration certificates, previous measurement data, experience with the behaviour of the measurements, manufacturers' specifications and all other relevant information.

There are many possible sources of uncertainty in testing, which can come from the test instrument, the item being tested, the test procedure, the test environment, the operator skill and the sampling issues (ASTM E8/E8M-16a, 2016). These sources are not necessarily independent as unrecognised systematic effects may exist that cannot be considered but contribute to error. The existence of such effects may sometimes be evident from a re-examination of the results of an inter-laboratory comparison programme. Therefore, the sources can be further elaborated as follows (Salah *et al.*, 2015; UKAS, 2016):

I. Incomplete definition of the test; the requirement is not clearly described, *e.g.* temperature may be given at room temperature;
II. Imperfect realisations of the test procedure; even when the test conditions are clearly defined it may not be possible to produce the required conditions;
III. Sampling – the sample may not be fully repetitive;
IV. Inadequate knowledge of the effects of measurement of environmental conditions of the measurement process; or imperfect measurement of environmental conditions;
V. Personal bias in reading analogue instruments;
VI. Instrument resolution or discrimination threshold, or errors in graduation of a scale;
VII. Values of constants and other parameters used in data evaluations;
VIII. Values assigned to measurement standards (both reference and working) and reference materials;
IX. Changes in the characteristics of or performance of a measuring instrument since the last calibration;
X. Approximations and assumptions incorporated in the measurement method and procedure;
XI. Variations in repeated observations of a measurement value made under apparently identical conditions – such random effects may be caused by, for example, short term fluctuations in the local environment*, e.g.*, temperature, humidity and air pressure, variability in the performance of the tester.

In addition, computer models for post processing and analyzing measurement data are also prone to producing errors and a method proposed by Bayarri *et al.* (2017) is worth examination to ensure computer models are properly validated.

6.2 Design of experiments

Experiments and measurements made can rely upon standard methods. However, for example for offshore structures, non-standard parameters might be investigated using experimental methods. For example, Adedipe *et al.* (2015, 2016) developed an experimental procedure for investigation of cyclic fatigue load frequency on the corrosion fatigue of offshore structural steels. In this example standard compact tension specimens were tested following the relevant

ASTM standard however, no method existed to measure crack length for a specimen in seawater. A compliance method using an electrical resistance strain gauge was devised; the method calibrated against a known approach and an error analysis established.

Roessle and Fatemi (2000) examined strain-controlled fatigue properties of steels and the sensitivity or otherwise with approximations made and Salah *et al.* (2015) reported on uncertainty estimation of mechanical testing properties using sensitivity analysis and stochastic modelling. Sankararaman *et al.* (2011) detailed an uncertainty quantification and model validation of fatigue crack growth prediction.

Experiments can be designed in addition to support design methods. For example, Grell and Laz (2010) applied a probabilistic fatigue life prediction using AFGROW (Air Force GROW, a life prediction software) and accounting for material variability.

Numerous similar examples exist however the increasing development of SHM of real structures in the field have led to renewed interest in the uncertainty of measurements as often sensors and transducers are installed in the field under non-ideal conditions with sometimes the expectation of gaining "laboratory standard" precision. A number of authors have studied various aspect of this issue including Farrar and Warden (2013) proposing a machine learning approach, Guzman and Cheng (2016) sharing experience of the use of statistical date from a monitoring programme on Alpha Ventus (an offshore wind farm in the German sector) and Scheu *et al.* (2017) who examined the influence of statistical uncertainty of component reliability estimations on offshore wind farm availability.

6.3 Quality standards

Standards for testing materials and structural parameters are abundant, however frequently uncertainty is not specified nor quantified. Some useful standards are: ASTM (2016) which describes uncertainty measurement in standard test methods for tension testing of metallic materials; ASTM (2015) which is the Standard Practice for Statistical Analysis of Linear or Linearized Stress-Life (S-N) and Strain-Life (E-N) Fatigue Data; JCGM Standard (2012) which is an evaluation of measurement data setting out the role of measurement uncertainty in conformity assessment.

SHM is a developing practice, Buren *et al.* (2017) published a paper concerning guaranteeing robustness of structural condition monitoring to environmental variability which is concerned with the practical implementation of transducers in a hostile offshore environment. A whole host of offshore wind SHM papers and the uses of measured data have recently emerged. Some of these are: Ioannou *et al.* (2017a, 2017b), Kaufer and Cheng (2014) and a very useful review by Van des Bas and Sanderse (2017) of uncertainty quantification for wind energy applications.

Finally, Hafele *et al.* (2017) describe the efficient fatigue limit state design load sets for jacket substructures considering probability distributions of environmental states, Kim *et al.* (2016) the probabilistic fatigue integrity assessment in multiple crack growth analysis associated with equivalent initial flaw and material variability and Larsen *et al.* (2013) on reducing uncertainty in fatigue life limits of turbine engine alloys.

7. CONTEMPORARY AND EMERGING TECHNIQUES

An important aspect of experimental tests are the measurement techniques used to record the particular data of interest. Each experiment is challenged by the test unit loading, size, sample rate, physical location and test scope. For each test challenge there are existing and emerging technologies to address them. The following sections summarize current and emerging techniques to meet experimental test requirements and address test challenges. An interesting development over the past few years is the reduced sensor size, increased data sample rate and multi-faceted test scopes. When combined, these factors are conceptualized as 'Big Data'; however, one must understand the criteria required before an experimental test can be considered 'Big Data'. The

concept of Big Data has been a buzz word in many industries. A review of 'Big Data' as it applies to marine and offshore structures is provided.

7.1 Overview of current techniques

There are various physical quantity measurement sensing technologies currently developed and applied to structures for different experimental test scales and data measurement requirements. This section summarizes current measurement techniques used to measure displacements (7.1.1), stress & strain (7.1.2), force (7.1.3), pressure (7.1.4), acceleration (7.1.5) and multi-variable measurements, including fibre-optics measurement and digital image correlation (7.1.6).

Table 4: Features of specimen level displacement sensors

Contents	Contact sensor	Non-contact sensor			
		Optical	Eddy current	Ultrasonic	Laser
Measurement object	Solid	Almost all	Metal	Almost all	Almost all
Measurement distance	Short	Normal	Short	Long	Short
Measurement accuracy	High	High	High	Low	High

Table 5: 3D measurement methods (Shinoda and Nagata, 2015)

Type	Method	Accuracy	Work Size	Characteristic	Application Examples
Laser Radiation	Pattern projection method	~ 0.05 mm	Several meters	High precision measurement	Assembly improvement
	Light-section method	~ 0.08 mm	Dozens of meters	Portable measurement	Process improvement of manufacture
	Time-of-flight method	~ 2.00 mm	Several meters	Wide range measurement	Measurement in a house
Digital Photograph	Photometric-stereo method	~0.085mm	Several meters	Inline point measurement	Calibration of construction equipment
	Structure from motion (SfM)	~0.025mm	Several meters	Easy point measurement	Measurement of flatness of sheet-metal
	SfM & MVS (multi-view stereo)	~ 10.00 mm	Several hundred meters	Camera + software Cheap & wide range	Large scale measurement

7.1.1 Displacement measurement

Displacement measurement can be divided into the high accuracy measurement generally used at the specimen level and large-scale level used for monitoring. At the specimen level, displacements are measured using contact and noncontact systems, as reported in Table 4.

At the large-scale level, three dimensional (3D) measuring devices are well suited for measuring displacements. Measurement systems can be classified into the laser irradiation and camera photographing types shown in Table 5 following Shinoda and Nagata (2015); employed to determine the construction position for large structural projects, 3D shape measurement, etc.

7.1.2 Strain/stress measurement

Strain measurement is commonly acquired using electrical resistance strain-gauges and optical methods such as the photoelastic method. In addition to electrical resistance and optical methods, there are various measurement methods applied in accordance with specific test purposes. These are divided into point measurement (point-by-point local measurement) and full field measurement relative to a finite area size. Each feature is summarized in Table 6 and 7.

Table 6: Point strain measurement methods

Method	Measured value	Conversion to Strain/Stress	Measurement Range
Electrical resistance strain gauges	Gauge metal electrical resistance change. Resistance change is converted to voltage using a Wheatstone bridge circuit.	Point Strain By using change of electrical resistance and gauge factor.	Normal type: +/- 2% ε Post yield type: +/- 20% ε (-20 ~ 80 °C)
Displacement meter Contact type Non-contact (laser) type	Change of gauge length.	Point Strain = (change of gauge length) / (gauge length)	Dependent on the resolution of the displacement-meter.
X-ray stress measurement	Change of distance between lattice planes based on crystal diffraction.	Point Stress/Strain using the angle between normal line of lattice plane and that of specimen surface, and the diffraction angle.	Elastic-Plastic stress can be measured.
Neutron diffraction measurement	Change between lattice planes based on crystal diffraction.	Point Stress/Strain. Measures the stress at a deeper location than X-Rays.	Elastic-Plastic stress can be measured.

Table 7: Field strain/stress measurement methods

Method	Measured value	Conversion to Strain/Stress	Measurement Range
Photo-elastic	Stress distribution by the double reflex of polymer material.	Stress distribution (principal stress difference).	It is dependent on the model size.
Moire	Distance between Moire pattern. The grid which were attached to the object surface and reference grid are superimposed optically, and the Moire pattern arises due to deformation of the object.	Strain distribution ε = p / d p: pitch of reference grid d: distance between Moire pattern	Surface of object attached grid; • Geometric Moire = 0.025 ~ 0.05 mm • Moire Interferometry = .001 ~ 0.01 mm
Holographic	Diffracted light field scattered from the object.	Strain distribution (out-of-plane displacement)	Measuring range is small (< several cm Accuracy < 0.1 μm)
Speckle	Movement of the speckle pattern which arises laser beam interference.	Strain distribution	Accuracy < 10 με Measurement time < 10ms
Thermo-elastic	Temperature change accompanying elastic deformation.	Stress distribution Cyclic loading is required.	Dependent on the resolution of the Thermo-viewer.
Stress Paint	State of paint crack on surface of objects: Number and direction of crack.	Maximum strain distribution (principle stress).	Sensitivity is low (700 - 800 με)
Image Correlation	Distance between dots on material surface.	Stress distribution on the surface of object.	It is dependent on the resolution of the CCD camera.

Residual stress can also be measured using some of the techniques listed in Tables 3 and 4. Ficquet *et al.* (2013) presented a classification of various measurement methods for residual stresses based on the measurement depth and the depth of removed material. High accuracy in the residual stress measurement is important for the evaluation of fatigue and buckling strength. Kleiman *et al.* (2012, 2013) developed an ultrasonic computerized complex for the measurement of residual stresses. The average through thickness stresses can be measured using the acoustic-elasticity effect; according to which the velocity of elastic wave propagation in solids is dependent on the mechanical stress. Examples of non-destructive evaluation of stresses are shown in this paper as well as the verification of the method effectiveness. Sotoudeh *et al.* (2013) investigated residual stresses in steel-to-nickel dissimilar joints by using Neutron Diffraction Technique.

7.1.3 Force measurement

There are basically two kinds of load cells to measure forces:

- Strain-gauge (SG) type
- Piezo-electric (piezo) type

The SG-type load cell consists of a transducer element, deformed by the applied force, on which the strain gages are attached. The voltage output signal from the strain gages is related to the applied force. A piezo-electric sensor (crystal piezo electricity sensor) consists of two sets of quartz plates and an electrode foil in the middle. Since the crystal generates an electric charge proportional to the load applied along a specific crystal direction, the strain can be measured via the piezo-electric effect. Using a charge amplifier, the electric charge is converted into a voltage signal related to the applied load. The strain-gauge type sensor has little data drift and is therefore well suited for long-term monitoring applications. On the contrary, the piezo-electric type sensor presents a small amount of drift requiring zeroing before measurements and dedicated processing. In comparison with the strain-gauge type sensor, the piezo crystal element generates an electric charge only when the applied force is changed and the piezo-electric sensor itself has a higher natural frequency; making it well suited for dynamic motion and time-varying force measurement.

7.1.4 Pressure measurement

There are various kinds of pressure sensors used for different measurement conditions, pressure range and sensing material. Due to the bending deformation of the sensor diaphragm in contact with the fluid, pressure can be convertible into other physical quantities such as deformation. In turn, this deformation is transduced into an electrical output like voltage or current depending on the device. Pressure can then be calculated based upon the area of the loaded diaphragm. The most common types of pressure transducers are reported below.

(*i*) *Wheatstone bridge*
The strain-gages connected to a Wheatstone bridge configuration is the most common pressure sensor. This type of sensor can meet the demand of various accuracy, size, strong nature, and cost testing requirements. The bridge base sensor can measure absolute pressure, gauge pressure, and differential pressure in high or low voltage applications. The strain gauges are used for detection of deformation of the pressured diaphragm.

(*ii*) *Electrical capacitance*
The electrical capacitance pressure sensor utilizes the capacitance change between a metal diaphragm and a fixed metal plate. The capacitance between the two metal plates changes with the distance between metal plates resulting from the applied pressure.

(*iii*) *Piezoelectric*
The piezoelectric type sensor uses only the electrical property of the crystal oscillator. The crystal generates an electric charge when deformation takes place. This charge is then converted to a proportional output voltage with the aid of an amplifier. The applied pressure is measured by output voltage. Piezoelectric sensors are sensitive to the influence of shock and vibration.

(*iv*) *Optical fibre*
Optical fibre type sensors can also be used to measure pressure. Wakahara *et al.* (2008) developed the affix-type multipoint pressure sensor by using Fibre Bragg Grating (FBG) technology. In this study, the FBG pressure sensor was affixed to the fore and aft-body surfaces of a model ship during resistance tests. The optical fibre sensor allowed for the measurement of multi-point pressure on curved surfaces of a ship with temperature compensation. The measured pressures were compared with the result of CFD calculations and found that the FBG pressure sensor effectively measured multipoint pressure on the surface of the model ship during resistance tests.

The bridge-based and the piezoelectric type sensors are most commonly used as pressure transducers because of their simple structure and excellent durability. Thus, they are comparatively low cost and well suited for a multi-channel system. Generally, the foil strain gauge is used with high pressure (up to 700 MPa) application. The electric capacity type and the piezoelectric type pressure transducer are generally stable and linear; however, when compared with other pressure sensors, the setup is complicated and can be easily subject to the influence of heat. The piezoelectric type sensor is excellent when the response to pressure change is measured. It is therefore well suited for pressure measurement of fast phenomena, such as explosion problems.

7.1.5 Acceleration measurement

Accelerometers are used to measure the acceleration (velocity change rate) of an object. Accelerometers are classified in Table 8.

Table 8: Acceleration measurement methods.

Method	Frequency	Max. Acceleration (G)	Sensitivity	Principle/Characteristic
Piezoelectric type	~10 kHz	50,000	+/-1~2 %	The piezoelectric acceleration sensor is measuring acceleration using the piezo-electric effect.
Servo type	DC ~ 300 Hz	10	+/-1 %	Since small and high-accuracy measurement is possible, it is used in broad fields such as vibration measurement and seismic observation
Strain gauge type	DC ~ kHz level	1,000	+/-1 %	There are metal type and semiconductor type which use the strain gauge for the relative-displacement detection sensor.
Semiconductor-type	Hz~10 kHz level	20,000	+/-1 %	These use MEMS (Micro Electro Mechanical Systems) technology. • Capacitance type • Piezoresistance type • Thermal detection type

Table 9: Comparison between Optical Sensing Technologies (distances are approximate).

Technologies	Topology	Range	Temperature	Strain	Pressure	Vibration
OTDR	Distributed	< 70 m	Yes	Yes	No	No
ROTDR	Distributed	< 20 km	Yes	No	No	No
BOTDR	Distributed	< 50 km	Yes	Yes	No	No
FBG	Multi-Point	< 50 km	Yes	Yes	Yes	Yes
Fabry-Perot	Single-Point	< 10 km	Yes	Yes	Yes	Yes

7.1.6 Multi-variable measurements

(1) Fibre Optic

The fibre optic sensor has an optical fibre connected to a light source to allow for detection in tight spaces. The fibre optic sensor is available for measuring most physical data such as temperature, strain, pressure, vibration, etc. Since the sensor assembly is constituted from glass, the optical fibre sensor does not require electric supply, shows excellent explosion-proof performance and resistance to thunderbolt and electromagnetic induction noise. A particular feature

of fibre optic sensors is its ability to connect multipoint sensors using one optical fibre. Some typical optical fibre sensors are listed below and summarized in Table 9.

- OTDR (Optical Time Domain reflectometer). The fracture location and bending point of an optical fibre are detectable. Example: Maintenance of fibre optic cable, Falling-stone detection, Watergate opening-and-closing detection.
- ROTDR (Raman Optical Time Domain Reflectometer). The temperature distribution along optical fibre is measured. Example: Temperature monitoring of a power cable, fire detection in a tunnel.
- BOTOR (Brillouin Optical Time Domain Reflectometry). The strain and temperature distribution along optical fibre are measured. Example: Measurement of strain distribution of bridge / large structures, slope failure detection.
- FBG (Fibre Bragg Grating). Distortion, temperature, pressure, etc. are measured using the reflected light of the diffraction grating formed in optical fibre. Application: strain, vibration, displacement, temperature, pressure measurement of the structure.
- Interferometric sensor (Fabry-Perot optical fibre). The interference phenomenon by composition of two waves is extracted. Application: strain, vibration, temperature, pressure, shock strain measurement of the structure, sonar.

(2) *Digital Image Correlation*
Digital Image Correlation (DIC) is a full-field image analysis method based on grey-scale digital images that can determine the contour and displacement field of an object in three dimensions under load. The accuracy of the Digital Image Correlation system with high-speed digital cameras was thoroughly investigated in both field and laboratory conditions by Schmidt *et al.* (2005a). Rigid body panel translation results, conducted in-situ on a test range, matched a calibrated micrometer within 1.09% for 0.1-inch increments from 0.1 to 1.0 inches with greater accuracy for most increments. The dynamic displacements from a bend and release laboratory test closely matched those from a laser interferometer, and strains from the same test matched both strain gauges and calculated values. The worst-case error for dynamic displacement was 1.27 %. The technique is broadly applicable for air blast deformation measurements, crash testing, high strain rate testing, and other dynamic phenomena. Catalanotti (2010) applied the DIC method to measure the crack resistance curves in CT and CC test specimens manufactured using cross-ply CFRP composite laminates. The measurement fields are the basis for the rigorous determination of the surface crack or kink-band tip (in the absence of delamination) location, and for the automatic computation of the J-integral. The comparison between the R-curves obtained in CT specimens using the FE-based post-processing and the DIC-based method indicates that the results are virtually the same and that the DIC method proposed is a valid alternative to measure R-curves associated with longitudinal tensile failure mechanisms in composite materials.

7.2 Novel measurement Techniques

This section concerns the most significant advances made in sensor technology to address sensor size, network configuration and power consumption challenges. More specifically, microelectromechanical systems have reduced sensor size significantly, wireless sensor networks have expanded the scope of sensor applications, and energy harvesting devices on-board sensor systems now support remote sensing capabilities. The following sections provide a summary of microelectromechanical systems, wireless sensor networks and energy harvesting devices.

7.2.1 MEMS

Microelectromechanical systems (MEMS) are sensor systems micro-machined into silicon, glass, ceramics, polymers, titanium or tungsten. MEMS are commonly micro-machined out of silicon due to its affordability and the availability of micro-machining infrastructure within the electronic integrated circuit industry (Maluf *et al.*, 2004)). MEMS machined shape and design

are customized for a particular application to utilize piezoresistive, piezoelectric and thermoelectric effects. Examples of MEMS pressure, accelerometer and angular rate sensors are also reported in Maluf *et al.* (2004). The pressure sensor in Figure 7 utilizes piezoresistors on the N-type (negatively charged silicon) layer to convert the stress in the N-type layer (produced by pressure on the layer) to voltage. The sensitivity of the pressure sensor can be adjusted by the N-type layer thickness and piezoresistor positioning in the areas of highest stress concentration with identical resistance (Maluf *et al.*, 2004). Piezoresistors without identical resistance will result in zero offset and affect the quality of the sensor measurement. The accelerometer shown in Figure 8 also utilizes piezoresistors to convert the acceleration of the MEMS inertial mass to voltage. Acceleration of the MEMS sensor causes the inertial mass to rotate about the hinge, displacing the piezoresistors.

The size and relatively inexpensive cost of MEMS sensors make them an attractive alternative to conventional sensors. Calibration and accuracy of the MEMS sensors is one challenge that may result in poor sensor system performance. The following sections present methods and challenges of MEMS calibration as well as some examples of MEMS application.

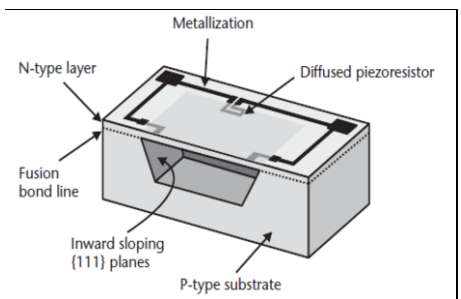

Figure 7: Piezoresistive pressure sensor (400 µm x 800 µm x 150 µm) converting stress in N-type layer to voltage (from Maluf *et al.,* 2004).

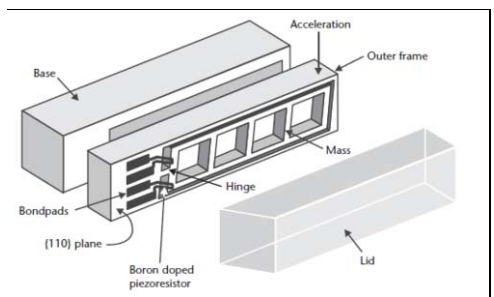

Figure 8: Piezoresistive accelerometer converting inertial mass displacement to voltage through piezoresistors (from Maluf *et al.,* 2004).

(1) *MEMS Sensor Error and Calibration*

One particular application of MEMS sensors is within a navigation aid inertia measurement unit (IMU). An IMU consists of accelerometers and gyroscopes (angular-rate sensors) to measure the position of an object in six degrees of freedom. The accuracy of the IMU gyroscope and accelerometer is important when considering the amount of drift that develops from an accelerometer or gyroscope with bias offset or noise. As such, it is important to verify the MEMS-based IMU is sufficiently accurate for its application. To quantify the accuracy of an IMU, a grade scheme is proposed in (Barbour, 2010) (shown in Table 10) as a function of the MEMS bias stability (bias rate).

Table 10: Navigation IMU grade levels (reproduced from Barbour, 2010).

Application Grade	Commercial	Tactical	Navigation	Strategic	
Gyroscope	> 1 deg/s	~ 1 deg/h	0.01 deg/h	~0.001 deg/h	
Accelerometer	> 50 mg	~ 1 mg	25 µg	~1 µg	

Generally, MEMS inertial sensors are calibrated within the laboratory before deployment into the field. Unfortunately, the installed environmental conditions, age of the sensor and run-to-run biases and thermal drifts are dynamic in nature and require infield calibration (Barbour, 2010). This is especially accurate for low-cost MEMS-based inertial sensors which suffer from large errors due to temperature dependence (Barbour, 2010). The review paper by Barbour (2010) provides an extensive summary of inertial sensor errors and calibration techniques in the laboratory and field.

MEMS-based inertial sensors are subject to deterministic and random classes of errors. Deterministic errors are a result of the system properties or manufacturing defects and removed through calibration (Barbour, 2010). Deterministic errors include:

- Bias: A nonzero output when no load input is applied. Bias is divided into static (offset), dynamic time varying (bias drift) and dynamic temperature varying (temperature drift).
- Scale Factor Error: When the ratio between the rate of change of output to the rate of change of input in is not consistent.
- Non-orthogonality Misalignment Error: The misalignment of the sensor sensitive axis with the platform axis.

Unlike deterministic errors, random errors cannot be corrected through calibration algorithms. Random errors require a stochastic modelling approximation in order to minimize their effect on the system reading. The calibration techniques reviewed in Barbour (2010) are generally categorized as:

- Calibration with High-Precision Equipment: Installing the IMU onto a levelled turntable (single or multi-axial) coupled with specific techniques, Kalman filtering and optimization algorithms to determine the precise inertial sensor error coefficients
- Calibration without Equipment Multiposition-based: Utilizes the Earth's gravity and rotation rate during infield calibration to determine the error coefficient
- Calibration without Equipment Kalman Filter-based: Utilizes Kalman filtering techniques to estimate the navigation state as well as the calibration error coefficient
- Camera-IMU Self-Calibration: IMU self-calibration via joint camera utilizing object shape and motion to estimate calibration parameters

Some of the concluding remarks indicate additional work is required to incorporate nonlinear scale factors, magnetic disturbances and g-dependent bias in the calibration algorithms. When reviewing the different calibration methods within (Barbour, 2010) it is important to consider that the paper focuses on low-cost MEMS. Different grades of IMUs will have different sensitivities and calibration requirements. The following section on MEMS applications highlights several comparisons between conventional and MEMS-based sensor systems. Once the sensor systems were compared they were used on a normal and abnormal motor to detect the associated faults using a wireless sensor system. Test results indicated that low-cost MEMS-based sensors are sufficiently accurate to replace conventional sensors.

(2) *MEMS application examples*

An example of a MEMS application in a harsh environment is the early work of Stauffer (2006). In this paper, the MEMS accelerometer is subject to 10,000 successive shocks of 1,000 g (sensor mounted onto a M16 gun) and remains within the required specification, unfortunately not further clarified. In addition to the extreme shock loads, the MEMS products were demonstrated to fully function from -120ºC to 180ºC. The grade of the MEMS sensors or the specification tolerances are not provided; however, this is a promising example of MEMS applications in harsh environments.

A comparison of MEMS-based accelerometers and current sensors was reported in Son *et al.* (2016) for machinery fault diagnosis applications. Conventional and MEMS-based accelerometers were subject to periodic and impulsive excitation using a calibration exciter and modal

impact hammer, respectively. The MEMS-based accelerometer was consistent with the conventional accelerometer for the frequency excitation; however, some variation was observed in the impulsive test amplitude and wave form. Variations observed in the impulsive excitation were likely a result of difference in mass between the two accelerometers. The paper also evaluated the performance of a MEMS-based current sensor with two conventional current sensors using different magnitudes of 60Hz AC electricity. Test results showed that the MEMS-based sensor had higher noise levels and showed more sensitivity at lower frequencies.

The works by Bryne *et al.* (2016) evaluated two low-cost MEMS IMUs using nonlinear observer (NLO) theory for attitude estimation and virtual vertical reference (VVR) measurement in heave estimation. Performance of the MEMS-based IMUs were compared to measurements by proven sensor systems for marine surface vessels. In the works of Bryne *et al.* (2016) they acknowledge that MEMS sensor errors include: bias, noise (internal and external), nonlinearity, scale factors, cross-coupling and g-sensitivity. It was assumed that the nonlinearity, scale factors, cross-coupling and g-sensitivity sensor error were accounted for by the IMU manufacturer and neglected in this study. An offshore supply vessel operating in the North Sea with a Rolls-Royce Marine dynamic positioning (DP) system was used to evaluate one STIM300 and ADIS16485 MEMS IMU. The MEMS IMUs (and NLO theories) were compared using station keeping with the DP system and manoeuvring over two hours. The study found that the choice of NLO theory has a greater influence on the sensor performance than the IMU. The results of the manoeuvring study found that the attitude estimation of the MEMS IMU was within acceptable limits; however, the heave estimate was 'marginally acceptable'.

7.2.2 WSN

The advent of wireless sensor networks (WSNs) has provided a solution for sensor networks in environments too harsh for or without access to a consistent power source. A WSN consists of sensor nodes to measure, store, process and transmit data wirelessly to a base station(s) which receives, compiles, stores and transmits the sensor data to a server network. Generally, the base station and server network have access to a constant power source with the sensor node relying on its own power source to perform its duty. Some application examples include:

- Railway condition monitoring (Hodge *et al.*, 2015): WSN utilizing fixed MEMS sensors with energy harvesting and mobile base station on the locomotive.
- Animal tracking (Zebranet) (Puccinelli and Haenggi, 2005): WSN using mobile low-power global positioning system with peer-to-peer data swaps for improved database reliability.
- Smart power grid (Fadel *et al.*, 2015): Groups of WSNs to monitor power generation, transmission and consumption.
- Building response to seismic events (Torfs *et al.*, 2013): WSN using MEMS accelerometers and strain gauges with line-of-site linkage with base station.
- Self-healing mine field (Rolader *et al.*, 2004): WSN which uses RF to autonomously reposition mines in an anti-tank mine field.
- Sniper locator (Maroti *et al.*, 2004): WSN utilizing hundreds of sensors to self-localize and use acoustic principals to locate a sniper in an urban multi-path environment.

The performance of the WSN is highly dependent on the capability and reliability of the sensor nodes ability to measure, process, store and transmit data to the base station. The following sections will focus on the sensor to base station layout, protocols, challenges and potential solutions of WSN.

(1) *Sensor Node*
The sensor node is required to perform its specific measurement function as well as process and store the data until it is transmitted to the base station while using a remote power supply. According to Rawat *et al.* (2014), a sensor node consists of:

- Sensor suited for its application,
- Energy source and storage,
- Processor/microcontroller for data manipulation,
- System protocols,
- Memory for data storage, and
- Transceiver to transmit data to the base station.

Some available sensor node examples are IRIS (Memsic (2017a)) and MICAz (Memsic, 2017b), both used in large scale networks (over 1000 nodes) for building monitoring/security to measure high speed acoustic, video and vibration data, IMote2 (Crossbow, 2017), used for condition health, vibration and seismic monitoring and analysis as well as digital image processing, Waspmote (Libelium, 2017), highly customizable sensor node with 120 different sensor applications and 16 different wireless communication interfaces, and WiSMote (WiSMote, 2017), used for measuring temperature, luminosity and acceleration (3-axis). For each sensor node component listed above there are layouts, specialized components and protocols developed to optimize the node and network capability and reliability.

(2) *Sensors*
The low power requirements of WSNs mean MEMS sensors are well suited; however, many applications include traditional sensor devices. A detailed review of sensor types is listed in Section 7.1.

Table 11: Energy consumption of common sensor node platforms (from Shaikh and Zeadally, 2016).

	IRIS	MicaZ	IMote2	Waspmote	WiSMote
Radio Standard	802.15.4/ ZigBee	802.15.4/ZigBee	802.15.4	802.15.4/ZigBee	802.15.4/ZigBee/6LoWPAN
Microcontroller	Atmega1281	ATMEGA128	Marvell PXA271	Atmel Atmega 1281	MSP430F5437
Sleep	8µA	15µA	390µA	55µA	12µA
Processing	8mA	8mA	31-53mA	15mA	2.2mA
Receive	16mA	19.7mA	44mA	30mA	18.5mA
Transmit	15mA	17.4mA	44mA	30 mA	18.5mA
Idle	-	-	-	-	1.6mA
Supply	2.7-3.3V (2x AA Battery)	2.7V (2x AA Battery)	3.2V (3x AAA Battery)	3.4-4.2 V (battery)	2.2-3.6V (2x AA battery)
Average	-	2.8mW	12mW	-	-

(3) *Energy Source/Storage*
Sensor nodes require a remote source of power from either battery, USB or energy harvesting device. Sensor nodes equipped with energy harvesting capability need a converter to convert the energy and store it in a supercapacitor or recharge a battery (Shaikh and Zeadally, 2016). The power requirements of currently available sensor node platforms are listed in Table 11.

Each sensor platform is customizable to the project measurement and transmission requirements. The sample and transmission rates will increase the power requirements of the unit. Therefore, assume the listed power requirements are a minimum for the listed platforms.

(4) *Microcontroller*

Sensor nodes are generally equipped with a microcontroller or processer to manage/compute the data processing as well as store and send data to the base station. The sensor node instructions (sampling, transmission and storage rate and range), updates and protocols are managed by the microcontroller. Sensor node data processing includes data validation (Hodge *et al.*, 2015) by analysing sensor and data status to determine the presence of sensor faults, data noise or null values and minimize communication errors.

Table 12: Summary of WSN standards and technical details (from Rawat *et al.*, 2014).

	Frequency (ISM)	Max Data Rate	Range	Battery Life	Network Topology	Power Consumption	Target Market/Application
IEEE 802.15.4 (ZigBee)	868/915 MHz: 2.4 GHz	250 kbps	100 m	Days-years	Star, P2P, Mesh	Low	Smart-meter, Smart grid devices
UWB IEEE 802.15.4a	3.1-10.6 GHz	110 Mbps	10 m	Multi-year		Low	Real-time monitor and track location (Indoor)
Blue-tooth	2.4 GHz	3 Mbps	10-100 m		P2P	Low	Consumer electronics
BLE	2.4 GHz	1 Mbps	200 m	Months - Years	P2P	Ultra-low	Health fitness, Smart devices
Z-wave	sub - 1 GHz	40 kbps	30 m	Multi-year	Mesh	Low	Home automation, security, consumer electronics
ANT	2.4 GHz	1 Mbps		Year	Star, P2P, Tree, Mesh	Ultra-low	Health Fitness, Heart-rate monitor, Speed sensors
Wavenis	868, 915, 433 MHz	100 kbps	1-4 km	Multi-year	P2P	Ultra-low	M2M, smart meter, Telemetry, Home automation
Dash7	433 MHz	200 kbps	2 km	Multi-year		Low	Mobile payments, Smart meter, Supply chain
EnOcean	868; 315 MHz	125 kbps	300 m	Battery-less		Ultra-low	Building, Industrial automation self-powered sensors, switches.

(5) *Protocols*

The data transmission component of the WSN consumes the most power (Magno *et al.*, 2013). It is therefore important to set the sensor node protocols to minimize data transmission and extend battery life. Protocols are the procedures the WSN follows to optimize the battery life of the sensor nodes and meet the requirements of the application. The following protocol examples from an open system interconnection model (Hodge *et al.*, 2015) consisting of five layers in the protocol stack with data transmission planes:

- Physical layer: Manages how data is transmitted to the network from the sensors.
- Data link layer: Manages the network topology (tree, mesh, etc.)
- Network layer: Manages how the data is transmitted through the data (in data packets for example).

- Transport layer: Manages sending and receiving of data.
- Application layer: Manages software data access.
- Power management plane: Manages sensor node power consumption.
- Mobility management plane: Manages the location of the sensor nodes (especially important in mobile WSNs).
- Task management plane: Manages node groups to ensure power and data generation levels are in line.

(6) *Memory and data transmission*
Data storage volume on board the sensor node is customizable to the application sample rate, data processing and transmission rate. The sensor node may be required to store and process/prepare large volumes of data before the transceiver is able to transmit the data to the base station. Data transmission between the sensor node and the base station is generally transmitted via wireless communication standards such as IEEE 802.11 (WiFi) and IEEE 802.15.4 (short range, low power and low data rate wireless sensor communication) (Rawat *et al.*, 2014). IEEE 802.15.4 specifies the physical and medium access control (MAC) lower layers of the protocol stack. The upper layers of the protocol stack are defined by 6LoWPAN (Montenegro *et al.*, 2007), Zigbee, ISA1001.11a and WirelessHART (Kim *et al.*, 2008). Some examples of emerging wireless technologies include; Bluetooth low energy, ZigBee green power, Wi-Fi direct and EnOcean (Rawat *et al.*, 2014). A technical summary of the WSN standards/technologies are provided in Table 12.

7.2.3 Energy Harvesting Devices

There are many energy harvesting devices that can be used in sensor nodes to support power requirements. Available energy sources include radio frequency (RF), solar, thermal, fluid flow-based, wind, microbial fuel cell (using microorganisms to convert chemical energy to electrical energy) and mechanical-based energy (vibrations, pressure and stress-strain) which utilize electromagnetic, electrostatic and piezoelectric methods to convert the energy to electricity. Each energy source can be harvested and used to charge a battery or supercapacitor or directly power the sensor node (assuming the energy source is constant and regular).

RF-based energy harvesting converts radio waves from a radar or antenna to DC power through a conditioning phase (Kausar *et al.*, 2014). The type of condition and efficiency is dependent on input power range (distance between source and receiver), application requirements, source power and antenna gain. The RF source may be the base station in a WSN, data mule or dedicated source in positions throughout the sensor field when a reliable external power source is available. As the distance between the source and sensor node increases, the converted power decreases. In order to boost the power, the sensor node conditioning phase can include: Multistage Villard Voltage Multiplier circuit, Multistage Dickson Charge Pump, or Multistage Cockcroft-Walton Multiplier (Shaikh and Zeadally, 2016). Examples of RF-based energy harvester are passive radio frequency identification tags used to track animals or near field communications between smartphones.

Solar energy harvesters utilize the photovoltaic effect to convert solar rays to DC power through silicon-based cells. The most effective way of utilizing a solar harvester is by storing the energy in a supercapacitor or battery and using the energy when required (Shaikh and Zeadally, 2016). Similar to the customization of WSN for a particular application, the solar panel size, cell composition and efficiency are also customizable for off-the-shelf sensor nodes. Some challenges with respect to photovoltaic cells are the variability of sunlight and cleaning frequency (Hodge *et al.*, 2015).

Thermal energy harvesters utilize the Seebeck effect to convert the temperature differential across a thermoelectric generator (TEG) to power (Shaikh and Zeadally, 2016). The usability

of thermal harvesters is a balance of the TEG characteristically low efficiency and high reliability. Some examples of thermoelectric harvesters include wearable TEG used in wireless area body networks to monitor physiological parameters. Wearable TEGs use the temperature differential between the room and body to produce approximately 0.026 mW for 36ºC/30ºC temperature differential (Shaikh and Zeadally, 2016).

A comparison between different energy harvesting sources and associated power density are listed in Table 13. By comparing the power density in Table 13 with the average power requirement of the MicaZ node platform in Table 12, one can compute the proportion of the node power supplied by an individual or series of energy harvesters for a particular application.

Table 13: Energy harvesting methods used for WSNs (reproduced from Kausar *et al.*, 2014).

Energy Source	Classification	Power Density	Weakness	Strengths
Solar power	Radiant Energy	100 mW/cm^3	Require exposure to light, low efficiency for indoor devices	Limitless use
RF waves	Radiant Energy	0.02 μW/cm^2 at 5km	Low efficiency for indoor	Limitless use
RF energy	Radiant Energy	40 μW/cm^2 at 10m	Low efficiency for out of line of sight	Limitless use
Body heat	Thermal Energy	60 μW/cm^2 at 5ºC	Available only for high temperature differences	Easy to build using thermocouple
External heat	Thermal Energy	135 μW/cm^2 at 10ºC	Available only for high temperature differences	Easy to build using thermocouple
Body motion	Mechanical Energy	800 μW/cm^3	Dependent on motion	High power density
Blood flow	Mechanical Energy	0.93 W at 100 mmHg	Energy conversion efficiency is low	High power density
Air flow	Mechanical Energy	177 μW/cm^3	Low efficiency for indoor	High power density
Vibration	Mechanical Energy	4 μW/cm^3		High power density
Piezoelectric	Mechanical Energy	50 μJ/N		High power density

7.3 Big-data analysis

The reduction in sensor size, sensor application variability, sample rate and network means that the collected data from experimental tests of health monitoring has the potential to get to Big Data levels. Examples of Big Data volume, veracity, variety and visualization in the literature with respect to marine and offshore structures is limited. The available literature consists of news articles and marketing material for different companies and class societies offering their services in the Big Data space (*e.g.*, Antuit, 2016). The initial goal of this section is to capture the technical details of Big Data applications to marine and offshore structures. Unfortunately, the bulk of the literature pertains to data collection, sorting, storage and retrieval on an electrical or network system level (*e.g.*, Pantelimon *et al.*, 2016; Perner, 2015; Spaho *et al.*, 2015; Simms, 2015; Tan *et al.*, 2016); outside the scope of ISSC. Alternatively, a high-level review of Big Data and its role in the maritime industry is provided.

7.3.1 Values of Big Data as a Technology

Today, Big Data (technology) is considered valuable to address the following challenges in and of data (DNV-GL, 2014; IBM, 2014; Huang *et al.*, 2014; Kambatla *et al.*, 2014; Koga, 2015; Lovoll and Kadal, 2014; Tableau, 2017; Wang, 2017) – Volume, Velocity, Variety, Veracity and Visualization.

- *Volume*
  Volume is the value of Big Data that most believe (Lu *et al.*, 2015). The reality is that most of our maritime data is remotely comparable in size with those in the financial or pharmaceutical industry.

- *Velocity*
  Velocity of data in motion makes data bigger. With the current costs of satellite communication, it is not feasible to "stream" data from a remote offshore rig every single second. Usually, a ship exchanges data onshore via satellites once every two to three hours or a few minutes. This pragmatism slows down the move of the maritime data, and consequentially, prevents our data from becoming "big".
- *Variety*
  It characterizes the daily routines of the brave souls offshore. Sailors steering a powered ship in rough seas rely on a variety of information or data, such as forecast of weather and seas, route and location, vessel speed, fuel consumption, emission, machine health and efficiency, cargo delivery and so on.
- *Veracity*
  Veracity of data is a challenge. Maritime data is inherently associated with uncertainties and flaws. Like all other industries, it is a lasting challenge to deal with data quality (Hazen *et al.*, 2014; Kwon *et al.*, 2014; Lin *et al.*, 2015).
- *Visualization*
  This is an opportunity being explored. Charts, diagrams and dashboards are proven marvels for visualizing insights gained from data analysis. If delivered in a secured cyber space, the modern visualizations would enable faster decision-making that leads to better operational efficiency.

The maritime industry is busy harnessing the technological advantages in Variety, Veracity and Visualization, while keeping an eye on the rising opportunities in Volume and Velocity.

7.3.2 Recent Activities in the Maritime Industry

Activities in development and adoption of Big Data are seen in classification societies, OEMs, in addition to technology start-up companies.

(*i*) *Classification societies*
Classification societies see the importance in data and have identified data as a strategically important area for future shipping industry and class services. The American Bureau of Shipping (ABS) views Big Data as one of the key technologies that support future classification services (ABS, 2015; Howard, 2016). They conducted a Proof of Concept project (Wang and Hu, 2016a) to investigate the feasibility of Big Data for maritime use and the gap in adoption of Big Data technologies. DNV-GL (2017) has launched a new industry data platform – "Veracity" – to help the maritime industry improve its profitability and explore new business models through digitalization. This data platform is designed to help companies improve data quality and manage the ownership, security, sharing and use of data. Lloyd's Register (2014,a,b) describes the importance of Big Data in shipping and offshore oil and gas industries, and listed data management and data analytics as key technologies that the industries will invest in now and in the near future (LR, 2016). Class NK (2015, 2016) established a Ship Data Center with partners of IT companies and Japan's shipping companies. The intent is to collect shipping related data.

(*ii*) *OEMs*
OEMs intend to build technology-driven services for maintenance of equipment and systems. With more and more "smart" products sold, OEMs are trying to capitalize the large volume of data from sensors that are built into their machinery products. Predictive analytics are used more and more to support condition-based maintenance (CBM) and alike to rationalize the maintenance scheme that has been largely age or calendar-based. Big Data as a technology is increasingly integrated into CBM to:

- Extract, move, store data related to machinery condition
- Assess the machine's health and efficiency
- Predict the future condition
- Optimize the maintenance program
- Report for regulatory compliance

A notable example is GE Predix (GE, 2015; Dittrick, 2016), an industrial IoT platform, which is specifically designed for the unique and complex challenges of industrial data. Predix is developed to drive the digital transformation of GE's own businesses across 10 industries. This unique and flexible platform is built with some Big Data technology for managing the entire flow of data.

(*iii*) *Start-ups*

Big Data has been favoured by companies building new services. Some have shown tangible promises. AIS data service deals with vessel tracking data (or AIS data) in a similar way to GPS data and has become free and available to the general public. Some companies have gone one step further - generating operational profiles from many vessel's AIS data (Armstrong, 2013; Mathews, 2016). This leap forward was made possible with Big Data, where AIS data (with inherent uncertainties) are collected and processed at scale and speed. The insights gained from analysis would tell how a vessel is most likely operated, which is a key input to optimization of ship operations and designs. Another example is provided by performance benchmarking. As more organizations adopt performance evaluation schemes in guiding designs and operations, how to quickly gather data from a large pool of vessels is identified as a challenge. Big Data offers tools that meet the required agility in data extracting, transformation and processing. Industrial projects and start-up companies have demonstrated the great potential of Big Data as a cost-effective, agile tool for gathering and aggregating data in different formats from various sources (Tan *et al.*, 2015; Wang and Hu, 2016).

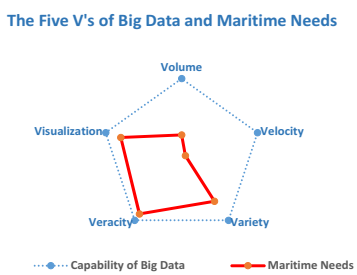

Figure. 9: The power (5 V's) of Big Data to the maritime industry versus its full potential as a technology (Wang, 2017).

7.3.3 Status of Maritime Application of Big Data

Big Data as an IT has advanced to a great level of maturity as Gartner's Hyper Cycle claimed over the last few years (Gartner, 2017). At briefly explained in the last sub-section, the maritime industry is now mostly exploring Big Data with growing expectation (Dugan *et al.*, 2014), and has not yet reached the stage when our industry enjoys the fruits that Big Data as a technology can bring to us (Wang, 2016b).

7.3.4 Future Potentials of R&D

As the industry is increasingly digitized, Big Data and technologies that support data will continue to be a focal point of R&D (Wang *et al.*, 2015; Wang, 2016b). As the maritime industry is still exploring the vast possibilities that Big Data may offer, we can foresee continued interest in research and product development. As always, some areas are promising, and some are yet to prove the values. Expectedly, opportunities of Big Data come from at least the following areas

- Near term potentials are in AIS data, predictive analytics, and performance evaluation.
- Long term potentials are in data management (Hadoop, data lake, data mart, etc.), cybersecurity (ABS, 2016), IoT (Le *et al.*, 2015), autonomous shipping, and alternative inspections.

Worth noting the challenges of Big Data adoption. They come from a variety of angles, from resistance to data sharing, costs of emerging technologies, knowledge and skill gaps, to reluctance to investing in R&D during the current economy with prolonged low oil prices.

7.3.5 Conclusions

Big Data has been a buzz word in the maritime industry for some time. Many have come to realize that the technology will greatly improve how we manage data at scale and how we use data. The industry is undergoing a tremendous change towards digitalization (Aspera, 2017). Emerging technologies such as Big Data will lead to transformation of the maritime industry.

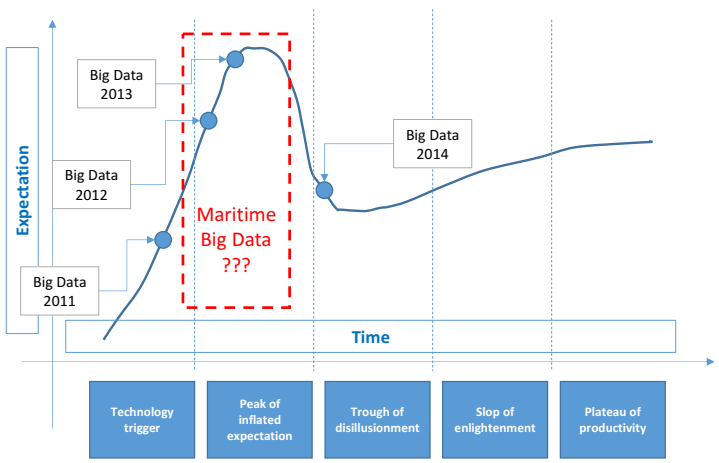

Figure. 10: Big Data as an IT has matured to the stage of "slop of enlightenment", while the maritime industry still views it with great expectations (Wang, 2016).

8. CONCLUSIONS AND RECOMMENDATIONS FOR FUTURE WORK

Following the path set by the mandate, this report has presented in a systematic and orderly manner basic concepts and recent advancements in structural testing related to ship and offshore structures.

Most of the techniques for 'dry' testing of structures at a specimen or component level share a common background with mechanical or civil engineering, and for this reason benefit of well-established approaches coded by standards over time. Notwithstanding these similarities, the importance of accurate experimental investigations supporting design and maintenance of ship and offshore structures is the reason for further improvements of techniques for material testing. As attention moves to 'large scale' (here the expression denotes also the scaled representations

of full-scale structures) or the sea environment becomes part of the experimentation, the peculiarity of the naval constructions emerges, and experimentation must find its own way to address specific issues and needs (welded structures, likely presence of defects, corrosion, testing under water and ice environmental conditions, etc.). Challenges in structural scaling are still ahead and improvements in scaling laws may add more value to certain type of tests in the future.

Miniaturization of sensors as well as the decrease in equipment cost invite us to plan experiments with sensor arrays instead of using just few sensors. As the number of sensor increases, efficient transmission of information becomes critical, and each sensor as a source of data becomes the node of a network. Each node may even provide multiple outputs, integrated or not in the same sensor, or even more complex information as in the case of the fatigue damage sensor (FDS). This concept is at the foundation of the wireless sensor networks, where the concern for cabling issues is reduced to a minimum. Aiming to increase the spatial resolution or to cover a larger domain, field measurements like digital image correlation (DIC) provide a contactless approach to the measurement of deformations and crack propagation. Extending the DIC capability to track dynamical problems and to sense multiple domains (*e.g.*, solid & fluid) is probably the next step but calibration and accuracy requirements of DIC are still a concern. The huge amount of data made available by complex measurement systems, especially if sparse and heterogeneous, fall typically into the 'Big Data' problem. Applications in the maritime field seem promising (monitoring of climate and metocean conditions by means of the ship-buoy concept, optimal routing, SHM of fleets) but data sharing and assessment of data quality are issues requiring further assessment also in ship and offshore engineering.

Another valuable trend is provided by the integration of experiments and numerical simulations. Traditionally, the link has been 'one-way', with data flowing from experiments to the validation of numerical simulations. In the opposite sense, also experimentation often benefits of numerical simulations for the design of experimental setups and for performing a sensitivity analysis to estimate the propagation of experimental uncertainties. Also for Structural Health systems, the cross-flow of experimental, monitoring and design data is essential. Hybrid methods instead pave the way for bi-directional 'coupling' between experimentation and simulations. In this perspective, virtual sensors can be defined expanding numerically the measurement datasets, different sources of information (data fusion) can be mixed, missing physics can be inserted into the experiment by driving dedicated hardware (*e.g.*, as in the hardware-in the-loop approach).

A committee's growing perception has been that full-coverage of the topics related to structural experimentation cannot be achieved without continuing the committee activity; as a leading example, composite materials testing, neglected in this report due to lack of space and specific expertise, call for being prioritized in the next committee mandate. Moreover, selected benchmarks – addressing for instance scaling, test reproducibility, miniaturization and integration of sensors along with new emerging techniques - will undoubtedly provide the opportunity to get a qualified insight into challenging experimental problems and techniques in a more critical way.

REFERENCES

Aalberts P., van der Cammen J., Kaminski M. (2010). The Monitas system for the Glas Dowr FPSO, 2010 Offshore Technology Conference, Houston, TX.

ABS (2003). Guide for surveys using risk-based inspection for the offshore industry, American Bureau of Shipping

ABS (2014). Guide for Fatigue Assessment of Offshore Structures, American Bureau of Shipping.

ABS (2015). Data Analytics: Setting the Foundation for a Data-driven Business http://www.abs-group.com/Knowledge-Center/Insights/Data-Analytics-Setting-the-Foundation-for-a-Datadriven-Business/, American Bureau of Shipping.

ABS (2016). Guidance Notes on Structural Monitoring Using Acoustic Emissions, American Bureau of Shipping.

Achtarides, T. (1979). Wave excited two-node vertical resonant vibration (springing) of flexible ships, Marine Tech.79: Ocean Energy, Marine Tech. Soc.Annual Conf., New Orleans, LA.

Adedipe O., Brennan F., Kolios A. (2015). Corrosion fatigue load frequency sensitivity analysis, Marine Structures, 42, 115-136.

Adedipe O., Brennan F., Kolios A. (2016). Review of corrosion fatigue in offshore structures: present status and challenges in the offshore wind sector, Renewable and Sustainable Energy Reviews, 61, 141-154.

Aggelis D., Kordatos E., Matikas T. (2011). Monitoring of Metal Fatigue Damage using Acoustic Emission and Thermography, Journal of Acoustic Emission, 29, 29-113.

Akai A., Inaba K., Shiozawa D., Sakagami T. (2015). Estimation of fatigue crack initiation location based on dissipated energy measurement, Journal of the Society of Materials Science, 64(8), 668-674.

Aldous L., Smith T., Bucknall R., Thompson P. (2015). Uncertainty analysis in ship performance monitoring, Ocean Engineering, 110, 29-38.

Alsos H. S. (2008). Analysis of Ship Grounding – Assessment of ship damage, fracture and hull girder behaviour, Doctoral Thesis, Norwegian University of Science and Technology.

Alsos H. S., Amdahl J. (2009). On the resistance to penetration of stiffened plates – Part I: Experiment, International Journal of Impact Engineering, 36 (6), 799-807.

Andrieu A., Pineau A., Besson J., Ryckelynck D., Bouziz O. (2012). Beremin model: Methodology and application to the prediction of the Euro toughness data set, Engineering Fracture Mechanics, 95, 102-117.

Antuit (2016). Datalytyx and Antuit to Launch Offshore Big Data Delivery Centre. http://www.antuit.com/about-us/news/datalytyx-and-antuit-to-launch-offshore-big-data-delivery-centre/.

API (2016a). API RP 580, Risk Based Inspection. American Petroleum Institute.

API (2016b). API RP 581, Risk-Based Inspection Technology, American Petroleum Institute.

Armstrong V. (2013). Vessel Optimisation for Low Carbon Shipping, Ocean Engineering, 73, 195-207.

ASTM E1820-17 (2017). Standard Test Method for Measurement of Fracture Toughness.

ASTM E1921-17 (2017). Standard Test Method for Determination of Reference Temperature, T0, for Ferritic Steels in the Transition Range.

ASTM E208-06 (2012). Standard Test Method for Conducting Drop-Weight Test to Determine Nil-Ductility Transition Temperature of Ferritic Steels.

ASTM E23-16b (2016). Standard Test Methods for Notched Bar Impact Testing of Metallic Materials.

ASTM E399-17 (2017). Standard Test Method for Linear-Elastic Plane-Stain Fracture Toughness KIc of Metallic Materials.

ASTM E739-10 (2015). Standard Practice for Statistical Analysis of Linear or Linearized Stress-Life (S-N) and Strain-Life (E-N) Fatigue Data 1. Annual Book of ASTM Standards, (Reapproved), 1-7.

ASTM E8/E8M-16a. (2016). Standard Test Methods for Tension Testing of Metallic Materials.

Azcona J., Bouchotrouch F., González M., Garciandia J., Munduate X., Kelberlau F., Nygaard T.A. (2014). Aerodynamic thrust modelling in wave tank tests of offshore floating wind turbines using a ducted fan, Journal of Physics: Conference Series 524 (2014), 012089.

Azcona J., Munduate X., González L., Nygaard T. (2017). Experimental validation of a dynamic mooring lines code with tension and motion measurements of a submerged chain, Ocean Engineering, 129, 415-427.

Badino A., Borelli, D., Gaggero, T., Rizzuto, E., Schenone, E., (2012). Normative framework for ship noise: present situation and future trends, Noise Control Engineering Journal, 60(6), 740-762.

Banabic D. (2000). Forming limits of sheet metal, Formability of Metallic Materials, D. Banabic, Ed., Springer, Berlin, 173-214.

Barbour N. M. (2010). Inertial Navigation Sensors, NATO report No. RTO-EN-SET-116, Charles Stark Draper Laboratory, Cambridge, MA.

Barsoum F., Suleman J., Korcak A., Hill E. (2009). Acoustic emission monitoring and fatigue life prediction in axially loaded notched steel specimens, Journal of Acoustic Emission, 27, 40-63.

Bayarri M. J., Berger J. O., Paulo R., Sacks J., Cafeo J. A., Cavendish J., Lin C. H., Tu J. (2017). A framework for validation of computer models. Technometrics, 49, 138-154.

Bell, S. (2001). Good practice guide no. 11 Issue 2 - A beginner's guide to uncertainty of measurement, Project UNCERT, NPL, UK.

Bennett S., Brooks C., Winden B., Taunton D., Forrester A., Turnock S., Hudson D. (2014). Measurement of ship hydroelastic response using multiple wireless sensor nodes, Ocean Engineering, 79, 67-80.

Bennet S., Phillips A. (2017). Experimental investigation of the influence of floodwater due to ship grounding on motions and global loads, Ocean Engineering, 130, 49-63.

Benzerga A. A., Leblond, J. B. (2010). Ductile Fracture by Void Growth to Coalescence, Advances in Applied Mechanics, 44, 169-305.

Blekkenhorst R., Ferrari G. M., Van der Wekken C. J., Ijsseling, F.P. (1986). Development of high strength low alloy steels for marine applications, British Corrosion Journal, 21, 163.

Borelli D., GaggeroT., Rizzuto E., Schenone C. (2015). Analysis of noise on board a ship during navigation and manoeuvres, Ocean Engineering 105, 256-269.

Bracco G., Giorcelli E., Mattiazzo G., Orlando V., Raffero M. (2015). Hardware-In-the-Loop test rig for the ISWEC wave energy system, Mechatronics, 25, 11-17.

Brennan F., de Leeuw B. (2008). The use of inspection and monitoring reliability information in criticality and defect assessments of ship and offshore structures, 27th International Conference on Offshore Mechanics and Arctic Engineering, Estoril, Portugal.

Bristow J. W., Irving P. E. (2007). Safety factors in civil aircraft design requirements, Engineering Failure Analysis, 14(3), 459-470.

Bryne T., Rogne R., Fossen T., Johansen T. (2016). Attitude and heave estimation for ships using mems-based inertial measurements, IFAC Conference Paper Archive, 49(23), 568-575.

BS 7448. Fracture mechanics toughness tests, The British Standards Institution.

BS 7910:2013+A1: (2015). Guide to methods for assessing the acceptability of flaws in metallic structures, The British Standards Institution.

BS 8571:2014 (2014). Method of test for determination of fracture toughness in metallic materials using single edge notched tension (SENT) specimens, The British Standards Institution.

Buren K. Van, Reilly J., Neal K., Edwards H., Hemez F. (2017). Guaranteeing robustness of structural condition monitoring to environmental variability. Journal of Sound and Vibration, 386, 134-148.

Calle M., Alves M. (2015). A review-analysis on material failure modeling in ship collision, Ocean Engineering, 106, 20–38.

Calle M., Oshiro R. E., Alves M. (2017a). Ship Collision and Grounding: Scaled Experiments and Numerical Analysis, International Journal of Impact Engineering, 103, 195-210.

Calle M., Verleysen P., Alves M. (2017b). Benchmark study of failure criteria for ship collision modelling using purpose-designed tensile specimen geometries, Marine Structures, 53, 68-85.

Cao Y., Hui H., Wang G., Xuan F. (2011). Inferring the temperature dependence of Beremin cleavage model parameters from the Master Curve, Nuclear Engineering and Design, 241 (1), 39-45.

Cao B. T., Hou B., Li Y. L., Zhao H. (2017). An experimental study on the impact behaviour of multilayer sandwich with corrugated cores, International Journal of Solids and Structures, 109, 35-45.

Carroll, G. P. (2006). Radiated acoustic power of model ship hull sections estimated from scanning laser Doppler vibrometer vibration response measurements, The Journal of the Acoustical Society of America, 119(5).

Catalanotti, C. (2010) Measurement of resistance curves in the longitudinal failure of composites using digital image correlation, Composites Science and Technology, 70, 1986-1993.

CCS (2015). Rules for intelligent ships, China Classification Society.

Cerik B. C., Shin H. K., Cho S. R. (2016). A comparative study on damage assessment of tubular members subjected to mass impact, Marine Structures, 46, 1-29.

Chen Q., Zimmerman T., Deeger D. (1997). Strength and stability testing of stiffened plate components, Ship Structure Committee Report, SSC-339.

Chen Y., Chen F., Zhang W., Du Z. P., Hua H. X. (2016). influence of solid rubber coating on the response of floating structure to underwater shock wave, Journal of Offshore Mechanics and Arctic Engineering, 138(6), 297-307.

Cheng F. (1997). Some results from Lloyd Register's open water model experiments for high speed craft, 4th International Conference on Fast Sea Transportation (FAST97*)*, Sydney, Australia.

Cheng SQ., Chen GJ., Wang SL. (2016). Trial study on dynamic responses of scaled ship model subjected to underwater explosions, Blasting, 32(1), 22-27.

Cho S. R., Song S. U., Park S. H., Shin H. K. (2017). Plastic and fracture damages of double hull structures under lateral collisions, 6th International Conference on Marine Structures, Lisbon, Portugal.

Class NK (2015). Ship Data Center. Nippon Kaiji Kyokai (Japanese Classification Society).

Class NK (2016). ClassNK Awarded Big Data Award at the Lloyd's List Asia Awards, Press Release, Nippon Kaiji Kyokai (Japanese Classification Society).

Choung J., Shim C. S., Song H. C. (2012). Estimation of failure strain of EH36 high strength marine structural steel using average stress triaxiality, Marine Stuctures, 29 (1), 1-21.

Choung J., Nam W., Lee J. Y. (2013). Dynamic hardening behaviours of various marine structural steels considering dependencies on strain rate and temperature, Marine Structures, 32, 49-67.

Coppejans O., Walters C. (2017). determination of parameters for the damage mechanics approach to ductile fracture based on a single fracture mechanics test, 36th International Conference on Ocean, Offshore and Arctic Engineering, Trondheim, Norway.

Coppotelli G., Dessi D., Mariani R., Rimondi M. (2008). Output-only analysis for modal parameters estimation of an elastically scaled ship. Journal of Ship Research, 52(1), 45-56.

Coutinho C.P., Baptista A.J., Rodrigues J.D. (2016). Reduced scale models based on similitude theory: A review up to 2015, Engineering Structures, 119, 81-94.

Crintea A. Moore P. (2016). Ensuring the Strain Capacity in Threaded-End Single Edge Notched Tension (SENT) Specimens, 22nd International Offshore and Polar Engineering Conference, Rhodes, Greece.

Crossbow (2017). Imote2 High-Performance Wireless Sensor Network Node (IPR2400). Document part number: 6020-0117-02 RevA.

Cui P., Zhang A.M., Wang S.P. (2016). Small-charge underwater explosion bubble experiments under various boundary conditions, Physics of fluids, 28(11), 117103.

Decò A., Frangopol D. (2015). Real-time risk of ship structures integrating structural health monitoring data: Application to multi-objective optimal ship routing, Ocean Engineering, 96, 312-329.

Dessi D., Mariani R. (2008). Analysis and prediction of slamming-induced loads of a high-speed monohull in regular waves, Journal of Ship Research, 52(1), 71-86.

Dessi D., De Luca M., Mariani R. (2009). Correlation of model-scale and full-scale analysis of the ship elastic response in waves. International Conference on Hydroelasticity in Marine Technology, Southampton, UK.

Dessi D., Faiella E. (2015). Damping identification of an elastic panel coupled to a fluid: model-scale and full-scale investigations for ships. Conf. on Noise and Vibration Emerging Technologies, Dubrovnik, Croatia.

Dessi D., Faiella E., Geiser J., Alley E., Dukes J. (2016). Design, assessment and testing of a fast catamaran for FSI investigation, 31st Symposium on Naval Hydrodynamics, 11-16 September, Monterey, California.

Dessi D., Faiella E., Geiser J., Alley E., Dukes J. (2017a). Design and structural testing of a physical model for wetdeck slamming analysis, 6th International Conference on Marine Structures, 8-10 May, Lisbon, Portugal.

Dessi D., Faiella E. (2017b). Experimental analysis of the station keeping response of a double-barge float-over system with an elastically scaled physical model, International Ocean and Polar Engineering Conf., San Francisco, CA.

Dittrick, R. (2016) BP, GE launch offshore big-data system starting with Atlantis in gulf, Oil & Gas Journal.

Diznab M., Mohajernassab S., Seif M., Tabeshpour M., Mehdigholi H. (2014). Assessment of offshore structures under extreme wave conditions by Modified Endurance Wave Analysis, Marine Structures, 39, 50-69.

Det Norske Veritas (2010). DNV-OSS-300-3:2010. Risk Based Verification of Offshore Structures. Oslo, Norway.

DNV-GL (2014) Strategic Research and innovation Position Paper 4-2014.

DNV-GL (2015). Fatigue assessment of ship structures, Class Guideline DNVGL-CG-0129.

DNV-GL (2017). Veracity Industry Data Platform.

Dragt R. C., Van den Heuvel W., Gelink E. R. M., Slot H.M. (2015). Testing of full scale composite journal bearings for offshore underwater applications, 34th International Conference on Ocean, Offshore and Arctic Engineering, St. John's, Newfoundland, Canada.

Drummen I., Storhaug G., Moan T. (2008). Experimental and numerical investigation of fatigue damage due to wave-induced vibrations in a containership in head seas, Journal of Marine Science and Technology, 13(4), 428-445.

Dugan P., Zollweg J., Popescu M., Risch D., Glotin H., LeCun Y., Clark. C. (2014). High performance computer acoustic data accelerator: A new system for exploring marine mammal acoustics for big data applications, International Conference on Machine Learning Applications, Bejing, China.

Eaton A., Safdarnejad S., Hedengren J., Moffat K., Hubbell C., Brower D., Brower A. (2015). Post-installed fiber optic pressure sensors on subsea production risers for severe slugging control, 34th International Conference on Ocean, Offshore and Arctic Engineering, St. John's, Newfoundland, Canada.

Ehlers S., Broekhuijsen J., Alsos H. S., Biehl F., Tabri K. (2008). Simulating collision response of ship side structures: a failure criteria benchmark study, International Shipbuilding Progress, 55 (1-2), 127-144.

Ehlers S., Ostby E. (2012a). Increased crashworthiness due to arctic conditions – the influence of sub-zero temperetature, Marine Structures, 28 (1), 86-100.

Ehlers S., Tabri K., Romanoff J., Varsta, P. (2012b). Numerical and experimental investigation on the collision resistance of the X-core structure, Ships and Offshore Structures, 7 (1), 21-29.

Endo H., Yamada Y., Kitamura O., Suzuki K. (2002). Model test on the collapse strength of the buffer bow structures, Marine Structures, 15 (4), 365–81.

Fadel E., Gungor V., Nassef L., Akkari N., Abbas Malik M., Almasri S., Akyildiz I. (2015) A survey on wireless sensor netowrks for smart grid, Computer Communications, 71, 22-33.

Farrar C. R., Warden, K. (2013). Structural health monitoring: a machine learning perspective, Wiley, UK.

Ficquet X., Hossain S., Kingston E. (2013). Residual stresses measurement in various joint welding, 32nd International Conference on Ocean, Offshore and Arctic Engineering, Nantes, France.

Franz von Bock, Polach R. U., Ehlers S., Kujala P. (2013). Model-scale ice — Part A: Experiments, Cold Regions Science and Technology, 94, 74-81

Franz von Bock, Polach R. U., Ehlers S., (2015). on the scalability of model-scale ice experiments, J. Offshore Mech. Arct. Eng., 137(5).

Fras T., Roth C. C., Mohr D. (2017). Fracture of high-strength armor steel under impact loading, International Journal of Impact Engineering, 111, 147-164.

Frazer G., Reagan D., Ruf W., Cheng J. (2011). Top tension riser fatigue monitoring system, 30th International Conference on Ocean, Offshore and Arctic Engineering, Rotterdam, Netherland.

Fricke W., Paetzold H. (2010). Full-scale fatigue tests of ship structures to validate the S–N approaches for fatigue strength assessment, Marine Structures, 23, 115-130.

Gao X., Ruggieri C., Dodds R. H. (1998). Calibration of weibull stress parameter using fracture toughness data, International Journal of Fracture, 92 (2), 175-200.

Gao Y., Fu S., Ma L., Chen Y. (2016). Experimental investigation of the response performance of VIV on a flexible riser with helical strakes, Ships and Offshore Structures, 11(2), 113–128.

Gartner (2017). Hyper Cycle of Emerging Technologies. http://www.gartner.com/technology/research/methodologies/hype-cycle.jsp

GE (2015). Predix – The Premier Industrial Internet Platform Connecting Machines, Intelligence, and People to Drive Operational and Business Outcomes that Matter, https://www.ge.com/digital/predix.

Getter D. J., Kantrales G. C., Consolazio G. R., Eudy S., Fallaha S. (2015). Strain rate sensitive steel constitutive models for finite element analysis of vessel-structure impacts, Marine Structures, 44, 171-202.

Gong Y., Gao Y., Xie D., Liu J. (2015). Deflection and fracture of a clamped plate under lateral indentation by a sphere, Ocean Engineering, 103, 21-30.

Gorbatov Y., Tekgoz M., Guedes Soares C. (2017). Experimental and numerical strength assessment of stiffened plates subjected to severe non-uniform corrosion degradation and compressive load, Ship and Offshore Structures, 12(4), 461-473.

Grell, W. A., Laz, P. J. (2010). Probabilistic fatigue life prediction using AFGROW and accounting for material variability, International Journal of Fatigue, 32(7), 1042-1049.

Gruben G., Solvernes S., Berstad T., Morin D., Hopperstad O. S., Langseth, M. (2017). Low-velocity impact behaviour and failure of stiffened steel plates, Marine Structures, 54, 73-91.

Guan S. (2015). Current and future tendency of monitoring technology for integrity assessment and life extension of the hull structure of floating production, storage and offloading (FPSO) vessel, 34th International Conference on Ocean, Offshore and Arctic Engineering, St. John's, Newfoundland, Canada.

Guzman R. F., Cheng P. W. (2016). Recommendations for load validation of an offshore wind turbine with the use of statistical data: experience from alpha ventus, Journal of Physics: Conference Series 749, 012017.

Haag S., Hoogeland, M. G., Vredeveldt, A.W. (2017). Grounding damage estimate through acceleration measurements, 36th International Conference on Ocean, Offshore and Arctic Engineering, San Francisco, CA.

Hafele J., Hi C., Gebhardt C. G., Rolfes R. (2017). Efficient fatigue limit state design load sets for jacket substructures considering probability distributions of environmental states, 27th International Ocean and Polar Engineering Conference, San Francisco, California, USA.

Halswell P. K., Wilson P. A., Taunton D. J., Austen S. (2016). An experimental investigation into whole body vibration generated during the hydroelastic slamming of a high-speed craft during the hydroelastic slamming of a high speed craft, Ocean Engineering, 126, 115-128.

Hara T., Fujishiro T. (2010). Effect of separation on ductile crack propagation behavior during drop weight tear test, 8th International Pipeline Conference, Calgary, Alberta, Canada.

Hashimoto K., Fujino M., Motora S. (1978). On the wave induced ship-hull vibration springing caused by higher-order exciting force, J. of the Soc. of Naval Arch. of Japan, 144, 183–194. Written in japanese.

Hauge M., Walters C. L., Zanfir C., Maier M., Ostby E., Kordonets S. M., Osvoll H. (2015). Status Update of ISO TC67/SC8/WG5: Materials for Arctic Applications, 25th International Ocean and Polar Engineering Conference, Kona, Big Island, Hawaii, USA.

Hazen B., Boone C., Ezell, J., Jones-Farmer A. (2014). Data quality for data science, predictive analytics, and big data in supply chain management: an introduction to the problem and suggestions for research and applications, International Journal of Production Economics, 154, 72-80.

Hermundstad O., Aarsnes J., Moan T. (1994). Hydroelastic response analysis of high speed monohull, 1st Conference on Hydroelasticity in Marine Tech., NTNU, Trondheim, Norway, 245–259.

Heshmati M., Zamani A. J., Mozafari A. (2017). Experimental and numerical study of isotropic circular plates response to underwater explosive loading, created by conic shock tube, Materialwissenschaft Und Werkstofftechnic, 48, 106-121.

Hessner K., Reichert K., Borge J., Stevens C., Smith M. (2014). High-resolution X-band radar measurement of currents, bathymetry and sea state in highly inhomogeneous coastal areas, Ocean Dynamics, 64(7), 989-998

Hiekata K., Mitsuyuki T., Enomoto M., Okada K., Furukawa Y. (2016). A study of projection mapping on ship plate using 3d laser scanner, Annual Autumn Meeting and Conference of the Japan Society of Naval Architects and Ocean Engineers (JASNAOE), Japan

Hodge V. J., O'Keefe S., Weeks M., Moulds A. (2015). Wireless sensor networks for condition monitoring in the railway industry: A survey, IEEE Transactions on Intelligent Transportation Systems, 16, 3.

Hong S.Y., Kim B.W., Nam B.W. (2011). Experimental study on torsion springing and whipping of large container ship, 21st International Offshore and Polar Engineering Conference, Maui, HI.

Hong S.Y., Kim B.W., Nam B.W. (2012). Experimental study on torsion springing and whipping of large container ship, International Journal of Offshore and Polar Engineering, 22(2), 97-107.

Hong S. Y., Kim B. W. (2014). Experimental investigations of higher-order springing and whipping-WILS project, Intl. J. Nav. Archit. Ocean Eng., 6, 1160-1181.

Hoogeland M. G., Vredeveldt A. W. (2017). Full thickness material tests for impact analysis verification, 6th International Conference on Marine Structures, Lisbon, Portugal.

Hosseinlou F., Mojtahedi A. (2016). Developing a robust simplified method for structural integrity monitoring of offshore jacket-type platform using recorded dynamic responses, Applied Ocean Research, 56, 107-118.

Howard F. (2016). The Maritime 20-20-20, Keynote presentation, International Symposium on Practical Design of Ships and Other Floating Structures (PRADS). Copenhagen, Denmark.

Huang D., Zhao D:, Wei L., Wang Z., Du Y. (2014). Modelling and analysis in marine big data: Advances and challenges. College of Information, Shanghai Ocean University. China.

Hutchison E. K., Moore P. L., Bath W. P. (2015). SENT Stable tearing crack path deviation and its influence on J, ASME 2015 Pressure Vessels & Piping Conference, Boston, MA.

Iafrati A., Grizzi S., Benitez-Montanes L., Siemann M. (2015). High-speed ditching of a flat plate: Experimental data and uncertainty assessment, Journal of Fluids and Structures, 55, 501-525.

Iafrati A. (2016). Experimental investigation of the water entry of a rectangular plate at high horizontal velocity, Journal of Fluid Mechanics, 799, 637-672.

IBM (2014). Big Data. http://www.ibmbigdatahub.com/infographic/extracting-business-value-4-vs-big-data.
IEEE 802.15.4. (2006). Standard for information technology part 15.4: wireless medium access control (MAC) and physical layer (PHY) specifications for low rate wireless personal area networks (LR-WPANs).
Ince S. T., Kumar A., Park D. K., Paik J. K. (2017). An advanced technology for structural crashworthiness analysis of ship colliding with ice ridge: Numerical modelling and experiments, International Journal of Impact Engineering, 110, 112-122.
International Ship and Offshore Structures Congress 2015 III.2.
ISA (2009). ISA-100.11: Wireless systems for industrial automation: process control and related applications, International Society of Automation.
Ioannou A., Angus A., Brennan F. (2017a). Stochastic prediction of offshore wind farm lcoe through an integrated cost model, Energy Procedia, 107, 383-389.
Ioannou A., Wang L., Brennan F. (2017b). Design implications towards inspection reduction of large scale structures, Procedia CIRP, 60, 434-439.
Irkal M., Nallayarasu S., Bhattacharyya S. (2016). CFD approach to roll damping of ship with bilge keel with experimental validation, Applied Ocean Research, 55, 1-17.
Ishikawa T., Inoue T., Funatsu Y., Otani J. (2012). Evaluation method for crack arrestability of steel plates using small-scale fracture test results, 22nd International Offshore and Polar Engineering Conference, Rhodes, Greece.
IMO MSC.337(91) (2012). Resolution MSC.337(91). Adoption of the code on noise levels on board ships.
IMO Res. MSC.337(91), Code on noise on board ships.
ISO 12135:2016 (2016). Metallic materials - Unified method of test for the determination of quasistatic fracture toughness, International Organization for Standardization.
ISO 14556:2015 (2015). Metallic materials – Charpy V-notch pendulum impact test – Instrumented test method, International Organization for Standardization.
ISO 148 (2009) Metallic materials – Charpy pendulum Impact Test – Part 1: Test Method
ISO 2631-1 (1997). Evaluation of human exposure to whole-body vibration -Part 1: General requirements.
ISO 2631-2 (1997). Evaluation of human exposure to whole-body vibration -Part 2: Continuous and shock-induced vibration in buildings (1 to 80 Hz).
ISO 27306:2016 (2016). Metallic materials – method of constraint loss correction of CTOD fracture toughness for fracture assessment of steel components.
ISO 6954 (1984). Mechanical vibration and shock- Guidelines for the overall evaluation of vibration in merchant ships.
ISO 6954 (2000). Mechanical vibration - Guidelines for the measurement, reporting and evaluation of vibration with regard to habitability on passenger and merchant ships.
ISO 8041-1:2017 (2017). Human response to vibration -- Measuring instrumentation -- Part 1: General purpose vibration meters.
ISSC (2015). ISSC Report of the Technical Committee III.2: Ultimate Strength. 19th International Ship and Offshore Structure Congress, Lisbon, Portugal.
Jalonen R., Ruponen P., Weryk M., Naar H., Vaher S. (2017). A study on leakage and collapse of non-watertight ship doors under floodwater pressure, Marine Structures, 51, 188-201.
Jang B.S., Ito H., Kim K.S., Suh Y.S., Jeon H.T., Ha Y.S. (2010). A study of fatigue crack propagation at a web stiffener on a longitudinal stiffener, Journal of Marine Science and Technology, 15, 176-189.
JCGM 106:2012 (2012). Evaluation of measurement data - The role of measurement uncertainty in conformity assessment, Joint Committee for Guides in Metrology.
Jiang M., Ren B., Wang G., Wang Y. (2014). Laboratory investigation of the hydroelastic effect on liquid sloshing in rectangular tanks, Journal of Hydrodynamics, 26(5), 751-761.

Jiao J., Ren H., Adenya C. A. (2015). Experimental and numerical analysis of hull girder vibrations and bow impact of a large ship sailing in waves, Shock and Vibration, 2015(3), 1-10.

Jensen A.E., Havsg G.B., Pran K., Wang G., Vohra S. T., Davis M. A., Dandridge A. (2000). Wet deck slamming experiments with a FRP sandwich panel using a network of 16 fibre optic Bragg grating strain sensors, Composites / Part B, 31, 187-198.

Jullumstrø E., Aarsnes J. (1993). Hull loads and response on high speed craft. RINA International Conference on High Speed Passenger Craft, London, UK.

Kambatla K., Kollias G.., Vand K., Grama A. (2014). Trends in big data analytics. Journal of Parallel Distribution Computation.74, 2561-2573.

Kandasamy R., Cuia F., Townsend N., Foo C., Guo J., Shenoi A., Xiong Y. (2016). A review of vibration control methods for marine offshore structures, Ocean Engineering, 127, 279-297.

Kandil F. A. (2000a). Glossary of definitions and symbols. Project UNCERT, (1), National Physical Laboratory, UK.

Kandil F. A. (2000b). Introduction to the evaluation of uncertainty. Project UNCERT, (1) National Physical Laboratory, UK.

Kaufer D., Cheng P.W. (2014). Validation of an integrated simulation method with high-resolution load measurements of the offshore wind turbine Repower 5M at Alpha Ventus. Journal of Ocean and Wind Energy, 1, 30-40.

Kausar Z. A. W., Reza M. U., Saleh H., Ramiah (2014). Energizing wireless sensor networks by energy harvesting systems: Scopes, challenges and approaches, Renewable and Sustainable Energy Reviews, 38, 973-989.

Kellner T. (2015). Deep Machine Learning: GE and BP will connect thousands of subsea oil wells to the industrial internet, GE report (http://www.ge.com/reports/post/123572457345 /deep-machine-learning-ge-and-bp-will-connect).

Kim A., Hekland F., Petersen S., Doyle P. (2008). When HART goes wireless: understanding and implementing the WirelessHART standard, IEEE International Conference on Emerging Technologies and Factory Automation, Hamburg, Germany.

Kim K. J., Lee J. H., Park D. K., Jung B. G., Han X., Paik J. K. (2016a). An experimental and numerical study on non-linear impact responses of steel-plated structures in an Arctic environment, International Journal of Impact Engineering, 93, 99-115.

Kim J. FL, Chau-Dinh, T., Zi, G., Lee, W. W., Kong, J. S. (2016b). Probabilistic fatigue integrity assessment in multiple crack growth analysis associated with equivalent initial flaw and material variability, Engineering Fracture Mechanics, 156, 182-196.

Kim Y., Park S-G, Kim B-H, Ahn I-G (2016c). Operational modal analysis on the hydroelastic response of a segmented container carrier model under oblique waves, Ocean Engineering, 127, 357-367.

Kim N.W., Nam, B.W., Kwon, Y.J., Cho, S.K., Park, I.B., Sung, H.G. (2017). Experimental investigation on mating operation during float-over installation of a large topside in waves, International Ocean and Polar Engineering Conference, San Francisco, CA, USA, June 25-30, 1162-1167.

Kitamura O. (1997). Comparative study on collision resistance of side structure, Marine Technology, 34 (4), 293-308.

Kleiman J., Kudryavtev Y. (2012). Residual stress management in welding: residual stress measurement and improvement treatments, 31st International Conference on Ocean, Offshore and Arctic Engineering, Rio de Janeiro, Brazil.

Kleiman J., Kudryavtev Y., Smilenko V. (2013). Non-destructive measurement of residual stresses by an ultrasonic method, 32nd International Conference on Ocean, Offshore and Arctic Engineering, Nantes, France.

Kobayashi T., Takaoka Y., Nihei K., Osawa N., De Gracia L., Ichihashi D. (2016). Improvement of prediction accuracy of hull fatigue life by a fatigue damage sensor under a storm model

loading, Journal of the Japan Society of Naval Architects and Ocean Engineers, 23, 153-157.

Kong X., Li X., Zheng C., Liu F., Wu W-G. (2017). Similarity considerations for scale-down model versus prototype on impact response of plates under blast loads, International Journal of Impact Engineering, 101, 32-41.

Koga, S. (2015). major challenges and solutions for utilizing big data in the maritime industry, World Maritime University Dissertations Paper 490.

Koo J. B., Jang K.B., Suh Y.S., Kim Y.S., Kim M.S., Yu H., Tai J.S.C. (2011). fatigue damage assessment based on full scale measurement data for a large container ship, 21st International Offshore and Polar Engineering Conference, Maui, HI.

Körgesaar M., Tabri K., Naar H., Reinhold E. (2014). Ship collision simulations using different fracture criteria and mesh size, 33rd International Conference on Ocean, Offshore and Arctic Engineering, San Francisco, CA.

Kostenko K. V., Kryukov Y. S. (2016). Technique for detecting a direct signal pulse from an underwater explosive source in a waveguide, Acoustical Physics, 62(1), 112-116.

Kyyro K., Hakala M.H. (1997). Determination of structural dimensioning loads of a fast catamaran, using rigid backbone segmented model testing techniques, 4th International Conference on Fast Sea Transportation (FAST97), Sydney, Australia.

Kubiczek J.M., Burchard K.S., Ehlers S., Schöttelndreyer M. (2017). Material relationship identification for finite element analysis at intermediate strain rates using optimal measurements, 6th International Conference on Marine Structures, Lisbon, Portugal.

Kubo A., Yajima H., Aihara S., Yoshinari H., Hirota K., Toyoda M., Kiyosue T., Inoue T., Handa T., Kawabata T., Tani T., Yamaguchi T. (2012). Experimental study on brittle crack propagation behavior with large scale structural component model tests - Brittle crack arrest design for large container ships, 22nd International Offshore and Polar Engineering Conference, Rhodes, Greece.

Kvåle K., Øiseth O. (2017). Structural monitoring of an end-supported pontoon bridge, Marine Structures, 52, 188-207.

Kwon Y. W., Priest E.M., Gordis J.H. (2013). Investigation of vibrational characteristics of composite beams with fluid-structure interaction, Composite Structures, 105, 269-278.

Kwon, O., N. Lee and B. Shin (2014). Data quality management, data usage experience and acquisition intention of big data analytics, International Journal of Information Management, 34, 387-394.

Kwon Y.J., Nam B.W., Kim N. W., Kwak H. W., Park I. B., Jung D. H., Sung H.G. (2017). A model test for docking operations of a transportation vessel during float-over installation, 27th International Ocean and Polar Engineering Conference, San Francisco, CA.

Larsen J. M., Jha S. K., Szczepanski C. J., Caton M. J., John R., Rosenberger A. H., Jira, J. R. (2013). Reducing uncertainty in fatigue life limits of turbine engine alloys, International Journal of Fatigue, 57, 103-112.

Lau T., Kelso R. (2016). A scaling law for thrust generating unsteady hydrofoils, Journal of Fluids and Structures, 65, 455-471.

Lavroff J., Davis M., Holloway D., Thomas G. (2007). The whipping vibratory response of a hydroelastic segmented catamaran model, 9th International Conference on Fast Sea Transportation (FAST2007), Shanghai, China.

Le Gall, F., Vallet Chevillard S., Gluhak A., Walravens N., Xueli Z., Hadji H.B. (2015). Benchmarking internet of things deployment: Frameworks, best practices and experiences, Modeling And Processing For Next-Generation Big-Data Technologies, Springer, 473-496.

Ledezma D., Amer A., Abdellatif F., Outa A., Trigui H., Patel S., Roba, B. (2015). A market survey of offshore underwater robotic inspection technologies for the oil and gas industry, SPE Saudi Arabia Section Annual Technical Symposium and Exhibition, Al-Khobar, Saudi Arabia.

Lee K., Cho S., Kim K., Kim J., Lee P. (2015a). Hydroelastic analysis of floating structures with liquid tanks and comparison with experimental tests, Applied Ocean Research, 52, 167-187.
Lee G. J. (2015b). Dynamic orifice flow model and compartment models for flooding simulation of a damaged ship, Ocean Engineering, 109, 635-653.
Lee P.S. (2017). Underwater explosion experiments using pentolite, Explosives & Blasting, 35(3), 21-30. (In Korean)
Lehmann E., Pschmann J. (2002). Energy absorption by the steel structure of ships in the event of collisions, Marine Structures, 15 (4), 491-441.
Li X., Li Y., Zheng Y. (2014). Effects of stress wave effects on the damage behavior of marine low carbon steel based on the low-speed Taylor rod experiment, Ship Mechanics,12, 1495-1504.
Li Y., Wang Y., Wu W., Du Z., Li X., Zhang W. (2015a). Dynamic mechanical properties and constitutive relations of marine 907+A steel, Journal of Harbin Engineering University, 127-129. (In Chinese)
Li S., Zhang A. M., Yao X. L. (2015b). Experimental and numerical study on the dynamic pressure caused by the bubble jet, Journal of Physics, COnf. Series, 656(1), 12-25.
Li S., Zhang A. M., Han R., Liu Y. (2017). Experimental and numerical study on bubble-sphere interaction near a rigid wall, Physics of Fluids, 29(9), 092-102.
Lin J-C., Leu F-Y., Chen Y. (2015). ReHRS: A hybrid redundant system for improving MapReduce reliability and availability, Modeling and Processing for Next-Generation Big-Data Technologies, 4, Springer.
Libelium (2017). Waspmote Technical Guide. Libelium Comunicaciones Distribuidas S.L. v7.4. Zaragoza, Spain.
Liu K., Wang Z., Tang W., Zhang Y., Wang G. (2015a). Experimental and numerical analysis of laterally impacted stiffened plates considering the effect of strain rate, Ocean Engineering, 99, 44-54.
Liu B., Villacencio R., Guedes Soares V. (2015b). Simplified method for quasi-static collision assessment of a damaged tanker side panel, Marine Structures, 40, 267-288.
Liu F., Li H., Lu H. (2016). Weak-mode identification and time-series reconstruction from high-level noisy measured data of offshore structures, Applied Ocean Research, 56, 92-106.
Liu N. N., Wu W. B., Zhang A. M., Liu Y. L., Liu N. N., Wu W. B. (2017). Experimental and numerical investigation on bubble dynamics near a free surface and a circular opening of plate, Physics of Fluids, 29(10), 107-102.
LR (2010). Guidance Notes for Risk Based Inspection for Hull Structures, Lloyd's Register.
Lloyds Register Energy (2014a). Asset Management: From Data to Decision. Lloyd's Register Group Limited.
Lloyd's Register Foundation (2014b). Foresight Review of Big Data. Lloyd's Register Foundation Report Series: No. 2014.2.
LR (2016). Global Marine Technology Trends 2030, Lloyd's Register.
LMS (2015). FPSO JIP on Life Cycle Management Hull, http://www.fpsoforum.com/jips/completed-jips/.
Lovoll G., Kadal J.C. (2014). Big Data - the new data reality and industry impact, DNV-GL.
Lu, P., Zhang L., Liu X., Yao J., Zhu Z. (2015). Highly efficient data migration and backup for big data applications, in elastic optical inter-data-center networks, IEEE Network, 29(5), 36-42.
Lupton R.C., Langley R.S. (2017). Scaling of slow-drift motion with platform size and its importance for floating wind turbines, Renevable Energy, 101, 1013-1020.
Lugni C., Bardazzi A., Faltinsen O. M., Graziani G. (2014). Hydroelastic slamming response in the evolution of a flip-thourgh event during shallow-liquid sloshing, Physics of fluids, 26.
Lugni C., Greco M., Faltinsen O. (2015). Influence of yaw-roll coupling on the behavior of a FPSO: An experimental and numerical investigation, Applied Ocean Research, 51, 25-37.

Magno M., Jackson N., Mathewson A., Benini L., Popovici E. (2013). Combination of hybrid energy harvesters with MEMS piezoelectric and nano-Watt radio wake up to extend lifetime of system for wireless sensor nodes, Architecture of Computing Systems, 26th International Conference. Prague, Czeck Republic.

Maljaars J. Pijpers R., Slot H., (2015). Load sequence effects in fatigue crack growth of thick-walled welded C-Mn steel members, International Journal of Fatigue, 79, 10-24.

Maluf N., Williams K. (2004). An Introduction to microelectromechanical systems engineering, Second Edition, Artech House, Inc. Norwood, MA.

Mariani R., Dessi D. (2012). Analysis of the global bending modes of a floating structure using the proper orthogonal decomposition, Journal of fluids and structures, 28, 115-134.

Maron A., Kapsenberg G. (2014). Design of a ship model for hydro-elastic experiments in waves, International Journal of Naval Architecture and Ocean Engineering, 6, 1130-1147.

Maroti M., Simon G., Ledeczi A., Sztipanovits J. (2004). Shooter localization in urban terrain. Computer, IEEE Journal, 37(8), 60-61.

Matsuo K., Fujimoto S., Shiraishi K. (2015). Introduction of AR technologies to ship building works, National Maritime Research Institute (NMRI), Technical Report 14, Japan.

Mc Goldrick R., Russo V. (1956). Hull vibration investigation on SS-Gopher Mariner, Technical Report, Report No. 1060, David Taylor Model Basin.

Memsic Inc. (2017a). IRIS Wireless Measurement System (XM2110CA), www.aceinna.com.

Memsic Inc. (2017b). MICAz Wireless Measurement System (MPR2400CB), www.aceinna.com.

Minami F., Takashima Y., Ohata M., Yamashita Y. (2013). Constraint-based assessment of fracture in welded components, Welding in the World, 57, 707-718.

Ming F.R., Zhang A.M., Xue Y.Z., Wang S.P. (2016). Damage characteristics of ship structures subjected to shockwaves of underwater contact explosions, Ocean Engineering, 117, 359–382.

Minorsky V. U. (1959). An analysis of ship collisions with reference to protection of nuclear plants, Journal of Ship research, 1-4.

Moan T., Amdahl J, Ersdal G. (2017). Assessment of ship impact risk to offshore structures – New NORSOK N-003 guidelines, Marine Structures, in press, https://doi.org/10.1016/j.marstruc.2017.05.003.

Mohr D., Marcadet S. J. (2015). Micromechanically-motivated phenomenological Hosford-Coulomb model for predicting ductile fracture initiation at low stress triaxialities, International Journal of Solids and Structures, 67-68, 40-55.

Mondoro A., Soliman M., Frangopol D. (2016). Prediction of structural response of naval vessels based on available structural health monitoring data, Ocean Engineering, 125, 295-307.

Montenegro G., Kushalnagar N., Hui J., Culler D. (2007). Transmission of IPv6 packets over IEEE 802.15.4.

Moon S. J., Kwon J. I., Park J. W., Chung J. H. (2017). Assessment on shock pressure acquisition from underwater explosion using uncertainty of measurement, International Journal of Naval Architecture and Ocean Engineering, 9, 589-597.

Moore P., Hutchison E. (2016). Comparison of J equations for SENT Specimens, 1st European Conference on Fracture, Catania, Italy.

Nematbakhsh A., Michailides C., Gao Z., Moan T. (2015). comparison of experimental data of a moored multibody wave energy device with a hybrid cfd and biem numerical analysis framework, 34th International Conference on Ocean, Offshore and Arctic Engineering, St. John's, Newfoundland, Canada.

Niklas K., Kozak J. (2016). Experimental investigation of Steel–Concrete–Polymercomposite barrier for the ship internal tank construction, Ocean Engineering, 111, 449-460.

Osawa N., Nakamura T., Yamamoto N., and Sawamura J. (2013). Development of a new fatigue testing machine for high frequency fatigue damage assessment, 32nd International

Oshiro R., Calle M., Mazzariol L., Alves, M. (2017). Experimental study of collision in scaled naval structures, International Journal of Impact Engineering, 110, 1-13.

Otani J., Works O., Funatsu Y., Inoue T., Shirarata H. (2011). Improvement of arrestability for brittle crack for welded joint: development of higher toughness YP47 (460N/mm2) Class steel plate for large container ships-3, 21st International Offshore and Polar Engineering Conference, Maui, HI, USA.

Ouyang D. H., Zhang Q. T., Wang, F. (2016). Experimental and numerical investigation of effects of charge density on the bubble characteristics originating from the combustion of pyrotechnic mixtures, Flow Turbulence & Combustion, 97(3), 1-10.

Paik J. K., Thayamballi A. K. (2003). An experimental investigation on the dynamic ultimate compressive strength of ship plating, International Journal of Impact Engineering, 28 (7), 803-811.

Paik J. K., Kim K.J., Lee J.H., Jung B.J., Kim S.J. (2017). Test database of the mechanical properties of mild, high-tensile and stainless steel and aluminium alloy associated with cold temperatures and strain rates, Ships and Offshore Structures, 12, 230-256.

Pan J., Farag, N., Lin T., Juniper, R. (2002). Propeller induced structural vibration through the thrust bearing, Annual Conference of the Australian Acoustical Society, Adelaide, Australia.

Panapakidis I., Michailides C., Angelides D. (2016). Missing wind speed data: clustering techniques for completion and computational intelligence models for forecasting, 26th International Offshore and Polar Engineering Conference, Rhodes, Greece.

Panapakidis I., Michailides C., Angelides D. (2017). Clustering techniques for data analysis and completion of monitored structural responses of a floating structure, 27th International Offshore and Polar Engineering Conference, San Francisco, CA.

Park J. Y, Jo E., Kim M. S , Lee S. J, Lee Y. H. (2016). Dynamic behavior of a steel plate subjected to blast loading, Transactions Of The Canadian Society For Mechanical Engineering, 40, 575-583.

Park D. K., Kim K. J., Lee J. H., Jung B. G., Han X., Kim B. J., Seo J. K., Ha Y. C., Paik J. K., Matsumoto T., Byeon S. H., Kim M. S. (2015). Collision tests on steel plated structures in low temperatures, 34th International Conference on Ocean, Offshore and Arctic Engineering, St. John's New Foundland, Canada.

Pasquier R., Berthon C.F. (2012). Model-scale test vs. full-scale measurement: findings from the full-scale measurement sloshing project. 22nd International Offshore and Polar Engineering Conference, Rhodes, Greece, 17-22 June.

Pedersen P.T., Zhang, S. (2000). Effect of ship structure and size on grounding and collision damage distributions, Ocean Engineering, 27, 1161-1179.

Pedersen C., Deshpande V., Fleck N. (2006). Compressive response of Y-shaped sandwich core, European Journal of Mechanics-A/Solids, 25, 125-141.

Perner, P. (2015). Decision tree induction methods and their application to Big-Data, Modeling and Processing for Next-Generation Big-Data Technologies, 4, Springer.

Popescu P., Slusanschi E., Iancu V., Pop F. (2016). A new upper bound for Shannon entropy. A novel approach in modeling of Big Data applications. Concurrency and computation: Practice and Experience, 28, 351-359.

Puccinelli D., Haenggi M. (2005). Wireless sensor networks: applications and challenges of ubiquitous sensing, IEEE Circuits and Systems Magazine, 5(3), 19-31.

Pussegoda L., Tiku S., Tyson W., Park D-Y., Gianetto J., Shen G., Pisarki H. (2013). Comparison of resistance curves from multi-specimen and single-specimen SEN(T) Tests, 23rd International Offshore and Polar Engineering, Anchorage, Alaska.

Puzak P. P., Babecki A. J. (1959). Normalization procedures for nrl drop-weight test, Welding Journal, 38, 209-.

Qian G., González-Albuixech V., Niffenegger M. (2015). Calibration of Beremin model with the Master Curve, Engineering Fracture Mechanics, 136, 15-25.

Quinton B. W. T., Daley C. G., Colbourne B. B., Cagnon R. E. (2017). Experimental investigation of accidental sliding loads on the response of hull plating, 6th International Conference on Marine Structures, Lisbon, Portugal.

Qiu X., Zhu L., Yan M., Liu B. (2017). Structural response and energy absorption of the simplified ship side under the impact of rigid indenters with different shapes, 6th International Conference on Marine Structures, Lisbon, Portugal.

Rawat P., Singh K., Chaouchi H., Bonnin J. M. (2014). Wireless sensor networks: a survey on recent developments and potential synergies. The Journal of Supercomputing, 68(1). 1-48.

Ren P., Zhou J., Tian A., Zhang W., Huang W. (2017). Experimental and numerical investigation of the dynamic behavior of clamped thin panel subjected to underwater impulsive loading, Latin American Journal of Solids and Structures, 14(6), 978-999.

Rodd J. L. (1996). Observations on conventional and advanced double hull grounding experiments, International Conference on Designs and Methodologies for Collision and Grounding protection of Ships, San Francisco, CA.

Roessle M. L., Fatemi A. (2000). Strain-controlled fatigue properties of steels and some simple approximations, International Journal of Fatigue, 22(6), 495-511.

Rolader G.E., Rogers J., Batteh J. (2004). Self-healing minefield. SPIE Proceedings 5441, Battlespace Digitization and Network-Centric Systems IV, Defense and Security, Orlando, FL.

Roth C. C., Gary G., Mohr D. (2015). Compact SHPB system for intermediate and high strain rate plasticity and fracture testing of sheet metal, Experimental Mechanics, 55(9), 1803-1811.

Roth C. C., Mohr D. (2016). Ductile fracture experiments with locally proportional loading histories, International Journal of Plasticity, 79, 328-354.

Roubos A., Groenewegen L., Peters D. J. (2017). Berthing velocity of large seagoing vessels in the port of Rotterdam, Marine Structures, 51, 202-219.

Rubino V., Deshpande V. S., Fleck N. A. (2008a). The dynamics response of end-clamped sandwich beams with Y-shaped or corrugated core, International Journal of Impact Engineering, 35, 829-844.

Rubino V., Deshpande V. S., Fleck N. A. (2008b). The collapse response of sandwich beams with Y-frame core subjected to distributed and local loading, International Journal of Mechanical Sciences, 50, 233-246.

Rubino V., Deshpande V. S., Fleck N. A. (2009). The dynamic response of clamped Y-frame and corrugated core sandwich plates, European Journal of Mechanics-A/Solids, 28, 14-24.

Rubino V., Deshpande V. S., Fleck N. A. (2010). The three-point bending of Y-frame and corrugated core sandwich beams, International Journal of Mechanical Sciences, 52, 485-494.

Ruponen P., Kurvinen P., Saisto I., Harras J. (2013). Air compression in a flooded tank of a damaged ship, Ocean Engineering, 57, 64-71.

Saad-Eldeen S., Garbatov Y., GuedesS oares C. (2016a). Experimental strength assessment of thin steel plates with a central elongated circular opening, Journal of Constructional Steel Research, 118, 135-144.

Saad-Eldeen S., Garbatov Y., Guedes Soares C. (2016b). Experimental strength analysis of steel plates with a large circular opening accounting for corrosion degradation and cracks subjected to compressive load along the short edges, Marine Structures, 48, 52-67.

Saad-Eldeen S., Garbatov Y., Guedes Soares C. (2017). Experimental compressive strength analyses of high tensile steel thin-walled stiffened panels with a large lightening opening, Thin-Walled Structures, 113, 61-68.

Salah B., Slimane Z., Zoheir M., Jurgen, B. (2015). Uncertainty estimation of mechanical testing properties using sensitivity analysis and stochastic modelling, Measurement, 62, 149-154.

Sankararaman S., Ling, Y., Mahadevan, S. (2011). Uncertainty quantification and model validation of fatigue crack growth prediction, Engineering Fracture Mechanics, 78(7), 1487-1504.

Sarzosa D., Souza R., Ruggieri C. (2015). J-CTOD relations in clamped SE(T) fracture specimens including 3-D stationary and growth analysis, Engineering Fracture Mechanics 147, 331-354.

Sauder T., Chabaud V., Thys M., Bachynski E.E., Sæther L.O. (2016). real-time hybrid model testing of a braceless semi-submersible wind turbine. Part I: The Hybrid Approach, 35th International Conference on Ocean, Offshore and Arctic Engineering, Busan, South Korea.

Scheu M.N., Kolios A., Fischer T., Brennan F. (2017). Influence of statistical uncertainty of component reliability estimations on offshore wind farm availability, Reliability Engineering and System Safety, 168 28-39.

Schiere M., Bosman T., Derbanne Q., Stambaugh K., Drummen I. (2017). Sectional load effects derived from strain measurements using the modal approach, Marine Structures 54, 188-209.

Schmidt T., Tyson J., Revilock D., Padula S., Pereira J., Melis M., Lyle K. (2005). performance verification of 3d image correlation using digital high-speed cameras, 2005 SEM Annual Conference and Exposition, Portland.

Schmidt T. Tyson J., Galanulis K., Revilock D., Melis M. (2005). Full-field dynamic deformation and strain measurements using high-speed digital cameras, Proc. of SPIE, 5580, 175-.

Schöttelndreyer M., Tautz I., Kubiczek. J. M., Fricke W., Lehmann E. (2011). Influence of Bulbous bow structures on their collision behavior, Analysis and Design of Marine Structures, Hamburg.

Schöttelndreyer M., Tautz I., Fricke W., Werner B., Daske C., Heyer H., Sander M. (2013). Experimental and numerical investigations of an alternative stiffening system for ship side structures to increase collision safety, Analysis and Design of Marine Structures, Espoo.

Shaikh F., Zeadally S. (2016). Energy harvesting in wireless sensor networks: A comprehensive review, Renewable and Sustainable Energy Reviews, 55, 1041-1054.

Shi X. H., Zhang J., Guedes Soares, C. (2017). Experimental study on collapse of cracked stiffened plate with initial imperfections under compression, Thin-Walled Structures, 114, 39-51.

Shibahara, M. (2012). Measurement of Welding Deformation Based on Stereo Imaging Technique, 22nd International Offshore and Polar Engineering Conference, Rhodes, Greece.

Shinoda T., Nagata Y. (2015). Trend of 3D Measurement Technology and Its Application, Komatsu Technical Report Vol.61, No168, Japan. (in Japanese).

SILENV (2012). Ships oriented innovative solutions to reduce noise and vibrations, FP7. http://www.silenv.eu/.

Simms D. (2015). Big Data, Unstructured Data, and the Cloud: Perspectives on Internal Controls, Modelling and Processing for Next-Generation Big-Data Technologies, 4.

Son J-D., Ahn B-H, Ha J-M, Choi B-K (2016). An Availability of MEMS-based Accelerometers and Current Sensors in Machinery Fault Diagnosis, Measurement, 94, 680-691.

Sormunen O., Castrén A., Romanoff J., Kujala P. (2016a). Estimating sea bottom shapes for grounding damage calculations, Marine Structures, 45, 85-109.

Sormunen O., Körgesaar M., Tabri K., Heinvee M., Urbel A., Kujala P. (2016b). Comparing rock shape models in grounding damage modelling, Marine Structures, 50, 205-223.

Sormunen O. (2017). Impact of sea bottom shape in rounding damage, suitability of modelling with Gaussian processes, Progress in the Analysis and Design of Marine Structures, International Conference on Marine Structures, Lisbon, Portugal.

Sotoudeh K., Zhang S., Eren S., Kabra S., Milititsky M., Gittos M. (2013). evaluation of residual stresses in steel-to-nickel dissimilar joints, 32nd 3International Conference on Ocean, Offshore and Arctic Engineering, Nantes, France.

Spaho, E., Barolli A., Xhafa F., Barolli L. (2015). P2P Data Replication: Techniques and Applications. Modeling and Processing for Next-Generation Big-Data Technologies, 4, Springer.

Stauffer J-M. (2006). Current capabilities of mems capacitive accelerometers in a harsh environment. IEEE Aerospace and Electronics Systems Magazine, 21(11), 29-32.

Stenius I., Rosén A., Battley M., Allen T. (2003). Experimental hydroelastic characterization of slamming loaded marine panels, Ocean Engineering, 74, 1-15.

Storhaug G., Mathisen, J., Heggelund, S.E. (2009). Model tests and full-scale measurements of whipping on container vessels in the North Atlantic. 28th International Conference on Offshore Mechanics and Arctic Engineering, Honolulu, HI.

Storhaug G., Haraide O. (2013). Assessment of hull monitoring measurements for a large blunt vessel, 32nd International Conference on Ocean, Offshore and Arctic Engineering, Nantes, France.

Storheim M., Amdahl J., Martens I. (2015). On the accuracy of fracture estimation in collision analysis of ship and offshore structures, Marine Structures, 44, 254-287.

St-Pierre L., Deshpande V. S., Fleck N.A. (2015). The low velocity impact response of sandwich beams with corrugated core or a Y-frame, International Journal of Mechanical Sciences, 91, 71-80.

Suàrez J.C., Townsend P., Sanz E., Diez de Ulzrrum I., Pinilla P. (2016). The effect of slamming impact on out-of-autoclave cured prepregs of GFRP composite panels for hulls, Procedia Engineering 167, 252-264.

Sugimoto K., Yajima H., Aihara S., Yoshinari H., Hirota K., Toyoda M., Kiyosue T., Inoue T., Handa T., Kawabata T., Tani T., Usami A. (2012). Thickness effect on the brittle crack arrest toughness value (Kca) - Brittle crack arrest design for large container ships, 22nd International Offshore and Polar Engineering Conference, Rhodes, Greece.

Sun J., Hiekata K. (2014a). Efficient point cloud data processing in shipbuilding: Reformative component extraction method and registration method, J. of Computational and Engineering, 1(3), 202-212.

Sun J., Hiekata K. (2014b). development of curved shell plate's processing plan generation system using 3D measured data and virtual templates, Annual Autumn Meeting and Conference of the Japan Society of Naval Architects and Ocean Engineers (JASNAOE), Japan.

Suominen M., Kujala P., Romanoff J., Remes H. (2017a). The effect of the extension of the instrumentation on the measured ice-induced load on a ship hull, Ocean Engineering 144, 327–339.

Suominen M., Kujala P., Romanoff J., Remes H. (2017b). Influence of load length on short-term ice load statistics in full-scale, Marine Structures 52, 153-172.

Swartz R. A., Zimmerman A. T., Lynch J. P., Rosario J., Brady T., Salvino L., Law K. H. (2012). Hybrid wireless hull monitoring system for naval combat vessels. Structure and Infrastructure Engineering: Maintenance, Management, Life-Cycle Design and Performance, 8(7), 621-638.

Tableau (2017). Top Ten Big Data Trend for 2017. www.tableau.com

Tabri K., Määttänen J., Ranta J. (2008). Model-scale experiments of symmetric ship collisions, Journal of Marine Science and Technology, 13, 71-84.

Tabri K., Matusiak J., Varsta P. (2009). Sloshing interaction in ship collision an experimental and numerical study, Ocean Engineering, 36, 1366–1376.

Tabri K., Varsta P., Matusiak J. (2010). Numerical and experimental motion simulations of non-symmetric ship collisions, Journal of Marine Science and Technology, 15, 87-101.

Tammer M, Kaminski M. (2013). Fatigue oriented risk based inspection and structural health monitoring of FPSOs, 23rd International Offshore and Polar Engineering Conference, Anchorage, AK, USA.

Tammer M., Kaminski M. L., Koopmans M., Tang J. (2014). Current performance and future practices in FPSO hull condition assessments, 24th International Offshore and Polar Engineering Conference, Busan, Korea.

Tan K. H., Zhan Y-Z, Ji G., Ye F., Chang C. (2015). Harvesting big data to enhance supply chain innovation capabilities: An analytic infrastructure based on deduction graph. International Journal of Production Economics, 165, 223-233.

Tanaka Y., Ogawa H., Tatsumi A., Fujikubo M. (2015). Analysis method of ultimate hull girder strength under combined loads. Ships and Offshore Structures, 10(5), 587-598.

Tasai F. (1974). On the calculation methods of wave induced vibrations of ships, Trans. of the West-Japan Soc. of Naval Arch., 48, 163–180. (in japanese).

Tautz I., Schöttelndreyer M., Lehmann E., Fricke W. (2013). Collision tests with rigid and deformable bulbous bows driven against double hull side structures, Collision and Grounding of Ships and Offshore Structures, Trondheim, Norway.

Thomas G., Winkler S., Davis M., Holloway D., Matsubara S., Lavroff J., French B. (2011). Slam events of high-speed catamarans in irregular waves, J Mar Sci Technol, 16(1), 8–21.

Turan O., Helvacioglu I.H., Insel M., Khalid H., Kurt R.E. (2011). Crew noise exposure on board ships and comparative study of applicable standards. Ship and Offshire Strctures, 6(4), 323-338.

Torfs T., Sterken T., Brebels S., Santana J., van der Hoven R., Spiering V., Bertsch N., Trapani D., Zonta D., (2013). Low Power Wireless Sensor Network for Building Monitoring. IEEE Sensors Journal, 13(3), 909-915.

Tveiten B., Wang X., Berge S. (2007). Fatigue assessment of aluminium ship details by hot-spot stress approach, SNAME 2007 Conference, Fort Lauderdale, Florida.

UK HSE (2001). Probabilistic methods: Uses and abuses in structural integrity, Report for the Safety and Health Executive, Bomel Limited, ISBN 0 7176 2238 X.

UKAS (2016). The Expression of Uncertainty in Testing. Edition 2: M 3003, United Kingdom Accredation Service, 1–14.

Van den Bas L, Sanderse B. (2017). Uncertainty quantification for wind energy applications—literature review. Technical Report SC-1701, Centrum Wiskunde & Informatica, Amsterdam.

Von Bock und Polach F. R. U., Ehlers S., (2015). On the scalability of model-scale ice experiments, J. Offshore Mech. Arct. Eng. 137(5).

Voormeeren L., Walters C., Tang L., Vredeveldt A. (2014). estimation of failure parameters for finite element simulations based on a single state of stress and arbitrary stress-strain relation, 33rd Internation Conference on Ocean, Offshore and Arctic Engineering, San Francisco, CA.

Vredeveldt A. W., Wevers L. J. (1992). Full scale ship collision tests, Conference on the Prediction Methodology of Tanker Structural Failure.

Wakahara M., Nakajima M., Fukasawa T. (2008). Development of an affix-type multipoint pressure sensor by use of FBG (1st Report), The Japan Society of Naval Architects and Ocean Engineers, 7, 1-7. (in Japanese).

Wallin K., Karjalainen-Roikonen P., Suikkanen P. (2016). Crack arrest toughness estimation for high strength steels from sub-sized instrumented Charpy-V Tests, 26th International Ocean and Polar Engineering Conference, Rhodes, Greece.

Walters C., van der Weijde G. (2013). Development and validation of a low-cost CTOD procedure, 23rd International Offshore and Polar Engineering, Anchorage, AK.

Walters C., Bruchhausen M., Lapetite J., Duvalois W. (2017) Fracture testing of existing structures without the need for repairs, 36th International Conference on Ocean, Offshore and Arctic Engineering, Trondheim, Norway.

Wang X., Koh C., Zhang J. (2014). Substructural identification of jack-up platform in time and frequency domains, Applied Ocean Research, 44, 53-62.

Wang S., Li Y., Li H. (2015a). Structural model updating of an offshore platform using the cross model cross mode method: An experimental study, Ocean Engineering, 97, 57-64.

Wang Z. X., Gu W. B., Liu J. Q. (2015b). Experimental study on peak pressure of shock waves in quasi-shallow water, Mathematical Problems In Engineering, 1-8.

Wang G., Hu K., (2016a). To establish ship performance assessment scheme in a dynamically changing environment, International Symposium on Practical Design of Ships and Other Floating Structures (PRADS), Copenhagen, Denmark.

Wang G. (2016b). Maritime Big Data – Where are we on the Gartner Hype Cycle? https://www.linkedin.com/pulse/maritime-big-data-where-we-gartner-hype-cycle-ge-george-wilwwwang reinserirla adopo gratner

Wang Z., Liu K., Chunyan J., Chen D., Wang G., Guedes Soares C. (2016c). Experimental and numerical investigations on the T joint of jack-up platform laterally punched by a knife edge indenter, Ocean Engineering, 127, 212-225.

Wang J., Xiang S., Fu S., Cao P., Yang, Y., He J. (2016d). Experimental investigation on the dynamic responses of a free-hanging water intake riser under vessel motion, Marine Structures, 50, 1-19.

Wang G. (2017). What values does Big Data bring to the Maritime Industry? https://www.linkedin.com/pulse/what-values-does-big-data-bring-maritime-industry-ge-george-wang.

Wei Z.J., Faltinsen O.M., Lugni C., Yue Q.J. (2015). Sloshing-induced slamming in screen-equipped rectangular tanks in shallow-water conditions, Physics of Fluids, 27(3).

WES 2815:2014 (2014). Test method for brittle crack arrest toughness, Kca. The Japan Welding Engineering Society, Tokyo, Japan.

Wevers L. J., Vredeveldt A. W. (1999). Full scale ship collision experiments, TNO, report 98-CMC-R1725 Delft, The Netherlands.

WiSMote (2017) WiSMote. www.wismote.com.

Woisin G. (1979). Konstruktion gegen kollisionsauswirkungen – design against collision, Schiff & Hafen, 12, 1059-1069.

Wolf M. (2003). Full-scale collision experiment, X-type Sandwich side hull, EU Sandwich project report, Deliverable TRD448, EU Sandwich project.

Woo J., Kim D., Na W.B. (2015). Damage assessment of a tunnel-type structure to protect submarine power cables during anchor, Marine Structures, 44, 19-42.

Wu W., Wang Y., Tang D., Yue Q., Du Y., Fan Z., Lin Y., Zhang Y. (2016). Design, implementation and analysis of full coupled monitoring system of FPSO with soft yoke mooring system, Ocean Engineering, 113, 255-263.

Xie Y. G., Guo J., Xin-Fei L. I., Cui H. B., Yao X. L. (2015). Analysis of time-frequency characteristics of wall pressure signals of hull structure subjected to underwater explosion, Journal of Dalian University of Technology, 55, 492-497. (In Chinese)

Xie Yaoguo, Cui Hongbin, Li Xinfei, Yao Xiongliang. (2016). Analysis of time-frequency characteristics of free-field pressure under underwater explosion, Chinese Journal of Ship Research, 11 (2), 27-32. (In Chinese)

Xue J., Zhang Z., Ostby E., Nyhus B., Sun D. (2009). Effects of crack depth and specimen size on ductile crack growth of SENT and SENB specimens for fracture mechanics evaluation of pipeline steels, International Journal of Pressure Vessels and Piping, 86, 787-797.

Yamada Y., Endo. H. (2005). Collapse mechanism of the buffer bow structure on axial crushing, International Journal of Offshore and Polar Engineering, 15 (2), 147-154.

Yamada Y. (2006). Bulbous buffer bows: a measure to reduce oil spill in tanker collisions, PhD thesis, Department of Mechanical Engineering, Technical University of Denmark, DTU.

Yamada Y., Endo H. (2007). Experimental and numerical study on the collapse strength of the bulbous bow structure in oblique collision, Marine Technology, 45(1), 42–53.

Yamamoto N., Negayama H., Furukawa N., Mouri M., Yasunaga R., Inami A., Nakamura T., Okada T., Mori T., Tanaka S., Shimanuki H., Sumi Y., Sugimura T., Morikage Y. (2012).

Analytical and experimental study on the thickness effect to fatigue strength, 22nd International Offshore and Polar Engineers, Rhodes, Greece.

Yanuka D., Shafer D., Krasik Y. (2015). Shock wave convergence in water with parabolic wall boundaries, Journal of Applied Physics, 117(16), 632-641.

Yi J-H. (2016). Laboratory tests on local damage detection for jacket-type offshore structures using optical FBG sensors based on statistical approaches, Ocean Engineering, 124, 94-103.

Yue J., Dong Y., Zhou H. (2012). Fatigue analysis on a multi-planer tubular kk joints based on scaled model test, 22nd International Society of Offshore and Polar Engineers, Rhodes, Greece.

Zhang A. M., Cui P., Cui J., Wang Q. X. (2015a). Experimental study on bubble dynamics subject to buoyancy, Journal of Fluid Mechanics, 776, 137-160.

Zhang P., Cheng Y., Liu J., Wang C., Hou H., Li Y. (2015b). Experimental and numerical investigations on laser-welded corrugated-core sandwich panels subjected to blast loading, Marine Structures, 40, 225-246.

Zhang S. H., Quan L., Jin H., Jia, Z. (2015c). Research on positioning method of underwater explosion source, Blasting, 32, 118-121. (In Chinese)

Zhang Z., Wang Y., Zhao H., Qian H., Mou J. (2015d). An experimental study on the dynamic response of a hull girder subjected to near field underwater explosion, Marine Structures, 44, 43-60.

Zhang X., Noel N., Ferrari G., Hoogeland M. (2016), Corrosion behaviour of mooring chain steel in seawater, Eurocorr 2016, Montpellier, France.

Zhang A. M., Wu W. B., Liu Y. L., Wang Q. X. (2017a). Nonlinear interaction between underwater explosion bubble and structure based on fully coupled model, Physics of Fluids, 29(8), 082-111.

Zhang C., Suo T., Tan W., Zhang X., Liu J., Wang C., Li Y. (2017b). An experimental method for determination of dynamic mechanical behavior of materials at high temperatures, International Journal of Impact Engineering, 102, 27-35.

Zhang S., Villavicencio R., Zhu L., Pedersen P. T. (2017c) Impact mechanics of ship collisions and validations with experimental results, Marine Structures, 52, 69-81.

Zhang Y., Huang Y., Wei Y. (2017d). Ultimate strength experiment of hull structural plate with pitting corrosion damage under uniaxial compression, Ocean Engineering, 130, 103-114.

Zhao W., Yang J., Hu Z., Tao L. (2014). Prediction of hydrodynamic performance of an FLNG system in side-by-side offloading operation, Journal of Fluids and Structures, 46, 89-110.

Ziemer G., Evers K. U. (2014). Ice model tests with a compliant cylindrical structure to investigate ice-induced vibrations, 33rd International Conference on Offshore Mechanics and Arctic Engineering, San Francisco, CA.

This page intentionally left blank

Proceedings of the 20th International Ship and Offshore Structures Congress (ISSC 2018) Volume II – M.L. Kaminski and P. Rigo (Eds.)

doi:10.3233/978-1-61499-864-8-143

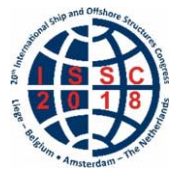

COMMITTEE V.3

MATERIALS AND FABRICATION TECHNOLOGY

COMMITTEE MANDATE

The committee shall give an overview about new developments in the field of ship and offshore materials and fabrication techniques with a focus on trends which are highly relevant for practical applications in the industry in the recent and coming years. Particular emphasis shall be given to the impact of welding and corrosion protection techniques for structural performance, and on the development of lighter structures.

AUTHORS/COMMITTEE MEMBERS

Chairman: Lennart Josefson, *Sweden*
Stephen van Duin, *Australia*
Bianca de Carvalho Pinheiro, *Brazil*
Nana Yang, *China*
Luo Yu, *China*
Albert Zamarin, *Croatia*
Heikki Remes, *Finland*
Frank Roland, *Germany*
Marco Gaiotti, *Italy*
Naoki Osawa, *Japan*
Agnes Marie Horn, *Norway*
Myung Hyun Kim, *South Korea*
Brajendra Mishra, *USA*

KEYWORDS

Lightweight, composites, adhesive, welding, residual stress, distortions, fatigue, steels, arctic, qualification, approval, high frequency mechanical impact (HFMI)

CONTENTS

1. INTRODUCTION 146

2. GENERAL TRENDS 146
2.1 Ongoing research programmes on materials and fabrication technology 148
2.1.1 China 148
2.1.2 Europe 148
2.1.3 Australia 149

3. MATERIALS 149
3.1 Low temperature steels 149
3.1.1 Nickel steels 150
3.1.2 Stainless steels and aluminum 151
3.1.3 High manganese steel 151
3.2 High strength steels 151
3.3 Steels for use in the arctic 152
3.4 Composite materials 155
3.4.1 Mechanical aspects 155
3.4.2 Recent technological innovations 156
3.4.3 Composites for subsea applications 156
3.5 Weight reducing materials 157

4. JOINING AND FABRICATION 158
4.1 Advances in joining technology 159
4.1.1 Low heat input welding processes 159
4.1.2 Secondary Processes - Active distortion control 160
4.2 Automation and robotic programming 162
4.3 Additive Manufacturing 163
4.4 Fabrication and joining of composites 164
4.4.1 Air inclusions 164
4.4.2 Exothermic peak 164
4.4.3 Bending response of infusion made composites 165
4.4.4 Prepregs 165
4.4.5 Fibre-matrix interface 165
4.4.6 Epoxy matrix 165
4.4.7 Non-crimp fibers 166
4.4.8 Joining of composites 166
4.4.9 Influence of the ply orientation 166
4.4.10 Nanoparticles 167
4.4.11 Fire resistance 167

5. QUALIFICATION AND APPROVAL 167
5.1 Qualification of composites 168
5.1.1 Hamburg meeting on qualification on composites 168
5.1.2 Best practice of qualification of composites 169
5.2 Qualification and approval processes by the class societies 171
5.2.1 DNV GL 171
5.2.2 ABS 171
5.2.3 Bureau Veritas 172
5.2.4 Lloyds 172
5.2.5 IMO 172

6. BENCHMARKS AND CASE STUDIES 172
6.1 Uncertainness in welding simulation 172
6.2 Sensitivity analysis on the cohesive parameters of a carbon-steel single lap 174
6.2.1 Model Description, material properties and mesh size 175
6.2.2 Cohesive model 175
6.2.3 Reference cohesive parameters 176
6.2.4 Experimental/numerical comparison and influence of parameter k 176
6.2.5 Influence of G_c 177
6.2.6 Influence of α 177
6.3 Fatigue life improvement using HFMI treatment 177
6.3.1 Multiple impact simulation of the HFMI process on stress-free steel sheets 178
6.3.2 Single impact simulation of the HFMI process on stress-free steel sheets 182
6.3.3 Summary and future plans 183

7. CONCLUSIONS AND RECOMMENDATIONS 183

REFERENCES 184

1. INTRODUCTION

This report presents recent developments in materials and fabrication technology in the shipping and offshore fields. This field is under strong pressure due to a decline in orders in particular in the offshore sectors, and also a drop in new build prices. But this also drives a strong development of new materials, fabrications processes and also means for qualifying and approving new materials and processes.

Chapter 2 shows recent trends in ship and offshore production, and in research in these fields, primarily publicly funded. The development of new metallic materials and composites are dealt with in Chapter 3. Chapter 4 gives an overview of welding methods for steels, and fabrication of composites, as well as advances in additive manufacturing. One new area for this Committee is the work with qualification and approval of new materials and processes. This is discussed in Chapter 5 with special focus on approval of composites, what tests are needed for approval and how can this be carried out in an efficient and time-consuming manner.

The V.3 Committee reports three benchmarks, the first is a continuation of the benchmark in the ISSC 2015 V.3 report, welding of a stiffener to a plate (T-Joint) and reports FE-computed residual stresses and deformations, which are compared with experimental results. It gives guidelines for the use of both heat source and model parameters. The second benchmark deals with a single carbon / steel lap joint using a specific adhesive. The sensitivity of parameters that define the separation law for the adhesive on the debonding of the single lap joint is assessed. Computed results are compared with experimental results, and some aspects of material modelling is discussed. The third benchmark deals with fatigue life improvement of fillet welds by use of HFMI (High Frequency Mechanical Impact) treatments. Based on a test case, peening of a stress-free flat steel plate, a best practice guide for simulating a HFMI treatment is given including the use of material model and element mesh size.

The Committee's mandate includes corrosion protection techniques. However, as this topic was covered extensively in the previous 2015 Committee report, it was decided not cover this area in the current report.

2. GENERAL TRENDS

The shipping market has seen a continued decrease in new orders in 2015 and 2016. This fall in orders is combined with a strong drop in new building prices. Figure 1 (total) and Table 1 (broken down in ship categories) clearly show this change in new orders. It is seen that the low order intake during the last years is not equally distributed over all maritime markets. While the orders for standard transport ships (tanker, bulk, container) has partly dramatically decreased, orders for RoRo, cruise, ferries (and yachts) have remained stable and tend to increase. The offshore oil and gas sector has suffered from low oil prices. Spending by oil companies is estimated to have dropped 35% since the end of 2013, but new sectors like offshore wind, marine renewable energies, aquafarming and deep-sea mining are increasing as well as specialized vessels for arctic operation. Even though currently niche markets, this market segments may grow further in the future.

New orders in 2017 are likely to be on par or slightly more than in 2016, given the general poor freight markets; the increased difficulty in arranging debt financing and also raising equity; the consolidation through take-overs or alliances; the prevailing price gap between newbuilding and second-hand tonnage (BRGS Group, 2017). The expansion of the Panama Canal completed in 2016 could encourage new types of ships. Shipbuilding may also be influenced by a predicted increase (by IMF) in global exports from 2.2 % 2016 to 3.5 % (Braura and Mittal, 2017). Also for tankers and LNG there seems to be an increase in demand.

There is a pressure from international and national authorities, banks and creditors, ship owners and shipyards to consolidate and reduce, in an organized way, the worldwide shipping and shipbuilding capacity. For 2016 a decline in shipbuilding capacity is seen, with more than 15

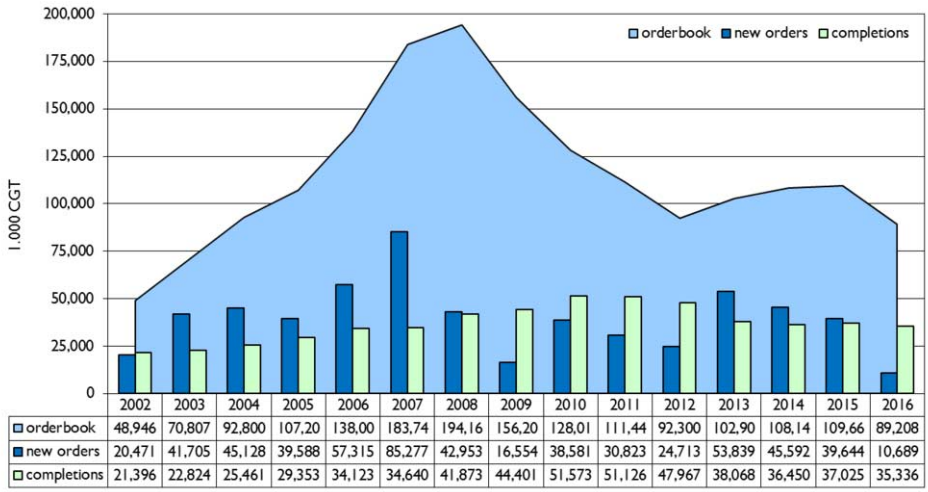

	2002	2003	2004	2005	2006	2007	2008	2009	2010	2011	2012	2013	2014	2015	2016
orderbook	48,946	70,807	92,800	107,20	138,00	183,74	194,16	156,20	128,01	111,44	92,300	102,90	108,14	109,66	89,208
new orders	20,471	41,705	45,128	39,588	57,315	85,277	42,953	16,554	38,581	30,823	24,713	53,839	45,592	39,644	10,689
completions	21,396	22,824	25,461	29,353	34,123	34,640	41,873	44,401	51,573	51,126	47,967	38,068	36,450	37,025	35,336

Figure. 1: Global commercial shipbuilding activity in CGT for the years 2002- 2016. From SEA Europe (2017), data source IHS Fairplay.

Table 1: New orders for different ship categories for the years 2006 – 2016 in M Dwt. From BRS Group (2017).

New Orders 2006 - 2016											
M Dwt	2006	2007	2008	2009	2010	2011	2012	2013	2014	2015	2016
Tanker	77,6	48,5	35,8	8,9	29,4	8,6	13,1	33,4	32,8	48,9	13,2
Bulk	47,6	142,9	85,4	23,4	88,4	39,6	24,0	75,6	58,1	24,5	15,5
Container	19,2	35,4	11,6	0,3	7,3	20,7	3,5	22,5	12,8	26,9	3,3
Other ships	10,4	14,3	6,3	1,3	4,4	6,7	5,9	8,7	12,3	7,4	2,0
Total	154,8	241,1	139,1	33,9	129,5	75,6	46,5	140,2	116,0	107,7	34,0

Orders for specialised vessels 2009 - 2016								
	2009	2010	2011	2012	2013	2014	2015	2016
Chemical carriers stainless steel (k Dwt)	137	265	202	370	939	2207	2138	737
LPG carriers (k cbm)	76	933	692	1424	5095	5360	5121	200
LNG carriers (k cbm)	313	2262	7875	6294	5531	11857	4090	1078
Ferries and Ro-pax (k gt)	124	568	57	214	183	299	301	559
Ro-ro (k Dwt)	198	41	246	659	152	41	151	284
Car carriers (k cars)	2	133	58	193	288	168	447	-
Cruise vessels (k gt)	130	1069	819	1510	733	2241	2485	1864

liquidations in 2016 compared to a few in 2015, and also a very low vessel ordering capacity. The decline in shipbuilding capacity can be exemplified as a change from an estimated 1,150 active yards in 2000 to around 630 yards in 2016, which represents a 35% decline to an estimated 45 million Compensated Gross Tons (CGT). The trend continues with an estimated 3 million CGT set to disappear in 2017. This development has also changed the focus of shipbuilding activities in the world. Thus, many countries and regions aim to enter new market segments of complex high-technology ships and initiated corresponding long-term research and development initiatives (Chen, 2014). This includes developments of new materials and production techniques, e.g. for lighter ships (composite materials), reduced drag and resistance (coatings and air lubrication), retrofitting (e.g. propulsion improvement devices, exhaust gas treatment) and new fuels (gas and methanol). On the legislative side new clean water ballast restrictions coming into force, new Sulphur Emission Control Area (SECA) zones and navigational speed may also push for a replacement and renewal of the fleet.

Table 2 visualizes the market focus, in terms of ship production and orders, as expressed by the different countries and regions. The Table is in a sense relative, but it shows also the dominance of China in the first three categories, where China managed to obtain half the new orders 2016. The Table also shows Korea's strong position in orders for LNG carriers and the strong focus in Europe on cruise, ferries and mega yachts.

Table 2: Activities in ship production and orders in different in different countries and regions. • = some activity, •• =considerable activity.

Type of Ships	China	Korea	Japan	Europe	Brasil	AUS	US
Crude oil tankers	••	••	•				
Bulk carriers	••		•				
Product & chemical tankers	••	••	•				
LNG and LPG carriers	•	•	•				•
Container vessels	••	•					
RoRo and other cargo	••		•				•
Cruise, PAX and ferries	•		•	••		••	
Mega Yachts	•			••		•	
Offshore vessels	••				••		
Naval vessels				•		••	••

2.1 Ongoing research programmes on materials and fabrication technology

2.1.1 China

Besides projects funded by the National Natural Science Foundation, there are strong research activities at several universities, on materials for ship and offshore structures (for wind energy, renewable energy, aquafarming and deep sea mining), on welding methods including laser welding and underwater welding, and on controlling distortions during welding.

2.1.2 Europe

Public funding of maritime R&D projects in Europe comes primarily from the member states and the European Union. Some European countries like Germany have own national maritime research funding schemes, while others fund maritime research through generic programs. The MARTEC II network has analyzed maritime R&D funding programs in the different countries (MARTEC II, 2017). On the European level, research is funded through the Framework Programs, such as FP7 (2007-2013, ca. 50 billion €) and HORIZON 2020 (2014-2020, estimated budget ca. 80 billion €). Maritime projects in HORIZON 2020 are primarily funded under the priorities of Transport (under Mobility for Growth) and Blue Growth (under Societal Challenge 2). Horizon 2020 aim at encourage innovation at higher Technology Readiness levels (TRL) and also include specific funding instruments for small and medium enterprises (SME:s), all aiming to promote the market uptake of research results and industrial competitiveness.

The following list gives an overview on some important maritime projects with relevance to materials and fabrication which were or are active in the period between 2015 and 2018 (European Commission, 2017).

Acronym	Title
HILDA	High Integrity Low Distortion Assembly (friction stir welding)
CARLOS	CooperAtive Robot for Large Spaces manufacturing
ADAM4EVE	Adaptive and Smart Materials and Structures for more efficient vessels
MOSAIC	Materials Onboard: Steel Advancements and Integrated Composites
LEAF	Low Emission Anti Fouling
SMARTYards	Developing Smart Technologies for productivity Improvement of European Small and Medium Sized Shipyards
HOLISHIP	Holistic Optimisation of Ship Design and Operation for Life cycle
SHIPLYS	Ship Life Cycle Software Solutions
RAMSSES	Realisation and Demonstration of Advanced Material Solutions for Sustainable and Efficient Ships
FIBRESHIP	Integral Composite Ship
SHIPTEST	Fully Automated Laser Guided Inspection Robot for Weld Defect Detection on Ship Hulls

Beside the large programs, there is an intense network activity between European companies (with increasing numbers of SME:s) , research institutes and academia, often financed by EU, it stretches beyond research into regulations and commercial activities. One example of such a network is E-LASS an European network fort lightweight applications at sea (www.e-lass.eu).

2.1.3 Australia

The main source of R&D funding for maritime in Australia is related to Defense and the Federal Government's Australian Continuous Shipbuilding Plan. Two new sources of funding have been provided through The Defense Innovation Hub investing $640 million over the decade in maturing and further developing technologies.

The future Frigate program is developing technologies in the areas of welding and joining, additive manufacturing, corrosion coatings and corrosion prognostic health monitoring, single crystal sonar ceramics, toughened composites and blast and shock modelling software tools. navigational speed may also push for a replacement and renewal of the fleet.

Table 3 visualizes research efforts in materials and fabrication technology as expressed by the different countries and regions. Steels, and welding methods still have strong position in several countries and regions, though research on non-metallic materials, eg composites and also additive materials and ICT / digitalization are emerging areas.

3. MATERIALS

3.1 Low temperature steels

Recent efforts to avoid the serious environmental pollution reinforced the International Maritime Organization (IMO) regulations for nitrogen oxide (NOx). In particular, the Marine Environmental Protection Committee (MEPC) of the IMO agreed upon progressively stricter limitations for NOx emissions from ocean going vessels (Azzara et al., 2014). In this trend, various types of LNG carriers such as liquefied natural gas carriers (LNGC), floating liquefied natural gas (FLNG), LNG-floating storage regasification unit (LNG-FSRU) and very large gas carrier (VLGC) have been developed and are currently operating worldwide.

Table 3: Research efforts in different countries and regions.
• = some activity, •• =considerable activity.

Research projects / programs	China	Korea	Japan	Europe	Brasil	AUS	US
Materials							
Steels	•	••	••	•	••	••	•
Other metallic materials	•	••			•	•	••
Non-metallic materials	•	•	•	••	••	•	•
Coatings	•	•		••		•	
Fabrication and joining							
Welding	••	•	••	•	••	••	••
Adhesive bonding	•	•		••		•	
Automation	••	•	•	•	•	•	•
Additive materials	•	•	••	•	••	•	•
Qualitative control and management	•	•		••	••		
ICT, digitalization	••	•	••	••	•		

One of the most important issues in the design of LNG carriers is the structural integrity of storage tanks under cryogenic temperature. Therefore, LNG storage tanks are typically manufactured using low temperature steels considering the operation temperature of LNG. In terms of the structural integrity of storage tanks, researches of low temperature steels mainly have focused on fatigue and fracture performances at cryogenic temperature. Also, further research of high manganese steel is being carried out to register the steel in International Gas Carrier (IGC) code. The most common low temperature steels are:

- Nickel steels (The contents of 3.5%, 5%, 7%, 9% nickel)
- Stainless steel (SUS 304L, SUS316L)
- Aluminum alloy (Al 5083-O)
- High manganese steel

3.1.1 Nickel steels

Nickel is one of the most utilized and important major industrial metals. In particular, nickel-iron alloys are commonly used in demanding corrosion-resistant and heat-resistant applications. Therefore, nickel steels have been used mainly for the primary barrier of LNG storage tanks. In this respect, some researches have been carried out to assess the fatigue and fracture performances of nickel steel. Pusan National University (PNU), Hanjin Heavy Industry and POSCO (2016) studied material characteristics of 9% nickel such as material properties, fatigue and fracture performances for the application of IMO Type C LNG Cargo Containment System (CCS). They performed tensile, Fatigue Crack Growth Rate (FCGR) and fracture toughness tests considering three different welding consumables and two welding processes. Scheid et al. (2016) assessed fracture toughness of 5.5% and 9% nickel steels regarding the effect of heat treatment. In addition, Park et al. (2016) evaluated material characteristics of 3.5 to 9 wt% nickel steels. Fatigue Ductile to Brittle Transition (FDBT) phenomenon was investigated to determine the requirement of classification. In addition, the fatigue and fracture performances are compared among 3.5% to 9 wt% nickel steels for both room and cryogenic temperatures. In order to find the suitable FCGR design curve, material constants of nickel steels are compared with the value in BS 7910 standard.

3.1.2 Stainless steels and aluminum

Stainless steels and aluminum are being considered as possible material candidates for primary barrier in IMO Type-B tank. In order to ensure the structural integrity of such tanks, it is very important to evaluate the fatigue and fracture performances at cryogenic temperature. Kumar et al. (2016) investigated impact toughness behavior at Heat Affected Zone (HAZ) and weld metal considering three different heat inputs as well as two thermal aging conditions. This study conducted Charpy V-notch (CVN) test at room and cryogenic temperatures. Chaves et al. (2017) evaluated fatigue limits for SUS and Aluminum from pure tension to pure torsion. In this study, the geometry of specimen is a thin-walled tube with a passing-through hole. Jesus et al. (2016) assessed the influence of Friction Stir Processing (FSP) on the fatigue behavior of Gas Metal Arc Welding (GMAW) T-welds in AA 5083-H111 plates. As a result, the fatigue strength of GMAW T-welds is found to be significantly improved. Ilman et al. (2016) investigated improving fatigue performance in AA 5083 metal inert gas (MIG) welded joints through mitigated distortion and residual stress using static thermal tensioning (STT).

3.1.3 High manganese steel

The increasing demand for strong and tough steels for cryogenic applications leads to the development of high-Mn austenitic steels utilizing Twining Induced Plasticity (TWIP) effect. Song et al. (2016a) performed to clarify the effect of Al addition on Low-Cycle Fatigue (LCF) properties of high - Mn TWIP steels, which were electro chemically charged by hydrogen. In addition, Song et al. (2016b) investigated the effect of cold-drawing on the fatigue properties of austenitic TWIP steels, and the results were compared with those of conventional Fully Pearlitic (FP) steel. Jeong et al. (2016) evaluated the FCGR behavior of high-Mn steels with a variety of chemical compositions in order to understand the controlling factors determining the near-threshold characteristics of crack propagation.

3.2 High strength steels

Many researches have been carried out to assess the fatigue and fracture performances of high strength steels. It is well known that the interior of a thick plate is in a plane strain state with the plastic region decreased in size (Kaneko et al., 2011). As a result, a stress greater than its yield stress is generated, and fatigue and fracture performances significantly decrease. The main topics of high strength steel are brittle crack arrest and improvement of fatigue strength. An et al. (2014) investigated brittle crack arrest fracture toughness with a high heat-input welding. Hase et al. (2014) developed a heavy thick YP460 steel plate with excellent brittle crack arrestability for the upper deck and hatch side coaming areas in mega container carriers. The fatigue strength improvement as a function of the yield strength was observed also for post-weld treated joints in Yildirim and Marquis (2012). Laitinen et al. (2013) showed that an increased fatigue strength can be obtained for cut plate edges without treatment, when cutting quality is good.

Recently, ultra large container ship that can carry more than about 20,000 TEU are being constructed. According to this trend, ships and offshore structures are under more demands for thicker plates to ensure the sufficient strength. In the case of large container ships (above 12,000 TEU), in particular, the high strength steels with a thickness of 80 mm are commonly applied to the hatch coaming section.

Liu et al. (2016) evaluated the effect of step quenching on microstructures and mechanical properties of High Strength Low Alloy (HSLA). Shibanuma et al. (2016) proposed a new model formulation to predict brittle crack propagation and arrest behaviors. Usami et al. (2016) reported the process and results of a risk analysis of cryogenic fluid leaks as well as the study on a prospective measure to mitigate the risk by use of a newly developed TMCP steel having brittle fracture arrestability. Kumar et al. (2016) investigated Ductile to Brittle Transition Temperature (DBTT) for HY 85 steel which is a high strength low alloy steel used in the

quenched and tempered condition specially developed for ship hulls. Lan et al. (2016) evaluated the impact toughness of HSLA steel with multi-pass Submerged Arc Welding (SAW). The effect of hydrogen on the fracture and impact toughness of ultra-high-strength steels at sub-zero temperatures were investigated by Pallaspuro et al. (2017). The influence of welding thermal cycles produced by reheating processing on mechanical properties was evaluated by Wang et al. (2017).

Shiozaki et al. (2015) assessed the relationship between residual stress and fatigue strength for as-punched specimens and specimens subjected to stress relief heat treatment after punching a hole. Mora et al. (2015) focused on the effect of sea water corrosion on the Giga-cycle fatigue strength of a martensitic–bainitic hot rolled steel R5 used for manufacturing off-shore mooring chains for petroleum platforms in the North Sea. Harati et al. (2015) compared the fatigue strength of as welded with that of High Frequency Mechanical Impact (HFMI) treated fillet welds in a 1300 MPa yield strength steel. Ottersböck et al. (2016) investigated the effect of single undercuts as characteristic weld defects on the fatigue behavior of high quality ultra-high-strength steel welds. The fatigue strength of TIG-dressed Ultra High Strength Steel (UHSS) fillet weld joints at different stress ratios was determined by experimental testing, and a statistical analysis was applied to local geometric factors and variables of manually TIG-dressed fillet welds (Mikkola et al., 2016). Harati et al., (2017) evaluated residual stress and fatigue strength of high strength steel welded joint considering difference in four Low Transformation Temperature (LTT) welding consumables. Leitner et al. (2017) contributed to quantify the influence of the local mean stress condition and the local weld geometry on the high-cycle fatigue strength of welded and high frequency mechanical impact (HFMI) treated S960 high-strength steel joints.

3.3 Steels for use in the arctic

It is well known that when the temperature decreases, steel becomes more brittle. In addition, the yield and tensile stress increase with decreasing temperature (Østby et. al. 2015) and the detailed shape of the stress-strain curve may change, e.g. the length of possible Lüders plateau may change (will elongate with lower temperatures). The benefit of an increased yield strength is not considered in design in the offshore and maritime industry today.

A structure or component need adequate toughness for the loading seen at low temperatures to prevent brittle fracture in the Arctic. None of the common offshore design codes today consistently addresses low temperature applications; EN 10225 is applied down to -10°C, NORSOK specifies a lower bound design temperature of -14°C while ISO 19902 does not state a lower bound of the design temperature and operate with requirement to material testing at lowest anticipated service temperature (LAST). ISO 19906 “Arctic Offshore Structures” requires that the Design Class (DC) approach in ISO 19902 shall be applied, which for the highest toughness class of materials requires steel to be tested 30 °C below LAST. Hence, for a design temperature of -40ºC would then typically require Charpy testing at -70ºC. Both Norsok and DC in ISO 19902 specify material per EN 10225 where Charpy testing at -40°C is the lowest test temperature required. It can be noted that EN 10225 currently are under revision with an aim to include materials for arctic offshore application. There is also an ISO working group, ISO TC67/SC8/WG5, drawing up standardized material requirements for Arctic Operations (Hauge et. al 2015). The committee has representatives from Russia, Canada, the Netherlands, Italy, France, Germany and Norway.

“Recognized Class Societies” (RCS) defines the temperature to be used for material selection to be based on the lowest Mean Daily Average Temperature (LMDAT). This temperature is used for structural material selection and should be based on several years of observations. While ISO 19906 for Arctic offshore structure defines the lowest anticipated service temperature (LAST) as the minimum hourly average temperature with a return period of 100

years. ISO 19904-1 opens for either using the LAST or LMDAT (RCS approach) for setting the material temperature.

Setting the material test temperature based on LAST or MDAT provide large difference as shown for a location in the Barents Sea, see Figure 2, where LMDAT gives a temperature of -7°C and -30°C for LAST respectively (Horn et al., 2016).

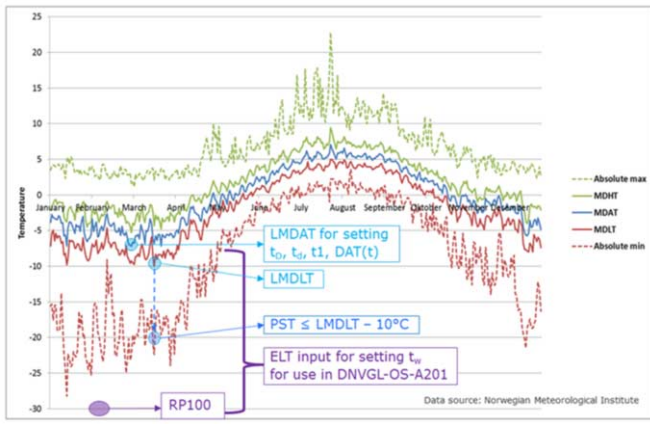

Figure 2: Temperature observations at Bjørnøya from 1998 to 2012. From Horn et al. (2016).

In general, ship and vessels are built to a fixed temperature, which often is set to -10ºC regardless of the location, transport rut etc., except for polar vessels, which are regulated under SOLAS and MARPOL. The same goes for jack-ups which in many cases are specified for -10ºC or for some extreme cases down to -20ºC. These design temperatures are in line with the -10 to -14ºC "qualification of steel materials in Offshore" per EN 10225 and Norsok M-101.

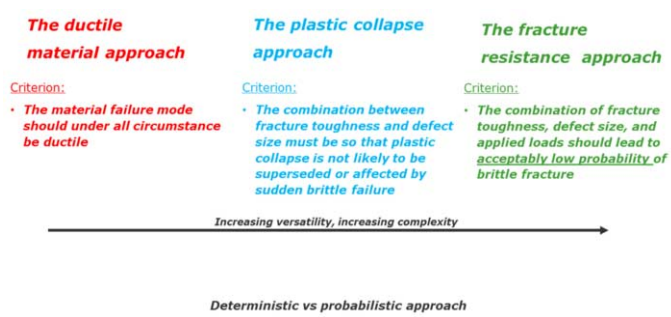

Figure 3: Material approaches. From Østby et al. (2015).

For lower temperatures than -10ºC it is up to the designer to demonstrate adequate toughness at lower temperature, some guidance can be found in Østby et al. (2015) and Horn et al. (2016) and is shown in Figure 3.

Today, it is common to test fracture toughness (CTOD) for the actual design temperature regardless of the utilization at the minimum design temperature. Horn et al. (2017) discuss the toughness in relation to CTOD and thickness and temperature effect. Based on the assumption of absolute stress level controlling the initiation of brittle fracture and an empirical representation of the yield stress dependence on temperature which increases at low temperature, a simplified scheme to transfer toughness levels between different temperatures has been discussed and compared with e.g. the master curve, see Figure 4. The proposed scheme

may have application when having to considered design scenarios with different temperatures, like transportation, installation and operation.

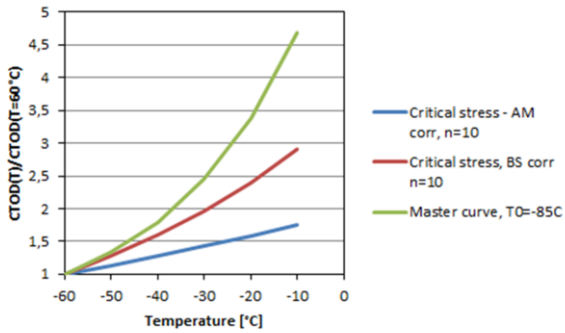

Figure 4: Comparisons of relative critical CTOD as a function of temperature using different models/assumptions. From Horn et al. (2017).

There is currently a focus towards materials behavior under Arctic conditions like the Arctic Materials project managed by SINTEF (2008-2017) (Akselsen at al., 2017). The research project has shown that good toughness values can be demonstrated by the base material, however generally the HAZ and weld metal show lower toughness values, especially in inter critical region in the HAZ, Østby et al (2014). Large scatter in the toughness results have been seen for low temperature toughness testing, (Akselsen et al., 2017) and in Østby et al. (2015) when more than 10 CTOD tests are run. In the Arctic Material project guidance toughness criteria given as CTOD values have been proposed by Østby et al. (2015). In Figure 5, the effect of temperature on toughness is shown for the two different weld thermal simulated

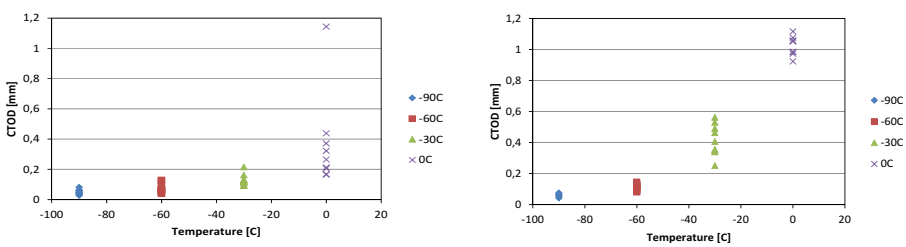

(a) (b)

Figure 5: CTOD values as function of temperature. a) CGHAZ (b) ICCGHAZ. From Østby et al. (2013).

HAZ microstructures CGHAZ and ICCGHAZ. As expected, the fracture toughness increases with increasing temperature (Østby et al., 2013).

Vessels that intend to operate within the Arctic and Antarctic areas as defined in the Polar Code need to comply with the Polar Code which entered force on 1 January 2017. For ship structures intended to operate in low air temperature, materials used shall be suitable for operation at the ships polar service temperature. The Polar Code refers to IACS UR S6 Use of Steel Grades for Various Hull Members – Ships of 90 m in Length and Above (latest version) or IACS URI Requirements concerning Polar Class (latest version), as applicable. IACS UR S6.3 has selection criteria for minimum steel grade requirements of ships operating in low air temperature environments. Based on the ship's design temperature, a structural member's

thickness and material category (i.e., criticality), minimum steel grades are prescribed. The most stringent material quality is use of F class for $35 \leq t \leq 50$ for PC1-3 (most stringent is PC 1 with Year-round operation in all polar waters).

3.4 Composite materials

Marine composites are typically constituted by multi-layered laminates, where each ply can be represented by an orthotropic layer. An orthotropic material admits three symmetry planes; thus, the resulting elastic matrix is defined by 9 independent elastic constants in 3 space, and by 4 elastic constants considering a plane stress condition, which is often the case for marine structures applications, characterized by relatively small thicknesses if compared to other dimensions.

The typical fiber reinforced composite is constituted by a polymeric matrix, which cures on the reinforcing fibers on a mold. The fibers sustain the load, in terms of stress, and provide the stiffness; moreover, the fibers also act as crack stopper limiting the fracture propagation, originating both in the matrix and in the fiber.

On the other hand, the matrix equally distributes the loads among fibers and provide the inter-laminar shear strength. Its tasks are also to resist against chemical aggressions and to allow an ultimate deformation higher than the one of fibers, to prevent from matrix failure at low fiber stress.

In the following, some peculiars aspects are considered resulting from the literature review of the last three years. Earlier findings and general descriptions may be found in Tsai and Hahn (1980), Shenoi and Wellicome (1993) and Jones (1998).

3.4.1 Mechanical aspects

The micro-mechanics considers the interaction between fiber and matrix in the isolated ply, assumed as linear-elastic orthotropic, and defines the elastic constants derived from analytical formulations or, when available, from experiments. Analytical formulations like the so called “mixture rule” are well-established and provide reliable results in terms of axial modulus and in-plane Poisson coefficients, starting from fiber and matrix properties. On the other hand, empirical corrections derived from experimental campaigns are still necessary to overcame limits originating from simplified assumptions in order to define the remaining elastic constants. Among the others, the Halpin-Tsai correction is still likely the most popular in current literature (Halpin and Kardos 1976).

More difficult is to predict reliable data for the strength of the lamina, as the manufacturing process has a strong impact on such parameters and composites obtained from very same fibers and matrix can show completely different behaviors. Manufacturing imperfections, like air inclusions, de-cohesions and fiber misalignment, and chemical features, i.e. the influence of ambient and laminate temperature while curing and humidity, may seriously affect the composite strength as well as its failure modes. This aspect is widely covered in literature, and confirmed in recent works by Godani et al. (2014), Kim et al. (2014), Kalantari and Dong (2017), in addition to earlier references.

The macro-mechanics allows the prediction of the laminate response when subjected to forces and moments, and is based on the so-called “Classic Laminate Theory”, which linearly adds the contribution of each ply to obtain the global stiffness of the composite laminate, given its stacking sequence. The theory is well established and implemented by most of the commercial finite element software when modelling multi-layered composites: it provides reliable results within the material elastic range of each ply. In practice, the mid-plane strains are calculated, as well as the laminate curvatures, from equilibrium considerations. A thru thickness linear variation of strain is assumed and the stresses are computed at each ply. Different failure models can be adopted to asses for the ply failure: the most commonly adopted currently by leisure

boat industry is the maximum strain failure criterion. Other criteria include maximum stress, Tsai-Hill, Tsai Wu and their derivations.

Nonlinear response associated to material failure still represent a challenging task for composite materials. In order to predict the post first ply failure and collapse behavior, orthotropic "plastic" models, with a close to zero admissible plastic deformation, were successfully adopted by Maggiani et al. (2017).

It is worth noting that composite materials present a number of failure modes, which is much higher if compared to traditional isotropic ductile materials, and current theories only provide reliable results to asses for the first ply failure only of laminates: among failure modes, the most critical to assess is the delamination.

Relevant works were conducted in recent years to predict the opening and the growth of delaminations in fiber-reinforced composites, and to assess for their effect in terms of global response of the structure. Gaiotti et al. (2014) compared different numerical strategies to determine the buckling capacity of delaminated composite panels and Colombo and Vergani (2014) studied the effect of delamination on fatigue behavior. Considering the advances of numerical simulations in this field, although the theory was developed in the past decades, due to the high computational efforts cohesive elements have become available in finite element software only recently. This fact has introduced a new tool to simulate delamination opening and growth; by the way, current applications only limits to small-scale models because of two main reasons, both related to computational limits: primarily because of the higher number of elements required to simulate cohesive layers, and secondarily since cohesive are solid elements requiring a 3D-solid modelling strategy.

In general, cohesive models currently represent a powerful instrument to investigate the influence of cohesive parameters in small scale model, while their implementation in large scale design is still far from being achieved due to computational limits. Some promising applications include the analysis of local problems, as well as the numerical characterization of the material capacity to resist against delaminating stresses as reported by Cricrì and Perrella (2016) and Woo et al. (2017).

3.4.2 Recent technological innovations

Another innovation related to reinforcing fiber were led by the introduction of the stitched fibers or non-crimp fabrics that are able to maintain the planarity of the reinforcement. The benefit of non-crimp fabrics leads to an increment of the tensile strength of about 20 to 30 %, being equal the glass content with respect to a woven fabric, according to an investigation conducted by the author upon reinforcements currently available on the market. Moreover, the lower number of interstitial space between non-crimp fibers also allows an increment in the composite fiber content, leading to a further improvement in terms of material properties. On the other hand, non-crimp fibers are more expensive than traditional woven roving, thus their application is limited to high performance composites. Another critical aspect was highlighted by Shiino et al. (2017) in delamination problems, which found a decrease in the surface propagation energy because the stitch yarn replaced the carbon fiber/epoxy interface, which has better chemical affinities

3.4.3 Composites for subsea applications

Composite risers are expected to be a high-impact technology that will be mainstream in the medium term. Nevertheless, due to the complex behavior and damage mechanisms presented by composite materials, when compared to metallic materials, the use of composite risers represents new challenges in terms of design and analysis procedures. There are still few references addressing the behavior of these composite risers in deep water. Pham et al. (2015) presents a comprehensive literature review on manufacture, testing and numerical simulations

of composite risers in deep water conditions, indicating some of the gaps and key challenges for their near future application growth.

FRP composites offer good potential for the design of deep-water risers. Thermoplastic composite risers (TPCR) offer good solutions to current limited technologies in metal Top Tensioned Risers (TTRs) and Steel Catenary Risers (SCRs), related to high costs for buoyancy and compensation system used to support their own weights at deep-waters. Composite risers demand lower top-tension and less or even no buoyancy, leading to a significant weight hanging reduction from the platform deck, this is economically beneficial which increase with increasing length. Furthermore, the size of the tensioner joint and tapered stress joint needed at the top and bottom of the composite riser system are considerably smaller than that of the steel riser system.

When compared to steel risers, composite risers have shown better resistance against many failure modes, including burst, collapse, leakage and crack through the liner and composite tube. Tan et al. (2015) stated that composite risers are more vulnerable to vortex-induced-vibrations (VIV), and therefore fatigue damage, than steel risers. This strength deterioration arises from a temperature increase, which is worst for deeper reservoirs. These effects can be avoided by increasing the fiber-winding angle, increasing the load bearing properties and raising eigenfrequencies, mitigating the VIV. Chen et al. (2013) found that the high stiffness of the liner reduces the overall performance the composite riser under VIV, as the high strength of the composite cannot be fully utilized.

Tan et al. (2015) carried out full-scale study experiments and numerical simulations aiming to compare steel risers and composite risers (with aluminum, steel and titanium liners). The results showed the liner is the weakest link for composite riser design. The titanium liner riser yielded 20% lower RMS strains than the aluminum liner riser and 10% lower RMS stress than the steel liner riser. It was then concluded that titanium alloys are a better choice than steel due to their density, wear and corrosion resistance.

Moreover, composite risers can be classified into two main types: bonded and unbonded. In the first type, the riser's layers are bonded, while in the second type, the relative movements between riser's components are not restrained. Bonded risers often include a core fiber-reinforced angle ply laminate sandwiched between an inner liner of metallic/elastomeric material and an outer liner of thermoplastic/ thermoset material or metal alloy, with the primary role of the liners being to prevent weeping and fluid leakage. DNV-OSS-302 (Det Norske Veritas, 2010) gives detailed design criteria for bonded FRP risers.

The metal-to-composite interface (MCI) is mainly used to provide an adequate contact between the composite pipe body and the metallic end fittings at pipe's terminations, which helps to effectively transfer loads between the pipes. An efficient design of the MCI is important since their length and mass may significantly affect the weight-effective use of composite risers and failure often occurs at this point. Efficient designs for end fitting are crucial for minimizing damage at the MCI, as well as guarantee good load transferring between the composite tube and metal components.

3.5 Weight reducing materials

The weight reduction we typically associate with replacing traditional materials with composites has different implications for ships. For military customers, the potential to incorporate smart functionality and reduce magnetic, radar and infra-red signatures is an obvious advantage. Composites are already used in military ships in several applications including: superstructure, masks, radomes, hangar and so on. However, it is noticed that composites are usually applied in non-main component in ships. One did not see a larger fighting naval vessel after Swedish Visby.

Composites are already used in commercial ships in several applications including: masts and radomes, lifeboats, pipework. Complete composite valve and pipework systems are available which have a major benefit in terms of corrosion resistance for seawater cooling systems. In commercial ships, taking account of the high cost, composites have not large-scale used. Recently, the concept of composite hatch, which was developed by Oshima Shipyard, has been raised. These bulk carrier hatch covers are 17 m by 8 m for each half and would weigh 36 tonnes in steel, but just 12 tonnes in GRP. Most of the top reasons for insurance claims for damage to cargo are related to hatch covers-problems with seals, corrosion, etc. The GRP covers would reduce many of these problems, and allow for smaller electric motors and lighter craneage.

A huge problem in steel ships is corrosion in ballast tanks. The tanks are integral to the structure of the hull, so structural beams pass through them, creating complex surfaces that are very difficult to maintain. A fully composite structure could solve this problem, but to suggest a composite hull for a large ship is a big step from where we are now. Because of its advantage in weight reduction, composites were applied in submersible vehicles. American 'Alvin', French 'Nautile' and Japanese 'Shinkai' manned submersible adopt composite to their outer hull shell. Outer hull shell doesn't bear huge underwater pressure and its major function is keeping structure outer shape to improve hydrodynamics performance and protect inter equipment. As composites low density and high strength advantage, it almost fits all of requirement of submersible vehicle outer hull shell.

Properties of cast aluminum components can be improved by strategically placing ferrous inserts to locally improve properties such as wear resistance and stiffness. A cost-effective production method is to cast-in the insert using the solidification of the molten aluminum as a joining method. Metallurgical bonding between the metals could potentially improve both load and heat transfer across the interface. The metallurgical bond between the steel and the aluminum has to be strong enough to withstand stresses related to solidification, residual stresses, thermal expansion stresses, and all other stresses coupled with the use of the component. Formation of a continuous defect free bond is inhibited by the wetting behavior of aluminum and is governed by a diffusion process which requires both energy and time. Due to the diffusional nature of the bond growth in combination with post manufacturing heat treatments defects such as Kirkendall voids can form.

The effect of aluminum alloying elements during liquid-solid bond formation in regards to microstructural changes and growth kinetics has been described (Soderhjelm and Apelian 2016). A timeframe for defect formation during heat treatments as well as microstructural changes has been established. The effect of low melting point coatings (zinc and tin) on the nucleation of the metallurgical bond has been studied as well the use of a titanium coating for microstructural modification. A set of guidelines for successful metallurgical bonding during multi-material metal casting has also been constructed.

In another research effort relating to light-weighting, aluminum based nano-composites containing, AlN, TiC, SiC and Si_3N_2 second-phase has been studied as an alternative for higher impact and fatigue strength material for structural applications (Udvardy, et.al. 2012).

4. JOINING AND FABRICATION

With certification and qualification of welds being a fundamental input for ship structural integrity, shipbuilders have generally persisted with the classic joining technologies as a proven fabrication option. But as ship designers more commonly use higher strength steels with thinner panels to lighten ship's hulls, distortion becomes a prominent issue for both assembly and ship operations, and so new advances in low heat input welding and joining technology need to be considered.

4.1 Advances in joining technology

There are three key areas shipbuilders use to control distortion: 1) during the design phase where increased stiffness and steel choices affect rigidity, 2) during the welding and joining process itself, and 3) through costly rework to correct distortion after it has occurred. When considering the joining process, the ability to either lower the heat input and/or carefully control the distribution of heat, has the potential to reduce residual stresses remaining after the assembly process.

4.1.1 Low heat input welding processes

In recent years, there are several low heat input processes which have been studied and/or made commercially available as an alternative to the higher heat input process Submerged Arc Welding (SAW). Some of these include Double Electrode (DE-GMAW), Tandem welding (T-GMAW), Double Sided processes (DSAW), Plasma Arc Welding (PAW), Keyhole TIG welding (K-TIG), Laser Beam Welding (LBW), Laser Hybrid welding (HL-GMAW) and Friction Stir Welding (FSW). However, the latter three will not be discussed, since these processes have been covered in previous report.

Tandem processes, on the other hand, include any process that duplicates the number of wire fed electrode and thus the deposition rate. Like hybrid laser or double electrode processes, several variants of the tandem process exist. The Pulsed Tandem Gas Metal Arc Welding (PT-GMAW) and Tandem Gas Tungsten Arc (T-GTAW) are the main studied processes and are commercially available. For the PT-GMAW, two welding wires are independently controlled wires are fed into the same weld pool. The synchronized pulse and electrically isolated electrodes allows the process to independently alter the leading and trailing wire feed and current/voltage settings. The effect is a controlled distribution of energy within the weld pool which results in lower overall heat input and resultant distortion. Doubling the number of electrodes also allows to reduce the number of passes and thus the production cost. Sproesser et al. (2016) showed that indirect savings are also achieved with a comparison of GMAW and PT-GMAW multi-pass processes on a 30mm 355J2+N butt weld. Besides the 55% reduction of the welding time, a 23% reduction of the electricity consumption and a 5% reduction of the total used filler wire was obtained, making it a more cost-effective and sustainable process (Sproesser et al., 2016).

Double electrode processes include any process that uses as second electrode. Generally, a Plasma Arc or GMAW torch is used to bypass some of the current, as shown in Figure 6, resulting in a reduced heat input in the weld pool. It also decouples the deposition rate from the heat input. Estifen et al. (2010) compared DE-GMAW with GMAW on 19 mm butt welds of ASTM 131 grade A shipbuilding ferritic steel and showed a reduction of the number of passes from 11 to 3 and a 40% reduction in the out-of-plane distortion. However, there was no significant reduction in angular distortion.

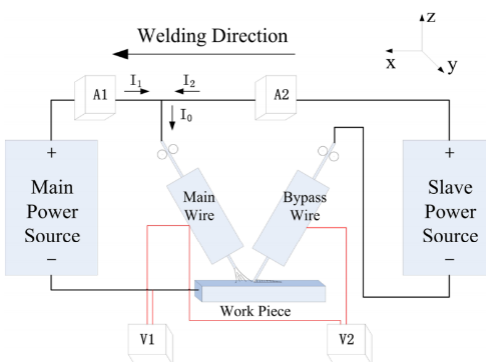

Figure 6: Schematic drawing of the Double Electrode Gas Metal Arc Welding process. From Wei et al. (2015).

The European research fund for coal and steel funded a three year study of the tandem processes (Thompson et al., 2008). Their main conclusion was that tandem processes lead to productivity increase from 50 to 100% without any detrimental effect on fatigue or toughness. They also concluded that T-GMAW was not efficient to reduce buckling distortion in comparison to single

GMAW but was efficient to reduce angular and bending distortion. They produced butt welds, fillet welds, and lap welds for S355 plates varying from 3 to 12 mm thicknesses.

A study and technology implementation by Larkin et al. (2011) showed that when using T-GMAW instead of SAW, angular distortion can be reduced by 60% on a 5mm DH36 single sided butt weld for naval ship panels. Similarly, the out-of-plane longitudinal distortion was reduced by 20% while doubling the welding speed up to 1.4 m/min with a 30% reduction in weight of filler material required (Larkin et. al., 2011). More recent work by Sterjovski et al. (2011) on 8 mm HSLA65 butt weld showed that distortion was reduced by more than 50% in comparison to standard GMAW process (Sterjovski et al., 2011).

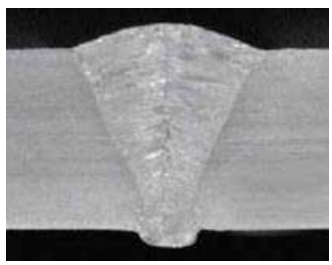

Figure 7: Macrograph of 8mm BW 316Ti Keyhole plasma arc welding. From Knautz (2017).

Plasma arc welding (PAW) is very similar to GTAW except that the arc is constricted in a plasma gas making it a very high-density energy process. The plasma gas itself is maintained in a classic inert gas flux. It is useful for welding thick plates with minimal joint preparation due to high-density of the beam. The process is defined as a Keyhole-Plasma Arc Welding (K-PAW) when the plasma jet penetrates completely through the work-piece. Without backing, the plasma can produce a uniform butt weld with a narrow Heat Affected Zone (HAZ) with reduced heat input. In a single pass, it can weld up to 0.5 m/min with a thickness up to 8 mm, as shown in Figure 7.

Double sided arc welding processes differ from tandem processes as the two welding heat sources are on opposite sides with the aim of balancing the heat input (Mochizuki and Toyoda, 2007). Their research investigates the effect of introducing a distance between the two torches. The advantage of having a fore and a rear torch, besides the balancing effect, is to induce a preheating effect (Mochizuki and Toyoda, 2007) like in tandem processes. Angular distortions could be completely removed using optimised welding parameters (Zhang et al., 2008)

Most recent research use two identical torches, whether they are GMAW (Li et al., 2015) or GTAW (Zhang et al., 2008). However, reported welding speeds are quite low in the literature (0.1 to 0.4 m/min) and the double-sided processes seem to have found more interest in thick plates applications. Thicknesses up to 50 mm have been welded using multi-pass DSAW with SAW (Yang et al., 2014) or DSAW with GMAW (Chen et al., 2015).

A similar process is the *Keyhole Tungsten Inert Gas (K-TIG)* welding process*;* although no plasma is required, making it an easier process to implement. According to the manufacturer, the process can weld up to 16mm thick steel plates and weld at 0.75m/min on 4 mm plates. Both PAW and K-TIG offer an alternative to the costlier laser key hole processes.

In summary, the uptake of each of these described low heat input processes within shipbuilding is varied. Besides laser beam welding, there are few instances of alternate low heat input welding methods being routinely used in production. For the Australian and US naval shipbuilding, there are two examples of panel line construction using PT-GMAW, and ongoing research (Leviel et al., 2017) on fillet welds for stiffened panels. For all other processes, production trials are generally the extent of their implementation.

4.1.2 Secondary Processes - Active distortion control

Low Stress No Distortion (LSND) processes use secondary heating or cooling sources to modify the local thermal profile of the resultant weld. These secondary thermal inputs are not used to influence the weld fusion process but instead only to modify the residual stress state and the structure distortion. The first distinction that has to be made within various forms of LSND processes is whether the heating or cooling source is moving or not.

In *Static-Low Stress No Distortion (S-LSND)*, fixed heating and cooling sources are used to balance the thermal profile to impede the plastic strain accumulation during the heating stage of welding and thus the stress formation. To obtain the adequate thermal profile, cooling is applied to the weld zone area. In some applications, the surrounding zone is also heated. A 170˚C difference is sufficient to prevent buckling in 4.8 mm DH36 stiffened panels (Conrardy et al., 2006). With optimised parameters, it can result in very low stress and almost distortion-free samples. However, generating the optimised thermal field evenly on the whole structure requires devices that are industrially impractical, costly and environmentally unfriendly. It is therefore recommend using transient heating discussed later.

A recent application to 3 mm aluminium butt-welded plates was published by Bajpei et al. (2016). They compare the cooling effect of a heat sink backing plate, of compressed air and of atomised water applied to the back of the weld. By using a numerical model validated with residual stress measurements, they show that angular distortion can be reduced by 50% and that shrinkage is almost eliminated.

In contrast to S-LSND, Transient - Low Stress No Distortion (T-LSND) processes use a moving secondary source. They are further categorised between processes using heating sources, known as transient heating and the processes that use a cooling source immediately behind the welding source. Because the heating or cooling sources are moving, the induced mechanisms, stress, and distortions results are completely different to S-LSND. Side heating is one method used, and although it has been shown to be very efficient to reduce buckling distortion (Pazooki et al., 2016), it has some drawbacks that need to be overcome. Because the plates are heated on one surface, the through-thickness thermal gradient is increased which causes more angular distortion. Although it can be controlled through severe clamping, it is unlikely that this solution would be used to weld large structures. Secondly, the reported welding speed in the literature are low (0.27-0.38 m/min). Transient reverse-side heating, or line heating, consist of applying a heat source on the opposite side of the weld. The process is thus very similar to asymmetric double-sided processes except that only one of the two torches is effectively welding. Mochizuki and Toyoda applied reverse side heating to reduce the angular distortion of fillet welds (Mochizuki and Toyoda, 2007). A relatively high welding speed of 1.8 m/min have been reported. The main drawback is that it only corrects the angular distortion.

Dynamically Controlled Low Stress No Distortion (DC-LSND) process uses the principle of a welding process trailed by a cooling source to reduce buckling distortion. Rotational distortions in fillet welds, caused by the bending of the plate and the stiffener, can also be reduced (Mochizuki et al., 2006). Several recent studies have used different cooling agents (Sudheesh and Prasad, 2015, Van der Aa, 2007, Okano and Mochizuki, 2016), however, CO_2 snow has been widely reported as being the most effective (Shen, 2013, Van der Aa, 2007). The CO_2 becomes solid at -78°C producing a snow jet. Part of the efficiency of the CO_2 snow as a cooling agent is attributed to its temporary solid state which induces good contact with the weld metal surface (Van der Aa, 2007). However, application of CO_2, produces an undesirable effect of disturbing the welding shielding gas flow as result of a turbulent flow of gas/liquid/solid being applied to the metal surface in close proximity to the welding process. For this reason, application with laser welding or FSW is easier. For application with GMAW or GTAW processes, several approaches have been tried to separate the two sources including intermittent welding or shielding as shown in Figure 8 (Holder, 2011, O'Brien et al., 2015 and Nagy, 2012).

Figure 8: Roller with silica based woven textile Refrasil® wool. From Holder (2011).

A study by Price et al. (2004) achieved an 80% reduction of the distortion index (average measured distortion) using CO_2 cooling for 5 mm DH36 plates (Price et al., 2004, Nagy, 2012). Nagy's own experiments, which focussed on buckling distortion, adapted a patented vacuum shield. He achieved butt welds on 4 mm DH36 with a 50% reduction of the out-of–plane peak longitudinal distortion when compared to the classic GMAW process. Currently there is no reported manufacturing use of this technology in shipbuilding production.

Table 4 summarises the main features of the different welding processes discussed above for the case of butt welding of DH36 steel. It is seen that the laser beam welding (LBW) gives the thinnest HAZ but also for the highest investment cost. Submerged arc welding (SAW) gives the widest HAZ and also large residual longitudinal stresses.

Table 4: Summary of the main characteristics of welding processes in DH36 butt welds.

Process	Vickers hardness peak value [kgf/mm2]	Longitudinal residual stress peak value [Mpa]	Typical welding speed [m/min]	Comparative investment cost from low ($) to high ($$$$)	Fusion zone area / Fusion zone area of the SAW process
GMAW	210-240	350	0.4-0.8	$	0.6
T-GMAW	210-240	320	0.7-1.6	$$	0.6
DC-LSND	235-245	350	0.25-1.4	$$	0.6
K-TIG	230		0.3-0.75	$$	0.3
DE-GMAW		350-550	0.3-1.27	$$$	0.2-0.3
LBW	400-420		1-2.5	$$$$	0.1
HL-GMAW	257-270		0.7-2.5	$$$$	0.2-0.3
SAW	215-226	450	0.4-1.1	$$$	1
FSW	290-350	355	0.1-0.5	$$$	0.6-1.1
DSAW	200-220		0.1-0.35	$$$	0.2-1.2

4.2 Automation and robotic programming

Robotic welding automation allows manufacturers to increase quality, flexibility with the ultimate aim of reducing costs. Many advanced welding processes also rely almost exclusively on robotic manipulation to provide the required control and posture. However, the challenges involved in programming welding robots for either complex environments or low volume production runs have been a significant barrier to shipbuilding. New advancements in the way robots can be automatically programmed are being used to generate robot programs directly from Computer Aided Design models with minimum human input. This now makes it possible for robot welding to be more cost effective than manual welding, even for once-off tasks.

Automated Offline Programming (AOLP) Larkin et. al. (2018) is an approach which extends Offline Programming (OLP) by using algorithms to automate much of the robot programming process. This can drastically reduce or even eliminate the human effort required for robot programming and allows for the generation of complex motions to access challenging areas, as well as integrating sensing to deal with part placement inaccuracies. Several shipyards have implemented AOLP with some level of automatic program generation. Kranendonk commercially offer RinasWeld™ as a weld planner, where robot type, position, configuration of external axis, and tooling are all 'hard coded' into a specific version of the software supplied for the end user. Bickendorf (2014) also describes a motion planner termed MOSES for the robotic welding of ship-subassemblies. The general approach taken for each of these AOLP software solutions is shown in Figure 9.

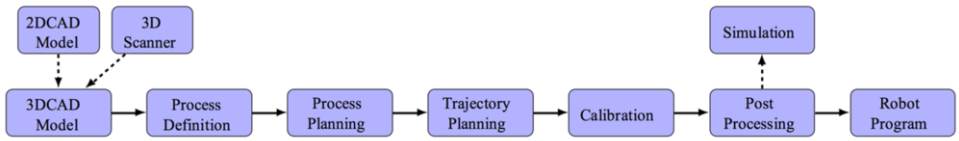

Figure 9: AOLP process for welding. From Larkin et al. (2018).

Unlike Computer Aided Manufacture with conventional multi-axis CNC tools, common industrial robots have a joint configuration which creates redundant motions. When coupled with requirement to provide specific weld gun orientations and other external axes, testing all possible solutions becomes computationally inefficient. By decomposing the welding task space problem, Larkin et. al. (2018) significantly reduce the computational complexity required and significantly simplify the tool path planning problem. This allows for dynamic programming to be handled for changing environments (calibration) and for higher degree of freedom manipulators such as multi-legged crawling robots used for bulk head and ballast tank inspection (Short et. al., 2017). Ding et, al. (2016) use this approach to apply adaptive robotic programming for the wire arc additive manufacture (WAAM) of ship's components. In these instances, AOLP is simultaneously used with CAD part slicing and decomposition algorithms to rapidly generate layered robot welding motion paths.

4.3 Additive Manufacturing

Additive Manufacturing or 3D-Printing (AM) is a technology that produces three-dimensional parts layer-by-layer, generally from polymeric or metallic materials. The method relies on a CAD protocol created digitally and transmitted to a machine that builds the component. Additive Manufacturing offers several advantages in the production of complicated and intricate parts, presenting design freedom with the ability to manufacture single or multiple components from a wide range of materials. The process allows the fabrication of parts from materials, such as refractory metals, titanium alloys, Ni- and Co-based super-alloys, tool steels, stainless steels as well as aluminum alloys, in near-net shape, requiring minimal post-processing. While the process has significant advantages over metal casting, wrought processing or powder-met techniques that require further post-processing (heat treatment and subtractive steps), AM provides easy manufacturing of engineering components that can be used by any industry, including shipbuilding.

For Ingalls Shipbuilding (Ingalls), the Integrated Project Team (IPT) has assessed and demonstrated the use of AM during ship construction activities, quantify the expected benefits, and provide a recommended path toward implementation. For General Dynamics Electric Boat (EB), the IPT has developed and demonstrated a process map that will allow the rapid production of tools and fixtures using AM. Additive Manufacturing (AM) is rapidly becoming a versatile tool in the manufacturing industry as the cost of acquiring and implementing the technology decreases. The Navy Metalworking Center (NMC) has conducted a project that has demonstrated the cost and time benefits of AM to support the construction of Navy platforms. Ingalls and EB are interested in using AM for several potential applications, such as visual aids for manufacturing, planning and staging; and production aids for temporary construction and templates. Using AM for these applications will lead to cost and time benefits, as well as improvements to first-time quality during ship construction (Wang X and Whitworth J, 2016).

On-site testing at Ingalls of three-dimensional (3-D) printed parts has been used to develop an implementation plan and to support a business case. At EB, the project-validated process map has been used as the basis for a procedure to instruct shipyard personnel on how to rapidly deploy new tooling / fixtures using AM. Ingalls has estimated a minimum acquisition cost savings of US$800,000 per year by utilizing AM for the construction of DDG, LHA and LPD. EB has estimated a minimum acquisition cost savings of US$200,000 per Virginia class

submarine (VCS) by using AM technology to rapidly deploy new tooling and fixtures. Implementation at Ingalls is planned in FY17 for DDG 121, LHA, and all future surface combatants produced there. Implementation at EB is planned for FY 17 on VCS (SSN 794) (Ingalls, 2017).

Engineers at Netherlands' Port of Rotterdam have begun experimenting with 3D printing processes to carry out repairs on damaged ships. The Port has opened the Rotterdam Additive Manufacturing Lab (RAMLAB), which has a pair of 6-axis robotic arms capable of additively manufacturing large metal industrial parts. The port is working alongside Autodesk which presented a scaled down 3D printed ship's propeller at Hannover Messe in Germany (World Industrial Reporter, 2017).

Some of the specialized component examples that have been produced via AM include brackets for aircrafts, micro-turbines, medical devices, fuel nozzles for jet engines, vacuum calibration sleeve, wing profile, turbine rotor, hydraulic crossing, etc. The AM industry products and services worldwide are projected at over $11 billion.

Herzog D, et al. (2016) has discussed the methods and materials for AM. In this context, the overview article describes the complex relationship between AM processes, microstructure and resulting properties for metals. It explains the fundamentals of Laser Beam Melting, Electron Beam Melting and Laser Metal Deposition, and introduces the commercially available materials for the different processes. Special attention is paid to AM specific grain structures, resulting from the complex thermal cycle and high cooling rates. The properties evolving as a consequence of the microstructure are elaborated under static and dynamic loading.

4.4 Fabrication and joining of composites

Manufacturing imperfections, like air inclusions, de-cohesions and fiber misalignment, and chemical features, i.e. the influence of ambient and laminate temperature while curing and humidity, may seriously affect the composite strength as well as its failure modes. This aspect is widely covered in literature, and confirmed in recent works by Godani et al. (2014), Kim et al. (2014), and Kalantari and Dong (2017), in addition to earlier references.

4.4.1 Air inclusions

The presence of air bubbles of various size is common in hand lay-up manufacturing method. The spherical shape of the bubbles make them less critical than sharp de-cohesions originating from impregnability issues, in terms of stress concentration, although they can influence the inter-laminar shear strength up to 25 % as investigated by Di Landro et al. (2017). Shipyards are gradually abandoning the manual impregnation, which is still very common indeed, in favor of the impregnation machines.

4.4.2 Exothermic peak

The exothermic peak often results in the need of splitting the lamination of thick stacking sequences into multiple stages. The peak mainly depends on the resin curing process, which is a fixed parameter once the matrix is chosen. Relevant investigations include Vargas et al. (2015) for polyester and Park et al. (2015) for epoxy. Other governing parameters are the ambient temperature which can seldom be controlled in shipyards, especially when laminating outdoor, and mostly the laminate thickness, since the heat transfer rate is less efficient in thicker laminates. Infusion method requires expensive consumables that have to be disposed after the process, thus splitting the lamination into different stages significantly increases the manufacturing cost. Moreover, the cured surfaces will not bond over fresh resin by chemical adhesion when produced by infusion, and only mechanical adhesion onto wrought surfaces will be possible. Hence, the vacuum infusion is still limited to decks, super-structures and components for naval applications. In leisure boat industry instead, the thickness involved is

usually not critical in term of exothermic peak, even in the bottom shell, and the manufacturing method choice is governed by a cost-benefit analysis.

4.4.3 Bending response of infusion made composites

Infusion-made composites present better quality towards embedded imperfection such as decohesions, air inclusions and delaminations. If on one side the higher fiber content associated to the infusion method leads to higher specific mechanical properties, the lower thickness diminishes the inertial contribution on the other. Hence, the resulting laminate will show a reduced bending response. Such assumption has recently found experimental evidence in Yaacob et al. (2017), where a small 12 feet fishing boat was built by both hand lay-up and infusion, with identical stacking sequence. The experiments showed that the resin infusion technique performed better upon ultimate tensile strength (+27%) but less satisfactory for in compressive stress (-12%) and flexural stress (-34%). The thickness reduction also gives rise to concerns about elastic stability issues. In conclusion, the potential benefits led by infusion method are out of discussion and well assessed in terms of composite quality.

4.4.4 Prepregs

Prepregs represent the state of the art in terms of composite performance, as they can maximize the fiber content leading to outstanding material properties. The extremely high cost and the need for refrigerated storage rooms limit their application to racing yachts and high-performance components. Manufacturing cost of prepreg is also a critical aspect, as to achieve outstanding material performances vacuum bag technology in controlled environment shall be adopted. Godani et al. (2015) highlighted poor inter-laminar performances of prepregs specimens due to air inclusions, with respect to a similar fiberglass composite produced by infusion. Gangloff et al. (2017) showed that imperfections related to air inclusion mainly originate in prepreg production, while the curing process inside the vacuum bag has a scarce influence on the overall quality.

4.4.5 Fibre-matrix interface

The interface between fibre and matrix is a governing parameter when dealing with fatigue and fracture, as well as dynamic loading. Due to chemical issues related to the different ionicity of matrix and fiberglass, a sizing is always necessary to improve fiber impregnability and fiber-matrix bonding. Carbon fiber is less critical and does not require sizing application in general, although recent innovations made available sizing for carbon, to improve the laminate performance (Andideh and Esfandeh, 2017) and Kobayashi et al. (2017). The fiber-matrix cohesive parameters may determine the predominant damage mode in particular stress conditions, as recently investigated by Ma and Liu (2016). Fiber bridging effects in fatigue problems were investigated by Olave at al. (2015), while Airoldi et al. (2015) showed the influence of fiber bridging in delamination problems

4.4.6 Epoxy matrix

Vinyl-ester matrices are nowadays characterized by outstanding performances in terms of elongation at break (above 4.5 %), as well as inter-laminar adhesion. These features close the gap with epoxy resin, considered the top performing matrix. Besides the higher cost of epoxy, correct handling of an epoxy matrix is a challenging task, as epoxy requires fixed thermal profiles in the post-curing stage, in order to show clear advantages with respect to a vinyl-ester matrix. Hüther and Brøndsted (2017) found that fatigue performance of unidirectional glass fiber reinforced epoxy composites, for loading at 0° with respect to fiber orientation, is highly influenced by the curing cycle. Relatively small components can be built in pressurized ovens, while large hulls require mold heating: in conclusion, the handling difficulties are still limiting the widespread use of epoxy for large marine structures mainly to racing yachts and naval applications.

4.4.7 Non-crimp fibers

Non-crimp fabrics maintain the planarity of the reinforcement leading to an increment of the tensile strength of about 20 to 30 %, being equal the glass content with respect to a woven fabric, according to an investigation conducted by the author upon reinforcements currently available on the market. Moreover, the lower number of interstitial space between non-crimp fibers also allows an increment in the composite fiber content, leading to a further improvement in terms of mechanical properties. On the other hand, non-crimp fibers are more expensive than traditional woven roving, thus their application is limited to high performance composites. Critical aspects were highlighted by Shiino et al. (2017) in delamination problems, which found a decrease in the surface propagation energy because the stitch yarn replaced the carbon fiber/epoxy interface, which has better chemical affinities.

4.4.8 Joining of composites

Fabrication of the hull either metal or composite is by no means the end of production; the bare hull must be turned into the finished vessel through the addition of stiffeners, decks, superstructure, bulkheads and fittings, all of which must be joined together. This may require up to 50% of the total time and building costs. Joining of fiber reinforced plastic can be achieved by surface bonding, bolted connection or combined solution. When large composite components are considered, bolting is not usually cost-effective since, as the number of bolts increases, the manufacturing process of the joint becomes slow and costly. Also, the bolts are adding weight to composite components. Bonding is cheaper, lighter, needs significantly less assembly time, can join dissimilar materials and FRP, does not change the base material properties, allows the use of thinner plating, can be performed from one side of the panel, and spreads the load over a greater area. Flexible adhesives can also reduce vibrations, compensate for tolerance problems in large component assembly, accommodate thermal expansion differences and reduce stresses due to deformations. Importantly in a marine context, bonding may also replace over-laminating to fix stiffeners to panels, significantly reducing the labour and time required.

Sutherland et al. (2017) conducted a large test program of statistical experimental design techniques, used to study the strength of ‘T’-Joints representative of various connections of marine composite. The effects of different surface preparations, cleaning methods and adhesives were investigated. An analysis of variance was conducted, giving an extremely good fit to the experimental data while statistical methods identified significant interaction effects. A way to overcome these problems is to prefabricate metallic joint elements (special profiles), which are adhesively bonded to the composite substructure by the FRP manufacturer and then welded to the ship structure. Such a procedure allows the adhesive joint to be manufactured in a suitable environment and, on the other hand, the shipyard to weld the FRP parts to the ship in an equivalent manner as corresponding metal parts. The majority of research carried out on metal-to-composite connections has been on secondary process joints. Some assessment strategies for composite-metal joining technologies is reviewed by Jahna et al. (2016). This involves the manufacturing of a composite structure and subsequent adhesive bonding to the metallic structure. There is increasing interest in producing joints by the co-curing method, which involves the making of the joint while consolidating the composite material.

4.4.9 Influence of the ply orientation

Hazimeh et al. (2016) was investigated the influence of composite laminates’ orientation on the peel and shear stresses in the adhesive layer of composite double lap joints. The highest adhesive stresses are achieved when fibers are all or mostly oriented along the loading/axial direction [0°] and the lowest adhesive stresses are obtained when the fibers are oriented perpendicular to the applied load [90°]. It is concluded that the adhesive stresses increase as the substrates longitudinal stiffness increases. Stress in the adhesive layer is mostly influenced by the closest laminate plies and almost not affected by the far plies.

4.4.10 Nanoparticles

Findings from nanoscience and nanotechnology, influence adhesives sciences significantly. Akpinar et al. (2017) added nanoparticles to the adhesive to increase the damage load of adhesively bonded single lap composite joints. Tensile and bending moment damage loads were experimentally investigated. In his study, carbon fiber fabric reinforced composites (0/90°) with Plain Weave were used as the adherend; rigid, tough and flexible adhesive types were used as the adhesive and 1 wt% Graphene-COOH, Carbon Nanotube-COOH and Fullerene C60 were used as the nanoparticles. The use of carbon fiber fabric reinforced composites as the adherend considerably increases the damage load of the joint, depending on the adhesive type. The addition of nanoparticles to the adhesive was also shown to increase the tensile and four-point bending damage load of joint, depending on the adhesive and nanoparticle type.

4.4.11 Fire resistance

According to the IMO (2009), composites must be considered combustible materials resulting in critical safety issues. Relevant published works include Evegren at al. (2014), Evegren and Hertzberg (2017). Current researches focus on flame-retardant additives: hybrids of aluminum hypophosphite and ammonium polyphosphate proved to be very effective by Lin et al. (2016), as well as phosphorus-containing star-shaped flame retardant included in the polyester matrix as tested by Bai et al. (2014), by the way their impact on mechanical properties was not assessed. Saat et al. (2017) tested the influence on mechanical properties of aluminum phosphate, used as fire retardant in fiberglass reinforced polyester matrix for leisure boat applications, indicating promising results.

5. QUALIFICATION AND APPROVAL

Technology qualification is all about building confidence for the stakeholders. New materials (e.g. composites) and related fabrication processes offer several benefits like weight saving, integrated functions etc. which finally result in reduced life cycle cost of ships and marine structures. They also offer a large variety of materials, fabrication and assembly processes which will in future lead to a much larger material mix in ships and offshore structures.

On the other hand, marine structures need to survive under extreme environments and operational conditions (loads, exposure to sea water, chemicals, UV radiation) for long life spans with limited possibilities of human interaction at sea. This imposes high risks on human life, maritime assets and the marine environment. To manage those risks rules and regulations by IMO, SOLAS (supervised by the flag states) as well as the classification societies have been issued, against which any new material and fabrication process needs to be benchmarked and approved.

In relation to the approval of new materials and related fabrication processes currently the maritime industry is facing the following challenges:

- New materials offer a wide variety of options which all influence their properties. Long term experiences on their operational performance are often missing;
- Prescriptive rules and regulations are often not applicable to new materials. Therefore, equivalent safety needs to be demonstrated for alternative designs, arrangements and innovative solutions. While this process as such is well known, its implementation is case specific and currently not harmonized, knowledge intensive, lengthy and costly;
- The speed of innovation in the maritime industry as well as in its suppliers (e.g. material sciences) is increasing and becomes a competitive factor. Current approval practices become more and more obstacles for innovation or slow down the innovation process significantly. A new – faster and simplified - procedure to approve new materials is necessary.

Putting into practice new materials or technology will need to be proven and qualified prior to be set in production and operation to minimize risk for its developers, manufacturers, vendors, operators and end-users. New goal based design codes give more options for material and process selection.

This chapter is divided into two main parts; one presenting the outcome from an ISSC meeting with the industry and example of qualification of composites for the offshore industry and the second part show the different class society approval and qualification schemes.

5.1 Qualification of composites

Lack of rules and guidelines can be a showstopper for implementing new material solutions. For the maritime sector, guidance related to use of composites has been limited. However, the issuing of the IMO guidelines for use of fiber reinforced plastic (FRP) within ship structures were formally approved without objections at MSC 98 the 16 June 2017 are welcome guidance for designers. The guidelines will be "interim" for a period of four years to allow for feed-back and modifications based on experiences from applying the guidelines. The guidelines particularly address fire when FRP composite is used to replace non-combustible structures. The document provides guidance when developing lightweight ships of the future with focus on recommendation regarding the needed assessment to prove equivalency by compliance with the prescriptive requirements provided by SOLAS with focus on risk assessment and uncertainty treatment. Still there will be challenges the industry will face and in order to map and discuss these, a joint workshop facilitated by this ISSC committee were held in April 2017, see below for a summary.

5.1.1 Hamburg meeting on qualification on composites

With the aim to discuss obstacles and possible new approaches for the approval of new materials in the shipbuilding and offshore sectors a joint workshop was arranged between the ISSC “Fabrication” committee, the European research projects RAMSSES and FIBRESHIP, see Chapter 2.1.2, and other participants including the classification societies DNVGL, Bureau Veritas and Lloyds Register and a representative of the IMO Correspondence Group on Composite Materials. The participants presented different approaches to improve the approval process for new materials which are either in use by the classification societies or under development in research projects. In addition, the group consisting of some 15 participants developed a list of issues to be addressed. This topic list was discussed and prioritized after the workshop. The discussion will continue using the E-LASS platform (www.e-lass.eu) which is open to external participants at no cost.

The following list gives an overview on the outcomes of the joint workshop conducted in Hamburg in April 2017:

- Spreading knowledge and establishing a “Maritime Materials Innovation Platform”
  - Establish a platform for information exchange and discussion;
  - Demonstrate and showcase successful applications of composite materials in the maritime sector;
  - Provide a better overview on existing rules and regulations related to new materials in shipbuilding and offshore, harmonize rules and approaches for shipbuilding and offshore;
  - Improve information exchange with other sectors and cross-industry standardization;
  - Develop materials, component and test data bases and define access rules for joint use.

  Note: The European RAMSSES project together with the existing E-LASS network for maritime lightweight materials are in a process to establish and extend such a platform which is accessible to any interested party, see www.e-lass.eu

- Research and research infrastructure
  - Research to better understand failure mechanisms of new materials and components under maritime conditions, with focus on ageing;
  - Assess defects in mock-ups from previous research and application;
  - Improve and share infrastructure for long term testing under real-life conditions;
  - Better correlate long-term testing, accelerated lab tests and develop numerical methods to reduce expensive tests;
- Supporting the prove of equivalent safety per SOLAS:
  - Collect success stories for the use of composite materials and submit to IMO;
  - Develop standard risk scenarios, which can be re-used for similar cases to reduce the effort and time for risk assessments;
  - Develop and harmonize rules on required tests depending on risks across classification societies and sectors;
  - Define "experience classes" and a concept to implement them in the approval process;
  - Define procedures how condition monitoring in operation can be considered in the approval process;
  - Develop a list of "qualified service suppliers" for inspection, NDT, repair and eventually recycling of composite and hybrid material solutions;
  - Develop lists of approved NDT methods and numerical methods for design;
  - Extend the list of type approved solutions for materials, components and processes.
- Develop new prescriptive rules for low risk composite applications with sufficient experience;
- Develop new business models for risk sharing in the introduction of innovative solutions between

5.1.2 Best practice of qualification of composites

Composites is an attractive material due to its strength, light weight and enhanced resistance to CO_2 and H_2S. Certification and qualification of composite components qualification requires extensive testing including full scale testing to document especially long-term properties.

A typical qualification campaign for a subsea composite component is costly and can range from 10 to 100 MNOK and an approximately cost distribution is shown in Figure 10 and reply on physical testing and very limited analytical work.

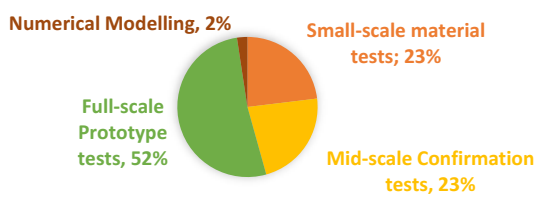

Figure 10: Approximate cost distribution for a typical qualification program for use in an oil & gas application

Since a test campaign is both costly and time consuming, qualification by simulation to reduce the need for testing would be of high value for both offshore and the maritime industry. Today industry phase the challenge to develop and qualify advanced material models to predict long-term performance of composites structures. Multi-scale modelling is important and should address important factors like the effect of aging of material at various medial, temperature and failure mechanisms to be assed under both short term and long term loading conditions (cyclic and static fatigue). DNVGL-ST-C501 "Composite Components", 2017 is a generic composite standards which give guidance on required test scope and acceptance criteria. The standard

opens for several ways of documenting the material properties like; direct measurements, qualification against representative data, qualification against manufacturer's data, data from the open literature and by component testing. The standard is adopting a multiscale approach where the results from smaller scales can be reused for various applications with different load scenarios, see Figure 11 for a possible test scheme.

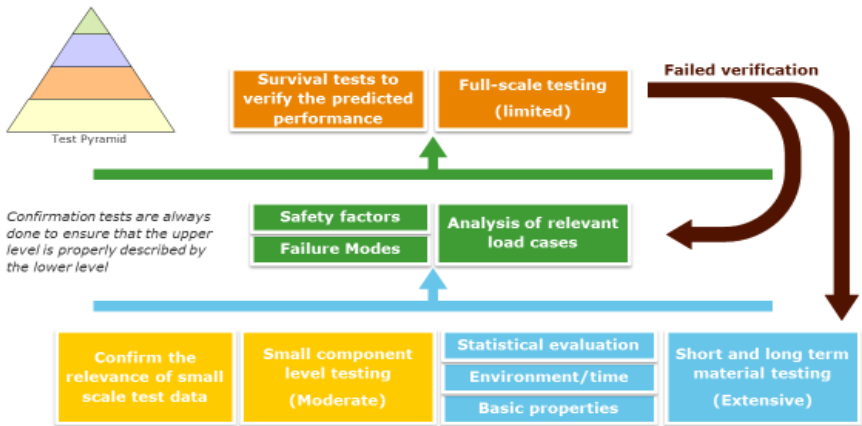

Figure 11: Overview of a proposed test campaign for composite material

Below some different theories and modelling assumptions have been pretended.
Performance based qualification approach can be useful for application where a well-known simple performance is required;

- Many full-scale tests are typically required depending of the targeted performance accounting for environmental effects such as temperature and degradation.
- The qualification is only valid for the tested conditions.
- Not a practical option when a complex long term performance is required.

Short and Long Term Small-scale Material Testing is demanding and may become expensive;

- Flexible with statistically determined characteristic values are used.
- Long term material strength is determined by small-scale testing.
- All determined properties are used in the analysis phase.
- Results of material tests depending on their scatter are used to choose the right set of calibrated partial safety factors.

Confirmation Testing on Representative Component;

- To ensure the relevance of material tests to the actual component.
- Static tests: Stresses/strains to failure should be within one standard deviation of the predicted mean stresses/strains.
- Long-term tests: Time/cycles to failure should be within one standard deviation of the predicted mean Time/cycles.
- Can be used for determination of the model factor accounting for the deviations between tests and analysis predictions.

Survival tests are required to verify the long-term strength calculations;

- Required only for safety classes high and medium.
- Should be performed for the loads which FRPs are expected to experience.
- Two survival tests for safety class high for each load case.
- One survival tests for safety class medium for each load case.

There has been activity the last years to qualify composites pipes for use subsea like a spolable reinforced thermoplastic pipes (RTP) as a cost-effective solution compared to carbon steel or CRA material (Adam et al., 2016). Anderson et al. (2016) investigated the use of flexible composites risers for 3000 m water depths where weight and installation cost can be reduced by use of composite pressure armour/tensile armours to replace steel. Wilkins et al. (2016) presented a qualification program for composite pipes based on a risk based approach (DNVGL-RP-A203 Technology Qualification 2017) in combination with generic composites requirements given in DNVGL-ST-C501. The test campaign consisted of small, medium and large scale testing. The paper addresses the challenging related to different acceptable small scale test methods to measure strength of composites materials, depending on method mean strength of 400 MPa up to 1000 MPa were reported. The data from small scale tests were input to finite element models of the pipe, and the medium scale testing was validating and adjusting the numerical models to capture the damage and failure mechanisms. To appropriate address the failure criteria is challenging when modelling composites; from assuming simple linear material behavior up to the point of brittle failure "fiber strain models" to progressive damage models allowing for matrix cracking.

5.2 Qualification and approval processes by the class societies

Technology qualification is a process of defining an adequate set of acceptance criteria for delivery and limits to operations, to assure defined technical performance of solutions. In the following the qualification and approval schemes by the different class society is briefly presented and discussed.

5.2.1 DNV GL

Technology Qualification comprises services for qualifying, assessing and developing new technology, as well as failure investigation. These services typically involve laboratories and physical testing. DNV GL has two recommended practices which addresses new technology; Technology Qualification / DNVGL-RP-A203, 2017 / and Technology Qualification Management / DNVGL-SE-0160, 2015 /DNV-DSS-401, 2012/. These practices have successfully been used by the offshore and the maritime industries. To focus on where uncertainty is greatest, the novelty categorization of Table 5 can be used. Both the novelty of the technology itself and its application area affect the uncertainty associated with the technology.

Table 5: Technology Categorization

Technology Categorization (table 7-1 in DNV-RP-A203)			
Application Area	Degree of novelty of technology		
	Proven	Limited Field History	New or Unproven
Known	1	2	3
Limited Knowledge	2	3	4
New	3	4	4

Category 1 technology elements are proven with no new technical uncertainties, where proven methods for verification, tests, calculations and analysis can be used to provide the required qualification evidence. Elements in category 2 to 4 require technology qualification and have an increasing degree of technical uncertainty.

5.2.2 ABS

ABS has two documents that deals with new technology; Qualifying new technologies and Guidance Notes on Review and Approval of Novel concepts (April 2017). The guidance is based on an engineering approach for qualification and is divided into a multi-stage process that is aligned with the typical product development phases of a new technology. For the

validation system integration and operational stage typically engineering evaluations and risk assessments are carried out. For both certification and classification approval concepts the acceptance will be based on safety and includes vendor, system integrator and end-user. The process covers the following qualification steps; feasibility, concept verification and prototype.

5.2.3 Bureau Veritas

The qualification of new technologies or existing technologies used in a new context is described in Bureau Veritas guidance note NI525 from 2010. The basic principle of qualification is to simulate, as realistically as possible, the service conditions for which a novel technology is designed. The qualification process opens for combining both theoretical, analytical modelling and physical tests. The process is divided into five steps; (1) identification of new technology, (2) functional description, (3) failure mode effect and criticality analysis (FMECA), (4) cost/benefit analysis and (5) recommendations regarding design, qualification and inspection/maintenance of equipment as to reduce/maintain the deviation from specified performances and/or risk to/under an acceptable level.

5.2.4 Lloyds

The qualification process is divided into three steps; technology appraisal, technology qualification (TQ) plan and execution, review and certification and described in Guidance Notes for Technology Qualification from 2017. The TQ is a goal based approach to risk that can be applied to any technology, ranging from the unconventional LNG offloading arrangements to the integration of marinised gas turbines into topside process plants, as well as aerial vehicles and various renewable technologies.

5.2.5 IMO

The IMO guidelines for how to manage fire safety in association with use of fibre reinforced plastic (FRP) within ship structures (MSC.1/Circ.1574) were formally approved without objections at MSC 98 in 16 June 2017. The guidelines will be "interim" for a period of four years to allow for feed-back and modifications based on experiences from applying the guidelines. This is hence a challenge to the industry to demonstrate interest in lightweight structures and to apply and evaluate the guidelines. The guidelines particularly address necessary fire safety considerations when FRP composite is used to replace non-combustible structures. The document provides guidance when developing lightweight ship structures, with focus on recommendations for the required assessment to prove fire safety equivalency to compliance with the prescriptive requirements. This approval process for alternative design and arrangements is provided by SOLAS II-2/17 (fire safety) and by SOLAS I/5 (general) and is based on risk assessment evaluation of introduced hazards and achievement of fire safety functions. The guidelines for example describe typical FRP composite materials and compositions used in shipbuilding with regards to fire behavior and give recommendations for relevant fire testing and for the fire risk assessment methodology. Furthermore, potential deviations against prescriptive fire safety regulations are described and issues other than related to fire safety are exemplified. The guidelines are intended for the approving Administrations when reviewing alternative designs involving FRP composite, but the guidelines will not less be used to support ship design and preliminary evaluations.

6. BENCHMARKS AND CASE STUDIES

6.1 Uncertainness in welding simulation

In numerical welding simulations, each selected parameter such as mesh size, material modelling, heat input, boundary conditions play an important role. In order to understand the influence of the modeler's practice and FEM codes on the welding simulation, the benchmark study was initiated in the ISSC 2015 V.3 Committee. Only the preliminary results were reported

in the previous committee's and thus, a short summary is included into the ISSC 2018 report. The details of the study is published in Caprace et al. (2017).

The geometry considered was a T-joint typically used for stiffened panels in ships and offshore structures. A 12-mm-thick stiffener was welded to the base plate that has a length of 500 mm. Both base plate and stiffener were the low carbon grade DH36 ferric steel plate. The welding residual stress and distortion were analyzed numerically, and the results were compared to the experiments. In welding experiments, (FCAW) single-side one pass welding procedure with a heat flux of 10.7 kJ/cm were applied. All the benchmark participants received the same technical specification about welding experiments. The responsibility to interpret this document, considering the limitation of each software, relied on the modelers. Thus, the variability of the solutions (S1-S6) adopted by the experts to solve the same problem; see Table 6. There are the combination of 4 different software, 3 thermal boundary conditions, 3 mechanical boundary conditions, 2 similar material models, 4 equivalent heat sources and 4 meshing. As seen from Table 7 an average element size was about one millimeter for all cases. To simulate the material deposition during the welding process, the element birth & death technique was employed.

Table 6: Simulation matrix. From Caprace et al. (2017).

Sim Id	Software	Therm. BC	Mec. BC	Material Prop.	Hardening Model	Phase Transf.	EHS Model	Elem. Type
S1	Ansys	conv.+rad.	MBC1	M_1	Isotropic	No	USHF	8N-Parallelepiped
S2	Ansys	conv.+rad.	MBC1	M_1	Kinematic	No	USHF	8N-Parallelepiped
S3	Sysweld	conv.+rad.	MBC1	M_1	Isotropic	Yes	Goldak's	8N-Parallelepiped
S4	Sysweld	conv.+rad.	MBC1	M_1	Isotropic	No	Goldak's	8N-Parallelepiped
S5	Virfac	conv.	MBC3	M_1	Isotropic	No	Goldak's	4N-Tetrahedral
S6	Abaqus	conv.+rad.	MBC2	M_2	Isotropic	No	Goldak's	8N-Parallelepiped

Table 7: Meshing parameters for finite element models. From Caprace et al. (2017).

Sim Id	Elem. Type	Therm. Elem. Order	Mech. Elem. Order	Node Nbr	Elem. Nbr	l•w•hmm•mm•mm	Elem Kill & Alive
S1	8N-Parallelepiped	1st	1st	33337	28392	9.60•1.00•0.75	Yes
S2	8N-Parallelepiped	1st	1st	33337	28392	9.60•1.00•0.75	Yes
S3	8N-Parallelepiped	1st	1st	194568	171600	9.60•1.00•0.75	Yes
S4	8N-Parallelepiped	1st	1st	194568	171600	9.60•1.00•0.75	Yes
S5	4N-Tetrahedral	1st	1st	127155	103302	0.78•0.78•0.78	Yes
S6	8N-Parallelepiped	1st	1st	82614	70760	2.25•2.25•1.0	Yes

Figure 12 shows the results for the temperature comparison. A good agreement for the maximum temperatures between the experimental measurements and numerical simulations although S6 presents a moderate overestimation. The reason for this might be the difference of thermal boundary condition (heat transfer coefficient) and thermo- mechanical properties (conductivity at high temperature). The cooling rate is also a good agreement with the experiments for the majority of the simulations. The simulations S3 and S4 with uniform surface heat flux (USHF) presents a higher cooling rate than that of the experiments. The simulation S6 maintain the gap observed in the peak temperature almost constant during the cooling. The comparison of fusion zone showed some discrepancies in penetrations, but the size of fusion zone was similar for the simulations and experiments. The results indicates that the change of heat source type and parameters affects peak temperatures and the fusion shape. Furthermore, it seems that the surface convection and radiation (S5) had little effect on the fusion zone shape.

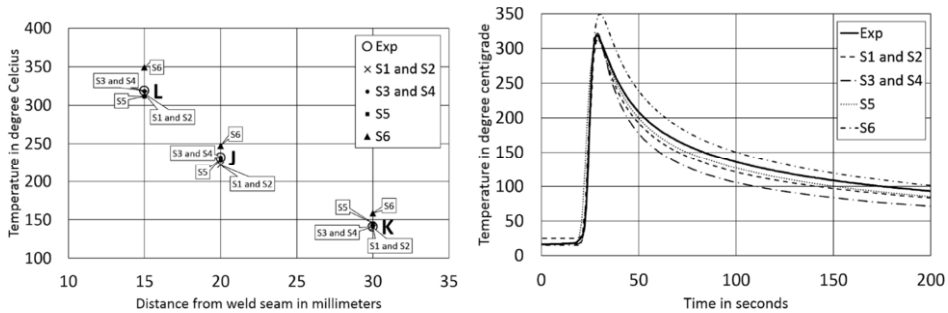

Figure 12: Comparison of the maximum temperatures (left) and Cooling rate for first weld at the point L (right). From Caprace et al. (2017).

The comparison of the welding angular distortions did not revels significant differences, less than 12%, that modeller practices had a small influence on the simulated welding distortion. Simulated residual stress showed higher difference. The measured and simulated residual stress are shown in Figure 13. The highest tensile longitudinal residual stresses were observed in the fusion zone and heat-affected zone as expected. The transverse residual stress induced in the weld and plate is much smaller than the longitudinal residual stress. The distribution of the longitudinal stress is not symmetrical due to the effects of the welding sequence. The longitudinal residual stresses present a good predictability, i.e. less than ≈18% difference. The transversal residual stresses are largely underestimated, i.e. difference largely higher than 35%. This discrepancies can partly due to the imperfect material model. This highlights the need of extensive material testing for welding simulations. The benchmark study show also that the results obtained with the double ellipsoidal heat course model (S3-S6; Goldak's) are closer to the experiments than that of USHF (S1-S2). The insignificant differences between the results S1 and S2 indicates that the kinematic hardening model can be replaced by an isotropic hardening model in this peculiar case. In addition, the effect of phase transformation on residual stresses and distortion seems to be insignificant since the difference between models S3 and S4 was small. Therefore, the phase-transformation can neglected for low-carbon steels (Deng, 2009). The differences due to software's and boundary conditions was less sensitive than other parameters.

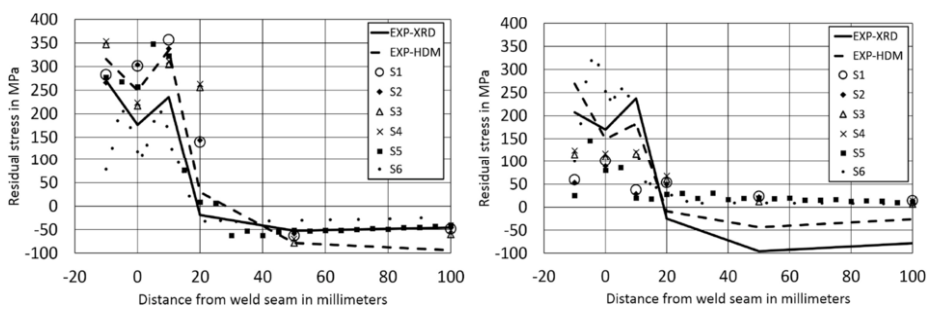

Figure 13: Longitudinal (left) and transversal (right) residual stress comparisons. From Caprace et al. (2017).

6.2 Sensitivity analysis on the cohesive parameters of a carbon-steel single lap

The present investigation aims at assessing the sensitivity of the parameters that define the traction separation law on the de-bonding of a single lap joint. Namely, two finite element software were compared, ADINA and LS-DYNA: the former adopts a bilinear traction separation laws, while in the latter both bilinear and trilinear curves were tested. The results were compared to previous experiments by Tomaso et al. (2014), available in literature.

6.2.1 Model Description, material properties and mesh size

The specimen, which measures 25 mm in width, is described in Figure 14. The resulting cohesive area is 12.5 x 25.0 mm^2. The specimen is clamped at both ends with fixes rotations, whereas one end can experience axial translation to apply the tensile force. The composite is made mostly by unidirectional carbon fibres in an epoxy matrix, with a negligible amount of ±45° layers and other non-structural plies to improve impregnation and resin distribution.

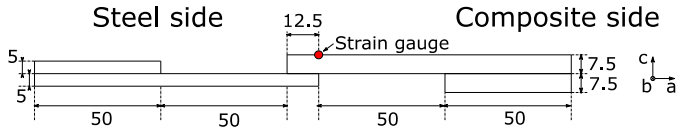

Figure 14: Model description

Steel is modelled as plastic-isotropic, with Young Modulus E=203 GPa and ν=0.3 [-]. The yield stress is σ_y=315 MPa and the ultimate stress σ_u=455 MPa. The hardening modulus is E_t=0,717 GPa.

The carbon reinforced plastic is modelled as elastic orthotropic, the elastic moduli are respectively E_a=38.7 GPa, E_b=E_c=6.5 GPa; the Poisson coefficients are ν_{ba}=0.35, ν_{ca}=0.059, ν_{cb}=0.34.

An eight-node solid element was used in both software due to compatibility issues with the cohesive element. The maximum element edge size was set to 1.07 mm after a preliminary mesh sensitivity analysis, resulting in five layers of elements through the thickness for the steel, and seven for the composite.

6.2.2 Cohesive model

Cohesive elements are modelled in the overlapping area between steel and composite. In ADINA, the element has an initial thickness equal to zero, while LS-DYNA requires a non-null initial thickness, which was set to 0.5 mm. The cohesive element is defined by a traction separation law, which relate the interface traction to the nodal displacement, such law is triangular by default in ADINA, while LS-DYNA allows more complex functions: in the present work both triangular and trapezoidal laws were tested.

In a triangular traction separation law, three parameters define the cohesive separation:

- The penalty stiffness k, which defines the steepness of the initial linear part of the law
- The energy release rate G_{ic}, which is the signed area under the curve up to the maximum opening displacement, at which separation occurs
- The peak traction τ_{max}, defining the maximum point in the traction-separation law

A trapezoidal law can be defined by the same parameters, although once the peak traction is reached, it remains constant in the so-called plateau region for a certain range of displacements, before dropping to zero.

Once k and τ_{max}, are defined, the parameter G_c also defines the maximum opening displacement.

The cohesive law can be defined separately for mode I and mode II. The cohesive behaviour can act independently for the two modes, or it can consider a mixed mode opening behaviour. In the present work, the power law defined in Equation 1 is considered, and the influence of parameter α investigated.

$$\left(\frac{G_I}{G_{IC}}\right)^{\alpha} + \left(\frac{G_{II}}{G_{IIC}}\right)^{\alpha} < 1 \quad (1)$$

The separation occurs once the inequality 1 is no longer satisfied. G_i is the signed area defined by the separation law at a specific load step.

6.2.3 Reference cohesive parameters

The following reference parameters, derived from literature work and previously adopted by Tomaso et al. (2014) were chosen:

- G_{Ic}=140 Jm^{-2}; G_{IIc}=280 Jm^{-2}
- Peak traction, mode I: τ_I=7.6 MPa Peak traction, mode II: τ_{II}=54 MPa
- K=5.6·10^{14} Nm^{-3} (Initial opening displacement: v_c=0.0000135 mm)
- α=0

6.2.4 Experimental/numerical comparison and influence of parameter k

The results, in terms of axial strains, are compared to those achieved by strain gauges placed at different spots in the specimen. For sake of shortness, only the comparison with the strain gauge shown in figure 14 is reported. The penalty stiffness is varied in the range [3.8·10^{12}- 5.6·10^{14}] for LS-DYNA and [10^{11}-10^{16}] for ADINA.

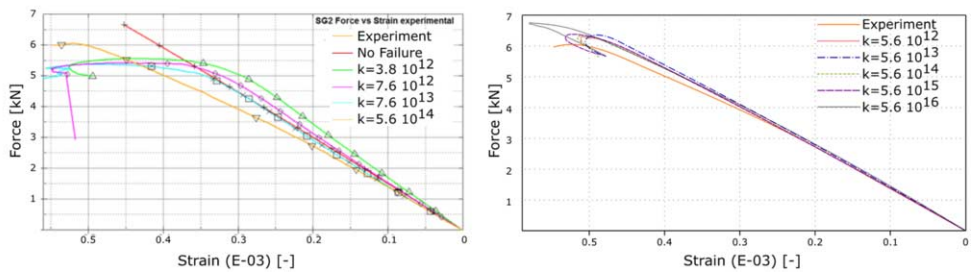

Figure 15: Axial strain for different k, LS-DYNA left and ADINA right

From Figure 15, it can be seen how LS-DYNA model is more sensitive towards the penalty stiffness with respect to the ADINA model, by the way the influence of this parameter is quite poor in both cases. ADINA matches the experimental data better, while LS-DYNA underestimates the local axial strains for the strain gage data reported. Data from other strain gauges show opposite behaviour, where LS-DYNA overestimate axial strains, while ADINA still show good experimental matching. In terms of axial force, ADINA generally over-estimate the ultimate force, while LS-DYNA underestimates it.

The failure load, for the models with different penalty stiffness k, is also plotted and reported in figure 16. Figure 16 shows a quite constant value of axial force at failure in the range 10^{11}-10^{16}, though LS-DYNA covers a smaller range. Outside such range the numerical results quickly diverge, in agreement to the behaviour described by Song et al. (2007). In conclusion, it can be said that the penalty stiffness, if chosen in a reasonable wide range, has poor influence on the numerical results, and a rough approximation of such value is sufficient.

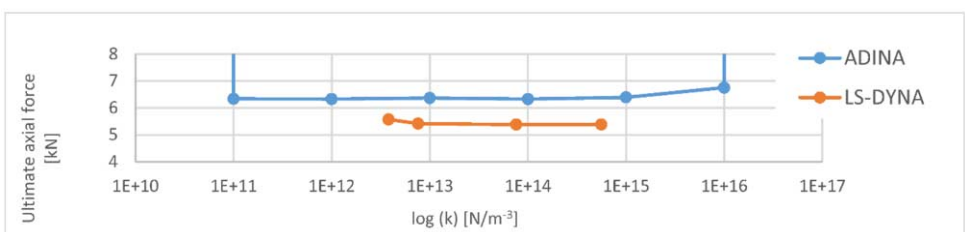

Figure 16: Axial force at failure, function of k

6.2.5 Influence of G_c

The influence of the parameter G_c on the failure load of the single lap joint is then shown in Figure 17 considering a contemporary variation for both G_{Ic} and G_{IIc}, expressed in % value. The bilinear traction-separation law shows a fairly linear trend in the area around the reference value in both ADINA and LS-DYNA, although in ADINA the parameter has a greater impact in the determination of the failure load. The LS-DYNA trilinear law leads to slightly different behaviour, but the impact is minimal in terms of failure force.

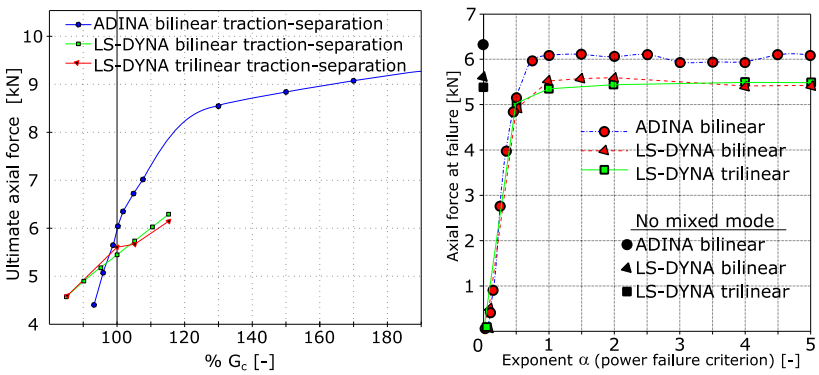

Figure 17: Impact of G_c (left) and α (right)

6.2.6 Influence of α

Finally, the parameter α described in equation 1 is investigated. It is worth nothing that in the present case a predominant mode II opening behaviour is expected, although the bending moment, led by the misalignment of the two parts of the joint, also induces some mode I components. For $0<\alpha<1$, the mixed mode leads to a quick drop in the failure force due to the increment of the contribution of each mode in Equation 1. The parameter has similar impact on both ADINA and LS-DYNA software, with similar decrement for $\alpha<1$.

6.3 Fatigue life improvement using HFMI treatment

This benchmark studies on numerical simulation technique for fatigue life improvement of welded joints by High Frequency Mechanical Impact (HFMI) treatment. Its analyses are conducted as a joint project of Chalmers University of Technology (CUT), Osaka University (OU) and Pusan National University (PNU).

HFMI makes use of cylindrical indenters which are accelerated against a component or structure with high-frequency (> 90 Hz). The introduction of compressive residual stresses (RS), work hardening, and reduce the notch effect at the weld toe are the three main contributions from this HFMI treatment e.g., Marquis (2013). However, there is concern that this compressive RS might deteriorate due to RS relaxation under cyclic loading, and the HFMI treatment might lose its effectiveness. It is needed to develop a numerical simulation technique for compressive RS's development (in welding and HFMI treatment) and relaxation (under cyclic loadings).

Numerical simulations of the HFMI-process have been investigated by many researchers e.g., Foehrenbach et al. (2016), Shengsun et al., (2016), Khurshid et al. (2017). Explicit elastic-plastic finite element (EPFE) code (e.g., Abaqus Explicit) was utilized in order to take into account dynamic effect in those studies. They examined the influence of the FE mesh and various analysis parameters (e.g., friction model, tool indentations, boundary conditions, etc.) on RS distribution, but recommendations on FE meshing and choice of simulation parameters for practical applications to marine structures has not been presented yet.

The objective of this study is set out best practice guides with respect to those simulations. This study is composed of three parts: a) HFMI simulation for stress-free steel sheet; b) welding-HFMI simulation of a welded joint; c) residual stress relaxation under cyclic loadings.

6.3.1 Multiple impact simulation of the HFMI process on stress-free steel sheets

The analysis target is HFMI-treated flat sheets of S355J2H (10 mm thickness) studied by Ernould et al. (2017). These sheets were manually treated along a path of 30 mm. A pin with a tip radius of 2 mm and a travel speed of 12 cm/min were used. RS were measured at the groove center by means of X-ray and neutron diffraction up to a depth of 5 mm. RS at the surface were respectively -200 and -400 MPa along the transverse and longitudinal (x-dir.) direction. Maximum compressive residual stress of -550 MPa is obtained at 0.8 mm depth in the transverse direction.

HFMI simulations are either displacement controlled simulations (DCS) or force controlled simulations (FCS). The pin's impact velocity has to be prescribed in FCS, but is difficult as a matter of practice, especially for manually treated cases. Therefore, DCS is chosen in this study. For simplicity, the pin is modelled as a rigid, and it is assumed that the indentation depth and impact period are constant.

Ernould et al. (2017) performed DCS of the target flat sheets, and reported fair agreements in RS profile with the experiments observed with combined isotropic-kinematic hardening law. The effectiveness of the analysis parameters chosen in their report was examined in this study.

The FE mesh shown in Figure 18 is used in the analyses. (x, y, z) coordinates shown in this figure are used in following discussions. This model features the same specification as those of Ernould's model. It is composed of hexahedron brick elements. All nodal displacements are constrained on the bottom face, and the transverse (y-dir.) motion is fixed on the symmetric plane. Peening tools are modeled by rigid shell elements. The peening pin is given an enforced oscillating motion along its axis with a constant frequency, such that the pin impacts the center of the plate. The indentation depth of D=0.2 mm is assumed. A linear motion in x-direction with a velocity such that every impacts are spaced by the given pitch P for the given pin frequency f. Friction coefficient of μ = 0.3 between pin and workpiece, and radii of pin nose of R = 2.0 mm are given. Hereafter, this procedure is called 'multiple impact' simulation (MIS).

The Chaboche's combined isotropic-kinematic and strain rate dependent hardening raw is adopted. In this hardening law, back stress tensor is given by the equation below:

$$d\boldsymbol{\alpha} = \sum_{i=1}^{M} d\boldsymbol{\alpha}_i \,;\; d\boldsymbol{\alpha}_i = C_i \frac{dp}{\sigma_o}\left(\boldsymbol{\sigma} - \boldsymbol{\alpha}\right) - \gamma_i \boldsymbol{\alpha}_i dp \tag{2}$$

where, $\boldsymbol{\alpha}$ is back stress tensor, $\boldsymbol{\sigma}$ is the stress tensor, $\boldsymbol{\varepsilon}^p$ plastic strain tensor, C_i, γ_i are material parameters, dp accumulated equivalent plastic strain increment, M number of kinematic parts, and i part number. M = 2 is used in this study. σ_o is the yield stress, and its developing equation is given as:

$$\sigma_o = \sigma_{o,0}\, F(\dot{\varepsilon_{\mathrm{p}}})\, G(\varepsilon_{\mathrm{p}});\;\; F(\dot{\varepsilon_{\mathrm{p}}}) = 1 + \left(\dot{\epsilon_{\mathrm{p}}}/_{H}\right)^{1/\rho}, G(\varepsilon_{\mathrm{p}}) = 1 + a(\varepsilon_{\mathrm{p}})^{b} \tag{3}$$

Here $\sigma_{o,0}$ is the initial yield stress, H and ρ are Cowper-Symonds strain hardening parameters, and a and b are isotropic strain hardening parameters. Material parameters are the same as those adopted in Ernould et al. (2017), and are listed in 'Optimized' column of Table 8.

Young's modulus E = 210 GPa, and Poison's ratio ν = 0.3. In Equation 2, $\gamma_1 = 2.19 \cdot 10^2$ and $\gamma_2 = 1.07 \cdot 10^2$. For Equation 3, $a = 1.0 \cdot 10^{-6}$ and b=0.6. ρ = 5.80 in accordance with Yasuda and Rashed (2016). Peening is carried out on the intersection between the top face and the

symmetric plane over 10 mm. f = 100 Hz is assumed because it was found that the peening response is not depending much on the frequency in the preliminary analysis.

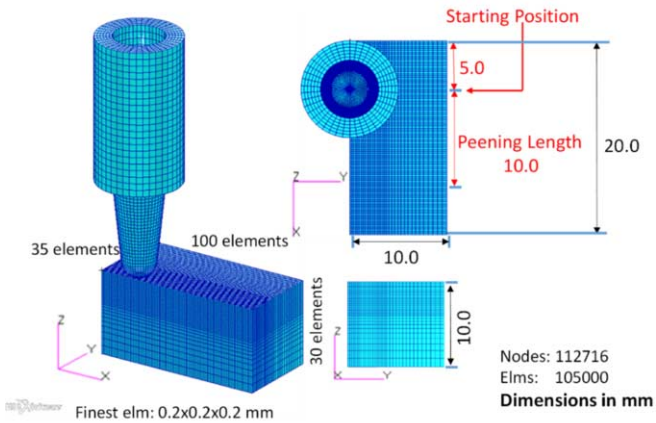

Figure 18: FE mesh of the flat sheet and peening tools used in multiple impact simulations.

OU and PNU performed peening analyses using different explicit EPFE codes (OU: MSC DYTRAN (MSC Software, 2017), PNU: Abaqus Explicit (ABAQUS Inc., 2016)). They searched optimal simulation parameters, and found that simulated RS profile agreed well with that measured when the 'optimized' parameters listed in Table 8 were adopted. These values are about the same as those of Ernould et al. (2017), but strain rate effects are not considered in the'Optimized' condition.

Table 8: Parameters used in flat sheet analyses.

	Optimized	Variations
Pitch P (mm)	0.4	0.2
Indentation depth D (mm)	0.2	0.1, 0.3
Yield stress σ_o [MPa]	435	210, 650
C_1 [MPa]	8.97E+03	4.49E+03, 0.0
C_2 [MPa]	1.27E+04	6.33E+03, 0.0
H [1/s]	∞	4000
Radius of pin nose R [mm]	2.0	3.0

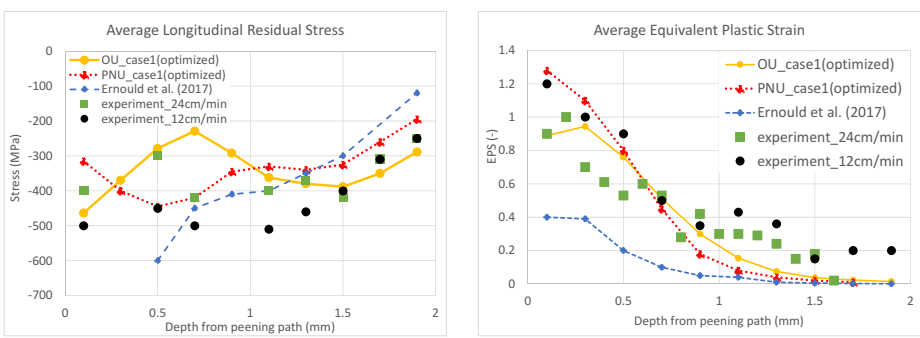

Figure 19: Comparison of residual stress and equivalent plastic strain profiles using optimized parameters with those measured (experiments: measured in Ernould et al. (2017)).

Let LRS be RS's longitudinal (x-dir.) component. Figure 19 shows comparisons of profiles for RS and equivalent plastic strain (EPS) in through-thickness direction calculated by OU (MSC DYTRAN) and PNU (Abaqus Explicit) using the 'optimized' parameters and those measured. In this figure, averaged LRS and EPS of elements with the same depth on the 5 mm section in model's middle part are plotted. It is shown that RS and EPS calculated in this study agree well with those measured, and FE code dependency is acceptably small. The accuracies of RS near the top face and EPS over the entire area are improved compared with Ernould et al. (2017). These results demonstrates the effectiveness of the adopted FE mesh and 'optimized' parameters in Table 8.

Sensitivity analyses of simulation parameters are performed. Variations in parameters are listed in Table 8. Eleven cases in total listed in Table 9 are examined. The FE mesh of Figure 18 is used. Case 1 is the optimized one which gives the simulation results shown in Figure 19.

Comparisons in RS (and EPS) profiles are shown in Figure 20. The following is found in these analyses:

- Neither RS (for depth < 1mm) and EPS almost never change when the kinematic hardening becomes smaller (Cases 2 and 7).
- RS's peak moves deeper and EPS becomes larger when D becomes larger (Cases 3 and 4) or R becomes larger (Cases 9; Figure 20 (a)).
- RS's absolute value (|LRS|) becomes smaller while EPS almost never change when σ_o becomes smaller (Cases 5 and 6; Figure 20 (b)).
- |LRS| raises substantially while EPS almost never change when the strain rate dependency is taken into account (Case 8; Figure 20 (c)).
- Neither RS and EPS almost never change when P becomes smaller (Cases 10 and 11).

Table 9: Parameters given in the sensitivity analyses.

Case	Pitch P (mm)		Indentation depth D (mm)			Material properties								Pin radi R (mm)	
						Yield Stress σ_o (MPa)			Hardening coeffs.			Strain rate dependency			
	0.2	0.4	0.1	0.2	0.3	210	435	650	Optimi-zed	x 0.0	x 0.5	Yes	No	2.0	3.0
1		*		*			*		*				*	*	
2		*		*			*			*			*	*	
3		*			*		*		*				*	*	
4		*	*				*		*				*	*	
5		*		*		*			*				*	*	
6		*		*				*	*				*	*	
7		*		*			*				*		*	*	
8		*		*			*		*			*		*	
9		*		*			*		*				*		*
10	*			*			*		*				*	*	
11	*			*			*			*			*	*	

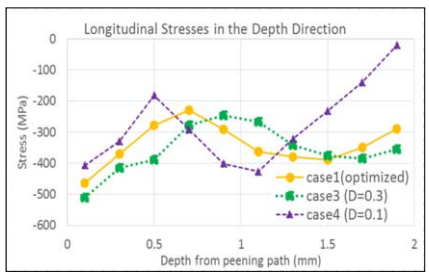

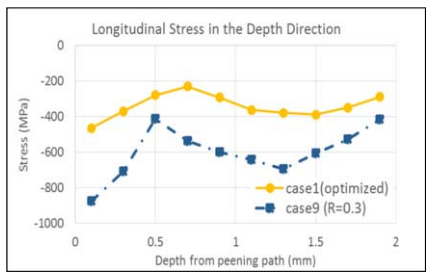

(a) Dependency on indentation depth D and pin's radi R.

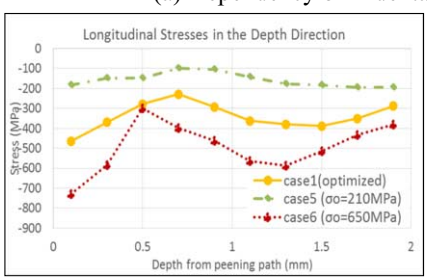

(b) Dependency on yield stress σ_o.

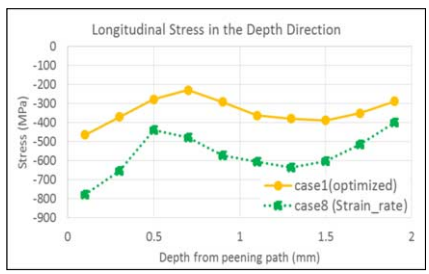

(c) Dependency on strain rate dependency.

Figure 20: Comparisons of residual stress and equivalent plastic strain profiles calculated in the sensitivity analyses.

Hereafter, the FE model of Figure 18 is called 'fine model.' Mesh sensitivity is studied by using 'intermediate model' and 'coarse model,' with larger element size. Let n_e be the number of elements, l_{min} the smallest element's sizes in x, y, z-direction (n_e, l_{min}) = (105,000, 0.2 x 0.2 x 0.2 mm) for 'fine' model. For compared models, (n_e, l_{min}) = (20,625, 0.6 x 0.4 x 0.4 mm) for 'intermediate,' and (n_e, l_{min}) = (4,480, 1.25 x 0.5 x 0.5 mm) for 'coarse' models. The 'Coarse' mesh element size is about the same as that used in the welded joint peening simulation performed by Leitner et al. (2016). This is a typical mesh size adopted in thermal-elasto-plastic welding FE analyses.

For each model, peening responses are calculated using 'optimized' simulation parameters in Table 8. Frequency f = 100Hz Let $l_{min,x}$ be the minimum longitudinal element size. The ratios $l_{min,x}/P$ for fine / intermediate / coarse models are 0.1, 0.3, and 0.625. The comparisons of RS's longitudinal (x-direction) and transversal (y-direction) components, σ_{xx} and σ_{yy}, are shown in Figure 21.

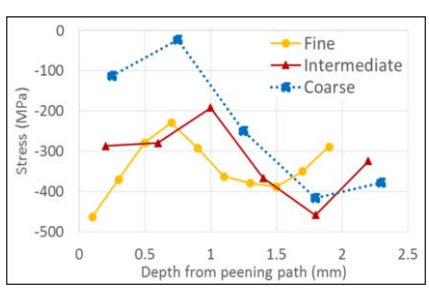

(a) longitudinal component σ_{xx}

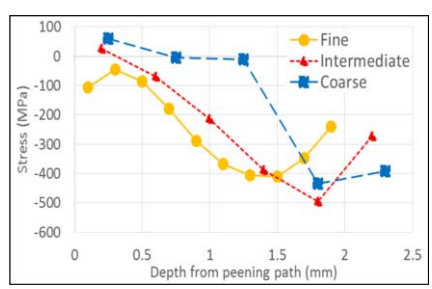

(b) transversal component σ_{yy}

Figure 21: Comparisons of residual stress components calculated by different meshes.

This figure shows that σ_{xx} drastically decreases with the increase in element size (>450MPa for 'fine' mesh, <100MPa for 'coarse' mesh) while the change in σ_{yy} is relatively small. This suggests that element size smaller than 1/10 of pin radius should be used if the longitudinal RS becomes a critical.

6.3.2 Single impact simulation of the HFMI process on stress-free steel sheets

It takes a lot of man-hour and computational time to perform a 'multiple impact' simulation (MIS) presented above. This man-hour and computational time can be reduced considerably if multiple impacts by a moving pin can be replaced by a single impact by a straight blade. Hereafter, this procedure is called 'single impact' simulation (SIS).

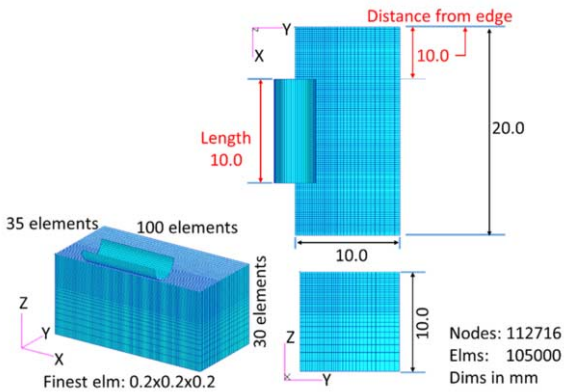

Figure 22: FE mesh of the flat sheet and peening blade used in single impact simulations.

CUT, OU and PNU performed SIS of the steel sheet model. The FE model for SIS is shown in Figure 22. The sheet mesh is the same as that of 'fine' model for MIS. The peening 'blade' with the length of 10 mm is modeled by rigid shell elements. 'Optimized' parameters (excluding pitch P) of Table 8 were adopted. For the friction coefficient μ is 0.30 (same as MIS) and 0.15 (1/2 of MIS). Analyses were performed using different EPFE codes. CUT: Abaqus standard version 6.14.2 (quasi-static), OU: MSC DYTRAN and PNU: Abaqus explicit. Calculated RS profiles are shown in Figure 23. Figure 23 (a) shows calculated averaged longitudinal (LRS) and (b) transversal (TRS) RS. The following are shown in these figures:

- SIS's |LRS| near the top face ranges from -500MPa to -300MPa, which are comparable to the measured ones and the MIS result. However, LRS profiles between 0.5~1.5mm show variations depending on EPFE codes and analysis method (quasi-static vs. explicit). It is also shown that |LRS| near the top face depends on μ.
- SIS's TRS near the top face and TRS profiles show very large variations depending on EPFE codes and analysis method.

These results show that RS calculated by SIS show wide variations depending on EPFE codes and analysis method. More investigations are needed to put SIS HFMI simulation into practical use. Additional experimental data for the transversal RS are also needed.

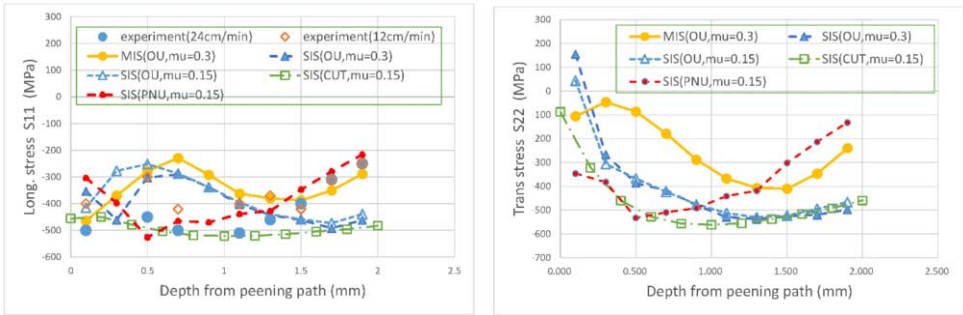

(a) Averaged longitudinal RS. (b) Averaged transversal RS

Figure 23: Comparison of residual stresses calculated by multiple and single impact simulations (experiments: measured in Ernould et al. (2017)).

6.3.3 Summary and future plans

It is shown that the measured RS profile can be reproduced by performing rate-independent explicit displacement controlled FE analysis. The simulation result shows significant mesh sensitivity, and it is found that element size should be smaller than peening pin's radius. Strain hardening does not affect RS profile, but RS's absolute value becomes smaller with the decrease of the yield stress. Both longitudinal and transversal stress profiles can be simulated in multiple impact simulation, while single impact simulation should not be adopted to cases where transversal stress is important. More investigations are needed for the single impact simulation to clarify the transversal stress behaviour. From the benchmark results, a best practice guide with respect to HFMI simulation procedure for the chosen peening tool has been set.

The benchmark group (CUT, OU and PNU) will perform welding-peening simulation of out-of-gusset welded joints following the proposed guideline, and examine the change in RS profile under cyclic loading condition. These results will be published in the near future.

7. CONCLUSIONS AND RECOMMENDATIONS

An overview of recent research and development on materials and fabrication technology is presented. Compared to the previous report we have focussed on some new areas, and also refrained from some areas covered in the previous V.3 Committee report, ie line heating, corrosion and simulation based production.

Ship production is still struggling, although with some exceptions like RoRo, cruise and ferries. Also offshore production is very low due to, so far, very low prices on oil. Several legislative initiatives, clean water ballast restrictions, new sulphur emission control area are pushing for a renewal of the fleet. There are also strong research programs on steels and joining methods, and recently on fabricating lighter ships using composites to a larger extent.

The developments of different steels is presented, in particular means of improving the fatigue life for high strength steels. The development of steels and pertinent material properties (eg fracture toughness, CTOD) for use in the arctic is also emphasized, as well as the development of composite materials for marine and subsea applications. We also give some good examples of the use of weight reduction materials.

Welding is still the main joining method for steels. One key outcome of the welding is the distortion of the welded components. With that in mind, several different processes are investigated including use of lower heat input, or use of secondary processes for distortion control. Summarizing, we find that laser beam welding gives the thinnest fusion zone, for the case of butt welding of steel D36. Additive manufacturing is starting to be used also in the maritime sector, we give some examples where it has advantages over other manufacturing methods. Possible applications where additive manufacturing uses automation are also given.

Different manufacturing imperfections appearing in composites have been discussed thoroughly, also joining of composites. Introducing non-crimp fibres are beneficial, it may increase the tensile strength, though it is more expensive than traditional woven rowing. Nano particles which are quite important for the cohesive strength of the matrix (delamination strength and fiber to matrix strength) is also recommended. The infusion method for manufacturing is often better from a cost/benefit analysis when the thickness of the composite is small.

New materials and related fabrication processes offer several benefits like weight saving, integrated functions which may give a reduced life cycle cost of ships and marine structures. However, long term experience of operational performance is not available. The problem of qualification of new materials have been addressed by the V.3 Committee, we arranged a meeting in Hamburg with stakeholders for two European projects, using new materials in ships and classification societies to find what measures that have to be addressed. A suggested best practice for qualification of FRP composites is presented together with a recently issued standard, which opens for several ways of documenting material properties. It also has a multi-scale approach where results from smaller scale tests can be reused for different applications. The use of different levels of verifying material behavior may also limit the number of expensive full-scale long terms tests needed. A survey of qualification and approval processes by different class societies is also given.

The benchmark about the uncertainness in welding simulations indicate good results for the prediction of welding distortions and residual stresses. However, a notable difficulty is the calibration of the equivalent heat course model that required high skilled experts and standards for experimental procedures. A small variation of the model parameters may cause considerable discrepancies on the residual stresses prediction. Moreover, obtaining reliable thermomechanical material properties is a big challenge.

For the adhesive carbon / steel lap joint benchmark, it was found that in general, ADINA tends to overestimate the experimental failure force, while LS-DYNA underestimates it. Good matching is found for axial strains, with better results from ADINA. The failure force is sensitive to G_c (fracture energy) variation, especially in ADINA, while a negligible influence is found for the parameter k (the initial steepness in the cohesive law for the adherend). Use of trilinear or bilinear traction-separation laws lead to comparable results. A similar influence is found for the parameter α (in the mixed mode I and II law) in both software.

For the High Frequency Mechanical Impact (HFMI) benchmark, where peening of a stress-free steel plate (sheet) was simulated numerically, a best practice guide with respect to the HFMI simulation procedure for the chosen peening tool has been set. It was shown that the measured residual stress profiles can be reproduced by performing a rate-independent explicit displacement controlled FE analysis. The simulation results show a significant mesh sensitivity, and it is found that element size should be smaller than peening pin's radius. Strain hardening does not affect the residual stress profiles, but the absolute values of the residual stresses become smaller with the decrease of the yield stress. A complete multiple impact simulation can simulate both longitudinal and transversal stress profiles with good agreement with experiments, while a less computationally intensive single impact simulation should not be adopted to cases where the transversal stress is important.

REFERENCES

Abaqus/Explicit Reference Manual, 2016, Dassault Systèmes Simulia Corp.

Adam, S. and Ghosh, S., 2016, March. Application of Flexible Composite Pipe as a Cost Effective Alternative to Carbon Steel-Design Experience. In Offshore Technology Conference Asia. Offshore Technology Conference.

Affdl, J.C. and Kardos, J.L., 1976. The Halpin-Tsai equations: a review. Polymer Engineering & Science, 16(5), pp.344-352.

Airoldi, A., Baldi, A., Bettini, P. and Sala, G., 2015. Efficient modelling of forces and local strain evolution during delamination of composite laminates. Composites Part B: Engineering, 72, pp.137-149.

Akpinar, I.A., Gültekin, K., Akpinar, S., Akbulut, H. and Ozel, A., 2017. Research on strength of nanocomposite adhesively bonded composite joints. Composites Part B: Engineering, 126, pp. 143-152.

Akselsen, O.M. and Østby, E., 2014. Evaluation of Welding Consumables for Application down to -60°C. In the 24th International Ocean and Polar Engineering Conference. International Society of Offshore and Polar Engineers.

Akselsen, O.M., Ren, X., Alvaro, A. and Nyhus, B., 2017, July. Key Challenges in Materials and Welding for Application of Steel Structures in Arctic. In The 27th International Ocean and Polar Engineering Conference. International Society of Offshore and Polar Engineers.

An, G.B., Woo, W. and Park, J.U., 2014. Brittle crack-arrest fracture toughness in a high heat-input thick steel weld. International Journal of Fracture, 185(1-2), pp.179-185.

Andena, L., Castellani, L., Castiglioni, A., Mendogni, A., Rink, M. and Sacchetti, F., 2013. Determination of environmental stress cracking resistance of polymers: Effects of loading history and testing configuration. Engineering Fracture Mechanics, 101, pp.33-46.

Anderson, T.A., Fang, B., Attia, M., Jha, V., Dodds, N., Finch, D. and Latto, J., 2016, May. Progress in the Development of Test Methods and Flexible Composite Risers for 3000 m Water Depths. In Offshore Technology Conference. Offshore Technology Conference.

Andideh, M. and Esfandeh, M., 2017. Effect of surface modification of electrochemically oxidized carbon fibers by grafting hydroxyl and amine functionalized hyperbranched polyurethanes on interlaminar shear strength of epoxy composites. Carbon, 123, pp.233-242.

Azzara, A., Rutherford, D. and Wang, H., 2014. Feasibility of imo annex vi tier iii implementation using selective catalytic reduction. International Council on Clean Transportation.

Bai, Z., Song, L., Hu, Y., Gong, X. and Yuen, R.K., 2014. Investigation on flame retardancy, combustion and pyrolysis behavior of flame retarded unsaturated polyester resin with a star-shaped phosphorus-containing compound. Journal of Analytical and Applied Pyrolysis, 105, pp.317-326.

Bajpei, T., Chelladurai, H. and Ansari, M.Z., 2016. Mitigation of residual stresses and distortions in thin aluminium alloy GMAW plates using different heat sink models. Journal of Manufacturing Processes, 22, pp.199-210.

Braura, A. and Mittal, A., 2017. Shipping: Sailing in Troubled Waters, in Global Economic Outlook 2017, 1st Quarter, Deloitte University Press, pp. 56-67.

BRS Group, 2017. Shipping and Shipbuilding Markets – Annual review 2017, www.brsbrokers.com /flipbook en2017.

Caprace, J.D., Fu, G., Carrara, J.F., Remes, H. and Shin, S.B., 2017. A benchmark study of uncertainness in welding simulation. Marine Structures, 56, pp.69-84.

Chaves, V., Beretta, G. and Navarro, A., 2017. Biaxial fatigue limits and crack directions for stainless steel specimens with circular holes. Engineering Fracture Mechanics, 174, pp.139-154.

Chen, L., 2014. Analysis on Situation and Strategy of Chinese Shipbuilding Industry Development. Research Institute of Machinery Industry Economic Management, pp.88-91.

Chen, Y., Tan, L.B., Jaiman, R.K., Sun, X., Tay, T.E. and Tan, V.B.C., 2013, June. Global-local analysis of a full-scale composite riser during vortex-induced vibration. In ASME 2013 32nd International Conference on Ocean, Offshore and Arctic Engineering (pp. V007T08A084-V007T08A084). American Society of Mechanical Engineers.

Chen, Y., Yang, C., Chen, H., Zhang, H. and Chen, S., 2015. Microstructure and mechanical properties of HSLA thick plates welded by novel double-sided gas metal arc welding. The International Journal of Advanced Manufacturing Technology, 78(1-4), pp.457-464.

Colombo, C. and Vergani, L., 2014. Influence of delamination on fatigue properties of a fibreglass composite. Composite Structures, 107, pp.325-333.

Conrardy, C., Huang, T.D., Harwig, D., Dong, P., Kvidahl, L., Evans, N. and Treaster, A., 2006. Practical welding techniques to minimize distortion in lightweight ship structures. Journal of Ship production, 22(4), pp.239-247.

Cricrì, G. and Perrella, M., 2017. Investigation of mode III fracture behaviour in bonded pultruded GFRP composite joints. Composites Part B: Engineering, 112, pp.176-184.

Deng, D., 2009. FEM prediction of welding residual stress and distortion in carbon steel considering phase transformation effects. Materials & Design, 30(2), pp.359-366.

Det Norske Veritas, 2010. Offshore riser system. In: Proceedings of the Offshore service specification. DNV-OSS-302.

Di Landro, L., Montalto, A., Bettini, P., Guerra, S., Montagnoli, F. and Rigamonti, M., 2017. Detection of Voids in Carbon/Epoxy Laminates and Their Influence on Mechanical Properties. Polymers & Polymer Composites, 25(5), p.371.

Ding, D., Shen, C., Pan, Z., Cuiuri, D., Li, H., Larkin, N. and van Duin, S., 2016. Towards an automated robotic arc-welding-based additive manufacturing system from CAD to finished part. Computer-Aided Design, 73, pp.66-75.

Ernould, C., Schubnell, J., Simunek, D., Leitner, M., Maciolek, A., Farajian, M., and Stoschka, M., 2017. Application of Different Simulation Approaches to Numerically Optimize High-Frequency Mechanical Impact (HFMI) Post-Treatment Process, IIW Document XIII-2684-17. International Institute of Welding.

Estefen, S.F., Gurova, T., Castello, X. and Leontiev, A., 2010. Surface residual stress evaluation in double-electrode butt welded steel plates. Materials & Design, 31(3), pp.1622-1627.

European Commission, 2017. CORDIS Community Research and Development Information Service, http://cordis.europa.eu

Evegren, F. and Hertzberg, T., 2017. Fire safety regulations and performance of fibre-reinforced polymer composite ship structures. Proceedings of the Institution of Mechanical Engineers, Part M: Journal of Engineering for the Maritime Environment, 231(1), pp.46-56.

Evegren, F., Rahm, M., Arvidson, M. and Hertzberg, T., 2014. Fire testing of external combustible ship surfaces. Fire Safety Science, 11, pp.905-918.

Foehrenbach J, Hardenacke, V., and Farajian, M., 2016. High Frequency Mechanical Impact Treatment (HFMI) for the fatigue improvement: numerical and experimental investigations to describe the condition in the surface layers, Welding in the World, 60 (4), pp. 749-755.

Gaiotti, M., Rizzo, C.M., Branner, K. and Berring, P., 2014. An high order Mixed Interpolation Tensorial Components (MITC) shell element approach for modeling the buckling behavior of delaminated composites. Composite Structures, 108, pp.657-666.

Gangloff Jr, J.J., Cender, T.A., Eskizeybek, V., Simacek, P. and Advani, S.G., 2017. Entrapment and venting of bubbles during vacuum bag prepreg processing. Journal of Composite Materials, 51(19), pp.2757-2768.

Godani, M., Gaiotti, M. and Rizzo, C.M., 2014. Interlaminar shear strength of marine composite laminates: Tests and numerical simulations. Composite Structures, 112, pp.122-133.

Godani, M., Gaiotti, M. and Rizzo, C.M., 2015, July. Influence of air inclusions on marine composites inter-laminar shear strength. In The Twenty-fifth International Ocean and Polar Engineering Conference. International Society of Offshore and Polar Engineers.

Hahn, H.T. and Tsai, S.W., 1980. Introduction to composite materials. CRC Press.

Han, W.T., Wan, F.R., Li, G., Dong, C.L. and Tong, J.H., 2011. Effect of trailing heat sink on residual stresses and welding distortion in friction stir welding Al sheets. Science and Technology of Welding and Joining, 16(5), pp.453-458.

Harati, E., Karlsson, L., Svensson, L.E. and Dalaei, K., 2017. Applicability of low transformation temperature welding consumables to increase fatigue strength of welded high strength steels. International Journal of Fatigue, 97, pp.39-47.

Harati, E., Svensson, L.E., Karlsson, L. and Widmark, M., 2016. Effect of high frequency mechanical impact treatment on fatigue strength of welded 1300 MPa yield strength steel. International Journal of Fatigue, 92, pp.96-106.

Hase, K., Handa, T. and Eto, T., 2014. Development of YP460 N/mm2 Class Heavy Thick Plate with Excellent Brittle Crack Arrestability for Mega Container Carriers. JFE Technical Report, 20, pp. 8-13.

Hauge, M., Maier, M., Walters, C.L., Østby, E., Kordonets, S.M., Zanfir, C. and Osvoll, H., 2015, July. Status update of ISO TC67/SC8/WG5: Materials for arctic applications. In The Twenty-fifth International Ocean and Polar Engineering Conference. International Society of Offshore and Polar Engineers.

Hazimeh, R., Othman, R., Khalil, K. and Challita, G., 2016. Influence of plies' orientations on the stress distribution in adhesively bonded laminate composite joints subjected to impact loadings. Composite Structures, 152, pp.654-664.

Herzog, D., Seyda, V., Wycisk, E. and Emmelmann, C., 2016. Additive manufacturing of metals. Acta Materialia, 117, pp.371-392.

Holder, R., Larkin, N., Li, H., Kuzmikova, L., Pan, Z. and Norrish, J., 2011. Development of a DC-LSND welding process for GMAW on DH-36 Steel. In 56th WTIA annual conference. Welding Technology Institute of Australia.

Horn, A.M., Østby, E., Moslet, P.O. and Hauge, M., 2016, June. The Fracture Resistance Approach in Order to Prevent Brittle Failure of Offshore Structures Under Arctic Environments. In ASME 2016 35th International Conference on Ocean, Offshore and Arctic Engineering (pp. V004T03A021-V004T03A021). American Society of Mechanical Engineers.

Hüther, J. and Brøndsted, P., 2016, July. Influence of the curing cycles on the fatigue performance of unidirectional glass fiber reinforced epoxy composites. In IOP Conference Series: Materials Science and Engineering (Vol. 139, No. 1, p. 012023). IOP Publishing.

Ilman, M.N., Muslih, M.R., Subeki, N. and Wibowo, H., 2016. Mitigating distortion and residual stress by static thermal tensioning to improve fatigue crack growth performance of MIG AA5083 welds. Materials & Design, 99, pp.273-283.

IMO, 2016. Suitability of High Manganese Austenitic Steel for Cryogenic Service and Development of any Necessary Amendments to the IGC Code and IGF Code, International Maritime Organisation.

Ingalls, 2017. http://www.nmc.ctc.com/index.cfm?fuseaction=projects.details&projectID=288

Jeong, D., Seo, W., Sung, H. and Kim, S., 2016. Near-threshold fatigue crack propagation behavior of austenitic high-Mn steels. Materials Characterization, 121, pp.103-111.

Jesus, J.S., Costa, J.M., Loureiro, A. and Ferreira, J.M., 2017. Fatigue strength improvement of GMAW T-welds in AA 5083 by friction-stir processing. International Journal of Fatigue, 97, pp.124-134.

Jones, R.M., 1998. Mechanics of composite materials. CRC press.

Kalantari, M., Dong, C. and Davies, I.J., 2017. Effect of matrix voids, fibre misalignment and thickness variation on multi-objective robust optimization of carbon/glass fibre-reinforced hybrid composites under flexural loading. Composites Part B: Engineering, 123, pp.136-147.

Kaneko, M. and Tani, T., 2011. Characteristics of Brittle Crack Arrest Steel Plate for Large Heat-input Welding for large Container Ships. Kobelco Technology Review, 30, pp.66-69.

Khurshid, M., Leitner, M., Barsoum, Z., and Schneider, C., 2016. Residual stress state induced by high frequency mechanical impact treatment in different steel grades - Numerical and experimental study. International Journal of Mechanical Sciences, 123, pp. 34-42.

Kim, S.Y., Shim, C.S., Sturtevant, C. and Song, H.C., 2014. Mechanical properties and production quality of hand-layup and vacuum infusion processed hybrid composite materials for GFRP marine structures. International Journal of Naval Architecture and Ocean Engineering, 6(3), pp.723-736.

Knautz, 2017. Procedural principle plasma key hole-welding. URL http://www.schweissmaschinen.net/en/schweissmaschinen/plasma-welding-machines/procedural-principle-plasma-key-hole-welding/ (accessed 2.14.17).

Kobayashi, S., Tsukada, T. and Morimoto, T., 2017. Resin impregnation behavior in carbon fiber reinforced polyamide 6 composite: Effects of yarn thickness, fabric lamination and sizing agent. Composites Part A: Applied Science and Manufacturing, 101, pp.283-289.

Kumar, S. and Nath, S.K., 2016. Effect of heat input on impact toughness in transition temperature region of weld CGHAZ of a HY 85 steel. Journal of Materials Processing Technology, 236, pp.216-224.

Kumar, S. and Shahi, A.S., 2016. Studies on metallurgical and impact toughness behavior of variably sensitized weld metal and heat affected zone of AISI 304L welds. Materials & Design, 89, pp.399-412.

Laitinen, R., Valkonen, I. and Kömi, J., 2013. Influence of the base material strength and edge preparation on the fatigue strength of the structures made by high and ultra-high strength steels. Procedia Engineering, 66, pp.282-291.

Lan, L., Kong, X., Qiu, C. and Zhao, D., 2016. Influence of microstructural aspects on impact toughness of multi-pass submerged arc welded HSLA steel joints. Materials & Design, 90, pp.488-498.

Larkin, N., Pan, Z.X., Van Duin, S., Callaghan, M., Li, H.J. and Norrish, J., 2011. Tandem gas metal arc welding for low distortion butt welds. In Advanced Materials Research (Vol. 337, pp. 511-516). Trans Tech Publications.

Larkin, N., Short, A., Pan, Z. and van Duin, S., 2018. Automated Programming for Robotic Welding. In Transactions on Intelligent Welding Manufacturing (pp. 48-59). Springer, Singapore.

Leitner, M., Khurshid, M., and Barsoum, Z., 2016. Stability of HFMI-treatment induced residual stresses during fatigue. IIW Document XIII-2633-16. International Institute of Welding.

Leitner, M., 2017. Influence of effective stress ratio on the fatigue strength of welded and HFMI-treated high-strength steel joints. International Journal of Fatigue, 102, pp. 158-170.

Levieil, B., Edwards, L., Cortial, F., Sterjovski, Z. and van Duin, S., 2017. Towards thickness reduction and performance improvement: development of low distortion welding processes for naval shipbuilding, FAST 2017, 14th International Conference on Fast Sea Transportation, Nantes, France.

Levieil, B., van Duin, S., Cortial, F., Edwards, L. and Sterjovski, Z., 2017. Low distortion welding for shipbuilding, Pacific 2017, International Maritime Conference, Sydney.

Lin, Y., Jiang, S., Hu, Y., Chen, G., Shi, X. and Peng, X., 2016. Hybrids of aluminum hypophosphite and ammonium polyphosphate: Highly effective flame retardant system for unsaturated polyester resin. Polymer Composites.

Liu, Y., Shi, L., Liu, C., Yu, L., Yan, Z. and Li, H., 2016. Effect of step quenching on microstructures and mechanical properties of HSLA steel. Materials Science and Engineering: A, 675, pp.371-378.

Ma, L. and Liu, D., 2016. Delamination and fiber-bridging damage analysis of angle-ply laminates subjected to transverse loading. Journal of Composite Materials, 50(22), pp.3063-3075.

Maggiani, G., Boote, D., Gaggero, T., Gaiotti, M. and Rizzo, C.M., 2017. Calibration of the Cohesive Parameters of Fiberglass Reinforced Plastic Plates with an Embedded Delamination by Experiments. In The Twenty-seventh International Ocean and Polar Engineering Conference. International Society of Offshore and Polar Engineers.

Marquis, G.B., and Barsoum, Z., 2013. A guideline for fatigue strength improvement of high strength steel welded structures using high-frequency mechanical impact, Procedia Engineering, 66, pp. 98-107.

MARTEC II, 2017. https://www.martec-era.net/index.php?index=21.

Mochizuki, M. and Toyoda, M., 2007. Weld distortion control during welding process with reverse-side heating. Journal of Engineering Materials and Technology, 129(2), pp.265-270.

Mochizuki, M., Yamasaki, H., Okano, S. and Toyoda, M., 2006. Distortion behaviour of fillet T-joint during in-process control welding by additional cooling. Welding in the World, 50(5-6), pp.46-50.

MSC Software. 2017. MSC DYTRAN2017 Reference Manual.

Muren, J., Caveny, K., Eriksen, M., Müller-Allers, J., Engelbreth, K.I. and Eide, J., 2013. Petroleum Safety Authority Norway: Un-bonded Flexible Risers–Recent Field Experience and Actions for Increased Robustness.

Nagy, T., 2012. Investigation of thermal techniques to mitigate buckling distortion in welding panels. Cranfield University, UK.

O'Brien, R., Veldsman, W. and Elmarakbi, A., 2015. The development of an industrial robotic Low Stress No Distortion (LSND) welding system. The IIW International Conference on High Strength Materials - Challenges and Applications, Helsinki. International Institute of Welding.

Okano, S. and Mochizuki, M., 2016. Experimental and Numerical Investigation of Trailing Heat Sink Effect on Weld Residual Stress and Distortion of Austenitic Stainless Steel. ISIJ International, 56(4), pp.647-653.

Olave, M., Vara, I., Husabiaga, H., Aretxabaleta, L., Lomov, S.V. and Vandepitte, D., 2015. Nesting effect on the mode I fracture toughness of woven laminates. Composites Part A: Applied Science and Manufacturing, 74, pp.166-173.

Ottersböck, M.J., Leitner, M., Stoschka, M. and Maurer, W., 2016. Effect of Weld Defects on the Fatigue Strength of Ultra High-strength Steels. Procedia Engineering, 160, pp.214-222.

Pallaspuro, S., Yu, H., Kisko, A., Porter, D. and Zhang, Z., 2017. Fracture toughness of hydrogen charged as-quenched ultra-high-strength steels at low temperatures. Materials Science and Engineering: A, 688, pp.190-201.

Park, J.Y. and Kim, M.H., 2016, June. Fatigue Crack Propagation Characteristics of 3.5 to 9 wt% Nickel Steels for Low Temperature Applications. In ASME 2016 35th International Conference on Ocean, Offshore and Arctic Engineering (pp. V004T03A010-V004T03A010). American Society of Mechanical Engineers.

Park, S.J., Heo, G.Y. and Jin, F.L., 2015. Cure behaviors and thermal stabilities of tetrafunctional epoxy resin toughened by polyamide. Macromolecular Research, 23(4), pp.320-324.

Pazooki, A.M.A., Hermans, M.J.M. and Richardson, I.M., 2017. Control of welding distortion during gas metal arc welding of AH36 plates by stress engineering. The International Journal of Advanced Manufacturing Technology, 88(5-8), pp.1439-1457.

Pérez-Mora, R., Palin-Luc, T., Bathias, C. and Paris, P.C., 2015. Very high cycle fatigue of a high strength steel under sea water corrosion: A strong corrosion and mechanical damage coupling. International Journal of Fatigue, 74, pp.156-165.

Pham, D.C., Sridhar, N., Qian, X., Sobey, A.J., Achintha, M. and Shenoi, A., 2016. A review on design, manufacture and mechanics of composite risers. Ocean Engineering, 112, pp.82-96.

Saat, A.M., Malik, A.A., Azmi, A., Latif, M.F.A., Ramlee, N.E. and Johan, M.R., 2017. Effect of aluminum phosphate on mechanical and flame retardant properties of composites fiberglass. ARPN Journal of Engineering and Applied Sciences, 12, pp. 1315-1318.

Scheid, A., Félix, L.M., Martinazzi, D., Renck, T. and Kwietniewski, C.E.F., 2016. The microstructure effect on the fracture toughness of ferritic Ni-alloyed steels. Materials Science and Engineering: A, 661, pp.96-104.

SEA Europe, 2017. Shipbuilding market monitoring report No 42, SEA Europe – Shipyards & Maritime Equipment Association (www.seaeurope.nu).

Shen, C., 2013. Low distortion welding for shipbuilding industry. University of Wollongong, Australia

Shengsun, H., Guo, C., Wang, D., and Wang, Z., 2016. 3D Dynamic Finite Element Analysis of the Nonuniform Residual Stress in Ultrasonic Impact Treatment Process, Journal of Materials Engineering of Performance, 25, pp. 4004-4015.

Shenoi, R.A. and Wellicome, J.F. eds., 1993. Composite Materials in Maritime Structures: Volume 1, Fundamental Aspects. Cambridge University Press.

Shibanuma, K., Yanagimoto, F., Namegawa, T., Suzuki, K. and Aihara, S., 2016. Brittle crack propagation/arrest behavior in steel plate–Part I: Model formulation. Engineering Fracture Mechanics, 162, pp.324-340.

Shiino, M.Y., Pelosi, T.S., Cioffi, M.O.H. and Donadon, M.V., 2017. The Role of Stitch Yarn on the Delamination Resistance in Non-crimp Fabric: Chemical and Physical Interpretation. Journal of Materials Engineering and Performance, 26(3), pp.978-986.

Shiozaki, T., Tamai, Y. and Urabe, T., 2015. Effect of residual stresses on fatigue strength of high strength steel sheets with punched holes. International Journal of Fatigue, 80, pp.324-331.

Skriko, T., Ghafouri, M. and Björk, T., 2017. Fatigue strength of TIG-dressed ultra-high-strength steel fillet weld joints at high stress ratio. International Journal of Fatigue, 94, pp.110-120.

Soderhjelm, C. and Apelian, D., 2016. Metallurgical bonding between cast-in ferrous inserts and aluminum, La Metallurgia Italiana, 6, pp. 93-100.

Song, K., Dávila, C.G. and Rose, C.A., 2008, May. Guidelines and parameter selection for the simulation of progressive delamination. In ABAQUS User's Conference (Vol. 41, pp. 43-44).

Song, S.W., Kwon, Y.J., Lee, T. and Lee, C.S., 2016a. Effect of Al addition on low-cycle fatigue properties of hydrogen-charged high-Mn TWIP steels. Materials Science and Engineering: A, 677, pp.421-430.

Song, S.W., Lee, J.H., Lee, H.J., Bae, C.M. and Lee, C.S., 2016b. Enhancing high-cycle fatigue properties of cold-drawn Fe–Mn–C TWIP steels. International Journal of Fatigue, 85, pp.57-64.

Sproesser, G., Pittner, A. and Rethmeier, M., 2016. Increasing performance and energy efficiency of gas metal arc welding by a high power tandem process. Procedia CIRP, 40, pp.642-647.

Sterjovski, Z., Donato, J., Munro, C., Luzin, V., Lane, N., and Larkin, N., 2011. An evaluation of pulsed tandem gas metal arc welding of high-strength HSLA65 steel for naval shipbuilding, In 56th WTIA annual conference. Welding Technology Institute of Australia.

Sudheesh, R.S. and Prasad, N.S., 2015. Comparative Study of Heat Transfer Parameter Estimation Using Inverse Heat Transfer Models of a Trailing Liquid Nitrogen Jet in Welding. Heat Transfer Engineering, 36(2), pp.178-185.

Sutherland, L.S., Amado, C. and Soares, C.G., 2017. Statistical experimental design techniques to investigate the strength of adhesively bonded T-joints. Composite Structures, 159, pp.445-454.

Tan, L.B., Chen, Y., Jaiman, R.K., Sun, X., Tan, V.B.C. and Tay, T.E., 2015. Coupled fluid–structure simulations for evaluating a performance of full-scale deepwater composite riser. Ocean Engineering, 94, pp.19-35.

Thompson, A.M., Dilthey, U., Fersini, M., Richardson, I., Dos Santos, J., Yapp, D. and Hedegård, J., 2008. Improving the competitiveness of the European steel fabrication industry using synchronised tandem wire welding technology. Brussels: European Commission, Directorate-General for Research, Research Fund for Coal and Steel Unit.

Tomaso, E., Risso, G., Gaiotti, M. and Rizzo, C.M., 2014, August. Numerical Simulation Strategies of Single Lap Joints. In The Twenty-fourth International Ocean and Polar Engineering Conference. International Society of Offshore and Polar Engineers.

Udvardy, S., Nuechterlein, J. and Makhlouf M., 2012, Development of High Performance Nano-Composite Materials, North America Die Casting Association, Super Weapons Systems through castings Report, pp. 133-148.

Usami, A., Kishimoto N., Kusumoto H., Kaneko F. and Inoue T., 2016. Cryogenic leakage risk analysis for FLNG and use of brittle crack arresting material as a risk mitigation measure, Proceedings of the Society for Naval Architects and Marine Engineers.

Van der Aa, E.M., 2007. Local cooling during welding: prediction and control of residual stresses and buckling distortion. Delft University of Technology, The Netherlands..

Wang, X.L., Nan, Y.R., Xie, Z.J., Tsai, Y.T., Yang, J.R. and Shang, C.J., 2017. Influence of welding pass on microstructure and toughness in the reheated zone of multi-pass weld metal of 550 MPa offshore engineering steel. Materials Science and Engineering: A, 702, pp.196-205.

Wang, X.Y. and Whitworth, J.R., 2016. Using additive manufacturing to mitigate the risks of limited key ship components of the Zumwalt-class destroyer (Doctoral dissertation, Monterey, California: Naval Postgraduate School).

Vargas, M.A., Vázquez, H. and Guthausen, G., 2015. Non-isothermal curing kinetics and physical properties of MMT-reinforced unsaturated polyester (UP) resins. Thermochimica Acta, 611, pp.10-19.

Wei, H.L., Li, H., Gao, Y., Ding, X.P. and Yang, L.J., 2015. Welding process of consumable double electrode with a single arc GMAW. The International Journal of Advanced Manufacturing Technology, 76(1-4), pp.435-446.

Wilkins, J., 2016, May. Qualification of Composite Pipe. In Offshore Technology Conference.

Woo K., Nelson J.W., Cairns D.S. and Riddle T.W., 2013. Effects of Defects: Part B—Progressive Damage Modeling of Fiberglass/Epoxy Composite Structures with Manufacturing Induced Flaws Utilizing Cohesive Zone Elements. In 54th AIAA/ASME/ASCE/AHS/ASC Structures, Structural Dynamics, and Materials Conference 2013 Apr (p. 1628).

World Industrial Reporter, 2017. https://worldindustrialreporter.com/port-of-rotterdam-uses-3d-printing-to-repair-damaged-ship-parts/.

Yaacob, M., Zakaria, I., Koto, J., Zarina, P. and Mun'aim, M.A.M.K., 2017. Comparative mechanical properties study of resin infusion versus hand laminating for the construction of 12-ft fishing boat. ARPN Journal of Engineering and Applied Sciences, 12, pp. 1954-1960.

Yang, C., Zhang, H., Zhong, J., Chen, Y. and Chen, S., 2014. The effect of DSAW on preheating temperature in welding thick plate of high-strength low-alloy steel. The International Journal of Advanced Manufacturing Technology, 71(1-4), pp.421-428.

Yasuda, A., and Rashed, S., 2016. Efficient Collapse Analysis of Ductile Components Subjected to Impact Loads in ASME 2016 35nd International Conference on Ocean, Offshore and Arctic Engineering, paper OMAE2016-54480. American Society of Mechanical Engineers.

Yildirim, H.C. and Marquis, G.B., 2012. Fatigue strength improvement factors for high strength steel welded joints treated by high frequency mechanical impact. International Journal of Fatigue, 44, pp.168-176.

Zhang, H., Zhang, G., Cai, C., Gao, H. and Wu, L., 2008. Fundamental studies on in-process controlling angular distortion in asymmetrical double-sided double arc welding. Journal of Materials Processing Technology, 205(1), pp.214-223.

Østby, E., Akselsen, O.M., Hauge, M. and Horn, A.M., 2013, June. Fracture mechanics design criteria for low temperature applications of steel weldments. In The Twenty-third International Offshore and Polar Engineering Conference. International Society of Offshore and Polar Engineers.

Østby, E., Hauge, M. and Horn, A.M., 2015, July. Development of materials requirement philosophies for design to avoid brittle behaviour in steel structures under Arctic conditions. In The Twenty-fifth International Ocean and Polar Engineering Conference. International Society of Offshore and Polar Engineers.

This page intentionally left blank

Proceedings of the 20th International Ship and Offshore Structures Congress (ISSC 2018) Volume II – M.L. Kaminski and P. Rigo (Eds.)

doi:10.3233/978-1-61499-864-8-193

COMMITTEE V.4

OFFSHORE RENEWABLE ENERGY

COMMITTEE MANDATE

Concern for load analysis and structural design of offshore renewable energy devices. Attention shall be given to the interaction between the load and structural response of fixed and floating installations taking due consideration of the stochastic nature of the ocean environment. Aspects related to prototype testing, certification, marine operations and total cost of energy shall be considered.

COMMITTEE MEMBERS

Zhen Gao, *Norway* (*Chairman*)
Harry B. Bingham, *Denmark*
David Ingram, *UK*
Athanasios Kolios, *UK*
Debabrata Karmakar, *India*
Tomoaki Utsunomiya, *Japan*
Ivan Catipovic, *Croatia*
Giuseppina Colicchio, *Italy*
José Miguel Rodrigues, *Portugal*
Frank Adam, *Germany*
Dale G. Karr, *USA*
Chuang Fang, *China*
Hyun-Kyoung Shin, *Korea*
Johan Slätte, *Norway*
Chunyan Ji, *China*
Wanan Sheng, *Ireland*
Pengfei Liu, *Australia*
Lyudmil Stoev, *Bulgaria*

KEYWORDS

Offshore wind turbine, floating wind turbine, wave energy converter, tidal turbine, ocean current turbine, design, integrated dynamic analysis, model test, hybrid testing method, field measurement, marine operations

CONTENTS

1. INTRODUCTION 195

2. OFFSHORE WIND TURBINES 196
2.1 Recent industry development 196
2.2 Numerical modelling and analysis 198
2.2.1 Numerical tools – state-of-the-art and validation 198
2.2.2 Loads and response analysis of bottom-fixed wind turbines 199
2.2.3 Loads and response analysis of floating wind turbines 203
2.3 Physical testing 208
2.3.1 Lab testing 208
2.3.2 Field testing 215
2.4 Transport, installation, operation and maintenance 216
2.4.1 Transport and installation 216
2.4.2 Operation and maintenance 219
2.5 Design standards and guidelines 220
2.6 Comparative study of optimal offshore wind turbine support structure configurations in varying water depths 221

3. WAVE ENERGY CONVERTERS 224
3.1 Numerical modelling and analysis 224
3.1.1 Load and motion response analysis 225
3.1.2 Power take-off analysis 227
3.1.3 Mooring analysis 229
3.2 Physical testing 231
3.2.1 Laboratory testing and validation of numerical tools 231
3.2.2 Field testing 237
3.3 Design rules and standards 239
3.4 ISSC contribution to the IEA OES benchmark study 240

4. TIDAL AND OCEAN CURRENT TURBINES 241
4.1 Recent development 241
4.2 Environmental Conditions 242
4.3 Tidal turbine loads and response analysis 244
4.3.1 Numerical methods 244
4.3.2 Laboratory tests and field measurements 246

5. OTHER OFFSHORE RENEWABLE ENERGY TECHNOLOGIES 249

6. COST OF OFFSHORE RENEWABLE ENERGY 250
6.1 General aspects 250
6.2 Current status and potential for cost reduction 251
6.3 Cost models and analysis tools 254

7. MAIN CONCLUSIONS AND RECOMMENDATIONS FOR FUTURE WORK 255

REFERENCES 257

1. INTRODUCTION

This is the fifth time that ISSC has included the Specialist Committee V.4 Offshore Renewable Energy, which started in 2006. Two-thirds of the committee members for this term (2016-2018) were involved in the work for the previous term (2013-2015), which formulates a good base for the cooperative work in the last three years.

The mandate of the committee was discussed at the beginning of the work and it was slightly modified to explicitly state that the total cost of energy, which has been the central question for developing offshore renewable energy, should be discussed in the committee report. This is important and we allocated one chapter (Chapter 6) to discuss the status of the levelized cost of energy (LCOE) for different energy conversion technologies (offshore wind turbines, wave energy converters and marine current turbines) and the potential for cost reduction in the future through research and development.

It is worth mentioning today's technological maturity and industrial development of different offshore renewable energies. Offshore wind is by far the most developed technology and promising cost reduction has been achieved in the last few years, which makes it possible to consider larger installations at even less cost for the near future. Both wave energy and marine current energy are still in a phase of intensive research and early development. We have seen a number of commercial-size tidal turbines installed for testing in recent years, but very few large-scale wave energy converters.

As compared to the ship and offshore oil & gas industry, the offshore renewable energy community is facing a lot of new challenges in a wide range of research areas, including resource and environmental condition assessment, conceptual design, aerodynamic and hydrodynamic loads calculation, structural response analysis, automatic control, marine installation and operation/maintenance, and various mechanical components. In view of the relevance to ISSC and the competences of the members, we focus on response analysis of offshore renewable energy devices under simultaneous wind, wave and/or current loads for design purposes based on numerical studies, lab and field measurements. Both operational conditions and transit phases such as transport and installation were considered. We have limited discussion about the ultimate and fatigue strengths of these structures (for which similar research on ships and offshore structures can be applicable) and have not considered resource assessment (which was discussed in the previous report) nor electrical grid issues (which are out of the scope for ISSC). Because of extensive research in this field, there exists a vast number of publications that deal with offshore renewable energy technologies. Therefore, the intention was not to cover all of these publications, but to focus on more solid and complete work from reports published by international associations and papers published in well-established journals and proceedings of important conferences.

Three chapters are allocated for three major technologies, i.e. offshore wind turbines (which is the most developed technology and is main focus of our report as in the previous ones), wave energy converters and tidal and ocean current turbines. For offshore wind turbines in Chapter 2, the main discussions are on the development of floating wind turbine concepts, continuous validation of developed numerical codes, new experimental techniques for testing floating wind turbines, as well as marine operations related to transport and installation of offshore wind turbines. The results from a comparative study of optimal offshore wind turbine support structures for varying water depths are presented. Chapter 3 discusses the recent research and development of wave energy converters, with focus on novel concept validation, numerical codes for component and system evaluation, model testing of stand-alone devices and devices in a farm configuration, field testing of a few prototypes, as well as the initial results from the IEA OES benchmark study. In Chapter 4, the recent development of commercial-size tidal current turbines is presented. In particular, numerical methods for turbine loads due to both current and waves are discussed in detail. We also briefly mention the develop-

ment of other technologies for utilization of offshore renewable energy in Chapter 5. The important aspects related to LCOE are discussed in Chapter 6, with focus on the offshore wind industry. In Chapter 7, a short summary of the main conclusions and recommendations for future research are presented.

2. OFFSHORE WIND TURBINES

2.1 Recent industry development

In the last few years, the offshore wind industry continues to grow and there is a promising significant cost reduction for some of offshore wind farms in the bidding phase. Cost of offshore wind farms will be discussed in detail along with the costs of other offshore renewable energies in Chapter 6. Here, we focus on the industrial development of offshore wind farms.

As shown in Figure 2.1 (GWEC, 2017a), by the end of 2016, the total installed offshore wind capacity reached 14.384GW worldwide and 12.631GW in Europe. Among them, 2.217GW were installed in 2016 worldwide and 1.558GW in Europe, which is 39% less than those installed in 2015 worldwide and 48% less in Europe. However, the number of offshore wind farms under construction and planned indicates a promising increase in installed capacity for the coming years (BVGA, 2017). Most of the offshore wind farms installed are located in Europe (in particular in the UK and Germany). There was a significant development in China in recent years, which lead China to be the third largest country in terms of installed offshore wind capacity in 2016, replacing Denmark. The US built their first offshore wind farm (The Block Island Wind Farm) in 2016, with five 6MW Alstom Haliade wind turbines on jacket foundations.

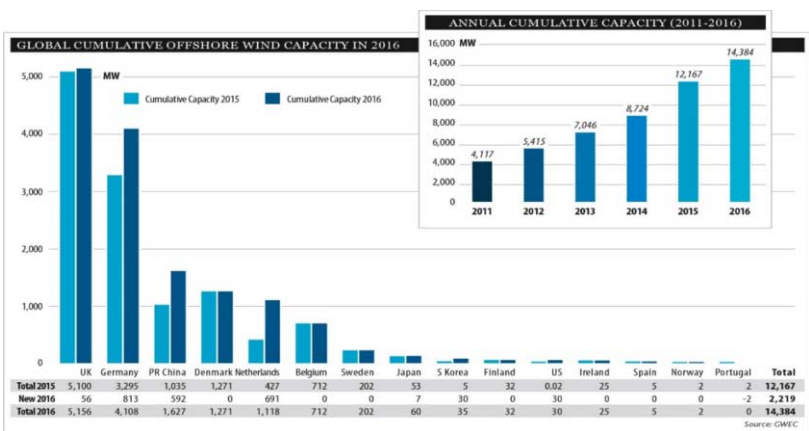

Figure 2.1: Global installed offshore wind capacity in 2016 (GWEC, 2017a)

The recent trend of offshore wind development shows that more wind turbines are being installed in deeper waters, farther from shore and in a bigger farm configuration. Most importantly, the rated power and the turbine size are continuously increasing. The average rated power for those installed in 2016 is 4.8MW (WindEurope, 2017), which is a 15% increase as compared to those in 2015. The first 8MW turbines (thirty-two Vestas' V164 turbines, with a rotor diameter of 164 m) have entered the market in 2016 and have been installed at the Burbo Bank Wind Farm Extension in the Irish Sea in UK. As shown below in Figure 2.2, the trend of increasing turbine size seems to continue, which will be beneficial to the overall cost reduction, but will lead to a lot of challenges for offshore installation, due to longer blades and larger lifting height.

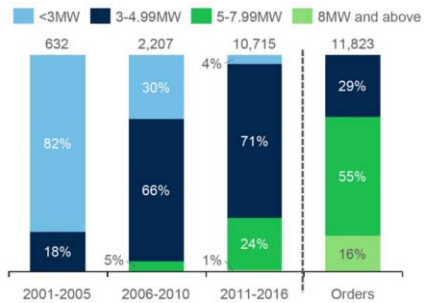

Figure 2.2: Increasing size of offshore wind turbines through years (Green Tech Media, 2017)

In the recent years, floating wind turbine technology has further developed. With the first small farm of five 6MW spar wind turbines installed by Statoil in Scotland (Statoil, 2017a), an important step towards the commercialization of floating wind farms was achieved. As per the presentation from Moeller (2017), in the next several years, a number of floating offshore wind projects will be commissioned, as shown in Figure 2.3. This includes the existing prototypes in Norway, Portugal and Japan and a few more prototypes that are already under construction in Japan, France and Germany. In addition to the Statoil Hywind Scotland wind farm, two small floating wind farms will be developed under the WindFloat 2 project in Europe and the Maine Aqua Ventus I project in the US.

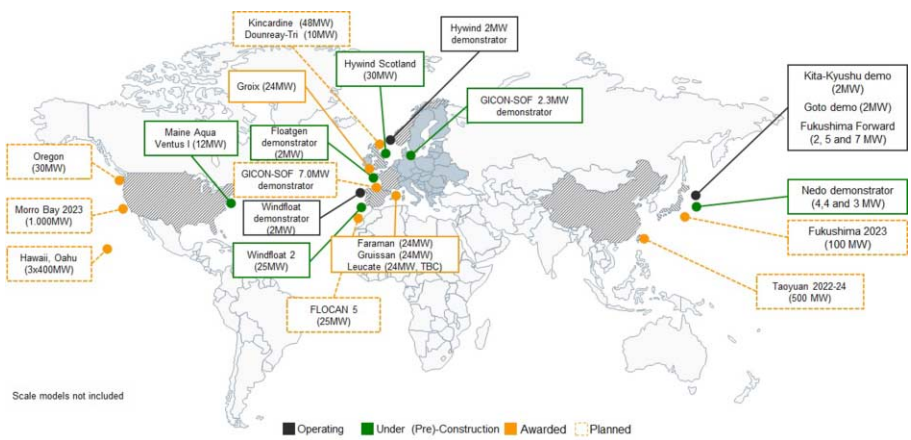

Figure 2.3: Current market situation of offshore floating wind turbines (Moeller, 2017)

As for long-term plans, the European Union set a legally binding target in 2014, to achieve at least 27% renewable energy in final energy consumption in Europe by 2030, which corresponds to 46-49% of electricity generated by renewables (EC, 2017). Accordingly, a wind energy development scenario towards 2030 was presented by EWEA (2015) and indicates that the total installed capacity of wind power could reach 320GW in 2030, comprising 254GW of onshore wind and 66GW of offshore wind. If we consider the total installed offshore wind capacity of 12GW up to 2016, an average annual increase of 15% is needed to reach this goal. This is probably achievable in view of the average annual increase of 25-30% in recent years. However, it also implies a significant number of offshore wind turbines that need to be installed, which is in the order of 650 6MW turbines per year.

Outside Europe, both China and the US have the potential and also the plans for offshore wind development (GWEC, 2017b).

China has a long coastline with rich offshore wind resources and the estimated technical potential of offshore wind power in China within 50km range offshore is up to 758GW (Wen, 2016). After several years of development, China's offshore wind farms have begun to take shape. In 2016, China was ranked as No. 3 in terms of the total installed capacity. In comparison with the total installed offshore wind capacity of 1.63GW by 2016, the Chinese government aims to achieve the total capacity of 5GW installed and 10GW under construction by 2020 (Offshore Wind, 2017).

In the US, the total technical potential of offshore wind in the five coastal regions (North Atlantic, South Atlantic, Great Lakes, Gulf of Mexico and Pacific regions) are estimated to be 2059GW (Musial et al., 2016). On the other hand, there is a big market for electricity demand in these coastal regions in the next thirty years, as indicated in Figure 2.4 by Marcy & Beiter (2016). The figure shows the difference between the electricity projected to be generated by various power plants and the projected electricity demand along the US coastlines. Thus, it shows the opportunity for energy developments, which in some regions offer potential for offshore wind farms. The North Atlantic coast of the US has the best potential for further development because of the proximity to high demand centers, relatively shallow waters, and higher wind speeds. Presently several projects are in the planning stages in the US, including the 90MW South Fork Wind Farm off the coast of New York and the 120MW wind farm offshore Maryland.

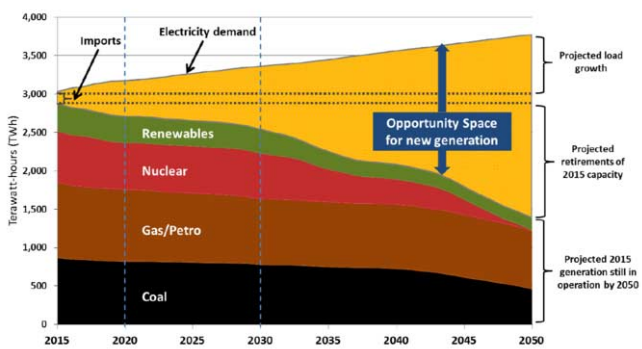

Figure 2.4: Future projected electricity demand and generation in the US coastal regions with the difference being the 'opportunity space' (Marcy & Beiter, 2016)

2.2 Numerical modelling and analysis

2.2.1 Numerical tools – state-of-the-art and validation

In the last decade, many numerical tools were developed for coupled dynamic analysis of both bottom-fixed and floating wind turbines for design purposes. Validation of numerical codes is an important step before they are widely used in the industry.

The International Energy Agency (IEA) initiated a code validation study through Wind Tasks 23 and 30, called OC3 (2005-2009) and OC4 (2010-2013), with focus on code-to-code comparison. As a continuation, the current OC5 (Offshore Code Comparison Collaboration Continuation, with Correlation) (2014-2018) project aims for validation of offshore wind modelling tools through the comparison of simulated responses to physical response data from actual measurements. It consists of three phases, including Phase I using the data for validation from the model-scale tank tests of monopile foundations at MARINTEK (Robertson

et al., 2015) and at DHI (Robertson et al., 2016), Phase II comparing the data from the model test of a semi-submersible floating wind turbine at MARIN (Robertson et al., 2017) and Phase III considering the field measurement data of a jacket wind turbine from the Alpha Ventus Wind Farm in Germany.

The work in Phase I has been concluded. The Phase II work was completed in mid-2017, but no reports were available at the time of this report writing. In 2018, they will focus on the Phase III comparison. Therefore, we discuss some of the Phase I results in our report. This benchmark study attracts most of the code developers and users for offshore wind turbine analysis and therefore it will be interesting and important to follow up this benchmark study for the future ISSC committee.

In the ISSC report (Brennan et al., 2012) in 2012, we discussed the codes that were compared in the OC3 and OC4 studies. It should be noted that most of the codes in this benchmark study were the global loads and response analysis codes. Wind turbine aerodynamics in such codes are based on the Blade Element Momentum (BEM) theory, while hydrodynamics are based on potential flow theory or the Morison's formula. The codes also have the ability to do platform motion and structural response analysis. Table 2.1 shows the codes that participated in the OC5 Phase I comparison against the results of a flexible monopile under wave loads from the model test at DHI (Robertson et al., 2016). Since this phase focused on linear and nonlinear hydrodynamic loads on a flexible monopile, the main features of wave kinematics models and loads models are compared in the table. Most of the codes are now able to simulate nonlinear waves in both regular and irregular seas and the hydrodynamic loads are mainly based on the Morison's formula. Typically, finite element models are implemented in these codes to capture vibrational responses, which are important for offshore wind turbines.

Figures 2.5 shows the monopile model considered in the test (which was designed so that the first bending mode of the structure was properly scaled). The time series of the wave elevation and the total shear force at the bottom are compared in the figure for large irregular waves (Hs=0.104m, Tp=1.4s at model scale and Hs=8.32m, Tp=12.5s at full scale) of moderate water depth (0.51m at model scale and 40.8m at full scale). The comparison was made directly at the model scale and the scaling ratio was 1:80. Most of the codes can predict well the nonlinear wave elevation and the corresponding loads under the non-breaking condition. This is also shown in Figure 2.6 (top plot) by the exceedance probability of the total shear force. However, the numerical predictions deviate more significantly from the measurements for breaking waves (Hs=0.133m, Tp=1.56s) in shallow water (with a depth of 0.26m at model scale), as shown by the exceedance probability of the total shear force in the same figure (bottom plot).

Individual code developers are also doing code validation against different types of model test and field measurements. These research activities are discussed below in the sections of analysis for bottom-fixed and floating wind turbines, as well as physical testing.

Classification societies are developing guidelines or recommended practice for coupled analysis of floating wind turbines, such as the JIP run by DNV-GL (2017a). This guidance will include setting up minimum requirements for the design of new concepts that can help investors' evaluation, and supporting the more mature technologies towards a safe and secure commercialization. It also covers the methodology to validate numerical models in relation to requirements in the standards from tank test results.

2.2.2 Loads and response analysis of bottom-fixed wind turbines

Bottom-fixed wind turbines are installed in the majority of today's offshore wind farms. The technology related to bottom-fixed wind turbines is relatively mature. Therefore, the research focuses on different aspects of wind turbine analysis where large uncertainties still exist (including soil-pile interaction, nonlinear wave loads) or where efficient methods are needed (for example for fatigue analysis or optimization).

Table 2.1: Numerical codes benchmarked in OC5 and their features (Robertson et al., 2016)

Participant	Code	Wave Model (Reg/Irr)	Wave Elevation	Hydro Model	Structural Model	Number DOFs
4Subsea	OrcaFlex	FNPF kinematics	FNPF kinematics	ME	FE, RDS	160 elements 960 DOFs
GE	Samcef Wind Turbines	5th-Order Stokes/ Linear Airy	Stretching	ME	FE (TS), RD	13 elements 84 DOFs
DNV GL-ME	Bladed 4.6	6th- and 8th-Order SF/ Linear Airy	Measured	ME	FE (TS), MD	8 (CB)
DNV GL-PF	Bladed 4.6	Linear Airy	Measured	1st Order PF	Rigid	N/A
DTU-HAWC2	HAWC2	6th-and 8th-Order SF/Linear Airy and FNPF kinematics	Stretching and FNPF kinematics	ME	FE (TS), RDS	20 elements, 126 DOFs
DTU-HAWC2-PF	HAWC2	6th-and 8th-Order SF/Linear Airy	Stretching	McCamy & Fuchs	FE (TS), RDS	31 elements, 192 DOF
DTU-BEAM	OceanWave3D	FNPF kinematics	FNPF kinematics	ME+Rainey	FE (EB), RD	160 DOFs
IFE	3Dfloat	FNPF kinematics	FNPF kinematics	ME	FE (EB), RDS	62 elements, 378 DOFs
IFE-CFD	STAR CCM	CFD	CFD-derived	CFD	Rigid	N/A
IFP-PRI	DeeplinesWind	3rd-Order SF/ Linear Airy	Measured	ME	FE	200 elements
UC-IHC	IH2VOF	FNPF kinematics	FNPF kinematics	ME	Rigid	N/A
MARINTEK	RIFLEX	2nd-Order Stokes and FNPF kinematics	Measured and FNPF kin.	ME	FE(E-B), RDS, FS	167 elements, 1002 DOFs
NREL-ME	FAST	2nd-Order Stokes and FNPF kinematics	Measured and FNPF kin.	ME	FE (TS), MD	4 (CB)
NREL-PF	FAST	2nd-Order Stokes	Measured	2nd-Order PF	Rigid	N/A
NTNU-Lin	FEDEM 7.1	Linear Airy	None	ME	FE (EB), RD	13 elements, 84 DOFs
NTNU-Stokes5	FEDEM 7.1	5th-Order Stokes	None	ME	FE (EB), RD	13 elements, 84 DOFs
NTNU-Stream	FEDEM 7.1	Stream Function	None	ME	FE (EB), RD	13 elements, 84 DOFs
PoliMi	POLI-HydroWind	2nd-Order Stokes	None	ME	FE (EB), RD	23 elements, 69 DOFs
SWE	SIMPACK +HydroDyn	2nd-Order Stokes	None	ME	FE (TS), MD	50
UOU	UOU + FAST	2nd-Order Stokes	None	ME	Rigid	N/A
WavEC	Wavec2Wire	2nd-Order Stokes	Measured	2nd-/1st-Order PF	Rigid	N/A
WMC	FOCUS6 (PHATAS)	FNPF kinematics	FNPF kinematics	ME	FE (TS), MD	12 (CB)

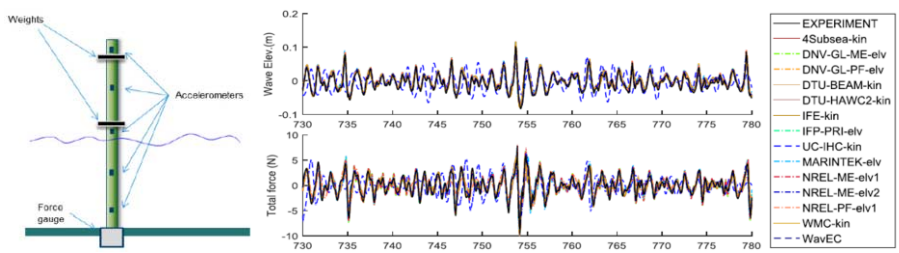

Figure 2.5: The flexible test model (left) and examples of wave elevation (middle, top) and total shear force (middle, bottom) at the monopile bottom for large waves (Hs=0.104m, TP=1.4s model scale (Hs=8.32m, Tp=12.5s full scale)) in moderate waters (with a depth of 0.51m, model scale (40.8m full scale)) (Robertson et al., 2016)

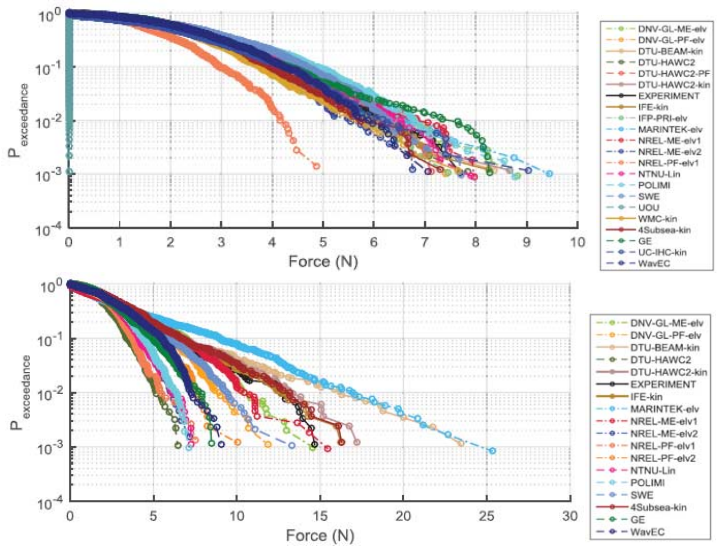

Figure 2.6: Exceedance probability of the total shear force at the monopile bottom under non-breaking waves in moderate water (top) and breaking waves in shallow water (bottom) (Robertson et al., 2016)

Soil-pile interaction

The p-y curve approach is the commonly applied method for analyses of laterally loaded piles. With its heritage from the offshore oil & gas industry, where the loading situation is substantially different and piles with smaller diameters are used as compared to offshore wind, such method is not suitable for large-diameter monopile foundations for offshore wind turbines. In the PISA (Pile Soil Analysis) project (Byrne et al., 2015), a new design methodology for monopile foundations was developed to overcome the shortcomings of the current methods. This new design method, as shown in Figure 2.7, is based on the use of numerical finite element models which are validated through a campaign of large scale field tests.

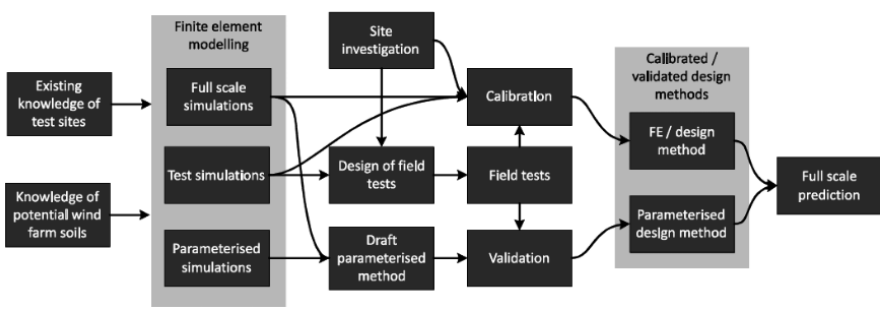

Figure 2.7: The new design methodology developed in the PISA project (Byrne et al., 2015)

The numerical analysis of the long-term performance of offshore wind turbines supported by monopiles is performed by Ma et al. (2017) considering cyclic loading of wind and waves. The study shows that under the serviceability limit state, the deflection and rotation at pile head considering the effect of long-term cyclic loading are notably greater than those computed for the case where this long-term effect is ignored.

Nonlinear wave loads and seismic loads

Bottom-fixed wind turbines installed in the shallow water regions are exposed to nonlinear wave loads. The breaking wave forces on jacket type structures and slamming wave loads on truss structures were analysed by Jose et al. (2016a, 2016b). In the case of jacket structures the wave kinematics calculated by the CFD model show a very good agreement with the experimental results. However, the CFD model overestimates slightly the total force calculations compared with the experimental results.

Wei et al. (2017) analyzed the dynamic effects in the response of offshore wind turbine supported by jackets under wave loading considering series of time domain dynamic analysis based on loading from regular and irregular wave histories and OWT support structures. The study shows that the dynamic amplification factor decreases with the increase in wave height.

Morato et al. (2017) studied the ultimate loads and responses of a monopile supported offshore wind turbine using fully coupled simulations. The structural response to different ultimate limit states is analyzed and the design load cases are ranked based on the three response parameters.

Horn et al. (2016) identified that hydro-elasticity contributes to the fatigue damage on large volume monopiles in the offshore wind energy industry. The study shows that the large third/fourth order moment and fatigue contribution is due to an incident wave elevation influenced by the sum-frequency components.

The offshore wind turbine model resting on multiple piles under seismic, wind, wave and current loads is investigated by Wang et al. (2017) and it is observed that the structural responses increase proportionally under the normalized seismic excitations with different peak ground accelerations.

Fatigue analysis and optimization

In the SLIC (Structural Lifecycle Industry Collaboration) project, a number of fatigue tests were carried out for welded steel foundations (such as monopile) for offshore wind turbines in air and seawater (Mehmanparast et al., 2017). It was found that for a given value of the stress intensity factor range (ΔK), the fatigue crack growth rate (da/dN) is on average around 2 times higher in seawater compared to the rate in air for the base metal and weldments, which is almost half of the value recommended by the current standards.

Ziegler et al. (2016) presented the influence of load sequence and weather seasonality on the fatigue crack growth for monopile-based OWT. The study indicates that loading sequence does not influence the long-term crack propagation considering fatigue relevant load cases only.

Muller et al. (2016) presented the study on the validation of load assumptions for both fatigue and ultimate loads. The study showed that, as compared to the wind loads, the wave loads have less influence on the structural responses at the tower base and even at the locations of the upper jacket.

Ong et al. (2017) investigated the dynamic responses of two jacket-type offshore wind turbines using both decoupled and coupled numerical models under wind and wave loadings. In the decoupled model, the thrust and torque of an isolated rotor model are used as wind loads and in addition a linear aerodynamic damping effect is considered.

The correlation between the tower top axial acceleration and the load effects in drivetrain segments of a monopile offshore wind turbine is investigated by Nejad et al. (2016). The study shows no correlation between the maximum axial force in the drivetrain and the maximum axial acceleration at the tower top. The tower-top bending moment was found to increase as the wind increases.

Wind turbine foundation optimization (monopile, jacket or floating foundations) is a hot topic in recent years. Considering the fact that there is a large number of simulations required for design analysis, such optimization analysis relies on the development of efficient numerical methods, for example those based on frequency-domain models.

Feyzollahzadeh et al. (2016) presented the responses of a wind turbine due to wind loads acting on it using an analytical transfer matrix method (TMM). The comparison of TMM result with the conventional methods shows that TMM can be used for the wind induced vibration analysis of the wind turbine as it gives a high value of accuracy.

Chew et al. (2016) developed an analytical gradient-based optimization framework for the design of OWT support structure, minimizing the overall structural mass and considering the design checks for member sizing, eigen-frequencies, extreme and fatigue load effects as constraints. It was applied to the UpWind and OC4 jacket wind turbines, supporting the NREL 5MW rotor. The optimization analysis was carried out with respect to diameter and thickness of the jacket legs and braces. Figure 2.8 shows the results of the initial and optimal designs obtained using both the analytical method and the central difference numerical method.

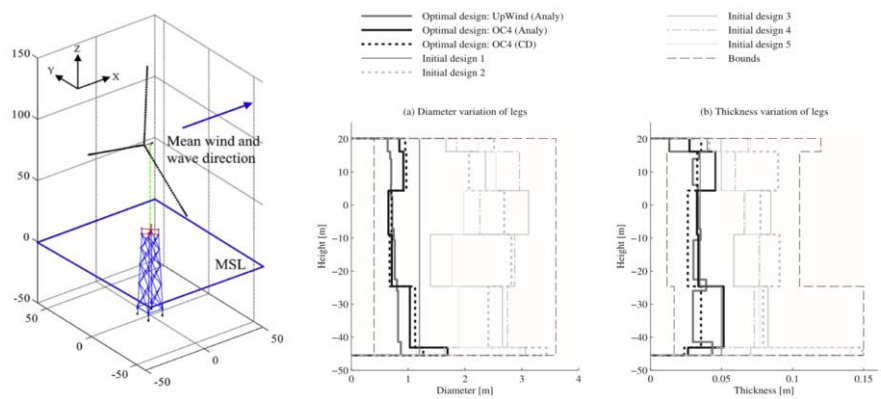

Figure 2.8 Initial and optimal designs of the UpWind and OC4 jacket support structures (Left: jacket wind turbine; middle: diameter of legs; right: thickness of legs. Analy: analytical method; CD: central difference method.)

2.2.3 Loads and response analysis of floating wind turbines

In the recent years, a significant number of studies on offshore floating wind turbines for deep waters (with a depth more than 50m) have been performed. The development and installation of multi-MW wind turbines started in early 2000 and are still in progress. Various floater concepts are developed and analysed to understand the dynamic behaviour under simultaneous wind/wave/current loads and to find a cost-effective solution. The focuses were on the development of novel floater concepts, CFD analysis of floating wind turbines, mooring system design and analysis, etc.

Global response analysis

Different modelling techniques to predict loads acting on the offshore floating wind turbines and induced motions and structural responses have been proposed and applied. Nygaard et al. (2016) presented the theory behind the structural model, aerodynamic and hydrodynamic load modules, control system and coupling with an optimizer. The verification and validation of the code 3DFoat for a floating platform was performed. Guignier et al. (2016) presented multibody modelling of a floating offshore wind turbine foundation for global load analysis induced by wind and wave loads. The validation of the numerical model was performed by

comparing the obtained results with the classical rigid body floater model. Lemmer et al. (2016) presented a linear time-invariant (LTI) model for a floating wind turbine (FOWT) coupled with a linear structural FOWT model. The LTI model fitted to the linear wave excitation force coefficient from a panel code which has been compared to the original panel code data in frequency and time domains.

Most of the developed floating wind turbine concepts are either spar, semisubmersible or TLP floaters. The dynamic characteristics of the truss Spar-type floating foundation used to support the offshore vertical-axis wind turbine (VAWT) were analyzed by Liu et al. (2016b). The effects of foundation parameters on the hydrodynamic performance of the offshore floating foundation were investigated. The motion performances were analyzed and compared for the two floating VAWTs, S-1 (the VAWT supported by FS-1) and S-2 (the VAWT supported by FS-2).

Leimeister et al. (2016) examined the procedure of up scaling of a semi-submersible platform in order to support a predefined wind turbine. The stability analysis, frequency-dependent hydrodynamic coefficients, natural periods and motion responses of the floating semisubmersible platform are thoroughly investigated under this study. Luan et al. (2016) explained the design data and numerical analysis of a braceless steel semi-submersible wind turbine. A numerical analysis is performed to analyze the intact stability, natural periods and modes and global dynamic responses in the combination of wind and waves. Wandji et al. (2016) developed a semi-floater concept for installation of a floating offshore wind turbine support structure under a moderate water depth. The reliability analysis and fatigue load calculations are performed to ensure a desired life expectancy of the structure. It is shown that the semi-floater design is fulfilling the necessary design requirements for supporting floating wind turbines. Karimirad and Michailides (2015) examined a V-shaped braceless semisubmersible wind turbine, similar to the concept of Fukushima FORWARD.

Walia et al. (2017) performed a FAST simulation for a TLP substructure with new material. It was shown that the deflections for all six DOFs are very small for the operating status as well as for an extreme storm surge. As one important result of the paper, the resulting internal forces and moments at the transition piece from the FAST simulations were taken as an input for the analyses of the steel reinforced pre-stressed ultra-high performance concrete pipes. These assumptions are conservative, and further investigations are needed.

Hydrodynamic effects, including second-order wave loads and viscous effects, on the motion responses of floating wind turbines are still being studied in detail. Antonutti et al. (2014) have shown the importance of including the heave plate excursion effects as a result of wind-induced inclination in a semi-submersible FOWT. Lopez-Pavon and Souto-Iglesias (2015) discussed hydrodynamic coefficients and pressure loads on heave plates for semi-submersible type FOWT using large scale models (1m diameter discs).

Liu et al. (2016c) examined modelling of a semi-submersible with slender bracings. Four different numerical methods (pure panel method, pure Morison's formula, combination of panel method and Morison's formula where inertia forces for slender bracings are modelled either by Morison's formula or panel method) are compared with experiments.

Karmakar et al. (2016) analyzed the reliability-based design loads based on the environmental contour method to estimate the long-term extreme loads for FOWT of spar-type and semi-submersible-type. In the case of 1D model, 10-min mean wind speed was considered as random, whereas wave height and 10-min maximum response load were held at their mean levels. In the case of 2D model, 10-min mean wind speed and wave height was considered random while the load variable was considered to be deterministic at its mean level. Basically, 1D and 2D models gave consistent results for the design loads.

Fatigue analysis

Considering the fact that thousands of time-domain simulations need to be carried out for fatigue design of wind turbines, developing efficient simulation techniques or numerical methods are always interesting.

Kvittem and Moan (2015) dealt with fatigue analysis for a semi-submersible wind turbine. Here, a wide range of environmental conditions were considered in order to study the effect of simulation length, the number of realizations of wind and wave loads, bin size and wind-wave misalignment.

Graf et al. (2015) proposed a high-throughput computation method in fatigue load estimation of floating offshore wind turbines using a Monte Carlo integration instead of using traditional grid-based methods. They showed that the Monte Carlo integration method can reduce the number of aeroelastic simulations drastically, but as nonlinearity increases, the effectiveness of the Monte Carlo approach is reduced.

Nejad et al. (2015) performed load and fatigue damage analysis of drivetrains in floating wind turbines of TLP, spar and semi-submersible. A de-coupled analysis approach was employed for the drivetrain analysis. First, the global response analysis was made, and motions, moments and forces from the global analysis were applied on the gearbox multibody model.

CFD analysis of floating wind turbines

Nowadays, a common approach for evaluation of aerodynamic loads acting on an offshore wind turbine is based on blade element momentum theory (BEMT). On the other hand, a common approach for hydrodynamic analysis for floating wind turbines is to use either the Morison's formula, potential flow theory or combinations thereof. However, alternative CFD approaches might be used possibly for validation of the above-mentioned methods. CFD calculations of aerodynamics and hydrodynamics are expensive and not suitable for engineering design in which a significant number of load cases need to be simulated. However, they are useful for special loading conditions for which detailed flow around the aero-foil and the floater needs to be resolved. For example, for a floating offshore wind turbine, the motion of a floating body may affect the flow fields, and thus the underlying assumptions in BEMT might be violated.

Sant and Cuschieri (2016) compared three aerodynamic models – the blade element momentum theory (BEM), the general dynamic wake (GDW) method implemented in FAST and a free-wake vortex method (FWVM) - for predicting the thrust and power characteristics of a yawed floating wind turbine rotor.

Liu et al. (2016d) investigated the effects of platform motions on the aerodynamics of a FOWT using the open source CFD code OpenFOAM. The aerodynamic thrust and torque on the wind turbine are compared and analyzed for platform motion patterns with the flow field.

Tran and Kim (2015) studied the periodic pitching motion caused by the rotation of turbine blades. The unsteady computational fluid dynamics (CFD) simulation based on the dynamic mesh technique is used for analysis of the pitching motion of wind turbine due to the platform motion. Tran and Kim (2016) then performed an unsteady aerodynamic analysis for both the blade alone and the full configuration wind turbine models considering the periodic surge motions of a floating wind turbine platform using both CFD and unsteady BEM.

Jeon et al. (2014) investigated the flow states of a floating wind turbine during platform pitching motion using the vortex lattice method. They showed that a turbulent wake state, which is unwanted aerodynamic phenomena, may arise when the floating platform is pitching in the upwind direction.

Quallen et al. (2014) performed CFD simulations of the OC3-Hywind model using a quasi-static crowfoot mooring-line model. They compared the results with the predictions by the NREL FAST code. Dunbar et al. (2015) developed and validated a tightly coupled CFD/6-DOF solver using the computational continuum mechanics library OpenFOAM, and then applied it to the DeepCwind semisubmersible offshore floating wind turbine platform. They also compared the results with the NREL FAST/HydroDyn code.

Leble and Barakos (2016a; 2016b) presented the study on the hydrodynamics load computation on the supporting structure using the Smoothed Particle Hydrodynamics (SPH) method and the aerodynamic load computations are performed using HMB3 CFD solver. The coupled analysis is performed for offshore wind turbine and it is showed that the weak coupling is adequate for the load computations.

Mooring system design and analysis

Lopez-Pavon et al. (2015) examined time-domain simulations with different models for the second-order forces for catenary mooring design of a semi-submersible FOWT. The models were full 6DOF quadratic transfer functions (QTF), Newman's approximations (6DOF), no slow-drift forces, and full 2DOF QTFs. Comparison between numerical and experimental results showed that, although the main trend is well captured by the numerical estimations, numerical results under predicted the measured loads to some extent, even when full 6DOF QTFs were computed.

Hall and Goupee (2015) introduced a lumped-mass mooring line model with DeepCwind semisubmersible FOWT, and validated it against scale-model test data. For the uncoupled validation, in which the fairlead kinematics are prescribed based on the test data, the mooring line tension at the fairlead agreed well with the experimental data. In coupled simulations of the entire FOWT system, the surge and pitch motions agreed well with the test data, but the heave motions were under predicted.

Gutierrez-Romero et al. (2016) presented a non-linear FEM solver for the analysis of the response of moored floating structures, in particular floating wind turbines. The model was based on an updated Lagrangian formulation. The OC3-Hywind FOWT was analyzed under operational conditions considering second-order waves. The results suggest that using a quasi-static model for fatigue assessment of the mooring lines could overestimate their fatigue life, whereas a first-order seakeeping approach could underestimate tension values on the mooring systems.

Azcona et al. (2017) quantified the influence of mooring dynamic models (either dynamic or quasi-static) on the calculation of fatigue and ultimate loads of three offshore FOWTs (spar, semisubmersible and tension-leg platform). More than 3500 simulations for each platform and mooring model were launched and post-processed according to the IEC 61400-3 guideline (IEC, 2009). It was revealed that the additional damping introduced by the mooring dynamics plays an important role on the differences of the models.

Hsu et al. (2017) investigated the extreme value distributions of a FOWT mooring tensions, where special attention was paid to snap-induced tensions in mooring lines. A composite Weibull distribution model with different shape and scale parameters was proposed that appeared to fit available data well.

Floating vertical axis wind turbines

Paulsen et al. (2014) summarizes the results from the DeepWind project on the development of a 5 MW spar vertical axis wind turbine (VAWT), with focus on the state-of-the-art design improvements, new simulation tools HAWC2 and results, and the feasibility for up-scaling to 20 MW. The aspects on structural mechanics, generator, floater & mooring system, control system design and rotor design were discussed in detail using the integrated tools. The design

has a rotating floater (spar) and the study found that the Magnus forces on the rotating floater have a limited influence.

Wang et al. (2016a) presented a stochastic dynamic response analysis of a 5MW floating vertical-axis wind turbine (FVAWT) based on fully coupled nonlinear time domain simulations. They used Simo-Riflex-Double Multiple Streamtube (DMS) coupled solver under different environmental conditions.

An integrated numerical tool (Simo-Riflex-AC) was developed for modelling and analysis of floating vertical axis wind turbines (Cheng et al., 2017a; 2017b; 2017c). AC stands for Actuator Cylinder flow model for aerodynamics of VAWT. The AC model was validated against experimental data and compared to another model DMS (Double Multiple Streamtube). The numerical model was used to study a VAWT with a two-bladed Darrieus rotor and found that the 2P (twice per revolution) responses are significant. Increasing the number of blades from 2 to 3 and 4 would reduce such responses. It is also used to compare the responses of a VAWT and a horizontal axis wind turbine (HAWT).

Borg and Collu (2015a) presented a literature review to understand the coupled dynamics involved in floating vertical axis wind turbines (VAWTs). They focused on the approaches to develop an efficient coupled model of dynamics for floating VAWTs. Emphasis was also placed on utilizing computationally efficient models and programming strategies. Borg and Collu (2015b) investigated the frequency-domain characteristics of floating vertical axis wind turbine aerodynamic loads. They presented through a case study the influence of unsteady platform motion on global frequency-domain aerodynamic loads generated by the VAWT on a floating support structure.

Chowdhury et al. (2016) carried out numerical validation of an experimental work of VAWT in upright and tilted conditions for applications like Floating Axis Wind Turbine. The numerical validation was accomplished by CFD analysis by solving Unsteady Reynolds Averaged Navier-Stokes (URANS) equation.

Floating wind turbine under abnormal loads

Special load conditions for offshore wind turbines are earthquakes, icing or component faults. These special load conditions are well defined in the load case tables from the ICE 61400-3 standard or in the DNV-GL guidelines.

Jiang et al. (2015) presented a comparative study of shutdown procedures on the dynamic responses of wind turbines which may induces excessive loads on the support structure. The short-term extreme response and the annual fatigue damage to the structural components were compared under normal and parked condition. The procedure of three blade shutdown is recommended for both the turbine cases because one or two blade shutdown with grid loss may results in a significant rotor over speed. Etemaddar et al. (2016) performed response analysis of spar-type FOWT under blade pitch controller faults, and made comparison with an onshore wind turbine, using the OC3-Hywind model.

Bae et al. (2017) performed numerical simulations of the performance of a floating offshore wind turbine (FOWT) with broken mooring line. An aero-hydro-servo-elastic-mooring coupled dynamic analysis in the time domain is performed for the simulation. It is observed that due to loss of one mooring line, the orientation of the platform and turbine can be changed which leads to large error in the nacelle yaw motion and affects the FOWT negatively.

The fuzzy-based damage detection method for TLP and Spar floating wind turbines was performed by Jamalkia et al. (2016) for the dynamic response of the structure. The variation values of the mean amplitude of dynamic response and frequency characteristics of the structure due to stiffness changes of mooring lines are considered as input parameters to the fuzzy system.

2.3 Physical testing

In the last few years, there is an increasing research interest in physical testing including lab testing of offshore wind turbines and in particular floating wind turbines. Todays' wind turbines are designed using first principles and the external loads and structural responses are explicitly calculated typically using time-domain numerical codes. Validation of such codes against measurements from lab tests under controlled and usually easily-known environmental conditions is an important part of the recent research work. However, there are a number of challenges in lab testing of offshore wind turbines (Muller et al., 2014):

- Quality of wind field generation in ocean basin or towing tank
- Conflicts in the scaling laws for aerodynamics (Reynolds scaling) and hydrodynamics (Froude scaling) and therefore how to match both mean and dynamic wind turbine aerodynamic loads for a wide range of wind speeds
- Simulation of wind turbine faults in model tests
- Consideration of structural flexibility

The recently-developed real-time hybrid testing technique (Azcona et al., 2014; Chabaud, 2016; Kanner, 2015) which combines physical testing with numerical simulations solves some of the problems mentioned above.

Field measurements of prototype offshore wind turbines are always useful since there are no scaling problems. However, the main challenge is the uncertainties in the measurements. From the validation of numerical codes point of view, both environmental conditions (here mainly wind and waves) and wind turbine responses must be simultaneously and accurately measured. Measurement of wind speed at the rotor swept area is particularly challenging and there are ongoing research projects, developing for example LIDAR systems. Moreover, prototype testing at sea is costly and the measurement data are often not publically available.

In this section, we will mainly discuss the recent work on lab testing of offshore wind turbines. Wind tunnel tests for rotor aerodynamic design and tests of mechanical components (such as drivetrains) are excluded because of less relevance for ISSC. Moreover, we focus on dynamic behavior tests of offshore wind turbines in wind and waves, rather than ultimate or fatigue strength tests of wind turbine blades or other structural components.

2.3.1 Lab testing

Bottom-fixed wind turbines

Offshore wind turbines with a bottom-fixed foundation (such as monopile, tripod, jacket or GBS) have been well developed and widely used in the industry. But, the development of large-scale (8-10MW) wind turbines in larger water depths (40-60m) leads to large-diameter monopile design and therefore hydrodynamic loads become more important. The recent experimental work on bottom-fixed foundations are related to nonlinear wave loads on monopile and jacket, foundation-soil interaction and seismic loads and responses.

Suja-Thauvin et al. (2017) presented the experimental results from MARIN on a monopile foundation (at 1:30.6 scale) considering a fully flexible model in which the first and second eigen-frequencies are properly scaled. Both breaking and nonbreaking waves are considered. It is found (as shown in Figure 2.9) that in addition to the quasi-static responses due to the first-order wave loads and the ringing responses of the first eigen-mode, the resonant responses of the second eigen-mode are excited by the breaking wave loads. The corresponding contributions to the largest response are about 40-50%, 30-40% and 20%, respectively.

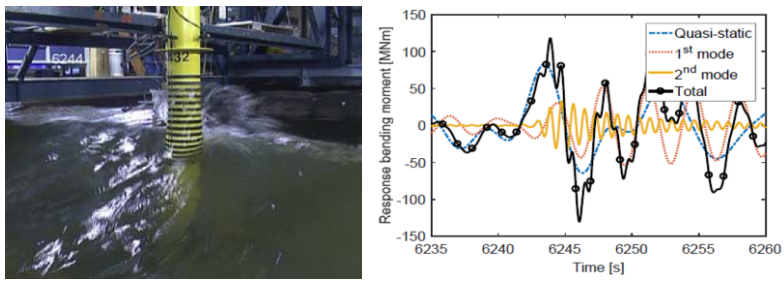

Figure 2.9: The flexible monopile model tested in MARIN (left) and examples of the bending moment response time series at the bottom (right) (Suja-Thauvin et al., 2017)

An extensive experimental campaign (Bachynski et al., 2017) on a 1:48 scale monopile was carried out at SINTEF OCEAN (previously MARINTEK) for Statoil in connection with the development of the Dudgeon wind farm in UK, as shown in Figure 2.10 (left picture). The focus was on the nonlinear wave loads and ringing-type resonant responses in nonbreaking extreme waves. The comparison with the experimental results indicates that numerical methods using a beam element model with a modified Morison wave load model and second-order wave kinematics gave reasonable prediction of the ringing responses of the fully flexible model. In addition, the results from three monopile models (including a rigid, a rigid with an equivalent rotational spring at bottom and a fully flexible model) are compared and the rigid model with rotational spring behaves similarly as the fully flexible model.

Loukogeorgaki et al. (2016) performed a model test of wave slamming loads on a three-legged jacket foundation (at 1:18 scale) for offshore wind turbines in the CNR-INSEAN wave tank in Italy, as shown in Figure 2.10 (right picture). The load components at the bottom of the jacket were measured. Their experiments for the focused wave cases revealed that there exists an additional impact on the leeward jacket legs slightly after the first impact on the windward leg. This induces complex dynamic responses of the complete structure.

Figure 2.10: The monopile model tested in SINTEF OCEAN (left) (Bachynski et al., 2017) and the jacket model tested in CNR-INSEAN (right) (Loukogeorgaki et al., 2016)

Soil-structure interaction is a traditional research topic for bottom-fixed wind turbines. In particular, a proper modelling of the soil resistance in terms of both nonlinear and time-dependent spring and damping effects on the dynamic responses of the bottom-fixed wind turbines is very important. Randomness in soil property at the offshore wind farm sites is another challenge. Therefore, lab tests or field tests are developed to validate numerical models.

An interesting field test of a monopile foundation under excitation of an eccentric-mass shaker was carried out by Versteijlen et al. (2017) to investigate the lateral dynamic soil-stiffness in real conditions. The measured response of the monopile is used to validate an effective 1D stiffness method and the current employed p-y stiffness method for small strain conditions. The results show that the effective stiffness method seems to overestimate the actual low-frequency stiffness while the p-y method will significantly underestimate it. In addition, a damping ratio of 20% for the monopile only (equivalent to 0.14% for the full structure) was identified from the field test.

Besides normal monopile foundations, suction buckets are recently developed for offshore wind turbines. In the work done by Foglia et al. (2015), thirteen monotonic and cyclic lab tests on a skirted footing bucket model (with a diameter of 0.3m and an embedment ratio of 1) were carried out to study the drained behavior of the soil considering the typical loading conditions with large overturning moment and horizontal force for an offshore wind turbine. The test results were used to validate a complete macro-element approach for both monotonic and cyclic loadings. A large-scale model test on a novel hybrid bucket foundation (with a diameter of 3.5m and a height of 0.9m) for offshore wind turbines has been performed by Ding et al. (2015), in which the horizontal load-displacement curve and the horizontal bearing capacity of the bucket in saturated clay were determined by tests. A numerical model based on finite element method for predicting the load-displacement curve was validated against the test results.

Besides wind and wave loads on bottom-fixed wind turbines, earthquake loads is another important design consideration for some geographical areas. Zheng et al. (2015) performed a test of a scaled (1:30) monopile wind turbine under joint earthquake and wave loads, with focus on the nacelle acceleration response, in the towing tank equipped with a shake table at Dalian University of Technology. They found that it is important to consider wave loads simultaneously when predicting the dynamic responses under earthquake loads. In the same lab, Wang et al. (2016c) performed a similar test on a bottom-fixed penta-pod wind turbine at a scale ratio of 1:30. The numerical FE simulations using the measured acceleration at the shake table as input predict quite accurate responses of the complete structure under seismic loads.

Floating wind turbines

Model testing of floating wind turbines in hydrodynamic labs became one of the hot research topics in recent years. Some of these studies focus on the effect of nonlinear hydrodynamic loads on the motion responses of floating wind turbines. In Simos et al. (2018), the wave-induced slow-drift motions of a three-column semi-submersible wind turbine were studied experimentally and numerically. The comparisons against the experimental results indicate that the full QTF model gives better predictions of the slow-drift motions than the Newman's approximation, which underestimates the second-order responses. In the study carried out by Pegalajar-Jurado et al. (2017) on the motion responses of a TLP wind turbine, different nonlinear wave kinematics were applied, including the second-order wave kinematics, the fully nonlinear wave kinematics and the linear waves with an extrapolation of the wave kinematics up to the instantaneous wave surface. It was found that the numerical models based on the Morison's formula considering nonlinear wave kinematics predict the motion responses better than the pure linear wave model.

In model tests, hydrodynamic loads on floaters are typically scaled according to the Froude law and then the main challenges are related to the modelling of wind turbines and the scaling of aerodynamic loads. The scaling issue has been thoroughly studied by Make & Vaz (2015) in which they investigated the flow over two (floating) wind turbines using RANS CFD calculations at model and full-scale Reynolds numbers conditions. The NREL 5MW and MARIN Stock Wind Turbine (which was designed to have the same thrust at model scale as the NREL turbine at full scale) were considered. Good agreement between the CFD and the ex-

perimental results was obtained for the model-scale turbine for the thrust coefficient, but not the power coefficient. The large Reynolds effects on the flow passing these two turbines are shown and explained.

Muller et al. (2014) and Stewart & Muskulus (2016) summarize the different experimental practices for modelling of wind turbines in labs. It includes the passive methods (concentrated masses with added point forces, over drag disks with a rotating body), the physical turbine methods (geometrically-scaled but pitch angle-redistributed rotor blades, redesigned performance-match rotor blades) and the hybrid methods (controlled duct fan to simulate thrust force only, other actuators (for example multiple hydraulic actuators) to simulate integrated wind turbine loads in multiple degrees of freedoms).

In the previous ISSC report (Gao et al., 2015), we discussed some of these methods and in this report, we will mainly review the new experimental techniques developed in recent years. This includes:

- Physical turbine model testing method
- Real-time hybrid model testing method

- ***Physical turbine model testing method***

To reproduce the equivalent thrust force is the first step in model testing of floating wind turbines, for which the thrust-induced pitch moment is the most important aerodynamic load effect with respect to motion responses of floating wind turbines. In recent years, attempts have been made to improve the reproduction of both mean and dynamic thrust force for a wider range of wind speeds, in particular by active blade pitch control at model scale.

Huijs et al. (2014) reported the results of the model tests for the GustoMSC Tri-Floater semi-submersible wind turbine concept at a scale ratio of 1:50 at MARIN (as shown in Figure 2.11) using the NREL 5MW wind turbine, in which both Froude-scaled thrust force and active blade pitch control at model scale were realized. Their study indicates that a Froude-scaled model with active blade pitch control is feasible and can significantly improve the mean thrust force reproduction in tests for typical operational conditions, while such model still cannot represent the dynamic responses of the turbine in full scale.

In another study by Goupee et al. (2017) at MARIN, the influence of different blade pitch and generator controls on the global responses of the DeepCwind-OC5 semi-submersible floating wind turbine was investigated experimentally for a model at 1:50 scale with the NREL 5MW turbine, as shown in Figure 2.11. This includes a fixed blade pitch with a constant rotor speed (no control), a collective blade pitch integral control with a constant rotor speed, and a variable speed generator control. The active blade controls with a Froude-scaled performance-matched wind turbine can reproduce the general trends of the motions one would observe for a full-scaled floating turbine.

Hara et al. (2017) discussed the model-based design of a blade pitch controller for a FOWT scale model. A linear state-space model of the FOWT scale model was created by using system identification, and the linear model was used to design a blade pitch controller.

Duan et al. (2017b) conducted the model tests of the OC3 spar floating wind turbine using both a thrust-matched blade-redesigned rotor and a geometrically-scaled rotor at 1:50 scale in the Ocean Basin at Shanghai Jiao Tong University, as shown in Figure 2.11. The study revealed the significant differences in the motion responses and the tower bending moments of the spar concept using two different model-scale rotors. This suggests the unsuitability of the geometrically-scaled rotor for model testing.

In the ongoing EU INNWIND project, a series of model test campaigns have been carried out on floating wind turbine concepts (a TLP (Pegalajar Jurado et al., 2016)), the scaled OC4

semi-submersible (Koch et al., 2016) and the Triple-Spar semi-submersible (Bredmose et al., 2017)), all supporting a 1:60 scale DTU 10MW wind turbine. The TLP test was carried out in the wave tank at DHI, Denmark, while the two semi-submersible tests were performed in the ocean basin of ECN, France (as shown in Figure 2.11). A performance-matched redesigned rotor was considered and active blade pitch control was applied. The design of the real-time blade pitch control system for model testing was detailed in Bredmose et al. (2017). Numerical simulations using FLEX5 were conducted and compared with the test results for the TLP concept (Pegalajar Jurado et al., 2016). It is found that FLEX5 gives good predictions of the surge motion and the mooring line tension, while it does not predict the pitch resonant motions reasonably well for the wave only cases. In the study of the scaled OC4 semi-submersible (Koch et al., 2016), the validation of a SIMPACK numerical model against the test results was performed. Moreover, the test data will be made publically available for future research work on floating wind turbines.

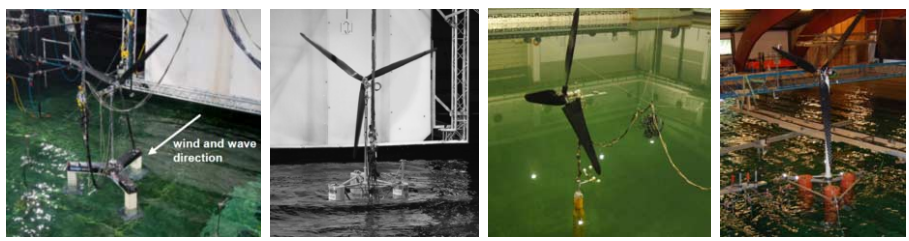

Figure 2.11: Floating wind turbine models tested at different hydrodynamic labs (from left: GustoMSC Tri-Floater at MARIN (Huijs et al., 2014); DeepCwind-OC5 semi-submersible at MARIN (Goupee et al., 2017); OC3 spar at SJTU (Duan et al., 2017a); Triple-Spar semi-submersible at ECN (Bredmose et al., 2017))

- ***Real-time hybrid model testing method***

One of the major developments in the last few years in experimental techniques for floating wind turbines are the real-time hybrid model testing methods (Azcona et al., 2014; Chabaud, 2016; Kanner, 2015). The basic idea of the hybrid testing is to combine physical experiments with numerical simulations, as shown in Figure 2.12 by Sauder et al. (2016) for testing a braceless semi-submersible floating wind turbine. The physics of the waves, current and their induced hydrodynamic loads and responses of the semi-submersible floater are realized, while the aerodynamic loads on the wind turbine in a turbulent wind field are numerically simulated and applied through actuators on the test model in real time. This method avoids the scaling issue of aerodynamic loads in a hydrodynamic lab test and allows us to study the coupling effect of the wind, wave and current induced loads and responses of floating wind turbines (Hall et al., 2017). It also opens the opportunities to study complex loading conditions that are required by design rules, such as wind turbine fault conditions, start-up and shut-down events.

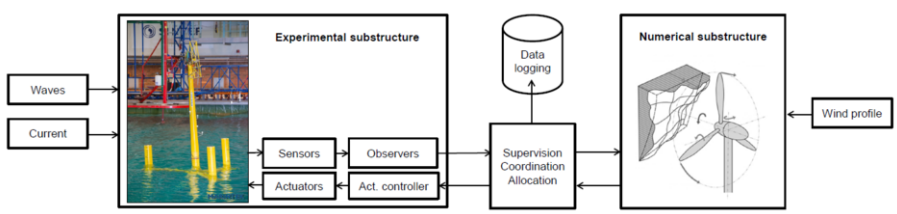

Figure 2.12: The methodology of real-time hybrid model testing for offshore wind turbines (Sauder et al., 2016)

The basic assumption is that the numerical simulation part (wind field generation and wind turbine aerodynamics in this case) typically using a numerical code should be already validated and correct. Such validation can be carried out by wind tunnel tests or field measurements of onland and offshore wind farms. The numerical code should be fast enough to calculate the demanded loads based on the motion measurements of the floating wind turbine in the lab test. The actuators should respond quickly to apply the demanded loads in real time or any delay in the actuation system should be compensated for in the actuator controller design. In Sauder et al. (2016), the frequency limit for actuators was set to achieve to a quick response to the wave-induced motions of the floater since the total integrated wind loads are of concern as shown in Figure 2.13. Moreover, the eigen-frequency of the actuation system needs to be designed away from any frequency of interest in wind and wave excitations. For bottom-fixed wind turbines, the feasibility of such experimental technique to capture the high-frequency resonant responses of the first bending mode needs to be investigated.

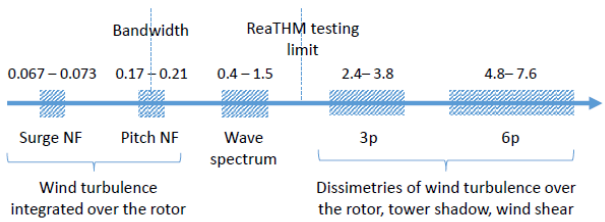

Figure 2.13: Frequency map for real-time hybrid model testing of floating wind turbines (Frequency values are in Hz, model scale. p denotes the rotational speed of the rotor. NF denotes natural frequency) (Sauder et al., 2016)

The developed real-time hybrid model testing method (Chabaud, 2016) was applied to test a braceless semi-submersible 5MW NREL wind turbine at 1:30 scale in the Ocean Basin at SINTEF OCEAN through the research centre NOWITECH (Sauder et al., 2016; Bachynski et al., 2016; Berthelsen et al., 2016). Six actuators with pulleys via thin lines connected to the frame on the semi-submersible were used to produce the integrated wind turbine loads in 5 DOFs (except the vertical force, which is shown to be less important for motion responses (Bachynski et al., 2015)). A detailed verification of the actuators and the calibration of a numerical model were carried out through the basic test cases (decay, wind-only and regular wave tests). The test results were then used to validate numerical models for conditions with irregular waves and turbulent wind, with focus on motion responses (Karimirad et al., 2017) and cross-sectional loads in the floater (Luan et al., 2017). Karimirad et al. (2017) obtained a good agreement between the numerical simulations and the experimental measurements of pitch motion responses and also demonstrated the limited effect of second-order wave orders for this braceless semi-submersible wind turbine, as shown in Figure 2.14.

A simpler real-time hybrid testing method was presented by Azcona et al. (2014), in which they used a ducted fan at the nacelle position of a semi-submersible floating wind turbine to provide the variable desired thrust force based on the numerical simulations, as shown in Figure 2.15. A 6MW wind turbine model was tested at a scale ratio of 1:40 at ECN, France. A good agreement between the experimental results of the platform motions and the recalculations from the numerical code FAST was obtained, showing the validity of this experimental technique.

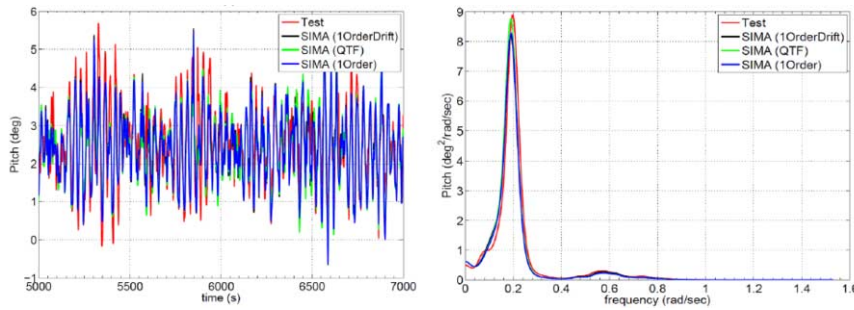

Figure 2.14: Comparison of the time series (left) and spectra (right) of pitch motions obtained by simulations (SIMA) and experiments (Test) (Uw=25m/s, Hs=5.9m, Tp=11.3s) (Karimirad et al., 2017)

Kanner (2015) developed a hybrid testing method, called the Multiple Integrated and Synchronized Turbines, to test a semi-submersible floater at 1:82 scale with two counter-rotating vertical-axis wind turbines (VAWTs), as shown in Figure 2.15. The two synchronized counter-rotating turbines can produce zero net yaw moment on the floater. The test was carried out at the UC Berkeley Physical-Model Testing Facility. The aerodynamic loads on two VAWTS were calculated using high-order, implicit, large-eddy simulation and applied through two pairs of spinning, controllable actuators (fans) in the model test. The developed time-domain numerical simulation tool is able to confirm some of the experimental findings, taking into account the decoupled properties of the slow-drift hydrodynamics and wind turbine aerodynamics.

Alternatively, hybrid testing methods are also developed for wind tunnel tests of floating wind turbines (Bayati et al., 2016; Giberti & Ferrari, 2015), in which the floater motions are imposed by a movable foundation and the wind field and the wind loads are generated physically. Such methods were developed in the wind tunnel at the Polytechnic University of Milan for the study about the effect of surge and pitch motions on the aerodynamics of the 1:75 scale DTU 10MW wind turbine using a 2DOF test rig (Bayati et al., 2016), as shown in Figure 2.15. The tests with platform surge and pitch motions at both a low and wave frequency and up to rated conditions were conducted. The results show hysteretic behaviours in the force-velocity plots, always of dissipative nature. They are now developing a 6DOF robotic platform for testing floating wind turbines (Bayati et al., 2014).

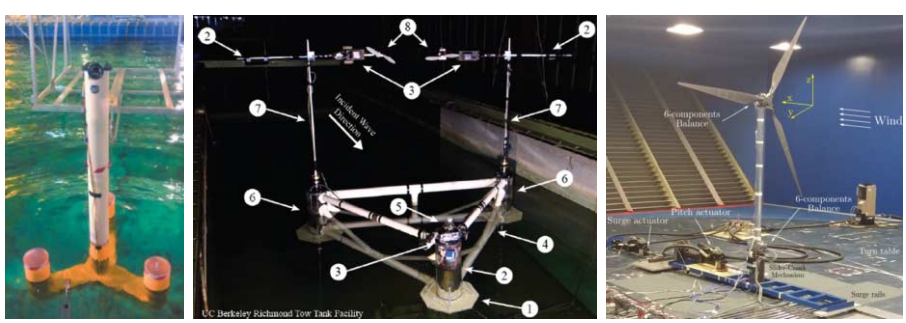

Figure 2.15: Other examples of hybrid testing of floating wind turbines (from left: semi-submersible wind turbine with a ducted fan (Azcona et al., 2014); counter-rotating vertical axis wind turbine with controllable fans (Kanner, 2015); wind tunnel testing with a movable foundation (Bayati et al., 2016))

2.3.2 Field testing

Bottom-fixed wind turbine technology is relatively mature. However, there is a need for testing of large-scale wind turbines and validation of the numerical codes for such turbines. There exists an extensive field measurement campaign (called RAVE) with research purposes at Alpha Ventus wind farm in Germany, see Muller & Cheng (2016), Muller et al. (2016), Lott & Cheng (2017).

Guzman & Cheng (2016) reported a comprehensive comparison of the measured and simulated structural responses of a tripod AD5-116 5MW wind turbine (NO.7 turbine in as shown Figure 2.16) considering 13 months of data. The bending moments in tower and at blade root were compared in detail. The numerical simulations were carried out in the coupled Flex5-Poseidon tool (Kaufer et al., 2009) using simulated (rather than measured) wind and wave conditions. However, in the simulations, similar turbulence intensity factor and significant wave height/spectral peak period for a given mean wind speed were considered and response statistics were compared, as shown in Figure 2.17. The 10-minute extreme values of the tower fore-aft bending moment, including both the mean and the ranges of predictions, agree very well with the measurements for different mean wind speed. Figure 2.17 also shows the comparison of the fatigue damage equivalent loads (DEL) of the blade flap-wise bending moment. The numerical tool predicts a good general trend, but less scatter of the blade responses for the mean wind speed close to the rated value.

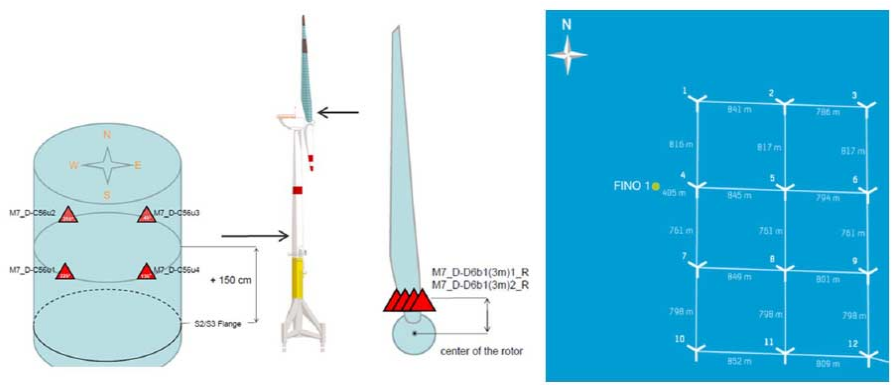

Figure 2.16: Illustration of the tripod wind turbine, its measurements and the Alpha Ventus wind farm configuration (Guzman & Cheng, 2016)

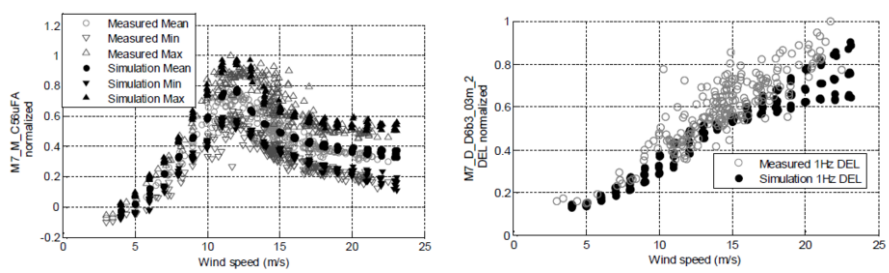

Figure 2.17: Comparison of the 10-minute extreme responses of the tower fore-aft bending moment (left) and the damage equivalent loads (DEL) of the blade flap-wise bending moment (right) (Guzman & Cheng, 2016)

As for floating wind turbines, there are quite a few prototypes that were tested and are under testing in Norway, Portugal, Japan and US. The WindFloat prototype with a 2MW Vestas

turbine was tested in Portugal since 2011 and decommissioned in 2016 (Principle Power, 2017). A complete lifecycle of development (from design, fabrication, installation, operation/maintenance and decommissioning) was successfully demonstrated. Similarly, the VolturnUS 1:8 prototype with 20kW turbine was tested in US for 18 months between 2013 and 2014 (Viselli et al., 2015).

As discussed in the last ISSC report (Gao et al., 2015), lack of publically-available full-scale field measurements was and remains a general problem for the research community in the area of offshore wind turbines and in particular, floating wind turbines. The subject of floating wind turbines attract a significant number of researchers in recent years to develop numerical codes and experimental techniques. There are very limited publications on validation of numerical simulations against field measurements, although several prototypes of floating wind turbines exist. This might be because most of these prototypes are developed by companies with the aim for commercialization. Besides the competition between the turbine manufacturers that already exist in the market for onshore and offshore bottom-fixed wind turbines, the floating wind turbine market could also become a very competitive market with regards to the foundation technology. In the ongoing OC5 benchmark study, the data from lab tests were used for validation of a variety of numerical codes and it is also planned to compare simulations against the measurement data from a bottom-fixed wind turbine farm. In the their future work, using the measurements from an existing prototype of floating wind turbines could be considered and would be beneficial for most of the code developers.

Nevertheless, validation of numerical simulations against field measurements were carried out for the Statoil Hywind Demo using a FAST model (Driscoll et al., 2016). The numerical simulations were carried out using reproduced wind speed time series from measurements and similar wave spectrum. The comparison shows that the wave-frequency motion responses for both low (Hs=1.4m) and moderate (Hs=4m) seas can be accurately predicted by the numerical model. However, the low-frequency roll responses and the yaw responses do not agree well with the measurements, indicating a need for a more advanced mooring line model (rather than a linear yaw stiffness model) and a model with short-crested waves.

2.4 Transport, installation, operation and maintenance

In order to reduce the cost of offshore wind farms, it is important to look at marine operations related to different phases of offshore project, including transport, installation, operation, maintenance and decommissioning. In view of the significant development plan, the offshore wind industry is an area where the ship and offshore technology community like ISSC should and can contribute. In particular, there is a need to develop purpose-built installation vessels, accommodation vessels, Service Operation Vessels (SOVs) and Crew Transfer Vessels (CTVs) (Turner, 2012). Moreover, the existing jack-up installation vessels have to be upgraded in terms of crane capacity and leg length in order to meet the market needs with increasing turbine size and water depth (MAKE Consulting, 2016). Since a commercial offshore wind farm normally consists of 50-100 turbines, logistics planning becomes very important for such installation and maintenance activities (Barlow et al., 2017; Vis & Ursavas, 2016; Dalgic et al., 2015). In this report, we will focus more on offshore wind installation and less on maintenance activities.

2.4.1 Transport and installation

Although tripod, jacket, GBS and even floating foundations have been developed and used to support wind turbines, bottom-fixed monopile wind turbines are still the majority in today's offshore wind farms. The transport and installation methods strongly depend on the type of foundations (Asgarpour, 2016). Monopile, tripod and jacket wind turbines are normally transported by barges and installed component-by-component at the offshore site. Large floating crane vessels have been used to install foundations, but wind turbine blades, nacelle and tow-

er are typically installed using jack-up vessels due to the high precision required in the mating operation of the blades into the hub, as shown in Figure 2.18 for one of the largest offshore wind farms in Europe under construction.

US installed their first offshore wind farm at the Block Island site in 2016 (Clean Technica, 2016), which consists of five 6MW wind turbines, as shown in Figure 2.18. Fred. Olsen Windcarrier did the offshore installation. The substructure foundation includes lower jacket and upper transition deck sections to reduce the weight of the assembly lifts, which was considered necessary to utilize the available assembly systems and vessels with limited lift capacity. ISO standards and design loads from IEC 61400-3 (2009) and API Recommend Practice 2A-WSD (2014) were employed with consideration of robustness levels of ultimate strength for Atlantic hurricane winds (Finucane & Hall, 2016).

The world's first small-scale farm of floating wind turbines was commissioned in Scotland in late 2017 based on the Hywind technology from Statoil, Norway. It consists of five 6MW Siemens turbines. Turbine blades, nacelles and towers are pre-assembled onshore before they are installed by one of the largest floating crane vessel, semi-submersible SAIPEM 7000, onto the spar floaters in the fjord in Norway, see Figure 2.18. Then, they are wet-towed to offshore Scotland and hooked up with mooring systems. A similar process using a large floating crane was adopted in the installation of the downwind 2MW hybrid spar wind turbine in 2013 in Japan (Utsunomiya et al., 2015). However, when developing commercial wind farms, the cost should be further reduced and new installation methods which rely less on expensive large crane vessels are preferred. In that respect, semi-submersible floating wind turbines have the advantage of being pre-assembled in one piece in the shipyard and towed to the offshore deployment site, as the WindFloat prototype project did (Principle Power, 2012). They also demonstrated the decommissioning process in 2016, disconnecting power cables/mooring lines as well as decommissioning the turbine at Sines quay side in Portugal (Principle Power, 2017; Roddier et al., 2017), see Figure 2.18.

Figure 2.18: Examples of offshore wind farms during installation (from left: Gemini Wind Farm in the Netherland, installed by Van Oord (Irving, 2017); Block Island Wind Farm in the US, installed by Fred. Olsen Windcarrier (Finucane & Hall, 2016); Statoil Hywind Wind Farm in Scotland, during assembly in Norway by SAIPEM 7000 (Statoil, 2017b); WindFloat prototype at Sines quay side in Portugal, under decommissioning (Roddier et al., 2017))

Different installation vessels were reviewed by Paterson et al. (2017), with focus on the vessels that performed the tasks in UK Offshore Wind Round 1 and Round 2, and Ahn et al. (2016), considering other vessels that were used in offshore wind farms in Europe. Paterson et al. (2017) also demonstrated a probabilistic simulation tool for optimal selection of vessel fleet, while Ahn et al. (2016) focused on the best installation method for a Korea offshore site.

One of the main challenges in the installation phase is to increase the weather window and to avoid any unexpected delays. This requires a good understanding of the performance of the installation vessels in waves. Therefore, numerical methods and models have been developed to estimate systems' dynamic responses during installation. Most of the studies focused on

static (Collu et al., 2014) or steady-state dynamic responses (Li et al., 2016), while in a few studies, the nonstationary features of the installation process are considered (Li et al., 2015). Li (2016) developed a numerical method for analyzing the dynamic responses of the monopile when it is lowered from the air into the water, considering the submergence-dependent hydrodynamic loads on the monopile and the vessel shielding effect. Regarding wind turbine blade installation, a numerical tool was developed by Zhao et al. (2017) to simulate the blade rigid-body motion responses in turbulent wind conditions using either jack-up or floating installation vessels.

There exist few model tests for complex marine operations in hydrodynamic labs and experimental techniques have not been extensively developed for assessment of the feasibility and safety of marine operations. The challenge is to scale both hydrodynamic loads and mechanical components and to simulate the actual operational phases involving transient hydrodynamic loads and structural responses. However, this is certainly an interesting area to develop and it will be very useful for validation of novel concepts for marine operations, for example installation of floating wind turbines (Hatledal et al., 2017).

For any marine operation, there exists one or multiple operational limits due to the safety requirements (e.g. personnel and property safety) which are often expressed as sea state limits. Most of wind turbine installation operations can be only performed in benign sea states (for example with Hs in order of 1-3 m), depending on vessels and tasks. Detailed information about the limiting environmental conditions for different construction vessels can be found in Table 2.2 (Ahn et al., 2017).

Such environmental limits should be established preferably using response-based criteria, but currently they are based on industrial experiences. A generic methodology for assessment of the operational limits and operability of marine operations was proposed (Guachamin-Acero et al., 2016; Guachamin-Acero, 2016). The basic idea is to estimate structural dynamic responses during operations in all possible sea states using numerical models and then backwards derive the limiting environmental conditions that will lead to the allowable response level. This methodology was applied to monopile foundation installation (Li et al., 2016) and transition piece installation (Guachamin-Acero et al., 2017a). A similar approach, called reliability-based decision support model, was developed by Gintautas et al. (2016), in which response statistics of the installation equipment were obtained based on simulations and used to estimate the weather windows in combination with the ensemble weather forecast model.

Table 2.2: Limiting environmental conditions for construction vessels (Ahn et al., 2017)

Vessel type	Operating equipment	Capacity	Transit condition		Operating condition	
			Speed (knots)	Wave height (Hs, m)	Wave height (Hs, m)	Wind speed (m/s)
WTIV	Jack up/down + crane	Crane capacity: 800–1500 ton	12	3.0	2.5	16
Jack-up barge	Jack up/down + crane	Crane capacity: 800 ton	4	2.5	1.65	16
Crane barge	Shear crane	Crane capacity: 3000 ton	4	1.5	1.0	10
Cargo barge	Stacking (without crane)	2000-5,000p	4	1.5	1.5	14
Tug boat	Towing	750 hp, 1000 p	13	2.5	1.0-1.65	14

One of the principles to reduce the installation cost is to reduce the number of operations (in particular crane operations) at the offshore site. Therefore, many novel installation methods or concepts were developed considering a pre-assembled rotor-nacelle-tower structure. Guacha-

min-Acero et al. (2017b) developed an installation concept for small crane vessels using the inverted pendulum principle in which the pre-assembled rotor, nacelle and tower can be installed via rotation through a rotating frame at the tower base. In the research centre SFI MOVE at NTNU, Hatledal et al. (2017) developed a catamaran installation vessel concept which can carry 3-4 pre-assembled rotor, nacelle and tower and install them on top of a monopile or a spar foundation through its onboard lifting mechanism. This is a similar concept as Ulstein's Windlifter concept (Ulstein, 2017).

Moreover, some foundation concepts, such as GBS (Esteban et al., 2015), allow the onsite installation with one completely pre-assembled structure. Zhang et al. (2016) developed a hybrid suction bucket foundation with seven compartments for offshore wind turbines. The sinking of the foundation with a complete wind turbine installed on it is realized by depressurizing the compartments and the verticality of the foundation is achieved by adjusting the pressures in different compartments. A model test at 1:10 scale was performed to demonstrate the feasibility of this technology.

2.4.2 Operation and maintenance

There is a wide range of topics related to offshore wind turbine operation and maintenance (O&M) of interest. However, in this report, we will only give a short discussion. It is suggested that the V.4 committee for the next term work more on this topic, probably together with the committees that deal with structural heath monitoring for marine structures in general since there are many common challenges.

Condition monitoring and structural heath monitoring of offshore wind turbine components (such as gearbox, blade, tower and foundation) has become a hot topic for research (Yang, 2016; Wymore et al., 2015; Romero et al., 2017; Mieloszyk & Ostachowicz, 2017). This is in line with the increased use of sensors, SCADA (Supervisory Control and Data Acquisition)-based and purpose-designed condition monitoring systems for commercial offshore wind farms. One of the main purposes of such system is to detect degradations or damages in wind turbine components in an early stage to prevent them from developing into component or system failures. Therefore, different condition monitoring techniques and signal processing methods have been used for fault detection in wind turbine components (Martinez-Luengo et al., 2016).

From marine operations point of view, the access systems for maintenance and repair are of concern. In particular, crew and equipment transfer are the most important operations for scheduled and emergency maintenance and repair work for offshore wind turbines. On one hand, increasing the reliability of wind turbine components is one of the crucial aspects for offshore wind projects. On the other hand, high accessibility in most of the sea conditions becomes very important to reduce the downtime caused by component failure and shutdown of the wind turbines. A review of the existing offshore wind access systems was carried out by Katsouris & Savenije (2017), including crew transfer vessels (CTVs) with a conventional method of access to the boat landing and recently developed service operation vessels (SOVs) equipped with motion compensated gangways. They also found that CTVs can typically provide access up to sea states of Hs of 1.5-2 m, while SOVs with motion compensation could be operated up to sea states of Hs of 3 m. In addition, helicopter support can be very beneficial due to fast response time and almost unlimited accessibility. Guanche et al. (2016) presented a methodology to assess limiting wave heights for safe personnel transfer between different service vessels and a floating wind turbine. The vessel and the floating wind turbine platform were modelled as a rigid, constrained multibody hydrodynamic model in the frequency domain.

Similar to installation, logistics planning for offshore wind farm operation and maintenance activities is also very important and many studies have been performed to optimize the fleet

selection for such activities at the wind farm level (Halvorsen-Weare et al., 2013; Sperstad et al., 2017). O&M simulation tools have been developed to (Katsouris & Savenije, 2017) estimate the maintenance cost for a selection of O&M fleet and the wind farm availability. Such tools are also used to find the most cost-effective O&M and logistics strategy. In particular, an advanced logistics planning tool was developed by Dalgic et al. (2015) using a time-domain Monte-Carlo simulation approach which takes into account environmental conditions, operability of transportation systems, component failure type and frequency, and simulation of repairs.

2.5 Design standards and guidelines

In the last ISSC report (Gao et al., 2015), the existing design standards and guidelines were discussed. In this report, the discussion will focus on the updates in recent years.

The IEC 61400 set of standards are the commonly used standards in the wind and offshore wind industry in particular in Europe. The current version of the IEC61400-3 (IEC, 2009) standard considers only bottom-fixed offshore wind turbines and a revision will be published in 2018. Accordingly, a technical specification of IEC 61400-3-2 for floating wind turbines will also be published in 2018.

Additional standards from API, ISO, and guidelines from classification societies such as DNV-GL, ABS, BV, are also considered essential to address key aspects in the development, deployment and operation of offshore wind projects.

These standards and guidelines address many key project aspects, including safety; site condition assessment; design evaluation of wind turbines, blades and support structures; manufacturing; transportation; installation, commissioning and certification; and operation. Sirnivas et al. (2014) made a thorough review of these standards and guidelines and assessed the major differences between them.

DNVGL-ST-0126 (DNV-GL, 2016) is a fully updated version of the standard for onshore and offshore wind turbine support structures, which was developed based on long experience in DNV-GL. This standard is applicable to bottom-fixed wind turbines and covers design of steel and concrete towers, gravity-based concrete foundations and steel foundations such as monopile, jacket structures and suction buckets. DNV-OS-J103 (2013) is an early version of the DNV-GL offshore standard for design of floating wind turbines. A new version of the standard, DNVGL-ST-0119, will be released during 2018. DNV-GL (2017a) is now running a JIP with focus on specifications for coupled analysis of floating wind turbines using numerical tools and experimental methods. The outcome of this JIP will be a Recommendation Practice, named DNVGL-RP-0286, Coupled Analysis of Floating Wind Turbines.

ABS published the revision of the Guides (ABS #176, 2015a; ABS #195, 2015b) in October, 2015. The two Guides provide the design, inspection, classification and certification requirements for bottom-fixed and floating offshore wind turbines. In particular, tropical cyclone conditions (such as hurricane and typhoon) are specified based on the measurements of tropical cyclone wind in the past 20 years. For bottom-fixed offshore wind turbines, a return period of 100 years was suggested for the design check. The Guidance Notes published in 2014 (ABS #206, 2014) provide suggested global performance analysis methodologies, modelling strategies and numerical simulation approaches for floating wind turbines.

Guidance Note NI 571 (2015), developed by BV, provides specific guidance and recommendations for the classification and certification of floating wind turbines. This Guidance Note is intended to cover floating platforms of different types (column-stabilized units, spar, TLP and barge) supporting single or multiple turbines with horizontal or vertical axis.

AWEA (American Wind Energy Association) published a recommended practice (AWEA, 2012) for bottom-fixed offshore wind turbines in the US waters (both state and federal), ad-

dressing all areas for offshore wind farm development, i.e. structural reliability, manufacturing, qualification testing, installation, construction, safety of equipment, operation and inspection, and decommissioning.

Up to now, although some guidelines exist, there still lacks detailed and specific rules or guidelines for offshore wind turbine transport, installation, operation & maintenance and decommissioning.

Most of the offshore wind turbines today are bottom-fixed wind turbines and they are installed mainly using jack-up vessels. LR (2014) developed a guidance note specific for offshore wind turbine installation vessels.

RenewableUK (2013) provided the second edition of Guidelines for the Selection and Operation of Jack-ups in the Marine Renewable Energy Industry in 2013. This guidance is intended to be relevant to all organizations contributing to the operation of jack-ups, but it is particularly relevant to jack-up owners'/operators' technical staff and crews responsible for the operation of jack-ups, and to project managers in the marine renewable energy industry.

A standard DNVGL-ST-0054 (2017) is published to provide general safety principles, requirements and guidance for offshore wind power plants during transport, installation and decommissioning operations.

GL Garrad Hassan (2013) developed the Guide to UK Offshore Wind Operations and Maintenance to meet the need for standardized technical and commercial practices for offshore wind operation and maintenance.

2.6 Comparative study of optimal offshore wind turbine support structure configurations in varying water depths

This study aims to compare the weight (as an indicator for cost) of different configurations of support structures with respect to their deployment in different water depths. It is mainly carried out by the ISSC committee member, Dr. Athanasios Kolios, and his group from Cranfield University in UK. Two types of support structures, i.e. monopile and jacket, are considered in this study and an optimisation algorithm has been applied in order to compare concepts on a fair basis.

The response of the structure (based on FE analysis) for each case study under given loads is obtained through validated parametric models that have been developed for each case. The monopile consists of two parts, i.e. 1) monopile substructure, which is submerged into the water; and 2) monopile foundation, which is embedded into the soil. The soil profile considered in this study consists of three layers of sandy soil with given properties. In this study, the monopile support structure is modelled using beam elements. The soil-structure interaction is taken into account by modelling the soil using distributed springs, of which stiffness is derived from the p-y method defined in API standard. The springs are applied with 1m intervals along the monopile foundation in order to achieve good accuracy. Additionally, the RNA (Rotor-Nacelle Assembly) is treated as a point mass on the tower top. In this study, the transition piece is ignored for simplification. The parametric FEA model for OWT monopile support structures is used to calculate the natural frequencies of the NREL 5MW OWT on the OC3 monopile (Passon, 2006). The modal frequency results from the FEA model are compared against the results reported in Jonkman & Bir (2010), showing good agreement, with a maximum relative difference (1.55%) observed at 1st SS model. Comparison of deflection also show good agreement with a maximum relative difference (5.31%) observed for deflection of monopile foundation on mudline. This confirms the validity of the present FEA model of OWT monopile support structures.

The jacket structure model consists of mud-braces as well as several levels of legs and X-braces. The number of levels depends on the water depth. The RNA (Rotor-Nacelle Assem-

bly) is treated as a point mass on the tower top, and the transition piece is taken into account as a point mass attaching to the tower bottom. For simplification, the soil is not considered, and the bottom of the jacket is assumed to be fixed at the mudline. The parametric FEA model for OWT jacket support structures is used to calculate the natural frequencies of the NREL 5MW OWT on the OC4 jacket. The results from the FEA model show good agreement with those from Damiani et al. (2013), with a maximum relative difference (3.04%) observed at 2nd SS and FA modes. Similarly to the monopile, a comparison of deflections show good agreement with the results reported, with a maximum relative difference (8.23%) observed for deflection at RNA under load case 2. This confirms the validity of the present FEA model of OWT jacket support structures.

According to DNV-OS-J101 (DNV, 2014), the loads on OWT support structures can be categorized into eight groups, i.e. 1) wind loads; 2) wave loads; 3) current loads; 4) hydrostatic pressure loads; 5) inertia loads; 6) sea ice loads; 7) loads due to marine growth; 8) loads due to exceptional events (e.g. earthquake, ship impact etc.). The wind, waves, current, hydrostatic pressure and inertia loads are considered in this study. Other loads associated with sea ice, marine growth and exceptional events are ignored. These effects may play a significant role for more detailed investigation or certain offshore locations; however, for the purpose of this generic study they are deemed negligible. In this study, both ultimate and fatigue load cases are considered. For the ultimate load case, the extreme sea condition (i.e. 50-year extreme wind condition combined with extreme significant wave height and extreme current velocity) represents a severe load and therefore is taken as a critical ultimate load case. For the fatigue load case, both wind and wave fatigue loads for the normal operation of OWTs are considered. Table 2.3 presents both extreme and normal sea condition considered in this study. The rotor aerodynamic loads are presented in Table 2.4 and are taken from LaNier (2005) for a typical 5MW wind turbine. The wave loads on monopile submerged in water are calculated using the Morison's formula. The current loads are taken into account by adding the current velocity to the wave particle velocity in the drag term of the Morison's formula.

Table 2.3 Sea conditions

Item	Values	
	Extreme sea condition	Normal sea condition
Wind speed [m/s]	59.5	10
Significant wave height [m]	8.40	1.00
Wave period [s]	10.50	5.55
Current speed [m/s]	1.42	-

Table 2.4 Rotor aerodynamic loads

Load case	Thrust [kN]	Bending moment [kN-m]	Torsion [kN-m]
Ultimate	781	38.567	7,876
Fatigue	197	3,687	3,483

The optimisation algorithm that has been selected is based on Genetic Algorithms, which is a search procedure based on genetics and natural selection mechanisms, in order to search for optimum solutions, as shown in Figure 2.19. In the GA, a population of candidate solutions (also called individuals) to an optimisation problem is evolved toward better solutions. The evolution generally begins with a population of randomly generated individuals. It is an iterative process, and the population in each iteration is called a generation. In each generation, the fitness of each individual in the population is assessed, and the fitness is generally the value of the objective function in the optimisation problem. The individuals having good fitness are stochastically selected from the population, and the genome of each individual is modified through mutation and crossover operators to form a new generation. The new generation of

individuals is then used in the next iteration of the algorithm. Generally, the algorithm terminates when either a satisfactory fitness level has been reached for the population, or a maximum number of generation has been produced. The objective function to be minimised for this problem is that of the total mass subject to a series of the criteria which include (i) a deflection constraint, (ii) a stress constraint for ultimate strength, (iii) fatigue constraint based on the SN curve approach, and (iv) buckling constraint and (v) frequency constraint.

The structural optimization model of OWT monopiles is applied to NREL 5MW OWT (Jonkman et al., 2009) on monopile support structures in seven water depths, ranging from 20m to 50m. The diameter of the monopile is assumed to be increased from 5.5m to 8.5m as water depth increase from 20m to 50m. The length of the monopile substructure is assumed identical to the length of the monopile foundation. The monopile foundation is designed with a uniform thickness to facilitate its installation. The monoopile substructure consists of several five-meter-length segments, and the number of segments depends on the water depth. The thickness of the monopile foundation and the thickness of each segment of the monopile substructure are taken as design variables, of which optimum values are determined using the design optimization model, which has been developed by combining the parametric FEA model and GA (genetic algorithm). The results from the optimization algorithm for the seven water depths for the monopile structure are depicted in Figure 2.20 (left plot).

The structural optimization model of OWT jacket support structure is applied to NREL 5MW OWT on jacket support structures in three water depths, i.e. 40m, 55m and 75m. For all cases, the angle between the two adjacent braces of X-braces is 110 deg, and the angle between the legs and X-braces is 37 deg. The legs are oriented with an angle of 2 deg with respect to the vertical axis. The diameter of legs is assumed to be 1.2m, and the diameter of both X-braces and mud-braces is assumed to be 0.8m. In this study, the thickness of X-braces and the thicknesses of legs at each level are taken as design variables, of which values are determined using the design optimization model. The thickness of mud-braces is assumed to be identical to that of X-braces. The results from the optimization algorithm for the three water depths for the jacket structure are depicted in Figure 2.20 (right plot).

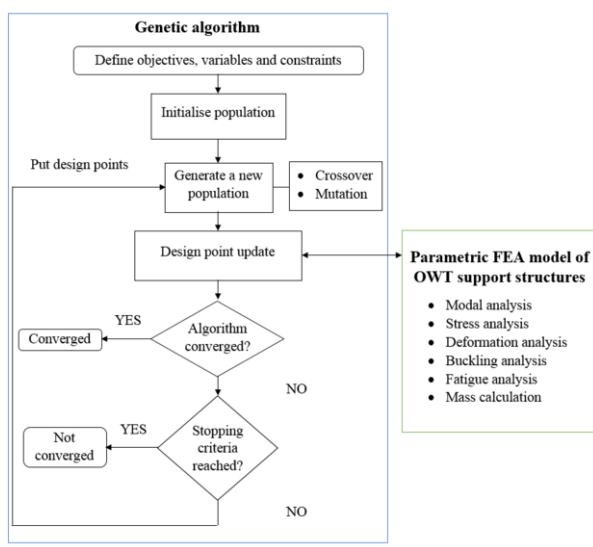

Figure 2.19: Genetic Algorithm for optimization of offshore wind turbine support structures

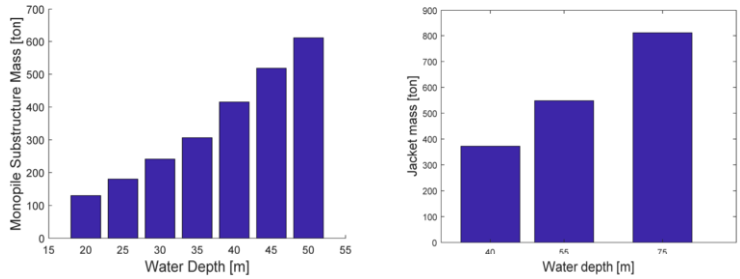

Figure 2.20: Mass of the support structures as function of water depth obtained from the optimization analysis (left: monopile; right: jacket)

3. WAVE ENERGY CONVERTERS

As compared to the offshore wind industry, there are no commercial wave energy converters yet. Extensive research has been carried out and led to the development of many WEC prototypes that were tested at sea. Most of these prototypes have a relatively small rated power (typically less than 300kW-500kW for a single device at small-scale, not full-scale) and have not been tested for long times (Astariz & Iglesias, 2015). However, we expect to see more WEC prototypes with increasing sizes, which may lead to a total installed capacity of as much as 26MW in Europe by 2018 (Magagna & Uihlein, 2015). We will mainly review the recent work on wave energy devices regarding numerical modelling and analysis with focus on nonlinear hydrodynamic effects, CFD analysis, PTO and mooring systems, as well as model testing of single WEC devices or arrays. The initial results from the IEA OES benchmark study are summarized at the end of this section. The main categories of wave energy conversion technologies considered here are: point absorbers, Oscillating Water Column (OWC) and overtopping devices.

3.1 Numerical modelling and analysis

Numerical modelling and analysis are vital for WEC design, validation and optimization. Mathematical models are essential for assessing power production, device motions, model-based control strategies and survivability. As for other offshore structures, two main modes of operation are commonly assessed: power production mode and survival mode. However, in contrast to traditional offshore engineering applications, WECs are designed to maximise power absorption with large motions, which are, therefore, intrinsic to most normal operations. Thus, nonlinear dynamics may appear, not only in survival mode, but also during power production mode. Accordingly, linear approaches originally created for traditional offshore engineering applications, may not be accurate to reproduce the behaviour of WECs (Penalba et al., 2017).

In a recent review of nonlinear numerical approaches applied to WEC behavior modelling, Penalba et al. (2017) suggest a modelling validity discretization in terms of three regions with increasing velocities, motion amplitudes and forces: 1) Linear region; 2) Nonlinear region; 3) Highly nonlinear region. 1) and 2) refer to power production mode, whereas 3) is valid for the survival mode.

Nonlinearities arise already in the wave modelling, particularly when assessing WECs in survival mode. However, Ransley et al. (2017b) reminds us that a fully nonlinear theoretical model of extreme waves does not yet exist and therefore use in their work a ‘NewWave’ linear formulation for simulating focused waves impacts on generic WEC hull forms, resorting to a fully nonlinear CFD tool.

Nonlinearities also arise in the PTO (Section 3.1.2), moorings (Section 3.1.3), and in the hydrodynamics of the fluid interaction with the WEC devices themselves. WEC control model-

ling is often coupled with the PTO system and is therefore not subject to extensive review in this section. However, recently published predictive control techniques which have an intrinsic hydrodynamic numerical model are worth mentioning. Such is the case of the study on the near-optimal control of a WEC with a deterministic-model driven incident wave prediction technique by Korde (2015). Another example is the straightforward process of assessing the impact of latching control technologies on the performance of a WEC presented by Sheng et al. (2015b). In their approach, a 'time-out' method is applied, where the time at which the system is latched is removed and then an 'equivalent' motion of the device is transformed to an approximately linear solution.

In this section, the numerical modelling and analysis of the WEC hydrodynamic loads and induced motion, PTO and mooring responses will be discussed with focus on nonlinear analysis methods.

3.1.1 Load and motion response analysis

Nonlinear hydrodynamic analysis of WECs

Approaches to solve the nonlinear hydrodynamics of the fluid interaction with the WEC bodies are addressed in what follows.

Froude-Krylov forces become nonlinear as the relative motion of the devices increases. Occurrence of parametrically excited motions can then arise, which may have drastic effects if damping is not sufficient. Furthermore, when amplitudes increase, so will the nonlinear nature of the drag forces. In this respect, Tarrant and Meskell (2016) presented an investigation on parametrically excited motions of point absorbers in regular waves, where a weakly nonlinear method was used to assess the instability regions in the roll and pitch modes of a 'WaveBob' model. Nonlinear drag was accounted for by a quadratic (in velocity) relationship, similar to the Morison's formula.

Sloshing is also an important source of nonlinearities. These, however, are limited to OWC devices or other WECs which include internal fluid motion. Elhanafi (2016) studied the wave loads on a fixed offshore OWC using 2D and 3D CFD models based on RANS-VOF. Results showed that under high frequency waves, the chamber's free surface motion is no longer flat and nonlinear effects as well as water sloshing increase, influencing the resultant forces. Furthermore, from 108 test cases in total, it was concluded that there are non-negligible differences between 2-D and 3-D computations, and between different models of the action of the PTO in an OWC.

Device slamming on the free surface, as well as wave slamming is a highly nonlinear phenomenon, very common in WECs. Of particular interest is the review on the phenomenon by Saincher and Banerjee (2016), who, among several other important conclusions, conclude that viscous effects arising from breaking-induced turbulence would increase the coefficient of radiation damping on the WEC motion equations, and thus lead to damped oscillations of the WEC. This would induce nonlinearity in the system response even in a regular wave field. Paradoxically, this additional damping could actually be beneficial if the turbulence generation is consistent and occurs for a sufficiently long duration, as an over-damped (point absorber) WEC would respond to a wider range of frequencies compared to an optimally damped WEC.

Approaches to include nonlinearities in the models can be more or less sophisticated, where increased complexity and accuracy always comes with increasing computational demand. In general, the level classification by Hirdaris et al. (2014) for more general floaters regarding numerical methods is valid also for WECs: 1) Linear; 2) Froude-Krylov nonlinear; 3) Body nonlinear; 4) Body exact - weak scatter; 5) Fully nonlinear - smooth waves; 6) Fully nonlinear.

Yet another way to include nonlinearities is through system identification models or related procedures. Ringwood et al. (2015) examined the range of tests available in a numerical wave tank from which linear and nonlinear dynamic models can be derived, from a system identification perspective. Davidson et al. (2016) proposed the use of discrete-time nonlinear autoregressive with exogenous input (NARX) models, as an alternative to continuous-time models of WEC behavior, with techniques of model identification being also presented and applied to a case study. Also related is the work by Spanos et al. (2016) who proposed a statistical linearization technique for conducting expeditiously random vibration analyses of single-point harvesters. The technique is developed by relying on the determination of a surrogate linear system identified by minimizing the mean square error between the linear system and the nonlinear one.

Unfortunately, at this point only a few WECs have been deployed at full scale and no, or very limited, data is publically available from these deployments that could be used to provide validation of a numerical model from system identification (Folley, 2016).

On the other hand, potential flow based linear methods are still commonly used as a standard tool - Folley (2016) estimates that these comprise approx. 90% of WEC hydrodynamic modelling. In addition, analytical methods are also used in initial estimates of WEC performance, particularly in assessing their main design characteristics, resorting to more or less sophisticated optimization algorithms.

Analytical or theoretical formulations are device specific. Some are formulated from first principles, whose derivation easily allows adaption to other designs at some point. Such is the exposition made by Stansby et al. (2015a), who studied a three-float broad-band resonant line absorber with surge for wave energy conversion. Other formulations address not so common WEC types with the originality or complexity of their derivation being, therefore, intrinsic. Examples of these are the study on the performance of a rigid open-ended pipe serving as an artificial upwelling pump, by Fan et al. (2016), and the prediction of ocean wave harvesting, with a piezoelectric coupled buoy structure by Wu et al. (2015). Also worth mentioning is the analysis of a cycloidal WEC performance from its radiated waves using a very simplified, yet experimentally validated, analytic formulation, by Siegel (2015), and Noad & Porter (2017), who aim at providing a more general analytic formulation to assess the performance of articulated raft WECs, avoiding its validity to very specific existing designs of this type.

The control strategy is becoming one of the key research topics for wave energy. In fact, a good control can improve the device efficiency, possibly more than doubling the average annual harvested power. For this reason, new control strategies are continuously introduced (Wilson et al., 2016).

However, control strategies rely on a model of the WEC behavior, and almost all of them are based on linear approximation of the motions. As described in Giorgi & Ringwood (2016), this may lead far from the optimum solution and in fact, nonlinearities are amplified by the control, with increased amplitude of motion of the WEC or with abrupt forces applied to it.

CFD analysis and validation

In Giorgi & Ringwood (2016), a 2D simulation of a cylindrical device in waves was run with OpenFoam (Weller et al., 1998) to optimize the control strategy. The authors found that the actual optimum is obtained with a smaller latching period than that for the linear simulation.

However, running 3D simulations of wave energy devices can be very time consuming. Bhinder et al. (2015) shows the differences in the results and computational time for a CFD calculation (with FLOW-3D) and a linear BEM solution with ANSYS AQWA of a pitching wave energy converter, as compared to the experimental data. Both solutions predict well the body motion, even though the CFD solution could take up to 3 days to run, while the linear one

takes only 8 minutes. The main difference in the solution is the higher amplitude of oscillation of the BEM that could be avoided by including a model of viscous effects, for example obtaining a damping coefficient from a free decay analysis.

In a thorough review of the computational methods by Penalba et al. (2017), they recognize that CFD calculations are necessary in some cases, for example the analysis of survival mode situations. In other cases, where the high fidelity can be sacrificed for a fast solution, it is possible to model the nonlinear effects by conducting a series of representative tests, selecting the representative data of the 'system', defining the fitting criteria, and identifying the system parameters.

Recent publications comparing numerical and experimental results include Penalba et al. (2017), Bhinder et al. (2017), Ransley et al. (2017a) and Ransley et al. (2017b). The CFD calculations here have been done using several solvers, namely: FLOW-3D, OpenFoam, STAR-CCM+. Most of these solvers have already been validated for a wide range of fluid flows, so, as long as an adequate mesh is used, their solutions tend to compare well with experimental data. Using CFD simulations for operational conditions can introduce significant numerical viscosity (see Penalba et al., 2017) and a poor approximation of the free surface (see Bhinder et al., 2017) or of the vorticity region (see Ransley et al., 2017b), if the mesh is too coarse. This makes the CFD calculation less appealing than linear or weakly nonlinear potential flow solutions, which are much less computationally demanding. CFD simulations are, however, critical to the study of survivability conditions (for example see Ransley et al., 2017b). In that case, small discrepancies with experimental data do not jeopardize the reliability of the fully nonlinear fluid dynamics solver in terms of free-surface behavior around structures, pressure on the device, motion of floating WEC and the loading in mooring lines.

3.1.2 Power take-off analysis

Numerical models

Xu et al. (2016) studied experimentally and theoretically the wave power extraction of a cylindrical oscillating water column (OWC) device with a quadratic power take-off (PTO). In numerical simulations, the quadratic PTO model was linearized based on the Lorenz's principle of equivalent work. The developed model adequately predicted the effects of wave length and wave height on capture width ratio. Additionally, a semi-analytical model based on the work done by the drag force is able to reasonably predict the variation of the viscous loss with wave period.

Weia et al. (2017) developed a numerical model in order to investigate the adaptability of the multi-pump multi-piston power take-off system of a novel WEC. The proposed model takes into account the diffraction and radiation effects as well as the inclusion of multiple degrees of freedom for the floater elements. The model was validated by comparing the dynamics of the floater and pistons with experimental results.

Kamath et al. (2015) used CFD to simulate an OWC in a 2D numerical wave tank. Darcy's law for flow through porous media was used to model the PTO damping on the device chamber. The model was validated by comparing the chamber pressure, variation of the free surface inside the chamber and the vertical velocity of the free surface with the experimental data. The PTO damping has a large influence on the hydrodynamics of the OWC, so the PTO damping can be used to attain the maximum possible hydrodynamic efficiency (for a given wavelength of the incident waves).

Liu et al. (2017) proposed a combined hydrodynamic and hydraulic PTO unit model in order to investigate the performance of the two-raft-type WEC. It was found that the time histories of the hydraulic PTO force resembled square waves. Thus, in regular waves, the hydraulic

PTO generally has a higher peak power capture width ratio than that obtained by using a linear PTO unit. However, this advantage was not found for irregular waves.

Nielsen et al. (2015) considered a gyroscopic PTO within a point absorber which consists of a float rigidly connected to a lever (where the other end of the lever is supported by a hinge). This type of WEC may have subharmonic or even chaotic response under harmonic wave excitation. However, when synchronization of the angular frequency of the ring to the angular frequency of the wave loading takes place, the response of the float becomes almost harmonic. This means that the generated electric power becomes almost constant in time so additional power electronics is unnecessary. The study also provides the stability conditions for the synchronized motion.

Shi et al. (2016) presented a theoretical analysis on the power take-off of a heaving buoy WEC. The governing equations were developed considering hydraulic damping of the PTO as well as the analytic solutions to describe the motion and maximum power output. Displacements and average output power of the buoy with different values of damping and inertia coefficients are presented.

Energy efficiency

Lopez et al. (2017) investigated the performance of the CECO wave energy converter including its wave energy conversion stages and the influence of the PTO system. The performance of CECO was simulated in the time domain with a BEM code. The numerical model was calibrated with the results obtained in the previous wave basin experiments. For irregular wave conditions, CECO can absorb more than 30% of the incident wave power and transmit to the electric generator up to 18% of the incident wave power.

Liermann et al. (2016) investigated the energy efficiency of a pneumatic PTO for small-scale, low cost, portable wave energy converter. Energy losses were found from: the pneumatic motor, the generator, the air preparation unit, the pumping cylinder and the accumulator.

Hansen and Pedersen (2016) presented a method for determining the optimal configuration of a discrete fluid power force system for the PTO system. The number of discrete forces and the level of these are varied within the observed configuration. The multi-chamber cylinder, the number of pressure lines and the value of the pressure in the common pressure lines were determined based on time series simulation.

Schmitt et al. (2016) presented an optimization of the PTO for an oscillating wave surge converter (OWSC). A novel method to determine the instantaneous wave excitation of an OWSC was developed based on RANS CFD simulations. Results for two regular waves were presented. Additionally, the method was used to find the optimum damping settings for an OWSC.

Negative springs is a hot topic for wave energy conversion. The reason for this is that most practical wave energy converters have relatively large restoring coefficients, which lead to large resonance frequencies and a mismatch with the wave conditions at the deployment site. Application of a negative spring could reduce the device restoring coefficient so to reduce its resonance frequency to better match the wave conditions and increase the wave energy production. The physical implementation of a negative spring in a wave energy converter may use hydraulic actuators. Todalshaug et al. (2016) have shown that it is possible to implement a system such that a negative spring could automatically be implemented, and the experimental results show an increase of more than 300% in the extracted wave energy compared to a conventional wave energy converter.

Another example of applying a negative spring in a wave energy converter has been implemented in an oscillating water column (OWC) using so called Hydrodynamic Negative Spring (HNS) (Gradowski et al., 2017). Accordingly, when the device moves downward, due to the

expanded air chamber (see Figure 3.1, left), less seawater is displaced by the floater. This reduces the buoyancy force pushing it back up, increasing its time spent below the mean water level. When the floater moves upward, the stored seawater in the expanded air chamber is returned to the sea, displacing an increased volume of seawater (see the right plot in Figure 3.1). This special design of an expanded air chamber in the spar OWC could increase the buoyancy force pushing up on the floater, and prolong its upward oscillation, that is, the resonance period of the device can be increased for a better match to the target waves.

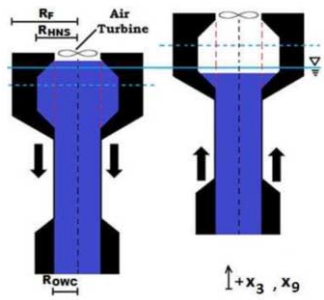

Figure 3.1: Negative spring implementation in a spar OWC (Gradowski et al., 2017)

3.1.3 Mooring analysis

Effects of mooring systems on WEC operability and survivability

Accurate assessment of the mooring lines is fundamental both in survivability conditions and in normal operating conditions, especially when the mooring is part of the energy harvesting process. The importance of the interconnection between the device motion and the mooring line was shown in Hann et al. (2015). There, the response to extreme waves of a single taut moored floating point absorber was measured when mooring lines purposely designed to generate a snatch load where in place. The extreme waves were generated by focused wave groups. It was found that for a dynamically responding floating body, the mooring loads are dependent on the displacement history, thus a single focused wave alone cannot be used to obtain an accurate assessment of extreme mooring loads.

Another example of the of strong interconnection among the different parts of a WEC device can be found in Fonseca et al. (2016), where an oscillating water column spar-buoy WEC was experimentally investigated. It was noticed that the closure of a stop valve (in order to protect the WEC turbine) may reduce the turbine-induced damping effect and cause amplification of the WEC movements. Consequently, in the more energetic sea states this might aggravate the loads on the mooring system and ultimately compromise the survival of the WEC system.

More general work by Paredes et al. (2016) shows how a better choice of mooring system can affect power production, displacements and extreme tensions.

A detailed validation of the numerical model of a wave energy mooring system against the tank test results was described by Harnois et al. (2015). A compliant three leg catenary mooring system using nylon ropes was investigated. Static, quasi-static, decay, regular and irregular wave tests were conducted. After the calibration of several hydrodynamic parameters, the numerical model demonstrated good agreement with the experiment. In addition, comparisons with the field test were conducted and large differences with numerical results were found, mainly because of uncertainties in the anchor position.

Yang et al. (2016b) investigated the effect of the superimposed wave-frequency random motion on the low-frequency mooring line damping through time domain simulations. Moreover, the random motions of the vessel were represented by an equivalent sinusoidal motion in or-

der to compare the effect of the superimposed sinusoidal motion and random motion. It was found that the response amplitude operator plays a dominant role in determining the amplification factor of the mooring line damping. The results also indicated that the effect of superimposed random motion is small as compared with the superimposed equivalent sinusoidal motion.

Palm et al. (2016) presented a fully coupled CFD mooring analysis of moored floating objects. A two-phase Navier-Stokes (VOF-RANS) model was coupled with a high-order finite element model of mooring cables. This study was made without the presence of a PTO system. An excellent match between the experimental and the numerical results for the surge decay test was found. Moreover, the model is able to capture the non-linear wave height dependence of the response amplitude operators seen in the experiments.

Fatigue assessment

A comparison of the simulation procedures for the fatigue analysis of WEC moorings was conducted by Yang et. al. (2016a). A floating cylindrical WEC with four spread mooring lines was chosen for the case studies. The dynamics of the WECs were simulated using both coupled and de-coupled models in the time-domain. The fatigue damage was calculated using the stress-based approach and the rain-flow counting method. It was established that the coupled and de-coupled simulation procedures generate different fatigue results for the studied cases under moderate wave conditions. Since the CPU times are about the same for the two simulation procedures, the coupled simulation procedure is considered as the better option for initial fatigue design assessment. Two different numerical implementations of the cable dynamics were considered and it was found that they have significant impact on final fatigue results.

The impact of biofouling on WEC systems with respect to energy absorption and fatigue lives of the cables and moorings was investigated by Yang et al. (2017). Coupled response analyses were conducted including hydrodynamic and structural response. The biofouling was modelled as an increase in the submerged weight and drag coefficients of the moorings and cables. The results showed that the biofouling can reduce the total power absorption by up to 10% for a WEC system which has been deployed for 25 years. Additionally, the fatigue life of the mooring lines decreased by approximately 20%.

Parametric studies and optimization

Optimization of a three-tether submerged point absorber wave energy converter was conducted by Sergiienko et al. (2016). The mooring configuration allows for the extraction of power from surge, heave and pitch motions where the relative contribution from each motion is different and depends on the inclination angle of the mooring lines. Two generic buoy shapes were considered, a sphere and a vertical cylinder. Optimization of the inclination angle was conducted through a frequency domain analysis. For the sphere, the optimal configuration was one where the tethers are orthogonal to each other. For the cylinder, an optimal angle between the tethers depends on the ratio between the cylinder height and diameter.

Wang et al. (2016b) studied a coaxial-cylinder WEC system consisting of a floating vertical inner cylinder and an annular outer cylinder. The study investigated the influence of the mooring line stiffness on the performance of the WEC system. The limiting cases of zero and infinite mooring line stiffness were also examined. It was concluded that the limiting cases can be viable, depending on the installation site depth, and that a poor choice of stiffness can eliminate the relative heave motion between the inner and the outer cylinders and lead to very low power extraction.

Novel concepts

A novel mooring tether was developed by Thies et al. (2014). The mooring tether combines soft elastomeric and stiff thermoplastic material components within a single assembly. Elastic

response through the elastomeric component is intended for operational conditions. Stiff, non-linear response, is achieved by the thermoplastic component to withstand higher loads during storm conditions. The point of transition from the elastic to the compressive element can be designed for a particular application. Fatigue and creep analysis showed that a lifetime of 5 to 10 years is feasible.

Luxmoore et al. (2016) presented the Intelligent Active Mooring System (IAMS). The main intention was to minimize extreme and fatigue loading in mooring lines through a load–extension curve that is variable during operation and can be adjusted to the prevailing environmental conditions. The IAMS design is based on a hollow braided wire rope. A flexible water filled bladder is set inside the hollow braid to resist reductions in the braid diameter, during rope extension, through controlled hydraulic pressure. An analytical model of IAMS was developed and validated against physical semi-static tests. Next, numerical validations were performed where a conventional mooring line is replaced by an IAMS. Fully dynamic simulations with real environmental data showed that the IAMS device can provide a significant reduction in the line tensions. Moreover, active control of IAMS can be used for tuning the mooring system to enhance the motions of a typical small WEC.

3.2 Physical testing

Physical testing is very important for verifying new concepts, validating numerical tools, and identifying technical problems and phenomena that were not fully understood or not revealed by analytical or numerical assessment. In this section, we will review some recent work on model testing and field testing of wave energy converters.

3.2.1 Laboratory testing and validation of numerical tools

Model testing of wave energy converters in hydrodynamic labs is performed mainly to verify new concepts in the early development stage with respect to the power absorption performance, and to validate numerical models for both operational and survival conditions. In 2014, the International Towing Tank Conference (ITTC) issued guidelines for wave energy device experiments (ITTC, 2014). It advises to use test facilities for devices with Technology Readiness Level (TRL) from 1 to 6, that is from the validation of concept to the sub-system and system validation in laboratories and/or simulated operational environments. According to the ITTC, for a higher TRL, tests should be carried out at large or full-scale.

The ITTC guidelines also highlight that even though towing tanks (suitable for long-crested waves), ocean basins (for both long- and short-crested waves) and ocean basins with wave and current facilities present a well controlled environment, a severe limit to their use is due to both wave heights and run durations for the large scale models required by WEC testing. In fact, it recommends that the corresponding duration of runs in full scale should be of 30 minutes in irregular waves for statistical validation and of 3 hours for the survivability tests. Both the physical limit of the maximum wave height generated by the wave makers and the need to minimize the build-up of reflected waves and to preserve the quality of the wave field, can severely limit the scale factor that is chosen for the model. In the end, however, it is necessary to compromise with the limits of the laboratories and the need for certain scale factors by taking into account the contamination from facility induced uncertainties. For example, in O'Boyle et al. (2017), where it was not possible to fully remove all tank contamination, the effect of WEC arrays on the wave field was studied by mapping the baseline variations in wave climate in the basin without any models installed. This has allowed the identification of the wave disturbance pattern and of its dependence on the array layout, on the wavelength to device spacing ratio, and on the applied PTO damping. In Costello et al. (2014), the uncertainty in the wave generated by the wave maker has been taken into account in the evaluation of the performance of a Model Predictive Control (MPC) strategy. The new strategy was applied to the study of a 1:20 scale model for the WaveStar machine in irregular sea, with wave

spectra representative of real-life conditions. The results sought to demonstrate that the estimated wave forces and the measured ones were close, and that this has allowed the maximization of the extracted power, disregarding the effects of the possible errors in the wave generation.

More importantly, the ITTC guidelines stressed that, whatever PTO model is used, a suitable characterization of the damping system should be carried out before the installation in the model. This should be done together with identifying the 'uncertainties associated with the reciprocating nature of many wave energy devices/PTOs', because the overall behavior may not be directly comparable with the individual behavior of single components under steady-state conditions.

Testing of power take-off (PTO) components

In a small-scale model test, it is important but difficult to design a representative power take-off (PTO) system corresponding to the full-scale concept. A PTO system is often simplified as a Coulomb or linear damper, an orifice load and sometimes an active control system in the lab tests. More details can be found in the 'Handbook of Ocean Wave Energy', edited by Pecher & Kofoed (2017).

An orifice plate is often used in the model test to represent the PTO (air turbines) for OWC devices. Fleming & Macfarlane (2017a) suggested to use separate flow coefficients for air inflow and outflow of an orifice to better estimate the air volume flux and therefore the power absorption. It also outlined a method to use the pressure measurements rather than the wave elevation data to estimate the air volume flux. In their second paper (Fleming & Macfarlane, 2017b), the detailed flow field around a 1:40 OWC model was revealed and assessed based on 2D PIV measurements.

Experimental and numerical studies (Colicchio et al., 2017) were carried out for a bottom-fixed OWC concept WaveSax at CNR-INSEAN, Italy. A 1:5 scale model equipped with an immersed Wells turbine was tested. In particular, the power performance of the three-blade, four-blade and five-blade turbines with angular speed control was studied in detail. The comparison between the numerical and experimental results indicates that the simplified porous disk is sufficiently accurate to model the Wells turbine.

Up to now, real-time hybrid testing techniques have not been used for testing WECs. In a hybrid test, parts of the system and the related dynamics are physically scaled and modelled in the lab, while the remaining parts and the related physics are numerically simulated and applied via actuators. In the chapter on offshore wind turbines, this technique has been discussed for testing of floating wind turbines (Chabaud, 2016). A similar technique might be applicable to represent PTO systems and loads in a model test for WECs. In an opposite way, when testing the PTO performance, the PTO loads might be obtained from a numerical WEC model and applied in the actual test. This was done by Li et al. (2017) for a PTO system of a point absorber with an electromagnetic generator and a mechanical motion rectifier (MMR) in a dry test. The MMR was used to convert bi-directional rotation into unidirectional rotation to improve the efficiency.

Unfortunately some errors in the PTO characterization and scaling have been noted in several cases, as highlighted in Falcao & Henriques (2014) for the correct scaling of the immersed part and the air chamber of OWCs. In particular, if Froude scaling applies to the immersed part, the air chamber either has the same scale factor, but the air inside it (and around it) has a reduced atmospheric pressure or the atmospheric pressure is kept unaltered and the size of the air chamber is scaled with a ratio that depends on the polytrophic behavior of the air. It is also noted that 'in many published papers reporting OWC model testing these similarity rules were simply ignored' with substantial errors in the prediction of the extracted power in full scale.

Testing of a single device

- ***Power performance tests***

When developing new WEC concepts, lab tests, in addition to numerical studies, are normally performed to verify the concepts with focus on power performance characterization.

At the University of Manchester, a three-body WEC (called M4) was developed and tested in their wave tank. The concept consists of a small bow float, a medium mid float and a large stern float in the direction of wave propagation. The bow and mid floats are rigidly connected, while the stern float is connected to the hinge point above the mid float, where a hydraulic PTO system is placed. This concept is shown by an experimental study at a scale ratio of 1:40 to have a high energy capture width ratio (Stansby et al., 2015b). A time-domain model based on the linear diffraction theory has been developed (Sun et al., 2017) and the comparison against the experimental results indicates an excellent prediction of relative rotation of the floats and beam bending moment and a slight over-prediction of power capture in unidirectional waves. In another study (Stansby et al., 2017), the power performance of multi-body configurations (from 1-1-1, 1-2-1, to 1-3-3, 1-3-4) are numerically studied and compared for four different offshore sites. Here, the number of buoys in the first, second and third rows of the system along the wave propagation direction was indicated, respectively. For example, the configuration 1-1-1 is shown in Figure 3.2. The capture width ratio increases significantly from the three-body system to the eight-body system.

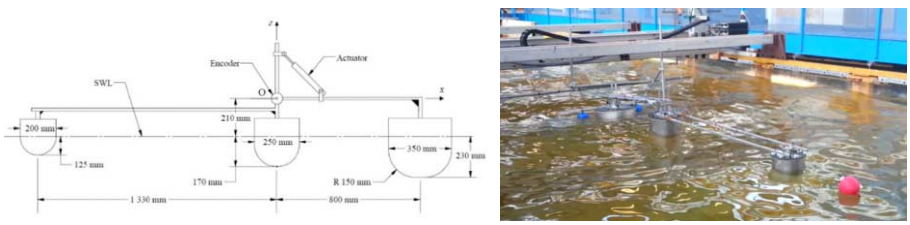

Figure 3.2: The three-body WEC concept M4 (Stansby et al., 2017)

A heaving-buoy concept (as shown in Figure 3.3) was developed by CorPower Ocean (Todalshaug et al., 2016) and tested at ECN in France, at a scale ratio of 1:16. A novel pneumatic solution (WaveSpring) for inherent phase control (that can provide a negative spring effect on heave motions), was developed and shown in the test to increase the absorbed energy by a factor of three as compared to a pure linear damper. On the other hand, the dynamic forces in the conversion machinery have the same magnitude as the operations without the negative spring module, as shown in Figure 3.3. Moreover, the WaveSpring unit can be tuned to give both resonant and broad-banded responses for operational conditions, while it can be detuned to reduce the responses in high-energy sea states.

Regarding OWCs, an experimental study (Vyzikas et al., 2017) on four bottom-fixed OWCs was performed with a scale ratio of 1:13, mainly to study the geometric effect on the power efficiency. They include a conventional OWC in a vertical seawall with a horizontal slit opening at the bottom, a conventional OWC combined with a submerged slope in the front representing part of a real breakwater, an improved design of the U-shape by Boccotti (2007a, 2007b), and the improved U-shape OWC combined with a submerged slope. Tests in regular and irregular waves from this study further confirmed the better power performance of the U-shape design as compared to the conventional one. Adding a submerged slope will also increase the power capture of the OWC.

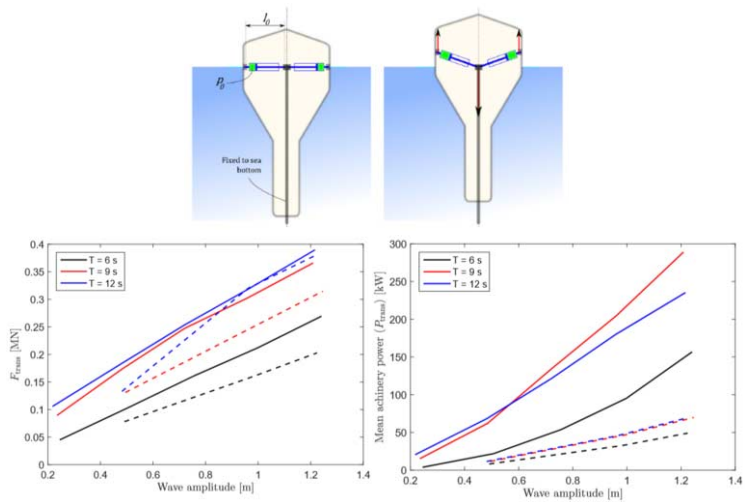

Figure 3.3: The heaving-buoy WEC concept (top) developed by CorPower Ocean and the dynamic force amplitude in the conversion machinery and the average absorbed power for regular wave conditions (Solid line: results with WaveSpring; dash lines: results without WaveSpring.) (Todalshaug et al., 2016)

- ***Numerical model validation tests***

Traditionally, numerical methods based on linear potential theory are the main tools to study the dynamic behaviour of WECs in operational and survival conditions. In recent years, CFD analyses have been more often applied and experimental results are used to validate CFD calculations. CFD analysis is more useful when nonlinear wave loads and responses become important.

A wave tank testing for the 1:33 scale model of a flap-type Floating Oscillating Surge Wave Energy Converter (FOSWEC) was performed at the Oregon State University's Directional Wave Basin (Bosma et al., 2016; Ruehl et al., 2016), as shown in Figure 3.4. The test was mainly to generate a large database for validation of the numerical tool WEC-Sim, developed by Sandia National Laboratories and the National Renewable Energy Laboratory (NREL). Up to now, a preliminary validation study was performed on motion decay results. A numerical model taking into account the nonlinear hydrostatic and hydrodynamic loads seems to agree much better with the experimental results as compared to the linear model.

Figure 3.4: The 1:33 scale model of the FOSWEC concept (Ruehl et al., 2016)

In the study by Rafiee & Fievez (2015) on their point absorber CETO, numerical predictions of the motions and the PTO loads using linear time-domain analyses and nonlinear OpenFOAM simulations were compared to the experimental data for operational wave conditions. The model test at 1:20 scale was performed at the FloWave tank at the University of Edinburgh, UK. The linear model is found to over-estimate the motions and the PTO loads because it does not consider the instantaneous wave elevation and position of the point absorber, while the CFD prediction agrees much better with the experimental results.

A novel overtopping WEC concept, WaveCat, was developed and tested at a scale ratio of 1:30 at the Ocean Basin of the University of Plymouth (Allen et al., 2017). It consists of two symmetrical hulls joined at the stern via a hinge (allowing the relative angle between the hulls to change depending on the sea state) and a catenary anchor leg mooring. No PTO system was modelled in the test. Unsteady RANS CFD analysis using STAR-CCM+ was performed to predict the heave and pitch motions of the device in regular waves. A good comparison with the measurements was obtained, but the accuracy of the CFD analysis was less for heave motions in large waves.

Elhanafi et al. (2017a) performed a model test of a 1:50 bottom-fixed OWC for regular wave conditions in the towing tank at the University of Tasmania, Australia. The wave elevation and the air pressure in the OWC chamber were measured and compared with the RANS CFD calculations using STAR-CCM+. A very good agreement was obtained for the 3D CFD model, while the 2D CFD model significantly over-estimates the hydrodynamic efficiency of the OWC device.

- ***Survivability tests***

In the EU FP7 MARINA Platform Project, model tests of the three combined wind and wave concepts were performed, including a test at CNR-INSEAN, Italy on the Spar-Torus-Combination (STC) concept and a test at ECN, Nantes on the Semi-submersible-Flap-Combination (SFC) concept. A summary of the experimental and numerical studies of these two combined concepts can be found in Gao et al. (2016).

In addition to the functionality test of the STC concept (Wan et al., 2016a) with focus on the single torus-type WEC power performance, the tests with two survival modes of the WEC (one with the torus fixed to the spar at the mean water level and the other at a submerged position) in extreme wind and wave conditions were also performed (Wan et al., 2015; Wan et al., 2016b). Large motions and water entry/exit of the torus (which leads to slamming loads on the bottom of the torus) were observed for the survival mode when the torus is placed at the mean water level, mainly due to the heave resonance. In this case, numerical simulations based on linear potential theory fail to predict the loads between the spar and the torus (Wan et al., 2015), while the numerical model with the consideration of slamming loads gives a much better agreement with the experimental results (Wan et al. 2017). The experiment also reveals that the STC has much smaller motions in the survival mode with the torus submerged. As compared to the STC concept, the SFC concept is a semi-submersible wind turbine with three submerged flap-type WECs, and the experiments indicate small motion responses in both operational and survival conditions (Michailides et al., 2016a and 2016b).

A survivability model test of a floating OWC concept with intact and damaged mooring lines was performed in the towing tank at the University of Tasmania (Elhanafi et al., 2017b). The mooring system used was a taut-line system with four vertical lines and the damaged condition had one broken line. A CFD analysis for both intact and damaged mooring conditions was performed and compared well to the experimental results of the regular wave cases. The experiment also revealed that the largest mooring line tension in either intact or damaged condition is not necessarily correlated to the largest waves in an irregular wave train. This is mainly due to the dynamic characteristics of the system.

Testing of an array

There is an increasing interest in studying the hydrodynamic interaction and the power performance of WEC arrays by lab testing. The WECs in an array might be mechanically connected, as in McDonald et al. (2017) or have independent motions as in Ruiz et al. (2017) and Stratigaki (2014).

In the work done by McDonald et al. (2017) and Ewart et al. (2017), model tests of the Albatern 12S WEC concept in a single-device configuration and a Hex-array configuration have been performed at 1:18 scale at the FloWave tank at the University of Edinburgh, UK, as shown in Figure 3.5. The single device is actually a floating WEC of four point absorbers connected via rigid beams and articulated joints, while the Hex array consists of nine interconnected point absorbers. The articulated joint allows for relative rotational motions of the point absorbers and an introduction of the PTO system with a linear damper. The experimental results show that the mechanical coupling as used in this study can potentially improve both the magnitude and the smoothness of the produced power per device and meanwhile reduce the mooring loads per float.

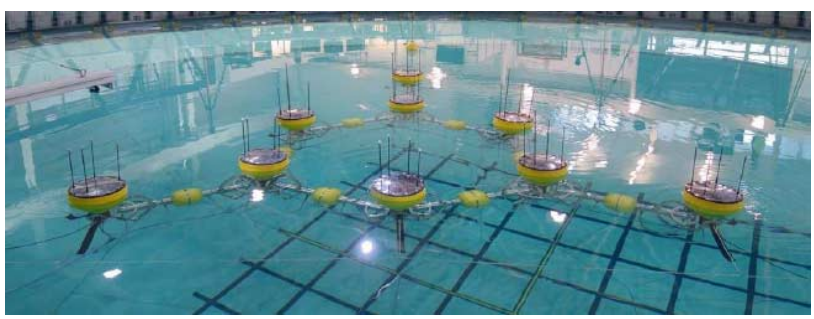

Figure 3.5: The Hex-array of the Albatern 12S WEC concept at the FloWave tank (McDonald et al., 2017)

Ruiz et al. (2017) did a model test on an array of five independent point absorbers (Wavestar WECs) under regular and irregular seas at a scale ratio of 1:20 at the deep-water wave basin at Aalborg University, see Figure 3.6 (left picture). Linear control strategies were accurately implemented in the PTO system via an electric motor. The purpose was to validate the numerical tool they developed for hydrodynamic analysis of WEC arrays. It was shown that the power prediction error from the numerical tool is typically less than 23% with a positive average error of 8%.

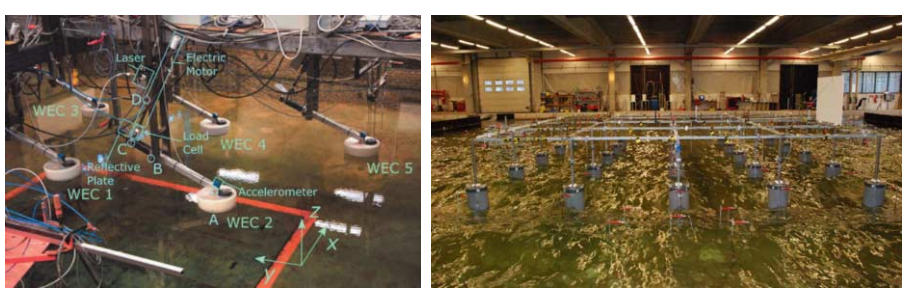

Figure 3.6: The array of five Wavestar WECs (left) in the deep-water ocean basin at Aalborg University (Ruiz et al., 2017) and the 5*5 array of points absorbers (right) at DHI (Stratigaki, 2014)

In the PhD thesis work by Stratigaki (2014), a large-scale experimental work has been performed on an array of 5*5 point absorbers with constrained heave motions at the DHI ocean basin, Denmark, as shown in Figure 3.6 (right picture).

The purpose was to study the intra-array interactions and the extra-array effect of the WECs in terms of wave field modifications. Therefore, the wave elevations inside the array and at the windward and leeward sides of the array were extensively measured. The motions of the WECs were also measured and used to derive the power production with an applied linear damping for each WEC. The time-averaged power output of the WECs in an array for long-crested and short-crested irregular waves are shown in Figure 3.7, as a percentage difference as compared to that of an individual WEC. The power output of the WECs in an array varies significantly. A positive effect on the power absorption was observed for almost half of the WECs for the long-crested wave conditions and the largest positive effect of about 50-55% increase was found for the WECs in the second and third rows inside the array. Only negative effect was found for all of the WECs for the short-crested wave conditions, with a largest decrease of 60%. A guideline on WEC array testing was recommended and the experimental data can be used for validation of numerical tools like WAMIT (2016) or MILDwave (Troch, 1998).

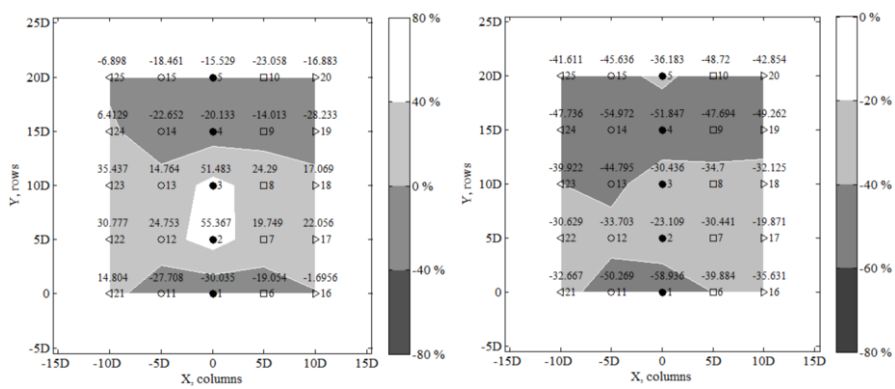

Figure 3.7: Difference percentages in non-dimensional time-averaged total power output between tests with an array and with an individual WEC for long-crested irregular waves of Hs=0.104m and Tp=1.26s at model scale (left) and for short-crested irregular waves of Hs=0.104m, Tp=1.26s and the spreading function s=10 (right) (Waves propagate from bottom to top and WECs are marked and numbered.) (Stratigaki, 2014)

3.2.2 Field testing

The use of real sea test sites for WECs is becoming compelling because of the limits in simultaneous scaling of mechanical, fluid-dynamic and electric components in labs. Most of the time, each part is tested separately and linearized models are used to take into account the others. The main problem comes from the non-linear nature of each of these parts or difficulties in reproducing the scaled effect (e.g. Falcao & Henriques, 2014; Falcao & Henriques, 2016). For these reasons, as soon as the WEC reaches a high TRL (technology readiness level) (Mankins, 1995), full (or almost full scale) tests are necessary to make sure that the full system is optimized and to implement the optimal control system in real sea conditions.

The availability of open-sea test sites is growing together with these needs. They are restricted regions of the sea possibly furnished with: 1) hydrographic and current surveys, 2) wave climate studies and/or historical collected wave data; 3) mooring configurations; 4) wave buoys, 5) grid connection; 6) observation towers; 7) instrumentation cables to onshore facilities, 8) data acquisition systems, 9) onshore facility; etc.

Most of these are shortlisted in the OES (Ocean Energy Systems) annual report (OES, 2016). There are eight of them in the US and eight in Europe (MARINET2, 2017), that can be used for R&D of new devices for a sufficiently long time. Among them, the BOLT Lifesaver was installed in March 2016 in the US and has been in operation for 78% of the 280 days of testing, producing a total of 17955kWh at an average power of 3.4 kW (OES, 2016).

New facilities are arising around the world, for example in Chile, where the Chilean Government's economic development organization CORFO (Corporación de Fomento de la Producción) is setting up a centre of marine energy R&D excellence in Chile, named Marine Energy Research and Innovation Centre (MERIC) (http://www.meric.cl).

Many other deployment sites have been chosen and equipped for the development of a specific technology. An outstanding example is the Carnegie Wave Energy Research Facility (http://www.carnegiece.com/wave/research-facility). It has been used for the development of the CETO technology that has been the world's first array of wave power generators to be connected to an electricity grid.

However, as shown in Cahill (2014), it is unlikely that a test site can reproduce, at reduced scale, the wave climate of the deployment site. However, a combined analysis of numerical data, wave basin and field testing can provide an accurate estimation of the expected performance, given a sufficiently long deployment time.

Once again, the CETO system is an outstanding example, it is using combined field testing, both in its own site and at the WaveHub later in 2018, and towing tank tests (at Plymouth University) to optimize some parts for its new generation technology (ASX, 2016).

In addition, in the last few years, there are many WEC devices that were deployed and tested in China (Xia et al., 2014). These field testing activities were coordinated by the Administrative Centre for Marine Renewable Energy (ACMRE) under the State Oceanic Administration (SOA) in China (Y.C. Chang et al. 2017). Some of the tested concepts are listed here, including the ones with a longer testing period at sea and the ones with a rated power larger than 100 kW, as shown in Figure 3.8.

The 10kW Jida I floating WEC of ten oscillating buoys (Wang et al., 2012) and the 10kW three-buoy WEC from Zhejiang Ocean University 15 (Xia et al., 2014) were tested for more than 150 days, both in 2015. However, the average efficiency of these two concepts was only about 15%. Similar to the Salter Duck concept, DUCK III (Yao et al., 2016), a 100kW floating WEC, was tested in 2013. The sea trial demonstrated a high energy capture efficiency, but the stability of the concept needs to be improved. As a continuation, the 100 kW prototype of Sharp Eagle Wanshan was deployed for testing offshore the Wanshan Islands in 2015. It was found in the test that at wave period between 4~6.5 seconds and at wave height between 0.6~1.8 meters, the energy conversion efficiency remains above 20% and the highest efficiency reached 37.7% (Sheng et al., 2015a).

Figure 3.8: Prototypes of the wave energy converters tested in China (from left, 10kW Jida I (Wang et al., 2012); 10kW three-buoy WEC (Xia et al., 2014); 100kW DUCK III (Yao et al., 2016); 100kW Sharp Eagle Wanshan (Sheng et al., 2015a))

3.3 Design rules and standards

As early as in 2005, Carbon Trust (UK) commissioned DNV to establish a standard for design and operation of wave energy converters (Carbon Trust, 2005). The standard essentially provides interpretation and guidance on the application of existing Codes and Standards (mainly from industries such as Offshore and Maritime). To streamline the development of this nascent sector, IEA-OES has organised international collaborations to implement guidelines and recommendations (reports can be downloaded at https://www.ocean-energy-systems.org/publications/oes-reports/), meanwhile the European project Equimar has also established similar practice and guidelines (deliverables can be downloaded at http://www.equimar.org/equimar-project-deliverables.html).

More recently, international efforts have been made to standardize the development of wave energy technologies and to provide a standardized assessment method, such as the rules and standards for marine renewable energy (wave and tidal energy (Cornett, 2014)). The International Electrotechnical Commission (IEC) has organized international experts from the relevant countries to work on the specific task of developing the technical specifications (which will finally be developed to be standards). The development of a technical specification must undergo the following stages: from the proposal of the task, to committee draft (CD), to draft technical specification (DTS) and technical specification (TS), and finally to standard. In the staged development, the member countries will make recommendations and comments on the documents, and the project team will make all the modifications, but the Technical Specification (TS) must be approved by the voters from the relevant countries. So far, the published TS includes:

- Marine energy- Wave, tidal and other water current converters- Part 100: Electricity producing wave energy converters- power performance assessment, published in August 2012.
- Marine energy- Wave, tidal and other water current converters- Part 10: Assessment of mooring system for marine energy converters (MECs), published in March 2015.
- Marine energy- Wave, tidal and other water current converters- Part 101: Wave energy resource assessment and characterisation, published in June 2015.
- Marine energy- Wave, tidal and other water current converters- Part 102: Wave energy converter power performance assessment at a second location using measured assessment data, published in Aug. 2016.

Some of the TS are being applied in technology development or in research work. Some other technical specifications are still under development, including the guidelines for the early stage development of wave energy converters: Best practices and recommended procedures for the testing of pre-prototype scale devices (IEC62600-103); and the electrical power quality requirements for wave, tidal and other water current energy converters (IEC62600-30).

3.4 ISSC contribution to the IEA OES benchmark study

The Ocean Energy Systems technology collaboration programme (OES) is an intergovernmental collaboration between countries, which operates under a framework established by the International Energy Association (IEA) in 2001. There are currently 20 member countries, and the goal of the alliance is to advance research, development and demonstration of conversion technologies to harness all forms of renewable energy from the ocean. In September of 2016, OES Task 10 – WEC modelling verification and validation was kicked off with a meeting of 20 participants from 10 countries. The task will run for 5 years, and the goals of the task are:

1. To assess accuracy, and establish confidence in the use of numerical models
2. To validate a range of existing computational modelling tools
3. To identify uncertainty related to simulation methodologies in order to:
    a. Reduce risk in technology development
    b. Improve WEC energy capture estimates (IEC TC 102)
    c. Improve loads estimates
    d. Reduce uncertainty in LCOE models
4. Define future research and develop methods of verifying and validating the different types of numerical models required under both operational and survival conditions.

Participants from the National Renewable Energy Laboratories (NREL) and the Sandia National Laboratories, both in the USA, took a leading role in getting the benchmark study up and running. In particular, they emphasized important lessons learned from their experience with several earlier benchmarking efforts: WEC-Sim (2017), WEC3 (Combourieu et al., 2015) and FONSWEC (2017). Experience was also brought to bear from similar efforts carried out by the IEA on Wind energy: the OC3- OC5 projects (IEA, 2017). Based on these earlier studies, the following recommendations were made:

- Start simple, e.g. single body/single DOF/simple geometry
- Minimize the number of variables
- Experiments must be performed with validation of numerical models in mind
- Uncertainty must be assessed throughout the experimental campaign. Repeated tests are a minimum here
- Frequent working meetings should be held

It was also decided that all work considered during this task should be made publicly available in order to help all developers. Participants were encouraged to seek local funding to support their participation in the Task.

A summary from Phase I of the study was presented at the EWTEC2017 conference in Cork, Ireland (Wendt et al., 2017). Phase I considered a code-to-code comparison using a floating sphere with a single degree of freedom in heave (see Figure 3.9). Calculations were made first for a decay test, then using regular waves of three different steepness values, and finally with three irregular wave conditions. For each wave condition, the sphere response (and/or forcing) was computed in the free unrestrained case, with an external (linear) optimal PTO damping, and in the fixed (no motion) condition. Participants used numerical models based on linear, weakly nonlinear and fully nonlinear potential flow, as well as CFD. Agreement among different codes was generally very good. An example is shown in Figure 3.9, which shows a very large amplitude decay test with the initial displacement equal to the sphere radius. The linear, weakly nonlinear and fully nonlinear calculations show distinct grouping in their predictions. See Wendt et al. (2017) for more details on the comparisons.

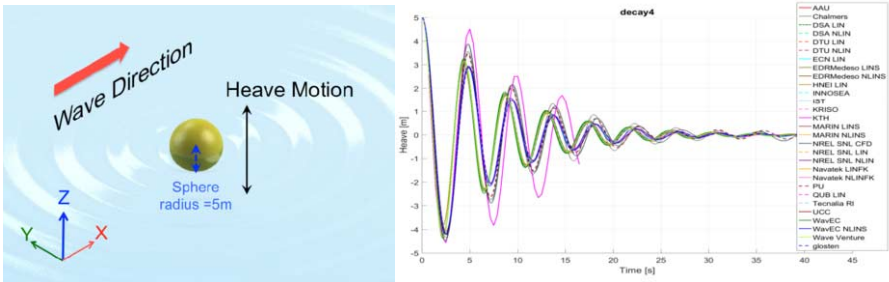

Figure 3.9: The Phase I case of a heaving sphere (left) (Courtesy of Kim Nielsen) and comparison of numerical solutions for a large-amplitude decay test (right) (Courtesy of Fabian Wendt)

Phase II of the project is currently being defined. Depending on the priorities of the participants, this could go in one of four possible directions:

- Focused wave interaction with either the floating sphere from Phase I, or a cylindrical buoy with a hemispherical bottom for which experimental measurements are available
- Comparison with experimental data for two more complicated WEC devices from the study by (Beatty et al., 2015)
- Introduction of control strategies for the case from Phase I
- Adding multiple complexities to the case from Phase I including: additional degrees of freedom, nonlinear PTO forcing (including end-stops) and a mooring system

Reporting from Phase II will appear in 2018. To participate in the study, contact Fabian Wendt (Fabian.Wendt@nrel.gov).

4. TIDAL AND OCEAN CURRENT TURBINES

Tidal range and tidal current technologies are the two basic technologies that convert the tidal energy into electricity. Tidal range devices harvest the potential energy due to the difference in head between ebb tide and flood tide, while tidal current turbines convert the kinetic energy due to tidal stream into electricity. In this report, we mainly discuss tidal current turbines. In addition, ocean current can also be used to generate electricity by current turbines, but this technology is less developed and will not be discussed here.

4.1 Recent development

In the last decade, there are a number of research studies on tidal current (or marine hydrokinetic) turbines worldwide and in particular in Europe. A list of the European projects under the FP7 and Horizon 2020 programmes can be found in Segura et al. (2018), including the completed projects, for example, CLEARWATER (http://cordis.europa.eu/project/rcn/185364_en.html) coordinated by Atlantis Operations Ltd., SEAMETEC (https://cordis.europa.eu/project/rcn/194749_en.html) by Eire Composites, and the ongoing projects, such as D2T2 (http://cordis.europa.eu/project/rcn/207451_en.html) coordinated by Nova Innovation, FLOTEC (https://cordis.europa.eu/project/rcn/199964_en.html) by Scotrenewables Tidal Power Limited, DEMOTIDE (https://cordis.europa.eu/project/rcn/207512_en.html) by DEME. Many of these projects focused on the demonstration of full-scale large-size tidal turbine systems, components (such as blades, drivetrain) or condition monitoring techniques. In particular, tidal current turbines are being deployed, at full scale in the marine environment.

The decommissioning of the 1.2MW SeaGen turbine will be conducted in 2018 (Figure 4.1) after 10 years of operation in the Strangford Narrows (Northern Ireland, UK). During operation SeaGen has delivered more than 10GWh to the local electricity grid. It is important to

note that the turbine is being decommissioned and removed at the end of the consented period for the demonstration project.

Figure 4.1: Wake behind the SeaGen monopile in Strangford Narrows (Northern Ireland, UK) (left) and blades that are out of water (right)

At the same time, Atlantis Resources recently deployed the forth megawatt scale turbine as part of the MeyGen project in the Pentland Firth (Scotland, UK) (Tidal Energy Today 2017), forming the highest capacity, grid connected, turbine array to date. Nova Innovations completed the first grid connected turbine array in Bluemull Sound (Shetland, UK) earlier the same year (Morton, 2017). Commercial turbines (as shown in Figure 4.2) are being developed by Atlantis, Voith Hydro, Alstom TGL, DCNS, Hammerfest, Schottel, Verdant and others and are being deployed in several countries including the UK, France, Canada, US and China. A full survey can be found in the annual report of the IEA Ocean Energy Systems group (OES, 2017).

Figure 4.2: Commercial turbines developed by Atlantis (top, left), Voith Hydro (top, right), Alstom TGL (bottom, left) and DCNS (bottom, right) (Kempener & Neumann, 2014)

4.2 Environmental Conditions

Tidal current turbines are preferably deployed in locations with a high mean tidal current speed, such as channels, for which strong variation in current speed might be expected due to ambient turbulence, wave-current interaction, and wake effect in a tidal turbine farm. Strong turbulence will lead to large variations in power output and dynamic loads on the turbine blades, which challenges the structural design of tidal turbines.

The work and experience gained by developers testing in the European Marine Energy Centre (EMEC) tidal test site in the Falls of Warness led to the Reliable Data Acquisition Platform

for Tidal (ReDAPT) project in the UK. Between 2011 and 2014, ReDAPT characterized the flow around Alstom Ocean Energy's 1MW, DEEP-Gen IV, tidal turbine, which has a rotor diameter of about 16m and was deployed at the mid water column in 40m deep water. ReDAPT primarily used Doppler profiling to characterize the flow. Seabed mounted diverging-beam acoustic Doppler profilers (DADP) and turbine-installed (mid-depth in the water column) single-beam acoustic Doppler profilers (SB-ADP), were deployed along with acoustic and pressured based wave measurement instruments mounted the sea floor. The need to characterize the turbulence in detail led to the development of a convergent-beam acoustic Doppler profiler (C-ADP) (Sellar et al., 2015) which was also deployed during ReDAPT. The resulting ReDAPT Environmental Conditions Database (see http://redapt.eng.ed.ac.uk) contains approximately five hundred Gigabytes of multi-seasonal raw and processed data (Sellar et al., 2018).

As part of ReDAPT Sutherland et al. (2017) analyzed the data obtained simultaneously, during the winter months, from two ADPs separated by 78m normal to the flow direction (see Figure 4.3). The analysis shows that there were significant differences of 49% in the available power between the two locations, with strongly sheared flow resulting in velocity differences of over 1m/s between the top and bottom of the rotor plane, and a velocity change at hub height of ±0.5m/s resulting from the waves.

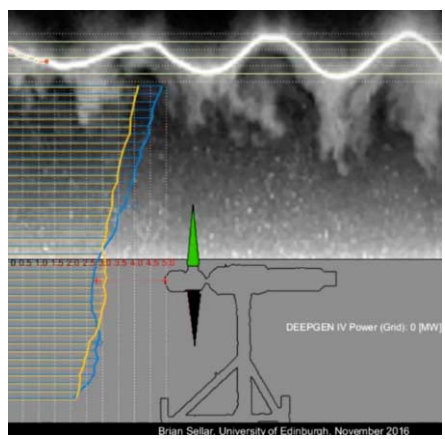

Figure 4.3: Measurements from two ADCPs deployed 78m apart by the DeepGEN IV turbine in the Falls of Warness

More field measurements of tidal currents with focus on turbulence intensity and vertical profile are needed for a better characterization of offshore sites for tidal turbine power and loads prediction. Nevertheless, the important of velocity shear and turbulence has gained much attention by the researchers in recent years. A numerical procedure was developed by Pyakurel et al. (2017) to generate a turbulent flow field based on the input of ambient turbulence intensity and mean flow velocity, which are integrated to a time-domain code for dynamic response analysis of tidal current turbines. It is found that the standard deviations of both power and axial loads increase by 4 times if the turbulence intensity increases from 5% to 20%. Generating a target turbulence intensity in towing tank or ocean basin for model testing is extremely difficult. In Blackmore et al. (2016), an experimental campaign using static grids to generate turbulence was performed in a circulating water flume. Turbulence decays with the distance downstream of the grid and therefore different turbulence intensities can be obtained by placing the tidal turbine model at different locations from the grid. In the extreme case, turbulence has an effect on the load fluctuations experienced by the blades with a 5-fold increase.

4.3 Tidal turbine loads and response analysis

4.3.1 Numerical methods

Similar for offshore wind turbines, numerical methods based on BEM (Blade Element Momentum) theory and CFD (Computational Fluid Dynamics) are being developed and partly validated against lab and field test results.

Due to the significant ambient turbulence and the presence of the waves, tidal turbines might be subjected to more dynamic loads as compared to offshore wind turbines. Faudot & Dahlhaug (2012) reported that wave loads are one of the main contributors to fatigue loading on turbine blades, and are a determining parameter in the calculation of turbine blade lifetime. Tatum et al. (2016) performed CFD simulations for a 10m-diameter tidal turbine in current and waves. They showed the significant fluctuations in both power and loadings, indicating the importance to consider waves in the modelling of the tidal turbines.

In many of the numerical studies, the focus was given to the overall power performance and the global loads (thrust and torque) of the turbine (Lust et al. 2013, Holst et al. 2015, Allsop et al. 2017). In some studies, detailed structural loads of the blades were obtained (Guo et al. 2017a, Barber et al. 2017).

Guo et al. (2017b) developed a BEM code for a three-blade tidal turbine in current and waves and compared both the mean and dynamic thrust and torque with the towing tank test results. A good agreement was obtained, but more validation work with respect to distributed loads along the blades should be considered. The BEM code is further used to study the blade loads in irregular waves (Guo et al. 2017a). Holst et al. (2015) performed CFD analyses of a two-blade tidal turbine using ANSYS-CFX and demonstrated the reasonably good accuracy of the CFD analysis when compared with the experimental results for both steady-state current condition and combined wave and current condition. As shown in Figure 4.4, the accuracy of the BEM code is comparable to that of the CFD analysis. Allsop et al. (2017) studied numerically a ducted, open central tidal turbine using BEM theory and an empirical model of the flow through the duct. They also show a good agreement between the BEM code and the CFD analysis for TSR (tip-speed-ratio) up to the optimal operating condition. It is also suggested that a more comprehensive validation work should be carried out. Barber et al. (2017) studied experimentally the performance of tidal turbines with adaptive pitch blades of composite material and compared it with the aluminum stiff blades. They found that the pitch-to-feather design can lead to lower blade loads, while the pitch-to-stall design has the potential of higher power generation, but also larger loads.

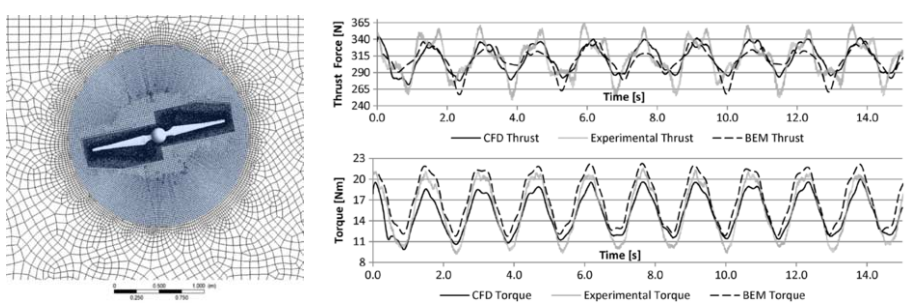

Figure 4.4: Mesh illustration for the CFD analysis of a two-blade rotor with the rotating domain highlighted in blue (left) and the comparison of the model-scale thrust and torque between BEM, CFD and measurements for a regular wave (H=0.25m, T=1.883s, model-scale) (Holst et al., 2015)

Machine data from ReDAPT was processed by Parkinson & Collier (2016) and compared with unsteady time-domain simulations performed using DNV-GL's Tidal Bladed software. Comparisons are reported for electrical power, pitch angle and blade near-root bending moment. The analysis shows that good agreement between the simulated and measured flapwise near root-bending damage equivalent loads and load spectra. The stochastic blade load data shows significant transient loadings.

CFD methods have been extensively used to study the detailed flow characteristics of the wake of a tidal turbine in uniform and constant flow (Liu et al., 2016a), which is important to understand and predict accurately the loads on turbine blades. CFD simulations for tidal turbines in shear and turbulent flow have also be performed. Ahmed et al. (2017) performed a series of RANS (Reynolds-Averaged Navier-Stokes) and LES (Large Eddy Simulation) CFD simulations on a 1MW tidal turbine and compared the results with the measurements from the test at the EWEC site. It was found that both RANS (with the SST k-ω model) and LES (with the Germano-Lilly dynamic subgrid model) simulations can predict similar phase-averaged loads and blade pressures for an ideal low-turbulence case. In addition, LES simulations with realistic inflow turbulence can satisfactorily reproduce the blade bending moment spectrum as compared to the field measurements.

Combined CFD/BEM numerical methods have also been developed to study the flow through a single rotor or multiple rotors in a channel. Schluntz & Willden (2015) developed an RANS solver with an embedded BEM model to study the effect of blockage (the ratio of the rotor swept area to channel cross-sectional area) on the power performance of a single rotor in a channel. In such method, RANS simulations of the flow in channel were performed considering the forcing of the rotor obtained by a BEM model. It is then further developed to investigate the performance of a closely spaced cross-stream fence of four turbines (Vogel & Willden, 2017). The mean fence power is found to be less than that predicted for a single turbine with the same local blockage ratio, but greater than that for a single turbine based on the global blockage ratio of the fence. Similar numerical techniques were used to predict the loads on a tidal turbine with contra-rotating rotors and its support structures (Creech et al., 2017) combing LES with Actuator Line Models for the rotors, and the loads on a ducted/open center tidal turbine (Allsop et al., 2017) combining RANS and BEM models.

For design of tidal turbine blades and support structures, structural responses due to hydrodynamic loads need to be predicted. Depending on the length and the flexibility of the blades, hydro-elastic responses of a tidal turbine might be less significant as compared to aero-elastic resonant responses of wind turbine blades in turbulent wind field. Arnold et al. (2016) performed a comparative study on a 1MW tidal turbine of 13m in diameter using both decoupled and coupled CFD and structural response analysis. They found that the flexibility of the blades and main shaft of this particular turbine are of minor importance. The hydro-elastic behavior is dominated by the tower bending and the nacelle nodding properties. However, with increasing turbine size and rotor diameter, the hydro-elastic behavior may become more important to consider for blade design.

Composite materials (mainly GFRP and CFRP) are most commonly used for wind turbine blades and are also suitable for tidal turbine blades. Although environmental loads acting on wind turbines and tidal turbines are quite different, experiences and research work on composite wind turbine blades should be used when developing methods for structural design and analysis of tidal turbine blades. A tidal turbine blade design methodology was proposed by Grogan et al. (2013). It consists of a hydrodynamic analysis of the rotor using the BEM method, a structural analysis to determine the strain distribution based on a FE (Finite Element) beam model of the blade and another structural stress analysis using a detailed shell model of the blade. In the second structural analysis, stress/strain-based failure criteria of the composite layup are considered. Murray et al. (2016) developed a coupled FE-BEM design tool based on

an iterative procedure for the determination of structural (deformation and stress) and hydrodynamic (power and thrust loads) responses of the blades and applied it to a tidal turbine with passively adaptive blades. The case study on a small-scale turbine with 360mm long shows that the rotor can operate optimally at design conditions, while reducing structural loads and power capture at flow speeds larger than the design conditions due to its large flexibility.

Fibre and matrix failure and delamination are the most common failure modes of composite materials. However, it is very challenging and time-consuming to incorporate all failure modes in blade structural analysis for design. A damage-based design and analysis methodology for fibre reinforced composite tidal turbine blades were developed by Fagan et al. (2016). In particular, the Puck phenomenological failure criteria for fibre and inter-fibre failure of GFRP and CFRP were used in the FE analysis of the blades using shell elements, with the distributed hydrodynamic loads obtained from a BEM model. In another study, an advanced numerical approach was proposed (Harper & Hallett, 2015), which explicitly models the cohesive material between the composite plies and incorporates stress and fracture based failure criteria related to both damage initiation and subsequent propagation to simulate delamination. This modelling approach is validated against the experimental result of a composite test sample, as shown in Figure 4.5.

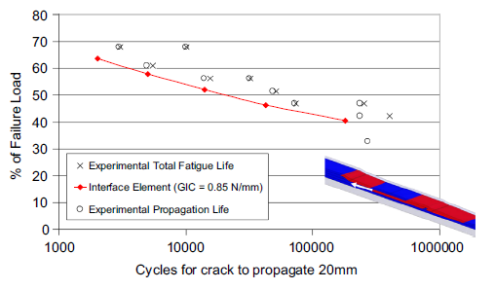

Figure 4.5 Cover ply specimen fatigue lives against normalized load level (Harper & Hallett, 2015)

Vertical axis or cross-flow tidal turbines have also been proposed and analysed. In some of the recent studies, structural response analyses of the blades and support structures were carried out using a coupled hydrodynamic/structural analysis. In the study by Wang et al. (2018), the structural analysis of an H-type three-blade vertical axis tidal turbine was performed using a beam model based on the geometric exact beam theory, which is coupled to the hydrodynamic loads analysis by a discrete vortex method. They also revealed the structural resonant responses due to the first few global vibrational modes of the support structure and the blades.

4.3.2 Laboratory tests and field measurements

A number of laboratory tests (mainly in towing tanks) of scaled horizontal axis tidal turbines have been performed in the last few years. This includes testing of scaled turbines in uniform and steady flow and in addition with oscillatory motions, regular or irregular wave conditions. Normally, the integrated thrust force and the blade root bending moment are measured. In such tests, a geometrically-scaled rotor, with a scaling factor of 1:20 - 1:30 is typically used with the hydrodynamic loads scaled by the Froude law and with the tip-speed-ratio kept the same as the full-scale one. Large-scale (1:5 - 1:10) or prototype field tests are also performed, providing valuable results for numerical model validation.

An interesting comparative ‘Round Robin’ test campaign (Gaurier et al., 2015) has been conducted in two flume tanks (at IFREMER and CNR-INSEAN) and two towing tanks (at KHL

and CNR-INSEAN) under the EU FP7 MARINET program. Tests of the same three-blade tidal turbine of 700mm in diameter with constant towing speeds of 0.6-1.2m/s were performed in these four testing facilities, as shown in Figure 4.6. Time series of the torsional moment and the axial force at the turbine shaft were measured and used to calculate the power and the thrust coefficients, which are compared in Figure 4.7 in terms of mean value and standard deviation. In general, the mean power and thrust coefficients compare well and the differences for high tip-speed-ratio is mainly related to the different blockage ratio of the four tanks. Even bigger differences in standard deviations were observed for both the power and the thrust coefficients, which might be caused by the different levels of ambient turbulence in the tanks and vibrations of the towing carriages. Overall, the ratio of the standard deviation to the mean value varies from 1.5% to 5% and from 3% to 13%, for the power and the thrust coefficients, respectively.

Figure 4.6 Views of the same turbine model in the IFREMER flume tank, in the KHL towing tank, in the CNR-INSEAN flume tank and in the CNR-INSEAN towing tank (from left)

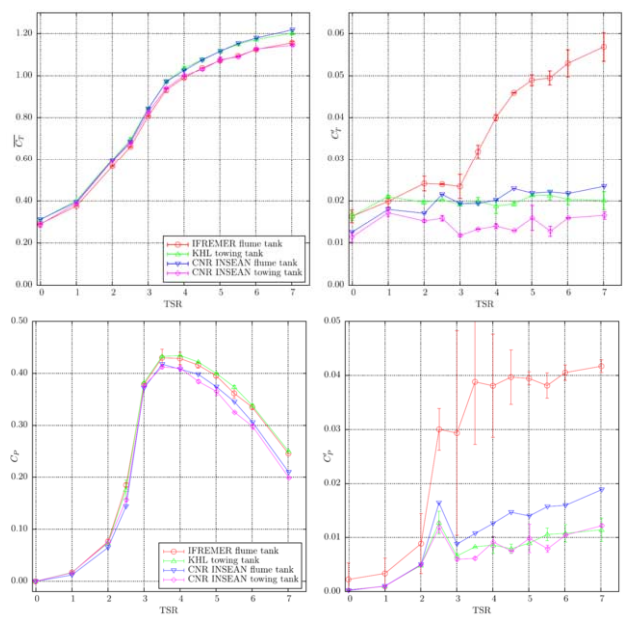

Figure 4.7 Mean (left) and standard deviation (right) of the power (top) and thrust (bottom) coefficients as function of tip-speed-ratio (TSR), obtained for every run at every tank for a mean current speed (towing speed) of 1.0m/s

Milne et al. (2013, 2015) performed model tests of a scaled tidal turbine in current with oscillatory motions to study the role of unsteadiness on the rotor loading (i.e. the blade root out-of-plane bending moment). They found that the hydrodynamic loads due to the oscillatory motions at high frequencies are in phase with acceleration, but the magnitudes are small as compared to the steady-flow loads. While, at low frequencies, the hydrodynamic loads are dominated by the dynamic inflow effect due to the oscillatory motions and a phase lead was observed. Moreover, at low tip-speed ratio, flow separation was observed, causing an increase and a phase lag in the hydrodynamic loads. They also found that the principle of superposition for turbine loads with multi-frequency oscillatory motions can be used based on the measurements from both the steady flow and the single frequency oscillatory tests, as long as the flow was attached. This is consistent with the findings by Guo et al. (2017a, 2017b), in which a model test of a scaled tidal turbine in combined current and waves was performed. A linear relationship between the wave amplitude and the turbine hydrodynamic load was observed and the superposition method can be used for turbine loads in linear irregular waves.

Most of the model tests of tidal turbines use aluminum. However, tests of composite or plastic turbines are also performed. Liu et al. (2015) performed a series of towing tank tests of a tidal turbine with a large solidity ratio and compared the performance of the metal and plastic rotors. As compared to the metal rotor, a maximum 40% decrease in the absorbed power was obtained for the plastic rotor, operating at a tip speed ratio of 3.0, which is mainly due to the high flexibility of the plastic rotor. On the other hand, Barber et al. (2017) have shown the potential to reduce the turbine loads when composite blades were used and pitched to feather for operation, based on their model test results of composite and aluminum rotors.

Field measurements of large-scale or prototypes of tidal turbines have been carried out and used to validate numerical predictions. The measurement data of the Alstom Ocean Energy's 1MW tidal turbine at the European Marine Energy Centre (EMEC) in Orkney, UK were analyzed by Parkinson & Collier (2016) and compared with the numerical simulations from the software DNV-GL Tidal Bladed. Normalized shaft power and near-root flapwise bending moment of the blade as function of the normalized inflow velocity are compared in Figure 4.8. In the numerical simulations, the onset flow turbulence is described using a von Karman velocity spectra and coherence functions. The comparison reveals a fairly good agreement between the field measurements and DNV-GL Tidal Blade, which is a BEM code.

Atcheson et al. (2015) performed a large-scale towing test in a lake for a 1:10 scale tidal turbine Evopod, which was carried by 16m long catamaran with a forward speed of 0.9-1.2m/s. The wake behind the rotor (the velocity field) was measured using Acoustic Doppler Velocimeters. The obtained maximum power coefficient is about 0.35 at a tip-speed-ratio around 3, which agrees well with the BEM prediction. A floating tidal turbine prototype GEM (Marine Electrical Generator) was developed and tested in the Venice lagoon, Italy (Coiro et al., 2017). It consists of a submerged two-hull floater, two counter-rotating ducted turbines and a tether mooring system. The field measurements of the prototype (which has a rated power of 100kW for single turbine at a current speed of 2.8m/s) indicate a maximum power of 7kW at the maximum measured current speed of 1.3m/s, which corresponds to a power coefficient of 0.6-0.65 due to the positive effect of the duct.

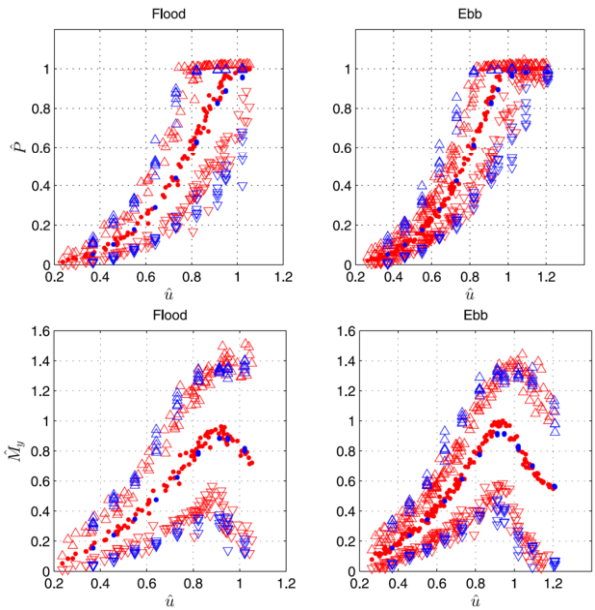

Figure 4.8 Comparison of the normalized shaft power (top) and near-root flapwise bending moment of the blade for flood (left) and ebb (right) flow conditions (Normalization performed with respect to the values at the rated condition. Max, mean, min denoted by upward pointing triangle, dot and downward pointing triangle.)

5. OTHER OFFSHORE RENEWABLE ENERGY TECHNOLOGIES

In addition to offshore wind, wave and marine current energy, ocean thermal energy conversion (OTEC) utilizes the temperature difference between the sea surface water and the colder, deep water to generate electricity. However, an OTEC device requires temperature differences of at least about 20 degrees Celsius to be effective (Mofor et al., 2014), which leads to the resources only applicable in the tropical waters. Moreover, a water depth of 1000m is expected to reach such level of temperature difference, which indicates a high cost for the need of extremely long pipes. A few small-scale land-based prototypes of OTEC have been built and tested, including the Okinawa Prefecture OTEC Demonstration Plant with two 50kW units in Japan (OTEC Okinawa, 2017) and the 105kW demo plant built by Makai Ocean Engineering and operated in Hawaii (Techxplore, 2017). Large-scale OTEC plants are under design and development, which includes a 16MW plant project that will be developed by Akuo Energy and DCNS in France with funding from the European Union's NER300 programme and a 10MW pilot plant that will be designed by Lockheed Martine in a project sponsored by the Reignwood Group in China (Mofor et al., 2014). In addition, MW-scale OTEC plant concepts with floating support structures (such as semi-submersible or mini-spar) have also be proposed (Stoev et al., 2017).

Similarly, a salinity gradient energy conversion plant harnesses the chemical potential due to salinity difference between freshwater and seawater, captured as pressure across a semi-permeable membrane (Mofor et al., 2014). River mouths are the most obvious locations for such resource. However, due to the high cost of membranes, this type of technology is still at a conceptual and early research and development stage. Most of the studies are conducted in labs. Only one small 4kW pilot plant was opened by Statkraft in Norway in 2009 (Statkraft, 2017), but no large-scale device exists.

Usually, commercial offshore renewable energy devices are developed with many units in a farm configuration, which occupies a large sea surface or ocean space. Combined use of ocean space for different types of offshore renewable energies and/or other sectors has become an important concern. Many research projects exist in particular in Europe and have been discussed in the previous ISSC report (Gao et al., 2015). However, as of today, there are no offshore wind farms that are combined with other use of the ocean space. It still remains to be seen how such combination is realized in actual development of commercial farms.

6. COST OF OFFSHORE RENEWABLE ENERGY

6.1 General aspects

Offshore renewable energy devices, such as wind turbines, wave energy converters and marine current turbines, are mainly designed to generate electricity for commercial development. In addition to being the green energy, cost of energy becomes the most important criterion for developing such technology. Since both wave energy and tidal turbine technologies are in the early stage of development, while offshore wind turbine technology has already been commercialized, we will discuss the cost issues separately. Due to the lack of industrial development, the cost estimations for wave energy converters and marine current turbines are subjected to significant uncertainties (IEA-OES, 2015). On the other hand, although some detailed data and analyses are available (Gonzalez-Rodriguez, 2017), the offshore wind industry today is a very competitive industry and therefore it is in general not easy to get the information about fabrication and installation costs of wind turbine components and operation and maintenance costs in specific wind farms. Herein, we aim for a review of the offshore wind cost from a general perspective.

Levelized Cost of Electricity or Energy (LCOE) is normally used for comparison of electricity generation cost, which is defined as the total lifetime cost divided by the total amount of electricity generated. Typically, the offshore renewable energy devices are designed with a lifetime of 25 years. The total cost consists of the capital expenditure (CAPEX) and the operational expenditure (OPEX), including the decommissioning cost. The total amount of electricity in terms of kWh is estimated or observed considering the fact that the device is not all time operational at the rated power due to the variation in the wind, wave and tidal current conditions. Typically, offshore wind turbines operate at a capacity factor (which is defined as the average generated power divided by the rated power) ranging from 40%-60%.

In addition to the LCOE, the cost of alternative sources is also a primary consideration when developing new technologies for electricity generation. The economic viability of course also depends on the prices and available capacity of electricity from alternative sources in the region being considered for offshore wind development. In the report by the US Department of the Interior and Department of Energy, Gilman et al. (2016) have considered these factors in terms of Levelized Avoided Costs of Energy (LACE). LACE is a measure of the potential revenue from electricity prices and capacity that is available to a new generator source and hence represents an estimate of the cost to generate the electricity that is displaced by a new project. The difference between LCOE and LACE indicates the net economic value. An example of the estimates was shown in Figure 6.1 for future wind farms in the US offshore regions.

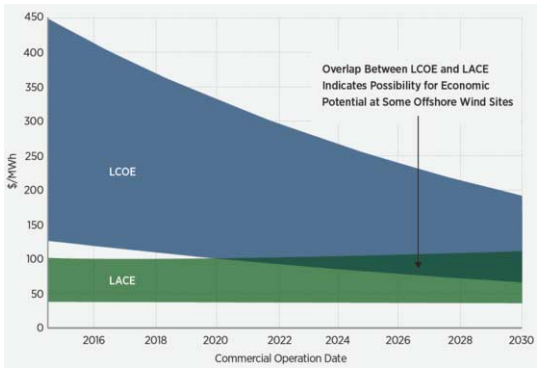

Figure 6.1: Comparison of levelized cost of energy and levelized avoided cost of energy estimates from 2015 to 2030 for future wind farms in the US offshore regions (Gilman et al., 2016)

6.2 Current status and potential for cost reduction

Based on the report from the Joint Research Centre, European Commission (Carlsson, 2014), Magagna & Uihlein (2015) compared the LCOE for alternative renewable energy and conventional energy technologies, as shown in Figure 6.2. The solid bars indicate the cost range as per 2015, while the shaded bars indicate the expected future cost reductions in 2050. As we can see, the LCOE of onshore wind farms is already comparable with that of the small-scale hydro power stations. The LCOE of offshore wind farms today (mainly bottom-fixed monopile wind turbines) is 12-18 Euro cent/kWh, about twice of the onshore counterpart (6.5-11 Euro cent/kWh) and potentially can be reduced to the same level by 2050. But the LCOE of both wave and tidal energy devices today is much higher than other technologies and also shows a larger scatter among the different devices. But there is a big potential for cost reduction if both technologies are commercially developed in large-scale farms.

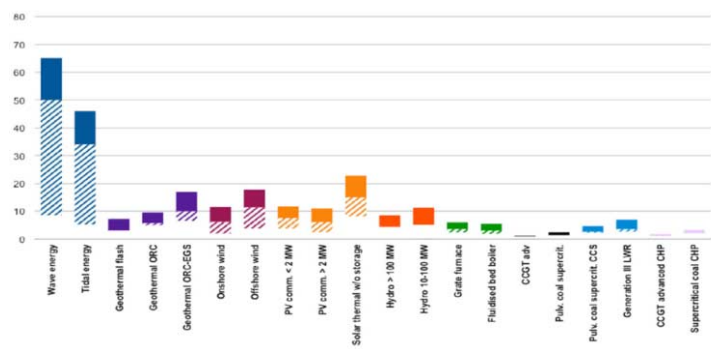

Figure 6.2: LCOE (Euro cent per kWh) for alternative renewable and conventional energy technologies (Magagna & Uihlein, 2015, reproduced based on Carlsson, 2014)

As opposite to the increasing cost in the previous years from 2005 to 2015, we have seen a clear falling trend in costs of offshore wind farms in the last two years (GWEC, 2017b). In particular in the auction for several offshore wind farms in 2016, including Borssele 3 & 4 in the Netherland, Krieger's Flak and Vesterhav in Denmark, the bidders gave very low bids, ranging from 72 Euro/MWh to 60 Euro/MWh as shown in Figure 6.3, which is even lower

than the normal bid for onshore wind farms (Hundleby & Freeman, 2017). In 2017, Dong Energy and EnBW won the bids to build first subsidy-free offshore wind farms in the North and Baltic Seas in Germany (Offshore Wind Industry, 2017). One of the reasons for the low bids is that the offshore wind farms in auction are to be completed by 2025 at the latest. The actual development remains to be seen. But, this reflects the general trend of cost reduction in this industry, due to the improvement and maturation of the offshore wind technology and management as well as the introduction of large-scale (6-8 MW) wind turbines. Moreover, such development is in line with the overall goal for offshore wind industry by 2030, as shown in Figure 6.3.

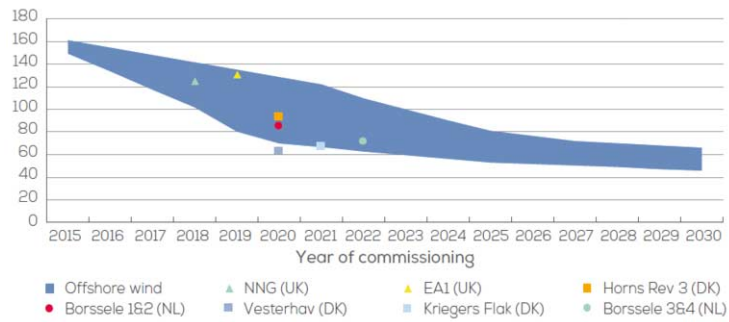

Figure 6.3: Offshore wind LCOE range and trajectory from 2015 to 2030 (Hundleby & Freeman, 2017)

The discussion above is mainly related to offshore bottom-fixed wind turbines. In terms of floating wind turbines, there are not so many turbines that are under testing out at the sea. In addition to the prototypes in Norway, Portugal, Japan and US, Statoil built the first floating wind farms in Scotland based on their Hywind technology with five 6 MW Siemens turbines, which started to operate since October 2017. The cost for developing prototype floating wind turbines is extremely high, but Statoil was able to cut the cost down in their Hywind Scotland project. They also aims for even lower LCOE at 40-60 Euro/MWh by 2030 for large-scale wind farm development (Statoil, 2017a), which will be comparable to bottom-fixed wind turbines.

The offshore wind industry needs further cut the cost down in order to provide cheaper electricity to the market by 2030. Then, it is important to understand the cost structure in today's offshore wind farms and the areas that have a potential for cost reduction. From the life cycle point of view, the cost includes CAPEX and OPEX. Typically, OPEX is about the 10-20% of the total cost. Figure 6.4 shows the CAPEX breakdown for different components and their installation for selected European farms (MAKE Consulting, 2016). As we can see, the wind turbine itself (including rotor, nacelle, gearbox and generator) accounts for 30%. The use of large-size turbines will reduce the average LCOE (Valpy & English, 2014), but probably will not reduce the cost share. The foundation cost is about 13% and could be potentially decreased. Moreover, the total installation cost is about 25%, which is an area that could be further reduced. These two areas with potential cost reduction are also relevant for the ISSC community, in terms of developing novel foundation structures and installation methods. Developing improved vessel access and condition monitoring systems are the ways to reduce the OPEX (Willow & Valpy, 2015).

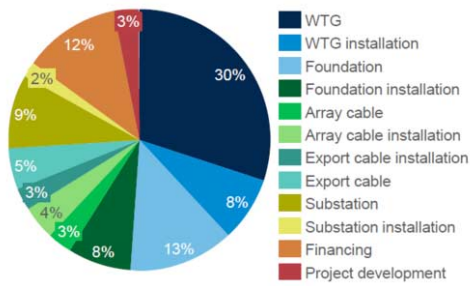

Figure 6.4: Cost breakdown for typical offshore bottom-fixed wind farms in Europe (MAKE Consulting, 2016)

It should be noted that the total cost and the cost breakdown vary significantly from project to project. In particular, an increase in water depth or distance from shore at the wind farm site would have a large impact on the cost share related to foundations and power cables (MAKE Consulting, 2016).

Most of the wave energy converter concepts today are still in the development phase with a typical Technology Readiness Level (TRL) of 5, which is defined as the technology validated (but not fully demonstrated) in relevant environment (industrially relevant environment in the case of key enabling technologies). Some leading WEC concepts have researched TRL 6 and 7, with demonstrations and prototypes at the sea, as shown in Figure 6.5 (Mofor et al., 2014). Individual large-scale tidal stream turbines have been developed and tested at sea, leading to a TRL of 7, but their performance in array needs to be demonstrated (Mofor et al., 2014). In general, the development of the wave energy sector lags that of the tidal energy (IEA-OES, 2015).

The current status about the LCOE for wave and tidal energy is available from the studies by IEA-OES (2015), Magagna & Uihlein (2015) and Astariz & Iglesias (2015). In particular, the study carried out by Astariz & Iglesias (2015) is a thorough review of all the factors that influence the LCOE of wave energy converters.

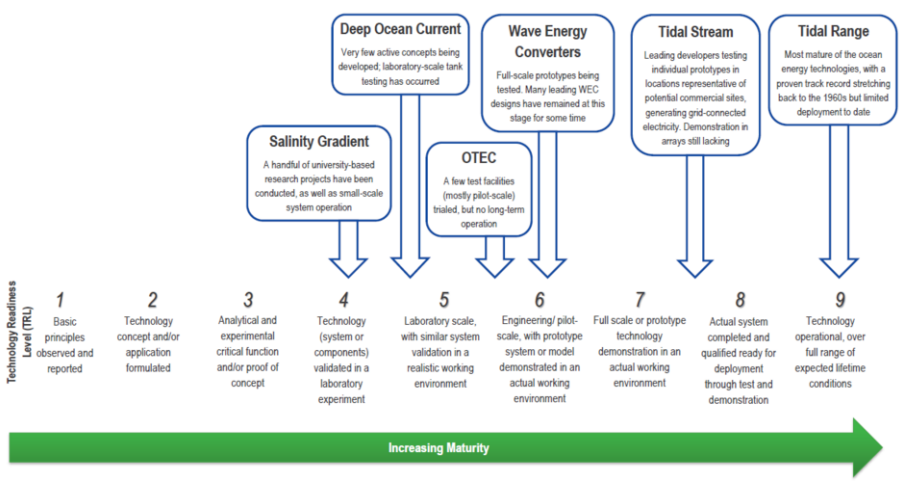

Figure 6.5: Technology Readiness Level (TRL) for ocean energy (Mofor et al., 2014)

Nevertheless, from the cost evaluation point of view, most of the analyses were based on predictions, not direct project experiences. A study (IEA-OES, 2015) was carried out by IEA Technology Collaboration Programme for Ocean Energy Systems (OES) about the LCOE of wave energy, tidal energy and Ocean Thermal Energy Conversion (OTEC) for the current stage of development and the future commercial development. It shows that the current LCOE for wave, tidal and OTEC technologies are very high, at a similar level as shown in Figure 6.2 (Magagna & Uihlein, 2015). The study also compares the cost share of different technologies. A very high OPEX share (40%) was found for tidal energy devices because of access difficulties, as compared to 14% for commercial wave energy devices and 23% for OTEC devices. The study also shows that the OTEC plants at a large scale are economically more attractive that wave and tidal energy technologies, but the geographic distribution of the OTEC resource is limited, similar to the tidal energy resource.

6.3 Cost models and analysis tools

Through years, many cost models and analysis tools have been developed for offshore wind farms (Van de Pieterman et al., 2010; DNV-GL, 2017b; Kaiser & Snyder, 2013) and some for wave energy converters and tidal turbines (Chozas et al, 2014, O'Sullivan & Ardanaz, 2012).

The tools for offshore wind farm development are mainly for operation & maintenance (O&M) planning and cost analysis, with a few for installation cost analysis. Dinwoodie et al. (2015) performed a review and a benchmark study of the O&M tools, including NOWIcob, University of Stavanger Offshore Wind Simulation Model, ECUME Model and Strathclyde University Offshore Wind OPEX Model. ECN has developed an Operation & Maintenance Cost Estimator (OMCE) (Van de Pieterman et al., 2010) since 2010 originally for the Dutch offshore wind industry and now becomes a standard tool for offshore wind farm developers. This tool uses data (including O&M, SCADA, load and response measurements, and condition monitoring data) and experiences gained by the wind farm under consideration and gives better estimate and control of the future O&M costs for the next 1 to 5 years. Based on the same methodology, ECN developed a tool, ECN Install 2.0 (2017), which can be used for installation cost analysis considering explicitly the effect of wind and wave conditions on offshore installation work. Based on the cost database from their projects and public information, DNV-GL recently developed an LCOE tool for offshore wind farms and used in their cost of energy modelling service (DNV-GL, 2017b). In the EERA DTOC project, a software tool, Wind & Economy (2017) was developed for optimization of offshore wind farms based on the integrated modelling of wind climate, large-scale and localized wind farm effects, electrical loss calculations and derivation of economic key figures.

In the EU FP7 research project MARINA Platform (O'Sullivan & Ardanaz, 2012), a cost evaluation tool was developed at the University College Cork and used for cost assessment and comparisons of combined offshore renewable energy devices (including combined wind/wave and combined wind/current devices). As for pure wave energy converters, an open-access tool (Chozas et al, 2014) was developed at Aalborg University for calculation of the LCOE based on the power production of a wave energy converter at a particular location. The users need to provide the power production data, which may derive from lab testing, numerical analysis or sea trials. As mentioned, due to the lack of industry experiences and data, cost evaluation for wave energy and tidal energy projects are subjected to large uncertainties. Research efforts were made to take into account such uncertainties and provide a probabilistic estimation of LCOE (Guanche et al., 2014).

The cost analysis tools are very useful for the developers to understand the cost breakdown of offshore renewable energy devices/farms and the potential areas for cost reduction. Such tools are also used for design optimization of offshore wind turbines (Ashuri et al., 2014; Martinez-Luengo et al., 2017), for minimization of the transport and installation cost (Sarker & Faiz, 2017) and the operation and maintenance cost (Sarker & Faiz, 2016; Martin et al., 2016), for

design optimization of wave energy converters (De Andres et al., 2016), for development of reference models for wave energy converters (Bull et al., 2016) and for comparison of different technologies (Castro-Santos et al., 2017).

7. MAIN CONCLUSIONS AND RECOMMENDATIONS FOR FUTURE WORK

In the last three years, we have seen a promising cost reduction in some of the offshore wind farms in Europe, which brightens the future of the offshore wind industry. This is mainly driven by the use of larger wind turbines and it seems that the turbine size will continuously grow in the near future. In addition to the European market, the offshore wind markets in China and the US are also developing very fast and show big plans ahead. This provides the traditional ship and offshore oil & gas industry a great opportunity to contribute to this green technology development in many ways. For the research point of view, the professional associations like ISSC shall also contribute.

In this report, we do not explicitly deal with resources and environmental conditions that are important for design and operation of offshore wind farms. It does not mean that there is no need for more advanced environmental models or for more measurement data. Joint distribution models of wind, waves and in some cases current (established based on the long-term measurement or hindcast data) are needed for both fatigue and extreme response analysis of offshore wind turbines. This is because time-domain simulations considering the strong coupling between these environmental loads and induced-responses of offshore wind turbines (in particular floating wind turbines) are normally required for design. Distribution models that consider the turbulence intensity factor and their validations against measurement are important to consider in the future. With respect to transport, installation and operation & maintenance of offshore wind turbines, accurate weather forecast models are needed and are important for making correct decisions on the relevant marine operations. A joint effort between this committee and the technical committee on environmental conditions should be made for the next term of ISSC.

Offshore wind turbine design relies on time-domain simulations using numerical codes. In the last ten years, many codes have been developed for both bottom-fixed and floating wind turbines. There is a still strong need for validation of the codes against field measurements. IEA OC3-5 benchmark studies have been the most important research effort on the comparison of these codes and on the validation of the codes against lab and field measurement data in the recent years. ISSC members in the future should still closely follow up this study. In particular, the OC5 study now enters a critical phase that the field measurement in the Alpha Ventus wind farm in Germany with bottom-fixed wind turbines will be used for validation. Because of the difficulty to correctly measure the real wind field and to represent it in numerical simulations, comparing the statistics and/or spectra of the measured responses with the simulated ones for the same short-term environmental parameters might be the best way for code validation. It might be difficult to conduct a direct comparison of response time series and to achieve a good agreement.

In addition to the field measurements, lab measurements are still very useful for feasibility studies of novel concepts and for validation of numerical codes with respect to nonlinear environmental loads and responses. Due to the conflict between the Froude and Reynolds scaling laws, it is not possible to up-scale correctly all of the test results for a geometrically-scale wind turbine. However, the recently developed real-time hybrid testing techniques enable us to focus on specific physical phenomena for testing (for example hydrodynamic loads), while still involving other physical loads (for example wind turbine aerodynamic loads) through numerical simulations and mechanical/hydraulic/electrical actuations. Such experimental techniques still need to be proven for bottom-fixed wind turbines for which high-frequency aerodynamic loads are difficult but need to be actuated in the model test. On the other hand,

the technique for testing wind turbines in a wind tunnel with a movable foundation to simulate the effect of rigid-body motions of a floating wind turbine should be further developed.

Bottom-fixed wind turbines are well developed. However, the challenges related to coupled dynamic response analysis remain in particular for design of larger-size wind turbines with larger foundations. This includes the uncertainties in dealing with the pile-soil interaction, nonlinear wave loads on large-diameter monopile and modelling of the wind field for large rotor plane. Floating wind turbines are the focus of the wind chapter in this report. More prototypes and even more small farms of floating concepts will be built in the near future. It is still not clear at which water depth, a floating wind turbine would be more cost-effective as compared to a bottom-fixed concept. A comparative study of optimal monopile and jacket foundations for varying water depths was conducted, as a first attempt to answer this question. Mooring system design is still one of the challenges for floating wind turbines at moderate water depths (50-100m). Optimization of offshore wind turbines becomes one of the hot topics in recent years and more work needs to be done. Eventually, cost optimization (rather than just weight optimization) and system optimization (rather than just component optimization) are needed.

With respect to marine operations for the offshore wind industry, there are some research in this direction. However, more work are needed. As mentioned, special vessels for transport and installation of offshore wind turbines and supply vessels for transfer of personnel and equipment for maintenance and repair of wind turbine components need to be developed. Again, ISSC with ship specialists can certainly contribute to this direction.

Condition monitoring, maintenance and repair of wind turbine drivetrain and blades are particularly important. It is suggested that this topic can be taken in the next term of the committee together with other committees, dealing with structural health monitoring for marine structures. In the future, this ISSC committee needs to involve the specialists on wind turbine aerodynamics, blade composite materials and mechanical components such as gearbox, to cover the topics related to these wind turbine components.

Extensive research efforts have been made in the sector of wave energy conversion technology, mainly focusing on the power performance and the survivability of WECs using numerical methods, experimental techniques and to some extent, field test data. However, on the other hand, we did not witness the launching of a truly commercial-scale product during the past three years. Lack of full-scale measurement data with good quality and long duration is a general problem for this sector. More efforts in developing large-scale prototypes to gain experiences towards commercialization and to test reliability of the system in real conditions are urgently needed.

There is still no consent in the research community regarding the ideal size of WECs for commercial development. In the offshore wind industry, a clear trend of developing larger-size wind turbines for cost reduction has been observed, and it is the main driving force for the development of novel foundations and new transport/installation vessels or methods. This trend might also be applicable to tidal turbines. To some extent, MW-size WECs are needed for commercial development. However, simply scaling up the dimension of a WEC will not work. Depending on the wave resource conditions, the length of an optimal point absorber or OWC in the wave propagation direction would be about 12-20m for average northern European wave conditions. However, the width of the device, along the direction perpendicular to the wave propagation, can be optimized for a determined rated power.

A number of numerical models and tools (so-called wave-to-wire models) have been developed for global hydrodynamic loads and response analysis as well as for power performance and survivability assessment. In the past, validation of these codes were performed mainly by individual researchers or concept developers. The ongoing IEA OES benchmark study is one

of the important efforts towards WEC modelling verification and validation. A few ISSC members attended this study and some initial results were reported here. ISSC members in the next terms should be continuously involved in this study and report their findings. The effects of nonlinear waves and induced nonlinear loads on the power performance and the responses of WECs in survival conditions have also been studied, using nonlinear potential flow theory and CFD analyses. Further validation against model test results and more importantly against field measurements are needed.

Lab testing of WECs mainly focuses on the hydrodynamic performance (converting the wave kinetic energy into the kinetic energy of the primary movers of the WECs). Survivability tests and complex array tests have also been performed. Power take-off (PTO) systems for WECs should be, in principle, tested at a relatively large scale, and therefore these have to be simplified in hydrodynamic tests of the WECs. The real-time hybrid testing techniques that were developed for floating wind turbines might be interesting to pursue for testing of WECs with simulated PTO behavior.

Mooring system is one of the important components for a floating WEC concept. Studies have been performed to investigate the mooring system effect on power absorption, particularly for point absorbers. The recent work on optimization of mooring systems for cost reduction and development of active mooring lines which can result into a positive power absorption, are promising and further work is encouraged.

Tidal current turbine technology is more mature than wave energy technology. Commercial MW-size tidal current turbines have been deployed and tested. In the near future, there will be more turbines that will be tested at sea. The next stage for the leading developers of tidal turbines is to deploy multiple turbines in a small array for testing.

The measurements at the test sites show significant variations of current speed in time and along the vertical profile. Moreover, the wave-current interaction adds the complexity in the velocity field which significantly influences the dynamic loads on turbine blades. Site measurements with sufficiently long duration are still needed.

Numerical codes based on BEM or CFD have been developed and used to predict hydrodynamic loads on tidal current turbines. Most of the codes are only validated against lab test results. Validation against field measurements is generally lacking or not available to the public. More efforts should be made in this direction. In particular, uncertainties in the field measurements of current conditions and tidal turbine performance and responses need to be well treated for numerical code validation. Numerical codes that can capture structural responses for design are also needed.

REFERENCES

ABS (2014) Guidance Notes on Global Performance Analysis for Floating Offshore Wind Turbine Installations. ABS #206. Houston, Texas, US.

ABS (2015a) Guide for Building and Classing Bottom-Founded Offshore Wind Turbine Installations. ABS #176. Houston, Texas, US.

ABS (2015b) Guide for Building and Classing Floating Offshore Wind Turbine Installations. ABS #195. Houston, Texas, US.

Ahmed, U., Apsley, D.D., Afgan, I., Stallard, T. & Stansby, P.K. (2017) Fluctuating Loads on a Tidal Turbine due to Velocity Shear and Turbulence: Comparison of CFD with Field Data. Renewable Energy, 112, 235-246.

Ahn, D., Shin, S.-C., Kim, S.-Y., Kharoufi, H. & Kim, H.-C. (2017) Comparative Evaluation of Different Offshore Wind Turbine Installation Vessels for Korean West-South Wind Farm. International Journal of Naval Architecture and Ocean Engineering, 9, 45-54.

Allen, J., Sampanis, K., Wan, J., Miles, J. Greaves, D. & Iglesias, G. (2017) Laboratory Tests and Numerical Modelling in the Development of WaveCat. In: Proceedings of the 12th European Wave and Tidal Energy Conference, Aug. 27-Sept. 1, Cork, Ireland.

Allsop, S., Peyrard, C., Thies, P.R., Boulougouris, E. & Harrison, G.P. (2017) Hydrodynamic Analysis of a Ducted, Open Centre Tidal Stream Turbine Using Blade Element Momentum Theory. Ocean Engineering; 141, 531-542.

Antonutti, R., Peyrard, C., Johanning, L., Incecik, A. & Ingram, D. (2014) An Investigation of the Effects of Wind-Induced Inclination on Floating Wind Turbine Dynamics: Heave Plate Excursion. Ocean Engineering, 91, 208-217.

API (2014) Planning, Designing, and Constructing Fixed Offshore Platforms - Working Stress Design. Recommended Practice 2A-WSD.

Arnold, M., Biskup, F. & Cheng, P.W. (2016) Impact of Structural Flexibility on Loads on Tidal Current Turbines. International Journal of Marine Energy, 15, 100-111.

Asgarpour, M. (2016) Assembly, Transportation, Installation and Commissioning of Offshore Wind Farms. In: Ng, C. & Ran, L. (Eds.) Offshore Wind Farms – Technologies, Design and Operation. Elsevier.

Ashuri, T., Zaaijer, M.B., Martins, J.R.R.A., van Bussel, G.J.W. & van Kuik, G.A.M. (2014) Multidisciplinary Design Optimization of Offshore Wind Turbines for Minimum Levelized Cost of Energy. Renewable Energy, 68, 893-905.

Astariz, S. & Iglesias, G. (2015) The Economics of Wave Energy: A Review. Renewable and Sustainable Energy Reviews, 45, 397-408.

ASX (2016) ASX Announcement - Carnegie Wave Energy Report to Shareholders for the Quarter Ended, June 30, 2016.

Atcheson, M., MacKinnon, P. & Elsaesser, B. (2015) A Large Scale Model Experimental Study of a Tidal Turbine in Uniform Steady Flow. Ocean Engineering, 110, 51-61.

AWEA (2012) Offshore Compliance Recommended Practices for Design, Deployment, and Operation of Offshore Wind Turbines in the United States.

Azcona, J., Bouchotrouch, F., Gonzalez, M., Garciandia, J., Munduate, X., Kelberlau, F. & Nygaard, T.A. (2014) Aerodynamic Thrust Modelling in Wave Tank Tests of Offshore Floating Wind Turbines Using a Ducted Fan. Journal of Physics - Conference Series, 524: 012089.

Azcona, J., Palacio, D., Munduate, X., Gonzalez, L. & Nygaard, T.A. (2017) Impact of Mooring Lines Dynamics on the Fatigue and Ultimate Loads of Three Offshore Floating Wind Turbines Computed with IEC 61400-3 Guideline. Wind Energy, 20 (5), 797-813.

Bachynski, E.E., Chabaud, V. & Sauder, T. (2015) Real-Time Hybrid Model Testing of Floating Wind Turbines - Sensitivity to Limited Actuation. Energy Procedia, 80, 2-12.

Bachynski, E.E., Kristiansen, T. & Thys, M. (2017) Experimental and Numerical Investigations of Monopile Ringing in Irregular Finite-Depth Water Waves. Applied Ocean Research, 68, 154-170.

Bachynski, E.E., Thys, M., Chabaud, V.B. & Sauder, T. (2016). Real-Time Hybrid Model Testing of a Braceless Semi-Submersible Wind Turbine. Part II: Experimental Results. In: Proceedings of the 35th International Conference on Ocean, Offshore and Arctic Engineering, Paper No. OMAE2016-54437, June 19-24, Busan, Korea.

Bae, Y.H., Kim, M.H. & Kim, H.C. (2017) Performance Changes of a Floating Offshore Wind Turbine with Broken Mooring Line. Renewable Energy, 101, 364-375.

Barber, R.B., Hill, C.S., Babuska, P.F., Aliseda, A., Wiebe, R. & Motley, M.R. (2017) Adaptive Composites for Load Control in Marine Turbine Blades. In: Proceedings of the ASME 2017 36th International Conference on Ocean, Offshore and Arctic Engineering, OMAE2017-62068, June 25-30, Trondheim, Norway.

Barlow, E., Ozturk D.T., Revie, M., Akartunali, K, Day, A.H. & Boulougouris, E. (2018) A Mixed-Method Optimization and Simulation Framework for Supporting Logistical

Decisions during Offshore Wind Farm Installations. European Journal of Operation Research, 264, 894-906.

Bayati, I., Belloli, M., Bernini, L. & Zasso, A. (2016) Wind Tunnel Validation of AeroDyn within LIFES50+ Project - Imposed Surge and Pitch Tests. Journal of Physics: Conference Series, 753, 092001.

Bayati, I., Belloli, M. & Facchinetti, A. (2017) Wind Tunnel 2-DOF Hybrid/HIL Tests on the OC5 Floating Offshore Wind Turbine. In: Proceedings of the ASME 2017 36th International Conference on Ocean, Offshore and Arctic Engineering, OMAE2017-61763, June 25-30, 2017, Trondheim, Norway.

Bayati, I., Belloli, M., Ferrari, D., Fossati, F. & Giberti, H. (2014). Design of a 6-DoF Robotic Platform for Wind Tunnel Tests of Floating Wind Turbines. Energy Procedia, 53: 313-323.

Battisti, L., Benini, E., Brighenti, A., Raciti Castelli, M., Dell'Anna, S., Dossena, V., Persico, G., Schmidt Paulsen, U. & Pedersen, T.F. (2016) Wind Tunnel Testing of the DeepWind Demonstrator in Design and Tilted Operating Conditions. Engery, 111, 484-497.

Beatty, S., Hall, M., Buckham, B.J., Wild, P. & Bocking, B. (2015) Experimental and Numerical Comparisons of Self-Reacting Point Absorber. Ocean Engineering, 104, 370-386.

Berthelsen, P.A., Bachynski, E.E., Karimirad, M. & Thys, M. (2016). Real-Time Hybrid Model Testing of a Braceless Semi-Submersible Wind Turbine. Part III: Calibration of a Numerical Model. In: Proceedings of the 35th International Conference on Ocean, Offshore and Arctic Engineering, Paper No. OMAE2016-54640, June 19-24, Busan, Korea.

Bhinder, M.A., Rahmati, M.T., Mingham, C.G. & Aggidis, G.A. (2015) Numerical Hydrodynamic Modelling of a Pitch Wave Energy Converter. European Journal of Computational Mechanics, 24 (4), 129-143.

Blackmore T., Myers, L.E. & Bahaj, A.S. (2016) Effects of Turbulence on Tidal Turbines: Implications to Performance, Blade Loads, and Condition Monitoring. International Journal of Marine Energy, 14, 1-26.

Boccotti, P. (2007a) Caisson Breakwaters Embodying an OWC with a Small Opening - Part I: Theory. Ocean Engineering, 34, 806-819.

Boccotti, P. (2007b) Caisson Breakwaters Embodying an OWC with a Small Opening - Part II: A Small-Scale Field Experiment. Ocean Engineering, 34, 820-841.

Borg, M. & Collu, M. (2015a) Frequency-Domain Characteristics of Aerodynamic Loads of Offshore Floating Vertical Axis Wind Turbines. Applied Energy, 155, 629-636.

Borg, M. & Collu, M. (2015b) Offshore Floating Vertical Axis Wind Turbines, Dynamics Modelling State of the Art, Part III: Hydrodynamics and Coupled Modelling Approaches. Renewable and Sustainable Energy Reviews, 46, 296-310.

Bosma, B., Simmons, A., Lomonaco, P., Ruehl, K. & Gunawan, B. (2016) WEC-Sim Phase 1 Validation Testing - Experimental Setup and Initial Results. In: Proceedings of the ASME 2016 35th International Conference on Ocean, Offshore and Arctic Engineering, OMAE2016-54984, June 19-24, Busan, South Korea.

Brennan, F.P., Gao, Z., Landet, E., Le Boulluec, M., Rim, C.W., Sirkar, J., Sun, L.P., Suzuki, H., Thiry, A., Trarieux, F. & Wang, C.M. (2012) Report of Specialist Committee V.4 Offshore Renewable Energy. In: Fricke, W. & Bronsart, R. (Eds.), Proceedings of the 18th International Ship and Offshore Structures Congress (ISSC 2012), 2, 153-199, September 9-13, Rostock, Germany.

Bredmose, H., Lemmer, F., Borg, M., Jurado, A.P., Mikkelsen, R., Larsen, T.S., Fjeldstrup, T., Wei, Y., Lomholt, A.K., Boehm, L. & Armendariz, J.A. (2017) The Triple Spar Campaign - Experiments with a Floating Wind Turbine in Wind, Waves and Blade Pitch Control. In: Proceedings of the EERA DeepWind'2017 Conference, January 18-20, Trondheim, Norway.

Bruinsma, N., Paulsen, B.T. & Jacobsen, N.G. (2017) Validation and Application of a Fully Nonlinear Numerical Wave Tank for Simulating Floating Offshore Wind Turbines. Ocean Engineering, DOI: 10.1016/j.oceaneng.2017.09.054

Bull, D., Jenne, D.S., Smith, C.S., Copping, A.E. & Copeland, G. (2016) Levelized Cost of Energy for a Backward Bent Duct Buoy. International Journal of Marine Energy, 16, 220-234.

BV (2015) Classification and Certification of Floating Offshore Wind Turbines. Guidance Note NI 572. Marine & Offshore Division, BV, Neuilly sur Seine Cedex, France.

Byrne, B.W., McAdam, R., Burd, H.J., Houlsby. G.T., Martin, C.M., Zdrakovic, L., Taborda, D.M.G., Potts, D.M., Jardine, R.J. Sideri, M., Schroeder, F.C., Gavin, K., Doherty, P., Igoe. D., Muir Wood, A., Kallehave, D. & Skov Gretlund, J. (2015) New Design Methods for Large Diameter Piles under Lateral Loading for Offshore Wind Applications. In: Proceedings of the Third International Symposium on Frontiers in Offshore Geotechnics (ISFOG 2015), June 12-15, Oslo Norway.

Cahill, B. (2014) Resource Scalability at Wave Energy Test Sites. In: Proceedings of the ASME 2014 33rd International Conference on Ocean, Offshore and Arctic Engineering. Paper No. OMAE2014-24628, June 8-13, San Francisco, California, USA.

Carbon Trust (2005) Guidelines on Design and Operation of Wave Energy Converters.

Carlsson, J. (2014) Energy Technology Reference Indicator Projections for 2010-2050. European Commission, Joint Research Centre (JRC), Institute for Energy and Transport.

Castro-Santos, L., Martins, E. & Guedes Soares, C. (2017) Economic Comparison of Technological Alternatives to Harness Offshore Wind and Wave Energies. Energy, 140, 1121-1130.

Chabaud, V. (2016) Real-Time Hybrid Model Testing of Floating Wind Turbines. PhD Thesis, Department of Marine Technology, Norwegian University of Science and Technology. Trondheim, Norway.

Cheng, Z.S. (2016). Integrated Dynamic Analysis of Floating Vertical Axis Wind Turbines. PhD Thesis. Department of Marine Technology, Norwegian University of Science and Technology.

Cheng, Z.S., Madsen, H.A., Gao, Z. & Moan, T. (2016) Aerodynamic Modelling of Floating Vertical Axis Wind Turbines Using the Actuator Cylinder Flow Method. Energy Procedia, 94, 531-543.

Cheng, Z.S., Madsen, H.A., Gao, Z. & Moan, T. (2017a) A Fully Coupled Method for Numerical Modelling and Dynamic Analysis of Floating Vertical Axis Wind Turbines. Renewable Energy, 107, 604-619.

Cheng, Z.S., Madsen, H. A., Chai, W., Gao, Z. & Moan, T. (2017b) A Comparison of Extreme Structural Responses and Fatigue Damage of Semi-Submersible Type Floating Horizontal and Vertical Axis Wind Turbines. Renewable Energy, 108, 207-219.

Cheng, Z.S., Wang, K., Gao, Z. & Moan, T. (2017c) A Comparative Study on Dynamic Responses of Spar-Type Floating Horizontal and Vertical Axis Wind Turbines. Wind Energy, 20 (2), 305-323.

Chew, K.-H., Tai, K., Ng, E.Y.K. & Muskulus, M. (2016). Analytical Gradient-Based Optimization of Offshore Wind Turbine Substructures under Fatigue and Extreme Loads. Marine Structures, 47: 23-41.

Chowdhury, A.M., Akimoto, H. & Hara, Y. (2016) Comparative CFD Analysis of Vertical Axis Wind Turbine in Upright and Tilted Configuration. Renewable Energy, 85, 327-337.

Chozas, J.F., Kofoed, J.P. & Jensen, N.E.H. (2014) User Guide – COE Calculation Tool for Wave Energy Converters. Aalborg University.

Clean Technica (2016) Turbine Blade Assembly at the Block Island Wind Farm. https://cleantechnica.com/2016/08/24/turbines-block-island-first-us-offshore-wind-farm/

Coiro, D.P., Troise, G., Scherillo, F., De Marco, A., Calise, G. & Bizzarrini, N. (2017) Development, Deployment and Experimental Test on the Novel Tethered System GEM for Tidal Current Energy Exploitation. Renewable Energy, 114, 323-336.

Colicchio, G., Santic, I., Peviani, M.A., Danelli, A. & Colucci, A. (2017) Numerical and Experimental Analysis of the Efficiency of an Oscillating Water Column. In: Proceedings of the 12th European Wave and Tidal Energy Conference, Aug. 27-Sept. 1, Cork, Ireland.

Collu, M., Maggi, A., Gualeni, P., Rizzo, C.M. & Brennan, F. (2014) Stability Requirements for Floating Offshore Wind Turbine (FOWT) during Assembly and Temporary Phases: Overview and Application. Ocean Engineering, 84, 164-175.

Combourieu, A., Lawson, M., Babarit, A., Ruehl, K., Roy, A., Costello, R., Laporte Weywada, P. & Bailey, H. (2015) WEC3: Wave Energy Converter Code Comparison Project. In: Proceedings of the 11th European Wave and Tidal Energy Conference (EWTEC), September 6-11, Nantes, France.

Cornett, A., Toupin, M., Baker, S., Piche, S. & Nistor, I. (2014) Appraisal of IEC Standards for Wave and Tidal Energy Resource Assessment. In: Proceedings of the International Conference on Ocean Energy, November 4-6, Halifax, Canada.

Correia da Fonseca, F.X., Gomes, R.P.F., Henriques, J.C.C., Gato, L.M.C. & Falcao, A.F.O. (2016) Model Testing of an Oscillating Water Column Spar-Buoy Wave Energy Converter Isolated and in Array: Motions and Mooring Forces. Energy, 112, 1207-1218.

Costello, R., Padeletti, D., Davidson, J. & Ringwood, J.V. (2016) Comparison of Numerical Simulations with Experimental Measurements for the Response of a Modified Submerged Horizontal Cylinder Moored in Waves. In: Proceedings of the ASME 2014 33rd International Conference on Ocean, Offshore and Arctic Engineering. Paper No. OMAE2014-24270, June 8-13, San Francisco, California, USA.

Creech, A.C.W., Borthwick, A.G.L. & Ingram, D. (2017) Effects of Support Structures in an LES Actuator Line Model of a Tidal Turbine with Contra-Rotating Rotors. Energies, 10, 726.

Dalgic, Y., Lazakis, I., Dinwoodie, I., McMillan, D. & Revie, M. (2015) Advanced Logistics Planning for Offshore Wind Farm Operation and Maintenance Activities. Ocean Engineering, 101, 211-226.

Damiani, R.R., Song, H., Robertson, A.N. & Jonkman, J.M. (2013) Assessing the Importance of Nonlinearities in the Development of a Substructure Model for the Wind Turbine CAE Tool FAST. In: Proceedings of the ASME 32nd International Conference on Ocean, Offshore and Arctic Engineering, June 9-14, Nantes, France.2013.

Davidson, J., Giorgi, S. & Ringwood, J.V. (2016) Identification of Wave Energy Device Models from Numerical Wave Tank Data - Part 1: Numerical Wave Tank Identification Tests. IEEE Transactions on Sustainable Energy, 7, 1012-1019.

De Andres, A., Maillet, J., Todalshaug, J.H., Moller, P. & Jeffrey, H. (2016) On the Optimum Sizing of a Real WEC from a Techno-Economic Perspective. In: Proceedings of the 35th International Conference on Ocean, Offshore and Arctic Engineering, Paper No. OMAE2016-54110, June 19-24, Busan, Korea.

De Ridder, E.-J., Otto, W., Zondervan, G.-J., Huijs, F. & Vaz, G. (2014) Development of a Scaled-Down Floating Wind Turbine for Offshore Basin Testing. In: Proceedings of the 33rd International Conference on Ocean, Offshore and Arctic Engineering, Paper No. OMAE2014-23441, June 8-13, San Francisco, California, USA.

Ding, H.Y., Liu, Y.G., Zhang, P.Y. & Le, C.H. (2015) Model Tests on the Bearing Capacity of Wide-Shallow Composite Bucket Foundations for Offshore Wind Turbines in Clay. Ocean Engineering, 103, 114-122.

Dinwoodie, I., van Endrerud, O.-E., Hofmann, M., Martin, R. & Sperstad, I.B. (2015) Reference Cases for Verification of Operation and Maintenance Simulation Models for Offshore Wind Farms. Wind Engineering, 39, 1-14.

DNV (2013) Design of Floating Wind Turbine structure. DNV-OS-J103. Hovik, Norway.

DNV (2014) Offshore Standard: Design of Offshore Wind Turbine Structures, DNV-OS-J101. Høvik, Norway.

DNV-GL (2016) Support Structures for Wind Turbines. DNVGL-ST-0126. Hovik, Norway.

DNV-GL (2017a) https://www.dnvgl.com/cases/coupled-analysis-of-floating-wind-turbines-86622

DNV-GL (2017b) https://www.dnvgl.com/services/cost-of-energy-modelling-for-offshore-wind-farms-5298

Driscoll, F., Jonkman, J., Robertson, A., Sirnivas, S., Skaare, B. & Nielsen, F.G. (2016) Validation of a FAST Model of the Statoil-Hywind Demo Floating Wind Turbine. Energy Procedia, 94, 3-19.

Duan, F., Hu, Z.Q., Liu, G.L. & Wang, J. (2016a) Experimental Comparisons of Dynamic Properties of Floating Wind Turbine Systems based on Two Different Rotor Concepts. Applied Ocean Research, 58, 266-280.

Duan, F., Hu, Z.Q. & Niedzwecki, J.M. (2016b) Model Test Investigation of a Spar Floating Wind Turbine. Marine Structures, 49, 76-96.

Dunbar, A.J., Craven, B.A. & Paterson, E.G. (2015) Development and Validation of a Tightly Coupled CFD/6-DOF Solver for Simulating Floating Offshore Wind Turbine Platforms. Ocean Engineering, 110, 98-105.

EC (2017) European Commision - 2030 Energy Strategy. https://ec.europa.eu/energy/node/163

ECN Install 2.0 (2017) https://www.ecn.nl/news/item/ecn-install-20-smart-planning-saves-costs-offshore-1

Elhanafi, A. (2016) Prediction of Regular Wave Loads on a Fixed Offshore Oscillating Water Column - Wave Energy Converter Using CFD. Journal of Ocean Engineering and Science, 1 (4), 268-283.

Elhanafi, A., Macfarlane, G., Fleming, A. & Leong, Z. (2017a) Investigations on 3D Effects and Correlation between Wave Height and Lip Submergence of an Offshore Stationary OWC Wave Energy Converter. Applied Ocean Research, 64, 203-216.

Elhanafi, A., Macfarlane, G. Fleming, A. & Leong Z. (2017b) Experimental and Numerical Investigations on the Intact and Damage Survivability of a Floating–moored Oscillating Water Column Device. Applied Ocean Research, 68, 276-292.

Esteban, M.D., Counago, B., Lopez-Gutierrez, J.S., Negro, V. & Vellisco, F. (2015) Gravity Based Support Structures for Offshore Wind Turbine Generators: Review of the Installation Process. Ocean Engineering, 110, 281-291.

Etemaddar, M., Blanke, M., Gao, Z. & Moan, T. (2016) Response Analysis and Comparison of a Spar-Type Floating Offshore Wind Turbine and an Onshore Wind Turbine under Blade Pitch Controller Faults. Wind Energy, 19 (1), 35-50.

Ewart, L.B., Thies, P.R., Stratford, T. & Barltrop, N. (2017) Optimising Structural Loading and Power Production for Floating Wave Energy Converters. In: Proceedings of the 12th European Wave and Tidal Energy Conference, Aug. 27-Sept. 1, Cork, Ireland.

EWEA (2015) Wind Energy Scenarios for 2030. European Wind Energy Association,

Fagan, E.M., Kennedy, C.R., Leen, S.B. & Goggins, J. (2016) Damage Mechanics Based Design Methodology for Tidal Current Turbine Composite Blades. Renewable Energy, 97, 358-372.

Falcao, A.F.O. & Henriques, J.C.C. (2014) Model-Prototype Similarity of Oscillating-Water-Column Wave Energy Converters. International Journal of Marine Energy, 6, 18-34.

Falcao, A.F.O. & Henriques, J.C.C. (2016) Oscillating-Water-Column Wave Energy Converters and Air Turbines: A Review. Renewable Energy, 85, 1391-1424.

Fan, W., Pan, Y., Zhang, D., Xu, C., Qiang, Y. & Chen, Y. (2016). Experimental Study on the Performance of a Wave Pump for Artificial Upwelling. Ocean Engineering, 113, 191-200.

Faudot, C. & Dahlhaug, O.G. (2012) Prediction of Wave Loads on Tidal Turbine Blades. Energy Procedia, 20, 116-133.

Feyzollahzadeh, M., Mahmooda, M.J., Nikravesh, S.M.Y. & Jamali, J. (2016) Wind Load Response of Offshore Wind Turbine Towers with Fixed Monopile Platform. Journal of Wind Engineering and Industrial Aerodynamics, 158, 122-138.

Finucane, Z. & Hall, R.A. (2016) Practical Aspects of the Block Island Wind Plant Structures. In: Proceedings of the OCEANS 2016 MTS/IEEE Monterey, IEEE Xplore Digital Library.

Fleming, A. & Macfarlane, G. (2017a) In-Situ Orifice Calibration for Reversing Oscillating Flow and Improved Performance Prediction for Oscillating Water Column Model Test Experiments. International Journal of Marine Energy, 17, 147-155.

Fleming, A. & Macfarlane, G. (2017b) Experimental Flow Field Comparison for a Series of Scale Model Oscillating Water Column Wave Energy Converters. Marine Structures, 52, 108-125.

Foglia, A., Gottardi, G., Govoni, L. & Ibsen, L.B. (2015) Modelling the Drained Response of Bucket Foundations for Offshore Wind Turbines under General Monotonic and Cyclic Loading. Applied Ocean Research, 52, 80-91.

Folley, M. (2016) Numerical Modelling of Wave Energy Converters: State-of-the-Art Techniques for Single Devices and Arrays, Elsevier / Academic Press.

FONSWEC (2017) http://research.engr.oregonstate.edu/nnmrec-data/opendata/wave/WEC-Sim/

Fowler, M.J., Goupee, A.J., Allen, C., Viselli, A. & Dagher, H. (2017) 1:52 Scale Testing of the First US Commerical Scale Floating Wind Turbine, VolturnUS – Testing Overview and the Evolution of Scale Model Testing Methods. In: Proceedings of the ASME 2017 36th International Conference on Ocean, Offshore and Arctic Engineering, OMAE2017-61864, June 25-30, 2017, Trondheim, Norway.

Gao, Z., Bingham, H.B., Nicholls-Lee, R., Adam, F., Karmakar, D., Karr, D.G., Catipovic, I., Colicchio, G., Sheng, W.A., Liu, P.F., Takaoka, Y., Slätte, J., Shin, H.K., Mavrakos, S.A., Jhan, Y.T. & Ren, H.R. (2015) Report of Specialist Committee V.4 Offshore Renewable Energy. In: Guedes Soares, C. & Garbatov, Y. (Eds.), Proceedings of the 19th International Ship and Offshore Structures Congress (ISSC 2015), 2, 669-722, September 7-10, Cascais, Portugal.

Gao, Z., Moan, T., Wan, L. & Michailides, C. (2016) Comparative Numerical and Experimental Study of Two Combined Wind and Wave Energy Concepts. Journal of Ocean Engineering and Science, 1 (1), 36-51.

Gaurier, B., Germain, G., Facq, J.V., Johnstone, C.M., Grant, A.D., Day, A.H., Nixon, E., Di Felice, F. & Costanzo, M. (2015) Tidal Energy 'Round Robin' Tests Comparisons between Towing Tank and Circulating Tank Results. International Journal of Marine Energy, 12, 87-109.

Giberti, H. & Ferrari, D. (2015) A Novel Hardware-In-the-Loop Device for Floating Offshore Wind Turbines and Sailing Boats. Mechanism and Machine Theory, 85, 82-105.

Gilman, P., Maurer, B., Feinberg, L., Duerr, A., Peterson, L., Musial, W., Beiter, P., Golladay, J., Stromberg, J., Johnson, I., Boren, D. & Moore, A. (2016) National Offshore Wind Strategy: Facilitating the Development of the Offshore Wind Industry in the U.S., Report of the US Department of the Interior and the US Department of Energy.

Gintautas, T., Sørensen, J.D. & Vatne, S.R. (2016) Towards a Risk-Based Decision Support for Offshore Wind Turbine Installation and Operation & Maintenance. Energy Procedia, 94, 207-217.

Giorgi, G. & Ringwood, J.V. (2016) Implementation of Latching Control in a Numerical Wave Tank with Regular Waves. Journal of Ocean Engineering and Marine Energy, 2, 211-226.

GL Garrad Hassan (2013) A Guide to UK Offshore Wind Operations and Maintenance.

Gonzalez-Rodriguez, A.G. (2017) Review of Offshore Wind Farm Cost Components. Energy for Sustainable Development, 37, 10-19.

Guo, X.X., Gao, Z., Yang, J.M. & Moan, T. (2017a) Hydrodynamic Loads on a Tidal Turbine in Random Seas. In: Proceedings of the 12th European Wave and Tidal Energy Conference, Aug. 27-Sept. 1, Cork, Ireland.

Guo, X.X., Gao, Z., Yang, J.M., Moan, T., Lu, H.N., Li, X. & Lu, W.Y. (2017b) The Effects of Surface Waves and Submergence on the Performance and Loading of a Tidal Turbine. In: Proceedings of the ASME 2017 36th International Conference on Ocean, Offshore and Arctic Engineering, OMAE2017-62233, June 25-30, Trondheim, Norway.

Goupee, A. J., Kimball, R.W. & Dagher, H.J. (2017) Experimental Observations of Active Blade Pitch and Generator Control Influence on Floating Wind Turbine Response. Renewable Energy, 104, 9-19.

Gradowski, M., Alves, M., Gomes, R.P.F. & Henrigues, J.C.C. (2017) Integration of a Hydrodynamic Negative Spring Concept into the OWC Spar Buoy. In: Proceedings of the 12th European Wave and Tidal Energy Conference, Aug. 27-Sept. 1, Cork, Ireland.

Graf, P.A., Stewart, G., Lackner, M., Dykes, K. & Veers, P. (2016) High-Throughput Computation and the Applicability of Monte Carlo Integration in Fatigue Load Estimation of Floating Offshore Wind Turbines. Wind Energy, 19 (5), 861-872.

Green Tech Media (2017) https://www.greentechmedia.com/articles/read/an-illustrated-guide-to-the-growing-size-of-wind-turbines#gs.QV0Ro3Q

Grogan, D.M., Leen, S.B., Kennedy, C.R. & Bradaigh, C.M. (2013) Design of Composite Tidal Turbine Blades. Renewable Energy, 57, 151-162.

Guachamin-Acero, W.I. (2016). Assessment of Marine Operations for Offshore Wind Turbine Installation with emphasis on Response-Based Operational Limits. PhD Thesis. Department of Marine Technology, Norwegian University of Science and Technology.

Guachamin-Acero, W., Gao, Z. & Moan, T. (2017a) Methodology for Assessment of the Allowable Sea States during Installation of an Offshore Wind Turbine Transition Piece Structure onto a Monopile Foundation. Journal of Offshore Mechanics and Arctic Engineering, 139 (6), 061901.

Guachamin-Acero, W., Gao, Z. & Moan, T. (2017b) Numerical Study of a Novel Concept for Installing the Tower and Rotor Nacelle Assembly of Offshore Wind Turbines Based on the Inverted Pendulum Principle. Journal of Marine Science and Application, 16 (3), 243-260.

Guachamin-Acero, W., Li, L., Gao, Z. & Moan, T. (2016). Methodology for Assessment of the Operational Limits and Operability of Marine Operations. Ocean Engineering, 125, 308-327.

Guanche, R., de Andres, A.D., Simal, P.D., Vidal, C. & Losada, I.J. (2014) Uncertainty Analysis of Wave Energy Farms Financial Indicators. Renewable Energy, 68, 570-580.

Guanche, R., Martini, M., Jurado, A. & Losada, I.J. (2016) Walk-to-Work Accessibility Assessment for Floating Offshore Wind Turbines. Ocean Engineering, 116, 216-225.

Guignier, L., Courbois, A., Mariani, R. & Choisnet, T. (2016) Multibody Modelling of Floating Offshore wind Turbine Foundation for Global Loads Analysis. In: Proceedings of the 26th International Ocean and Polar Engineering Conference, June 26-July 1, Rhodes, Greece.

Gutierrez-Romero, J.E., Garcia-Espinosa, J., Servan-Camas, B. & Zamora-Parra, B. (20169 Non-Linear Dynamic Analysis of the Response of Moored Floating Structures. Marine Structures, 49, 116-137.

Guzman, R.F. & Cheng, P.W. (2016) Recommendations for Load Validation of an Offshore Wind Turbine with the Use of Statistical Data: Experiences from Alpha Ventus. Journal of Physics – Conference Series, 749, 012017.

GWEC (2017a) http://gwec.net/global-figures/global-offshore/#

GWEC (2017b) Global Wind Report 2016 - Annual Market Update. Global Wind Energy Council, Brussels, Belgium.

Hall, M. & Goupee, A. (2015) Validation of a Lumped-Mass Mooring Line Model with DeepCwind Semi-Submersible Model Test Data. Ocean Engineering, 104, 590-603.

Hall, M., Goupee, A. & Jonkman, J. (2017) Development of Performance Specifications for Hybrid Modelling of Floating Wind Turbines in Wave Basin Tests. Journal of Ocean Engineering and Marine Energy, DOI: 10.1007/s40722-017-0089-3

Halvorsen-Weare, E.E., Gundegjerde, C., Halvorsen, I.B., Hvattum, L.M. & Nonås L.M. (2013) Vessel Fleet Analysis for Maintenance Operations at Offshore Wind Farms. Energy Procedia, 35, 167-176.

Hann, M., Greaves, D. & Raby, A. (2015) Snatch Loading of a Single Taut Moored Floating Wave Energy Converter due to Focussed Wave Groups. Ocean Engineering, 96, 258-271.

Hansen, A.H. & Pedersen, H.C. (2016) Optimal Configuration of a Discrete Fluid Power Force System Utilised in the PTO for WECs. Ocean Engineering, 117, 88-98.

Hara, N., Tsujimoto, S., Nihei, Y., Iijima, K. & Konishi, K. (2017) Experimental Validation of Model-Based Blade Pitch Controller Design for Floating Wind Turbines: System Identification Approach. Wind Energy, 20 (7), 1187-1206.

Harnois, V., Weller, S.D., Johanning, L., Thies, P.R., Le Boulluec, M., Le Roux, D., Soul, V. & Ohana, J. (2015) Numerical Model Validation for Mooring Systems: Method and Application for Wave Energy Converters. Renewable Energy, 75, 869-887.

Harper, P.W. & Hallett, S.R. (2015) Advanced Numerical Modelling Techniques for the Structural Design of Composite Tidal Turbine Blades. Ocean Engineering, 96, 272-283.

Hatledal, L.I., Zhang, H.X., Halse, K.H. & Hildre, H.P. (2017) Numerical Study for a Catamaran Gripper-Monopile Mechanism of a Novel Offshore Wind Turbine Assembly. In: Proceedings of the ASME 36th International Conference on Ocean, Offshore and Arctic Engineering, OMAE2017-62342, June 25-30, Trondheim, Norway.

Hirdaris, S.E., Bai, W., Dessi, D., Ergin, A., Gu, X., Hermundstad, O.A., Huijsmans, R., Iijima, K., Nielsen, U.D., Parunov, J., Fonseca, N., Papanikolaou, A., Argyriadis, K. & Incecik, A. (2014) Loads for Use in the Design of Ships and Offshore Structures. Ocean Engineering, 78, 131-174.

Holst, M.A., Dahlhaug, O.G. & Faudot, C. (2015) CFD Analysis of Wave-Induced Loads on Tidal Turbine Blades. IEEE Journal of Oceanic Engineering; 40 (3), 506-521.

Horn, J.T.H., Krokstad, J.R. & Amdahl, J. (2016) Hydroelastic Contributions to Fatigue Damage on a Large Monopile. Energy Procedia, 94, 102-114.

Hsu, W.-T., Thiagarajan, K.P. & Manuel, L. (2017) Extreme Mooring Tensions due to Snap Loads on a Floating Offshore Wind Turbine System. Marine Structures, 55, 182-199.

Hsu, W.Y., Yang, R.Y., Chang, F.N., Wu, H.T. & Chen, H.H. (2016) Experimental Study of Floating Offshore Platform in Combined Wind/Wave/Current Environment. International Journal of Offshore and Polar Engineering, 26 (2), 125-131.

Huijs, F., de Ridder, E.-J. & Savenije, F. (2014) Comparison of Model Tests and Coupled Simulations for a Semi-Submersible Floating Wind Turbine. In: Proceedings of the 33rd International Conference on Ocean, Offshore and Arctic Engineering, Paper No. OMAE2014-23217, June 8-13, San Francisco, California, USA.

Hundleby, G. & Freeman, K. (2017) Unleashing Europe's Offshore Wind Potential – A New Resource Assessment. BVG Associates.

IEA (2015). Projected Costs of Generating Electricity – 2015 Edition.

IEA (2017) https://community.ieawind.org/task30/home

IEA-OES (2015) International Levelized Cost of Energy for Ocean Energy Technologies – An Analysis of the Development Pathway and Levelized Cost of Energy Trajectories of Wave, Tidal and OTEC Technologies. IEA Technology Collaboration Programme for Ocean Energy Systems (OES).

IEA-OES (2016) Annual Report of Ocean Energy Systems (OES).

IEC (2009) Wind Turbines – Part 3: Design Requirements for Offshore Wind turbines, IEC 61400-3, First Edition. International Electrotechnical Commission.

Irving, M. (2017) Europe's Largest Offshore Wind Farm Boots up in the Netherlands. Available online. https://newatlas.com/gemini-wind-farm-netherlands-opens/49428/

ISO (2007) Petroleum and Natural Gas Industries - Fixed Steel Offshore Platforms. ISO 19902, First Edition.

ITTC (2014) Recommended Guideline on Wave Energy Converter Model Test Experiments. Specialist Committee on Testing of Marine Renewable Devices of the 27th ITTC, Report 7.5-02-07-03.7.

Jamalkia, A., Ettefagh, M.M. & Mojtahedi, A. (2016) Damage Detection of TLP and Spar Floating Wind Turbine Using Dynamic Response of the Structure. Ocean Engineering, 125, 191-202.

Kaufer, D., Cosack, N., Boker, C., Seidel, M. & Kuhn, M. (2009) Integrated Analysis of the Dynamics of Offshore Wind Turbines with Arbitrary Support Structures. In: Proceedings of the European Wind Energy Conference 2009, March 16-19, Marseille, France.

Jeon, M., Lee, S. & Lee, S. (2014) Unsteady Aerodynamics of Offshore Floating Wind Turbines in Platform Pitching Motion Using Vortex Lattice Method. Renewable Energy, 65, 207-212.

Jiang, Z., Moan, T. & Gao, Z. (2015) A Comparative Study of Shutdown Procedures on the Dynamic Responses of Wind Turbines. Journal of Offshore Mechanics and Arctic Engineering, 137, 011904.

Jonkman, J. & Bir, G. (2010) Recent Analysis Code Development at NREL. Sandia Blade Workshop.

Jonkman, J., Butterfield, S., Musial, W. & Scott, G. (2009) Definition of a 5-MW Reference Wind Turbine for Offshore System Development. National Renewable Energy Laboratory (NREL), Golden, CO, US.

Jose, J., Choi, S.J., Lee, K.H. & Gudmestad, O.T. (2016a) Breaking Wave Forces on an Offshore Wind Turbine Foundation (Jacket Type) in the Shallow Water. In: Proceedings of the 26th International Ocean and Polar Engineering Conference, June 26-July 1, Rhodes, Greece.

Jose, J., Podrazka, O., Obhrai, C., Gudmestad, O.T. & Cieslikiewicz, W. (2016b) Methods for Analysing Wave Slamming Loads on Truss Structures Used in Offshore Wind Applications based on Experimental Data. International Journal of Offshore and Polar Engineering, 26 (2), 100-108.

Kaiser, M.J. & Snyder, B.F. (2013) Modelling Offshore Wind Installation Costs on the U.S. Outer Continental Shelf. Renewable Energy, 50, 676-691.

Kamath, A., Bihs, H. & Arntsen., Ø.A. (2015) Numerical Modelling of Power Take-Off Damping in an Oscillating Water Column Device. International Journal of Marine Energy, 10, 1-16.

Kanner, S.A.C. (2015) Design, Analysis, Hybrid Testing and Orientation Control of a Floating Platform with Counter-Rotating Vertical-Axis Wind Turbines. PhD Thesis, Department of Mechanical Engineering, University of California, Berkeley.

Karimirad, M., Bachynski, E.E., Berthelsen, P.A. & Ormberg, H. (2017) Comparison of Real-Time Hybrid Model Testing of a Braceless Semi-Submersible Wind Turbine and Numerical Simulations. In: Proceedings of the ASME 2017 36th International Conference on Ocean, Offshore and Arctic Engineering, OMAE2017-61121, June 25-30, 2017, Trondheim, Norway.

Karimirad, M. & Michailides, C. (2015) V-Shaped Semi-Submersible Offshore Wind Turbine: An Alternative Concept for Offshore Wind Technology. Renewable Energy, 83, 126-143.

Karmakar, D., Bagbanci, H. & Guedes Soares, C. (2016) Long-Term Extreme Load Prediction of Spar and Semi-Submersible Floating Wind Turbines Using the Environmental Contour Method. Journal of Offshore Mechanics and Arctic Engineering, 138 (2), 021601.

Katsouris, G. & Savenije, L.B. (2017) Offshore Wind Access 2017. ECN-E-16-013.

Kempener, R. & Neumann, F. (2014) IRENA Ocean Energy Technology Brief - Tidal Energy. International Renewable Energy Agency.

Koch, C., Lemmer, F., Borisade, F., Matha, D. & Cheng, P.W. (2016) Validation of INNWIND.EU Scaled Model Tests of a Semisubmersible Floating Wind Turbine. In: Proceedings of the 26th (2016) International Ocean and Polar Engineering Conference, June 26-July 1, Rhodes, Greece.

Korde, U.A. (2015) Near-Optimal Control of a Wave Energy Device in Irregular Waves with Deterministic-Model Driven Incident Wave Prediction. Applied Ocean Research, 53, 31-45.

Kvittem, M.I. & Moan, T. (2015) Time Domain Analysis Procedures for Fatigue Assessment of a Semi-Submersible Wind Turbine. Marine Structures, 40, 38-59.

LaNier, M.W. (2005) LWST Phase I Project Conceptual Design Study: Evaluation of Design and Construction Approaches for Economical Hybrid Steel/Concrete Wind Turbine Towers. National Renewable Energy Laboratory, Golden, CO, US.

Leble, V. & Barakos, G. (2016a) Demonstration of a Coupled Floating Offshore Wind Turbine Analysis with High-Fidelity Methods. Journal of Fluids and Structures, 62, 272-293.

Leble, V. & Barakos, G.N. (2016b) A Coupled Floating Offshore Wind Turbine Analysis with High-Fidelity Methods. Energy Procedia, 94, 523-530.

Leimeister, M., Bachynski, E.E., Muskulus, M. & Thomas, P. (2016) Rational Upscaling of a Semi-Submersible Floating Platform Supporting a Wind Turbine. Energy Procedia, 94, 434-442.

Lemmer, F., Raach, S., Schlipf, D. & Cheng, P.W. (2016) Parametric Wave Excitation Model for Floating Wind Turbines. Energy Procedia, 94, 290-305.

Li, L. (2016). Dynamic Analysis of the Installation of Monopiles for Offshore Wind Turbines. PhD Thesis. Department of Marine Technology, Norwegian University of Science and Technology.

Li, L., Gao, Z. & Moan, T. (2015) Response Analysis of a Non-Stationary Lowering Operation for an Offshore Wind Turbine Monopile Substructure. Journal of Offshore Mechanics and Arctic Engineering, 137 (5), 051902.

Li, L., Guachamin-Acero, W.G., Gao, Z. & Moan, T. (2016) Assessment of Allowable Sea States during Installation of Offshore Wind Turbine Monopiles with Shallow Penetration in the Seabed. Journal of Offshore Mechanics and Arctic Engineering, 138 (4), 041902.

Li, Q., Kamada, Y., Maeda, T., Murata, J., Iida, K. & Okumura, Y. (2016) Fundamental Study on Aerodynamic Force of Floating Offshore Wind Turbine with Cyclic Pitch Mechanism. Energy, 99, 20-31.

Li, X.F., Liang, C.W., Boontanom, J., Martin, D., Ngo, K., Parker, R. & Zuo, L. (2017) Design, Fabrication and Testing of Wave Energy Converters (WECs) using Different Power Take-Off with Mechanical Motion Rectifier. In: Proceedings of the 12th European Wave and Tidal Energy Conference, Aug. 27-Sept. 1, Cork, Ireland.

Liermann, M., Samhoury, O. & Atshan, S. (2016) Energy Efficiency of Pneumatic Power Take-Off for Wave Energy Converter. International Journal of Marine Energy, 13, 62-79.

Liu, C.H., Yang, Q.J. & Bao, G. (2017) Performance Investigation of a Two-Raft-Type Wave Energy Converter with Hydraulic Power Take-Off Unit. Applied Ocean Research, 62, 139-155.

Liu, J., Lin, H. & Purimitla, S.R. (2016a) Wake Field Studies of Tidal Current Turbines with Different Numerical Methods. Ocean Engineering, 117, 383-397.

Liu, L.Q., Jin, W. & Guo, Y. (2016b) Dynamic Analysis of a Truss Spar-Type Floating Foundation for 5MW Vertical-Axis Wind Turbine. Journal of Offshore Mechanics and Arctic Engineering, 139, 061902.

Liu, P.F., Bose, N., Frost, R., Macfarlane, G., Lilienthal, T. & Penesis, I. (2015) Model Testing and Performance Comparison of Plastic and Metal Tidal Turbine Rotors. Applied Ocean Research, 53, 116-124.

Liu, Y., Hu, C., Sueyoshi, M., Iwashita, H. & Kashiwagi, M. (2016c) Motion Response Prediction by Hybrid Panel-Stick Models for a Semi-Submersible with Bracings. Journal of Marine Science and Technology, 21 (4), 742-757.

Liu, Y., Xiao, Q., Incecik, A., & Wan, D.C. (2016d) Investigation of the Effects of Platform Motion on the Aerodynamics of a Floating Offshore Wind Turbine. Journal of Hydrodynamics, 28 (1), 95-101.

Lombardi, D., Bhattacharya, S. & Nikitas, G. (2017) Physical Modelling of Offshore Wind Turbine Model for Prediction of Prototype Response. In: Letcher, T.M. (Ed.) Wind Energy Engineering: A Handbook for Onshore and Offshore Wind Turbines. Elsevier.

Lopez-Pavon, C. & Souto-Iglesias, A. (2015) Hydrodynamic Coefficients and Pressure Loads on Heave Plates for Semi-Submersible Floating Offshore Wind Turbines: A Comparative Analysis Using Large Scale Models. Renewable Energy, 81, 864-881.

Lopez-Pavon, C., Watai, R.A., Ruggeri, F., Simos, A.N. & Souto-Iglesias, A. (2015) Influence of Wave Induced Second-Order Forces in Semi-Submersible FOWT Mooring Design. Journal of Offshore Mechanics and Arctic Engineering, 137 (3), 031602.

Lopez-Pavon, M., Taveira-Pinto, F. & Rosa-Santos, P. (2017) Influence of the Power Take-Off Characteristics on the Performance of CECO Wave Energy Converter. Energy, 120, 686-697.

Lott, S. & Cheng, P.W. (2017) Load Extrapolations based on Measurements from an Offshore Wind Turbine at Alpha Ventus. Journal of Physics – Conference Series, 753, 072004.

Loukogeorgaki, E., Lentsiou, E. N. & Chatjigeorgiou, I.K. (2016) Experimental Investigation of Slamming Loading on a Three-Legged Jacket Support Structure of Offshore Wind Turbines. In: Proceedings of the Twenty-Sixth (2016) International Ocean and Polar Engineering Conference, June 26-July 1, Rhodes, Greece.

LR (2014) Guidance Notes for Wind Turbine Installation Vessels. Lloyd's Register Group Limited, London, UK.

Luan, C.Y., Chabaud, V., Bachynski, E.E., Gao, Z. & Moan, T. (2017) Experimental Validation of a Time-Domain Approach for Determining Sectional Loads in a Floating Wind Turbine Hull Subjected to Moderate Waves. In: Proceedings of the EERA DeepWind'2017 Conference, January 18-20, Trondheim, Norway.

Luan, C., Gao, Z. & Moan, T. (2016) Design and Analysis of a Braceless Steel 5-MW Semi-Submersible Wind Turbine. In: Proceedings of the 35th International Conference on Ocean, Offshore and Arctic Engineering, June 19-24, Busan, South Korea.

Lust, E.E., Luznik, L., Flack, K.A., Walker, J.M. & van Benthem, M.C. (2013) The Influence of Surface Gravity Waves on Marine Current Turbine Performance. International Journal of Marine Energy; 3-4, 27-40.

Luxmoore, J.F., Grey, S., Newsam, D. & Johanning, L. (2016) Analytical Performance Assessment of a Novel Active Mooring System for Load Reduction in Marine Energy Converters. Ocean Engineering, 124, 215-225.

Ma, H.W., Yang, J. & Chen, L.Z. (2017) Numerical Analysis of the Long-Term Performance of Offshore Wind Turbines Supported by Monopiles. Ocean Engineering, 136, 94-105.

Magagna, D. & Uihlein, A. (2015) Ocean Energy Development in Europe: Current Status and Future Perspectives. International Journal of Marine Energy, 11, 84-104.

MAKE Consulting (2016) Norwegian Opportunities in Offshore Wind. A Report for INTPOW, Export Credit Norway and Greater Stavanger.

Make, M. & Vaz, G. (2015). Analysing Scaling Effects on Offshore Wind Turbines using CFD. Renewable Energy, 83: 1326-1340.

Mankins, J.C. (1995) Technology Readiness Levels: A White Paper. NASA, Office of Space Access and Technology.

Marcy, C. & Beiter, P. (2016) Quantifying the Opportunity Space for Future Electricity Generation: An Application to Offshore Wind Energy in the United States (No.

NREL/TP-6A20-66522). National Renewable Energy Laboratory (NREL), Golden, CO, US.

MARINET2 (2017) http://www.marinet2.eu/facilities/wave/

Martin, R., Lazakis, I., Barbouchi, S. & Johanning, L. (2016) Sensitivity Analysis of Offshore Wind Farm Operation and Maintenance Cost and Availability. Renewable Energy, 85, 1226-1236.

Martinez-Luengo, M., Kolios, A. & Wang, L. (2016) Structural Health Monitoring of Offshore Wind Turbines: A Review through the Statistical Pattern Recognition Paradigm. Renewable and Sustainable Energy Reviews, 64, 91-105.

Martinez-Luengo, M., Kolios, A. & Wang, L. (2017) Parametric FEA Modelling of Offshore Wind Turbine Support Structures: Towards Scaling-Up and CAPEX Reduction. International Journal of Marine Energy, 19, 16-31.

McDonald, A. Xiao, Q., Forehand, D., Mavel, V. & Findlay, D. (2017)Experimental Investigation of Array Effects for a Mechanically Coupled WEC Array. In: Proceedings of the 12th European Wave and Tidal Energy Conference, Aug. 27-Sept. 1, Cork, Ireland.

McElman, S., Koop, A., de Ridder, E.-J. & Goupee, A. (2016) Simulation and Development of a Wind-Wave Facility for Scale Testing of Offshore Floating Wind Turbines. In: Proceedings of the ASME 2016 35th International Conference on Ocean, Offshore and Arctic Engineering, OMAE2016-54281, June 19-24, Busan, South Korea.

Mehmanparast, A., Brennan, F. & Tavares, I. (2017) Fatigue Crack Growth Rates for Offshore Wind Monopile Weldments in Air and Seawater: SLIC Inter-Laboratory Test Results. Materials and Design, 114, 494-504.

Michailides, C., Gao, Z. & Moan, T. (2016a) Experimental Study of the Functionality of a Semi-Submersible Wind Turbine Combined with Flap-Type Wave Energy Converters. Renewable Energy, 93, 675-690.

Michailides, C., Gao, Z. & Moan, T. (2016b) Experimental and Numerical Study of the Response of the Offshore Combined Wind/Wave Energy Concept SFC in Extreme Environmental Conditions. Marine Structures, 50, 35-54.

Mieloszyk, M. & Ostachowicz, W. (2017) An Application of Structural Heath Monitoring System based on FBG Sensors to Offshore Wind Turbine Support Structure Model. Marine Structures, 51, 65-86.

Milne, I.A., Day, A.H., Sharma, R.N. & Flay, R.G.J. (2013) Blade Loads on Tidal Turbines in Planar Oscillatory Flow. Ocean Engineering, 60, 163-174.

Milne, I.A., Day, A.H., Sharma, R.N. & Flay, R.G.J. (2015) Blade Loading on Tidal Turbines for Uniform Unsteady Flow. Ocean Engineering, 77, 338-350.

Moeller, J. (2017) What is Driving the Development of Floating Foundations from an OEM's Point of View. Presentation at the Offshore Wind Energy 2017 Conference, June 6-8, London, UK.

Mofor, L., Goldsmith, J. & Jones, F. (2014) Ocean Energy - Technology Readiness, Patents, Deployment Status and Outlook. IRENA Report. International Renewable Energy Agency (IRENA).

Morato, A., Sriramula, S., Krishnan, N. & Nichols, J. (2017) Ultimate Loads and Response Analysis of a Monopile Supported Offshore Wind Turbine Using Fully Coupled Simulation. Renewable Energy, 101, 126-143.

Morton, T. (2017) Third Tidal Turbine Deployed in Bluemull Sound. http://www.shetland.org/60n/blogs/posts/third-tidal-turbine-deployed-in-bluemull-sound

Muller, K. & Cheng, P.W. (2016) Validation of Uncertainty in IEC Damage Calculations based on Measurements from Alpha Ventus. Energy Procedia, 94, 133-145.

Muller, K., Reiber, M. & Cheng, P.W. (2016) Comparison of Measured and Simulated Structural Loads of an Offshore Wind Turbine at Alpha Ventus. International Journal of Offshore and Polar Engineering, 26 (3), 209-218.

Muller, K., Sandner, F., Bredmose, H., Azcona, J., Manjock, A. & Pereira, R. (2014) Improved Tank Test Procedures for Scaled Floating Offshore Wind Turbines. In: Proceedings of International Wind Engineering Conference - Support Structures & Electrical Systems. September 3-4, Hannover, Germany.

Murray, R.E., Nevalainen, T., Gracie-Orr, K., Doman, D.A., Pegg, M.J. & Johnstone, C.M. (2016) Passively Adaptive Tidal Turbine Blades: Design Tool Development and Initial Verification. International Journal of Marine Energy, 14, 101-124.

Musial, W., Heimiller, D., Beiter, P., Scott, G. & Draxl, C. (2016) 2016 Offshore Wind Energy Resource Assessment for the United States (No. NREL/TP-5000-66599). National Renewable Energy Laboratory (NREL), Golden, CO, US.

Nejad, A.M., Bachynski, E.E., Kvittem, M.I., Luan, C., Gao, Z. & Moan, T. (2015) Stochastic Dynamic Load Effect and Fatigue Damage Analysis of Drivetrains in Land-Based and TLP, Spar and Semi-Submersible Floating Wind Turbines. Marine Structures, 42, 137-153.

Nejad, A.R., Bachynski, E.E., Li, L. & Moan, T. (2016) Correlation between Acceleration and Drivetrain Load Effects for Monopile Offshore Wind Turbines. Energy Procedia, 94, 487-496.

Nielsen, S.R.K., Zhang, Z., Kramer, M.M. & Olsen, J. (2015) Stability Analysis of the Gyroscopic Power Take-Off Wave Energy Point Absorber. Journal of Sound and Vibration, 355, 418-433.

Noad, I.F. & Porter, R. (2017) Modelling an Articulated Raft Wave Energy Converter. Renewable Energy, 114, 1146-1159.

Nygaard, T.A., de Vaal, J., Pierella, F., Oggiano, L. & Stenbro, R. (2016) Development, Verification and Validation of 3DFloat Aero-Servo-Hydro-Elastic Computations of Offshore Structures. Energy Procedia, 94, 425-433.

O'Boyle, L., Elsaber, B. & Whttaker, T. (2017) Experimental Measurement of Wave Field Variations around Wave Energy Converter Arrays. Sustainability, 9 (1), 70.

OES (2017) IEA OES Annual Report. https://www.ocean-energy-systems.org/library/annual-reports/document/oes-annual-report-2017

Offshore Wind (2017) http://www.offshorewind.cn/news/show.php?itemid=13392

Offshore Wind Industry (2017) http://www.offshorewindindustry.com/news/germany-offshore-wind-farms-extremely-low

Oggiano, L., Pierella, F., Nygaard, T.A., De Vaal, J. & Arens, E. (2016) Comparison of Experiments and CFD Simulations of a Braceless Concrete Semi-Submersible Platform. Energy Procedia, 94, 278-289.

Ong, M.C., Bachynski, E.E., Økland, O.D. (2017) Dynamic Responses of Jacket-Type Offshore Wind Turbines Using Decoupled and Coupled Models. Journal of Offshore Mechanics and Arctic Engineering, 139, 041901.

O'Sullivan, K. & Ardanaz, I.A. (2012) Cost Model with the Parameters and Cost Drivers that Do Influence the Life Cycle Cost of Ocean Energy Systems. Report, WP6 – Economic Feasibility Assessment, EU FP7 MARINA Platform Project.

OTEC Okinawa (2017) http://otecokinawa.com/en/Project/index.html

Palm, J., Eskilsson, C., Paredes, G.M. & Bergdahl, L. (2016) Coupled Mooring Analysis for Floating Wave Energy Converters Using CFD: Formulation and Validation. International Journal of Marine Energy, 16, 83-99.

Paredes, G.M., Palm, J., Eskilsson, C., Bergdahl, L. & Taveira-Pinto, F. (2016) Experimental Investigation of Mooring Configurations for Wave Energy Converters. International Journal of Marine Energy, 15, 56-67.

Parkinson, S.G. & Collier, W.J. (2016) Model Validation of Hydrodynamic Loads and Performance of a Full-Scale Tidal Turbine Using Tidal Bladed. International Journal of Marine Energy, 16, 279-297.

Passon, P. (2006) Derivation and Description of the Soil–Pile Interaction Models. Memorandum, University of Stuttgart, Stuttgart, Germany.

Paterson, J., D'Amico, F., Thies, P.R., Kurt, E. & Harrison, G. (2017) Offshore Wind Installation Vessels – A Comparative Assessment for UK Offshore Rounds 1 and 2. Ocean Engineering, DOI: 10.1016/j.oceaneng.2017.08.008

Paulsen, U.S., Madsen, H.A., Kragh, K.A., Nielsen P.H., Baran, I., Hattel, J., Ritchie, E., Leban, K., Svendsen, H. & Berthelsen, P.A. (2014). DeepWind – From Idea to 5MW Concept. Energy Procedia, 53: 23-33.

Pecher, A. (2016) Experimental Testing and Evaluation of WECs. In: Pecher, A. & Kofoed, J.P. (Eds.), Handbook of Ocean Wave Energy. Springer Open.

Pegalajar-Jurado, A.M., Borg, M., Robertson, A., Jonkman, J. & Bredmose, H. (2017) Effect of Second-Order and Fully Nonlinear Wave Kinematics on a Tension-Leg-Platform Wind Turbine in Extreme Wave Conditions. In: Proceedings of the ASME 2017 36th International Conference on Ocean, Offshore and Arctic Engineering, OMAE2017-61798, June 25-30, 2017, Trondheim, Norway.

Pegalajar-Jurado, A.M., Hansen, A.M., Laugesen, R., Mikkelsen, R.F., Borg, M., Kim, T.S., Heilskov, N.F. & Bredmose, H. (2016) Experimental and Numerical Study of a 10MW TLP Wind Turbine in Waves and Wind. Journal of Physics – Conference Series, 753: 092007.

Penalba, M., Giorgi, G. & Ringwood, J.V. (2017). Mathematical Modelling of Wave Energy Converters: A Review of Nonlinear Approaches. Reneweable and Sustainable Energy Review, 78, 1188-1207.

Principle Power (2012) Principle Power's WindFloat Prototype. Available online. https://www.youtube.com/watch?v=i6pdp8wyQ8A

Principle Power (2017) http://www.principlepowerinc.com/en/windfloat

Pyakurel, P., Van Zwieten, J.H., Dhanak, M. & Xiros, N.I. (2017) Numerical Modelling of Turbulence and its Effect on Ocean Current Turbines. International Journal of Marine Energy, 17, 84-97.

Quallen, S. & Xing, T. (2016) CFD Simulation of a Floating Offshore Wind Turbine System using a Variable-Speed Generator-Torque Controller. Renewable Energy, 97, 230-242.

Quallen, S., Xing, T., Carrica, P., Li, Y. & Xu, J. (2014) CFD Simulation of a Floating Offshore Wind Turbine System Using a Quasi-Static Crowfoot Mooring-Line Model. Journal of Ocean and Wind Energy, 1 (3), 143-152.

Rafiee, A. & Fievez, J. (2015) Numerical Prediction of Extreme Loads on the CETO Wave Energy Converter. In: Proceedings of the 11th European Wave and Tidal Energy Conference, Sept. 6-11, Nantes, France.

Ransley, E.J., Greaves, D., Raby, A., Simmonds, D. & Hann, M. (2017a) Survivability of Wave Energy Converters Using CFD. Renewable Energy, 109, 235-247.

Ransley, E.J., Greaves, D.M., Raby, A., Simmonds, D., Jakobsen, M.M. & Kramer, M. (2017b) RANS-VOF Modelling of the Wavestar Point Absorber. Renewable Energy, 109, 49-65.

RenewableUK (2013) Guidelines for the Selection and Operation of Jack-Ups in the Marine Renewable Energy Industry, Issue 2.

Ringwood, J.V., Davidson, J. & Giorgi, S. (2015) Optimising Numerical Wave Tank Tests for the Parametric Identification of Wave Energy Device Models. In: Proceedings of the 34th International Conference on Ocean, Offshore and Arctic Engineering, OMAE2015-41529, May 31-June 5, St. John's, Newfoundland, Canada.

Robertson, A.N., Wendt, F., Jonkman, J.M., Popko, W., Borg, M., Bredmose, H., Schlutter, F., Qvist, J., Bergua, R., Harries, R., Yde, A., Nygaard, T.A., de Vaal, J.B., Oggiano, L., Bozonnet, P., Bouy, L., Sanchez, C.B., Garcia, R.G., Bachynski, E.E., Tu, Y., Bayati, I., Borisade, F., Shin, H.K., van der Zee, T. & Guerinel, M. (2016) OC5 Project Phase Ib: Validation of Hydrodynamic Loading on a Fixed, Flexible Cylinder for Offshore Wind Applications. Energy Procedia, 94, 82-101.

Robertson, A.N., Wendt, F., Jonkman, J.M., Popko, W., Dagher, H., Gueydon, S., Qvist, J., Vittori, F., Azcona, J., Uzunoglu, E., Guedes Soares, C., Harries, R., Yde, A., Galinos, C., Hermans, K., de Vaal, J.B., Bozonnet, P., Bouy, L., Bayati, I., Bergua, R., Galvan, J., Mendikoa, I., Sanchez, C.B., Shin, H.K., Oh, S., Molins, C. & Debruyne, Y. (2017) OC5 Project Phase II: Validation of Global Loads of the DeepCwind Floating Semisubmersible Wind Turbine. Presentation at the 14th EERA Deep Sea Offshore Wind R&D Conference (DeepWind'2017), January 18-20, Trondheim, Norway.

Robertson, A.N., Wendt, F., Jonkman, J.M., Popko, W., Vorpahl, F., Stansberg, C.T., Bachynski, E.E., Bayati, I., Beyer, F., de Vaal, J.B., Harries, R., Yamaguchi, A., Shin, H.K., Kim, B.C., van der Zee, T., Bozonnet, P., Aguilo, B., Bergua, R., Qvist, J., Wang, Q.J., Chen, X.L., Guerinel, M., Tu, Y., Huang, Y.T., Li, R.F. & Bouy, L. (2015) OC5 Project Phase I: Validation of Hydrodynamic Loading on a Fixed Cylinder. In: Proceedings of the 25th International Ocean and Polar Engineering Conference, June 21-26, Kona, Hawaii, USA.

Roddier, D., Cermelli, C., Aubault, A. & Peiffer, A. (2017) Summary and Conclusions of the Full Life-Cycle of the WindFloat FOWT Prototype Project. In: Proceedings of the ASME 2017 36th International Conference on Ocean, Offshore and Arctic Engineering, OMAE2017-62561, June 25-30, Trondheim, Norway.

Romero, A., Soua, S., Gan, T.-H. & Wang, B. (2017) Condition Monitoring of a Wind Turbine Drive Train based on Its Power Dependent Vibrations. Renewable Energy, DOI: 10.1016/j.renene.2017.07.086

Ruehl, K., Michelen, C., Bosma, B. & Yu, Y.H. (2016) WEC-Sim Phase 1 Validation Testing – Numerical Modelling of Experiments. In: Proceedings of the ASME 2016 35th International Conference on Ocean, Offshore and Arctic Engineering, OMAE2016-54986, June 19-24, Busan, South Korea.

Ruiz, P.M., Ferri, F. & Kofoed, J. P. (2017) Experimental Validation of a Wave Energy Converter Array Hydrodynamics Tool. Sustainability, 9 (115).

Saincher, S. & Banerjee, J. (2016) Influence of Wave Breaking on the Hydrodynamics of Wave Energy Converters: A Review. Renewable and Sustainable Energy Review, 58, 704-717.

Sang, L.Q., Takao, M., Kamada, Y. & Li, Q. (2017) Experimental Investigation of the Cyclic Pitch Control on a Horizontal Axis Wind Turbine in Diagonal Inflow Wind Condition. Energy, 134, 269-278.

Sant, T. & Cuschieri, K. (2016) Comparing Three Aerodynamic Models for Predicting the Thrust and Power Characteristics of a Yawed Floating Wind Turbine Rotor. Journal of Solar Energy Engineering, 138 (3), 031004.

Sarker, B.R. & Faiz, T.I. (2016) Minimizing Maintenance Cost for Offshore Wind Turbines Following Multi-Level Opportunistic Preventive Strategy. Renewable Energy, 85, 104-113.

Sarker, B.R. & Faiz, T.I. (2017) Minimizing Transportation and Installation Costs for Turbines in Offshore Wind Farms. Renewable Energy, 101, 667-679.

Sauder, T., Chabaud, V.B., Thys, M., Bachynski, E.E. & Sæther, L.O. (2016). Real-Time Hybrid Model Testing of a Braceless Semi-Submersible Wind Turbine. Part I: The Hybrid Approach. In: Proceedings of the 35th International Conference on Ocean, Offshore and Arctic Engineering, Paper No. OMAE2016-54435, June 19-24, Busan, Korea.

Schmitt, P., Asmuth, H. & Elsaber, B. (2016) Optimising Power Take-Off of an Oscillating Wave Surge Converter Using High Fidelity Numerical Simulations. International Journal of Marine Energy, 16, 196-208.

Segura, E., Morales, R. & Somolinos, J.A. (2018) A Strategic Analysis of Tidal Current Energy Conversion Systems in the European Union. Applied Energy, 212, 527-551.

Sellar, B., Wakelam, G., Sutherland, D., Ingram, D. & Venugopal, V. (2018) Characterisation of Tidal Flows at the European Marine Energy Centre in the Absence of Ocean Waves. Energies, 11 (1), 176.

Sellar, B., Harding, S. & Richmond, M. (2015) High-Resolution Velocimetry in Energetic Tidal Currents Using a Convergent-Beam Acoustic Doppler Profiler. Measurement Science and Technology 26 (8), 085801.

Sergiienko, N.Y., Cazzolato, B.S., Ding, B. & Arjomandi, M. (2016) An Optimal Arrangement of Mooring Lines for the Three-Tether Submerged Point-Absorbing Wave Energy Converter. Renewable Energy, 93, 27-37.

Sheng, S.W., Zhang, Y.Q., Wang, K.L., Lin, H.J., Wang, W.S. & Chen, A.J. (2015a) The Overall Design of Wave Energy Converter WanShan. Ship Engineering, 37 (1), 10-14.

Sheng, W., Alcorn, R. & Lewis, A. (2015b) On Improving Wave Energy Conversion, Part II: Development of Latching Control Technologies. Renewable Energy, 75, 935-944.

Shi, H., Cao, F., Liu, Z. & Qu, N. (2016) Theoretical Study on the Power Take-Off Estimation of Heaving Buoy Wave Energy Converter. Renewable Energy, 86, 441-448.

Siegel, S.G. (2015) Wave Radiation of a Cycloidal Wave Energy Converter. Applied Ocean Research, 49, 9-19.

Simos, A.N., Ruggeri, F., Watai, R.A., Souto-Iglesias, A. & Lopez-Pavon, C. (2018) Slow-Drift of a Floating Wind Turbine - An Assessment of Frequency-Domain Methods based on Model Tests. Renewable Energy, 116, 133-154.

Sirnivas, S., Musial, W., Bailey, B. & Filippelli, M. (2014) Assessment of Offshore Wind System Design, Safety, and Operation Standards. NREL/TP-5000-60573 Report. NREL, Golden, CO, US.

Spanos, P.D., Arena, F., Richichi, A. & Malara, G. (2016) Efficient Dynamic Analysis of a Nonlinear Wave Energy Harvester Model. Journal of Offshore Mechanics and Arctic Engineering, 138, 1-8.

Sperstad, I.B., Stalhane, M., Dinwoodie, I., Endrerud, O.-E.V., Martin, R. & Warner, E. (2017) Testing the Robustness of Optimal Access Vessel Fleet Selection for Operation and Maintenance of Offshore Wind Farms. Ocean Engineering, 145, 334-343.

Stansby, P., Carpintero Moreno, E. & Stallard, T. (2015a) Capture Width of the Three-Float Multi-Mode Multi-Resonance Broad-Band Wave Energy Line Absorber M4 from Laboratory Studies with Irregular Waves of Different Spectral Shape and Directional Spread. Journal of Ocean Engineering and Marine Energy, 1, 287–298.

Stansby, P., Carpintero Moreno, E. & Stallard, T. (2017) Large Capacity Multi-Float Configurations for the Wave Energy Converter M4 using a Time-Domain Linear Diffraction Model. Applied Ocean Research, 68, 53-64.

Stansby, P., Carpintero Moreno, E., Stallard, T. & Maggi, A. (2015b) Three-Float Broad-Band Resonant Line Absorber with Surge for Wave Energy Conversion. Renewable Energy, 78, 132-140.

Statkraft (2017) https://www.statkraft.com/media/news/News-archive/2009/the-worlds-first-osmotic-power-plant-opened/

Statoil (2017a) https://www.statoil.com/no/news/worlds-first-floating-wind-farm-started-production.html

Statoil (2017b) Statoil Hywind Mating. Available online. https://www.youtube.com/watch?v=-eZu_uNcVN4

Stewart, G. & Muskulus, M. (2016) A Review and Comparison of Floating Offshore Wind Turbine Model Experiments. Energy Procedia, 94, 227-231.

Stoev, L., Georgiev, P. & Garbatov, Y. (2017) Offshore Sulphide Power Plant for the Black Sea. In: Proceedings of the 17th Congress of International Maritime Association of the Mediterranean, October 9-13, Lisbon, Portugal.

Stratigaki, V. (2014) Experimental Study and Numerical Modelling of Intra-Array Interactions and Extra-Array Effects of Wave Energy Converter Arrays. PhD Thesis, Department of Civil Engineering, Ghent University. Ghent, Belgium.

Suja-Thauvin, L., Krokstad, J.R., Bachynski, E.E. & de Ridder, E.-J. (2017) Experimental Results of a Multimode Monopile Offshore Wind Turbine Support Structure Subjected to Steep and Breaking Irregular Waves. Ocean Engineering, 146, 339-351.

Suja-Thauvin, L., Krokstad, J.R. & Frimann-Dahl, J.F. (2016) Maximum Loads on a One Degree of Freedom Model-Scale Offshore Wind Turbine. Energy Procedia, 94, 329-338.

Sun, L., Zang, J., Stansby, P., Carpintero Moreno, E., Taylor, P.H. & Eatock Taylor, R. (2017) Linear Diffraction Analysis of the Three-Float Multi-Mode Wave Energy Converter M4 for Power Capture and Structural Analysis in Irregular Waves with Experimental Validation. Journal of Ocean Engineering and Marine Energy, 3, 51-68.

Sutherland, D., Sellar, B., Borthwick, A. & Venugopal, V. (2017) Turbulence Metrics in Wave-Current Interactions. In: Proceedings of the Twelfth European Wave and Tidal Energy Conference (EWTEC), Aug. 27-Sept. 1, Cork, Ireland.

Tarrant, K. & Meskell, C. (2016) Investigation on Parametrically Excited Motions of Point Absorbers in Regular Waves. Ocean Engineering, 111, 67-81.

Tatum, S.C., Frost, C.H., Allmark, M., O'Doherty, D.M., Mason-Jones, A., Prickett, P.W., Grosvenor, R.I., Byrne, C.B. & O'Doherty, T. (2016) Wave-Current Interaction Effects on Tidal Stream Turbine Performance and Loading Characteristics. International Journal of Marine Energy, 14, 161-179.

Techxplore (2017) https://techxplore.com/news/2015-08-celebrating-hawaii-ocean-thermal-energy.html

Thiagarajan, K.P., Urbina, R. & Hsu, W. (2015) Nonlinear Pitch Decay Motion of a Floating Offshore Wind Turbine Structure. Journal of Offshore Mechanics and Arctic Engineering, 137 (1), 011902.

Thies, P.R., Johanning, L. & McEvoy, P. (2014) A Novel Mooring Tether for Peak Load Mitigation: Initial Performance and Service Simulation Testing. International Journal of Marine Energy, 7, 43-56.

Tidal Energy Today (2017) Atlantis Resources has Reinstalled the Fourth Tidal Turbine in the Pentland Firth off Scotland, Wrapping up the Phase 1A of the MeyGen Project. http://tidalenergytoday.com/

Todalshaug, J.H., Asgeirsson, G.S., Hjalmarsson, E., Maillet, J., Moller, P., Pires, P., Guerinel, M. & Lopes, M. (2016) Tank Testing of an Inherently Phase-Controlled Wave Energy Converter. International Journal of Marine Energy, 15, 68-84.

Tom, N.M., Lawson, M.J., Yu, Y.H. & Wright, A.D. (2016) Development of a Nearshore Oscillating Surge Wave Energy Converter with Variable Geometry. Renewable Energy, 96, 410-424.

Tran, T.T. & Kim, D.H. (2015) The Platform Pitching Motion of Floating Offshore Wind Turbine: A Preliminary Unsteady Aerodynamic Analysis. Journal of Wind Engineering and Industrial Aerodynamics, 142, 65-81.

Tran, T.T. & Kim, D.-H. (2016) A CFD Study into the Influence of Unsteady Aerodynamic Interference on Wind Turbine Surge Motion. Renewable Energy, 90, 204-228.

Troch, P. (1998) MILDwave – A Numerical Model for Propagation and Transformation of Linear Water Waves. Internal Report, Department of Civil Engineering, Ghent University.

Turner, J. (2012) Healthy Competition: Demand Grows for Specialised Offshore Vessels. Available online. http://www.offshore-technology.com/features/featureoperation-maintenance-offshore-wind-oil-gas-hydrocarbons-installed-capacity-wind-farm-specialised-resources-ship-boat-vessel-installation/

Ulstein (2017) Windlifter. Available online. https://ulstein.com/equipment/ulstein-windlifter

Utsunomiya, T., Sato, I., Kobayashi, O., Shiraishi, T. & Harada, T. (2015) Design and Installation of a Hybrid-Spar Floating Wind Turbine Platform. In: Proceedings of the 34th International Conference on Ocean, Offshore and Arctic Engineering, OMAE2015-41544, May 31-June 5, St. John's, Newfoundland, Canada.

Utsunomiya, T., Sekita, K., Kita, K. & Sato, I. (2017) OMAE2017-62197 Demonstration Test for Using Suction Anchor and Polyester Rope in Floating Offshore Wind Turbine. In: Proceedings of the ASME 2017 36th International Conference on Ocean, Offshore and Arctic Engineering, OMAE2017-62197, June 25-30, 2017, Trondheim, Norway.

Valpy, B. & English, P. (2014) Future Renewable Energy Costs: Offshore Wind – How Technology Innovation is Anticipated to Reduce the Cost of Energy from European Offshore Wind Farms. A Report for Knowledge & Innovation Community (KIC) InnoEnergy. BVG Associates.

Van de Pieterman, R.P., Braam, H., Obdam, T.S., Rademakers, L.W.M.M. (2010) Operation & Maintenance Cost Estimator (OMCE) – Estimate Future O&M Cost for Offshore Wind Farms. Paper presented at the DEWEK 2010 Conference, November 17-18, Bremen, Germany.

Vaughan, S. & Ferreira, C.B. (2016) Determining Structural and Hydrodynamic Loads. In: Folley, M. (Ed.) Numerical Modelling of Wave Energy Converters - State-of-the-Art Techniques for Single Devices and Arrays. Elsevier.

Versteijlen, W.G., Renting, F.W., van der Valk, P.L.C., Bongers, J., van Dalen, K.N. & Metrikine, A.V. (2017) Effective Soil-Stiffness Validation - Shaker Excitation of an In-Situ Monopile Foundation. Soil Dynamics and Earthquake Engineering, 102, 241-262.

Vis, I.F.A. & Ursavas, E. (2016) Assessment Approaches to Logistics for Offshore Wind Energy Installation. Sustainable Energy Technologies and Assessment, 14, 80-91.

Viselli, A.M., Goupee, A.J., Dagher, H.J. & Allen, C.K. (2015) VOLTURNUS 1:8: Conclusion of 18-Months of Operation of the First Grid-Connected Floating Wind Turbine Prototype in the Americas. In: Proceedings of the 34th International Conference on Ocean, Offshore and Arctic Engineering, OMAE2015-41065, May 31-June 5, St. John's, Newfoundland, Canada.

Viselli, A.M., Goupee, A.J., Dagher, H.J. & Allen, C.K. (2016) Design and Model Confirmation of the Intermediate Scale VolturnUS Floating Wind Turbine Subjected to its Extreme Design Conditions Offshore Maine. Wind Energy, 19 (6), 1161-1177.

Vogel, C.R. & Willden, R.H.J. (2017) Multi-Rotor Tidal Stream Turbine Fence Performance and Operation. . International Journal of Marine Energy, 19, 198-206.

Vyzikas, T., Deshoulieres, S., Barton, M., Giroux, O., Greaves, D. & Simmonds, D. (2017) Experimental Investigation of Different Geometries of Fixed Oscillating Water Column Devices. Renewable Energy, 104, 248-258.

Walter, E.L., Gueydon, S. & Berthelsen, P.A. (2017) JIP on Coupled Analyses of FOWTs – Testing Philosophies for Floating Offshore Wind Turbines. In: Proceedings of the EERA DeepWind'2017 Conference, January 18-20, Trondheim, Norway.

WAMIT Inc. (2016) WAMIT User Manual Version 7.2. Available: http://www.wamit.com

Wan, L., Gao, Z. & Moan, T. (2015) Experimental and Numerical Study of Hydrodynamic Responses of a Combined Wind and Wave Concept in Survival Modes. Coastal Engineering, 104, 151-169.

Wan, L., Gao, Z., Moan, T. & Lugni, C. (2016a) Experimental and Numerical Comparisons of Hydrodynamic Responses for a Combined Wind and Wave Energy Converter Concept under Operational Conditions. Renewable Energy, 93, 87-100.

Wan, L., Gao, Z., Moan, T. & Lugni, C. (2016b) Comparative Experimental Study of the Survivability of a Combined Wind and Wave Energy Converter in Two Testing Facilities. Ocean Engineering, 111, 82-94.

Wan, L., Greco, M., Lugni, C., Gao, Z. & Moan, T. (2017) A Combined Wind and Wave Energy Converter Concept in Survival Mode: Numerical and Experimental Study in Regular Waves with a Focus on Water Entry and Exit. Applied Ocean Research, 63, 200-216.

Wandji, W.N., Natarajan, A. & Dimitrov, N. (2016) Development and Design of a Semi-Floater Substructure for Multi-Megawatt Wind Turbines at 50m+ Water Depths. Ocean Engineering, 125, 226-237.

Wang, J.P., Zheng, W.J. & Gao, F. (2012) Research Progress of International Marine Renewable Energy and the Implications for China. Renewable Energy Resources, 11, 123-127.

Wang, K., Moan, T. & Hansen, M.O.L. (2016a) Stochastic Dynamic Response Analysis of a Floating Vertical-Axis Wind Turbine with a Semi-Submersible Floater. Wind Energy, 19 (10), 1853-1870.

Wang, L., Son, D. & Yeung, R.W. (2016b) Effect of Mooring-Line Stiffness on the Performance of a Dual Coaxial-Cylinder Wave-Energy Converter. Applied Ocean Research, 59, 577-588.

Wang, Q., Zhang, P.K. & Li, Y. (2018) Structural Dynamic Analysis of a Tidal Current Turbine Using Geometrically Exact Beam Theory. Journal of Offshore Mechanics and Arctic Engineering, 140, 021903.

Wang, W.H., Gao, Z, Li, X. & Moan, T. (2017) Model Test and Numerical Analysis of a Multi-Pile Offshore Wind Turbine under Seismic, Wind, Wave and Current Loads. Journal of Offshore Mechanics and Arctic Engineering, 139, 031901.

Wang, W.H., Gao, Z., Li, X., Moan, T. & Wang, B. (2016c) Model Test of Offshore Bottom Fixed Pentapod Wind Turbine under Seismic Loads. In: Proceedings of the ASME 35th International Conference on Ocean, Offshore and Arctic Engineering, OMAE2016-54499, June 19-24, Busan, South Korea.

WEC-Sim (2017) http://wec-sim.github.io/WEC-Sim/index.html

Wei, K., Myers, A.T. & Arwade, S.R. (2017) Dynamic Effects in the Response of Offshore Wind Turbines Supported by Jackets under Wave Loading. Engineering Structures, 142, 36-45.

Weia, Y., Barradas-Berglindb, J.J., van Rooija, M., Prinsa, W.A., Jayawardhanab, B. & Vakisa A.I. (2017) Investigating the Adaptability of the Multi-Pump Multi-Piston Power Take-Off System for a Novel Wave Energy Converter. Renewable Energy, 111, 598-610.

Weller, H.G., Tabor, G., Jasak, H. & Fureby, C. (1998) A Tensorial Approach to Computational Continuum Mechanics Using Object-Oriented Techniques. Computers in Physics, 12 (6).

Wendt, F.F., Yu, Y.-H., Nielsen, K., Ruehl, K., Bunnik, T., Touzon, I., Nam, B.W., Kim, J.S., Kim, K.-H., Janson, C.E., Jakobsen, K.-R., Crowley, S., Vega, L., Rajagopalan, K., Mathai, T., Greaves, D., Ransley, E., Lamont-Kane, P., Sheng, W.A., Costello, R., Kennedy, B., Thomas, S., Heras, P., Bingham, H., Kurniawan, A., Kramer, M.M., Ogden, D., Girardin, S., Babarit, A., Wuillaume, P.-Y., Steinke, D., Roy, A., Beatty, S., Schofield, P., Jansson, J. & Hoffman, J. (2017) International Energy Agency Ocean Energy Systems Task 10 Wave Energy Converter Modelling Verification and Validation. In: Proceedings of the 12th European Wave and Tidal Energy Conference, Aug. 27-Sept. 1, Cork, Ireland.

Willow, C. & Valpy, B. (2015) Approaches to Cost-Reduction in Offshore Wind – A Report for the Committee on Climate Change. BVG Associates.

Wilson, D., Bacelli, G., Coe, R.G., Bull, D.L., Abdelkhalik, O., Korde, U.A. & Robinett III R.D. (2016) A Comparison of WEC Control Strategies. Sandia Report - SAND2016-4293, Sandia National Laboratories.

Wind & Economy (2017) http://www.wind-and-economy.com/home

WindEurope (2017). The European Offshore Wind Industry – Key Trends and Statistics 2016.

Wu, N., Wang, Q. & Xie, X. (2015) Ocean Wave Energy Harvesting with a Piezoelectric Coupled Buoy Structure. Applied Ocean Research, 50, 110-118.

Wymore, M.L., Van Dam, J.E., Ceylan, H. & Qiao, D.J. (2015) A Survey of Heath Monitoring Systems for Wind Turbines. Renewable and Sustainable Energy Reviews, 52, 976-990.

Xia, D.W., Gao, Y.B., Wang, J. & Xia, Q. (2014) Analysis of the Development of China's Marine Renewable Energy Industry. Marine Technology Society Journal, 48 (6), 419-427.

Xu, C., Huang, Z. & Deng, Z. (2016) Experimental and Theoretical Study of a Cylindrical Oscillating Water Column Device with a Quadratic Power Take-Off Model. Applied Ocean Research, 57, 19-29.

Yang, S.-H., Ringsberg, J.W., Johnson, E. & Hu, Z.Q. (2017) Biofouling on Mooring Lines and Power Cables Used in Wave Energy Converter Systems - Analysis of Fatigue Life and Energy Performance. Applied Ocean Research, 65, 166-177.

Yang, S.-H., Ringsberg, J.W., Johnson, E., Hu, Z.Q. & Palm, J. (2016a) A Comparison of Coupled and De-Coupled Simulation Procedures for the Fatigue Analysis of Wave Energy Converter Mooring Lines. Ocean Engineering, 117, 332-345.

Yang, W. (2016) Condition Monitoring of Offshore Wind Turbines. In: Ng, C. & Ran, L. (Eds.) Offshore Wind Farms – Technologies, Design and Operation. Elsevier.

Yang, Y., Chen, J.-X. & Huang, S. (2016b) Mooring Line Damping due to Low-Frequency Superimposed with Wave-Frequency Random Line Top End Motion. Ocean Engineering, 112, 243-252.

Yao, Y.X., Li, H.L., Wu, J.M. & Zhou, L. (2016) Numerical Simulation of Duck Wave Energy Converter. Key Engineering Materials, 693, 484-490.

Zhang, P.Y., Guo, Y.H., Liu, Y.G. & Ding, H.Y. (2016) Experimental Study on Installation of Hybrid Bucket Foundations for Offshore Wind Turbines in Silty Clay. Ocean Engineering, 114, 87-100.

Zhao, Y.N., Cheng, Z.S., Sandvik, P.C., Gao, Z. & Moan, T. (2017) An Integrated Dynamic Analysis Method for Simulating Installation of a Single Blade for Offshore Wind Turbines. Ocean Engineering, (under review).

Zheng, X.Y., Li, H.B., Rong, W.D. & Li, W. (2015) Joint Earthquake and Wave Action on the Monopile Wind Turbine Foundation - An Experimental Study. Marine Structures, 44, 125-141.

Ziegler, L., Schafhirt, S., Scheu, M. & Muskulus, M. (2016) Effect of Load Sequence and Weather Seasonality on Fatigue Crack Growth for Monopile Based Offshore Wind Turbines. Energy Procedia, 94, 115-123.

This page intentionally left blank

Proceedings of the 20th International Ship and Offshore Structures Congress (ISSC 2018) Volume II – M.L. Kaminski and P. Rigo (Eds.)

doi:10.3233/978-1-61499-864-8-279

COMMITTEE V.5

SPECIAL CRAFT

COMMITTEE MANDATE

Concern for structural challenges of non-conventional, special surface craft, including uncertainties in established design methods and modelling techniques. Particular attention shall be given to mega yachts, naval craft, offshore service vessels and work boats, which can be characterized by particular materials and structural configurations (wide openings, large unsupported structures, unconventionally shaped superstructures, etc.) and/or are to sustain specific loading conditions (harsh environment, severe cyclic loads or extreme operational ones).

AUTHORS/COMMITTEE MEMBERS

Chairman: D. Truelock
Z. Czaban
H. Luo
X. Wang
M. Holtmann
E. Begovic
A. Yasuda
M. Ventura
R. Nicholls-Lee
E. Oterkus
P. Sensharma

KEYWORDS

Special Craft, Structures, Naval Craft, Offshore Operation Vessels, Yachts, Motor Yachts, Sailing Yachts, Polar Ship, Icebreaker, HSC Rules, Naval Standards, Special Hull Structures, Free-Fall Lifeboat, Heavy Lift Ship, SWATH, Wave-Piercing Catamaran, Moonpools, Helideck Design, Autonomous Vessel, Total Cost of Ownership, 3D Structural Printing

CONTENTS

1 INTRODUCTION TO SPECIAL CRAFT 282
1.1 Definition of Special Craft and Types 282
1.1.1 Market Analysis of Naval Craft 282
1.1.2 Market Analysis of Offshore Operation Vessels 283
1.1.3 Market Analysis of Yachts 284

2 RULES AND STANDARDS 285
2.1 HSC Rules 285
2.1.1 ABS Rules for Classification of High-Speed Craft 2017 287
2.1.2 DNV GL Rules for Classification – High speed and light craft 2015c 287
2.1.3 LR Classification of Special Service Craft Rules 2016 288
2.1.4 CCS China Classification Society 2017 289
2.2 Yachts 289
2.3 Naval craft / Surface Combatant 291
2.3.1 NATO and national standards 291
2.3.2 Class Rules 293
2.4 Polar Ship / Icebreaker 294
2.5 Offshore Operations Vessels 295
2.6 Special Structures Rules and Standards 295
2.6.1 Moonpools 295
2.6.2 Helicopter Decks 296
2.6.3 Free-Fall lifeboats 298

3 NAVAL CRAFT 298
3.1 Why Naval Standards are Special 299
3.1.1 The Argument For Maintaining Naval Standards 301
3.1.2 The Cost-Benefit of Naval Standards. 305
3.2 Recommendations 307

4 OFFSHORE OPERATION VESSELS 307
4.1 Subsea Drilling/Construction Vessels 308
4.2 Self-Elevating Vessels (Lift Boats) 308
4.3 Heavy Lift (Semi-Submersible) Ships 309
4.4 Accommodation Vessels 309
4.5 SWATH Offshore Vessels 310

5 YACHTS 310
5.1 Motor Yachts 311
5.1.1 Megayachts and Gigayachts 311
5.1.2 Superyachts 313
5.1.3 Expedition Yachts 314
5.1.4 Small Yachts 316
5.2 Sailing Yachts 316
5.2.1 Giga, Mega and Superyachts 316
5.2.2 Racing Yachts 317
5.3 Recommendations 318

6 SPECIAL HULL AND APPURTENANCE STRUCTURES 319
6.1 Freefall Lifeboats 319
6.1.1 Impact Loads 320
6.1.2 Simulation 321

6.2 SWATH Hulls 321
6.3 Heavy Lift Hulls 322
6.4 Icebreaking Hulls 323
6.5 Wave-Piercing Catamaran Hulls 323
6.6 Moonpools 325
6.7 Offshore vessels Helideck Design and Integration 326
6.7.1 Materials and Analysis Techniques 327
6.7.2 Structural Configurations 328
6.7.3 Thermal Loads 328

7 CONCLUSIONS AND RECOMMENDATIONS 329
7.1 Recommended Research for Future Special Craft Committees 329
7.1.1 Autonomous and Unmanned Vessels 329
7.1.2 Research and Polar Vessels 330
7.2 Emerging Structural Trends to Watch 330
7.2.1 Total Cost of Ownership 330
7.2.2 3D Printing for Structures 330
7.3 Concluding Remarks 331

REFERENCES 331

1 INTRODUCTION TO SPECIAL CRAFT

The intent of this report is to highlight the wide range of vessels that operate around the world, as well as the unique structural variations and design aspects that grant them the privilege of being "Special." First of its kind, the ISSC 2018 Specialist Committee V.5 for Special Craft will attempt to cover the three major marine market sectors. The goal will be to highlight developments, published work and previous ISSC report writings over the last decade that warrant further discussion on these structural unique vessels. Previously, the Specialist Committee V.5 focused on Naval Vessel structural design developments. Although developments on this vessel type will be covered within the report, naval vessels will not be the focus of the report. The first Specialist Committee V.5 Special Craft report is broad in subject matter in order to cover a wide range of vessel types, developments over the last decade and focus on structural configurations that have been considered "special" by the V.5 Committee members in support of the current mandate. Recommendations are provided in Chapter 7 of this report which provide future V.5 Special Craft Committees suggested focus areas based on the vessel types. In order to allow future reports the ability to address more in-depth analyses of structural challenges and topics, current market trends are also included.

1.1 Definition of Special Craft and Types

For purposes of this report's discussion, Special Craft were chosen to be those vessels which perform a unique marine operational mission or function that requires the vessel to have a uniquely designed structural configuration. The structural arrangement and design is purpose-designed to consider a wide range of variables, including environment and loading scenarios. For thoroughness, the Committee members have chosen to cover all three of the marine market sectors: Military, Commercial and Pleasure. The definition of craft for the intents and purposes of this report is only pertaining to a surface vessel capable of self-propulsion. The implication that the definition of "craft" pertains to a small or high-speed vessel is not the intention within this report. All craft, including large full-displacement vessels as shown in Figure 1, were considered with regard to this Committee's mandate. Specialized hull forms and other structures that demand a detailed discussion are highlighted in Chapter 6.

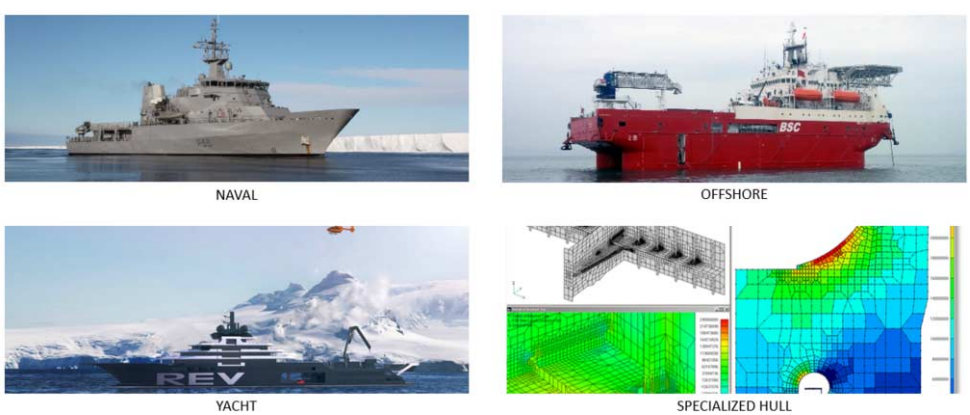

Figure 1: Markets and Specialized Hull Structures Addressed in Report

1.1.1 Market Analysis of Naval Craft

The previous three ISSC V.5 Specialist Committees have focused on Naval Vessel design specific to the Committee's report. Chapter 3 will address Naval Standards and the economic and structural design challenges involved in their utilization. This discussion is in part because the Official Discusser of the 2015 ISSC V.5 Report, Naval Ship Design, Jelle Keuning suggested a discussion in this area for Naval Ships is necessary. This Chapter will briefly

discuss the cost variations in naval vessels which make them not only special in structural complexity, but in economic impact to government budgets.

The current trends within the naval vessel market show the world's Navies are racing to repair and replace their existing capabilities, as well as further expand on their fleet to allow for new capabilities. Countries are discovering the cost of new construction programs is not advancing towards cost effective as it is extremely expensive to maintain an outdated platform beyond its designed service life. Navies are finding new construction is necessary to keep the industrial base alive for future programs as well as the vessels design is technologically and economically viable to maintain. Based on data collected by Maritime Affairs (2015) and shown in Figure 2, there are a substantial number of vessels planned in the next 15 years.

Table 1. World Naval Market Forecast 2013–2032.

	In progress		Planned		Projected		Total	
Vessel Type	No. of Hulls	US$B	No. of Hulls	US$B	No. of Hulls	US$B	No. of Hulls	US$B
Aircraft carrier	9	49.8	2	4.0	2	3.0	13	56.8
Amphibious	129	29.5	204	33.9	33	3.4	366	66.8
Auxiliary	57	8.1	112	40.1	16	3.1	185	51.3
Corvette	51	7.1	43	13.1	23	5.8	117	26.0
Cruiser	2	2.6	6	3.6	-	-	8	6.2
Destroyer	55	55.3	90	113.8	3	2.9	148	172.0
FAC	147	5.5	45	3.5	34	2.8	226	11.8
Frigate	193	68.8	75	42.4	44	17.0	312	128.2
MCMV	28	4.5	71	6.4	28	2.6	127	13.5
OPV	121	12.5	139	16.7	31	3.1	291	32.3
Patrol craft	1121	9.7	482	7.5	157	1.6	1760	18.8
Submarine	154	142.3	142	100.7	27	11.5	323	254.5
Total	**2067**	**395.7**	**1411**	**385.7**	**398**	**56.8**	**3876**	**838.2**

Source: AMI International, "2013 Naval Market Forecast", September 6, 2013, www.amiinter.com (accessed January 25, 2015).

MARITIME AFFAIRS Vol. 11 No. 1 Summer 2015

Figure 2: Forecasted Naval Craft Builds (Market Affairs 2015)

1.1.2 Market Analysis of Offshore Operation Vessels

The Offshore Oil & Gas market is supported by highly specialized vessels designed to perform very specific missions. These Offshore Operations vessels are required to be unique in hull and structural design which lends them to the "special" category. Chapter 4 touches on a few types of these specialized craft, their function and recent literary work that addresses the structural aspect of their on-board equipment, hulls and function. Chapter 2 will focus on the Rules that are relevant to these offshore vessels. Chapter 6 will go more in depth on the structural design of the hulls and other appurtenance.

Prior to the rapid oil and then offshore decline in late 2014, market predictions showed a steady uptick in offshore new construction on both offshore support vessels and specialized merchant vessels. The market has struggled to keep the industrial workers employed and companies learned quickly that diversified portfolios were extremely important to maintain. Clarkson's Research (2016) showed Offshore Supply Vessels (OSVs) have recently shown a sharp decline in the global order book due to the declining oil prices as shown in Figure 3. As a result, clientele will eliminate new build risk by focusing on acquisitions of highly specialized and multi-purpose vessels in order to allow for maximum flexibility in asset usefulness when oil prices dip once again.

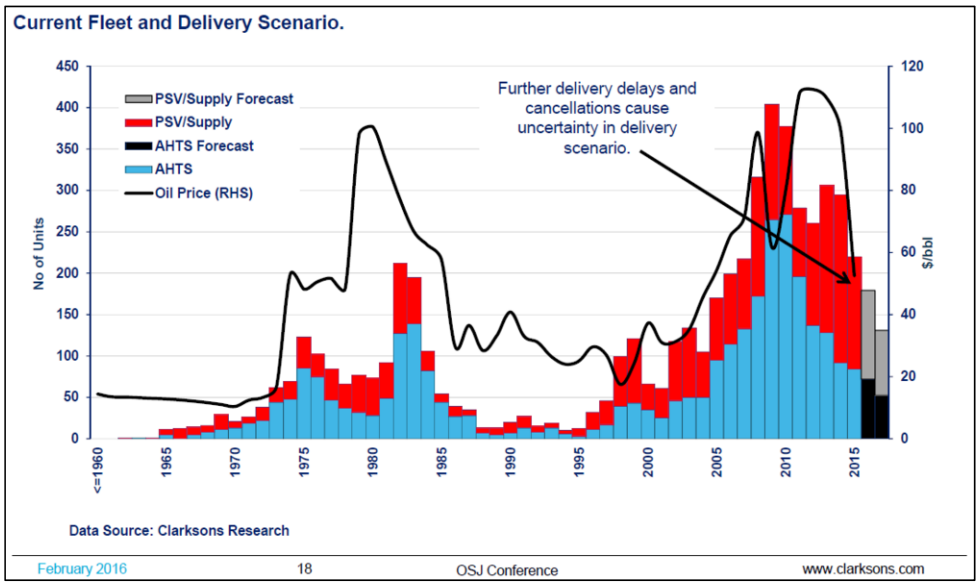

Figure 3: Rapid Decline in the Work Boat/OSV Market (Clarksons Research 2016)

1.1.3 Market Analysis of Yachts

The previous two ISSC V.8 yacht committees (2009 and 2012) focused on sailing and motor yachts respectively. This report focuses on larger pleasure yachts, primarily in excess of 30m, and so-called mega yachts – those at the extremes of the industry.

It is now widely recognized yachts over 24m length overall are considered to be superyachts, primarily due to the change in design regulations that occurs at this length. Despite the continuation of the struggling oil and gas industry, 2017 has seen a steadiness in the superyacht market with 760 yachts on order or under construction compared to 755 in 2016. These values are an advancement from previous years (refer to Table 1) indicating the market is improving.

Table 1: Build orders for Yachts >24m (Global order books 2013-2017)

Year	Build Orders
2013	692
2014	735
2015	734
2016	755
2017	760

Figure 4 shows the new yacht orders split into various categories for 2016. Evidently, there is significantly more demand for motor yachts with 74% of the market coming under this category.

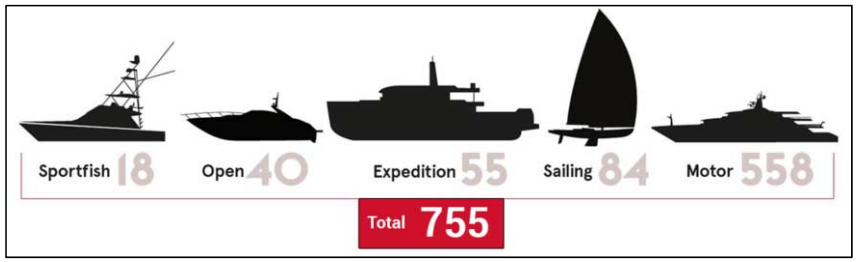

Figure 4: New yacht orders by type 2016 (Montigneaux, 2015)

The variation of market share with respect to yacht length, shown in Figure 5,shows the increase in demand for yachts over 40m in recent years. Some yachts are well in excess of 100m, the largest currently afloat being the Motor Yacht Azzam with an overall length of 180m and a gross tonnage of 12600te.

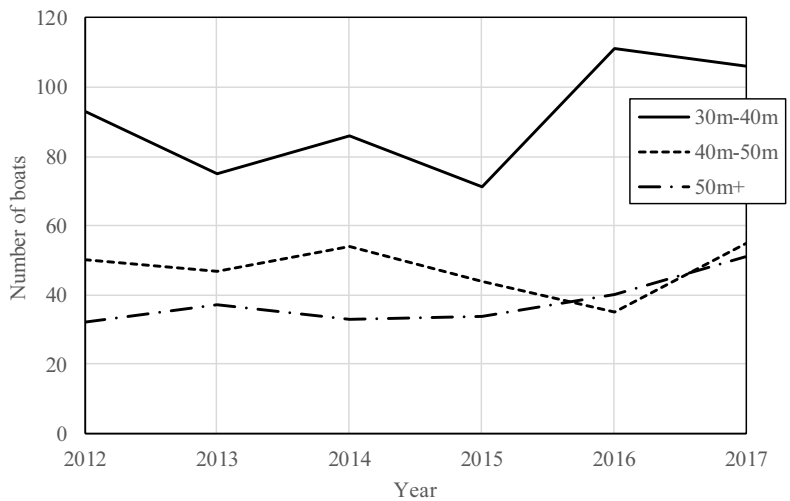

Figure 5: Yachts delivered > 30m from 2012-2017 (The Superyacht Intelligence, 2017)

2 RULES AND STANDARDS

This chapter highlights the most relevant rules and standards for the structural configurations of special craft covered by the Committee's mandate. Since this committee is a newly formed committee the aim is to give an overview of the existing regulations, its systematics and background rather than giving an insight in the technical details of the specific standard's requirements. To a certain extent related Rules and Regulations chapters from former ISSC reports of related committees were consolidated and updated.

2.1 HSC Rules

A set of rules that deals with several of the special craft covered by the committee's mandate are the International Code of Safety for High-Speed Craft (HSC Code) and the related adoptions from most classifications societies.

With the development of many new types of high speed craft in the 1980s and 1990s, IMO decided in 1994 to adopt the HSC Code (IMO 1994) and made it mandatory via a new SOLAS chapter X - Safety measures for high-speed craft.

The HSC Code applies to high-speed craft engaged on international voyages, including passenger craft which do not proceed for more than four hours at operational speed from a place of refuge when fully laden and cargo craft of 500 gross tonnage and above which do not go more than eight hours from a port of refuge.

According to the Code a High Speed Craft is defined as a craft that is capable of a maximum speed in knots equal to or exceeding

$$V = 7.16\ \Delta^{0.1667} \text{ (knots)} \quad (1)$$

Whereas Δ is the displacement corresponding to the design waterline in tons.

Due to rapid pace of development in the HSC sector, in December 2000, the Maritime Safety Committee adopted amendments to SOLAS chapter X to make the High-Speed Craft Code 2000 (IMO 2000) mandatory for new ships. The 2000 HSC Code updates the 1994 HSC Code and applies to all HSC built after the date of entry into force, 1 July 2002. The original Code will continue to apply to high-speed craft built before that date.

Almost all Classification Societies implemented the HSC Rules and extended it by further ship and/or special service types. This was especially true for Light Craft, Naval and naval support vessels are covered by most Societies' HSC Rules.

All societies except ABS follow the above IMO definition of a high-speed craft, whereas the ABS criteria is $V=2.36\sqrt{L}$. While it is not possible to directly compare the definitions as the IMO criteria is displacement vs. speed and the ABS criteria is length vs. speed it is nonetheless useful to show the two criteria together and to compare a specific vessel. Consider a corvette sized vessel that is classed as a HSC. It is 61 m long with a full load displacement of 950 tons. Under the IMO criteria a 950 tons vessel must have a design speed of at least 22.5 knots to be considered a high speed vessel. The same vessel, 61 m long, can have a design speed of only 18.4 knots under the ABS Rules and still be considered a high-speed craft.

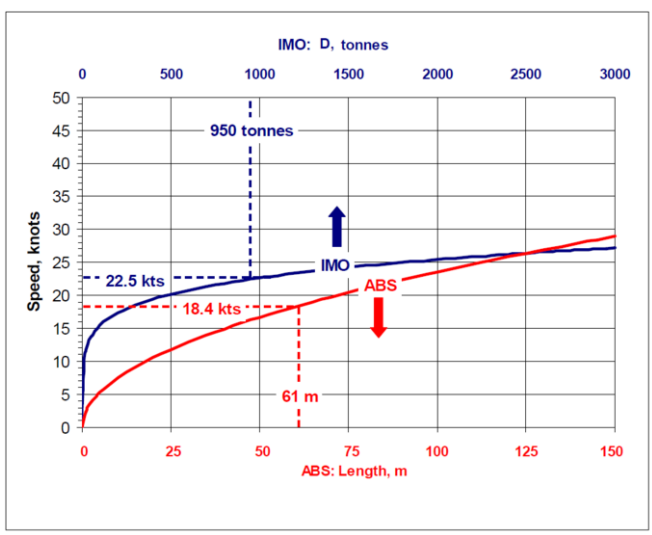

Figure 6: IMO and ABS Definitions of High Speed Craft (SSC 2005)

A light craft is defined as a craft with a full load displacement not exceeding

$$\Delta = (0.13\ L\ B)^{1.5} \text{ tons} \quad (2)$$

where L is the length at the design water line and B the full breadth at L/2 (m) (DNVGL 2015c).

2.1.1 ABS Rules for Classification of High-Speed Craft 2017

The HSC Rules or HSNC Rules are applicable to high-speed craft or high-speed naval craft constructed of steel, aluminium, or FRP. Applicable craft type and length are as follows:

Craft Type	Applicable Length
Mono-hull	< 130 m (427 ft)
Multi-hull	< 100 m (328 ft)
Surface Effects Ship (SES)	< 90 m (295 ft)
Hydrofoil	< 60 m (197 ft)

Further restrictions are given for coastal and riverine craft.

2.1.2 DNV GL Rules for Classification – High speed and light craft 2015c

In the DNV GL Rules it is distinguished between the High Speed Light Craft (HSLC) and Light Craft (LC) notation. All high speed, light craft and naval service craft shall, in addition to the main class, have a ship type notation as well as a service restriction notation as a part of their classification as defined in Table 2.

Table 2: Service area restrictions (DNVGL 2015c)

Service area notations	*Seasonal zones (nautical miles)*		
	Winter	*Summer*	*Tropical*
R0	250	No restrictions*	No restrictions*
R1	100	200	300
R2	50	100	200
R3	20	50	100
R4	5	10	20
R5	1	2	5
R6	0.2	0.3	0.5
*) Unrestricted service notation is not applicable for craft falling within the scope of the HSC Code, i.e. ship type notations **Passenger**, **Ferry** or **Cargo**			

Several ship types, specifically Passenger and Cargo Craft, Car Ferries, Crew – and Patrol Boats, Small Service Craft, Naval and Naval Support vessels as well as naval landing craft are addressed. The materials steel, aluminium, fibre composite and sandwich constructions are specifically addressed in individual Chapters.

Scantling reductions for high speed and light craft steel and aluminium structures as compared to the Rules for Classification of Ships, are captured within these Rules and based on:

- thorough corrosion protection of steel, carried out under indoor conditions
- a certain stiffener spacing reduction ratio s/sr

  s = chosen spacing in mm

  sr = basic spacing = 2(240 + L) for steel and 2(100 + L)/1000 [m] for aluminium
- longitudinal framing in bottom and strength deck
- extended global longitudinal and local buckling control
- sea and weather service restrictions

The reduction factor s/sr shall not be taken less than 0.5 or greater than 1.0.

For the Naval Landing Craft special structural requirements are defined. Bottom plating and stiffening within the beaching protection length shall be increased by 20%. For impact areas the spacing of longitudinals not to be greater than 500 mm. A formula for an average beaching pressure is given for dimensioning of the girders and web frames within the beach protection length. If the craft has to be pushed out from the beach, the front ramp shall have to be dimensioned for push-out loads. For the push out area a load corresponding to 50% of the displacement is proposed. The ramp structure is to be designed according to the rules for Car Ferries.

2.1.3 LR Classification of Special Service Craft Rules 2016

LR Rules distinguish between the High Speed Light Craft (HSC) and Light displacement Craft (LDC) notation. The notations are appended by a service area restriction, service type and a craft type notation. The following service types are possible: Cargo, Passenger, Passenger Yacht, Patrol, Pilot, Yacht or Support Yacht Craft, Wind Farm Service Vessel, Workboat.

The following craft types are foreseen: amphibious air cushion vehicles, catamarans including wave piercers, hydrofoil craft, rigid inflatable boats, surface effect ships, small waterplane area twin hull ships (SWATH).

The Rules are applicable to the following craft types constructed from steel, aluminium alloy, composite materials or combinations of these materials:

- High speed craft
- Light displacement craft
- Multi-hull craft
- Yachts of overall length, LOA, 24m or greater
- Craft with draught to depth ratio less than or equal to 0.55

The following craft types will be considered upon request on the basis of the Rules:

- Amphibious air cushion vehicles
- Rigid inflatable boats
- Hydrofoil craft

All craft classed under the LR SSC Rules are assigned a service area restriction and a service type notation as follows:

- G1: Craft intended for service in sheltered waters adjacent to sandbanks, estuaries, etc. and in reasonable weather where the range to refuge is, in general, 5 nm or less
- G2: Craft intended for service in reasonable weather, in waters where the range to refuge is 20 nm or less, e.g. craft operating in defined coastal waters
- G2A Service Group 2A covers craft intended for service in reasonable weather in waters where the range to refuge is 60 nautical miles or less.
- G3: Craft intended for service where the range to refuge is 150 nm or less
- G4: Craft intended for service where the range to refuge is 250 nm or less
- G5: Craft intended for service where the range to refuge is 350 nm or less
- G6: Yachts and patrol craft having unrestricted service.

Depending on the service type a correction factor $\omega > 1.0$ is defined for the determination of the minimum thickness of plating and stiffeners.

Table 3: Service type correction factor (ω)

Service type notation	ω
Cargo	1,1
Passenger	1,0
Patrol	1,0
Pilot	1,1
Yacht	1,0
Workboat MFV	1,2

2.1.4 CCS China Classification Society 2017

In 2017, CCS revised its Rules for Construction and Classification of Sea-Going High Speed Craft. The main revisions are:

- A craft assigned with the class notations does not necessarily have to comply with the requirements of the HSC Code
- Trimaran as well as Open Sea Service Restrictions are now also covered by the Rules
- Requirements for distance between butt welds and fillet welds have been included
- A new section covering Supplementary Requirements for Aluminium Alloy Stiffened Plates is introduced.

The structural requirements like design pressures, global cross sectional loads, and equipment number are strongly linked to the chosen service restriction for a vessel which is related to the maximum value $H_{1/3\,max}$ of the assumed wave heights.

Table 4 Service Restrictions

Service Restriction	Wave height
Greater Coastal Service Restriction	$H_{1/3\,max}$ = 6.0 m
Coastal Service Restriction	$H_{1/3\,max}$ = 4.0 m
Sheltered Water Service Restriction	$H_{1/3\,max}$ = 2.0 m
Calm Water Service Restriction	$H_{1/3\,max}$ = 1.0 m

2.2 Yachts

There is a wide variety of national and international rules and regulations which motor yachts must adhere to. In addition to the rules from classification societies, the International Maritime Organisation (IMO), National Regulations, and Port State Regulations, large motor yachts must meet the following International Conventions:

- Safety of Life at Sea (SOLAS);
- International Load Line Convention (ILLC);
- MARPOL, devoted to the control of the marine pollution;
- International Regulations for Preventing Collisions at Sea (COLREG), which
- provides requirements for steering and sailing, navigation lights and sound signals;

- Standards of Training, Certification and Watchkeeping (STCW).
- Maritime Labour Convention (MLC 2006)

The rule's applicability depends on yacht characteristics such as dimensions (represented mainly by load line length and gross tonnage), the type of service and the number of passengers. Yachts are subdivided into two main categories: superyachts with a freeboard length over 24m and yachts below 24m.

Rules and regulations governing commercialized pleasure craft were discussed in some detail in the ISSC 2012 Report of the V.8 Committee. The updates with regard to rules and regulations applicable to yachts over 24m in length (private and commercial) are shown in Figure 7.

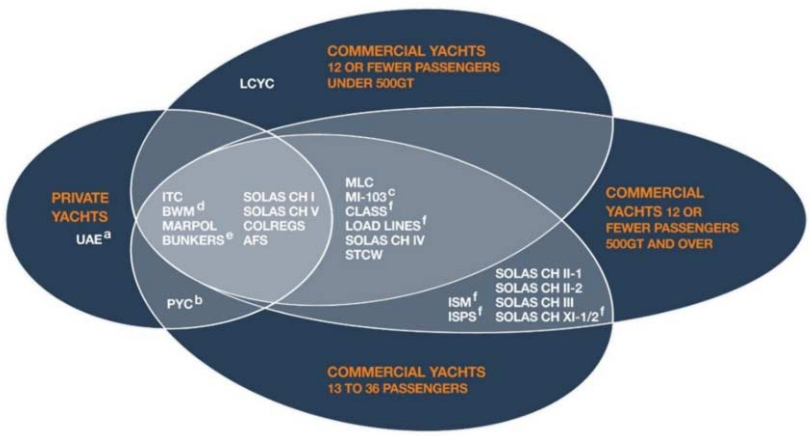

Figure 7: Rules and regulations applicable to yachts > 24m (Manta Maritime 2015)

The primary updates to the regulations for super and megayachts are the release of an update to the Large Yacht Code from the MCA in the form of LY3 (Maritime and Coastguard Agency 2012), yearly updates to the Passenger Yacht Code (PYC) and most recently the latest updates to both of these at the end of 2017 combined as two parts of the whole now known as REG-YC – the Red Ensign Group Yacht Code (ref REG-YC).

Except for the just recently released DNVGL Rules and the CCS Rules a synopsis of structural requirements and issues contained in the rules and regulations of most of the following Classification Societies Rules was already presented in ISSC 2012 and with respect to sailing yachts in ISSC 2009 report.

The DNVGL rules for Yachts (DNVGL 2016) cover all aspects of classification of yachts, including motor yachts, passenger yachts, sailing yachts and sail ships. The rules are based on the former GL rules and guidelines and the technical requirements are updated to represent the latest experience with classification of yacht projects. The structure of the rules is aligned with other rule books, and all applicable yacht types are included. Content from other rule books is reused as far as possible ensuring a consistent approach to classification. The structural design requirements are mainly covered in Part 3 Hull of the Rules. In Chapter 2 requirements with respect to subdivision, compartment and access arrangement are devoted. In Chapter 3, 'Hull design loads', it is stated that the wave-induced hull girder loads may be determined by direct calculation alternatively to the rules loads based on wave scatter diagrams. Chapter 4, 'Metallic hull girder strength', accounts for the special structural design of yachts characterized by many and large openings. It is described how structural members not contributing to hull girder sectional area are to be determined (e.g. shell large openings exceeding 2.5 m in length or 1.2 m in breadth are to be deducted from the sectional area used in hull girder moment of inertia and section modulus.) Chapter 6 describes generic modelling techniques, loads, acceptance

criteria and required documentation for finite element analysis of different type of yachts built in steel or aluminum. Methodologies for finite element analysis of yachts built in composites and other composite related requirements are defined in Chapter 5. In Chapter 7 the detailed requirements for rudder, foundations and appendages can be found.

The Chinese Classification Society (CCS) published in 2012 its Rules for Construction and Classification of Yachts. In line with the international regulations the Rules distinguish between yachts of less than 24 m in length and those above 24m but less than 90m. The structural requirements like design pressures, global cross sectional loads, and equipment number are strongly linked to the chosen service restriction for a vessel which is related to the maximum value H1/3 max of the assumed wave heights.

Table 5 CCS Yacht Service Restrictions

	Wave height	Distance to shore
Category I	$H_{1/3\ max}$ = 8.0 m	> 200 n miles
Category II	$H_{1/3\ max}$ = 6.0 m	< 200 n miles
Category III	$H_{1/3\ max}$ = 4.0 m	< 20 n miles
Category IV	$H_{1/3\ max}$ = 2.0 m	< 10 n miles
Category V	$H_{1/3\ max}$ = 1.0 m	< 5 n miles

2.3 Naval craft / Surface Combatant

Due to the increasing complexity of naval ships and the need to reduce ship construction costs in the face of ever decreasing defence budget funds, a great deal of attention has been given in recent years to addressing ways to improve Naval ship design and construction practice in many countries.

2.3.1 NATO and national standards

Naval ships have traditionally been designed to in-house standards. These standards and design approaches were developed by various navies based on extensive experience and research. An overview of the different national regulatory approaches was given in ISSC report 2006 (ISSC 2006). Since then two new German Naval Standard (BV) were issued. In 2007 the BV 1040-1 Structural Strength of Surface Ships was revised (BAAINBw 2007). These naval construction rules shall describe only that navy-specific portion of a naval vessel – for application on ships of the German Navy – that cannot be specified by industrial/class rules. The standard is not restricted and contains consequently no military loads. Those are specified e.g. in the classified standard BV 0230 Shock Resistance (BAAINBw 2017). This standard has been developed as a joint regulation with the Dutch Defence Materiel Organisation and under the Dutch designation D5050-0599. In contradiction to its revision 2004, which required threat and design specific determination of shock loads by direct global shock simulations, the 2017 revision contains again empirical shock design spectra.

Also the United Kingdom Royal Navy revised its Shock Manual. The former Shock Manual BR 3021, which was already superseded by the BR8470-8473, was revised by MAP 01-470, Shock Design Manual (MoD 2012). The shock loading to be withstood is associated with equipment location and based on Shock grade schemes. Each shock grade zone represents a different region within the vessel. From the Shock Response Grade Scheme also transient parameters can be derived allowing shock calculations in the time domain.

Standards developed within NATO have been written by committee membership representing various navies and aimed at providing a common minimum requirement. A Standardization Agreement (STANAG) is a NATO standardization document that specifies the agreement of member nations to implement a standard. Because of its consensual nature as an agreement between several countries a STANAG can often be considered as a minimum requirement only. Besides STANAG NATO publishes Allied Engineering Publications (ANEP). The most recognized ANEP is the ANEP-77 known as the Naval Ship Code (NSC). ANEP-77 forms a naval alternative to the commercial ship safety standard SOLAS. The code is a goal based standard that determines a minimum level of safety for naval vessels. It is however not intended to apply to combat operations or their associated threat conditions. The NSC contains three distinct parts as shown in Figure 8.

The code is primarily written as a "Standard for the selection of standards" rather than a standard for direct application. The goals are given on a high generic level and it is expected that the more detailed prescriptive requirements will be found in underlying technical standards such as Classification Rules. In practice, the code is aimed to act as calibration and a framework for rule development of Classification Rules for hull strength of naval craft.

Being a generic code, the ANEP-77 can be applied for any type of naval craft. The differences between the different ship types are mainly related to various functions and operating conditions of the ship.

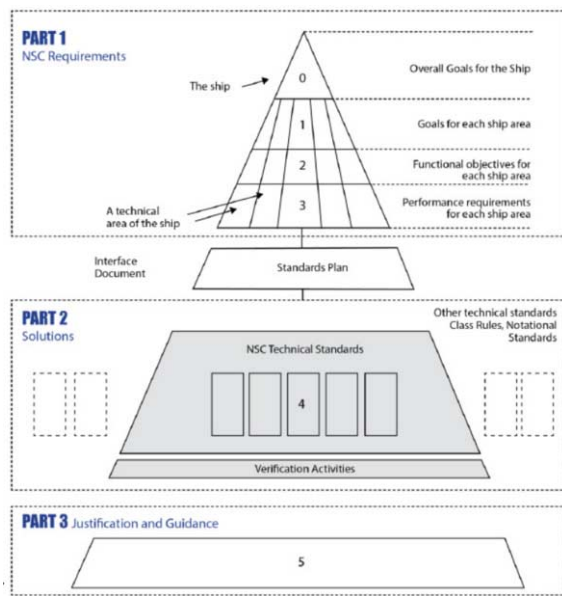

Figure 8: Arrangement of the Naval Ship Code

The structural requirements stipulated in Chapter II of ANEP-77 are that for the design life of the ship, the structure shall be designed, constructed and maintained to:

- Provide weathertight and watertight integrity;
- Carry all loads that may be foreseen;
- Permit embarked persons to carry out their duties safely;
- Protect the embarked persons and essential safety functions in the event of all foreseeable emergencies and accidents at least until the persons have reached a place of safety or the threat has receded;

- Minimise the risk of loss of the ship under non-combat related maritime scenarios.

The Goals relate to the main functions of the ship structure, and one may observe that the goals give a wider scope for the hull structure than is normally found in standards for structural strength.

2.3.2 Class Rules

Naval classification is a relatively new concept especially because naval ships are not required to comply with international Conventions and Codes, like IMO and other institutions. Over the last 25 years navies have however undergone significant changes in the pursuit of efficiencies in the areas of acquisition and support of their platforms. This included adapting their own approach to be more compatible with commercial standards and practices.

Naval Class Rules have been published by several members of the International Association of Classification Societies. An overview of the ship type related notations explicitly handled by the different societies' rules is shown in Table 6.

Some Classification Societies like ABS define only few higher-level categories embracing several different ship types. It should however be noticed that some societies offer the possibility to extend the notation by any further description which indicates the operational role for which the ship is designed.

ABS rules for naval ships are covered by the International Naval Ship Guide "INSG" (ABS 2017a) and High-Speed Naval Craft "HSNC" (ABS 2017b).

Both the former GL and DNV rules for naval vessels are brought forward as DNV GL rules. The GL naval rules were incorporated in the DNV GL rules as a separate rule book; "NAVAL" (DNVGL 2015a). The DNV rules for Naval are incorporated as an integral part of the rules for Ships "SHIP" (DNVGL 2015b) and the rules for High Speed and Light Craft "HSLC" (DNVGL 2015c).

Table 6: Coverage of Ship types notations by Class' Rules

	ABS	LR	BV	DNV GL		RINA
				DNV	GL	
NAVAL COMBATANT	INSG			SHIP		RINAMIL
- Cruisers		NS2			NAVAL	
- Destroyers		NS2			NAVAL	RINAMIL
- Frigates		NS2	NR483		NAVAL	RINAMIL
- Corvettes		NS2	NR483		NAVAL	RINAMIL
NAVAL FORCE PROJECTION	INSG					
- Aircraft carriers		NS1	NR483		NAVAL	RINAMIL
- Helicopter carriers		NS1				RINAMIL
- Amphibious assault vessels		NS1	NR483		NAVAL	RINAMIL
NAVAL SUPPORT	INSG		NR483	HSLC / SHIP		RINAMIL
- Fleet replenishment		NS (SR)				
- Landing ships		NS3		HSLC		
- Logistic support		NS (SR)				
- Mine warfare		NS3			NAVAL	RINAMIL
NAVAL CRAFT (high speed)	HSNC					FPV
- patrol craft		NS3		HSLC		
- fast attack craft		NS3				
COASTAL NAVAL CRAFT	HSNC	NS3	NR483	HSLC		RINAMIL
RIVERINE NAVAL CRAFT	HSNC	NS (SSC)		HSLC		
GOVERNMENT SPECIAL PURPOSE	INSG					
COAST GUARD	INSG					

In addition to its rules for Naval Ships "RINAMIL" (RINA 2017), RINA has published a special rule book only for fast patrol vessels (Rules for the Classification of Fast Patrol Vessels - FPV -, which are intended for the classification of high speed ships up to 65 m and built in steel, aluminium alloy or composite materials - RINA 2007). Specific rules also cover Combat System Physical Integration and existing naval ships. It is anyway to be noted that the approach to classification is generally more articulated, starting – for each new build – from the definition of a specific and comprehensive "Regulatory Framework", which outlines the complete set of reference rules and regulations to best fit the ship type and its operational features.

BV "NR483" (BV 2017) and Lloyd's "Nx" (2017a) compiled all navy Rules in one Rule book.

2.4 Polar Ship / Icebreaker

On 21 November 2014 and 15 May 2015, the International Maritime Organization (IMO 2014, IMO 2015) formally adopted the safety and environmental parts of the Polar Code at its Maritime Safety Committee (MSC) and Marine Environmental Protection Committee (MEPC) meetings. The goal based Polar Code introduces a broad spectrum of new binding regulations covering elements of ship design, construction, onboard equipment and machinery, operational procedures, training standards, and pollution prevention. The code entered into force for new ships on 1st January 2017 and for existing ships on 1st January 2018. Two primary hazards which pose risks to hull structures are addressed by the Polar Code in Chapter 3, low air temperature and the presence of ice, resulting in the ship structural goal to provide that material and scantlings of the structure retain their structural integrity based on global and local response due to environmental loads and conditions. Two IACS standards are referenced for demonstration of compliance.

- IACS Unified Requirement UR S6 - Use of Steel Grades for Various Hull Members – Ships of 90 m in Length and Above (IACS 2015)
- IACS Unified Requirements UR I Requirements Concerning Polar Class (IACS 2016)

IACS UR S6.3 has selection criteria for minimum steel grade requirements for ships operating in low air temperature environments. Based on the ship's design temperature, a structural member's thickness and material category, minimum steel grades are prescribed. IACS has incorporated changes to IACS UR S6.3 to account for the new definition of the Polar Service Temperature introduced by the Polar Code. If a ship has a Polar Class notation, IACS UR I2 contains ice class-dependent prescriptive material requirements that should be used.

Beside the first functional requirement of operation in low air temperature, the second functional requirement deals with appropriate levels of ice strengthening. The Polar Code established three categories linked to recognized IACS Polar ice classes. Table 3 shows which ice classes are required for each category.

Table 7: Polar Ship Categories (ABS 2016b)

Category	Description	Ice Class
A	Designed for operation in Polar waters in at least medium first-year ice which may include old ice inclusions	IACS PC1, PC2, PC3, PC4, PC5*
B	Designed for operation in Polar waters in at least thin first-year ice which may include old ice inclusions	IACS PC6 - PC7*
C	Designed to operate in open water or in ice conditions less severe than those included in Cat A or B	Scantlings adequate for intended ice types and concentrations

*Or alternative standard offering an equivalent level of safety

The Finnish-Swedish Ice Class Rules (FSICR) were generally considered as the industry standard for ships operating in first year ice. A detailed description on the evolution of the FSICR is given in Riska and Kämäräinen (2012).

Steel plastic design of hull structure has become the new norm for ice class ship design. The new IACS unified polar rules (IACS UR I), the Canadian Administration (ASPPR 1996) and the Russian Maritime Register all employ plastic design methods.

Navigation in coastal waters within Canadian jurisdiction north of latitude 60°N is governed by the Arctic Shipping Pollution Prevention Regulations (ASPPR). The ASPPR deal with the construction of ships (certain construction requirements for different navigation zones). Four Canadian Arctic Categories (CAC) have replaced the previous Arctic Classes. Details of the structural classifications are provided in the Transport Canada publication "Equivalent Standards for the Construction of Arctic Class Ships - TP 12260". Under the ASPPR no ship carrying more than 453 m^3 of oil shall navigate in any of the zones illustrated unless the ship itself meets prescribed construction standards as either an Arctic Class ship, or a Canadian Arctic Category (CAC) ship or a Type A, B, C, D or E ship.

The Northern Sea Route (NSR) is a significant issue not only for the Russian Federation but for the entire international community. The main regulatory act to be applied to the area in Russia is Federal Law 132-FZ of 28 July 2012 often referred to as the NSR Law. Regulatory measures vessels sailing along the NSR have to comply with are: Guide to Navigating through the NSR, Regulation for Icebreaker and Pilot Guiding of Vessels through the NSR, and Requirements for Design, Equipment and Supply of Vessels Navigating the NSR all adopted in 1996.

Winterisation measures are those which ensure an offshore vessel is prepared for operation in cold climates focusing on the adverse effects and the control of icing, freezing and wind chill. DNV GL developed a new offshore standard which came into effect in April 2014 and covers the technical requirements to control these adverse effects (DNVGL 2014).

2.5 Offshore Operations Vessels

A not necessarily exhaustive overview of some classification societies' rules and non-class standards addressing structural specialties of the offshore ships covered in Chapter 4 are shown in Table 8. Swath specific rules are incorporated by most Classification Societies in their High Speed Light Craft Rules, see above.

2.6 Special Structures Rules and Standards

2.6.1 Moonpools

A moonpool is a vertical well extending through the vessel from deck to bottom, providing a direct access to the sea and allowing safe and easy deployment of equipment used for drilling, diving, cable laying or any other subsea operation. The following Guidelines from Classification Societies address moonpools specifically in their rule requirements.

ABS (2014) provides prescriptive formulations for the dimensions of plates and stiffeners of longitudinal and transverse moonpool bulkheads. Guidance is also given for the strength assessment of the hull structure in the moonpool region based on a 3-D finite element model.

Bureau Veritas (BV 2016d) Guidelines for Moonpool address resonant pumping, sloshing, vortex generation as hydrodynamic phenomena having potential undesirable effects to be considered in the design of the vessel moonpool. As a rule the scantlings of moonpool bulkheads are to be calculated as side shell according to the Rules applicable to the vessel.

DNVGL's Offshore standard (2015i) requires that stress distribution in areas with global stress concentrations and discontinuities, e.g. moonpool openings, turret openings, etc. shall be derived from fine mesh FE analysis.

Table 8: Rules and Standards for Offshore service vessels and work boats

	Offshore Drilling Units	Self-Elevating Vessels (Liftboats)	Heavy Lift (Semi-Submersibles)
ABS	Rules for Building and Classing Mobile Offshore Drilling Units (ABS 2017c)	Guidance Notes on Structural Analysis of Self-Evaluating Units (ABS 2016a)	Guide for Building and Classing Semi-Submersible Heavy Lift Vessels (ABS 2017d)
BV	Classification of Drilling Ships (BV 2016a)	Rules for the Classification of Self-Elevating Units - Jack-ups and Liftboats (BV 2016c)	Rule Note Semi-Submersible Cargo Ships (BV 2016b)
CCS	Rules for Classification of Mobile Offshore Units (CCS 2016)	X	Rules for Classification of Sea-going-steel Ships (CCS 2015)
DNV GL	Rules for Classification Offshore drilling and support units (DNVGL 2015d)	Rules for Classification Self-elevating units (DNVGL 2015e) Structural design of self-elevating units - LRFD method (DNVGL 2015f)	Rules for Classification - Vessels for special operations (DNVGL 2015g)
LR	Rules for the Classification of Offshore Units (Lloyds 2017b)		
RINA	Rules for the Classification of Floating Offshore Units at Fixed Locations and Mobile Offshore Drilling Units (RINA 2013)		Rules for Checking the Arrangements intended for Sea Transportation of Special Cargoes (RINA 2014)
non-Class Standards	IMO – Resolution A.1023(26) MODU Code (IMO 2009)	Guidelines for Site Specific Assessment of Mobile Jack-Up Units (SNAME 2002)	X

2.6.2 Helicopter Decks

Table 9 gives an overview about load specification during helicopter landing while Table 10 relates to helicopter in the stowed position as specified by the referenced standards and Class' Rules.

With the assistance of experts from both the large yacht and aviation industries, the Maritime and Coastguard Agency of the United Kingdom has also developed technical standards for helicopter landing areas on board large commercial yachts. The standards were designed to amend section 24.2 of the Large Commercial Yacht Code (LY2). Lardner (2007) had explained the rationale behind the development of these standards, published as Amendment 1 to the Large Commercial Yacht Code. Further to this, the process of compliance is explained with an introduction to the newly appointed aviation inspection body delegated the responsibility for approving landing areas against aviation-specific criteria. In explaining the development of the Amendment, this paper outlines the main findings of a study group established to highlight issues and propose solutions.

The numbers of large offshore structures and fixed jacket type platforms are rapidly increasing for oil and gas companies. Generally, a shuttle vessel or helicopter is used to access offshore structures such as a fixed platform, floating platform, jack-up rig and so on. The helideck structure should be installed in these offshore structures for landing and taking-off of the helicopter. The helideck structure comprises of pancakes, girders using aluminium materials and supporting steel structures. The helideck structure should be designed to accommodate a safe landing area suitable for the largest and heaviest helicopter that is anticipated to land on the helideck. The helideck and its supporting structure are safety critical elements as a result of their role in emergency evacuation, as well as during normal operations. The codes and standards applicable for the structural design of the helideck will be determined by where the helideck is to be operated and the national jurisdiction governing the installation or vessel of which the helideck will become part. International standards such as ISO, Eurocodes, or

national standards, e.g. BS 5950, NORSOK N-004 or AISC (American Institute of Steel Construction) may be specified for detailed design. The results of structural analysis and design that has been performed for a 28.54 meter diameter octagonal standard aluminium helideck with support truss & lower steel support structure of jackup drilling rig based on the NORSOK requirements had been presented by Park et al.(2016). The supporting structure is designed to provide the adequate resistance to the external force produced by the design helicopter and environmental conditions.

The report is specifically targeting the structural configurations of free standing non-integrated helicopter decks, but there are many naval ship types with integrated helicopter decks structures or "flight decks". These ships can host organic and/or external aircraft, providing not only take-off, landing and shelter capabilities, but also other services like JP5 refuelling, Vertical Replenishment (VERTREP), afloat maintenance, etc. These flight decks were discussed in report V.5 of the 2015 ISSC Specialist Committee on Naval Vessels.

Table 9: Helideck Loading Specifications - Helicopter Landing

Authority	ISO 19901-3 (2014)	CAP 437. (2016)	HSE (2001)	ABS (2015)	BV (2000)	DNV·GL (2015h)	Lloyd's (2013)	CCS (2015)
Heavy Landing	-	1.5M	1.5M	-	1.5M	-	-	1.5M(6) 1.75M(7)
Emergency Landing	2.5M	2.5M	2.5M	1.5M(1)	3.0M	3.0M	1.5M(2) 2.5M(3)	-
Deck Response Factor	1.3	1.3(4)	1.3(4)	-	-	-	-	-
Super-imposed Load kN/m^2	0.5	0.5	0.5	2.0(5)	2.0(5)	As normal class	-(2) 0.2(3)	0.5
Lateral Load	0.5M	0.5M	0.5M	-	-	-	0.5M	0.5M
Wind Load	Max. Oper.	Sect'n 11	Sect'n 11	Normal design	-	vel=36m/s	-	-

M maximum take-off weight

(1) Or manufacture's recommended wheel impact loads

(2) For design of plating

(3) For design of stiffing and supporting structures

(4) Additional frequency dependent values given for the Chinook helicopter

(5) Considered independently

(6) For normal landing

Having activity of human under the helideck

Table 10: Helideck Loading Specifications - Helicopter at Rest

Authority	ISO 19901-3 (2014)	CAP 437. (2016)	HSE (2001)	ABS (2015)	BV (2000)	DNV·GL (2015h)	Lloyd's (2013)	CCS (2015)
Self-weight	M	M	M	M	M	M	-	M
Super-imposed Load kN/m^2	2.0	0.5	0.5	0.49	0.5	As normal class	2.0	0.5
Wind Load	100yr storm	Sect'n 11	Sect'n 11	Normal design	Normal Design	vel=51.5m/s	-	-
Platform Motions	As calc.	As calc.	As calc.	As calc.	As calc.	As calc.	-	As calc.(1)
M maximum take-off weight (1) Or 0.5M								

For standards regarding helicopters decks integrated into naval vessels, the overall configuration (including outfitting, provisions and lighting for night and day operations, safety matters, etc.) is generally ruled by NATO standards (NATO APP2). In terms of structural scantling, Classification Societies suggest possible approaches, which can also refer to FE verifications, but it is worth mentioning - as an internationally recognised reference - the US Design Data Sheet (DDS) 130-2, used to analyse the structural strength of helicopter flight and hangar decks on naval ships.

2.6.3 Free-Fall lifeboats

Free-Fall lifeboats are designed and built in accordance to the requirements of IMO SOLAS and LSA regulations and MODU codes.

Ronold & al (2009) presented a new standard for site-specific design of free fall lifeboats, developed aiming at providing for sufficiently safe lifeboat designs. The objective has been to develop a standard that follows the same reliability based safety philosophy and design principles as those implemented and used for design of conventional fixed and floating offshore structures. The standard is intended to cover all aspects involved in the design process for a free fall lifeboat, providing requirements that shall be met in design as well as guidance on how to meet these requirements. The following aspects are covered: Safety philosophy and design principles, metaocean conditions, loads, materials, structural design, operational requirements, occupant safety and comfort, model testing and full scale testing, installation, equipment, and qualification of lifeboat concepts. The new standard is published both as an OLF Guideline by the Norwegian Oil Industry Association OLF and as a DNVGL Standard (2016a). The paper presents the highlights of the new standard with emphasis on topics which are critical for design of free fall lifeboats, first of all structural safety, human safety and comfort, and headway.

3 NAVAL CRAFT

The ultimate purpose of naval craft is: "to deliver ordinance on target". This unique performance requirement distinguishes naval craft from other ship types and explains why they are special. The simple mission statement is compounded by the need for naval craft to perform while in harm's way and under arduous conditions. Unlike most commercial craft, there is no expectation of profit or financial return from the operation of naval craft and hence rather different criteria need apply to quantify their merits and justify design requirements. Commercial (e.g. profit driven) practice based on trade-off rationalization for cost saving

makes little sense when considering, for example, whether a warship's magnetic characteristics are more important than its radar cross section.

Jane's Fighting Ships (Saunders & Phillpott 2016) identify 27 types of naval craft in addition to a group of navy specific miscellaneous designs. The miscellaneous category covers specialized vessels including submarine and diving tenders, torpedo recovery boats, bridge erection vessels, barges, tug boats, fire boats, hospital ships, and many others. Naval vessels typically include coast guard ships and harbour craft that in all, number about 7,000 worldwide but comprised less than 10% of the more than 70,000 ocean going merchant and passenger ships registered in 2016. The range of ship types presented in Table 11 suggests a broad and complex set of potential design standards and specifications. Application of traditional (generic) classification society notation to such special craft requires significant interpretation of design rules.

Table 11: Types of Naval Craft

SUBMARINES	Ballistic missile	Cruise Missile	Fleet	Patrol
AIRCRAFT CARRIERS				
CRUISERS				
DESTROYERS				
FRIGATES				
CORVETTES				
FAST ATTACK CRAFT	Missile	Torpedo	Gun	
PATROL CRAFT				
MINELAYERS				
MINEHUNTERS	Ocean	Coastal	Inshore	Minesweeping
ASSAULT SHIPS				
LANDING	Ships	Craft		
DEPOT REPAIR SHIPS				
SURVEY RESEARCH SHIPS				
SUPPLY SHIPS				
TANKERS	Large	Small		
HYDROFOILS & ACV's				
MISCELLANEOUS				

3.1 Why Naval Standards are Special

Naval standards for the design and fabrication of the ship types listed in Table 12 have been developed by many navies, out of necessity, and apply to vessels owned and operated by naval forces. Of particular interest to, and in keeping with the ISSC special craft committee mandate, it turns out that naval standards specifically address the structural challenges and uncertainties in established design methods and modelling techniques with a focus to endure specific extreme loading conditions that arise from the environment as well as the threat of combat. Public access to naval design standards varies between countries depending on national classification restriction policies, however even a cursory examination of those in the public domain provide important insight into the type and nature of prescriptive design direction is not explicit in commercial classification society notation based standards. Naval standards tend to restrict the ship designers options of specific requirements and direct choices toward selection of materials and features that result in more: damage tolerant structural details; battle hardened electrical and mechanical system design detail; fail-safe design methods; structural optimization for weight reduction; compartmentalization to survive collisions and weapons effects and general arrangement criteria for inherent vulnerability reduction; stealth and susceptibility criteria; EMI/EMC/EMP compliance; underwater noise related vibration reduction; shock, blast, fragmentation, fire, flooding and smoke protection; verification and validation programs; among others.

Table 12: Naval Craft Type (Category) Definition

Ship Type	Role	Definition	Examples
I	Combatant	Ship intended to operate in harm's way: • Ships intended to engage in combat • Ships intended to deploy combat systems for offensive, defensive or surveillance purposes; and Troop transport vessels	Aircraft Carriers, Cruisers, Destroyers, Frigates, Patrol Boats, Troop transports
II	Combat Support	Ships expected to operate in harm's way in close support of combat operations. • Fleet Replenishment vessels • Ships considered of tactical or strategic "high value"	AOR's, Tankers, Hospital Ships
III	Naval Auxiliaries	Ships not intended to operate in harm's way (all Ships not type I or II)	Tugs, Ferries, Training Vessels, Research vessels, Work boats, Barges, Range vessels etc.

A good example that describes the nature of naval standards can be found in the UK Ministry of Defence Standard 02-154 dealing with Surface Ship Structures. Its scope covers:

"This NES (Naval Engineering Standard) defines the structural strength standards that are to be achieved in the design, construction and modification of all surface warships. It is also applicable to the military requirements of Royal Fleet Auxiliaries and other non-military craft owned by the MOD where these requirements are in addition to the Rules of Lloyd's or another Classification Society to which the ships are designed. The provisions of this NES apply only to conventional mono-hull vessels and not to multi-hulled or high-speed planing craft."

The NES-154 opening technical paragraph directs and delimits the choice of material for construction of naval ships to the 4 steel types listed in Table 13, with an immediate focus on why the selection is important:

"The particular concern in relation to material and assembly quality in the construction of steel ships is the avoidance of brittle fracture of the structure under high rates of loading or cold conditions. The choice of steel is therefore to be made in accordance with the following paragraphs. However, brittle failure may occur in all steels under specific, albeit rare, conditions and so the quality of construction is also important and the requirements of NES 147, NES 155 Part 1, NES 706 and NES 769 must be followed in addition to the requirements set out in the following clauses so as to ensure that avoidable crack initiating points are not built into the structure."

Table 13: NES-154 Steel Selection Table

Description	MOD Standard	Classification Society Grade	British Standard
Mild steel	NES 791 Part 1	A	BS 4360 grade 43A
Mild steel with guaranteed toughness	NES 791 Part 2	D	BS 4360 grade 43D
'B' Quality mild steel	NES 791 Part 3	EH32	BS 4360 grade 50EE
'BX' Quality steel	NES 791 part 4	no equivalent	

Of specific interest for steel selection and structural design detail, the NES goes on to state that for Hull Plating:

- Category A (Ship Type I)The whole external hull envelope, that is the hull shell, upper deck(s), and first level of superstructure (that is up to and including 01 deck) is to be of steel of guaranteed toughness, that is Part 2 or Part 3 steel. If Part 2 steel is used then crack arresting strakes of Part 3 steel of minimum width two metres must be introduced

to ensure that there is not more than 25% of the girth continuously in Part 2 steel, at any cross section along the length. This will usually mean introducing Part 3 steel at the sheer strakes, I deck margin strakes and at the turn of bilge and/or the garboard strakes and flat keel. Consideration is to be given to the use of Part 4 steel in thicknesses above 18mm where lamellar tearing is a possibility.

- Category B (Ship Type II) Any steel from Table 13 may be specified, but if Part 1 or Part 2 steels are used then crack arrestors must be fitted as for Category A ships. Note that this requirement is more severe than normal Classification Society rules for vessels less than 250m in length and for steel less than 15mm thickness.
- Category C (Ship Type III) These are to comply with the relevant Technical Requirements as laid down in the contract.

3.1.1 The Argument For Maintaining Naval Standards

Using the reference above, there is an important argument for properly maintaining and applying Naval Standards. As an example, the EH steel grade designation has outstanding notch tough ductility characteristics that allow the material to absorb a lot of energy through plastic elongation without propagating fracture cracks during a rapid elongation response as is common for shock, blast and fragmentation loading scenario. Arguments that cold temperature toughness is not required for ships not expected to see “Arctic" climates, simply fail to understand that any material with good low temperature notch toughness also has superior notch toughness at room temperature than materials specified for non-Arctic operations and hence build in superior ability to absorb damage from weapons effects without weight penalty. The NES hence avoids the typical commercial trade-off debate by simply directing the need to use EH material for warship construction. The merit of such direction is graphically illustrated by the USS Cole incident shown in Figure 9 for a USN design built to similar USN Gen Spec rules. Without the shear strake and other military features, the consequences of the improvised weapon contact detonation blast damage could have been far more severe. The standards include a need for not only retaining strength under damaged conditions, but stress the need for resisting the type of load arising from dynamic, rather than static application characteristics.

Figure 9: USS Cole following contact air blast detonation showing the protection against crack propagation afforded by the ~2m wide high strength steel sheer strake[1]

Legacy naval design standards tend to focus on lessons learned from combat. A good example of this was provided by Keil (1961) as shown in Figure 10. Classic analysis considers the need for longitudinal strength under intact conditions to be met using bending moment and shear arising from a static bending moment curve derived from placing the ship on a standard wave.

[1] e.g. as required by NES Category A Type I ship from Table 2.

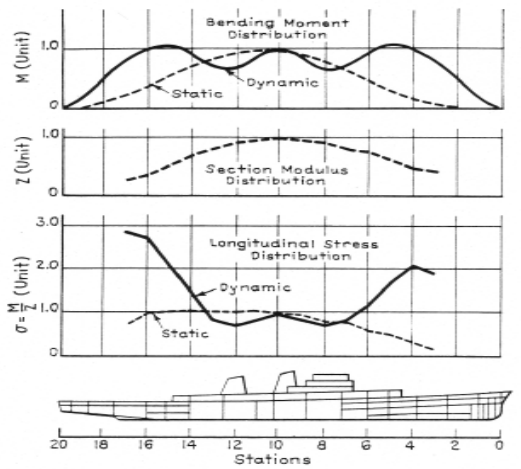

Figure 10: Illustration of load curves under static and dynamic response, (after Kiel 1961),

Under such a condition maximum stress, and hence section modulus peak at about midships (dashed line). Under the dynamic condition induced by underwater explosions however, the bending moment peaks not only at midships but also at the two quarter points (solid lines).

A review of ships lost to actual underwater weapon whipping effects shows the need to strengthen the forward and aft quarters in addition and more so than midships. Such strengthening using higher strength notch tough steels or specially designed box girders is even more important to retain longitudinal strength in damaged conditions as would arise from anti-ship missile or contact mine attacks. In general, naval standards tend to provide more "positive guidance" than "performance based requirements". They tend to be based on previous experience and extensive verification (albeit not well publicized) by naval staff. Such direction avoids potential degradation of proven performance and nugatory work in debate over better options during the exceedingly short duration design cycle. While it is acknowledged that naval design and construction experience may have degraded somewhat during extended peacetime (e.g. disbandment of the British Corps of Naval Constructors in the mid 2000's), the benefit of a non-partisan, not-for-profit skilled organization with a research budget in this field cannot be overstated.

Many Naval forces (e.g. UK, US, CA, IT, FR, AUS, GER, NL...) maintain in-house Ship Design Authorities while others support integrated or co-operative Government/Industry teams. The military design offices maintain responsibility for regulating the navy's standards and are empowered by mandate to undertake various studies individually or co-operatively to advance state of the art knowledge and capability intended to exploit technological advancement. While classification society standards address naval rules for classification, such rules inevitably refer to the need to have naval staff participate or provide more specific requirements for combat survivability involving weapons effects and signature control among others.

Despite the shrinkage in allocated budgets for new builds and maintenance, which pushes towards the research of more and more cost-effective solutions and hence affordability, it is important to understand that the best value, in terms of naval use, is biased towards better through-life capability rather than simply lower acquisition price. Knowing that a naval platform expected to sail in harm’s way was designed, built and outfitted by the lowest bidder who was allowed to bypass "overly" demanding naval standards and test verification programs has proven time again to be a false economy that does not instil confidence in those who sail them. Accordingly, various nations have legislation requiring that warships undergo specific objective based verification. OPNAVINST 9070.1 issued under authority of Vice Chief Naval

Operations of the US Navy, defines roles and responsibilities for various naval organizations charged to uphold Public Law 95-485 under a series of orders to incorporate nuclear hardness, fire protection, damage control and shock hardening of surface ships as well as direction on how to achieve and verify appropriate levels of performance. OPNAVINST 9070.1 restates the mission as: *"Warships are expected to perform offensive missions, sustain battle damage and survive."* It goes on to identify hardening requirements and training to accomplish the goals of survivability by incorporating survivability features early in the ship design process with another goal of making the features affordable (e.g. rather than trading them off). The OPNAV defines three levels of affordable protection as follows:

Level I represents the least severe environment anticipated and excludes the need for enhanced survivability of designated ship classes to sustain operations in the immediate area of an engaged battle group or in the general war-at-sea region. In this category, the minimum design capability required shall, in addition to the inherent sea keeping mission, provide for Electro-Magnetic Pulse (EMP) and shock hardening, individual protection for Chemical Biological and Radiation (CBR), including decontamination stations and Damage Control as well as Fire Fighting (DC/FF) capability to control and recover from conflagrations and include the ability to operate in a high latitude environment.

Level II represents an increased severity that includes the ability of sustained operations when in support of a battle group and in the general war-at-sea area. This level provides the ability for sustained combat operations following damage from weapons impact. Capabilities include requirements of Level I plus primary and support system redundancy, collective protection system, improved structural integrity and subdivision, fragmentation protection, signature reduction, conventional and nuclear blast protection and nuclear hardening.

Level III, the most severe environment projected for combatant battle groups, includes the requirements of Level II plus the ability to deal with broad degrading effects of damage from anti-ship cruise missiles (ASCMs), torpedoes and mines.

The protection requirements by ship class are summarized below and provide a representative and consistent understanding accepted by most navies. Table 14 affirms the important distinction that exists between design requirements for vessels designated as warships and other non-military or auxiliary craft. In particular, requirements for “combatants” are distinct from those of non-combatants in that they rely on expectations of mission capability following action damage. Combatants are expected to retain some degree of mission capability (e.g. ability to place ordnance on target) following action damage whereas non-combatants do not. The degree and nature of warship hardening follows from a more precise understanding of exactly what the warship must be able to do following an attack; how quickly it must be able to do this; and for how long.

The need for warships to “fight-hurt” was highlighted by the official discusser (Keuning 2015) who, in his critique of the Naval Ship Design Committee V.5 report at the 2015 ISSC, stated that mixing military and commercial standards may result in unforeseen incompatibility and degrade overall performance, particularly given that general structural design aspects influence vulnerability. Material specifications including steel quality; structural details; welding specs; stiffener types; and quality control need to form part of an integrated package. In many cases, commercial standards rely on specialized direction from naval experts, yet those experts are not aware of specific details in the commercial standards. Legacy naval ship standards which evolved over many years do address such requirements and need to be better understood by the non-naval community in keeping with the intention to harmonize efforts and integrate initiatives undertaken by Classification Societies and NATO groups (e.g. ANEP 77) to establish more compatible, albeit, commercial-naval standards.

Table 14: Protection Requirements by Ship Class (per OPNAVINST 9070.1)

SHIP CLASS	NUCLEAR/CONVENTIONAL WEAPON PROTECTION LEVELS		CBR PROTECTION LEVELS	NUCLEAR/CONVENTIONAL PROTECTION LEVELS (1)
	SHIP	EQUIPMENT	SHIP	PERSONNEL
AIRCRAFT CARRIERS	III	III	III	III
BATTLE FORCE SURFACE COMBATANTS	III	III	III	III
FRIGATES	II	II	II	II
AMPHIBIOUS WARFARE SHIPS	II	II	II	II
UNDERWAY REPLENISHMENT STATION SHIPS	II	II	II	II
UNDERWAY REPLENISHMENT SHUTTLE SHIPS	I	I	I	I
PATROL COMBATANT AND MINE WARFARE SHIPS	I	I	I	I
NAVAL STRATEGIC SEALIFT	I	I	I	I
MATERIAL SUPPORT SHIPS	I	I	I	I
ALL OTHER AUXILIARY SHIPS/CRAFT	I	I	I	I
(1) Note that personnel hazard environments include fragments and debris, thermal radiation, initial and residual nuclear radiation, chemical and biological agents, temperature extremes, fire, smoke and toxic products of combustion and laser irradiation.				

ANEP-77 is a NATO document intended to "provide a standard for naval ship safety based on and benchmarked against IMO conventions ... it does not include measures specifically designed to address the effects of military attack." The ANEP philosophy is summarized as taking a goal based approach that is amenable to become prescriptive so long as decisions are based on meeting higher level intent. The General provisions of ANEP-77 require the Code to be applied as a comprehensive set of requirements and clearly state it contains requirements for design, construction and maintenance of naval ships, and set levels of safety which are equivalent to those of merchant ships (Chap. 1 Part a Reg. 1a, Art 2.). Given that the ANEP does not address the effects of military attack and limits provisions to those of merchant ships, the concern raised by Keuning (2015) regarding mixing military and commercial standards seems to be reinforced.

Similarly, not all current commercial rules for high speed vessels address hull girder whipping loads. Hull girder whipping due to ship bow slamming vertically into the sea occurs repeatedly in high speed over the service life of the ship. Semi-probabilistic approach can be used to account for slam-induced loads due to random nature of the sea environment and the variable nature of the operational service of naval craft. The initial whipping moment should be combined with the peak wave moment to form a combined design hull girder bending moment. This slam induced bow whipping load becomes even more critical for lightweight high speed multihull naval craft. The high speed naval combatant (HSNC) rules developed by ABS provide formula for calculating these dynamic loads including bow slamming but do not directly apply to multihull ships. In this instance, a navy would need to develop their own requirements and incorporate them within the program specification documents.

Combatant requirements clearly recognize the need to avoid brittle fracture at high strain rates and invoke the need to avoid stress concentrations and provide notch tough steel for crack arresting purposes as a priority. They (e.g. NES 154 Art. 1.3) recognize that long stalk symmetrical Tee section stiffeners show significant advantage over bulb flats and angle sections by avoiding premature tripping under compressive and lateral loads in response to weapon effects and enabling and thereby maintaining efficient light weight inherently stable structures. On the other hand, Tee sections are less production-friendly and do not ensure that shear stresses

can correctly flow from common stiffeners to primary ones. This often obliges to add a remarkable number of lugs, which unfortunately are quite difficult to weld, giving rise to potential crack initiations, especially in case of cyclic loading conditions. The ability of steel to absorb energy under high strain rate provides an important advantage for warship construction. So why would major new naval combatant programs select aluminium as a preferred material for construction?

3.1.2 The Cost-Benefit of Naval Standards.

Costs relating to combat and weapon systems are the single largest driver in shipbuilding even when costs of the weapons themselves are excluded (Sullivan 2006). Design trend aims for more sophisticated capability along with reduced crew size coupled with fewer but more capable ships of reduced displacement all lead to tighter volumes and accordingly, a commensurate and significant increase in fabrication and quality assurance costs. According to the US Secretary of the Navy, technology has provided us with extraordinarily capable ships but we cannot afford to buy as many of them as we would like (Winter 2006). While there may be some interest, it has been found that trends towards a globally integrated production system for naval shipbuilding are unlikely (Dombrowski 2002). The NATO Frigate Project (NFR-90) was cancelled, despite large investment by many navies, because inter-naval agreement on common requirements could not be reached, and only a few binational programs have been developed in the last twenty years (one example being the Horizon Destroyers, jointly developed by Italy and France).

Warship design in a way parallels several "expensive sports car" features. Warships need to be light, fast and stiff. Lightness is important to maximize payload. Extra weight added to structure reduces the payload capacity of the ship. The lighter the ship, the faster it could accelerate and enjoy the benefit of agility while avoiding weapon strikes. Stiffness adds a number of benefits for signature control, sea-keeping and machinery plant well-being. Accordingly, naval structural standards evolved more complex structures to improved structural continuity and optimize payload capacity at the cost of fabrication and schedule for construction. As an example, simulation studies conducted by Canadian Navy (late 1980's) found that comparable sized ships in terms of displacement and dimension built following Lloyds Rules would have a hull capable of surviving the same level of shock as one built to Canadian Naval Standards. The significant difference was found to be that the naval standard ship design had a payload capacity 30% greater than if it were designed using Lloyds Rules simply due to carrying 30% less structural weight to achieve the necessary strength of hull structure. Accordingly, a comparable ship built to commercial standard would require 30% greater displacement to carry the same payload as a naval design. Once again, the use of naval standards over commercial rules can yield structural efficiency benefits, but only if the navy or government is able to stomach the cost of time and money.

Weight reduction by use of aluminium, particular for warship superstructures, was popular for more than half a century. Issues began to emerge during nuclear simulation tests that found aluminium lost significant strength to the thermal pulse preceding the blast wave and required significant and costly measures to remain intact. In addition, shipboard fires such as the one that cost many lives on HMCS KOOTENAY in 1969 significantly reduced survivability of the aluminium construction. The KOOTNAY fire arose when a reduction gear casing exploded during full power trials and started a large oil spray fire in the main machinery space that rapidly spread to main passageways. The fire quickly melted the aluminium escape ladders and trapped machinery space operators and the rescue teams that fell through the weakened ladders and walkways. Also, the 5xxx-series aluminium alloys with magnesium content of greater than 3% are susceptible to sensitization and stress corrosion cracking at temperature higher than 50 °C. Highly sensitized aluminium alloys are not weldable and cannot be repaired. Figure 11 shows the damage to an aluminium superstructure arising from a collision with a steel ship bow.

Figure 11: On left: collision damage to aluminium superstructure. On right: only slight collision damage to the steel (naval) ship bow responsible for destroying the al superstructure.

Naval ships in many countries tend to remain in service for more than 35 years, or more than twice as long as merchant ships. Certainly a close watch on the fatigue life of aluminium vessels will be warranted on any naval vessel utilizing aluminium as a building material. The lessons from the KOOTENAY fire were applied by the Canadian Navy directly into ship design standards. Aluminium ladders and related structures were forbidden and a back-fit program implemented to correct the fleet. Secondary escape routes were verified suitable and back-fitted into the fleet as required. Electrical and communications systems were provided with improved action damage survivability features. Firefighting stations and practices were revised to account for a far greater range of "what-if" scenarios. While such efforts are possible within the context of naval practice, it is unclear how such lessons would find their way into quasi-commercial naval codes.

A good example of problems in this regard is emerging from the recent efforts to upgrade the survivability characteristics of the LCS (Littoral Combat Ship) variants (Eckstein 2016). Independence variant LCS ships are of trimaran hull form and are entirely constructed from aluminium including the main hull and are built to commercial ABS HSNC rules. These ABS rules are mainly applicable for mono-hull ships and do not address weapon or shock loading for ship platforms. Implications of commercial standards for structural design without augmenting with naval standards for shipbuilding clearly show the cost of performance penalties by recent attempts to “better militarize” the LCS project. The LCS project recently wrote down $115 million (USD) to comply with "arising" contractual requirements in order to meet the military shock standard and US Naval Vessel Rules that were introduced into the class performance requirement, likely in keeping with the OPNAVINST 9070.1 well after the initial fixed price contract was negotiated with the Pentagon. The USN LCS ships were originally contracted without call to follow military standards. Eventually the need to survive the naval combat environment and avoid cheap-kill was realized and extra-ordinary effort taken in an attempt to back fit appropriate combat survival capability. The recent shock trials (Figure 12) proved that back fitting can cost more than new build and unlikely to bring the LCS capability up to full grade (Eckstein 2016).

Figure 13 shows the relative effectiveness of naval opposed to commercial construction in that proper steel selection and scantling design remained relatively intact when compared to the extensive structural collapse in what should have been collision bulkheads in the bow of the much larger displacement merchant ship

Figure 12: USS Jackson (LCS 6) undergoing shot 1 of 3 full scale shock trial.

Figure 13: On left, collision between merchant and warship. Center: Warship damage. Right: Merchant damage.

Given the reliance of certain navies to adopt more commercial shipbuilding practice, there remains a need to better integrate naval design standards with those of commercial classification societies to ensure combat survivability does not degrade in an effort to save cost. The challenge remains on how to verify and address issues with commercial practice.

3.2 Recommendations

The design is the primary driver of quality, cost and schedule. Design variables become locked-in during early stages. The power of a fit-for-purpose structural design needs to be leveraged earlier, broader and deeper. That means that an early fix is less expensive than a later fix. Multi-functional teams are the key to solving the total design equation. There is a need to look at the life cycle from earliest stages. It must be recognized that since ship electronics and combat system are responsible for more than 60% of the program costs, a far greater saving can materialize by applying control measures there than by degrading structural requirements.

Most importantly it must be understood that the navy definition of "best value" differs from the commercial definition.

4 OFFSHORE OPERATION VESSELS

The Offshore industry is a vast and complex market that utilizes a number of various vessel types to support drilling, storage, processing, construction and other subsea activities. This chapter briefly highlights a few of the unique and recently relevant vessel types and their roles in offshore operations. These vessels each have their structural uniqueness that warrant them the title of "Special."

4.1 Subsea Drilling/Construction Vessels

Ships that are designed for the installation and construction of the shallow section of subsea wells and seafloor infrastructures providing support for activities such as:

- Subsea and well activity
- Conductor and casing installation
- Well de-risking
- Pre-drill activities
- Well decommissioning and abandonment

Construction and subsea support vessels are used to support complex offshore construction, installation, maintenance and other sophisticated operations. They are significantly larger and more specialized than other offshore vessels. Some sub-types can be identified, such as:

- Cable lay vessels, built to lay pipelines on the ocean floor.
- Pipe lay vessels, to lay pipelines on the ocean floor, linking floating or subsea oil production units with onshore facilities, at increasing values of water depth of 2,000 meters and more.
- Subsea Crane vessels

Recent examples of subsea crane construction vessels are the "Far Sleipner", of abt. 8,790 dwt and an overall length of 142 meters and the “Skandi Afrika”, of about 16,000 dwt, both designed and built by VARD (RINA, 2016). It is expected that ultra-deep-water activities will increase in the next decades, which raise new type of problems with the structural integration of above deck equipment and ever increasing subsea cranes. Graaf and Zandwijk (2014) have developed a new concept to handle the logistic of above deck pipe reeling operations. The concept of exchangeable reels has been developed and implemented in the multi-purpose vessel "Aegir" to increase flexibility in quick reel mobilization and elevated foundational design to eliminate reeling downtime.

4.2 Self-Elevating Vessels (Lift Boats)

Jack-up Barges, Self-elevating Platforms, Lift boats & Spud pontoons are a type of mobile unit that consists of a rectangular hull fitted with usually three or four legs. These legs can have either a round or square cross section or truss type construction, and can raise its hull over the surface of the sea. Jacking or lifting takes place by rack & pinion, hydraulic cylinders or wires. The hull enables towing of the unit and to a desired location although some units have self-propulsion. Once on location the hull is raised to the required elevation above the sea surface supported by the sea bed. The legs of these units require a sea bead surface which prevents them to sink into it, although some may be designed to slightly penetrate the sea bed or may be fitted with enlarged sections or footings. Except for the larger types, generally Jack-up Barges and Self-elevating platforms are not self-propelled and manoeuvre on site by means of mooring equipment consisting of four winches with long wires and anchors. Over long(er) distances transport takes place with tugs dedicated barges for transportation or with semi-submersible / heavy lift ships.

These types of units are used for all kinds of stationary activities in relative shallow waters such as:

- Marine construction
- Oil well intervention activities (e.g. wireline and coiled tubing)
- Maintenance and repairs of offshore platforms
- Upgrading of offshore platforms

- Removal of old platforms
- Operational support of offshore platforms
- Temporary housing for construction and service crews
- Salvage

4.3 Heavy Lift (Semi-Submersible) Ships

A brief history of the evolution of the heavy-lift ships, characterizing some configurations such as the semi-submersibles and dock ships can be found in Van Hoorn (2008).

Cullen (2007) has presented an analysis of the use of existing heavy-lift vessels to marine maintenance and repair applications, avoiding the need to build a dedicated ship. A system to provide support for ship maintenance and repair was developed to be adaptable to any heavy lift vessel configuration available commercially. The feasibility of the solutions was demonstrated using 3D CAD system and applying it to three existing ships with different configurations.

The operation of heavy lift ships raises critical stability considerations that need to be assessed prior to conducting a heavy lift task. Handler et al (2012) have focused on the analysis of the de-ballasting of a heavy lift carrying another vessel and discussed the critical stability phases of the operation and the methods and the methods and practices to reduce the effects of reduced stability during those phases.

Yasseri (2012) has discussed the importance of the perception of factors in the environment and the understanding of their meaning and impact during critical marine operations such as heavy-lift. A systems engineering approach to Marine Domain Awareness (MDA) is presented and a model for developing the information exchange system during complex marine operations is proposed. The objective is to develop safer procedures and training programs to promote the use of MDA as a decision support tool.

The dynamics of offshore heavy lift is complex due to the interaction between the ship and the lifting object under severe environmental loads. Khac et al (2014) proposed an analytical formula using the double pendulum, based on the Euler-Lagrangian equations, to explore the insight of the heavy lift dynamics. The paper presents a practical approach to obtain reasonable results to improve the safety of offshore heavy lift.

Hatecke et al (2014) presented a fast numerical method to analyse heavy-lift operations of ships in short crested waves. The developed seakeeping method takes into consideration the coupled motions of the heavy-lift vessel and a freely suspended load. The speed of the method makes it especially suitable to situations when very long or a very large number of simulations are required.

4.4 Accommodation Vessels

Accommodation units also known as Flotels have several typical configurations, which strongly depend on the intended operation sites. In order to operate in harsh environments, for instance, it is necessary to have great seakeeping performance, thus only semi-submersibles are usually operating in North Sea's Norwegian and British sectors. A few monohulls however have also operated in the North Sea (Danish sector and a state-of-the-art monohull for 600 POB in UK). Other regions more suitable to semi-submersibles are the Gulf of Mexico and Australia due to recurrent hurricanes and cyclones. Brazilian waters are considered benign, thus both semi-submersibles and monohulls may operate there. A Compact Semi-Submersible (CSS) in the accommodation vessel market had also operated in Brazil – Bacia de Campos. Lastly, barges do not have sufficient seakeeping performance to operate in any of the abovementioned seas and are usually not equipped with Dynamic Positioning Systems (DPS), thus they only operate in mild seas or close to the shore (Malaysia, Caspian Sea and West Africa). On the other hand, due to their relative low cost, they are actually the preferable solution for these operation sites.

Recent research done on the design of an accommodation unit was published starting from Pardo & Fernandez (2012), where a preliminary and strictly qualitative study on flotels was performed. It includes even accommodation units not designed for the offshore industry and coastal, i.e. accommodation units located by the coast and therefore built in accordance with different requirements, having to operate under different regulations, sometimes having also to meet luxury standards.

Research on the dimensioning of offshore platforms has also been performed, e.g. by Sharma et al (2010), where different optimization methods are discussed for the dimensioning of a semi-submersible platform. Their approach however is a general one and it does not consider the particularities of accommodation units.

A total of 72 dedicated floating accommodation units, 27 of them semi-submersibles – including 1 non-conventional compact semi-submersible (CSS), 27 barges, 17 monohulls currently operate within the offshore industry

4.5 SWATH Offshore Vessels

A review of the SWATH technology and market in general can be found in Grannemann (2015).

One of the applications of this type of vessel is crew transfer. Actually, the larger and fastest crew vessel available, the "Muslim Magomayev", is a semi-SWATH with 70 meters length, able to carry 150 passengers, a crew of 14 and 130 tonnes of deck cargo, in wind speeds up to 40 knots and seas of 3 meter significant wave height.

Smid et al (2014) presented a study where SWATH is compared with monohull and catamaran alternatives for the most cost-efficient crew transfer vessel to offshore wind park maintenance. The study concluded that the SWATH alternative could result in savings of about 50 million Euros over a one-year period.

Other offshore applications are the installation of wind turbines. The main design aspects of this concept, such as seakeeping, model testing in seakeeping tank, wind turbine landing sequence, and the workability are presented in Bereznitski (2011). One recent example of this type of vessels is the Wind Turbine Shuttle (WTS) developed and built by the Dutch company Huisman Equipment BV, which can transport and install two wind turbines simultaneously in high seas.

5 YACHTS

This chapter provides an update to the recent structural challenges faced in the field of yacht design and construction, with a focus on megayachts as stated in the committee mandate.

The ISSC 2012 V.8 committee was the last to discuss developments in yacht design, with the report focused primarily on motor yachts. The ISSC 2009 V.8 committee report mainly discussed sailing yachts, with a short update on the topic also included in the 2012 V.8 report.

As stated in Chapter 1, it is widely accepted that yachts in excess of 24m in length are classified as superyachts.

This gives rise to the most appropriate definition of yachts over 24m: as previously mentioned they are currently all widely regarded as superyachts, but terms such as ‘megayacht’ and ‘gigayacht’ are becoming more prevalent. The primary reason for the division at the 24m length is the significant change in regulations the vessel must adhere to for operation from (in Europe) the ISO standards to the Large Yacht Code (LY3) (Maritime and Coastguard Agency 2012), however with a significant number of vessels now in existence, and on order, up to, and well in excess of, 100m LOA this results in the newer terms being utilized. There is little consistent definition, however, of either the term ‘megayacht’ or ‘gigayacht’. Some state that megayacht applies to vessels over 60m LOA (Motta et al 2011) and some over 100m in length (Žanić 2015), however it is at this stage that not only length should be considered. Another big step in regulation change occurs for vessels in excess of 100m in length and with a gross tonnage of

3000te or more which are, in effect, classified as ships (Manta Maritime 2015, and previous V.8 report 2012). It is for this reason that the definitions stated in Table 15 have been applied and will be used throughout this Chapter.

Table 15: Yacht Types by Definition

Type	Definition
Superyacht	$24m \leq LOA < 60m$
Megayacht	$60m \leq LOA\ GT < 3000te$
Gigayacht	$LOA \geq 100m$ and $GT \geq 3000te$

5.1 Motor Yachts

The ISSC 2012 V.8 committee defined motor boats as 'vessels whose main propulsion is provided by a mechanic propulsion system represented, in most cases, by internal combustion engines but can include steam engines or more modern gas turbines'. This broadly still holds true; however, electric engines are also becoming more prevalent as battery technology improves and the engines themselves are more efficient. Owners of motor boats used for recreational purposes are also keen to be seen to be helping the environment with both hybrid and pure electric propulsion systems becoming more common in smaller craft.

1073 motor yachts over 30m LOA were delivered, launched or are in build from 2012-2021 (The Superyacht Intelligence 2017). 89% of these are superyachts, with only 8% qualifying as megayachts and 3% as gigayachts. The largest privately-owned motor yacht is Azzam, launched in 2013, Figure 14. She comes in at 180.61m LOA and gross tonnage of 13,136te.

Figure 14: 180m gigayacht MY Azzam (McNicoll 2013)

5.1.1 Megayachts and Gigayachts

The demand for increasing the size of pleasure craft has led those kind of vessels to reach, in recent years, the biggest dimensions ever seen, typical of small- to medium-sized passenger vessels. Recently, some yachts were even classified as passenger vessels instead of pleasure craft. However, this demand for growing dimension remains strictly linked to the design issues typical of a yacht (large glass surfaces, big openings in the shell due to the presence of shell doors, very irregular general arrangements with big unsupported spaces, etc.) and forces the structural designer to pay a deep and continuous attention to the structural details as well as to find every possible way to guarantee the structural continuity in both vertical and longitudinal

directions. Ivaldi (2015) gives a good overview of the main stages of the structural design highlighting its peculiarities and the principal differences with the design of other kinds of ships. Alternative propulsion systems also provide structural design challenges, from supports to insulation. Lamberti et al (2013) assessed the applicability of an onboard Fuel Cell system to reduce the environmental impact, testing the feasibility of the proposed design through design changes of a Mega Yacht draft called XProject based on a LNG fuelled engine provided by Fincantieri. Kikkila & Erkintalo (2017) state that the general expectation for electric propulsion vessels is that Azipod propulsion is considerably lighter compared to shaftline propulsion with the same thrust, especially when taking into account savings in hull steel weight and conventional shaftline equipment due to components such as rudders/sterntubes/shaftline etc. not being required.

Design methods used for megayachts are trending towards those used in modern ship structures, due to their ever increasing size and hence applicability of such methods utilized for ships. Žanić et al (2015) assessed the benefits of modern rational design support techniques in the form of Finite Element Modelling and optimisation techniques, on an example megayacht of 100.8m in length for the concept, preliminary and detailed design phases. Use of ship design techniques resulted in a reduction of weight/cost and increased safety of the vessel indicating that such methods are well suited to application to megayacht design.

Korbetis et al (2015) explored the ability of ship design software to output CAD models of varying levels of details for use in parametric design optimization using an automatically updated Finite Element model. Design information and details concerning material properties, stiffeners, cross sections, tank loading and equipment masses are kept through the design process and used as input data for the FE model. Ascic et al (2015) investigated the PYC and its probabilistic approach to damage stability by describing the methodology of calculating the probabilities for flooding and surviving as well as its application on a 90m megayacht. They compare the use of deterministic damage assessment method to the probabilistic method for the PYC for the 90m yacht in the case study and found less than 1% difference between the two.

Another approach suggested by Bosma (2013) is the implementation of human comfort factors into the preliminary megayacht design stage, as opposed to the detailed design stage. A new approach to concept mega yacht design is considered by presenting a framework of how these identified human comfort factors can be implemented as early as possible within existing classical process of mega yacht preliminary ship design.

Design-driven innovation, the development of a design scenario by engaging with a range of interpreters in technology and cultural production, is widely used in product design and more recently McCarten (2013) and McCarten & Edens (2013) promoted its use in the field of megayacht design. A multidisciplinary superyacht design project engaging in Design-Driven Innovation through the application of a technologically advanced high speed platform combined with the implementation of a culturally specific emotional design framework has developed an Art Deco high speed superyacht coastal cruiser for the Chinese market based on a 130m pentamaran concept (McCarten 2013). McCarten & Edens (2013) discussed the use of Design Driven Innovation to create a new market between luxury cruising and superyacht charter for the American Market consisting of a main entertainment vessel (cruise liner) acting as a mothership, which transports SWATH floating apartments to various destinations where they are launched and recovered similarly to standard dockwise yacht transport.

With the increase in size associated with megayachts, and gigayachts, and the increasing number of such vessels in the market construction materials have become a subject of interest in order to improve performance and facilitate construction. Composites have long been implemented in the small boat industry, marine renewables, transportation and civil engineering and, as such, the technical knowledge of advanced composite materials has grown rapidly. Dassi (2015) highlighted the benefits of utilization of composites in the mega and gigayacht

industry gained from these alternative industries, with focus on ease of processing and manufacture. Ghelardi et al (2015) assessed the concept of shear lag effective breadth of plating for a large composite hull comprised of stiffened plating. FE models were developed and validated to investigate the behaviour of the effective breadth of stiffened laminates when varying geometrical and other typical parameters of composite made ship structures. It was found that it is noted that boundary conditions, stacking sequences and structural configuration have an important influence on effective breadth.

A good understanding of the structural response of megayachts is key to proper optimization of the structure, be it globally or locally. In Pie et al (2015) the differences in structural response between a steel and aluminium mega yacht superstructure in waves are discussed. Larger overall deformations were observed in the aluminium structure, which then transmitted larger loads to the steel hull structure.

Comfort is a key design parameter for all luxury yachts, with maximum vibration levels being carefully assessed and minimized. Dellepiane & Boote (2013), Boote et al (2013) and Boote et al (2014) reviewed the so-called "Comfort Class Rules" – those issued by Classification Societies for the evaluation of vibration maximum levels. A detailed FE model of a 60m case study megayacht was carried out in order to investigate the dynamic behaviour of hull and superstructures. The results of modal and transient analyses are compared with a first series of experimental data gathered during the vessel construction. Noise Vibration Harshness (NVH) analysis, already well established in the automotive industry, and has only recently come into its own in the megayacht industry as part of Comfort Class Rules. Bermano et al (2015) investigated the dynamic behaviour of large yacht structures and applied an NVH methodology to a 60m megayacht in order to optimise a passive control device (a tuned mass damper system) or adaption to the deck geometry. This solution reduced vibration levels with the addition of only 600N of weight which is significantly less than the increase in structural mass and potential deck thickness in the conventional structural stiffening approach. Kikkila & Erkintalo (2017) found that the use of Azipod® propulsion systems, in place of conventional propellers and rudders, reduced perceived onboard noise and cavitation by 30-35%.

5.1.2 Superyachts

Various reasons have seen an increased level of caution from large yacht buyers recently; however, 122 sales of yachts over 24m in length were reported in the first four months of 2017 alone. This is similar to the 124 reported during the same period in 2016, and up 8% on 2015's figure of 113 sales suggesting that, even with increased caution, the industry is not showing any signs of slowing (Montigneaux 2017). As with megayachts, features only associated with the luxury yacht market govern the structural design of such vessels. A bespoke tender garage/beach club design and its impact on the vessel design is discussed by van Loon (2015), with Uithof et al (2015) proposing use of a Hull Vane ® on a 50m trimaran to reduce resistance – however this will bring structural challenges in itself.

McCartan et al (2015) employed the approach of Design-Driven Innovation to take advantage of the reduced regulatory framework for superyachts under 500GT which offers a significant opportunity for a greater percentage of interior volume to be assigned to guest activities, due to a reduction in both crew area requirements and fire insulation and the absence of certain requirements such as an emergency generator.

Archer & Roy (2013) investigated the application of Platform Engineering to the 25-50m yacht market and highlighted some of the barriers that result from production boat builders, traditionally focused on yachts of less than 24m, increasing the size of their product in order to enter the superyacht market.

Optimisation tools are becoming increasingly commonly suggested as a method for improving the design of large yachts. Mutlu et al (2017) explored various optimisation algorithms with

regards to the design of composite stiffened panels for large yachts. A top-hat stiffened composite plate was optimised for the objectives of mass/stiffness and mass/strength with Pareto fronts for each Genetic Algorithm, and their relationship to the variable space and computational times were compared. Nazarov (2013) presented the review of design experience for catamaran superyachts 30-35m long. Comparison of catamarans with traditional monohull motor yacht is presented in terms of usable space and layout concepts with parametric optimization of initial key design variables.

The industry is seeing more suggestion of the use of novel hull forms, such as SWATHS as a method of limiting slamming/seakeeping loads and bringing yachts in like with Comfort Class Rules. (Begovic & Bertorello, 2015; McCracken, 2015). Abeking & Rasmussen already construct SWATHS for commercial applications and have recently been collaborating with Reymond Langton Design to develop a luxury 62m SWATH with interior volumes equivalent to that of an 80m monohull.

Aesthetics are key for all luxury vessels, and defects such as bumps and hollows due to welding are not acceptable on the surface finish in the industry. Vessels of composite manufacture often have improved surface finishes, but this is highly dependent on the method of construction and type of mould used. All vessels require some level of filling and fairing to produce a surface suitable for painting. Giannarelli et al (2015) investigated of the influence of temperature on the mechanical behaviour of steel plates coated by filler layers. The study included FEM structural analyses calibrated by experimental measurements performed on laboratory specimens simulating yacht hulls exposed to solar radiation in various conditions. Gaiotti et al (2015) focused on the macro-mechanic properties of fillers currently applied on yacht hulls and superstructures. Two types of tests were carried out for different fillers: a compression strength test on isolated filler specimens and three-point bending test on specimens made by filler applied to a steel substrate. Load-displacement curves of test specimens were determined.

One common component throughout the luxury yacht industry is the large amount of glass incorporated in various ways in the design of vessels. This is key structurally, with the dynamic response of laminated glass to vibrations and the quasi-static response key in the structural assessment of the material used in each yacht. Gragnani et al (2015) presented a method for identifying a dynamic model of laminated glass that can be used to carry out acoustic calculations for a numerical yacht model. The owner's cabin windows of a superyacht are assessed using the proposed method.

5.1.3 Expedition Yachts

An expedition yacht is a versatile vessel which has the ability to cruise self-sufficiently for long periods of time at sea. The vessels travel through extremes of temperature, from the South Pacific to ice filled waters of Alaska, and are required to withstand a myriad of conditions for extended periods of time. Designed and built with power, stability and efficiency foremost to mind, with the addition of a deep displacement hull, they often incorporate extreme structural design challenges associated with ice breaking capabilities for example, whilst maintaining the same high standards of interior design of their shorter-range counterparts (Lyons 2015). Current expedition yachts are in the length range of super and megayachts, however there is one in development in excess of 160m putting it firmly in the gigayacht category. Nonetheless, the unique environmental challenges these yachts must withstand put them in a category on their own.

McCartan et al (2017) utilised their Design-Driven Innovation approach to present a 300m sustainable luxury Ice-Class Arctic explorer vessel which supports scientific research and curated luxury experiences. The vessel is to be hydrogen powered, incorporating a further level of structural challenge. Other propulsion solutions for the novel vessels include Azipods® (Kokkila, 2017), due to better vessel manoeuvrability, improved passenger and crew safety, greater fuel efficiency and lower total cost of ownership. Azipods ® are currently fitted on the

polar discovery yacht Scenic Eclipse – the world's first passenger vessel to be constructed explicitly to Polar Code standards.

In 2015, Damen developed a range of purpose built globally capable expedition yachts (65m, 90m and 100m) – the SeaXplorer. Designed specifically for the expedition market, the yacht has the operational profile of an expedition vessel, with Polar Code requirements implemented in the core design. The hull shape has been optimised, ice breaking capability defined alongside the propulsion system and other purpose specific requirements without compromising the safety and luxury comfort of the yacht in any way (Van der Velde et al, 2016). EYOS expeditions provided insight into the unique operational envelope for the vessel with in excess of 150 design criteria, and the hull form was assessed and optimised through HSVA model tests which helped define the ice strengthening regions along the hull with respect to the Polar Class Demands. The first SeaXplorer 65m has been sold for delivery in 2019. The vessel will be capable of full autonomy for 40 days and complies with the environmental and safety standards in the IMO Polar Code's B category.

Figure 15: The REV (http://rosellinisfour-10.no/)

VARD (2017) are also to enter the expedition vessel market with the 181.6-metre Research Expedition Vessel (REV), Figure 15. Construction of the vessel will take place in several stages, with the hull to be built at VARD's Tulcea facility in Romania. It will then be towed to the company's shipyard in Brattvaag, Norway for outfitting, and following hand over to her owner in Norway in the summer of 2020, the ship will be returned to Romania where fairing, deck-laying and finalisation of the accommodation areas will take place. The vessel has a length of 181.6m, Beam of 22m, draft of 5m and a gross tonnage of 16,000te. With a maximum speed of 17 knots, the vessel can hold up to 60 scientists and 40 crew members. During luxury expedition trips the REV is designed to host up to 36 guests together with a company of 54 crew members.

5.1.4 Small Yachts

With the committee mandate focussing emphasis on larger yacht structures, this section is a short update as to the developments in the small yacht (under 24m) industry. Of key note in the motor yacht industry is the use of Fluid structure interaction (FSI) methods to optimise the structural design of vessels. Fong & Chang (2014) and Fong (2011) used validated ALE and SPH simulation approaches to calculate slamming impact loads for a 58' planing yacht for use during structural design. Further discussion as to slamming loads on vessels is undertaken in the Sailing Yachts section.

5.2 Sailing Yachts

Sailing yachts differ from motor yachts insofar as they have a primary method of propulsion that uses sails, powered by the wind, to propel the vessel. While they comprise a much smaller share of the yacht market than motor yachts with only 123 yachts over 30m LOA were delivered, launched or are in build from 2012-2021 (The Superyacht Intelligence 2017), their size range these days is growing with 96% of these superyachts, 2.5% megayachts and 1.5% gigayachts.

5.2.1 Giga, Mega and Superyachts

The largest sailing yacht launched to date is SY A, Figure 20, which comes in at just under 143m in length and 12,600GT and is shown in Figure 20.

Figure 16: SY A (Horn 2015)

Whilst many design methodologies are just as applicable to sailing and motor yachts, some case studies have been carried out focusing wholly on sailing vessels. Shaw (2015) explored the possibilities for performance, function and form achievable through refocusing the design drivers in the development of a superyacht, with a fresh emphasis on the design and engineering aspects of construction, hull form, sail plan and appendages.

McCartan & Kvilums (2013) explored the principles of 'Passive Design' to produce a sailing catamaran design concept that addresses the 'green luxury' gap in the market for luxury charter performance orientated vessels, which implement ecological technologies that enhance the user experience and also benefit the environment.

Sail and rig system design is evidently key to the success of a sailing yacht. Gaiotti & Rizzo (2015) moved away from the more traditional empirical approach to rig design and applied numerical simulations to assess effects of load variations in time of a pre-tensioned slender

structure. The dynamic buckling of the bottom panel of a typical large mast is evaluated, showing significant differences from the widely applied quasi-static approach. The obtained results provide a new perspective for the scantling assessment of sail systems, overcoming the current empirical and prescriptive approach proposed by rules of classification societies and international standards. Fossati et al (2015) provided an overview of the experimental research carried out in the Politecnico di Milano Wind Tunnel aimed to support the sail inventory development for the high-performance superyacht Magic Carpet[3]. Sail shape and the effect of flexure on performance is discussed.

Composite materials have long been prevalent in the racing yacht industry, with sailing megayachts such as Mirabella V constructed from composite materials since 2002. With an increase in scale, autoclave production is negated and out-of-autoclave prepregs become the construction material of choice for high performance marine craft. Voids are not collapsed by the low external compaction pressure, and have potential to cause structural instabilities. Hickey & Bickerton (2015) presented the development of experimental techniques to accurately measure the as-laminated void content, compaction response and in-plane and through thickness air permeability of two prepreg materials.

While the majority of the motor yacht market is often seen as a competition for the largest yacht, the sailing industry produces some truly unique vessels. In 2012 BANQUE POPULAIRE V a 40 m LOA sailing trimaran circumnavigated the globe non-stop and without external assistance in 45 days and 13 hours at average speed of 26.5knots, which is a record at present unattainable by motorised craft. Bertorello & Begovic (2016) discussed the specific design aspects of the most recent boats for the circumnavigation record and showed how the latest available technical and technological resources have been exploited.

Köhlmoos et al (2012) reported on “Tûranor PlanetSolar”, the world’s largest solar powered vessel. The aim of the vessel was to demonstrate the capabilities of current photovoltaic solar cell technology. The vessel comprises a wave piercing catamaran hull design, powered by electric motors and semi-submerged carbon-fibre propellers. The combination of these technologies allows the 85te craft to cruise at 7knots consuming an average of 20 kW of installed power, buffered by lithium-ion batteries. Load prediction mechanisms for boats which do not fit the standard rules have been developed with the class society agreeing "best engineering principles" be employed for structural analysis.

5.2.2 Racing Yachts

Racing sailing yachts, especially America’s Cup vessels, are at the forefront of pushing technologies into the marine industry. Key developments in this field in recent years are primarily in the field of composite materials and their response to the loads imposed by the inherently harsh environment racing yacht are subjected to. Seo et al (2015a) investigated the current trends of composite applications in the marine and leisure fields to study the development of a 33ft America’s cup training CFRP sailing yacht. Lake et al (2012) used the manufacture of the AC45 catamarans as a case study of the efficiencies and accuracies gained by using CNC machining technology in manufacturing high performance racing yachts and multihulls. CNC machining was found to reduce the amount of time to manufacture the hulls by at least 15% and the costs by around 10%.

Different types of porosity found in traditional racing yacht structures were presented by Bayle et al (2015). Current developments to improve racing yacht composite quality such as thin ply technology, out-of-autoclave processing and automated fibre placement were assessed and their implications for porosity discussed.

Detailed assessment of the effects of salt water and xenon light, salt water spray test and xenon test were undertaken on CFRP specimens with a total of 15 plies by Seo et al (2015b). Tensile strength of each specimen was compared both before and after exposure to the environmental

conditions. The resulting tensile strength of composite specimens was adversely affected by salt water (2-9% decrease) but improved with exposure to xenon light by around 8%.

Slamming is an inherent issue with racing yachts which are being pushed to their design limits in a wide variety of environmental conditions. Allen & Battley (2015) characterised the variations in both applied pressure and panel response due to hydroelasticity of panels, previously assumed to be rigid. They found changes in both loads and responses were largest at the centre and chine edge of the panel. These variations were related to the significant changes in local velocity (centre) and deadrise angle (chine).

Goutard et al (2012) developed a Finite Element - Finite Volume (FE - FV) coupled method to assess slamming and the effect of hydroelasticity on slam induced pressures. It was shown that the coupled numerical model captured well the underlying physics of slamming, and the predicted pressure field and structural response agree well with the experimental results.

Weber et al (2015) and Battley et al (2012) both stated that the majority of slamming assessments to date have been carried out on flat panels; however, racing yachts are rarely comprised of flat panels and there is likely some difference in the reaction of curved panels to slamming as opposed to flat. Weber et al (2015) investigated the effect of curvature on slamming loads through the use of constant velocity experimental testing and coupled Finite Element-Smoothed Particle Hydrodynamics numerical simulations. The work showed that curved bodies experienced a much higher initial loading than rigid wedges, which then abated to a quasi-constant residual load. Battley et al (2012) described the results of a parametric study investigating the effects of stringer stiffness on panel skin stresses and core shear stress distributions for curved sandwich panels. Analytical results, finite element modelling and experiments were conducted on flat and curved sandwich panels, with various boundary conditions under a uniformly distributed load. The results showed that responses of curved sandwich panels differed significantly from those of flat panels, and that the stringer compliance had important effects on the panel responses.

Appendage design has long been a source of design for racing yachts, particularly with the advent of foiling multihull America's Cup contenders. Keel flutter, vibration which is due to the excitation forces of the fluid on the keel, has appeared as a major technical issue for designers with potentially catastrophic outcomes. In Mouton & Finkelstein (2015) an FSI method under assessment was validated through examination of three as built' keels, representing a wide range of known flutter behaviour. The presented results showed a good correlation between on-the-water experience and the calculated predictions.

5.3 Recommendations

The total number of yachts over 30m in length on order alone in 2017 up at 760 shows a positive increase in the superyacht market compared to 692 in 2013. There is also an increase in demand for longer, larger vessels with terms such as 'megayacht' and 'gigayacht', as defined by means of LOA and GT in this Chapter, becoming more prevalent. Such large vessels come with their own inherent structural challenges and it is these that the chapter have focused on, with an update as to new and novel work done in other areas of recreational yachting.

The development of large vessels that are capable of expeditions into hostile environments and comply with Polar Class rules is on the rise, and it is recommended that the next committee focus in on this expanding fleet with many structural challenges apparent balancing luxurious accommodation and facilities with practicalities of travel in hostile seas and use/storage of scientific exploration equipment. Alongside this, there are more Gigayachts in build, and it is recommended that the challenges of application of Ship Class rules to such large vessels are examined. Other areas that may be considered include fast pleasure craft and pleasure submersibles.

6 SPECIAL HULL AND APPURTENANCE STRUCTURES

Within the last decade there are numerous examples of innovative and special-purpose hull forms which require various structural configurations to achieve speed, payload capacity and mission complexity. As discussed from a regulatory stance in Chapter 2, the vessel types addressed in this Chapter include free-fall lifeboats, SWATH vessels, heavy lift vessels, icebreaking vessels, wave-piercing vessels and others. Their geometries, structural topologies and materials required for the structural configurations did not fit well with traditional design methods and procedures rooted in empirical approaches. Instead, these ships and their appurtenance structures, such as moonpools and helidecks, require direct analysis or first-principles approach, mainly requiring computer aided processing.

6.1 Freefall Lifeboats

Freefall lifeboats were designed to be fast and reliable evacuation systems. For example, the launching of a freefall lifeboat is to simply slide from a skid before the freefall. Immediately after the water impact, the propulsion system will start and the lifeboat will then sail away from the parent vessel. The trajectories of freefall lifeboats during the launching process depend on the headway and advance speed after water entry and surfacing of the lifeboats. In the years prior, research work has focused on the different aspects of the structural design, such as the materials and the loads (ice loads, impact loads).

Browne et al (2008) developed a practical design and prototype of an Ice-Strengthened Lifeboat (ISL). This lifeboat was designed to reduce the risk of damage or loss due to crushing by ice during evacuation from offshore installations or vessels in ice covered waters. This novel design combines new hull shape features with a composite shell, reinforced structurally to resist the ice loads.

Similarly, the work developed by Kennedy et al (2010) focused on the determination of the structural limitations of the existing freefall lifeboats (non ISL) which would be subject to ice impact loads in order to develop operating procedures for a safer operation in icy waters.

Based on field trials with conventional freefall lifeboats, Simões Ré et al (2011) investigated the extent of the ice limits operational capabilities. Measurements were made with ice loads from different ice conditions and in different types of operations.

A Freefall Lifeboat (FFLB) must be able to avoid irregular motion and resurface at a sufficient distance away from the host ship. In Tregde and Nestegård (2014), a FFLB drop simulator was developed and used to produce a database of random drops from a floating ship in storm conditions, intact or damaged. The database was used as a basis for regression analysis to estimate the responses for different wind, waves and host ship conditions. The objective of the study is to analyse the motion trajectory of the FFLB and to check its ability to escape the host after resurfacing in accordance with the design standard.

Hwang et al (2014) developed a method for design modification of structurally damaged FFLBs based on the results of skid launching freefall tests, analysing the four phases of the fall: sliding, rotation, free-fall and water entry. The aim of the work is the improvement of the structural design of existing FFLBs.

The work of Rahman et al (2015) presents an analysis of local ice loads measured during full-scale field trials conducted in 2014 with a totally enclosed motor propelled survival craft (TEMPSC) in controlled pack ice conditions. The event-maximum method of local ice pressure analysis was used to analyse the field data in order to improve the understanding of the nature of ice loads for such interactions. This analysis was also used to evaluate the suitability of the approach for design load estimation for TEMPSCs (i.e., lifeboats) in ice. The work established links between extreme loads and the exposure of the lifeboat to ice for different operating conditions. The work also concluded the event-maximum method provided a promising approach

for establishing risk-based design criteria for lifeboats if field data are available which adequately represent ice conditions encountered during the design life of the lifeboat.

Simões Ré et al (2012) presented ideas for improving the capabilities of lifeboats while complying with the regulations in the sea ice conditions, understanding they can be met in offshore operations. Model scale and full scale trials were carried out with special attention to select design aspects, such as powering and propulsion, manoeuvring, structural resistance to ice loads, and arrangement of the coxswain's cockpit.

Simões Ré & Veitch (2013) carried out full-scale field trials of a conventional lifeboat in pack ice to investigate design considerations such as powering and propulsion, hull form, manoeuvring, ice loads and ergonomics. This paper focuses on local ice loads measured on the hull during aggressive operations in pack ice. Field measurements are presented and the implications for design and safe operations are discussed.

Kennedy et al (2014) investigated design considerations for a conventional Totally Enclosed Motor Propelled Survival Craft (TEMPSC) operating in ice. Local ice impact forces were measured in field testing. The results are presented and the operational performance discussed.

Hwang el al (2016) presented design modifications to reduce the impact pressure during water entry of free-fall lifeboats (FFLB) based on full scale tests carried out with a damaged FFLB. The test analysed four phases of the launching process: sliding, rotation, free-fall and water entry. In the water entry phase, structural damage can be avoided by reducing the top deck impact area and by increasing the modular factor of the roof deck which ultimately modifies the structure of the deck and its shape.

6.1.1 Impact Loads

In the sequence of unacceptable structural deflections found in the roof of FFLB resulting from offshore installation tests, an extensive research project was carried out at MARINTEK to study the main performance factors in rough weather conditions (100-year storm - Kauczynski et al 2009). An extensive program of model tests for different types of FFLBs was carried out. FFLBs were launched by a vertical drop method or from a skid in different weather conditions, still water, regular and irregular waves. The results were then compared with full-scale tests and the conclusions were used to propose and discuss new structural performance and technical criteria for the hulls.

The work of Sauder and Fouques (2009) focused on the safety of occupants of FFLB during water impact. A theoretical method was developed to predict the trajectory in six degrees of freedom of a body entering water waves and to compute the slamming forces and moments. The model was validated by extensive model testing in calm water and irregular waves.

Luxcey et al (2010) focused on the numerical evaluation of acceleration loads during water impact of FFLB launched from the skid. Two wave models are considered. Linear waves are compared with regular Stokes waves of the 5th order and linear irregular waves are compared with irregular waves of the 2nd order. The modeling detail of the launching skid is also taken into consideration.

Tregde et al (2011) used CFD to obtain design loads on a FFLB. The results were then validated with full scale tests. The larger structural loads, such as those due to hydrostatic, dynamic and slamming pressure, correlated very well with the full scale testing results.

The work of Ji et al (2015) focused on the assessment of the structural integrity of lifeboats launched from FPSO vessels. The pressure distributions on the impact were computed by CFD simulations, for different load cases, and quasi-static finite element (FE) analyses were performed. The non-linear load/response effect when the load factor is applied to the load was studied by a sensitivity analysis. Also investigated was the time-varying pressure distribution for selected cases and the dynamic effects that resulted from them.

Designing against impact loads (slamming) can be challenging and time consuming, involving advanced analyses and complex calculations. In the work of Heggelund et al (2015), the application of simplified, quasi-static calculation approaches to the design of freefall lifeboats is discussed extensively. The authors concluded although the results are on the conservative side, simple hand calculations including non-linear geometry can be used to predict the maximum strain on the fiber reinforced plastic hull structure due to impact loads. They also investigated linear methods, but concluded they should be used with more rigid structures such as stiffened steel and aluminium panels.

Zakki et al (2016) developed a new type of FFLB for the quick evacuation from offshore platforms. A new hull form was designed and the acceleration response due to slamming was studied, using a Fluid Structure Interaction (FSI) analysis with the penalty coupling method. The numerical results were then compared with the requirements of the IMO regulations.

6.1.2 Simulation

Berchiche et al (2015) presented the results from model tests and CFD simulations of lifeboat launches in regular waves. The validation shows that predicted accelerations agree well with the measured ones. The simulations provided near accurate or relatively conservative estimates of the local pressure at various locations on the hull except on one location on top of the canopy where the pressure was slightly under-predicted. Furthermore, it has been shown to improve the predictions of the pressure loads on the aft wall of the lifeboat, the compressibility of air has to be taken into account in the simulations in order to capture the behaviour of the air-pocket behind the lifeboat.

Zakki et al (2015) investigated the influence of some launching parameters such as sliding distance, angle of skid and the falling height on the motion pattern of the freefall lifeboats by using Fluid Structure Interaction (FSI) analysis. The results of the numerical simulations provide the magnitude of launching parameters for safely launching of the freefall lifeboat.

6.2 SWATH Hulls

SWATH, Small Water-plane Area Twin Hull, typically have two submarine-like lower hulls which run completely submerged. When in the water, a SWATH resembles a catamaran. There are two other components to the hull: 1) the struts and 2) the haunches. The haunches, which blend into the decks and bridge, are connected to each submerged hull by one or two relatively thin vertical members, called struts. The longitudinal cross-section of each strut is roughly half the width of the submerged hull, and is streamlined to decrease wave-making resistance.

There are two key advantages for designed SWATHs: (1) the ability to provide big-ship platform stability and ride quality in a smaller vessel; (2) the ability to maintain normal cruising speed in rough head seas. The cross-structure load and strength is one of the key points from the view of the SWATH structure. Figure 17 shows the typical load cases that need to be considered (ABS, 1999).

Thomas Mathai (2006) carried out research on the Wave-induced cross-structure loads for a SWATH vessel. The hydrodynamic problem is solved using the higher-order boundary element method and the generalized modes approach available in the radiation-diffraction program WAMIT (Lee and Newman, 2001). The difference between cross-structure loads computed in earth-fixed coordinates and the same loads computed in body-fixed coordinates is illustrated. In the absence of any damping from viscous effects and separation, the computed free surface elevation in the gap between the hulls exhibits large sloshing at resonant frequencies. The effect of sloshing resonance on the computed loads is shown. A technique was proposed by Newman (2004) to simulate the additional damping and thereby obtain more realistic predictions of free surface elevations and cross-structure loads.

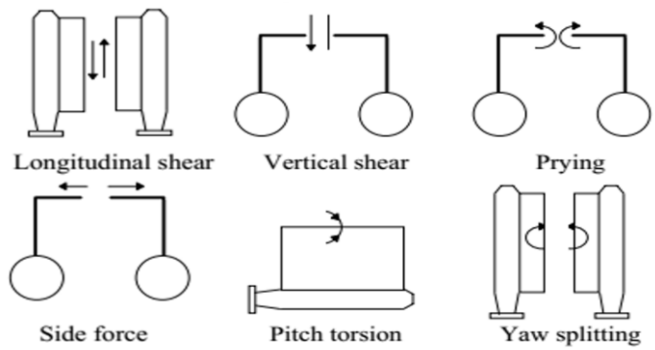

Figure 17: Considered Design Loads on SWATH Hull Structure

Chen Ying et al (2012) presented one corrected formula for the lateral force of the SWATH by comparing CCS Rules (2005), ABS Rules (1999) and model tests. Finite element analysis is carried out for the vessel in six typical load cases. One more dangerous load case - 60^0 oblique wave - is suggested for the structural strength.

The stress concentration of SWATH's cross-deck structure is serious. Zhen Chunbo et al. (2014) studied the structural strength in heading and oblique waves using the 3-D global FEA model. Ren Huilong et al (2015) analysed the high stress concentration problem of the SWATH connecting bridge local structures using FEA method. Sub-model method was used to analyse a fine mesh model of the connection of a sponson platform and pillar. The SWATH structure optimization solution using the parametric sub-model method is proposed.

Complex lateral load, special structural form and extensive use of high-strength steels cause serious fatigue strength problems of typical details of SWATH. Zhen Chunbo, Ren Huilong et al (2012) carried out a model test on the fatigue of a SWATH ship's cross deck structure.

6.3 Heavy Lift Hulls

The heavy lift vessel is also known as the floating crane. It is widely used in offshore large lifting, salvage, bridge construction and port construction, etc. Many heavy lifting vessels are used for offshore platform construction or demolition. With the gradual development of offshore oil and gas development to the deep sea, the offshore platform is becoming large-scale. Lifting capacity of the crane ship is increasing.

For the mono hull ships, more attention is paid to the overall strength of the hull and the local strength of the base. Xu Fan-fan et al (2015) analysed the strength of a 12000t heavy lift vessel by FEA, ZhenHua30, whose lift capability is the largest now among mono hull ships. The stress distribution of three cargo holds and crane foundation of a 12000t heavy lift vessel under some typical load cases were obtained.

The semi-submersible ship is another type of ship hull which is suitable for the heavy lift vessel. Yi Caiying et al (2012) analysed the global strength of one 16000t deep-water semi-submersible pipe-laying crane vessel. SESAM code was used to predict wave induced loads and corresponding structural responses. 35 wave load conditions together with four different loading conditions were considered. Stress concentration was obviously found in the connections of pontoon and pillar of the vessel. Structure strength was checked using ABS rules.

For twin-hull ships, more attention is paid to the strength of the joints of the two hulls. 'Pioneering Spirit', 382 meters length, 124 meters width, is one of the largest twin- hull ships ever built. The bow of the ship is equipped with a 48000 tons lifting capacity crane, which is the largest facility for the installation and removal of large offshore oil platforms. The ship, once equipped with the pipeline laying system, will become the largest vessel.

Two key recommendations for a heavy lift vessel's structure design are be wary of shear strength and stress concentrations. In order to avoid stress concentrations, the longitudinal components of floating crane hull should be strengthened, such as the longitudinal bulkhead and the inner bottom near the crane. The longitudinal bulkheads and side panels near the base of crane need to be properly thickened to ensure shear strength.

6.4 Icebreaking Hulls

Ships navigating in ice-covered waters experience local and global ice loads due to ice-hull interaction. The design of a ship with good ice performance requires adequate assessment of these ice forces, including distribution in time domain and also along the ship hull.

Erceg et al (2014) presented a quasi-static numerical approach to model the initiation of icebreaking pattern in level ice. The model accounts for the bow geometry and the properties of the encountered ice. The icebreaking pattern for a case study ship is simulated using the developed model. The sensitivity of the model with respect to the bow shape is discussed.

Li Zhou et al (2017) showed a method to simulate non-simultaneous crushing failure in time domain based on previous research on simulations of bending failure between intact ice and the hull. The simulated results are also compared with model test results. Simulated ice loads are in good agreement with the experimental results in terms of mean value, standard deviation, maximum and extreme force distributions, though there are some deviations between predicted and measured results for certain cases.

SY Jeong et al (2015) performed model tests in the ice model basin in Korea Research Institute of Ships and Ocean engineering (KRISO) with the model of icebreaking ship Araon. The Self-propulsion tests in level ice were performed with three different model ship speeds. Three tactile sensors were installed to measure the spatial distribution of ice load acting at different locations on a model ship, such as the bow and shoulder areas. Variation in the distribution of ice load acting on a model hull with ship speed is discussed.

In various ice conditions, icebreakers generally suffer significant ice load on ship's hull. Normal operating conditions are expected from the planned field ice trials and also from general ice transits. Sometimes an icebreaker may encounter extraordinary ice conditions during unplanned transits and / or unusual weather conditions.

Choi, Kyungsik et al (2015) revealed the peak ice pressures results recorded from the Korean icebreaking research vessel ARAON, during her normal operations and also unplanned ice transits trials in the Antarctic sea during the 2012 summer season. Strain gauge signals were recorded during her planned icebreaking performance tests and also during the unplanned ice transits in heavy ice conditions. The peak ice pressures on the ARAON's hull during the planned and the unusual ice transits were then compared.

In order to further optimize the hull forms and enable more efficient ship operations, Mård (2015) performed experimental studies on the icebreaking process of an ice breaking trimaran in Aker Arctic's model basin. The side hull encounters an ice field with micro cracks caused by the middle hull. These micro cracks enable the side hulls to break the ice with a small resistance. The model test results show the minimal ice resistance of the icebreaking outer hulls are due to a beneficial icebreaking efficiencies of the middle hull.

6.5 Wave-Piercing Catamaran Hulls

The Wave-piercing catamaran was developed on the basis of a high-speed catamaran, which is the product of the combination of small waterline and deep V ship's good navigation performance and the structure of the catamaran and hydrofoil arc struts. Wave-piercing catamarans are used extensively for both defence and commercial sea transportation. Advantages such as a large deck area, stability and high speed make these catamarans suitable for transporting roll-on roll-off

cargo and passengers. However, issues such as the impact of the bow into the water when operating in large waves, better known as wet deck slamming, can affect their mission capability and can cause structural damage. Slamming of the wave piercer bow is a complicated unsteady hydrodynamic process as the bow enters a wave. Slamming occurs due to the rapid unsteady confluence of water displaced by the demi-hulls and Centre bow at the top of the arches in the hull cross section.

A Shahraki, Jalal Rafie et al (2013) study focused on the centre bow design for a wave-piercing catamaran. In order to evaluate the effect of various centre bow hull forms on motions and slamming loads, a hydro elastic segmented model was designed and constructed. This segmented model is a scaled model of a 112m INCAT wave-piercing catamaran and has two transverse cuts and a separate Centre bow. The Centre bow segment was equipped with two six degree of freedom force/torque sensors to allow for slam loads to be measured. Three Centre bow volumes (lengths) were designed and tested in head seas in the AMC towing tank in regular waves. The results show a significant variation in slam loads when comparing the three Centre bow lengths, with the highest loads found on the longest Centre bow, caused by larger water volume constrained between the Centre bow and demi hulls. Results also showed that the longer Centre bows have higher pitch motions in slamming conditions.

Lavroff el al (2015) from Australia conducted research on slamming and corresponding whipping energy for wave-piercing catamarans. The model tests carried out were intended to identify the most severe slams possible. For a 112-m vessel with 2500 tonnes displacement slams in 5.4 m height, regular waves would reach a maximum force of 2115 tonnes weight with a duration of 1.14 seconds and an impulse of 918 tonne seconds. The energy imparted to structural deformation would reach 3.9 MJ at full scale, of which approximately 1.0 MJ would be transferred into structural whipping. The results obtained in these model tests are broadly consistent with the most severe slam loads observed during sea trials.

Lavroff et al (2017) studied the wave impact loads on wave-piercing catamarans. Wave slamming is investigated for the 112 m INCAT wave-piercer catamaran with reference to experimental work conducted at full scale, numerical computation by CFD and FEA and testing at model scale using a 2.5 m segmented hydro-elastic model. The segmented model was tested in regular head seas to investigate the magnitude and location of the dynamic wave slam force and slam induced hull bending moments. Scaled slam forces of up to 2150 t weight (21.1 MN) were measured during model tests for a full-scale vessel with a loaded displacement of 2500 t. These slams can impart impulses on the bow of up to 938 t weight-seconds (9.20 MNs) and strain energy of up to 3.5 MJ into the ship structure based on scaled model test data. The impact energy is transferred primarily to the main longitudinal whipping mode. Thisdecays with an overall structural damping ratio of 0.02–0.06, strongly dependent on internal frictional mechanisms within the ship structure.

In order to analyse the applicability of different high speed craft rules and select suitable ones for the design of a high speed wave piercing catamaran, Wang Xueliang et al (2010) evaluated the global design wave loads according to regulations in DNV, ABS, CCS and LR rules. Meanwhile, model tests of this catamaran are performed in the seakeeping basin of CSSRC to confirm the design values in heading and quartering seas. It is concluded that the methods from DNV and CCS rules are rational for the structure design while those from ABS and LR rules gave relatively conservative design value for this catamaran.

Wang Weiwei et al (2013) carried out research on fatigue strength assessment of typical spots in wave-piercing catamaran using Miner's rule of linear damage accumulation and S-N curves by employing spectral-based analysis. Fatigue strength assessment of the hot spots was conducted using wave scatter diagrams of the North Atlantic as the wave loading spectrum. The result is helpful to structural design of the joints of similar wave-piercing catamarans. The cumulative fatigue damage is relatively large for structures near the waterline. Appropriate measures should

be taken to strengthen the point to reduce the stress at the hot spots to meet the fatigue life design requirements.

6.6 Moonpools

One of the common characteristics of these types of vessels considered is the existence of a moonpool. Moonpools are vertical wells onboard floating vessels and offshore structures that provide open access for several types of underwater activities. The relative motions that occur inside the moonpool and their impact in several aspects of the ship design have been the subject of several research work.

Sharanabasappa and Surendran (2013) studied the influence of the shape and depth of a moonpool and the frequency range of the waves in the response of a drillship. Tank model testing has been carried out, with circular, square and rectangular moonpool shapes. The mooring lines have also been modelled. The different modes of oscillation of the water column were measured with a wave gauge and the corresponding response of the vessel determined.

Yang & Kwon (2013) carried out experimental work to investigate the effect of the operational performance of a floating offshore structure near the moonpool resonance frequency, both in fixed and motion free conditions. Special attention was given to the effect of the cofferdam inner structure inside the moonpool.

Industrial research has also been active in this field. Ulstein developed an innovative design of the moon pool doors, which differ from industry standards by a special foldable link mechanism, reducing the span of the centre door. This reduces the construction cost and increases safety during operation. The foldable link mechanism further allows these top hatches to be used more practically in combination with large bottom doors, as the compact design eliminates clashes in simultaneous opening positions. All moving parts and systems that require maintenance are accessible from a safe and practical position. Ulstein h developed the moon pool hatches to fit the offshore construction vessel Island Venture's main moon pool opening of 11.2 x 12 m and coping with a 450 tonne hang-off load.

Moon pools of large dimensions such as those found in drill ships have an impact in resistance and propulsion are difficult to estimate at the early stages of design. In Krijger and Chalkias (2016) RANSE CFD was used to optimize the hull and appendages of a drillship with a special hydrodynamically shaped moonpool. These authors claim this design reduces the added moonpool resistance by 37% compared to a conventional one while at the same time eliminates sloshing in transit.

Ma et al (2016) presented a real case study aimed at the reduction of the added resistance due to the moonpool in a drillship. Model tests and CFD simulations have shown that the ship resistance has large fluctuations due to the added resistance induced by the moonpool. This added resistance is mainly due to the vortices shed from the moonpool front wall, which enter into the moonpool and impinge on the rear wall. A parametric study revealed that smaller moonpool dimensions result in smaller added resistance.

Chalkias & Krijger (2017) performed potential flow frequency domain calculations to predict the natural frequencies and water motions for several moonpools. Two vessels with different moonpool dimensions and shapes were studied and model tests were carried out for one of them. Based on this work a motion reduction device was designed to increase the operability of the ships by reducing the motions in the moonpool.

Lohrmann et al (2017) investigated the dumping of waves in moonpools. Numerical simulations of the effect of perforated bulkheads were carried out using a viscous solver and the results were compared with those from model tests. The study found a dependency of the natural frequency of the surface elevation inside the moonpool on the ship speed. Based on this elevation, the resulting dumping of different layouts is discussed.

Yoo et al (2017) presented results from experimental and numerical simulation studies to reduce the internal flow of a moonpool. In particular, it was studied the effect of larger damping devices for four moonpool designs: ordinary plain moonpool, moonpool with a recess deck, moonpool with an isolated recess deck (island deck) and moonpool with a combination of island deck, splash plates and wave absorber. The internal flow of the moonpool has been investigated using RANS based CFD code. The CFD analysis considered regular waves, which calculated the water surface responses inside the moonpool. The flow pattern and resonance frequency were then compared with model test results and showed reasonably good agreements.

6.7 Offshore vessels Helideck Design and Integration

Generally, offshore vessels and floating structures have integrated a helideck structure in order to provide for offshore helicopter landing to transfer personnel and equipment to and from the drill or construction site. The helideck structure should satisfy key safety requirements in accordance with some offshore regulations and rule notations. The aim of these requirements and rule sets is to evaluate the buckling/ultimate strength of the developed pancake under helicopter landing impact and vessel motions. An example of this evaluation with regard to the structural safety and stability of the developed aluminium pancake was carried out by BS EN 19999-1-1:2007 to comply with the design requirement by Koo et al (2014). For verification with respect to an evaluation by EUROCODE 9, a 3-dimensional finite element analysis is performed with FEA program. Various offshore structures and vessels with helideck are shown in Figure 18.

Figure 18: Examples of Helidecks in Offshore Applications

Offshore helideck structures use aluminium because of its light weight, low maintenance requirements, cost effectiveness and easy installation. The aluminium helideck structure should satisfy requirements in accordance with some offshore regulations and rule notations such as the Australian/New Zealand Standard and EUROCODE 9. The width-to-thickness ratio and the yield stress are recognized as the governing design parameters in the design of cross sections in these specifications. The aluminium helideck design with relevant EUROCODE 9 was based on the strength calculation by Park et al (2015). Figure 19 shows the flow chart for the typical design process of an aluminium helideck structure.

However, section designs of aluminium pancakes tend to modify and/or change from the steel pancakes. Therefore, it is necessary to optimize section design and evaluate the safety requirements for aluminium helidecks. A design procedure was developed based on section optimization techniques with experimental studies, industrial regulations and nonlinear finite element analyses by Seo et al (2016). To validate and verify the procedure, a new aluminium section was developed and compared strength capacity with the existing helideck section profiles.

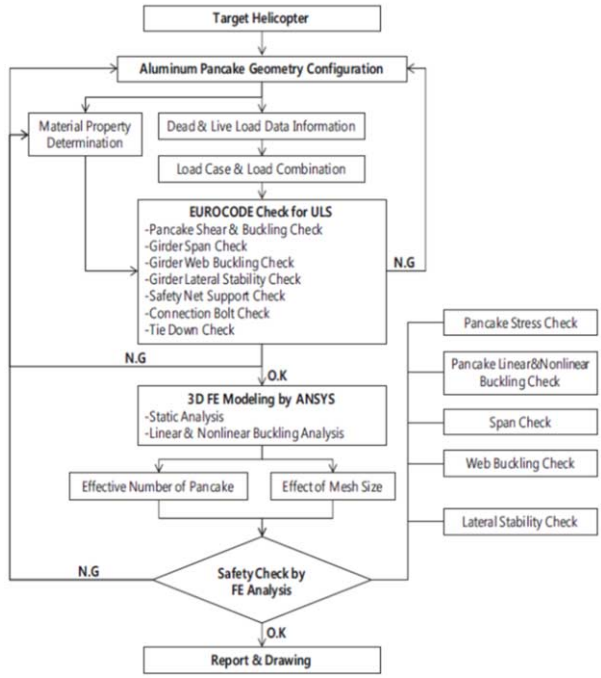

Figure 19: Flow chart showing the design process of an aluminium helideck structure

6.7.1 Materials and Analysis Techniques

Generally, offshore helideck structures are constructed by using steel material. However, aluminium helideck structure is widely used for reasons such as weight savings, no-maintenance, anti-corrosion, and convenience of assembly etc. Ha et al (2015) had mentioned the large scaled SAFE (Samsung Aluminium Fire-fighting Enhanced) helideck structure based on the code checked design through collaboration of experimental verification. In the structural engineering stage of the SAFE helideck, it was found the design factors in the EURCODE 9 were not clearly defined. Therefore, engineering decisions for some un-cleared design factors as well as methodology were carried out. Furthermore, it was strongly recommended to ensure safety for the SAFE helideck structure in accordance with offshore regulations such as CAP437, NMA, NORSOK etc. Through the experimental tests such as coupon load test, fire test and friction test, the SAFE helideck structure was verified by a certified authority. The newly designed large scale SAFE helideck structure displayed excellent benefits with regards to overall structural safety.

Since there is always the probability of helicopter emergency landing in a lifetime of such structures, evaluation of structural performance to achieve structural capacity beyond the elastic range by non-linear analysis can create new approaches in the design codes of offshore facilities. Despite the approaches of current design codes had changed from design-based on force method to design-based on performance method, the helideck design codes still recommended users to use the force method (Vaghefi et al 2013). Therefore, by using nonlinear analysis to review the capacity of structure in the elastic range, estimating its resistance and assessment of the current codes, appropriate results for the next generation of design codes could be reached.

Helidecks are vital structures acting as a last exit in an emergency. Helicopters transport people and goods to and from ships and offshore plants. When designing the structure of a helideck, it is necessary to comply with loading conditions and design parameters specified in existing

professional design standards and regulations. Finite element analysis (FEA) was conducted with regard to a steel helideck mounted on the upper deck of a ship considering the emergency landing of the helicopter by Park et al (2016). The superstructure and substructure were designed, and the influence of various design parameters was analysed on the basis of the FEA results.

6.7.2 Structural Configurations

The required helideck diameters for various classifications under NORMAN 27 are listed in Table 16 and an industry sampling of existing offshore helideck structural configurations are listed in Table 17.

Table 16: List of the NORMAN 27 Classifications of Helidecks

NORMAN27	DIAMETER OF HELICOPER DECK(metre)	<15	H1
		15~24	H2
		>24	H3

Table 17: Typical Helicopter Particulars

Classification	Helicopter deck diameter (m)	APPLIED	Helicopter deck type	Helicopter type	D-value (m)	Rotor diameter (m)	'T' value (t)	Landing net size (m ×m)
H3	25.24	Offshore platform	Vertical	EH101 Sikorsky S92A	22.8 20.88	18.6 17.17	14.6 12	15x15
H2	22.2	Offshore platform	Inclined	EC 155B1 Sikorsky S76	14.3 16	12.6 13.4	4.9 5.3	12x12
H2	22.2	Offshore platform	Inclined	Sikorsky S76 EC225	16 19.5	13.4 16.2	5.3 11	12x12
H3	25.24	Offshore platform	Vertical	EH101 Sikorsky S92A	22.8 20.88	18.6 17.17	14.6 12	15x15
H2	22.2	Offshore platform	Inclined	Sikorsky S76 Super Puma AS332L	16 18.7	13.4 15.6	5.3 8.6	12x12
H2	19.5	Offshore platform	Inclined	Sikorsky S76 EC155B1	16 14.3	13.4 12.6	5.3 4.9	12x12
H3	26.65	Shuttle Cruise	Vertical	Super Puma AS332L	18.7	5.6	8.6	15x15
H2	22.5	FSO	Vertical	EC225 Sikorsky S76	19.5 16	16.2 13.4	11 5.3	12x12
H2	22.8	Offshore platform	Vertical	EH101	22.8	18.6	14.6	12x12

6.7.3 Thermal Loads

API (2006) and DNV (2001) recommend fire safety facilities such as fire extinguishers, water sprays, fire resistant equipment, etc. are installed to prevent such a structural damage. Also, SOLAS (2015) suggests the fire-fighting appliances regarding categories in Regulation 18 (Helicopter facilities). There are only recommendations for fire suppression facilities in the rules and standards. The guidelines for structural fire safety, fire fighting and the definition of required design fire loading are very unclear and open to interpretation. In particular, a helideck made from aluminium is sensitive to temperature and heat flux, compared with other materials such as carbon steel, stainless steel, nickel alloy, etc. A structural design standard for an aluminium helideck should specifically address the risk of fires and the associated criterion. This makes such a standard's development critical.

The helideck structure must satisfy the safety requirements associated with various environmental and accidental loads. There have been a number of fire accidents offshore due to helicopter collision (take-off and/or landing) in recent decades. To prevent further accidents, a substantial amount of effort was directed toward the management of fire in the safety design of offshore helidecks. Kim et al (2015, 2016) introduced and applied a procedure for quantitative risk assessment and management of fires by defining the fire loads with an applied example. The frequency of helicopter accidents in the Gulf of Mexico and the North Sea were considered, and design accidental levels for both regions were suggested. The proposed procedures for determining design fire loads can be efficiently applied in offshore helideck

development projects, and the application includes the assessment of design fire loads and the quantification of the effects of risk control options, such as optimization of the helideck pancake profile, the location and the number of water deluge systems.

In recent years, the demand for ships and offshore platforms operating within the Arctic Ocean has been rapidly increasing due to global warming and the discovery of large reservoirs of oil and natural gas in the area. Bae et al (2015) discussed winterization design as a key issue to consider in the structural design and building of ships and their helidecks that have the possibility of operating in the Arctic and Sub-Arctic regions. International regulations for winterization design in Arctic conditions regulate only those ships and offshore platforms with a Polar Class designation and/or an equivalent standard. To cope with the rising demand for operations in the Arctic region, existing and new non Polar Class vessels were called to operation, but lacking adequate winterization design standards for refitting the vessels. These existing ships and offshore platforms were not designed utilizing reliable data based on numerical and experiment studies. These vessels were designed only to performance and functional criteria. Bae described the importance to obtain reliable data and to provide design guidance of the anti-icing criteria on structure, such as helidecks, by taking the effects of low temperature environments into consideration when evaluating the use of a specific vessel in a specific environment. Therefore, the main objective of this paper considered the retroactive anti-icing design of aluminium helidecks structures using heating cables. In the paper's discussion, finite element methods were carried out using thermal analysis with cold chamber testing for the required performance and capacity of the heating cables. According to the results, the method can be used as a standardized regulation and design guidance for retroactive winterization design of equipment, ships and offshore platforms. This will provide a more systematic, comprehensive guidance for helideck structural winterization design.

7 CONCLUSIONS AND RECOMMENDATIONS

7.1 Recommended Research for Future Special Craft Committees

The Committee members of the 2018 ISSC V.5 Special Craft Committee have created a list of recommended vessel types for future Special Craft Committees to address specifically in greater depth and detail. As stated, the maiden 2018 ISSC V.5 Special Craft report was intended to be a wider and more shallow discussion in order to cover many references and topics on specialized vessels as compared to follow on reports. The recommended vessels below and emerging research topics are based on current trends and evolving market demands in these areas. Papers, articles and other research material is expected to be more readily available over the next three years.

7.1.1 Autonomous and Unmanned Vessels

The need for marine drone-like vessels is now becoming a reality with many projects in both the naval and offshore industry currently underway. Soon vessels will travel point-to-point through the seaways without a human element on-board. Much like Aerial Unmanned Vehicles (AUVs), the controls will be held by a shore based pilot guided by a series of automation and surveillance equipment. The effects on the structural design will be profound for these new sea-going vessels as the emphasis and limitations of the human-element on board will have been removed. It is unclear whether these vessels will be fully automated or be piloted shore-side, but it is clear this shift can lighten the structural design aspects of these special craft. Conversely, it can also drive more robustly designed vessels able to encounter headings and sea states that are agnostic to on-board mariner safety.

Advances in autonomous vessels may soon allow the human factor to be eliminated in structural designs, ultimately opening any operational and service restrictions that limit performance. As these programs begin to emerge and materialize, it is recommended future Special Craft

Committees investigate the direct impacts to structural configurations, weights and loads on unmanned and autonomous marine vessels.

7.1.2 Research and Polar Vessels

Deep water and Polar Regions are being explored for new trade routes and natural resources. This is bringing future structural challenges to ship design, requiring a revamping of research and testing to support the need for research and heavy icebreaking vessels, larger vessels and cranes for subsea exploration, and extreme cold and pressure tolerant structural materials. New standards are being developed to aid in the surge of these required vessel types and their structural necessities. Both research and polar vessels are part of an aging worldwide fleet where knowledge is lacking and new research conducted by utilizing the latest technologies. It is recommended an emphasis be put on these vessel types for future reports.

7.2 Emerging Structural Trends to Watch

To help governments sustain new construction within their respective countries, advanced construction techniques for mitigating vessels lifecycle costs are now involving modular and multi-party production schemes. These new strategies will affect how designers and production teams design structural scantlings to ensure fiscal viability, adequate alignment and fitting of units. Also printing of structural material and possibly scantlings may possibly be the 3D printing techniques of the future for construction and repair.

7.2.1 Total Cost of Ownership

Economical solutions for vessels in the form of lighter structural configurations and designs with the vessels structural lifecycle maintenance and disposal in mind are becoming part of the acquisition conversation. Soon designers will need to consider the materials used in design and how the vessels' recyclability is economically advantageous to the owner. Where owners were only concerned on the initial capital cost of the vessel and her structure, they are now asking the structural design lend itself to fiscally viable repair and maintenance solutions. Consideration must be given to worldwide material availability for repair, multi-party construction and the overall reduction in complexity of the structural configuration. De-complicating structure would allow ease of maintenance and painting by eliminated such items as sharp corners to prevent coating failures leading to corrosion. Today, owners are more cash strapped, feeling the economic impacts of oil prices and new regulation, on vessel service lives' lasting much longer than the typical 25-30 years. Tomorrow they will ask for an evaluation of the total cost of ownership in the concept design phase, and demand creative foresight to reduce monetary burdens down the line.

7.2.2 3D Printing for Structures

Metal-based additive manufacturing, or three-dimensional (3D) printing, is an emerging technology across various industries including the marine industry. Manufacturing metal components layer by layer increases design freedom and manufacturing flexibility. Therefore, complex geometries can be easily created, product customisation can be enhanced and time to market can be shortened. However, only a few number of alloys can currently be reliably printed (Martin et al, 2017). Metal-based additive manufacturing often involves the deposition of layers of an alloy feedstock in the form of powders or wires, which are melted together by a rapidly moving heat source to form a solid mass. The rate of solidification is often an order of magnitude higher than that is seen during conventional casting techniques, and the process of building up layers causes non-uniform cooling. This leads to thermal stresses in the alloy which can generate cracks known as hot tears (Todd, 2017). A new approach has recently been proposed by introducing nanoparticles of nucleates that control solidification during additive manufacturing (Martin et al, 2017).

For the marine industry, 3D printing technology can enhance new product developments and reduce the cost of development by allowing to verify and improve design parameters and ideas so that design level and efficiency increases. Moreover, 3D printing technology makes the production of auxiliary products more economical and quicker. 3D printing technology can manufacture complex parts with higher accuracy and smoothness where traditional manufacturing methods may encounter difficulties. Currently, 3D printing technology is mainly used in shipbuilding industry in small-sized parts with a complicated structure such as impellers, engine blades, radiators and small propellers (Chao et al, 2017).

Complex and large components operate in harsh and corrosive marine environment. These components are assembled into various ship types. There is a significant potential of 3D printing technology to be used in marine sector. However, there are still substantial technological issues that need to be resolved before the mass acceptance and utilisation of additive manufacturing in marine industry (Strickland, 2016). In order to make all the components to be printed useful, it is essential to have printed material property at least the same as those made by traditional metallurgy.

7.3 Concluding Remarks

Technology is moving at an alarming pace and with new construction of specialized vessels requiring flexibility, collaboration and modularity to remain economically viable options for owners, the future is exciting for structural design techniques in addition to uncertainties.

The overall intent of this first report of the V.5 Special Craft Committee was to cover a very broad area of vessels across three major marine market segments and to highlight the ones considered “special” or “specialized” due to their unique operations and associated structural aspects. The difficulty but advantage of having the ability to choose craft that have specialized structural features is the abundance or lack of reference literature in which to evaluate from. Future Special Craft Committees now have a baseline report upon which they may focus on very specific vessels relevant or significant to current markets which would lead to the ability to perform useful benchmark studies for industry. As a lesson learned, it is the recommendation that the V.5 Special Craft Committee be considered under the naming V.5 Special Vessel Committee for future ISSC Specialist Committees in order to eliminate any reader expectations or confusion on the word “Craft”.

REFERENCES

ABS (2004). Guide for Building and Classing Naval Vessels, American Bureau of Shipping

ABS (2014). Guide for building and Classing Drillships – Hull Structural Design and Analysis. 2014.ed. Houston, TX, USA: American Bureau of Shipping.

ABS (2015). Rules for Building and Classing Part 3 Ch2 Sec11. 2015.ed. Houston, TX, USA: American Bureau of Shipping.

ABS (2016a). Guide for Building and Classing: Semi-submersible Heavy Lift Vessels. 2017. ed. Houston, TX, USA: American Bureau of Shipping.

ABS (2016b). IMO Polar Code Advisory. 2016. ed. Houston, TX, USA: American Bureau of Shipping.

ABS (2017a). ABS International Naval Ship Guide. 2017.ed. Houston, TX, USA: American Bureau of Shipping.

ABS (2017b). ABS Rules for Building and Classing High-Speed Naval Craft. 2017. ed. Houston, TX, USA: American Bureau of Shipping.

ABS (2017c). Rules for Building and Classing Part 3 Hull Construction and Equipment: Mobile Offshore Drilling Units 2017.ed. Houston, TX, USA: American Bureau of Shipping.

ABS (2017d). Guidance Notes on Structural Analysis of Self-Evaluating Units. April 2016.ed. Houston, TX, USA: American Bureau of Shipping.

ABS (2017d). Guide for Building and Classing: Semi-submersible Heavy Lift Vessels. 2017.ed. Houston, TX, USA: American Bureau of Shipping.

ABS 2014 Rules for building and Classing High Speed Naval Craft, ABS Houston, TX.

Allen, T., Battley, M. (2015) Hydroelasticity in Slamming Impacts of Flexible Composite Hull Panels, 5th High Performance Yacht Design Conference, Auckland, 10-12 March, 2015

ANEP-77 (2011) Naval Ship Code (Edition 3), North Atlantic Treaty Organization, NATO Standardization Agency (NSA)

API, (2012) Specification 2C: Offshore Pedestal-mounted Cranes. American Petroleum Institute, Washington D.C., USA.

API, (2006) Recommended Practice for Planning, Designing, and Constructing Heliports for Fixed Offshore Platforms. American Petroleum Institute, Washington D.C., USA.

Archer, L., Roy, J. (2013) Platform Engineering for Production and Semi-Custom Yachts, Design & Construction of Super & Mega Yachts, 8-9 May 2013, Genoa, Italy

ASPPR (1996) Arctic Shipping Pollution Prevention Regulations, Canada

Arena, M.V., Blickstein, I., Younossi, O., Grammich, C.A., (2006) Why has the cost of Navy Ships risen?, RAND Corporation, Santa Monica, CA.

Ascic, B., Acanfora, M., Boote, D. (2015) The Influence of Damaged Stability Probabilistic Approach on overall Megayacht Design, Towards Gren Marine Technology and Trasnsport, Ed. Guedes Soares, Dejhalla & Paveltić, Taylor & Francis Group, London, UK, ISBN 978-1-138-02887-6

Ashe, G. et al., (2006), ISSC Committee V.5 – Naval Ship Design, In: Proc. Of the 16th Intl. Ship and Offshore Structures Congress. Southampton: ISSC, pp213-262

Assael, J. (2017) New 'Red Ensign Group Yacht Code', Superyacht UK Technical Seminar 2017, 12th January 2017, London, UK.

Augier, B., Hauville, F., Bot, P., Durand, M. (2012) Numerical Investigation of the Unsteady Fluid Structure Interaction of a Yacht Sail Plan, 4th High Performance Yacht Design Conference, Auckland, 12-14 March, 2012

Bae S.Y., Kang G.H., Shin W.H., Park, J.S., Seo, J.K. (2015) Winterization design of aluminum helideck in artic environment. RINA, Royal Institution of Naval Architects - ICSOT Korea: Safety of Offshore and Subsea Structures in Extreme and Accidental Conditions 2015, Papers, p 121-126.

BAAINBw (2007) BV 1040-1 Festigkeitsberechnungen für Überwasserkampfschiffe, Federal Office of Bundeswehr Equipment, 31. October 2007, Koblenz, Germany

BAAINBw (2017) BV 0230 Shock Resistance, Federal Office of Bundeswehr Equipment, October 2017, Koblenz, Germany

Baley, C., Lan, M., Davies, P., Cartié, D. (2015) Porosity in Ocean Racing Yacht Composites: A Review, Applied Composite Materials, Vol. 22, Iss. 1, pp. 13-28, February 2015

Baral, N., Cartié, D.D.R., Partridge, I.K., Baley, C., Davies, P. (2010) Improved impact performance of marine sandwich panels using through-thickness reinforcement: Experimental results, Composites Part B: Engineering, Vol. 41, Iss. 2, March 2010, pp. 117-123

Barba Fau, C. (2017) Floodable Docking Garages, Design & Construction of Super & Mega Yachts, 10-11 May 2017, Genoa, Italy

Battley, M., Grossmann, E., Basset, T. (2012) Effect of Stiffener Compliance on Response of Curved Hull Panels, 4th High Performance Yacht Design Conference, Auckland, 12-14 March, 2012

Begovic, E., Bertorello, C. (2015) Small Waterplane Area Twin Hull for Maxi and Mega-Yacht Design, Design & Construction of Super & Mega Yachts, 13-14 May 2015, Genoa, Italy

Berchiche, N.; Östman, A.; Hermundstad, O.A.; Reinholdtsen, S-A (2015). Experimental validation of CFD simulations of free-fall lifeboat launches in regular waves. Ship Technology Research, Vol.62, No.3, pp.148-158.

Bereznitski, A. (2011). Wind turbine installation vessel of a new generation. Wind turbine installation vessel of a new generation. OMAE 2011, 30th International Conference on Ocean, Offshore and Arctic Engineering; 19-24 June 2011; Rotterdam, The Netherlands. Organised by ASME, New York, US. Vol.5, pp 329-334.

Bermano, C., Boote, D., Pais, T., McCartan, S. (2015) Development of an NVH methodology for superyacht structures, Design & Construction of Super & Mega Yachts, 13-14 May 2015, Genoa, Italy

Bertorello, C., Begovic, E. (2016) From Nuclear Submarine to Sailing Trimaran Record The Globe Circumnavigation, The Ultimate Marine Challenge, In the 10th Symposium on High Performance Marine Vehicles, 17-19 October, Cortona, Italy

Birkler, J. (2005) Differences between military and commercial shipbuilding. RAND Corporation, Santa Monica, CA.

Boote, D., Pais, T., Dellepiane, S. (2013) Vibrations of Superyacht Structures: Comfort Rules and Predictive Calculations, In C. Guedes Soares & J. Romanoff (eds.), Analysis and Design of Marine Structures; Proceedings of the 4th International Conference on Marine Structures (MARSTRUCT2013), Espoo, Finland, 25-27 March 2013. London: CRC Press, pp. 37-44

Boote, D., Pais, T., McCartan, S. (2014) Vibration Analysis of Large Yacht Structures, Proceedings of the 112th ATMA Session, Paris, 26-27 May 2014. Association Technique Maritime et Aeronautique

Bosma, T. (2013) A Human Factors' Approach to Mega Yacht Concept Design, Design & Construction of Super & Mega Yachts, 8-9 May 2013, Genoa, Italy

Bradbeer, N.I.C., (2013), Implications for underwater shock response of adopting simplified structural styles in warships, Ph.D. Thesis, Dept. Mech Eng, UCL.

Browne, Robin P.; Gatehouse, Evan G.; Reynolds, Alan (2008). Design of an ice strengthened lifeboat. International Conference and Exhibition on Performance of Ships and Structures in Ice 2008, ICETECH 2008, p 438-445.

Bureau Veritas (BV) 2016 Rules for classification of Naval Ships

BV (2000). Rules for Classification of Steel Vessels. 2000. ed. Paris, France: Bureau Veritas.

BV (2016a). NR 569 DT R01 E: Classification of Drilling Ships. 2016. ed. Paris, France: Bureau Veritas.

BV (2016b). NR 628: Semi-Submersible Cargo Ships. 2016. ed. Paris, France: Bureau Veritas.

BV (2016c). NR 534: Rules for the Classification of Self-Elevating Units - Jack-ups and Liftboats. 2016. ed. Paris, France: Bureau Veritas.

BV (2016d). Guidance Note NI 621 DT R00 E: Guidelines for Moonpool Assessment. 2016. ed. Paris, France: Bureau Veritas.

BV (2017). NR 483 2012: Rules for Classification of Naval Ships. June 2017. ed. Paris, France: Bureau Veritas.

CAP 437. (2016) Standards for offshore helicopter landing areas. e.d. December 2016, West Sussex, UK: Civil Aviation Authority,

CCS (2015). Rules for the Construction and Classification of Sea-going Steel Ships. ed. 2015. Beijing, China: China Classification Society

CCS (2016). Rules for Classification of Mobile Offshore Units. ed. 2016. Beijing, China: China Classification Society

CCS (2017). Rules for the Construction and Classification of Sea-going High speed craft. ed. July 2017. Beijing, China: China Classification Society

CCS, China Classification Society. (2005). Guide for SWATH vessels.

Chalkias, D. and Krijger, J.W. (2017). Moonpool Behavior of A Stationary Vessel in Waves and a Method to Increase Operability. Proceedings of the ASME 2017 36th International Conference on Ocean, Offshore and Arctic Engineering OMAE2017, June 25-30, 2017, Trondheim, Norway.

Chao, C., Liu, L. and Xu, J., 2017. Application of metal additive manufacturing in shipping and marine engineering, In Electromechanical Control Technology and Transportation: Proceedings of the 2nd International Conference on Electromechanical Control Technology and Transportation (ICECTT 2017), January 14-15, 2017, Zhuhai, China (p. 191). CRC Press.

Chen Ying, Yue Ya-Lin, Lin Ji-ru, Wei Peng-yu, (2012) Research on the design loads of the SWATH, Journal of Ship Mechanics. Vol 16, No 1-2, pp 101-107(in Chinese)

ChoiK., Cheon E–., Kim H–., Nam J–., Lee T–. (2015). Comparison of peak ice pressures on the IBRV ARAON during the planned and the unusual ice transits. Proceedings of the International Conference on Port and Ocean Engineering under Arctic Conditions, POAC,

Cullen, Robert (2007). Use of Heavy Lift Ship as a Maintenance and Repair Vessel. Ship Systems Integration & Design Department, Technical Report NSWCCD-CISD–2006/006.

Current trends in Naval Shipbuilding, http://www.aph.gov.au/Parliamentary_Business/Committees/Senate/Foreign_Affairs_Defence_and_Trade/Completed_inquiries/2004-07/shipping/report/c02

Dassi, P. (2015) Advanced Composites: A possible answer to mega yacht structural questions, Design & Construction of Super & Mega Yachts, 13-14 May 2015, Genoa, Italy

Dellepiane, S., Boote, D. (2013) Numerical and Experimental Analysis of the Dynamic Behaviour of Large Yacht Superstructures, Design & Construction of Super & Mega Yachts, 8-9 May 2013, Genoa, Italy

Det Norske Veritas (DNV) 2016 Rules for naval surface craft

DNV·GL. (2017) Pt6 Ch5. Rules for classification: Ships.

DNVGL (2015a). DNVGL-RU-NAVAL-P15Ch3: Rules for Classification – Naval vessels. December 2015 ed. Høvik, Norway: DNV GL.

DNVGL (2015b). DNVGL-RU-SHIP-Pt5Ch13: Rules for Classification – Ships. October 2015 ed. Høvik, Norway: DNV GL.

DNVGL (2015c). DNVGL-RU-HSLC-P1Ch2: Rules for Classification – High speed and light craft. December 2015 ed. Høvik, Norway: DNV GL.

DNVGL (2015d). DNVGL-RU-OU-0101: Offshore drilling and support units. July 2015 ed. Høvik, Norway: DNV GL.

DNVGL (2015e). DNVGL-RU-OU-0104: Rules for Classification Self-elevating units. 2015 ed. Høvik, Norway: DNV GL.

DNVGL (2015f). DNVGL-OS-C104: Structural design of self-elevating units - LRFD method. 2015 ed. Høvik, Norway: DNV GL.

DNVGL (2015g). DNVGL-RU-SHIP-Pt5Ch10: Vessels for special operations. 2015 ed. Høvik, Norway: DNV GL.

DNVGL (2015h). DNVGL-OS-E401: Helicopter Decks. July 2015 ed. Høvik, Norway: DNV GL.

DNVGL (2016a). DNVGL-ST-E406: Design of free-fall lifeboats January 2016 ed. Høvik, Norway: DNV GL.

DNVGL (2016b). DNVGL-ST-0378: Standard for offshore and platform lifting appliances May 2016 ed. Høvik, Norway: DNV GL.

Dombrowski, P. (2002) The Globalization of the Defense Sector? Naval Industrial Cases and Issues, Globalization and Maritime Power, ed. Sam J. Tangredi, Washington, D.C., National Defense University Press.

Eckstein, M., (2016) Navy says LCS shock trial had positive results; Pentagon still has concerns, USNI

EDNAY, L.A., (1988) Survivability policy for surface ships of the U.S. Navy, OPNAVINST 9070.1, Vice Chief of Naval Operations.

EN 13852 - Part1 (2013) Cranes - Offshore cranes - Part 1: General-purpose offshore cranes: EUROPEAN STANDARD

EN 13852 – Part2 (2014) Cranes - Offshore cranes - Part 2: Floating cranes: EUROPEAN STANDARD

Erceg, S.a, Ehlers, S.ab,Von Bock Und Polach, R.ac, Leira, Bernt . 2014. A numerical model to initiate the icebreaking pattern in level ice. Proceedings of the International Conference on Offshore Mechanics and Arctic Engineering - OMAE, v 10, 2014

Fong, R.-Y. (2011) A Comparison Study between ALE and SPH for Yacht Structure Design under Slamming Impact Loads, 16th ABAQUS Taiwan Users' Conference, 2011

Fong, R.-Y., Chang, H.-Y. (2014) Finite Element Analysis Project Proposal for Yacht Hydrodynamic Quantification

Forrester, C., (2016) Austal takes hit of LCS shock trial, HIS Jane's Defence Industry, London.

Fossati, F., Bayati, I., Orlandini, F., Muggiasca, S., Vandone, A., Mainetti, G., Sala, R., Bertorello, C., Begovic, E. (2015) A Novel Full Scale Laboratory for Yacht Engineering Research, Ocean Engineering, Vol. 104, pp. 219-337

Fossati, F., Muggiasca, S. (2012) An Experimental Investigation of Unsteady Sail Aerodynamics Including Sail Flexibility, 4th High Performance Yacht Design Conference, Auckland, 12-14 March, 2012

Fossati, F., Schito, P., Vandone, A., Malandra, M., Russo, G. (2015) Furling Sails Design for Super & Mega Sailing Yachts, Design & Construction of Super & Mega Yachts, 13-14 May 2015, Genoa, Italy

Gaiotti, M., Rizzo, C.M. (2015) Dynamic buckling of masts of large sail ships, Ships and Offshore Structures, Vol. 10, No. 3, 290–301

Gaiotti, M., Rizzo, C.M., Nebbia, G., Caleo, A., Ivaldi, A. (2015) Mechanical Behaviour of Fillers: Tests and Comparisons, Design & Construction of Super & Mega Yachts, 13-14 May 2015, Genoa, Italy

Gerard, R., Fajoui, J., Alila, F., Jacquemin, F., Casari, P. (2015) Updated Fatigue Test Methods for Structural Foams and Sandwich Beams, 5th High Performance Yacht Design Conference, Auckland, 10-12 March, 2015

Germanisher Lloyds (GL) 2015 Rules for classification and construction Naval Ship Technology

Ghelardi, S., Gaiotti, M., Rizzo, C.M. (2015) On the shear lag effective breadth concept for composite hull structures, Ships and Offshore Structures, Vol. 10, No. 3, 272–289

Giannarelli, D., Boote, D., Pais, T., Vergassola, G.M., Penco, G. (2015) Mechanical Behaviour of Steel Plates with Epoxy Coatings Exposed to Thermal Loads, Design & Construction of Super & Mega Yachts, 13-14 May 2015, Genoa, Italy

Goutard, M., Das, R., Battley, M., Allen, T., Norris, S. (2012) Evaluation of the Influence of Hydro-Elasticity in Slamming of Elastic Panels Using a Coupled FE-FV Method, 4th High Performance Yacht Design Conference, Auckland, 12-14 March, 2012

Graaf, J. van der, and Zandwijk, K. van (2014). Deepwater construction vessel AEGIR shifting the frontiers of reeling. OTC 2014, 45th Offshore Technology Conference; 5-8 May 2014; Houston, Texas, US.

Gragnani, L., Boote, D., Pais, T. (2015) Acoustic Characterisation of Laminated Glass for Superyachts Windows, Design & Construction of Super & Mega Yachts, 13-14 May 2015, Genoa, Italy

Grannemann, F. (2015). SWATH- a new concept for the safety and security at sea. Ship Science & Technology, v 8 n 17, 2015, pp.47-57.

Ha Y.S., Park J.S., Koo J.B., Jang K.B. Suh Y.S. Seo J.K., Shin W.H. Seo Y.L. (2015) Development of large scaled SAFE helideck structure. Proceedings of the 25th International Ocean and Polar Engineering Conference, ISOPE 2015.

Handler, P., Jarecki, V., Bruhns, H. (2012). FLO/FLO heavy lift critical stability phases. STAB 2012, 11th International Conference on Stability of Ships and Ocean Vehicles; 23-28 September 2012; Athens, Greece.

Hatecke, H., Kruger, S., et al (2014). A fast seakeeping simulation method for heavy-lift operations based on multi-body system dynamics. OMAE 2014, 33rd International Conference on Ocean, Offshore and Arctic Engineering; 8-13 June 2014; San Francisco, US. Organised by ASME, New York, US.

Heggelund, S.E.; Li, Z.; Jang, B-S and Ringsberg, J.W. (2015). Quasi-static assessment of response to slamming impact on free fall lifeboats. ASME 2015 34th International Conference on Ocean, Offshore and Arctic Engineering, OMAE 2015, May 31 - June 5, St. John's, NL, Canada.

Hickey, C., Bickerton, S. (2015) Characterisation of the Processing Properties of Out-of-Autoclave Prepregs, 5th High Performance Yacht Design Conference, Auckland, 10-12 March, 2015

Hootman, J.C., Tibbitts, B.F., (2004) Evolution of Naval Surface Combatant Design and Acquisition Policies, SNAME transactions.

Horn, K. (2015) Sailing Yacht A in der Kieler Förde, 28th September 2015

HSE. (2001) Offshore helideck design guidelines. Prepared by John Burt Associates Limited /BOMEL Limited for the Health and Safety Executive.

https://en.wikipedia.org/wiki/Pioneering_Spirit_(ship)

Hwang, J.-K., Roh, M.-I., & Cha, J.-H. (2016). Design Modification of a Damaged Free-Fall Lifeboat for Floating Production Storage and Offloading Through Free-Fall Tests. International Journal of Offshore and Polar Engineering, Vol.26, No.4.

Hwang, J-K; Roh, M-I and Cha, J-H (2014). Design modification of a damaged free-fall lifeboat for FPSO through the free-fall test. Proceedings of the 24th International Ocean and Polar Engineering Conference, ISOPE Busan.

IACS (2016) Req. UR I. Polar Class. April 2016 International Association of Classification Societies IACS, London, UK

IMO (1994). International Code of Safety for High Speed Craft - HSC Code 1994. 1994: IMO

IMO (2000). International Code of Safety for High Speed Craft - HSC Code 2000 (MSC resolution MSC.97(73)). 2000: IMO

IMO (2009). Code for the Construction and Equipment of Mobile Offshore Drilling Units - MODU– Resolution A.1023(26). 2009: IMO.

International Standards Organisation (2012) Small craft -- Hull construction and scantlings -- Part 9: Sailing craft appendages, ISO 12215-9:2012, Geneva, Switzerland

ISO 19901-3 (2014). Petroleum and natural gas industries – Specific requirements for offshore structures – Part: Topside structure. 2014

ISSC 2006 Committee V.5 Naval ship design

ISSC 2009 Committee V.5 Naval ship design

ISSC 2012 Committee V.5 Naval ship design

ISSC 2015 Committee V.5 Naval ship design

Ivaldi, A. (2015) Growing length in the megayacht industry and structure-related design topics, Ships and Offshore Structures, Vol. 10, No. 3, 221–231, 2015

Ji, G.; Berchiche, N.; Fouques, S.; Sauder, T.; Reinholdtsen, S-A (2015). Integrity assessment of a free-fall lifeboat launched from a FPSO. ASME 2015 34th International Conference on Ocean, Offshore and Arctic Engineering, OMAE 2015, May 31 - June 5, St. John's, NL, Canada.

Kauczynski, W.E.; Werenskiold, P. and Narten, F. (2009). Documentation of operational limits of free-fall lifeboats by combining model tests, fullscale tests, and computer simulation. Proceedings of the 28th International Conference on Ocean, Offshore and Arctic Engineering 2009, OMAE2009, May 31, 2009 - June 5, 2009, Honolulu, HI, USA.

Keil, A.H., (1961) The response of ships to underwater explosions, SNAME transactions, New York.

Kennedy, A.; Simões Ré, A.; Veitch, B. (2010). Operational limitations of conventional lifeboats operating in sea ice. International Conference and Exhibition on Performance of Ships and Structures in Ice 2010, ICETECH 2010, p 440-445.

Kennedy, Allison; Simões Ré, António; Veitch, Brian (2014). Peak ice loads on a lifeboat in pack ice conditions. Society of Petroleum Engineers - Arctic Technology Conference 2014, pp.536-543.

Keuning, P.J., (2015) Discussion, Committee V.5 Naval Ship Design, Volume 3.

Khac, K.V., Zhang, Y., Et al (2014). Monohull dynamics during heavy lift. OMAE 2014, 33rd International Conference on Ocean, Offshore and Arctic Engineering; 8-13 June 2014; San Francisco, US. Organised by ASME, New York, US.

Kim S. J., Lee J., Paik J.K., Seo J.K., Shin W.H., Park J.S. (2016) A study on fire design accidental loads for aluminum safety helidecks. International Journal of Naval Architecture and Ocean Engineering, 8(6):519-529.

Kim, S.J., Park, J.B., Kim, B.J., Seo, J.K., Paik, J.K., Shin, W.H., Park, J.S. (2015) Determination of fire accidental loads for aluminium safety helidecks. RINA, Royal Institution of Naval Architects - ICSOT Korea: Safety of Offshore and Subsea Structures in Extreme and Accidental Conditions, 109-119.

Köhlmoos, A., Bertram, V., Hoffmeister, H., Hansen, H., Moltschaniwskyj, A. (2012) Design by Best Engineering Principles for the Solar Catamaran Tûranor PlanetSolar, 4th High Performance Yacht Design Conference, Auckland, 12-14 March, 2012

Kokkila, K. (2017) Polar Expedition Ships: Ultimate in Passenger Safety and Comfort with Azipod® Propulsion, ABB Business Unit Marine & Ports White Paper, Document 3AJM005000-0076

Kokkila, K., Erkintalo, J. (2017) Relieving Yacht Desingers' Challenge by Integrating Azipod ® Propulsion and Onboard DC Grid Distribution: Increased Safety and Comfort, Considerable Footprint Savings (Over 40%) and Reduced Environmental Impact, Design & Construction of Super & Mega Yachts, 10-11 May 2017, Genoa, Italy

Koo J., Park J. Ha Y. Jang K. and Suh Y. (2014) Nonlinear structures response analysis for aluminium Helideck. Proceedings of the Twenty-forth International Ocean and Polar Engineering Conference, Busan, Koera.

Korbetis, G., Chatzimoisiadis, S., Drougkas, D. (2015) Automated Interprobability from Concept Design to Multidisciplinary FE Analysis, Design & Construction of Super & Mega Yachts, 13-14 May 2015, Genoa, Italy

Krijger, J.W. and Chalkias, D. (2016). CFD Driven Drillship Design. Proceedings of the ASME 2016 35th International Conference on Ocean, Offshore and Arctic Engineering OMAE 2016, June 19-24, 2016, Busan, South Korea.

Laguette, C., Battley, M., Basset, T., Isin, R. (2012) Damage Initiation and Evolution in Marine Composite Laminates, 4th High Performance Yacht Design Conference, Auckland, 12-14 March, 2012

Lake, S., Smyth, T., Mellow, C. (2012) AC45: A Study of High Performance Composite Construction, 4th High Performance Yacht Design Conference, Auckland, 12-14 March, 2012

Lamberti, T., Magistri, L., Gualeni, P., Da Chá, A., Calcagno, A. (2013) The Application of Fuel Cell System as Auxiliary Power Unit Onboard Mega Yacht Vessels: A Feasibility Study, Design & Construction of Super & Mega Yachts, 8-9 May 2013, Genoa, Italy

Lardner I. (2007) Development and implementation of helideck requirements for Yachts. RINA - International Conference - Modern Yacht, 31-35.

Lavroff, J. ; Davis, M.R. ; Holloway, D.S. ; Thomas, G.A. ; Mc Vicar, J.J. (2017). Wave impact loads on wave-piercing catamarans. Ocean Engineering, v 131, p 263-271

Lavroff, Jason; Davis, Michael Richard. (2015). Slamming kinematics, impulse and energy transfer for wave-piercing catamarans. Journal of Ship Research, v 59, n 3, p 145-161

Lee, J., Wilson, P. (2010) Experimental Study of the Hydro-Impact of Slamming in a Modern Racing Sailboat, Journal of Sailboat Technology, Article 2010-01, SNAME 2010

Li, L.; Gao, Z. and Moan, T. (2016). Operability Analysis of Monopile Lowering Operation Using Different Numerical Approaches. International Journal of Offshore and Polar Engineering, Vol. 26, No. 2, June 2016, pp. 88–99.

Lloyd's (2013). Rules and regulations for the classification of ships, incorporating notice No.1,2,3,4,5 & 6- Ship Structures(General)-Special Features-Helicopter landing areas. 2013. e.d. Southampton, UK: Lloyd's Register

Lloyd's (2016). Classification of Special Service Craft. July 2016. e.d. Southampton, UK: Lloyd's Register

Lloyd's (2017a). Classification of Naval Ships. January 2017. e.d. Southampton, UK: Lloyd's Register

Lloyd's (2017b). Rules for the Classification of Offshore Units. 2017. e.d. Southampton, UK: Lloyd's Register

Lloyd's Register. (2005) Vol1 Pt4 Ch2. Rules and regulations for the classification of naval ships.

Lloyds Register (LR) 2016, Rules and regulations for the classification of Naval ships.

Lohrmann, J; Carrica, P.M. and Cura-Hochbaum, A. (2017). Numerical and Experimental Damping of Piston and Sloshing Motions in Moonpools. Proceedings of the ASME 2017 36th International Conference on Ocean, Offshore and Arctic Engineering OMAE2017, June 25-30, 2017, Trondheim, Norway.

Lombardi, M., Cremonesi, M., Giampieri, A., Parolini, N., Quarteroni, A. (2012) A Strongly Coupled Fluid-Structure Interaction Model for Wind-Sail Simulation, 4th High Performance Yacht Design Conference, Auckland, 12-14 March, 2012

Lozej, M., Golob, D., Vrtič, B., Bokal, D. (2012) Pressure Distribution on Sail Surfaces in Real Sailing Conditions, 4th High Performance Yacht Design Conference, Auckland, 12-14 March, 2012

Luxcey, N.; Fouques, S.; Sauder, T. (2010). Computing acceleration loads on free-fall lifeboat occupants. Consequences of including nonlinearities in water waves and mother vessel motions. ASME 2010 29th International Conference on Ocean, Offshore and Arctic Engineering, OMAE2010, June 6-11, Shanghai, China.

Lyons, B. (2015) Building and Operating Expedition Vessels, EYOS Expeditions

Ma, P., Xing, X., Yan, D., Chien, H.-P., Lee, S.-K., Gu, H., Haihua Xu, H.; Choudhary, A.; Hussain, A. and Merchant, A. (2016). Drillship Moonpool Design to Reduce Added Resistance for Fuel Saving. Offshore Technology Conference, 2-5 May, Houston, Texas, USA.

Manta Maritime (2015) The rules and regulations applicable to yachts over 24m in length engaged on international voyages, Botley, UK

Mård, Anders. (2015). Experimental study of the icebreaking process of an ice breaking trimaran. Proceedings of the International Conference on Port and Ocean Engineering under Arctic Conditions, POAC,

Maritime and Coastguard Agency (2012) LY3 The Large Commercial Yacht Code, Southampton, UK.

Martin, J. H., Yahata, B. D., Hundley, J. M., Mayer, J. A., Schaedler, T. A. and Pollock, T. M., 2017. 3D printing of high-strength aluminium alloys, Nature, Vol. 349, 365-369.

McCartan, S., Barrett, A., Swinfield, L., Verheijden, B., Boote, D., More, L., Schouten, R. (2017) Sustainable Luxury Ice-Class Artic Explorer Vessel for Millenials, Design & Construction of Super & Mega Yachts, 10-11 May 2017, Genoa, Italy

McCartan, S., Edens, J. (2013) Design-Driven Innovation: A New Luxury Maritime Leisure Sector Between Cruising and Superyacht Charter, Design & Construction of Super & Mega Yachts, 8-9 May 2013, Genoa, Italy

McCartan, S., Kvilums, C. (2013) Development of an Eco-Catamaran for the Charter Market Through the Implementation of 'Passive Design' Technology, Design & Construction of Super & Mega Yachts, 8-9 May 2013, Genoa, Italy

McCartan, S., Stubbs, E., Crea, N., Rowles, D., Verheijden, B., Shouten, R. (2015) Design-Driven Innovation: Avant Garde 50m Superyacht under 500GT, Design & Construction of Super & Mega Yachts, 13-14 May 2015, Genoa, Italy

McCartan, S., Verheijden, B., Roy, J., Nuvolari, C. (2013) Design-Driven Innovation of a High Speed Art Deco Superyacht Coastal Cruiser for the Chinese Market, Design & Construction of Super & Mega Yachts, 8-9 May 2013, Genoa, Italy

McCracken, A. (2015) Are Swath platforms the ideal superyacht design?, Boat International, 21st January 2015, https://www.boatinternational.com/yachts/yacht-design/are-swath-platforms-the-ideal-superyacht-design--715

McNatt T., Ma M., Hunter S. (2013) Historical perspective on the structural design of special ships and the evolution of structural design methods. Ships and Offshore Structures, 8(3-4): 404-414.

McNicoll, A. (2013) Move over Abramovich: Meet 'Azzam', the world's largest, fastest superyacht, CNN Travel, 18th July 2013, http://edition.cnn.com/travel/article/move-over-abramovich-azzam/index.html

MoD (2012) Shock Design Manual. MAP 01-470, April 2012, UK Ministry of Defence.

Ministry of Defence, (2000) Design standards for surface ship structures. Defence Standard 02-154 (NES 154), UK: Sea Systems Controllerate, UK Ministry of Defence.

Montigneaux, R. (2013) 2013 Global Order Book, ShowBoats International, 19th January 2013

Montigneaux, R. (2014) 2014 Global Order Book, ShowBoats International, 19th January 2014

Montigneaux, R. (2015a) 2015 Global Order Book, ShowBoats International, 19th January 2015

Montigneaux, R. (2015b) 2016 Global Order Book, ShowBoats International, 8th December 2015

Montigneaux, R. (2017) 2017 Global Order Book, ShowBoats International, 6th January 2017

Moretti, P. (2013) RINA Sailing Rig Guidelines and Certification, Design & Construction of Super & Mega Yachts, 8-9 May 2013, Genoa, Italy

Motta, D., Caprace, J.-D., Rigo, P., Boote, D. (2011) Optimization of Hull Structures for a 60 meters MegaYacht, 11th International Conference on Fast Sea Transportation, FAST 2011, Honolulu, Hawaii, USA, September 2011

Mouton, L., Finkelstein, A. (2015) Exploratory Study on the Flutter Behaviour of Modern Yacht Keels and Appendages, 5th High Performance Yacht Design Conference, Auckland, 10-12 March, 2015

Mutlu, U., Grudniewski, P.A., Sobey, A., Blake, J.I.R. (2017) Selecting an Optimisation Methodology in the Context of Structural Design for Leisure Boats, Design & Construction of Super & Mega Yachts, 10-11 May 2017, Genoa, Italy

Nam, B-W; Kim, N-W; Young-Myung Choi, Y-M; Hong, S.Y. and Kim, J-W (2016). A Model Test for Deepwater Lifting and Lowering Operations of a Subsea Manifold. International Journal of Offshore and Polar Engineering, Vol. 26, No. 3, September 2016, pp. 263–27.

NATO Standard 2016 ANEP-77 Naval Ship Code,

Nazarov, A. (2013) Catamarans as Superyachts, Design & Construction of Super & Mega Yachts, 8-9 May 2013, Genoa, Italy

OPNAV (1988) OPNAVINST 9070.1, Survivability Policy for surfac ships of the U.S. Navy.

Pardo M.L. & Fernandez R.P. (2012). Accommodation Vessels. Journal of Shipping and Ocean Engineering, No.6, pp. 327-339.

Park D.H., Kim J.H., Park Y.J., Jeon J.H., Kim M.H., Lee J.M. (2016) Parametric study for suggestion of the design procedure for offshore plant helideck subjected to impact load. Structural Engineering and Mechanics, 60(5):851-873.

Park J.S., Kishore R. K, Ha Y. S., Jang K. B. (2016) Structural engineering of aluminum helideck structure based on the NORSOK requirement. Proceedings of the International Conference on Offshore Mechanics and Arctic Engineering - OMAE,3, ASME, 35th International Conference on Ocean, Offshore and Arctic Engineering.

Park, J.S., Ha, Y.S., Jang, K.B. (2015) Aluminium helideck design for EUROCODE9 with deformation based design. RINA, Royal Institution of Naval Architects - ICSOT Korea: Safety of Offshore and Subsea Structures in Extreme and Accidental Conditions,127-135.

Peer, D., (2012), Estimating the cost of naval ships, CANADIAN NAVAL REVIEW Vol 8 No 2

Pei, A., Zhang, S., Cai, W., Wu, W., Chen, K., Hu X. (2015) Structural Response of Mega Yacht in Waves, TEAM 2015, Oct. 12 - 15, 2015, Vladivostok, Russia

PEO LCS Public Affairs (2016) http://www.navsea.navy.mil/Media/News/Article/849527/uss-jackson-completes-full-ship-shock-trials/

Rahman, Md Samsur; Taylor, Rocky S.; Kennedy, Allison; Ré, António Simões; Veitch, Brian (2015). Probabilistic Analysis of Local Ice Loads on a Lifeboat Measured in Full-Scale Field Trials. Journal of Offshore Mechanics and Arctic Engineering, Vol.137, No.4, 2015.

Ren Huilong, Zhang Qingyue, Hu Yumeng, Jiang Xueyun. (2015). Optimization of small water plane are twin-hull ship structure based on parametric sub-model. Journal of Huazhong University Science and Technology (Natural Science Edition). Vol.43, No.11,. pp 88-93. (in Chinese)

RINA (2007). RINAMIL for FPV: Rules for the Classification of Fast Patrol Vessels. 2007. ed. Genova, Italy: RINA.

RINA (2011). RINAMIL: Rules for the Classification of Naval Ships. July 2011. ed. Genova, Italy: RINA.

RINA (2013). Res. 17: Rules for the Classification of Floating Offshore Units at Fixed Locations and Mobile Offshore Drilling Units. 2013.ed. Genova, Italy: RINA.

RINA (2014). NC/C 6: Rules for Checking the Arrangements intended for Sea Transportation of Special Cargoes. 2014.ed. Genova, Italy: RINA.

RINA (2015). FAR SLEIPNER: subsea construction vessel. Significant Ships of 2015. RINA, London, UK, 2016.

RINA, 2016 Rules for Naval ships Registro Italiano Navale.

Riska, K. & Kämäräinen, J. (2012). A Review of Ice Loading and the Evolution of the Finish-Swedish Ice Class Rules. SNAME Transactions. SNAME Annual Meeting & Expo and Ship Production Symposium, November 2011, Houston, TX, USA

Ronold KO, Nestegård A, McGeorge D, Ertsgaard A, Skjæveland R and Narten F (2009). New standard for design of free fall lifeboats. Proceedings of the 28th International Conference on Ocean, Offshore and Arctic Engineering 2009, OMAE2009, May 31, 2009 - June 5, 2009, Honolulu, HI, USA.

Russo, C. (2017) Passenger Yachts Outfitting Materials, Certification and Fire Load Calculation, Design & Construction of Super & Mega Yachts, 10-11 May 2017, Genoa, Italy

Sauder, T.and Fouques, S. (2009). Theoretical study of the water entry of a body in waves. Application to safety of occupants in free-fall lifeboats. Proceedings of the 28th International Conference on Ocean, Offshore and Arctic Engineering 2009, OMAE2009, May 31, 2009 - June 5, 2009, Honolulu, HI, USA.

Saunders, S., Philpott, T., (ed) (2016) Jane's Fighting Ships, IHS, London.

Seo, H., Jang, H., Chun, H. (2015b) Investigation of Tensile Strength of Composite Laminate under Diverse Environment Conditions, Materials Science Forum, Vol. 813, pp. 169-180

Seo, H.-S., Jang, H.-Y., Lee, I.-W., Choi, H.-S. (2015a) Development of 33feet Class America's Cup Training CFRP Sailing Yacht for Marine and Leisure Applications, Composites Research, Vol. 28, No. 1, pp. 15-21

Seo, J. K., Kyeom P. D, Jo S. W, Park J. S., Koo J. B., Ha Y. S, Jang K. B. (2016) A numerical and experimental approach for optimal structural section design of offshore aluminium helidecks. Structural Engineering and Mechanics, 59(6), 993-1017.

Shahraki, Jalal Rafie; Thomas, Giles ; Penesis, Irene ; Amin, Walid ; Davis, Michael ; Davidson, Gary. (2013). Centre bow design for wave-piercing catamarans. FAST 2013 - 12th International Conference on Fast Sea Transportation

Sharanabasappa, C.S. and Surendran, S. (2013). Model tests on the moored vessel with different moonpool shapes. Ocean Systems Engineering, Vol.3, No.2, pp.137-147.

Sharma R., Kim T.W., Sha O.P. and Misra S.C. (2010). Issues in Offshore Platform Research – Part 1: Semi-submersibles. International Journal of Naval Architecture & Ocean Engineering, No. 2, pp.155-170.

Shaw, R.G. (2015) Applying a Performance-Focused Race-Yacht Methodology to the Design of a Superyacht, Design & Construction of Super & Mega Yachts, 13-14 May 2015, Genoa, Italy

Shipping, Houston, Texas, USA.

Simões Ré, A. J. ; Veitch, Brian (2012). Evacuation in ice: Field trials of a conventional lifeboat in pack and level ice. Society of Petroleum Engineers - Arctic Technology Conference 2012, Vol.1, pp. 1-8.

Simões Ré, A. J.; Veitch, Brian (2013). Evacuation in ice: Ice loads on a lifeboat during field trials. Proceedings of the 32nd International Conference on Offshore Mechanics and Arctic Engineering – OMAE 2013, Vol. 6.

Simões Ré, A.; Veitch, B.; Kuczora, A.; Barker, A.; Sudom, D.; Gifford, P. (2011). Field trials of a lifeboat in ice and open water conditions. Proceedings of the 21st International Conference on Port and Ocean Engineering under Arctic Conditions, POAC, Vol.2, pp.1023-1033, 2011.

Smid, S., Mala, O., Rannala, M. (2014). Cost-benefit analysis on crew transfer vessels to minimize downtime of future wind parks. International Conference in the Design & Operation of Wind Farm Support Vessels; 29-30 January 2014; London, UK.

SNAME (2002) Guidelines for Site Specific Assessment of Mobile Jack-Up Units, Technical & Research Bulletin 5-5A Rev. 2. ed. Jan. 2002. SNAME.

SOLAS, (2015) Construction - Fire Protection, Fire Detection and Fire Extinction, Chapter II-2. International Convention for the Safety of Life at Sea, International Maritime Organization, London, UK.

SSC (2005). Report No. SSC-439 Comparative Structural Requirements for High Speed Craft. February 2005. ed. Springfield, VA, USA: National Technical Information Service U.S. Department of Commerce

Strickland, J. D., 2016. Applications of additive manufacturing in the marine industry, Proceedings of PRADS2016, September 4-8 2016, Copenhagen, Denmark.

SY Jeong, K Choi, EJ Cheon. (2015). An Analysis of Characteristic of Ice Load Distribution on Model Ship due to Ship and Ice Interaction. Journal of the Society of Naval Architects of Korea. 52 (6). p478-484.

The Red Ensign Group (2016) A Code of Practice for Yachts Carrying 13 to 36 Passengers (The Passenger Yacht Code), Sixth Edition, January 2016, Southampton, UK

The Superyacht Intelligence (2017) Vessels, http://www.superyachtintelligence.com/vessels/, Last Accessed: 15th September 2017.

Thomas Mathai (2006). Cross-Structure Loads of a Simple SWATH Vessel. Proceedings of the Sixteenth (2006) International Offshore and Polar Engineering Conference San Francisco, California, USA, May 28-June 2, 2006

Todd, I., 2017. No more tears for metal 3D printing, Nature, Vol. 549, 342-343.

Tregde, V. and Nestegård, A. (2014). Prediction of irregular motions of free-fall lifeboats during drops from damaged FPSO. Proceedings of the International Conference on Offshore Mechanics and Arctic Engineering - OMAE 2014, June 8, 2014 - June 13, 2014, San Francisco, CA, United states.

Tregde, V.; Halvorsen, T.E.; Underhaug, K.O. (2011). Simulation of free fall lifeboats impact forces, slamming and accelerations. 11th International Conference on Fast Sea Transportation, FAST 2011, September 26-29, Honolulu, HI, USA.

Uithof, K., van Oossanen, P.G., Bergsma, F. (2015) The Feasibility and Performance of a Trimaran Yacht Concept Equipped with a Hull Vane, Design & Construction of Super & Mega Yachts, 13-14 May 2015, Genoa, Italy

Vaghefi M., Bagheri H. and Mohebpour S.R. (2013) Nonlinear analysis of offshore helideck due to the helicopter emergency landing loads. Middle-East Journal of Scientific Research 13(10):1351-1358.

van der Velde, J., Di Donato, L., Ascic, B., McCallum, R. (2016) The Design of a Purpose Built Global Capable Expedition Yacht, in the 24th International HISWA Symposium on Yacht Design and Yacht Construction, 14-15 November 2016, Amsterdam, The Netherlands

Van Horn, F. (2008). Heavy Lift Transport Ships – Overview of Existing Fleet and Future Developments. Proceedings of the Marine Operations Specialty Symposium 2008 CORE, National University of Singapore, Singapore.

van Loon, P.T. (2015) Design of a Combined Tender Garage & Beach Club, Design & Construction of Super & Mega Yachts, 13-14 May 2015, Genoa, Italy

Vard (2017) Building a Sustainable Project Portfolio from Diverse Market Segments, Vard Q1 Press Release, Vard Asia

Vice Admiral Paul E. Sullivan, Ms Allison Stiller, Rear Admiral Charles Hamilton, II, statement before the Subcommittee on Projection Forces of the House Armed Services Committee on Shipbuilding, 5 April 2006, p. 6.

WangW.W., LiuJ.X., GongY.F., ZhaoY., ZhangZ. (2013). Assessment of Fatigue Strength of Typical Spots in Wave-Piercing Catamaran (WPC) Based on Spectral Method. Shipbuilding of China. 54(4):19-27. (in Chinese)

Wang Xueliang, Gu Xuekang. (2010). Evaluation of the global desing wave loads for a high speed wave piercing catamaran. Journal of Ship Mechanics. Vol.14, No.1-2. P56-65. (in Chinese)

Weber, J., Das, R., Battley, M. (2015) Slamming Induced Loads on a Rigid Cylinder and Comparison with Rigid Wedges, 5th High Performance Yacht Design Conference, Auckland, 10-12 March, 2015

Winter, D.C. (2006) 'Sea Air Space Exposition', Secretary of Navy, Washington, D.C.

Winton, J. (2012) New Material for Sail Production, 4th High Performance Yacht Design Conference, Auckland, 12-14 March, 2012

Xu F.F., Xia L.J., Li C.Y.. (2015) Strength Analysis and Evaluation of 12000t Self-propelled Revolving Heavy Lift Vessel. (in Chinese). Ship Engineering, 37(12):5-8.

Yang S.H.and Kwon S.H.(2013). Experimental Study on Moonpool Resonance of Offshore Floating Structure. International Journal of Naval Architecture and Ocean Engineering, Vol.5, Issue 2, June 2013, pp.313–323.

Yasseri, S. (2012). Marine domain awareness and safety of heavy lift operation. Marine Heavy Lift Transport & Lift III, International Conference; 24-25 October 2012; London, UK. Organised by RINA, London, UK.

YI Caiying, LIANG Yu,WANG Jifeng. (2012) Global Strength Analysis of Semi-Submerged Pipe-Laying Crane Vessel of 16000 Tons. Shipbuilding of China, Vol 53, special 2, pp1-7(in Chinese)

Yoo, S.O.; Kim, H.J.; Lee, D.Y.; Kim, B. and Yang, S.H. (2017). Experimental and Numerical Study on the Flow Reduction in the Moonpool of Floating Offshore Structure. Proceedings of the ASME 2017 36th International Conference on Ocean, Offshore and Arctic Engineering OMAE2017, June 25-30, 2017, Trondheim, Norway.

Zakki, A. F.; Windyandari, A.; Bae, D.M. (2016). The development of new type free-fall lifeboat using Fluid Structure Interaction analysis. Journal of Marine Science and Technology, Vol.24, No.3, pp.575-580.

Zakki, A.F.; Windyandari, A. and Bae, D.M. (2015). The Investigation of Launching Parameters on the Motion Pattern of Freefall Lifeboat Using FSI Analysis. Procedia Earth and Planetary Science, Vol.14, pp.110-117.

Žanić, V., Andrić, J., Prebeg, P., Pirić, K., Radić, L. (2015) Design Support System application to structural design of mega-yacht, Towards Green Marine Technology and Transport, Ed. Guedes Soares, Dejhalla & Paveltić, Taylor & Francis Group, London, UK, ISBN 978-1-138-02887-6

Zhen Chunbo, Feng Liang, Lu Guochun, Hou Yuanhang.(2014) Global Structure Strength Analysis of SWATH Based on Direct Calculate Method. Applied Mechanics and Materials. Vol.633-634, pp1002-1006. ABS, American Bureau of Shipping. (1999). Guide for building and classing SWATH vessels.

Zhen Chunbo, Ren Huilong, Feng Guoqing, Li Chenfeng. (2012). Fatigue strength test of a SWATH ship's cross-deck structure. Journal of Harbin Engineering University. Vol.33, No.4, pp414-418. (in Chinese).

Zhou L.; Riska, K., Ji C. (2017). Simulating transverse icebreaking process considering both crushing and bending failures,Marine Structures,Vol 54, July 2017, Pages 167-187

This page intentionally left blank

Proceedings of the 20th International Ship and Offshore Structures Congress (ISSC 2018) Volume II – M.L. Kaminski and P. Rigo (Eds.)

doi:10.3233/978-1-61499-864-8-347

COMMITTEE V.6

ARCTIC TECHNOLOGY

COMMITTEE MANDATE

Concern for development of technology of particular relevance for the safety of ships and offshore structures in Arctic regions and ice-covered waters. This includes the assessment of methods for calculating loads from sea ice and icebergs, and mitigation of their effects. On this basis, principles and methods for the safety design of ships and fixed and floating structures shall be considered. Recommendations shall also be made regarding priorities for research programmes and efficient implementation of new knowledge and tools.

AUTHORS/COMMITTEE MEMBERS

Chairman: S. Ehlers
A. Polojärvi
A. Vredeveldt
B. Quinton
E. Kim
F. Ralph
J. Sirkar
P.O. Moslet
T. Fukui
W. Kuehnlein
Z. Wan

KEYWORDS

Arctic Ships, Polar Class, probabilistic design, mission-based design, limit states design, ice mechanics, iceberg, sea ice, Arctic Sea transportation, Northern Sea Route, North West Passage, Polaris, IMO

CONTENTS

1. INTRODUCTION 349

2. DESIGN METHODS FOR MARINE STRUCTURES 351
2.1 Rules for ships 352
2.1.1 IMO Polar Code 352
2.1.2 IACS Polar Class Rules 353
2.1.3 IMO POLARIS 356
2.1.4 RMRS Rules 356
2.2 Rules for offshore structures 357
2.3 Mission-based analysis for ships 359
2.4 Difference between ship and offshore rules 361

3. STRUCTURAL CAPACITY 362
3.1 Limit states 362
3.2 Response to moving loads 363
3.3 Temperature definitions 364
3.4 Requirements of ductile to brittle transition 365
3.5 The effects of low temperature on fatigue and fracture properties 366
3.6 Repair limits 368

4. ICE LOAD MEASUREMENT AND MODELLING 368
4.1 Full-scale 368
4.2 Laboratory-scale 370
4.3 Ice load modelling and validation 371
4.4 Towards a benchmark data suite 373
4.5 Propeller ice interaction 374
4.6 Ice induced vibration (IIV) 375
4.7 Ice induced fatigue 376

5. SUMMARY AND RECOMMENDATIONS 377

REFERENCES 378

APPENDIX 387

A.1 GUIDELINES FOR THE NONLINEAR ANALYSIS OF MOVING ICE LOADS 387

A.2 SIMULATORS 389

1. INTRODUCTION

The abundance of commercial opportunity that exists in the arctic as well as observed changes in environmental conditions, we can expect substantial increase in offshore and marine transportation activity in the Arctic. A definition of Arctic regions is given in the preceding ISSC committee report on Arctic Technology V.6 (2015). Consequently, ships and offshore structures must be designed to comply with comply with regional conditions and design requirements. To ensure ships and offshore structures are safe, clear guidance is needed, which may include the definition of target reliability levels and corresponding structural failure modes and limit states. Guidance from other disciplines may be considered, such as aviation or nuclear engineering, but it must be ensured that guidelines are clear and not misleading to society. In the Arctic, ships and offshore structures should be a safe haven in the event of accidental actions. Aborting the ship or offshore structure should be avoided even if it is plausible to escape from the hazard (i.e. with the exception for example of a fire), because the persons placed in life boats will face severe environmental conditions. In conclusion, accidents in Arctic regions require a different mind-set, because the environment to evacuate into may be much more dangerous then to stay on the ship or offshore structure.

A general observation to be drawn from operations of ships and offshore structures is that heavy reinforcement is generally safer. In the case of offshore structures it may be lower life-cycle costs to design the hull to withstand ice impact rather than to include a disconnect option or to do repairs after incidents with ice. In case of ships, excessive strengthening is typically in conflict with the requirement to minimize initial expenditure. On the other hand, the maritime world links ice conditions to ice classes and insurance as well as ice breaker service following a cost/benefit-approach. The latter typically contains higher damage acceptance in ice class rules for ships, than what is often experienced for offshore structures.

The IACS Polar Code seeks to contribute to the safety of ships, yet it does not quantify safety in terms of reliability target (for instance in the terms of impacts per year or an annual failure rate). The introduced POLARIS system checks if the vessel journey is to be made safely and follows the concept of the Arctic Shipping Pollution Prevention Regulations (ASPPR), even though the background of the contained multipliers are not well defined and thus subjected to uncertainty when used. Another aspect not addressed sufficiently for ships and offshore structures is the design ice load prediction resulting from ice rubble. For the latter the simulations may serve as a fine purpose while complex phenomena can be analyzed also with the help of ice model tests.

In order to design and operate ships in the Arctic, an international legislative framework has to be followed. The main bodies of this framework are the United Nations Convention on the Laws of the Seas (UNCLOS), the International Maritime Organization (IMO), the maritime states, Recognized Organizations (ROs), and the International Association of Classification Societies (IACS) (DNV, 2012). In addition, there is the International Labour Organization (ILO, 2014). The enforcement of mandatory requirements of the IMO conventions depends upon the individual IMO members, which include most maritime states. The member state acts both as flag state and port state. A flag state has the authority and responsibility to enforce regulations over vessels registered under its flag. Since all ships have to meet the international requirements set by the IMO, flag states need to integrate their own statutory requirements with the requirements set by the IMO. "When a Government accepts an IMO Convention it agrees to make it a part of its own national law and to enforce it just like any other law". As a result, any IMO member (i.e. maritime state) has the authority to carry out so-called Port State Controls (PSC) to ensure that the condition and equipment of ships visiting their ports comply with the IMO standards). This complex framework regulates the design and operation of ships in general, which is further described by Bergström (2017) and in Figure 1.

The International Maritime Organization (IMO) Polar Code, being in force since January 2017, seeks to contribute to the safety of ships in the ice covered waters of the Arctic Sea (See Section 2.1.1). the International Association of Classification Societies (IACS) provides the "Unified Requirements (UR) for Polar Ships", which standardized global ice classification specifications in seven polar classes.

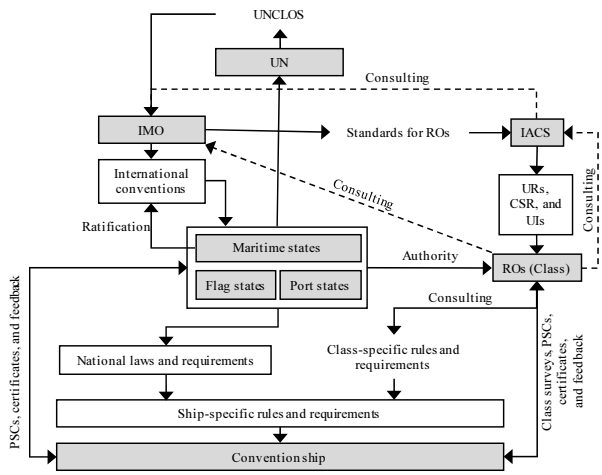

Figure 1: The current legislative framework for arctic ships (based on Bergström 2017)

Concerning offshore structures one challenge is to address the aspects involving disconnection versus stationary offshore structures with and without ice management. As outlined in ISO 19906, an offshore structure can be categorized in the following way:

- active: move-off capability, physical ice management capability;
- semi-active: move-off capability, no physical ice management capability;
- semi-passive: no move-off capability, physical ice management capability;
- passive: no move-off capability, no physical ice management capability.

For structures categorized as passive, the design approach is rather straight-forward. Other categories can make cost-benefit analysis to see how much shall be spent for a certain operational measure. For fixed structures in ice the load is defined through the probability of exceedance levels for ULS and ALS in ISO of 10^{-2} and 10^{-4}. These loads can be established using probabilistic models including all uncertainties of the parameters. Here, the target reliability levels based on analysis of failures have some level of human error integrated. However, to model human error in loads, without adjustment of target reliability levels will be overly conservative.

A robust operational philosophy is needed including an economic feasibility study. To have success in realizing new projects in Arctic or ice covered areas, these projects need to consider besides operational and technical also social, physiological and political aspects. This means prior such a project should be defined, all aspects need be heard, collected and included in the development of the project.

Further, given the limited availability of operational data, uncertainties limit the ability to exercise robust models and design in the following areas: sea spray icing; ice and iceberg forecasting; quantification of loads for floating structures in ice from managed and broken ice; ice in waves causing loads above and below the ice belt (relevant for marginal ice zone); and air temperature requirements. For example, wind and low temperature does not occur at the same time, thus the return period for each event is different and a 100-year maximum cannot occur

for both at the same time. Consideration for modeling human error in combination with this vast amount of contributing factors will be rather challenging. Further, attempts to address this issue must however be carried out very carefully ensuring consistency with estimates of design risk, and calibration of safety targets based on analysis of accidental data.

In conclusion, the objective of this committee report is to present the current state of the art in rules and regulations to be considered when designing ships and offshore structures for ice loads. The background and motivation of the presented rules will be presented to ensure their use in line with the design conditions and assumptions. In order to progress beyond the current rules, the report presents a mission-based approach to identify the design ice load and scantlings corresponding to target ice conditions and reliability targets. Allowing for a link back to the current ice classes will ensure a straightforward applicability of the proposed approach in terms of well-known measures. Furthermore, the mission-based approach will serve as decision support tool towards the most suitable ice capability of the ship of offshore structure by also addressing the uncertainties involved in the obstacles involved.

2. DESIGN METHODS FOR MARINE STRUCTURES

The design of marine structures need to consider in addition to operational and technical issues also social, physiological and political aspects (Kuehnlein 2016). Furthermore, ambitious and challenging offshore installations in harsh environments must be designed and optimized from an operational point of view taking into consideration the full range of determining factors, such as environmental sensitivity, operational aspects, technical possibilities, investment requirements, lifecycle and operational costs. Each project should be approached with a tailor-made solution, as it is not possible to copy one project from one location to another location, even if the defining parameters are quite similar. But of course, such an existing project might be a good start for developing a new tailor-made project solution. The design should be developed by an integrated team which consists at least of psychologists, sociologists, politicians, lawyers, operators, mariners, engineers and managers. Concerning the technical aspects of the project, the following aspects should be evaluated:

- Environmental conditions;
- Environmental protection and cleanup premises;
- Year around operations;
- Year around evacuation;
- Long periods without supply;
- Extreme ice loads;
- Ice management;
- Dynamic Positioning;
- Disconnectable solution versus non disconnectable solution in ice; and
- Minimized discharge (cuttings, solids, liquids, emissions, …).

Overall, the following multi-disciplinary aspects should be considered:

- 1st nations engagement: how they are involved in the project and how their fears and concerns are mitigated?
- What kind of psychological /social and physical environment will exist and/or has to be created in order to have efficient and satisfied people working there?
- What kind of legal and political environment will exist and/or has to be created in order to have an efficient and satisfying project performance?
- What environmental and environmental protection aspects could/should/need to be considered and maintained?

- What is the main purpose of the project and how can it be achieved?
- What operational aspects have to be considered and how can these be achieved?
- What technical challenges is the project facing and will the right technology be in place to overcome these?
- What are the risks of the project and does the chosen concept minimize these (ALARP)?

2.1 Rules for ships

The choice of a certain ice class depends on a variety of factors and is different for different stakeholders. While heavily reinforced ships generally work well in ice, they may not be economical for the majority of operations (von Bock und Polach *et al*., 2014, Bergström 2017). Possible motivations include the following:

- the need for a certain performance target certain ice condition,
- the need for a certain ice class certificate to operate in a specific geographical location,
- benefit of a higher ice class compared to the rest of the regional fleet comparing increased capital costs with otherwise increased operational costs.

While the first point requires a thorough analysis of all contributing aspects, partially covered in this report, the following points are mostly driven by economic measures, which are not covered in this report.

In general, it is important to understand the underlying assumptions in the specific rules, e.g. the Baltic Ice classes require open channels or icebreaker support and the ships are not supposed to ram ice, while the amount of acceptable rams with an ice edge increase exponentially to the highest IACS Polar Class, namely PC1. Furthermore, each ice class is created around a target ice condition and while the latter cannot be accurately monitored even when operating in it, the possibility to operate the vessel outside the design ice condition is given and thereby damages are possible. In terms of the FSICR rules, the possibility of damaging the vessels structure due to overloading from ice is apparent, because the return period of the design ice load is typically below 10 days. The IACS Polar Code seeks to contribute to this aspect of safety of ships operating in ice, but so far it does not quantify safety in terms of annual exposure and reliability targets (the only reference to probability is an assumption that at least one impact occurs each year).

2.1.1 IMO Polar Code

The Maritime Safety Committee of the International Maritime Organization (IMO) adopted the International Code for Ships Operating in Polar Waters (the Polar Code) in November 2014 and the Marine Environment Protection Committee adopted the Polar Code in May 2015. The Polar Code entered into force in January 2017. The requirements of the Polar Code are intended to address the particular hazards associated with operations in the Polar regions. The structural requirements are associated with the design capabilities based on the expected ice conditions – and are based on the Unified Requirements of IACS, Polar Classes 1 through 7. Most major classification societies have provided detailed guidance on the implementation of the Polar Code (See www.lr.org and www.eagle.org for examples). The Polar Code contains specific provisions for ship structure, subdivision, stability, equipment for life-saving, navigation, and communications, as well as crew training, and environmental protection for ships in the Arctic (N of 60°N) and Antarctic (S of 60°S). These provisions are in addition to the following IMO Conventions: Safety of Life at Sea (SOLAS), Prevention of Pollution from Ships (MARPOL), and Standards for Training, Certification, and Watch-keeping (STCW).

2.1.2 IACS Polar Class Rules

A preliminary review of the IACS Polar Class rules was carried out by Ralph (2017) including background derivations of fundamental equations (ARMARK and MUN 1998). A brief summary is included here.

Global impact forces are estimated using a closed form kinetic energy collision model where kinetic energy from a ship collision with ice is dissipated by crushing and inertial response of the vessel. A resultant equation for maximum normal force for a given interaction area (e.g. bow or shoulder) is given as

$$F_{N\,MAX} = P_0^{\frac{1}{3+2e_x}} \cdot f_a^{\frac{1+e_x}{3+2e_x}} \left((3+2e_x)\frac{1}{2}\frac{M}{C_0} \cdot V_n^{\,2} \right)^{\frac{2+2e_x}{3+2e_x}}$$

where

- P_0 is a class parameter scaling ice pressures;
- fa is an interaction shape parameter;
- e_x is the ice failure exponent;
- M is the vessel mass;
- C_0 is the Popov mass reduction coefficient accounting for vessel and ice rotation during a collision (See Appendix A); and
- Vn is the impact speed normal to the hull.

Many of these factors are given in Table 1 below although justification or calibration of the parameters are not provided.

Table 1. Class factors in IACS rules and governing parameters.

Polar Class	Crushing Failure Class Factor	Load Patch dimension Class Factor	Flex Failure Class Factor	Displ Class Factor	Long'l Strength Class Factor	Impact Speed (m/s)	Ice Strength (MPa)	Ice Thickness (m)	Flex Strength (MPa)
	CF_C	CF_D	CF_F	CF_{DIS}	CF_L	Vs	P_0	h_{ice}	flex
1	17.69	2.01	68.6	250	7.46	5.68	6.02	7.000	1.400
2	9.89	1.75	46.8	210	5.46	3.99	4.21	6.000	1.300
3	6.06	1.53	21.17	180	4.17	3.00	2.99	4.200	1.200
4	4.5	1.42	13.48	130	3.15	2.51	2.47	3.500	1.100
5	3.1	1.31	9	70	2.5	1.99	2.00	3.000	1.000
6	2.4	1.17	5.49	40	2.37	1.77	1.50	2.800	0.700
7	1.8	1.11	4.06	22	1.81	1.50	1.25	2.500	0.650

The interaction scenario considered in the rules is a shoulder collision (Daley 1999). Icebreaker design is not specifically considered. The force transmitted into the hull is limited by a flexure failure calculation based on some prescribed classed based flexure strength parameter and ice thickness (which is not yet measurable on transit through an ice prone region).

Given the global impact force is transferred into the structure through localized contact areas resulting from fracture and spalling processes, the nominal contact area is adjusted to estimate a semi-local contact area and corresponding pressure using a two dimensional (2D) brittle flaking model (Daley 1992). The resultant proportion of local area to global - was on average estimated to be on the order of 25-30%. Forces through this reduced semi-local area result in higher pressures that are very high compared with other codes.

Further localization is considered recognizing that pressures on smaller areas can significantly increase. Local pressures on plating between main frames are scaled higher using peak pressure

factors. The final local pressure and contact area used for plating design is based on some reduced height of the contact ice feature, and frame span.

To initially estimate the global contact area, a global pressure area model consistent with $P = Cp\ A^{-Dp}$ (written as $P = P_0 A^{-ex}$) is used except that the Polar Class rules only model a minimal scale effect with e_x = -0.1 unlike experimental results demonstrating a scale effect proportional to e_x (or Dp) = -0.4 (Riska 1987; Joensuu and Riska, 1989; Riska 1991; Jordaan *et al*. 2005). Interestingly if, one were to program the rule based equations and substitute e_x = -0.4, the trend in design is no longer correct: local pressures and plating thickness for lower exponents (e.g. e_x = -0.5) reduce for increasing vessel displacement. Although these reference global scale effects, for illustration, local design pressures from ship ram data follow a scale effect consistent with $A^{-0.7}$ as illustrated in Jordaan *et al*. (2007); Taylor *et al.* (2010); Masterson and Frederking 1993; Masterson et al. 1997; Palmer et al.,2009).

The final design equation for semi-local contact area models a pressure area effect with pressure increasing with increasing contact area and a scale effect proportional to $A^{+0.3}$. The intent of this empirical equation is to model the effect that higher penetrations and global contact area will result from higher energy collisions from larger moving faster ships which leads to increasing pressures locally. Contrary to Frederking (1998, 1999), Daley (2004) suggests that justification for this trend in the background literature to the Polar Class Rules is that there is no reason for traditional pressure area scale effects to exist and that with confinement, fracturing processes will be limited. But fracturing processes exist at all scales. The occurrence and behavior of HPZs either lead to very large stress localization that enhances fracture events or they undergo microstructure damage that softens the ice at the structure interface. In probabilistic extremal analysis, this design trend is entirely consistent with exposure modeling (i.e. faster larger ships will penetrate further increasing pressures locally). The resultant design trend in polar class rules is reasonable - increased pressures for larger vessels moving faster, the background ice mechanics needs improvement. We must be very careful to not confuse empirical equations of best practice with theory.

Preliminary Comparison with Exposure Based Calculations

As part of earlier work to review the Arctic Shipping Pollution Prevention Regulations (ASPPR) proposals, an extremal probabilistic design methodology was used to estimate exposure based ship ice ram design global forces and local pressures on the scantlings. The number of expected annual collisions with ice is key to modelling exposure among different class vessels (i.e. for benchmarking exercises, the annual number of expected interaction with CAC1, CAC2, CAC3 and CAC4 vessels was assumed to be 10000, 1000, 100 and 10 rams respectively). A ship ram software called FMAX (a dynamic time step ship ice structure interaction software) was developed during the ASPPR proposals review to model a “parent” distribution of impact forces for any ram, a model calibrated with full scale measurement of ship ram forces from Kigoriak, MV Arctic, Polar Sea, Manhattan and Oden trials (Carter et al. 1996). Using extremal analysis, estimates of the maximum force out of n rams in a year for a given vessel having a particular Arctic class can be estimated. Estimated design forces based on annual target exceedence probability were compared with deterministic design formulations in the Code to verify the design recommendations. Similarly, the methodology in ISO 19906 for local glacial ice design (ISO 19906, 2010) was used for designing the shuttle tankers for the White Rose development, traversing iceberg prone regions (Ralph et al., 2006). An exposure based first principle approach was developed to estimate local pressures on the hull(s) and an equivalent ship class selected (i.e. highest Baltic Class with extra ice shielding or belt around the bilge to consider deeper icebergs). Probabilistic methods were used to arrive at a suitable class as well as to verify the design adequacy. A parallel activity was to identify an equivalent ship class to assist the ship builder (see also Ralph and Jordaan 2013).

Using the extremal probabilistic approach outlined for the Arctic Shipping Pollution Prevention Regulations (ASPPR) work (ASPPR 1995, Carter et al. 1991 & 1996, Fuglem et al. 1996), the resultant recommendation for design pressures in the Polar Class rules and particularly the class coefficients that govern design pressures were reviewed by Ralph (2017). Consistent with the ASPPR proposals review, exposure levels were mapped to each of the highest Polar Classes (e.g. Polar Class 1 at 10,000 rams per year; Polar Class 2 at 1000 rams per year; Polar Class 3 at 100 rams per year; Polar Class 4 at 10 rams per year; Polar Class 5 at 1 ram per year). Local pressures were estimated based on probabilistic methods and compared with rule based design recommendations. As shown in Figure 2 and, preliminary results show that plating design pressures are reasonable (See also Tõns et al. 2015 and Erceg et al. 2015). Some lower classes with a potential risk of interaction with multiyear or glacial ice may consider possible increase in coefficients. A full comprehensive exposure based analysis of all classes is recommended particularly where a region is prone to multiyear ice.

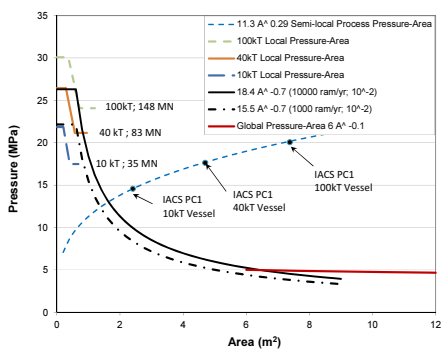

Figure 2: For shoulder impact model with contact 5 m from stem, comparison of ISO 10^{-2} exceedence, 10,000 ram local pressures on a 40 kTonne vessel with IACS Polar Class 1 local pressure-area predictions for 10, 40 and 100 kTonne vessels

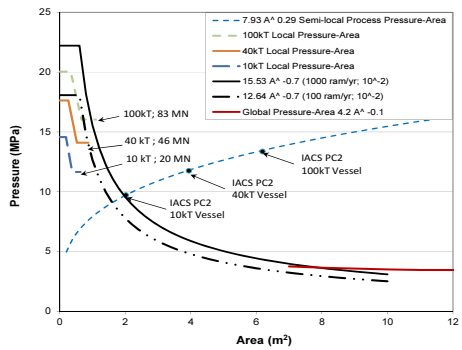

Figure 3: For shoulder geometry with contact reference 5 m from stem, comparison of ISO 10^{-2} exceedence, 1000 ram local 'bow' pressures on a 40 ktonne vessel with IACS Polar Class 2 local pressure-area predictions for 10, 40 and 100 kTonne vessels

Consideration for Probabilistic Design

As suggested above, once a Polar Class is selected, the development of scantlings following the empirical equations outlined in the rules is straight forward. Selection of the appropriate class based on exposure of the vessel to ice conditions is seen as an area for improvement. By exposure we mean consideration for the annual occurrence of ice conditions in the region of interest, potential impacts based on annual transects through the region, routing through the region, and application of risk mitigation measures (detection and avoidance). A probabilistic methodology for design of ships based on the principles of safety and consequences will allow the designer to estimate design pressures than can be compared with class pressures from exercising the rules. This way the sensitivity to increasing or decreasing a class and adding or reducing risk can be incorporated in the decision process. A higher classed stronger vessel will cost more, but have reduced risk of downtime. A weaker vessel will cost less, but with increased risk of delay or downtime. Hence the designer has a deeper understanding of risk supporting his final decision and opportunity to model operational risk mitigation in the design (i.e. detection and avoidance). He may need to justify the installation of a special ice detection radar, performance of which can be modeled in probabilistic methodology. As noted earlier, human performance may also be considered but not before an appropriate recalibration of performance targets has been carried out.

Consideration for Icebreaker Design and Concentric Bow Impacts
The design approach of future versions of the Polar Class rules should allow for the assumption that the captains will avoid ice impact, as well as specific consideration for concentric bow geometry, as opposed to shoulder only impacts. Interaction geometry and models for different alternative scenarios are formulated in Daley (1999). It is not entirely clear, however, that concentric bow impacts should be ignored even for conventional ship design. While glancing impacts with blunt hull geometry may have steep force penetration curves, shoulder impacts have a reduced Popov equivalent mass that reduces impact force as eccentric impacts result in subsequent yaw motion. further, the level of load resulting from shoulder impacts is based on an assumed ice angle of 150°. Loads are rather sensitive to this geometric interaction angle.

While the premise for this is that ship owners and captains will be motivated to avoid ice and any impacts from a manoeuvring attempt, multi-year ice embedded in level ice is largely undetectable and impact can occur anywhere across the whole bow. As a result, a designer would benefit from considering both. It is also noted that ramming events should not be assumed to only occur with an icebreaker during ice management or escort operations. Experience on bulk carriers (e.g. the MV Arctic and captain experience) demonstrates that there are times when delay in shipment of goods is not desirable, nor may the risk of getting stuck, and ramming be required to transect particular regions of ice.

2.1.3 IMO POLARIS

The IMO Polar Code requires the carriage of a valid Polar Ship Certificate that (among other items) establishes operational limitations, including limitations related to ship structural capabilities. IMO has developed general guidance (IMOb, 2016) on methodologies for operational limitations and capabilities in ice. The general guidance is that for developing any methodology, it should take into account hull structural capability, ice regimes, independent or escorted operations, and ice decay.

One methodology, considered acceptable to IMO, is the POLARIS (Polar Operational Limit Assessment Risk Indexing System), which has been developed incorporating experience and best practices from Canada, Russia, Finland and Sweden. POLARIS provides a risk assessment tool to evaluate the risk of operations for a given ship design in different ice conditions. The use of POLARIS is not mandatory – it is provided as one acceptable methodology to determine operational limitations. For detailed descriptions related to POLARIS, the reader is referred to www.eagle.org.

2.1.4 RMRS Rules

The Russian Maritime Register of Shipping or RMRS (listed in the bottom of figure) provides services for the classification of ships and offshore structures, including verification of their compliance with the applicable national and international standards. The regulatory framework of RMRS consists of rules, guidelines and other technical documentation and covers all types of modern ships and marine structures, including those suitable for operation in cold climate and in the Arctic. At present, full text electronic documents such as Rules for the Classification, Construction and Equipment of Mobile Offshore Drilling Units and Fixed Offshore Platforms, Rules for the Classification and Construction of Sea-Going Ships, Operating Experience of Ice Strengthened Tankers, among others are made available on the RMRS webpage in Russian and some are in English.

The focus is on hull scantling design in accordance with RMRS (2015). The standard approaches to limit states in RMRS ice class rules take either the yield point (elastic design) as the design limit state for the Baltic ice classes or the formation of a plastic mechanism (rigid-plastic design) as the design limit state for the Polar and RMRS ice classes.

The rules for RMRS ice class and Polar classes share much in common. For Polar classes the detailed derivation of the design loads can be found in the literature, along with the list of assumptions linking the ice class to physical values; see Daley (2000) for details. In contrast to Polar classes, the design formulae for RMRS ice classes can be difficult to understand because the explicit relationships between the physical parameters and class factors are not available in the open literature.

The ice class factors are selected to give values that are consistent with the range of desired ice class requirements for strength (i.e., PC1 should require plate and framing dimensions consistent with the hugest Arctic ice class in service). However, according to the discussion in Quinton et al. (2012), the real problem lies in the side shell pressures specified for PC1 and PC2. All evidence from various kinds of tests supports the thesis that these pressures are not reasonable but are excessively and unjustifiably high. Thus a real problem is created for higher class icebreaking ship hull design.

The Finnish-Swedish Ice Class (FSICR), IACS Polar Class (PC) and the Russian Ice Class (RMRS) rules, accept that some plastic deformation occurs during the ships' lifetime. The amount of plastic deformation (i.e. limit state) and the expected number of times it may be exceeded (exposure) is however not clearly defined, see also Kujala and Ehlers (2013) and Kämärainen and Riska (2012). Nevertheless, the critical deformation limit that requires repair can be found in the RMRS Instructions for Determination of the Technical Condition, Renovation and Repair of the Hulls of Sea-Going Ships (refer to Appendix 2 of the Rules for the Classification Surveys of Ships).

We are still a long way from being able to formulate ship rues strictly from theory. The Daley model and the Kurdyumov–Kheisin model for calculating ice crushing pressure lack some physical realism, thus making their use difficult outside the application range of the rules. For instance, as there is very little information in ISO 19906 around production floaters in sea ice, some parties may consider that designing vessels to ice class may be sufficient (see 13.5.1 in the ISO 19906). For detailed discussion on this topic refer to Kim and Amdahl (2016).

2.2 Rules for offshore structures

The section discussing the ISO standards 19900 series will be subjected to changes as the ISO19906 is currently under revision and some restructuring is anticipated. As a result, the information presented in this section may become outdated.

Historically, Russian standards have been prescriptive rather than goal based. On the other hand, incentives to apply new technology or to implement new research findings have not been prioritized through these standards. Russian standards include GOST and GOST R standards (national standards of the Russian Federation) as well as Russian and CIS countries standards and technical regulations for all major industries. These include Building Codes (SNiP, SN, GESN), Industry Codes and Safety Rules (RD, PB), Sanitation Regulations (SanPiN, GN, SP), Fire Codes (NPB, PPB), norms, instructions, methods, cost estimate standards, Russian federal and regional legislation and many others.

Additional standards relevant for Arctic operations, but not covered within this report, can be found in the Arctic Council working group report – Emergency, Prevention, Preparedness and Response (EPPR, 2015).

General and unifying principles for all types of offshore structures are provided in ISO19900 (2013). These principles include exposure levels, limit states design and the partial factor design approach, as well as considerations for structural configuration, robustness, hazards and environmental conditions. There is a relationship among the various International Standards applicable to offshore structures. One International Standard can reference the design provisions of

another International Standard in the ISO 19900-series. Users need to be aware of these cross-references when using any member of this set of International Standards.

ISO19906 (2010), published in December 2010, is written as one of the ISO 19900-series of international standards for offshore structures and focuses on supplementary provisions for conditions in the Arctic and cold climate. The standard was written to cover all structural types that could operate in waters subjected to sea ice and/or icebergs; this can include both waters in the Arctic Circle and more temperate latitudes such as the Caspian Sea, Barents Sea, East Coast of Canada. Civil engineering structures such as man-made islands are also included. ISO19906 is divided into Normative and Informative sections. The former sets specific safety levels commensurate with the 19900 series and methods for ice action calculation, while the latter provides guidance with depth on calculation of ice action values. ISO19906 (2010) uses the limit state design approach; for details refer to Thomas *et al*., (2011). For general requirements for the limit state design of floating structures, ISO 19906 relies on ISO19904-1 (2006). The OGP Report No. 422 (OGP, 2010) is to be considered as a supporting document to ISO 19906 as it presents the basis for the load factor calibration and presents case studies for different Arctic regions. The report is listed as bibliographic reference A.7-2 in ISO 19906. The calibration process accounts for weighted combinations of all action effects overall design equations, and load combinations for different resistance models, levels of action effect model uncertainties, levels of statistical uncertainty, and mean action event occurrence rates.

In Russia, ISO 19906:2010 Arctic offshore structures standard has been adopted as GOST R 56000-2014 Petroleum and natural gas industry. Other relevant standards are SNiP 2.06.04-82* Loads and forces on hydrotechnical structures (influence of ice, sea waves and ships) and VSN 41.88 Ice-resistant fixed platforms design.

Users need to be aware that in Russia, the standards are reviewed every 12 years, on average (according to RS Research Bulletin, 2015), thus there could be conflicting requirements and pluralism among some of the standards. One illustrative example of pluralism is the global ice loads formulations in Rules for the Classification, Construction and Equipment of Mobile Offshore Drilling Units and Fixed Offshore Platforms, (2014) and in SNiP 2.06.04-82* Loads and actions on hydraulic engineering constructions (wave and ice generated and from ships) (2014).

Several shortcomings of the ISO 19906 have been identified by the Barents2020 – a joint project between Russian and Norwegian scientists and engineers. Details can be found in Moslet et al. (2010) and Barents 2020 (2012), only a short summary is presented below. The guidance, which is offered for floating structures in the ISO 19906, is limited, e.g., only generalities are offered in the normative part, involving checklists and general recommendations for design, but no guidance on applicable methods on induced ice actions, including ice scenarios is offered. ISO 19906 is weak on guidance for moored structures in ice.

In most methods that concern ice loads, the load itself is assumed to be independent of the stiffness characteristics of the structure and the methods are to a very large extent based on measurements and research on fixed structures. Classically there are three distinctions made on the structures properties: 1) diameter, 2) whether the waterline shape is rectangular or circular and 3) the slope angle (different regime for vertical and sloped structures based on ice failure mechanisms). This could and should also be analogous to floating structures, but there is one principal difference. The structures response can change the properties, i.e. a ship riding up the ice edge during a ram, on the exerted load. This is a classic feedback effect, which may further change the load (see also Quinton 2015 and Herrnring et al. 2017).

Ice management (IM) and/or disconnection are important factors in reducing the magnitude and frequency of ice actions. IM can only reduce design action if it can be documented that the IM system is able to reliably detect and handle ice features causing the design action. However, there is no standard practice on documenting IM efficiency and reliability. ISO 19906 mentions IM by setting performance standards but gives no guidance on how to include IM in design.

Furthermore, there is no guidance (and only limited experience) from handling glacial features surrounded by or frozen into an ice sheet and how to quantify the effects of sea ice management.

Little guidance is provided on how to perform tests with offshore structures in ice and how to accurately model and produce ice ridges, which in many cases would yield the design load in the Barents region.

Ice load calculation methods are given, however little focus is given to the range and validity. Uncertainties are covered in detail, however unclear of the overall uncertainty compares to other offshore standards. For instance, OGP (2014) reports the safety factor calibration is highly dependent upon region and ice-type. For some regions there might be a zero load associated with a 10^{-2} ice event due to their rarity but abnormal ice events could still be significant. For floating platforms, the OGP reports that the current partial environmental action factor does not account for: flexibility of mooring systems; floating structure movement; non-linear interaction between a moored structure and ice; changes in direction of incoming ice for a turret-moored ship-shaped unit; relevant operational procedures (physical ice management and disconnection); action factors for local and global actions may be different from the L1 = 1.35 value which was calibrated for bottom-founded structures. It is also noted that the focus in terms of ice loading had been heavily towards level ice acting on vertical piles, but there was very little around ice effects on floaters. It is also noted that ISO 19906 provides LRFD (load and resistance factor design) environmental action factors, however, the ISO station keeping code for floating structures (ISO 19901-7) is based on a WSD (working stress design) approach.

2.3 Mission-based analysis for ships

Present design methods benefit from the vast experience of small to medium-sized transversely stiffened ships operating in first-year ice. Scantling determination requires a design pressure and occurrence for the target ice class or the operational area in question as well as a design criterion i.e. yield. The rule-based respectively target ice class-based concept is shown by Riska and Kämäräinen (2012). However, the current rule-based design methods are not necessarily transparent by means of design pressure and scantlings determination, because they use intrinsic design criteria.

Ice-induced loads can only be described with stochastic processes due to the unknown distribution in ice strength properties and local contact geometry in the ship-ice interaction process. Besides different operational modes, also the form of the ice influences the ice load directly (i.e. level ice, ice floes and ridged ice containing first-year and multi-year ice). Further, to date there is no mathematical, numerical or analytical model available to describe the physical process of ice breaking, i.e. ship-ice interaction.

Probabilistic, or site-specific, ice load determination allows for a link between statistical data from the operational area of the vessel and the design load. However, current ice class rules are not considering probabilistic methods for determining ice-induced loads, because the requirement to specify the mission of the vessel can be considered a shortcoming by means of liability from a regulator's perspective. The latter link between the design rules and the operation of the vessel is however created in IMO's POLARIS-System, which nevertheless lacks the specification by whom this will be controlled. Yet, probabilistic design methods can be used to enhance the design process by identifying the ice load in a continuous space in addition to the discrete rule-based load. Thereby more refined design decision can be made.

An example of such mission-based probabilistic ice-load determination is presented by Tõns et al. (2015) on the basis of a method by Jordaan et al. (1993), who showed how to use pressure area relationships, obtained from full-scale measurements, to predict extreme loads at a certain exceedance probability level level (see also Ralph and Jordaan (2013) and Ralph et al. 2006).

Erceg et al. (2015) presented the applicability of such probabilistic design load method to ice-going ships operating along the Northern Sea Route (NSR) in comparison to rule-based loads. The rule-based loads were calculated according to FSICR (Trafi, 2010). For the probabilistic local design load, a global ram analysis is first carried out from which an average ram duration and penetration is determined. The local pressures on individual panel areas is modelled using an exponential distribution for peak panel pressures given as:

$$F_x(x) = 1 - exp\left(-\frac{x - x_0}{\alpha}\right)$$

where x_0 and α are constants for a given area and x is a random quantity denoting pressure. To obtain the local peak pressure distribution, the number of events can be modelled as a Poisson-process resulting in

$$F_z(z) = exp\left\{-exp\left(\frac{z - x_0 - x_1}{\alpha}\right)\right\}$$

where $x_1 = \alpha(ln\mu)$ and x_0 is the panel exposure constant. Exposure is modelled as the proportion of events that represent actual impacts between the ice and the structure as

$$\mu = v \cdot r \cdot \frac{t}{t_k}$$

where v is the time period, r is the proportion of events resulting in "direct hits" on the structure, t is the duration of the impact, and t_k is the reference duration associated with a design curve from Jordaan et al. (1993). As a result, the design load z_e can now be calculated for a given exceedance probability $F_z(z_e)$ as

$$z_e = x_0 + \alpha\{-ln[-lnF_z(z_e)] + ln\mu\}$$

For design loads in multi-year ice it is suitable to use the envelope or upper bound curve described by $\alpha = 1.25a^{-0.7}$, where a represents the local contact area. For first-year ice, the following approach may be more appropriate, because the envelope curve overestimates local pressures by a considerable margin: the use of design equations corresponding to the datasets under ice loading conditions, similar to those expected for the design environment; see Taylor et al. (2009).

For illustration purposes, a mission-based example is now presented considering transits along the NSR from the Zhelaniya port (Kara Sea) to the Dezhnev port (Bering Strait), with a distance of approximately 4500 km. The average speed is considered to be seven knots resulting in an approximate duration of one transect of 15 days. In a given year, four months are considered a feasible operational window at a maximum level ice thickness of one meter, resulting in four round trips. Assumptions of stationary ice conditions and ice concentration of 0.5 are made. Additionally, the route is ice-free for two months in a given year. Using an event duration of 0.934 s, calculated as 1/frequency from Kujala et al. (2009), and Poisson's discrete probability for n events to occur, the expected number of events for the chosen period is 1.88 million. The ship is designed to an exceedance level of 10^{-2}, which corresponds to the design point of FSICR, i.e. reaching yield once in a winter. The proportion of true hits is chosen as $r = 0.5$. The exposure constant x_0, dependent on the design area, is calculated according to Taylor et al. (2009) for the North Bering Sea 1983 dataset. With 1.88 million events along the route and Equation (3) we can solve for the corresponding design pressure using Equation (4) and $\alpha = 0.28a^{-0.7}$ for the North Bearing Sea 1983 dataset. The resulting design pressure versus exposure, in comparison to the corresponding FSCIR load value for IA Super, is given in Figure 4. Therein, it can clearly be seen that the probabilistic ice load determination accounts for significantly more impacts resulting in an increase of the design load from 1.5 MPa to 5 MPa. The latter certainly results in higher scantling requirements and thus a heavier and more expensive structure, which in turn will be less vulnerable to ice induced damages.

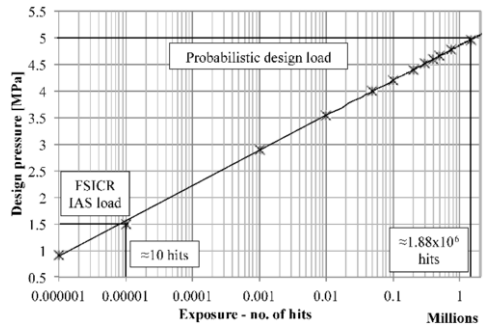

Figure 4: Design pressure for a local panel of ~ 1 m^2 (Erceg et al., 2015)

2.4 Difference between ship and offshore rules

Despite the fact that for an offshore structure, "*the designer may utilize the appropriate formulations in guidelines for ice-strengthened vessels of a recognized classification society*" (ISO 19906), the ice class rules are prescriptive and are not reliability-based in the same way as ISO 19906 where reliability targets have been used to calibrate the values of partial action factors. Ice class rules link ice conditions to the ice class, but ice condition descriptions are very vague. The ice class rules are rather more experience-based, linked to insurance and ice breaking service. Floating production unit in Norway does not need an ice class, but in Russia it needs an ice class. In each shelf state the mandatory requirements differ, i.e. in Canada they are required to follow the Canadian adoption of the ISO 19906 standard, but in Norway this is not the case. Similarities and differences between the methodologies of the Arctic offshore standards and the ice class rules are further discussed in Riska and Bridges (2017). A general finding is that prescriptive classification society rules are directly applicable, because they contain straightforward equations with a minimum of prescriptive text left for interpretation. While a general challenge is the fact that even the people writing standards can often disagree on how to use them, e.g. ISO lacks a certain validity of the proposed methods.

The definition of the ice load is the most important part of the hull rules. Summary of the RMRS approach to hull scantling design is presented below. For details refer to RMRS (2015), Riska and Kämäräinen (2011) and Daley (2000), Kurdyumov and Kheisin (1974).

Baltic ice classes - The requirements coincide with the requirements of the Finnish-Swedish Ice Class Rules, 2010 and apply to ships being in service in the Baltic Sea in winter. The design load corresponds to a collision with a level ice edge, a channel edge when the ship is escorted or with the consolidated layer of an ice ridge. The ice load is assumed to be described by uniform ice pressure p, on a rectangular load patch. The effect of the pressure distribution on the response of transversely framed plating is taken into account by introducing an effective plate ice pressure of $0.75p$. Limit state is yield limit, only the elastic response of the structures needs to be derived

Polar classes - The requirements coincide with the requirements of IACS PC, and apply to ships intended for navigation in ice-infested polar waters, except icebreakers. The design load corresponds to a glancing impact on the bow with an ice foe of infinite mass. The ice edge opening angle is assumed constant and equal to 150 degrees. The load is assumed to be described by uniform ice pressure p, on a rectangular load patch. Crushing and bending failure modes are considered. The Popov collision model and the Daley ice crushing model, where flaking is modelled to change nominal contact dimensions versus the actual contact area dimensions, are used. Ice edge spalling and non-uniform pressure distribution are taken into account

for by reducing the size of load patch and by introducing a pressure peak factors respectively. The limit state is the formation of a plastic mechanism.

RMRS ice class - Ice load formulations from RMRS Vol.1 Pt.2 Sec. 3.10. Design ice load correspond to a collision with ice floe with a rounded edge and infinite mass. Floe radius is 25 m. The load is assumed to be described by uniform ice pressure on a rectangular load patch. The Popov collision model and the Kurdyumov–Kheisin ice crushing model are used. Ice edge spalling and non-uniform pressure distribution are explicitly taken into account by the Kurdyumov–Kheisin model. The limit state is the formation of a plastic mechanism.

3. STRUCTURAL CAPACITY

3.1 Limit states

A limit state is a condition beyond which a structure or a part of a structure no longer satisfies a specified design requirement and is considered to be failed (DNVGL-OS-C101, ISO 2394, ISO 19900). According to ISO 19900 the performance of a structure, in whole or in part, shall be described with reference to a specified set of limit states.

There is much discussion on the definitions of limit states. Some discrepancies in limit state definitions have been noted. In ISO 19906, limit states are categorised as ultimate limit states (ULS), fatigue limit states(FLS), serviceability limit states (SLS), and accidental limit states (ALS), whereas for the revision of ISO 19900, the ALS category somewhat has been changed, and instead three ULS are introduced as shown in Table 2.

Leaving this discrepancy in limit states definition aside, the information below pertain specifically to ISO 19906 and ISO 19904-1.

Table 2: ULS (Thomas, 2017)

ULS(a):	ULS(b):	ULS(c):
failure of an individual structural component caused by design action effects exceeding design resistance (in some cases reduced by deterioration), including loss of structural stability (buckling, etc.);	loss of static equilibrium of the structure, or of a part of the structure, considered as a rigid body (e.g. overturning, sliding, sinking, or capsizing);	complete loss of integrity of the structure or vital parts of the structure when there is no further system ductility or reserve strength, including transformation of the structure into a mechanism (collapse or excessive deformation), loss of stationkeeping (free drifting);

According to ISO 19906, the ULS design condition shall be based on environmental events which result in extreme-level (EL) environmental actions, with both local and global ice actions considered. In addition, the expected effects of snow accumulation, icing and ice accretion shall be accounted for. For floating structures, it is necessary to consider pressure events due to convergence of surrounding ice (or presence of a coastline).

The combination of environmental actions, permanent actions and variable actions with corresponding partial safety factors are used in the ULS design. The representative values for environmental actions shall be determined based on an annual probability of exceedance not greater than 10^{-2} and include the principal action and relevant companion actions (e.g., ice, wind and waves). The latter can be stochastically independent or stochastically dependent. To determine the representative values probabilistic methods or deterministic methods are used. It is important to realize that selecting the appropriate design conditions for the ice environment may be challenging as neither the largest ice ridge nor the thickest ice necessarily give the largest

action effect. In other words, a 100−year environment conditions ≠ a 100−year action ≠ a 100−year action effect.

According to ISO 19906, the design procedures for ULS shall be based primarily on linear elastic methods of structural analysis. Some localized inelastic behaviour is accepted. For foundation design, ULS shall be analysed with the appropriate cyclic action effect history including ice actions. For hull design of floating structures, the designer may utilize the appropriate formulations for ice-strengthened vessels, and IMO national requirements shall be incorporated in the design when applicable.

In accordance with the ISO 19904-1, the following specific limit states are usually evaluated for floating structures within the ULS framework: yielding, global and local buckling instabilities. For ULS checks the representative value of the yield strength is used and the buckling strength is based upon formulations in the recognized classification society or equivalent code formulation.

In NORSOK N-004 (2013) it is added that when plastic or elastoplastic analyses are used for structures exposed to cyclic loading checks shall be carried out to verify that the structure will shake down without excessive plastic deformations or fracture due to repeated yielding. Note that the NORSOK has a temperature limitation to -14C.

It should be also noted that the RMRS's Rules for the Classification, Construction and Equipment of mobile offshore drilling units (MODU) and fixed offshore platforms (FOP) use limit state equations in a form that essentially differs from that in ISO 19900 series, mainly due to different systems of safety factors and load combination factors used and due to some extra factors in Russian version. In accordance with the RMRS rules, the dangerous states such as excessive deformations of material, buckling, fatigue cracks and brittle fracture shall be avoided.

According to ISO 19904-1, non-linear analysis may be used to determine the ultimate capacity of structural components, substructure or the complete structure. A non-linear analysis should include appropriate models for all significant non-linear effects, including elastoplastic behaviour large deflection and criteria for rupture, among others. Refer to ISSC (2015) for detailed information related to buckling and ultimate strength of components and systems of ships and offshore structures. The explicit limit state definition is practically non-existent. Interpretation/understanding of the limit state can be found in Riska and Bridges (2017).

3.2 Response to moving loads

Moving (or sliding) ice loads are hull loads arising from oblique impact, or continuous sliding contact, with an ice feature. They are characterised by both motion in the direction normal to the hull, as well as sliding motion tangential to the hull. Hull response to an oblique impact with ice depends on the relative masses of the hull and the ice, the compliance of each, the impact trajectory, and the speed of the impact. Continuous sliding contact generally occurs when either the ice, or both the ice and the hull, are undergoing considerable damage at the contact interface, and are unable to separate.

Many operational hull impacts (e.g. collision with a single ice floe having a mass considerably less than that of the hull) with ice result in a glancing collision, characterised by elastic hull structural response and little to no sliding action of the ice along the hull. Other operational ice loads (e.g. the hull interacting with level ice, or a ship ramming a multi-year ridge) involve considerable sliding contact between the ice and the hull.

With a few exceptions, practically all hull impacts involve some component of relative sliding motion between the hull and the struck (or striking) object; however, it is common practice to neglect the sliding component when the hull structural response to the load remains elastic.

This is evidenced by the fact that no international rules or guidelines for the design of ships or offshore hull structures presently consider moving loads as a design scenario.

For steel hulls, when the hull responds plastically, the sliding component of these loads has been shown to incite a considerable loss in hull structural capacity (up to approximately 50%), for hull plating and hull framing, when compared with hull response to stationary loads of equal magnitude. Specifically, the greater the amount of plastic damage on the trailing side of the moving load, the greater the loss in hull capacity. This was initially predicted numerically (Quinton 2008; Alsos 2008), then analytically (Hong and Amdahl 2012), and was recently verified experimentally (Quinton 2015). Additionally, Quinton (2008; 2015) showed that the web of a hull frame will plastically buckle under a moving load at a far lower load magnitude than for a stationary load. Huang et al. (2015) proposed a deterministic ice force function to predict the ice loads during icebreaking activity. They modelled a composite ice crushing mode where the icebreaker will interact with the ice face and develop radial cracks. The ice-ship interaction of a multi-purpose icebreaker was analyzed by using the MOSES software. The results revealed that the moving responses are different in heading current or adverse current with different ice velocities.

It is important to note that the structural design point for the hulls of polar class ships (IACS 2016) and Arctic offshore structures (ISO 19906 2010) is a plastic design point. That is, under the design load, these hulls are expected to sustain a small level of plastic damage (e.g. a small dent). The extent to which the capacity loss associated with moving loads affects arctic offshore structures and IACS polar class ships is presently unclear. The work by Quinton et al. (2012), using real-time and real-space moving loads recorded during the 1980s USCGC Polar Sea ice trials, indicates that the level of hull damage sustained from application of the design load is not sufficient to induce any great loss in hull structural capacity. In other words, Polar Sea icebreaker was suitably designed and no damage resulted from icebreaking trials.

3.3 Temperature definitions

There are many different temperature definitions used for the design of maritime and offshore units. Some of the most relevant are listed in Table 3.

One can differentiate between definitions used for selecting appropriate steel grades (i.e. material selection) or for setting winterization performance requirements. For material selection, there are in general two regimes:

- Lowest Mean Daily Average Temperature (LMDAT)
- Lowest Anticipated Service Temperature (LAST)

The LMDAT regime is in general used for ships and offshore units applicable to classification, while LAST originally comes from ISO 19902 and the definition became clarified in ISO 19906. The LMDAT is the basis for selecting the design temperature, where at least a 20-year data series should be used for calculating LMDAT. There are no minimum requirements (for instance minimum number of years of data) for determining LAST (being the extreme low hourly average temperature with an annual probability of exceedance not greater than 10^{-2}). Due to the difference in the definitions LAST can be about 20-30 degrees lower than LMDAT and for some offshore areas LAST can be as low as -40°C. However, as noted by Riska and Bridges the calculation of LAST needs better definition to ensure consistent use. For instance, the height of the measurement point is not specified.

Table 3: Common temperature definitions

Symbol	Meaning	Reference	Use
$t_{D,}$ t_d	Design temperature; Material design temperature	IACS UR S6.3 and DNVGL Rules for Ships	Ship winterization Selecting steel grade
tw	Winterization temperature	DNVGL-OS-A201	Offshore winterization
t1, t2	Design temperature (t1) and Extreme design temperature (t2)	DNV Rules for Ships (pre-July 2013)	Ship winterization
DAT(t)	Design ambient temperature	DNVGL Rules for Ships	Class notation for structural material selection
PST	Polar service temperature	IMO Polar Code	Polar Code compliance
LMDAT	Lowest mean daily average temperature	IACS UR S6.3, DNVGL Rules for Ships, and DNVGL-OS-A201	Setting tD, td, t1, DAT(t), selecting steel grade
LMDLT	Lowest mean daily low temperature	IMO Polar Code	Setting PST, PST ≤ LMDLT – 10°C
ELT	Extreme low temperature	DNVGL-OS-A201	Setting tw, no prescribed definition
LAST	Lowest anticipated service temperature	ISO 19902, ISO 19906	Offshore installation design
RP100	Extreme low temperature with an annual probability of exceedance not greater than 10−2	ISO 19906 and NORSOK N-003	Setting LAST

3.4 Requirements of ductile to brittle transition

While the strength of steel increases under cold temperatures, it is obvious that the inherent risk of unexpected brittle fracture increases as well. All ferritic structural steels suffer from reduced fracture toughness at low temperatures due to the ductile-to-brittle transition behavior (DBT), which is characteristic for steels with body-centered cubic (bcc) crystal structure, see also Figure 5. The figure shows a distinct shift in the ductile to brittle transition temperature due to the differences between the specimens and test conditions. At lower temperatures, the mechanism of stable crack growth behavior changes from plastic blunting and tearing to cleavage controlled brittle fracture. This transition occurs over a narrow range of temperature, typically 30 K (Billingham et al. 2003) and is often characterized by the T27J temperature. This is the temperature where the interpolation of Charpy V-notch impact toughness tests results yields an energy of 27J. Other measures for the ductile-to-brittle transition temperature (DBTT) are the fracture-appearance transition temperature (FATT), where 50% of the fractured surface is related to brittle fracture, or transitions in CTOD (BS 7448-1), KIc (ASTM E399), T0 (ASTM1921), or J-integral (ASTM E1820) test results.

Consider one example for a location where LMDAT is -10°C and LAST is -40°C. The structural design of a primary loading bearing member requires using a steel plate with thickness 70 mm with yield strength 355 MPa.

Using the specification in IACS, steel with such yield strength is denoted ‘higher strength’ steel and the standard further specifies that grade E steel can be used for the specified thickness. At a test temperature of -40°C, the DNVGL-OS-B101 standard specifies that 41 J and 27 J needs to be demonstrated in conventional Charpy V-notch tests (the DNVGL standards DNVGL-OS-C101 and DNVGL-OS-B101 are harmonized with the IACS rules).

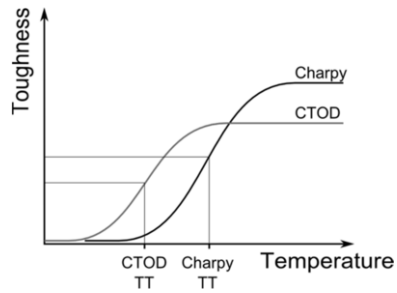

Figure 5: A schematic illustration of a Charpy and CTOD ductile to brittle transition curve.

Using the requirements in ISO 19902 of having Charpy V-notch test temperature 30°C lower than LAST would then mean test temperatures down to -70°C for group II, class CV2 steels. The required Charpy toughness is then specified to be a minimum of 35 J. The ISO 19902 standard recommends. then the EN 10225 standard as a material selection standard for steel plates

While the ISO 19906 standard specifies hourly average temperatures and an annual probability of exceedance not greater than 10^{-2}, the NORSOK N-003 standard specifies a 24-hour average and the same probability of exceedance. At this probability level there is little difference between using a 1-hour average and a 24-hour average. The NORSOK M-120 standard requires the EN 10225 standard to be used for rolled plates.

However, the EN 10225 standard however, only specifies steels with low temperature impact properties at temperatures down to -40°C so can strictly speaking not be applied with such low service temperatures as specified in this example.

Interestingly, the Canadian CSA S.473 standard specifies 35.5 J at a test temperature 30°C lower than the 'toughness design temperature' which is to be specified based on an annual probability of exceedance of 0.5. No attempts have been taken to relate this to LAST or LMDAT for this report.

This discrepancy between the standards regimes have not been under scrutiny much in past since a default design temperature for ships and offshore mobile units have been -10°C.

Ships and offshore structures operating in Arctic regions are exposed to low temperatures as defined above and are thus required to function reliably therein. Current regulations however do not cover the expected temperature range and thus the reliability of structures used in such conditions may be reduced. DNV GL provides some guidance down to -30°C (DNV, 2013), while NORSOK is limited to -14°C (Norsok, 2017). Consequently, there is a lack of guidance in structural behaviour at low temperatures, especially for welds.

3.5 The effects of low temperature on fatigue and fracture properties

For structural assessment, it is therefore required that the DBTT remains below the anticipated service temperatures at all times. However, low service temperatures also influence other limit states. Regarding fatigue limit state design, it is generally assumed that lower temperature will have no detrimental effect on the fatigue properties of steels, see Alvaro et al. (2014) or DNV (2013). This assumption is backed by extensive fatigue crack growth rate testing of base materials for a wide variety of steel grades. In plain steel structures without welds, fatigue life is divided into two parts, fatigue crack initiation and fatigue crack growth. Depending on the geometry, stress state and presence of material defects, one might dominate the other. The mechanism of fatigue damage is known to be the result of complex dislocation arrangement governed by local irreversible plastic flow (Alvaro et al., 2014). Since the static strength increases with

lower temperatures, the resistance against dislocation movement is increased and thus both the fatigue crack initiation and the crack propagation are hindered (Alvaro et al., 2014). However, for metals which feature a DBT, the fatigue crack growth rate increases again for temperatures below the fatigue transition temperature (FTT), which can be seen in Figure 6. This phenomenon is sometimes referred to as fatigue ductile-to-brittle transition (FDBT).

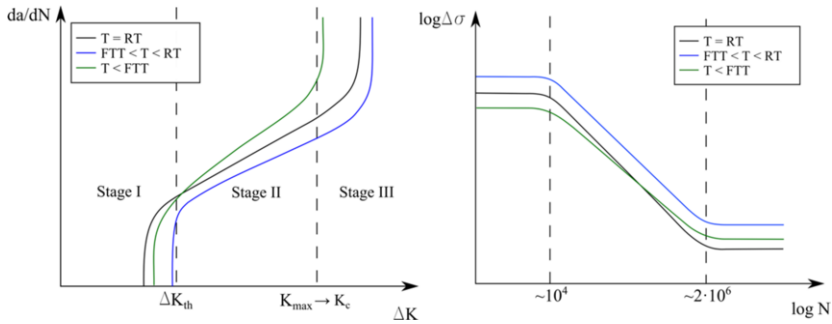

Figure 6: Schematic representation of the effect of low temperature on (a) the fatigue crack growth curves based on Alvaro et al. (2014) and (b) the expected SN-curves

Since low temperatures seem to increase the lifetime of a structure, this effect is usually neglected during fatigue assessment of steel structures at low temperatures. Using medium and high strength steel test, Walters et al. (2014 and 2015), demonstrated that this assumption is not generally true . It was found that the FTT seems to be lower than the FATT, but higher than the T27J temperature, which is usually used as indicator for the DBTT. The FTT is usually not considered in design, and any protection is obtained implicitly by using T27J as a quality control measure for fracture. It showed that the common belief that sufficient impact toughness of the base material at the design temperature will be enough to justify the use of a material at this temperature, might not be enough.

Based on the assumption that brittle fracture occurs before the changing fatigue behavior significantly affects the lifetime of a structure, current regulations for material qualifications are enforcing sufficient toughness values at the design temperature. The main objective of many research projects is therefore to provide a reliable basis for estimating the transition to brittle fracture of base materials and welded structures. On the other hand, compared to the well investigated fatigue crack initiation and growth behavior of plain steel specimens, the effect of temperature on fatigue properties of welded structures is scarcely mentioned in published literature. Experimental tests of Miki and Anami (2001) and Wahab and Sakano (2003) suggest that the DBTT is higher in the heat-affected-zone (HAZ) of welded structures than in the surrounding base material. However, the influence on the fatigue properties of welded structures for offshore applications is not evident, due to the lack of comprehensive studies regarding the change of static and dynamic properties of base material and welded structures at sub-zero temperatures. Bridges et al. (2012) carried out cyclic tension fatigue testing of welded specimens made from AH36 and DH32 steel grades under room and cold temperature conditions. The experimental results revealed that the mean fatigue strength of the tested steel specimens at low temperature is slightly higher than that at room temperature. Braun (2017) presented a first insight into static and dynamic material properties for different welded structural details and material strengths at changing temperatures from room temperature to -50°C in order to establish a physical model that explains the change of fatigue growth behavior at low temperatures based on the changing failure mechanism.

In welded steel structures, it has long been recognized that brittle fractures almost never propagate along the HAZ (Goldak et al., 1977). Charpy V-notch toughness testing of the HAZ is therefore difficult to perform, since the fracture path will not usually follow or stay in the zone being tested. Further, the DBTT varies with the state of stress e.g. the specimen size, type of

loading (bending versus tension), geometry, and rate of loading. Despite this, Charpy V-notch testing is the basic method prescribed in codes and standards to ensure sufficient impact and fracture toughness. Although the relation between impact and fracture toughness test results is mainly empirical in nature, the concept has been proven to yield satisfactory results for moderate thickness sections, see Banister (1998). Moreover, Charpy impact testing is usually preferred as a low-cost quality control measure. The latter was also identified by Hauge et al. (2015) addressing also the subject of corrosion control, aluminium structures and steel structural fabrication for low temperature applications in conjunction with the notion of crack arrestability. The paper states that current design codes require 'relatively low requirements to Charpy impact energy (e.g. 27 J)', which as such 'do not prove that brittle fracture can be avoided'. An approach is advocated where fracture mechanics tests are conducted for material qualification, in conjunction with Charpy impact tests during the design and qualification phase. The other subject addressed is corrosion. It is pointed out that the cold environment creates electro-chemical conditions which are rather different from non-arctic environments, which cannot be ignored. The other important influential parameters such as the thickness and load strain rate may also significantly influence both strength and toughness. For example, increased thickness may lead to so called plain-strain condition and therefore minimum possible toughness levels. Therefore, based on nominal toughness level and delivery condition for one structural steel grade and selected minimum design temperature, the maximum allowed thickness for utilization are defined.

3.6 Repair limits

A clear definition of the state of deformation requiring repair is not to be found in the current rules. The Russian Maritime Register of Shipping allows repair of smooth indentations in the hull plating during the next scheduled dry docking, if the following is met:

- the indentations are not larger than 20% of frame spacing and the depth to length ratio is not larger than 1:20;
- local dents are allowed if the depth is not greater than five times the thickness of the plating and the ratio of depth to frame spacing not greater than 1:20 (Benkovsky, 1970).

Further, surveyors may require repair, if the plate deflection is above 1/12 of the frame spacing (Hayward, 2007).

4. ICE LOAD MEASUREMENT AND MODELLING

4.1 Full-scale

Simulation of ice and ice loads, in general, is an extremely complex endeavour. It may appear that direct comparison of full-scale ice load measurements and data to modelling results is a straightforward approach for ice load model validation. This approach is, however, accompanied by several challenges: (1) the measured data on ice loads is somewhat scarce and observations often insufficient (Timco and Weeks, 2010), (2) sample sizes in the experiments are typically low but the ice loads are known to be stochastic and the scatter in data large (Daley at al., 1998; Jordaan, 2001), (3) interpretation of the measurement results is difficult and may have sometimes even been erroneous (Liferov, 2005), and, just simply due to (4) the ice loading processes in full-scale being very complex (Palmer, 1991; Daley at al., 1998).

The range of parameters measured in full-scale is often small and in nature the parameters vary through any given ice field which leaves the question; how to parameterize a model so that it represents the ice conditions during a field measurement? It is impractical and sometimes infeasible to measure all potentially interesting sea ice parameters during full-scale ice measurement set of trials (Palmer, 1991). This is due to the field conditions, the nature of measurements,

and often the cost of the measurements (Timco and Weeks, 2010). Even if such measurements could be made, it is likely that the ice properties change during an interaction process due to the inhomogeneity of sea ice. The mechanical properties of sea ice are poorly known and there is only a handful of reasonably well-understood properties.

Ice as a material demonstrates a myriad of mechanical behaviours; including creep, viscoelastic-viscoplastic deformation, and fracture into discrete media where interaction between all discrete and continuous ice pieces are important. With numerous factors influencing the behaviour of ice, modeling ice is exceedingly challenging; and to date, no general ice model, which can capture all the scenario dependent ice behaviours, has been developed. We can, however, limit the number of parameters needed by conducting a design of experiments. Simulations are a good platform for this type of study as they allow full control on parameters in ice-structure interaction. Ranta et al. (2016) used this approach and performed a 2D FEM-DEM study on ice-structure action. They investigated the sensitivity of maximum global ice loads in the process to variety of parameters related them. Namely, the ice-related parameters affecting the loads were: ice thickness, friction coefficient and yield strength of ice. Interestingly, the temperature, having a significant effect on HPZ failure strength, was not included.

Ranta et al. (2016) observed that the effect of ice thickness on the maximum loads far exceeded the effect of actual material parameters of ice. For example, while still showing in the results, increasing ice compressive strength value from 1 MPa to 2 MPa caused about 10-15 % increase in peak ice load values. This observation is in line with widely accepted view that ice thickness has an important role as it is closely related to ice loads, ice failure behaviour, and ship resistance in ice (Timco and Weeks, 2010; Palmer and Croasdale, 2013). One must notice that depending on the scale and application the interesting parameters may change: the compressive strength of ice is obviously of interest if we are interested on local ice pressures.

Another challenge for validation of numerical models is the inadequate sample sizes in field experiments. It would be crucial that the experiments would be repeated a number of times due to typical wide scatter in measurement results. This need is demonstrated by a recent simulation-based study on ice-structure interaction in Ranta et al. (2016): there may be need to run sets of tens of repeated measurements for reasonable error limits on measured loads in ice-structure interaction. These numbers are impossible to reach in well controlled full-scale experiments.

The problems related to interpretation of the full-scale data are discussed below using ice rubble as an example, but is due to limited knowledge on the most important sea ice failure mechanisms during a loading process, and the lack of opportunities for accurate observations in-situ being very limited. While the full-scale experimentation and measurements on ice loads has led to important data on the load values, the field tests remain difficult to analyze, understand and generalize due to the complexity of the ice loading processes: there have been no methods in receiving all the data needed (Palmer, 1999; Kendrick and Daley, 2011).

Ice load records are difficult to interpret in terms of mechanics of the process as they include numerous consecutive short-term peak load events. In statistical studies, short-term peak load events are defined using various techniques, in which commonly a threshold load level is prescribed and used to separate a number of peak load events from the data. One commonly used technique is Rayleigh separation: highest peak load value is first selected from the load record while the next peak load is not chosen until the load has decreased under the chosen threshold value. This definition clearly does not account for the mechanisms in the loading processes, and defining a single peak ice load event from a measured load signal is a challenge. Suominen and Kujala (2014) studied the short-term ice loads on the ship hull using Rayleigh separation, and their study shows that the method leads to load statistics that depend on the choice of the threshold value.

The short-term peak loads may appear and disappear due the ice-ship contact moving away from the load patch, or the peaks may simply be due to, for example, ambient water or ice fragments around the ship instead of the actual ice failing. Suominen et al. (2013) compared the results from the simulations on ice loads on a ship operating in level ice with their full-scale results on ice loads. The simulations mimicked their experiments. The measured full-scale data included a substantial number of peaks that were not predicted by the simulations. It is unclear, which of the peaks were due to actual ice loads.

The model should cover a lengthy interaction process in total and capture the most important mechanisms in this process in order to be truly predictive. There is no reason to assume that an interaction process reaches a steady state that produces a roughly constant maximum load (Palmer, 1991). This especially applies to ice loads on fixed structures, where the earlier sea ice failure and loading process itself affects the subsequent failure process (Määttänen, 1986; Sanderson, 1988; Daley at al., 1998). In short, the ice loading process evolves in time as discussed recently in Ranta et al. (2018). On the other hand, due to this, numerical models that repeat some prescribed failure behaviours and patterns may have only limited use in improving ice load predictions and understanding of ice mechanics.

4.2 Laboratory-scale

Laboratory-scale experiments are an attractive platform for validation of ice load models due to their relatively low expenses and more accurate control when compared to full-scale. Very detailed observations are possible laboratory-scale and, for example, Liferov and Bonnemaire (2005) suggest that the laboratory experiments may be the only practical possibility to get an insight about the failure process of ice rubble. In laboratory one can perform sets of repeated experiments, while having good control on parameterization. Laboratory tests also allow a relative ease for limiting the problem under study. An example of this type of study are the ice crushing experiments by Määttänen (2011) which were modeled using FEM and cohesive fracture by Kuutti et al. (2013).

This opportunity to isolate, at least up to certain length, phenomena of interest in laboratory is of crucial importance, if one of the aims of the experiments is in the development, validation or verification of an ice load model or a predictive simulation tool. In validation of a model, one wishes that the model would first repeat or predict the results, which are measured in a simple ice loading scenario, before advancing to more complex less well-defined ice loading scenarios. The gap in directly going reliably from a numerical model to a general ice loading scenario, in either laboratory-scale or full-scale, is often simply too large.

For validation purposes, it is thus of outmost importance, that properly scaled experiments that are suitable for validation are performed, and as will be suggested below, it would be beneficial that a suite of ice simulation benchmarking data be collected, organized, and made publicly available. The benchmark experiments should include very detailed reporting, and allow fairly simple interpretation through a manageable set of parameters and potential load mechanisms. These experiments should be done apart from the experiments on general ice loading scenarios that have their primary aim in design loads. A design load experiment is usually performed using a given type of model scale ice, they may be too complex for model validation even if useful for the design, and, unfortunately, their reporting may lack due to the goal of solely catching a design load (or some other design feature of interest).

It is a very challenging task to define a definite set of benchmark experiments, which an ice load model should fulfil for it to be validated for design, and for being able to claim that a given model suffices all different ice loading scenarios; There are several different types of ice load sources, loading mechanisms, and ice parameters, which may be important depending on an ice loading scenario and the task of planning benchmark experiments for all of them is difficult. In

addition, the importance of different parameters may change during a loading process (Palmer, 1991; Ranta, 2016). It can be said that partly the challenge is due to the complex ice loading processes and ice material behaviour, but also due to the need for better understanding of fundamental mechanical behaviour of various ice features themselves. The model validation is partly a challenge as we do not understand the ice loads and the mechanics of them well enough.

Apart from this, there are also short-comings, and related discussion, in performing just laboratory-scale experiments. A very obvious difference between the full-scale and laboratory-scale experiments is the physical dimensions. Another crucially important difference is in the type of ice used in the laboratory-scale studies. While some of the experiments are performed using normal sea ice, others are done using fresh water ice, ice grown in laboratory, or doped model scale ice with scaled material properties. Different ice types show different behaviour, which is why the type of ice must be accounted for when interpreting laboratory-scale experiments. A minimum standard ice sample production consideration, if attainable, would enable improved interpretation of laboratory test data.

Lubbad and Løset (2011) developed a level ice resistance on ship model for use in real time simulators on. a simplified ice failure model is used. The failure followed a closed form solution for a bending failure of a sheet on Winkler foundation. They found that the simulation results for mean ice resistance levels were in agreement with full-scale measurements in both, model and full-scale experiments. A simulation tool with very similar ice failure model was used by Dudal et al. (2015) for real time simulations on ice structure interaction. Su et al. (2010, 2011a, 2011b, 2014) performed simulations on ice resistance of a ship in continuous level ice breaking. The ice failure in their model was defined to follow a prescribed pattern, which was based on available work on crack patterns in ice. Also in their model, the cracks formed by bending and depended on the characteristic length of ice sheet, ship speed, the frame angle, and a normally distributed random variable. Su et al. (2014) compared the simulation results to model scale experiment results with some success, but note that limited amount of data somewhat restricts the validation of their model. Zhang et al. (2014) studied the interaction between side grillage of a ship and icebergs using finite element simulations and model tests. They were able to validate their simulation tool, which then was used in studies on ship bulbous bow-ice collisions with various velocities.

Having reliable full-scale validation is needed in the development of numerical modelling tools for design, even if they would be in agreement with laboratory experiments in these cases. There have been recent efforts that aim for better understanding of model scale ice behaviours (von Bock und Polach et al., 2013; von Bock und Polach and Ehlers, 2013; and von Bock und Polach and Ehlers 2013, 2015) as it is very important to understand the advantages and limitations of model tests.

4.3 Ice load modelling and validation

The understanding of the mechanics of ice loads is constantly increasing and numerical simulations have a role in this increase, since they may give understanding on the detailed mechanisms behind the ice loads. As described above, the validation of ice load models and simulations for taking them to the level of design is a challenging task. However, ice load simulations and modelling efforts have increased and computational ice mechanics has been performed using various techniques.

Recent numerical modelling work has been done using discrete element method (DEM) (Cundall and Strack, 1979), combined finite-discrete element method (FEM-DEM) (Munjiza, 2004), finite-element method (FEM) with various modelling frameworks, various types of cohesive elements (Camacho and Ortiz, 1996 and smoothed particle hydrodynamics (Gingold and

Monaghan, 1977; Lucy, 1977). In addition to these, modelling of hydrodynamics in ice-structure interaction has been developed using computational fluid dynamics (CFD) and potential flow theory.

Lubbad and Løset (2011) developed a model for use in real time simulators on level ice resistance on ships. The model uses a simplified model for the ice failure. The failure followed a closed form solution for a bending failure of a sheet on Winkler foundation. They found that the simulation results were in agreement with full-scale measurements on mean ice resistance levels in both, model and full-scale experiments. A simulation tool with a very similar ice failure model was used by Dudal et al. (2015) for real time simulations on ice structure interaction. Su et al. (2010, 2011a, 2011b, 2014) performed simulations on ice resistance of a ship in continuous level ice breaking. The ice failure patterns in their model were defined to follow a prescribed model, which was based on earlier work on crack patterns in ice. Also in their model, the cracks in the model formed by bending and depended on the characteristic length of ice sheet, ship speed, the frame angle, and a normally distributed random variable. Su et al. (2014) compared the simulation results to model scale experiment results with some success, but note that limited amount of data somewhat restricts the validation of their model. Zhang et al. (2014) studied the interaction between side grillage of a ship and icebergs using finite element simulations and model tests. They were able to validate their simulation tool, which then was used in studies on ship bulbous bow-ice collisions with various velocities.

Metrikin and Loset (2013), Metrikin (2014) and Metrikin et. al (2015) present a non-smooth DEM based model for modelling ice-structure interaction. According to the authors, the model is suitable for simulating station keeping in a field of ice floes. Recently van den Berg (2016) presented a random lattice based model for sea ice. The work aims to model a variety of ice mechanics problems based on lattice modelling, where discrete rigid bodies are glued together with initially elastic cohesive elements. When an ice sheet is modelled using this type of method, the basic mechanics of the model become similar to those in Paavilainen et al. (2010) who modelled the ice sheet using a lattice of beams that connected rigid discrete elements together. This model was further studied in Lilja et al. (2017a, b) in some fundamental mechanics problems. Further, van den Berg (2016) demonstrates the capability of the model to model consolidated ice ridges in a similar manner than Polojärvi and Tuhkuri (2013). The model is yet to be validated against experimental data.

Kuutti et. al (2013) modelled ice loads on structure using FEM and cohesive elements. The modelling was done on a level of local ice loads, and the authors claim that their model is the first model that able to describe continuous crushing of ice. The load levels from the model compared well against the laboratory experiments in Määttänen (2011), which were done for studying the distribution of local ice loads on a model hull structure. In the experiments by Määttänen (2011) the ice properties were not scaled, albeit the ice was laboratory made. Kuutti and Kolari (2010, 2011) also presented a damage-mechanics-based FEM model with local remeshing procedure, which allowed the cracks to propagate through the finite elements. There was no comparison of the latter model with ice load data. Ice crushing and local ice loads were also recently modelled using FEM by Jordaan et al. (2016) and Gagnon (2011) and by a combination of FEM and SPH by Kim (2014).

Modelling work related to on ice mechanics and, in more detail, ice rubble has been recently performed by Polojärvi and Tuhkuri (2009, 2013) and Polojärvi et al. (2012). The work concentrated on understanding the material behaviour of ice rubble and the model was validated against experimental data, both from model and full-scale. In this case, the model-scale experiments were performed using plastic rubble blocks with a goal in model development to achieve increased insight on the mechanics through exercising punch through tests. Kulyathkin and Polojärvi (2016, 2017) used numerical modelling to study the applicability of the continuum assumption on ice rubble using numerical modelling. Further work on more fundamental ice mechanics was done in von Bock und Polach et al. (2013), von Bock und Polach and Ehlers

(2013) and in von Bock und Polach and Ehlers (2013, 2015). The work aimed to tackle some of the above mentioned challenges in scaling of laboratory-scale results by using laboratory-scale experiments and numerical modelling in parallel to study model scale ice properties.

Role of the hydrodynamics on ice loads has been recently studied by several authors. Gagnon and Wong (2012) studied a simplified bergy bit-ship interaction accounting for hydrodynamics by using a CFD solver. Simulations yielded realistic bergy bit behaviour and ship grillage damage patterns for their model. Tsarau et al. (2014) introduced computationally efficient numerical tool, which combines DEM and a potential flow theory based solver. The model was first validated against simplified laboratory experiments and then applied to more complex ice loading scenario involving a ship and ice floes. Tsarau and Løset (2015) added a vortex element method solver to the same simulation tool to predict ice motion further and used visual observations on laboratory experiments in validation. Tsarau et al. (2016) also used a simplified hydrodynamics model to account for fluid drag forces on ice floes in a modelling study on the effect of propeller flow in ice management (Polojärvi and Tuhkuri (2009) and Polojärvi et al. (2012) presented a similar model for hydrodynamic pressure drag).

4.4 Towards a benchmark data suite

We suggest that a suite of ice simulation benchmarking data be collected, organized, and made publicly available – even if suggesting a set of definite experiments for this is out of scope of this report. One effective way to categorize the data base would be to divide it into three parts, based on simulation scale and ice engineering purpose: large, medium, and small; with large being on the order of kilometres scale, medium being at metres scale, and small being at centimetres scale. (Here we, even if important, leave out geophysical scale and concentrate on ice engineering scale.) Each scale has unique data measurement and availability challenges.

For large scale, some typical sources for data are satellite imagery, meteorological ice and weather records, ice flight observations, ice radar, and ship ice-trials databases. Much of this data, as well as data collecting philosophy is based in 20th century technology. Nowadays, with satellites, cell phones, GPS, and the internet of things, it is possible (and recommended) to have access to live-streaming real-time meteorological ice related data virtually everywhere. This access will enable development of onsite ice-operation related decision support tools; de-risking these operations and streamlining productivity.

Medium scale scenarios are typically on the order of metres, or tens of meters, and involve the interaction of a one or more ice pieces with a structure and other ice pieces. Models for this scale are dependent on ice physical properties, on relationships prescribing ice behaviour (such as ice friction models, or ice contact pressure as a function of contact area), and on understanding of the underlying mechanical phenomena. Benchmarking data for this scale should thus include measured, scenario dependent physical ice properties, and detailed observations on scenario-dependent mechanical processes.

Small scale scenarios occur at the scale of centimetres, and are typically centred on replicating small-scale laboratory experiments, or extrapolating/investigating ice behaviours that are difficult to study in the laboratory. These models strongly depend on the physical properties of ice and on the modelling assumptions. (Benchmarking data required for these types of simulations are similar to the physical properties data required for medium scale simulations, however, often more in-depth and higher quality data is required). Due to the extreme scenario-dependence of small scale simulations, it would be impractical to consider all possible small scale ice loading cases. For benchmark database, a table characterising the scenario and conditions, under which the data was collected, should be carefully contrived.

Regardless of scale, developing a suitable material model for ice is a key issue in order to run reliable simulations of different scenarios. At least for small and mid scale scenarios, the ideal

material model should be able to reproduce laboratory experiments in a simulation, regardless of the type of expected ice behaviour. For this purpose, experimental data could be put into a standard framework, such as the one proposed in Figure 7. Here, the peak stress ice can sustain is given as a function of the triaxiality of the stress state η. Moreover, exemplary stress-time curves are given for different types of behaviour.

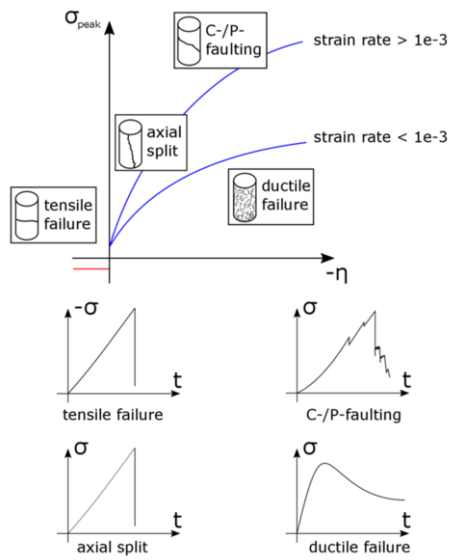

Figure 7: Concept proposal for a small scale benchmark data suite. Diagrams without scale. (Kellner et al. 2018).

Such a framework could be useful in many ways. Firstly, it could help to identify knowledge gaps of available experimental data. Secondly, it could serve as benchmark data for material models which aim at the simulation of small and mid scale scenarios. The ideal material model should be able to reflect the behaviour shown in Figure 7 for different states of stress with curves similar to the ones depicted. It could also help to show the limitation of current material models with a standardized "language". The triaxiality is suggested to be calculated based on principal stresses as follows:

$$\eta = \frac{\frac{1}{3}(\sigma_1 + \sigma_2 + \sigma_3)}{\frac{1}{\sqrt{2}}\sqrt{(\sigma_1 - \sigma_2)^2 + (\sigma_1 - \sigma_3)^2 + (\sigma_2 - \sigma_3)^2}}$$

4.5 Propeller ice interaction

One third of vessel repair cost following damages in ice are related to the machinery, of which 40% is related to the main engine and 25% to the propulsion system (Henderson, 2010). Current rules and ice-propeller prediction models do however not consider propulsion machinery as a coupled system even though the ice-propeller torque is not equal to the shaft response torque. Therefore, an inverse model of the propulsion machinery is required for transforming the propeller shaft torque response to the ice-propeller torque

Polic et al. (2016a, b and 2017) present a propulsion machinery model capable of transforming the propeller shaft response to the propeller load and present the following three objectives: a propulsion machinery model capable of calculating the propeller shaft response based on the known transient propeller load; the correlation between propeller shaft response and propeller

load within different propulsion machinery systems; and a reliable inverse propulsion machinery mode capable of calculating the propeller load based on the propeller shaft response. The propulsion machinery model that combines the complete rigid body motion of the crank mechanism, flexible crankshaft, flexible coupling, finite-mode propeller shaft with three flexible modes, and rigid propeller with rule based and random ice-related propeller torque load is presented and used for calculating the propeller shaft response. The calculated response is successfully transformed back to the propeller load by considering potential energy in flexible modes of the propeller shaft and rigid body (kinetic) energy from propeller and propeller shaft. In addition, robustness of the inverse model, used in transformation process, to noise in the propeller shaft response and starting time (static or transient state) is demonstrated. Yang et al. (2015) carried out the transient torsional vibration analysis of ship propulsion system for ship navigation in ice by using the Newmark method. It was found from numerical results that the transient torque is bigger than steady torque due to the ice impact, and its amplitude depends on the relationship between the natural frequency of the propulsion shaft and ice stimulated frequency. The blade frequency exciting component was found by time-frequency analysis and it is necessary to avoided the blade number order resonance of ice impact.

4.6 Ice induced vibration (IIV)

Besides static ice loads, significant load levels can occur due to periodic, dynamic loading. This is also called ice-induced-vibration (IIV). First cases of IIV were encountered about 50 years ago at the first Cook Inlet offshore structures in Alaska (Määttänen, 2015). Since then, many cases of IIV have been recorded. The consequences range from human discomfort and gas leakage to fatigue failure in secondary structures (Määttänen 2015, Yue et al. 2009, Wang et al. 2013). One event that almost led to the loss of a structure was recorded at the Molikpaq platform in 1986. Here, a floe was continuously crushed against the side of the platform. The resultant vibrations almost made the sand core lose its ability to withstand shear stress (Jefferies and Wrigth, 1988). The field monitoring data of ice-resistant platforms in Bohai (Yue and Bi, 2000) revealed that the risks induced by ice vibrations are more serious than the extreme static ice load. The significant ice-induced vibration not only causes significant cyclical stress of tube node but also great acceleration response, which can endanger the pipeline systems on the platform and discomfort the crew members (Zhang et al., 2015a).

In general, IIV events are not fully understood and some of the connected topics in ice mechanics are still at the heart of ongoing discussion. However, since the first IIV incidents, observations and measurements have led to some understanding of the involved processes. In the current ISO standard three types of crushing are described: intermittent, frequency lock-in and continuous brittle crushing (ISO 19906:2010). Of those types, a frequency lock-in is considered to be the most dangerous. Simply put, under certain conditions the ice crushing failure can synchronize around the structure and vibrations start to build up. In other words, the ice fracture sequence locks in to the oscillation of the structure (Ziemer and Deutsch 2015, Palmer and Bjerkås 2013).

Significant attention by the research community has been given to frequency lock-in vibrations. One of the first models to simulate IIV was introduced by Matlock in 1969. He proposed a simple spring mass damper system in connection with an ice crushing model. Most of the research in this area is still focused on a basic understanding of IIV and frequency lock-in, hence such simple models are still being developed today (Hendrikse and Metrikine 2015, McQueen and Srinil 2016, Withalm and Hoffmann 2010). Zhang et al. (2015b) performed the ice-induced dynamic response analysis of a jack-up platform in Bohai sea based on the field monitoring data of ice-resistant platforms and model experiment of ice loads on the jack-up platform. The results show that the acceleration response is lower than the displacement response of deck under steady ice force and it is necessary to pay attention to the effect of ice-induced vibration on structural fatigue.

A more sophisticated and verified numerical model does not exist yet (Määttänen, 2015). The reasons are the lack of publicly available full scale data and the complexity of the process. In addition a verified and reliable material model for sea ice is not available yet.

Taking everything into account it is reasonable to assume that a frequency lock-in can only be modelled with a coupled simulation. This simulation should take into account a flexible structure, a suitable material model for ice and a CFD simulation for the sea water.

Further, the design of OWTs has to account for localized and dynamic ice loads. The solution is to estimate possible ice loads for the desired installation location. The susceptibility of the structure to ice-induced-vibration can also be assessed in advance. One option is to engage an ice expert. Typically, he will estimate the loads based on experience and additional methods. IIV is still not well understood and there are a number of different developments and active discussion related to the topic. Due to the lack of full understanding, the estimates on the severity of IIV vary, and it may even appear that some of the approaches are not transparent enough for a designer (ISO 19906:2010). There have been several empirical and semi-empirical approaches in the design against IIV, and also new approaches that are based on phenomenological models are developed (Hendrikse and Metrikine, 2016). There is also IIV studies that use DEM, FEM with damage models, and FEM using a foam analogues and cohesive elements (Ziemer and Deutsch 2015, Palmer and Bjerkås 2013, Hendrikse and Metrikine 2015, McQueen and Srinil 2016, Withalm and Hoffmann 2010). Many of the current approaches focus on ice crushing and compressive failure, and some of the most recent ones, on buckling (Hendrikse and Metrikine, 2016).

Many formulas use a projected area multiplied with the ice pressure or the compressive strength of ice, respectively. An extensive early work was done by Korzhavin, based on measurements in Siberian rivers (Withalm and Hoffmann 2010). Subsequently, many works applied similar approaches, mostly based on field or laboratory measurements, for instance Croasdale et al., Michel and Toussaint or Frederking et al. (Croasdale et al., 1977, Michel and Toussaint, 1977, Frederking et al, 1999). The use of formulations based on project area and a nominal average ice pressure is used by several standards for instance the ISO 19906 standard.

Furthermore, some work has been done to compare the methodology and applicability of the different formulas. Masterson et al. (2003) investigated the methodology behind standards. Masterson and Tibbo (2011) compared ice loads for different fictitious cases, taken from (Timco and Croasdale, 2006, Tseng, 1998). Frederking evaluated different standards using typical offshore structures (Frederking, 2012). Popko et al. (2012) compared different guidelines and standards with focus on integrated sets of design loads. Overall it was shown that the results of different formulas can vary significantly. In order to presented the suitability of these empirical approaches. Kellner et al. (2017) compares them to each other and where possible to measurements. Previously, design ice loads with measured ice loads for the Nordströmsgrund lighthouse. This was done with three standards and for just one ice thickness (Määttänen, 2015).

In addition to numerical modelling of IIV events, research efforts have also been directed toward understating what happens in the ice and at ice/structure interface and how it affects response of the structure (Sodhi et al. 1998, Nord et al. 2015, O'Rourke et al. 2016).

4.7 Ice induced fatigue

Ships also experience fatigue and there is more experience and knowledge about ice-induced fatigue on ice going vessels, see for example Bridges et al., (2006) and Ehlers et al. (2012). Fatigue assessment of the lifetime of ship and offshore structures is generally performed by means of linear damage accumulation (Palmgren-Miner rule) since service loads and thereby stresses are stochastically distributed over time, see also Ehlers et al. (2010). When the long-term stress range distribution for the whole service life is expressed by a stress histogram it is possible to

calculate the fatigue damage by splitting the stress histogram into a number of representative blocks of equivalent stress range. This allows calculation of the damage contribution of each block individually. The fatigue life is consequently defined by the sum of damage accumulated in each block independently. However, blocks with high mean stress effects can lead to changes in fatigue crack growth (e.g. Führing, 1977) and therefore the hypothesis of linear damage accumulation loses its validity. In other words, sequences with high ice loads, which will cause such stress effects, invalidate the assumptions of independent damage accumulation. Current standards for fatigue design of ship and offshore structures introduce design fatigue factors to reduce the acceptable fatigue damage. Alternatively, a load history with its variation in amplitude accounting for the ice-structure interaction of the offshore structure besides the open water wave loads can be used. Consequently, the fatigue damage can be accumulated over this variable amplitude loading history and the life of the offshore structure can be assessed. The latter is however challenging, because the fatigue critical loading histories must be known for the specific design scenario. Furthermore, the influence of low temperatures must be assessed, due to exponentially increased crack growth at stress ranges that initiate crack extension by cleavage fracture modes, see also Braun (2017), Ritchie and Knott (1973) and Walters et al. (2016). Consequently, this also requires a definition of the design temperature, see chapter 3.3.

5. SUMMARY AND RECOMMENDATIONS

For ships and offshore structure, it is important to define the ice loading in order to design a compliant structure. Offshore structures are required to be designed for ULS and ALS with a corresponding probability of exceedance of 10^{-2} and 10^{-4} when establishing load levels. Therefore, probabilistic rules are often, but not always, applied to reach compliance with the location specific conditions, such as ice conditions and exposure. Ships are however designed differently using industry-wide rules and regulations, where the design load is based on the target ice class in a deterministic framework. Thereby, the design and scantlings of ships are obtained based on prescriptive and experience-based methods. Beneficial to this is approach for ships is the fact, that during their design life, they may experience different operators and missions. Therefore, such industry-wide ice class approach ensures that the experience from various conditions leads to safe designs. However, a first principle based approach, which defines the design load based on the vessel's mission including the target ice conditions and exposure allows for a more optimised design. The shortcoming is naturally that the life-time mission must be known and deviations (for instance that the ship is operated differently than what the probabilistic design assumed) may lead to structural failure. On the other hand, a probabilistic approach can be used to identify a vessel to be chartered for a specific mission to be accomplished. In other words, a link between the *assumed* operations and design for ice class can be established.

The rules currently cover good operational conditions with good visibility, but they fall short for accidental scenarios. Furthermore, the PC rules do not cover accidental impact with icebergs, nor specify a safe operating speed or how to check different hull arrangements and vessels for different scenarios. Therefore, it is useful to establish a connection between a safe operational envelope and physical construction of the vessel. Such a safe envelope must account for both, qualified experts operating the ship as well as somewhat uncertain operators, to identify the associated uncertainties. This could feed directly into the polar water operating manual as part of compliance to the Polar Code.

Generally, it would be very useful to instrument ships and offshore structures to monitor and record ice loads in addition to ice maps to learn from the behavior and make better predictions in the future. Together with shared damage reports on ice induced damages this would contribute to a solid basis for improved rules and regulations. In order to achieve such goal, the ice community should be more open to share knowledge and data, other than through publications with selected contents, which usually do not allow the reader to reproduce the results in full.

In order to make actual use of the presented simulation methods and models for design compared to the limited amount of large-scale experiments available we need agreed benchmarks test to validate numerical models. The experiments underlying these benchmarks need to be designed for numerical modelling and thus numerical modelling should drive the experiment to ensure that the required parameters are measured. Corresponding publications shall be accommodated with the numerical codes and numerical analysis should supplement the numerical model as well. Thereby a public community-based database containing ice data, experiments, as well as agreed standards for laboratory ice production and specimen geometries should be established. Thereby non-transparent ice load models can be avoided with unphysical parameters requiring validation for each application, which naturally makes them unusable for design load predictions.

In summary, the following strength-related research challenges can be identified:

- Definitions of limit states;
- Design procedures-based on ULS;
- Plastic effects of moving ice loads;
- Consistent design temperature definition;
- Fatigue and fracture of base material and welded structures at low temperatures; and
- Appropriate toughness evaluation method.

And further, the following ice load-related research challenges can be identified:

- Link between ice-related parameters and ice loads;
- Definition of design relevant events considering peak loads;
- Relationship between local HPZs and global pressure;
- Scaling of model versus full-scale ice including ice resistance;
- Agreed set of benchmark experiments for numerical models;
- Validated ice load models and simulations for design load predictions;
- Propulsion machinery model transforming propeller shaft response to propeller load;
- Simulation models for frequency lock-in vibration;
- Formulas for crushing type of ice failure; and
- Fatigue critical loading histories induced by ice load.

REFERENCES

Alsos, H.S. 2008. "Ship Grounding - Analysis of Ductile Fracture, Bottom Damage and Hull Girder Response." PhD, Norwegian University of Science and Technology (NTNU).

AMARK and MUN (1998). Unified Requirements Load Model – Synthesized Approach. Report for IACS Polar Harmonization Semi-Permanent Working Group on behalf of Canada/Russia Bilateral Project Steering Committee: Institute for Marine Dynamics, Transport Canada, and Russian Maritime Register.

ASPPR, 1995. Canadian Arctic Shipping Pollution Prevention Regulations, Equivalent Standards for Construction of Arctic Class Ships, Transport Canada Ship Safety, Report TP 12260.

Barents2020, 2012, Assessment of international standards for safe exploration, production and transportation of oil and gas in the Barents Sea. Harmonisation of Health, Safety, and Environmental Protection Standards for The Barents Sea Final Report Phase 4. Report no 2012-0690.

Benkovsky, D. D. (1970) Technology of Ship Repairing. Moscow: MIR Publishers. (In Russian)

Bergström M. A simulation-based design method for arctic maritime transport systems. Doctoral theses at NTNU, 2017:93

Braun M. Fatigue and fracture mechanics testing at sub-zero temperatures. DNV GL Workshop, Trondheim, Norway, 2017.

Braun M. Fatigue and fracture mechanics testing at sub-zero temperatures. DNV GL Workshop, Trondheim, Norway, 2017.

Brian J. O'Rourke, Ian J. Jordaan, Rocky S. Taylor, Arne Gürtner, Experimental investigation of oscillation of loads in ice high-pressure zones, part 1: Single indentor system, In Cold Regions Science and Technology, Volume 124, 2016, Pages 25-39,

Brian J. O'Rourke, Ian J. Jordaan, Rocky S. Taylor, Arne Gürtner, Experimental investigation of oscillation of loads in ice high-pressure zones, part 2: Double indentor system — Coupling and synchronization of high-pressure zones, In Cold Regions Science and Technology, Volume 124, 2016, Pages 11-24

Bridges R., Zhang S. and Shaposhnikov V., 2012, Experimental investigation on the effect of low temperatures on the fatigue strength of welded steel joints, Ships and Offshore Structures, 7:3, 311-319

Camacho, G., Ortiz, M., 1996. Computational modeling of impact damage in brittle materials. International Journal of Solids and Structures 33 (20–22), 2899–2938.

Carter, J.E., Daley, C., Fuglem, M., Jordaan, I.J. Keinonen, A., Revill, C., Butler, T., Muggeridge, K., Zou, B., 1996. Maximum Bow Force for Arctic Shipping Pollution Prevention Regulations Phase II. Report for Transport Canada Ship Safety, Northern Region by Memorial University of Newfoundland Ocean Engineering Research Center. Report TP12652.

Carter, J.E., Frederking, R., Jordaan, I.J., Milne,W.J., and Muggeridge, D.B., 1991. Review and Verification of Proposals for the Revision of the Arctic Shipping Pollution Prevention Regulations, Report on Phase I – Concept Review. Report for Canadian Coast Guard Northern, by Memorial University of Newfoundland Ocean Engineering Research Center. Report TP11472E.

Croasdale, K.; Morgenstern, N.; Nuttall, J. (1977): Indentation Tests To Investigate Ice Pressures On Vertical Piers. In Journal of Glaciology 19 (81).

Daley, C. 1999. ENERGY BASED ICE COLLISION FORCES, Proc. of the 15th International Conference on Port and Ocean Engineering under Arctic Conditions, Helsinki University of Technology in Espoo,Finland on August 23-27, 1999

Daley, C., 2000, Background notes to design ice loads. . IACS ad-hoc group on polar class ships, Transport Canada.

Daley, C., 2004. A Study of the Process-Spatial Link in Ice Pressure-Area Relationships. Prepared for National Research Council as part of its Program on Energy Research and Development. PERD/CHC Report 7-108.

Daley, C.G., Tuhkuri, J., and Riska, K., 1998. The role of discrete failures in local ice loads. Cold Regions Science and Technology, 27, 197–211.

Daley. C., 1992. Ice edge contact and failure. Cold Regions Science and Technology 21 (1992). 1–23.

Dudal A., Septseault, C. , Beal, P-A, Le Yaouanq, S., Roberts, B. (2015). A new arctic platform design tool for simulating ice-structure interaction. In Proceedings of the 23rd International Conference on Port and Ocean Engineering under Arctic Conditions (POAC), Trondheim, Norway (electronic publication).

Ehlers S, Remes H, Klanac A, Naar H. A multi-objective optimisation-based structural design procedure for the concept stage - a chemical product tanker case study. Ship Technology Research, Schiffstechnik, 2010; 57(3): 182-197.

Ehlers S., Cheng F., Kuehnlein W., Jordaan I., Kujala P., Luo Y., Riska K., Sirkar, Oh Y.T., Terai K., Valkonen J.: ISSC Report COMMITTEE V.6 ARCTIC TECHNOLOGY, 2015.

EPPR, 2015, Arctic Council - EPPR 1 st Draft report: Standards for the Prevention of Oil Spills from Offshore Oil and Maritime Activities in the Arctic.

Erceg, B., Ralph, F., Ehlers, S., and Jordaan, I., (2015). Structural Response of Ice Going Ships using Probabilistic Design Load Method. Proceedings of the 34th International Conference on Ocean, Offshore and Arctic Engineering (OMAE). St John's, Newfoundland. June 2015.

Frederking, R. (2012): Review of Standards for Ice Forces on Port Structures. In B. Morse, G. Doré (Eds.): Cold Regions Engineering. Quebec City, Canada, 2012, pp. 725–734.

Frederking, R., 1998. The pressure-area relation in the definition of ice forces, 8th Int. Offshore and Polar Engineering Conference, May 24-29, 1998, Montreal, Vol. II, pp. 431-437.

Frederking, R., 1999. The Local Pressure-Area Relation in Ship Impact with Ice. Proceedings 15th International Conference on Port and Ocean Engineering under Arctic Conditions, POAC'99, Vol.2, pp 687-696, Helsinki, Finland, August 23-27, 1999.

Frederking, R.; Timco, G.; Reid, S. (1999): Sea Ice Floe Impact Experiments. With assistance of NRC Canadian Hydraulics Centre, NRC Institute for Ocean Technology.

Führing, H. (1977): Calculation of elastic-plastic stresses in Dugdale crack sheets with crack flank contact on the basis of nonlinear fracture mechanics. No. 30, Statik und Stahlbau, TH Darmstadt.

Gagnon, R.E., 2011. A numerical model of ice crushing using a foam analogue. Cold Regions Science and Technology, 65 (3), pp. 335-350.

Gingold, R.A. and Monaghan, J.J, 1977. Smoothed particle hydrodynamics: theory and application to non-spherical stars, Monthly Notices of the Royal Astronomical Society, vol. 181, p. 375-389.

Hauge M. (2015), Maier M., Walters C. L., Østby E., Kordonets S.M., Zanfir C., Osvoll H., Status Update of ISO TC67/SC8/WG5: Materials for Arctic Applications, Proceedings of the Twenty-fifth (2015) International Ocean and Polar Engineering Conference Kona, Big Island, Hawaii, USA, June 21-26, 2015

HAYWARD, R. (2007). Principles of Plastic Design. In Increasing the Safety of Icebound Shipping (Vol. 2, pp. 197-213). Espoo: Helsinki University of Technology, Ship Laboratory, M-302.

Heinonen, J., 2004. Constitutive Modeling of Ice Rubble in First-Year Ridge Keel. (Doctoral Thesis), TKK, VTT Publications 1235-0621 536. VTT Technical Research Centre of Finland, Espoo, Finland (2004, 142 pp.).

Hendrikse H, Metrikine A. Interpretation and prediction of ice induced vibrations based on contact area variation. International Journal of Solids and Structures. 2015;75–76:336-48.

Hendrikse, H., Metrikine, A., 2016. Ice-induced vibrations and ice buckling. Cold Regions Science and Technology 131, 129–141.

Herrnring H, Kubiczek J, Ehlers S, Niclasen NO, Burmann M. Experimental investigation of an accidental ice impact on an aluminium high speed craft. 6th International Conference on Marine Structures (MARSTRUCRT), 8 – 10 May 2017, Lisbon Portugal.

Hillerborg, A., Modéer, M., Petersson, P., 1976. Analysis of crack formation and crack growth in concrete by means of fracture mechanics and finite elements. Cement and Concrete Research 6, 773–781.

Hong, L. and Amdahl, J. 2012. "Rapid Assessment of Ship Grounding Over Large Contact Surfaces." Ships and Offshore Structures 7 (1): 5-19.

Huang Y., Guan P. and Yu M., Study of the sailing's moving response of an icebreaker in ice, Mathematics in Practice and Theory, Vol.44 No.2, 2015, 149-160

IMOa, 2016, International Code for Ships Operating in Polar Waters (Polar Code), Resolution MSC. 385(94), and Resolution MEPC.264 (68).

IMOb, 2016, MSC.1/Circ.1519, Guidance on Methodologies for Assessing Operational Capabilities and Limitations in Ice.

ISO, 2010. Petroleum and natural gas industries — Arctic offshore structures, International Standard by The Organization for Standardization (ISO). Reference number ISO/FDIS 19906:2010(E).

ISO/FDIS/19906, 2010. Petroleum and natural gas industries – Arctic offshore structures. Standard.

ISO19900, 2013, Petroleum and natural gas industries - General requirements for offshore structures. International Organization for Standardization.

ISO19904-1, 2006, Petroleum and natural gas industries -- Floating offshore structures -- Part 1: Monohulls, semi-submersibles and spars. International Organization for Standardization.

ISO19906, 2010, Petroleum and natural gas industries – Arctic offshore structures. International Organization for Standardization.

ISSC, 2015, Ultimate Strength. Proc. 19th International Ship and Offshore Structures Congress, Cascais, Portugal, 1: 279-350.

Jefferies M. and W. Wright, “Dynamic Response of "Molikpaq" to ice-structure interaction,” in Proceedings of the 7th international conference on offshore mechanics and arctic engineering, 1988, pp. 201–220.

Joensuu, A., Riska, K., 1989. Contact between ice and structure in Finnish. Laboratory of Naval Architecture and Marine Engineering, Helsinki University of Technology, Espoo, Finland, Report M-88.

Jordaan, I. J., Li, C., Mackey, T., Stuckey, P., Sudom, D., and Taylor, R., 2007. “Ice Data Analysis and Mechanics for Design Load Estimation, Final Report”, prepared for NSERC, C-CORE, Chevron Canada Resources, National Research Council of Canada, Petro-Canada and Husky Energy.

Jordaan, I., O’Rourke, B., Turner, J., Moore, P., Ralph, F., 2016. Estimation of Ice Loads using Mechanics of Ice Failure in Compression. In Proceeding of the Arctic Technology Conference (ATC), St. John’s, Canada (electronic publication).

Jordaan, I., Sudom, D., Li, C., Stuckey, P., Ralph, F., 2005. Principles for local and Global Design using Pressure-area relationships. POAC’05 Conference, New York, June 2005.

Jordaan, I.J., 2001. Mechanics of ice-structure interaction. Engineering Fracture Mechanics, 68, pp. 1923–1960.

Kendrick, A., and Daley, C., 2011. Structural challenges faced by Arctic ships. Ship Structure Committee report SSC-461.

Kim, E. and Amdahl, J., 2016 Discussion of assumptions behind rule-based ice loads due to crushing. Ocean Engineering.

Kim, E., 2014. Experimental and numerical studies related to the coupled behavior of ice mass and steel structures during accidental collisions. Doctoral thesis, Norwegian University of Science and Technology.

Kim, HW and Quinton, B.W.T. 2016. "Evaluation of Moving Ice Loads on an Elastic Plate." Marine Structures 50: 127-142.

Kim, HW. 2014. "Ice Crushing Pressure on Non-Planar Surface." Ph. D., Memorial University of Newfoundland.

Kim, M.-C., Seung-Ki, L., Won-Joon, L., Jung-yong, W., 2013. Numerical and experimental investigation of the resistance performance of an icebreaking cargo vessel in pack ice conditions. International Journal of Naval Architecture and Ocean Engineering, 5 (1), 116-131.

Kolari, K., Kuutti, J. and Kurkela, J., 2009. FE-simulation of continuous ice failure based on model update technique. In the proceedings of the 20th International Conference on Port and Ocean Engineering under Arctic Conditions (POAC), Luleå, Sweden.

Kuehnlein, Walter L., Design and Development Philosophies for Arctic Projects Proceedings of Arctic Technology Conference, ATC 2016, held in St. John’s, New Foundland, Paper OTC 27328.

Kulyakhtin, S. and Polojärvi, A. (2016). Ice Rubble Stress in Virtual Experiments for Assessing Continuum Approach. In: The Proceedings of the 23rd IAHR International Symposium on Ice, Ann Arbor, Michigan, USA. Electronic publication.

Kulyathkin, S. and Høyland, K., 2015. Ice rubble frictional resistance by critical state theories. Cold Regions Science and Technology 119, 145–150

Kulyathkin, S. and Polojärvi, A (2017). Variation of Stress in Virtual Biaxial Compression Test of Ice Rubble. In: Proceedings of the 24th International Conference on Port and Ocean Engineering under Arctic Conditions, Busan, Korea. Electronic publication.

Kurdyumov, V.A. and Kheisin, D.E., 1974, About definition of ice loads acting on icebreaker hull under impact. Proc. Leningr. Shipbuild. Inst, 90. (in Russian)

Kuutti, J. and Kolari, K., 2010. Simulation of ice crushing experiment using FE-model update technique. In the Proceedings of the 20th International Symposium on Ice (IAHR), Lahti, Finland.

Kuutti, J., Kolari, K. and Marjavaara, 2013. Simulation of ice crushing experiments with cohesive surface methodology. Cold Regions Science and Technology 92, 17–28

Kuutti, J., Kolari, K., 2011. A local remeshing procedure to simulate crack propagation in quasi-brittle materials. Engineering Computations, 29 (2), 125-143.

Lensu, M., 2002. Short term prediction of ice loads experienced by ice going ships. Report M-269. Helsinki University of Technology, Ship Laboratory, Espoo, Finland.

Leppäranta, M., Hakala, R., 1989. Field measurements of the structure and strength of first-year ice ridges in the Baltic sea. Proceedings of the Eighth International Conference on Offshore Mechanics and Arctic Engineering, Hague, Netherlands. Vol. 4. pp. 169–174.

Leppäranta, M., Hakala, R., 1992. The structure and strength of first-year ice ridges in the Baltic sea. Cold Regions Science and Technology 20 (3), 295–311.

Liferov, P., Bonnemaire, B., 2005. Ice rubble behavior and strength: Part I. review of testing and interpretation of results. Cold Regions Science and Technology 41, 135–151.

Lilja V.-P., Polojärvi A., Tuhkuri, J. and Paavilainen, J. (2017a). A combined 3D FEM-DEM model for an ice sheet, in: Proceedings of the 24th International Conference on Port and Ocean Engineering under Arctic Conditions, Busan, Korea. Electronic publication.

Lilja V.-P., Polojärvi A., Tuhkuri, J. and Paavilainen, J. (2017b). Effective tensile strength of an ice sheet using a three-dimensional FEM-DEM approach, in: Proceedings of the 24th International Conference on Port and Ocean Engineering under Arctic Conditions, Busan, Korea. Electronic publication.

Lubbad, R., Løset, S., 2011. A numerical model for real-time simulation of ship – ice interaction. Cold Regions Science and Technology, 65, 111–127

Lucy, L.B., 1977. A numerical approach to the testing of the fission hypothesis Astronomical Journal, vol. 82, Dec. 1977, p. 1013-1024.

Masterson, D.; Kouzmitchev, K.; deWaal, J. (2003): Russian SNIP 2.06.04-82 and Western Global Ice Pressures - A Comparison. In : Proceedings of the 17th International Conference on Port and Ocean Engineering under Arctic Conditions. Trondheim.

Masterson, D.; Tibbo, S. (2011): Comparison of Ice Load Calculations Using ISO 19906, CSA, API and SNIP. In : Proceedings of the 21th International Conference on Port and Ocean Engineering under Arctic Conditions. Port and Ocean Engineering under Arctic Conditions. Montréal.

Masterson, D.M. and Frederking, R., 1993. Local contact pressures in ship/ice and structure/ice interactions, Cold Regions Science and Technology, Vol. 21, pp. 169-185.

Masterson, D.M., Frederking, R.M.W.,Wright, B., Kärnä, T., Maddock,W.P., 2007. A revised ice pressure-area curve. Proceedings, Nineteenth International Conf. on Port and Ocean Engineering under Arctic Conditions, Dalian, vol. 1. Dalian University of Technology Press, pp. 305–314

Matlock H., W. Dawkins, and J. Panak, "A Model for the Prediction of Ice-Structure Internation," in Offshore Technology Conference: Offshore Technology Conference, 1969.

Määttänen, M., 1986. Ice sheet failure against an inclined wall. IAHR 86 Proceedings of the 8th International Symposium on Ice, Iowa City, U.S.A., pp. 149–158.

McQueen H. and N. Srinil, "A Modified Matlock–Duffing Model for Two-Dimensional Ice-Induced Vibrations of Offshore Structures With Geometric Nonlinearities," J. Offshore Mech. Arct. Eng, vol. 138, no. 1, p. 11501, 2016.

Metrikin, I. and Løset, S., 2013. Nonsmooth 3d discrete element simulation of a drillship in discon- tinuous ice. In Proceedings of the 22nd International Conference on Port and Ocean Engineering under Arctic Conditions (POAC), Espoo, Finland (electronic publication).

Metrikin, I., 2014. A Software Framework for Simulating Stationkeeping of a Vessel in Discontinuous Ice Modeling, Identification and Control, 35 (4), 211–248.

Metrikin, I., Gurtner, A., Bonnemaire, B., Tan, X., Fredriksen, A., and Sapelnikov, D., 2015. SIBIS: a numerical environment for simulating offshore operations in discontinuous ice. In Proceedings of the 23rd International Conference on Port and Ocean Engineering under Arctic Conditions, POAC, in Trondheim, Norway (electronic publication).

Michel, B.; Toussaint, N. (1977): Mechanisms and Theory of Indentation of Ice Plates. In Journal of Glaciology 19 (81).

Mironov, M.E., 2013, Вопросы нормативно-правового регулирования при создании сооружений на континентальном шельфе РФ. Современные подходы и перспективные технологии в проектах освоения нефтегазовых месторождений российского шельфа, 3: 17-21. (In Russian)

Moslet, P.O., Masurov, M. and Eide, L.I., 2010, Barents 2020 RN02 – Design of Stationary Offshore Units against Ice Loads in the Barents Sea. 20th IAHR International Symposium on Ice, Lahti, Finland.

Muggeridge K.J, McKenna R.F, Spring, W. and Thomas G.A.N., 2017. ISO 19906 update – an international standard for Arctic offshore structures, POAC

Määttänen M., “Ice induced frequency lock-in vibrations - converging towards consensus,” in Proceedings of the 23th International Port and Ocean Engineering under Arctic Conditions, 2015.

Määttänen, M., Marjavaara, P., Saarinen, S. and Laakso, M., 2011. Ice crushing tests with variable structural flexibility. Cold Regions Science and Technology 67, 120–128.

Nord TS, Lourens E-M, Määttänen M, Øiseth O, Høyland KV. Laboratory experiments to study ice-induced vibrations of scaled model structures during their interaction with level ice at different ice velocities. Cold Regions Science and Technology. 2015;119:1-15.

OGP, 2010, Calibration of action factors for ISO 19906 Arctic offshore structures. International Association of Oil and Gas Producers, Report No. 422.

OGP, 2014, Reliability of offshore structures-current design and potential inconsistencies. Proc. of International Association of Oil and gas Producers, OGP Report No. 486.

Paavilainen, J., 2010. Jäälautan murtuminen kartiorakennetta vasten. In: J. Heinonen, ed. Jatkuvan murtumisprosessin mallinnus jää-rakenne vuorovaikutusprosessissa, Research report (in Finnish), Project: "STRUTSI". Technical Research Center of Finland, Espoo: VTT, pp. 25-27.

Paavilainen, J., Tuhkuri, J., 2012. Parameter effects on simulated ice rubbling forces on a wide sloping structure. Cold Regions Science and Technology 81, 1 – 10.

Paavilainen, J., Tuhkuri, J., 2013. Pressure distributions and force chains during simulated ice rub- bling against sloped structures. Cold Regions Science and Technology 85, 157 – 174.

Palmer A. and M. Bjerkås, “Synchronisation and the transition from intermittent to locked-in ice induced vibration,” in Proceedings of the 22th International Conference on Port and Ocean Engineering under Arctic Conditions, 2013.

Palmer, A. and Croasdale, K., 2013. Arctic Offshore Engineering. World Scientific Publishing.

Palmer, A. and Dempsey, J., 2009. Model tests in ice. In the proceedings of the 20th International Conference on Port and Ocean Engineering under Arctic Conditions (POAC), Luleå, Sweden.

Palmer, A., 1991. Fracture mechanics models in ice-structure interaction. In Jones, S.J., McKenna, R.F., Tillotson, J., Jordaan, I.J. (editors), Ice-Structure Interaction: IUTAM/IAHR Symposium St. John's, Newfoundland Canada 1989, p. 93-107, ISBN 978-3-642-84100-2.

Palmer, A.C., Dempsey, J.P., and Masterson, D.M., 2009. A revised ice pressure-area curve and a fracture mechanics explanation. Cold Regions Science and Technology 56 (2009) 73–76.

Polic D, V Æsøy, S Ehlers. Propeller torque load and propeller shaft torque response correlation during ice-propeller interaction. Accepted for publication in Journal of Marine Science and Application.

Polic D, V Æsøy, S Ehlers. Transformation of propeller shaft dynamic response to propeller torque load. To be submitted shortly.

Polic D, V Æsøy, S Ehlers. Transient simulation of the propulsion machinery system operating in ice – Modeling approach. Ocean Engineering, online 10. August 2016. Article in press.

Polojärvi, A. and Tuhkuri, J., 2012. Velocity effects in laboratory scale punch through experiments. Cold Regions Science and Technology, 70(1):81–93.

Polojärvi, A., Tuhkuri, J., 2009. 3D discrete numerical modeling of ridge keel punch through tests. Cold Regions Science and Technology 56 (1), 18–29.

Polojärvi, A., Tuhkuri, J., 2013. On modeling cohesive ridge keel punch through tests with a combined finite-discrete element method. Cold Regions Science and Technology 85, 191–205.

Polojärvi, A., Tuhkuri, J., and Korkalo, O., 2012. Comparison and analysis of experimental and virtual laboratory scale punch through tests. Cold Regions Science and Technology, 81:11–25.

Polojärvi, A., Tuhkuri, J., and Pustogvar, A., 2015. DEM simulations of direct shear box experiments of ice rubble: Force chains and peak loads. Cold Regions Science and Technology, 116:11–23.

Popko, W.; Heinonen, J.; Hetmanczyk, S.; Vorpahl, F. (2012): State-of-the-art Comparison of Standards in Terms of Dominant Sea Ice Loads for Offshore Wind Turbine Support Structures in the Baltic Sea. In Jin S. Chung (Ed.): ISOPE-2012 Rhodes. Proceedings of the 22nd International Offshore and Polar Engineering Conference;. Rhodes, Greece. International Society of Offshore and Polar Engineers. Cupertino, Calif.: International Society of Offshore and Polar Engineers (ISOPE).

Popov, Yu., Faddeyev, O., Kheisin, D., and Yalovlev, A., (1967) "Strength of Ships Sailing in Ice", Sudostroenie Publishing House, Leningrad, 223 p., Technical Translation, U.S. Army Foreign Science and technology Center, FSTC-HT-23-96-68.

Pustogvar, A., Høyland, K. V., Polojärvi, A., Bueide, I. M., 2014. Laboratory scale direct shear box experiments on ice rubble: the effect of block to box size ratio. In: Proceedings of OMAE14, 33th International Conference On Offshore Mechanics and Arctic Engineering. June 8-13, San Francisco, USA.

Quinton, B.W.T. 2008. "Progressive Damage to a Ship's Structure due to Ice Loading." Master of Engineering, Memorial University of Newfoundland.

Quinton, B.W.T. 2015. "Experimental and Numerical Investigation of Moving Loads on Hull Structures." PhD, Memorial University of Newfoundland.

Quinton, B.W.T., Daley, C.G. and Gagnon, R.E., 2012, Response of IACS URI Ship Structures to Real-time Full-scale Operational Ice Loads. Transactions. Society of Naval Architects and Marine Engineers, 120: 203-209.

Ralph, F. 2016. Design of Ships and Offshore Structures: A Probabilistic Approach for Multi-Year Ice and Iceberg Impact Loads for Decision-making with Uncertainty. A Thesis submitted to the School of Graduate Studies in partial fulfillment of the requirements for the degree of Doctor of Philosophy. Faculty of Engineering and Applied Science Memorial University, St. John's, NL. October 2016.

Ralph, F., and Jordaan, I. 2013. Probabilistic Methodology for Design of Arctic Ships. Proceedings of the 32nd International Conference on Ocean, Offshore and Arctic Engineering. June 9-14, 2013, Nantes, France

Ralph, F., and Jordaan, I. 2013. Probabilistic Methodology for Design of Arctic Ships. Proceedings of the 32nd International Conference on Ocean, Offshore and Arctic Engineering. June 9-14, 2013, Nantes, France

Ralph, F., Jordaan, I., Clarke, P. and Stuckey, P. 2006. Estimating Probabilistic Iceberg Design Loads on Ships Navigating in Ice Covered Waters. ICETECH Conference, Banff. Paper No. ICETECH06-05-006. July 2006.

Ranta, J., Polojärvi, A., and Tuhkuri, J. (2016). The statistical analysis of peak ice loads in a simulated ice-structure interaction process. Cold Regions Science and Technology, 133, 46–55

Ranta, J., Polojärvi, A., Tuhkuri, J. (2018). Ice loads on inclined marine structures - Virtual experiments on ice failure process evolution, Marine Structures, 57, 72-86.

Research Bulletin No 40/41, 2015, Russian Maritime Register of Shipping (In Russian)

Riska K, Bridges R, Limit state design and methodologies in ice class rules for ships and standards for Arctic offshore structures, In Marine Structures, 2017, ISSN 0951-8339, https://doi.org/10.1016/j.marstruc.2017.09.005.

Riska, K. and Kämäräinen, J., 2011, A Review of Ice Loading and the Evolution of the Finnish-Swedish Ice Class Rules. SNAME Transactions.

Riska, K., 1987. On the mechanics of the ramming interaction between a ship and a massive ice floe, Thesis for degree of Doctor of Technology, Technical Research Centre of Finland, Publication 43, Espoo, Finland.

Riska, K., 1991. Observations of the line-like nature of ship-ice contact. In: Proceedings, 11th International Conference on Port and Ocean Engineering Under Arctic Conditions, St. John's, Newfoundland, Canada, Vol. II, pp. 785–811.

Riska, K., Tuhkuri, J. (Eds.), 1999. Local ice cover deformation and mesoscale ice dynamics. Part 2: Synthesis Report. Helsinki University of Technology, Ship Laboratory, Espoo, Finland (Report M-243).

Ritchie R, Knott J. Mechanisms of fatigue crack growth in low alloy steel. Acta Metall 1973; 21:639–48.

RMRS, 2015, Правила классификации и постройки морских судов Российский морской регистр судоходства, 1-3. (In Russian)

Sawhill, S. (2015): Use of temperature in standards and classification rules for shIp and offshore installations. DNV GL memo 1XH3HD3-3/STESAW

Serré, N., 2011a. Mechanical properties of model ice ridge keels. Cold Regions Science and Technology 67 (3), 89–106.

Serré, N., 2011b. Numerical modeling of ice ridge keel action on subsea structures. Cold Regions Science and Technology 67 (3), 107–119.

Shunying, J., Shaocheng, D., and Shewen, L., 2015. Analysis of ice load on conical structure with discrete element method. Engineering Computations, 32(4):1121–1134.

Sodhi DS, Takeuchi T, Nakazawa N, Akagawa S, Saeki H. Medium-scale indentation tests on sea ice at various speeds. Cold Regions Science and Technology. 1998;28:pp.161-82.

Su, B., Skjetne, R., Berg, T. E., 2014. Numerical assessment of a double-acting offshore vessel's performance in level ice with experimental comparison. Cold Regions Science and Technology, 106–107, 96–109

Su. B., Skjetne, R., Berg, T.E., 2014. Numerical assessment of a double-acting offshore vessel's performance in level ice with experimental comparison. Cold Regions Science and Technology 106–107 (2014) 96–109

Suominen, M. and Kujala, P., 2014. Variation in short-term ice-induced load amplitudes on a ship's hull and related probability distributions. Cold Regions Science and Technology 106–107, 131–140.

Suominen, M., Su, B., Kujala, P. and Moan, T., 2013. Comparison of measured and simulated short term ice loads on ship hull. In the Proceedings of the 22nd International Conference on Port and Ocean Engineering under Arctic Conditions (POAC).

Taylor, R., Jordaan, I., Li, C., and Sudom, D., 2009. Local Design Pressures for Structures in Ice: Analysis of Full-Scale Data. Journal of Offshore Mechanics and Arctic Engineering AUGUST 2010, Vol. 132 / 031502-1.

Thomas, G.A.N., Bercha, F.G. and Jordaan, I.J., 2011, Reliability, Limit States and Action Factors for ISO 19906. OTC Arctic Technology Conference, Houston, Texas, USA (Document ID OTC-22072).

Timco, G. and Weeks, W., 2010. A review of the engineering properties of sea ice. Cold Regions Science and Technology, 60, 107–129.

Timco, G. W.; Croasdale, K. R. (2006): How well can we predict ice loads? In Proceedings 18th International Symposium on Ice, IAHR'06 1, pp. 167–174.

Timco, G., Frederking, R., Kamesaki, K. and Tada, H., 1999. Comparison of ice load calculation algorithms for first-year ridges, Proceedings International Workshop on Rational Evaluation of Ice Forces on Structures, REIFS'99, 88–102.

Tõns, T., Ralph, F., Ehlers, S., and Jordaan, I., (2015). Probabilistic Design Load Method for the Northern Sea Route. Proceedings of the 34th International Conference on Ocean, Offshore and Arctic Engineering (OMAE). St John's, Newfoundland. June 2015.

Tsarau, A., Lubbad, R., Løset, S., 2016. A numerical model for simulating the effect of propeller flow in ice management. Cold Regions Science and Technology. Article in press

Tsarau, A., Lubbad, R., Løset, S., 2016. A numerical model for simulation of the hydrodynamic interactions between a marine floater and fragmented sea ice. Cold Regions Science and Technology 103, 1–14.

Tsarau, A., Løset, S., 2015. Modelling the hydrodynamic effects associated with station-keeping in broken ice. Cold Regions Science and Technology, 118, 76–90.

Tseng, J. (1998): Comparison of International Codes for Ice Loads on Offshore Structures. With assistance of NRC Canadian Hydraulics Centre, Sandwell.

van den Berg, M., 2016. A 3-D random lattice model of sea ice. In Proceeding of the Arctic Technology Conference (ATC), St. John's, Canada (electronic publication).

von Bock und Polach RUF, Ehlers S, Erikstad SO. A decision-based design approach for ships operating in open water and ice. Journal of Ship Production and Design, 2014, 30(3):11

von Bock und Polach, R.U.F. and Ehlers, S., 2013. Model-scale ice - Part B Numerical Model. Cold Regions Science and Technology, 94, 53-60.

von Bock und Polach, R.U.F., 2015. Numerical analysis of the flexural strength of model-scale ice. Cold Regions Science and Technology, 118, 91-104.

von Bock und Polach, R.U.F., Ehlers, S. and Kujala, P., 2013. Model-scale ice - Part A Experiments. Cold Regions Science and Technology, 94, 74-81.

von Bock und Polach, R.U.F., Ehlers, S., 2015. On the scalability of model scale ice experiments. Journal of Offshore Mechanics and Arctic Engineering, 137, 5, 1-11.

Voormeeren L. (2014), Atli-Veltin B., Vredeveldt A.W., Impact resistance, cryogenic bunker fuel tanks, Proceedings of the ASME 2014 33rd International Conference on Ocean, Offshore and Arctic Engineering OMAE2014 June 8-13, 2014, San Francisco, California, USA

Walters, C.L.; Alvaro, A.; Maljaars, J.: The effect of low temperatures on the fatigue crack growth of S460 structural steel. International Journal of Fatigue, 82(1), pp. 110-118, 2016.

Wang S., Q. Yue, and D. Zhang, "Ice-induced non-structure vibration reduction of jacket platforms with isolation cone system," Ocean Engineering, vol. 70, pp. 118–123, 2013.

Withalm M. and N. P. Hoffmann, "Simulation of full-scale ice–structure-interaction by an extended Matlock-model," Cold Regions Science and Technology, vol. 60, no. 2, pp. 130–136, 2010.

Yang H.J., Che C.D., Zhang W.J. and Qiu T., 2015, Transient torsional vibration analysis for ice impact of ship propulsion shaft, J. Ship Mech., 19(1-2):176-181

Yue Q, Bi X. Ice-Induced Jacket Structure Vibrations in Bohai Sea. Journal of Cold Regions Engineering. 2000; 14:81-92.

Yue Q., F. Guo, and T. Kärnä, "Dynamic ice forces of slender vertical structures due to ice crushing," Cold Regions Science and Technology, vol. 56, no. 2-3, pp. 77–83, 2009.

Zhang D.Y., Yue Q.J., Liu D., Xu N., Wang D.Q. and Wang S.T., 2015a, "Structural ice-resistant performance evaluation of jack-up drilling platforms, J. Ship Mechanics, 19(7):850-858

Zhang J., Wan Z.Q., Chen C., 2014, Research on structure dynamic response of bulbous bow in ship-ice collision load, J. Ship Mech., 18(1-2):106-114

Zhang J., Wan Z.Q., Huang J.H. and Yin Q., 2014, Research on numerical simulation and model test of collision between side grillage and icebergs, J. Ship Mech., 18(4):424-433

Ziemer G. and C. Deutsch, "Study of Local Pressure Distribution and Synchronization During Frequency Lock-In," in Proceedings of the 23th International Port and Ocean Engineering under Arctic Conditions, 2015.

APPENDIX

A.1 GUIDELINES FOR THE NONLINEAR ANALYSIS OF MOVING ICE LOADS

This section presents guidelines (Quinton 2016) for the nonlinear finite element (FE) assessment of the structural capacity of the hull of a ship or steel hulled offshore structure subject to moving ice loads. The guidelines presented pertain primarily to the assessment of the hull structural response to a given moving load. A discussion of some existing finite element methods for modelling ice follows this discussion.

FE code type

Moving loads may induce highly nonlinear geometric and material behaviours, sliding contact, and short-duration structural instabilities. It is theoretically possible to model these behaviours using an implicit (static or dynamic) nonlinear finite element code, however, it is often practically difficult and highly inefficient. This is primarily due to the extremely short time-step that is required to adequately capture the structural deformations at the translating point of application of the load. Note: the fact that implicit codes are unconditionally stable does not imply that long timesteps will accurately model events of short duration. Even excepting all other practical considerations, the necessarily small time-step will generally render implicit codes inefficient for models of suitable scale to assess moving loads on hull structures.

Analyses of the nonlinear response of hull structures to moving loads are generally best suited to an explicit time-integration code with nonlinear geometric, material, and constraint capabilities. According to the stability criterion of the explicit time-integration, the time-step is less than or equal to the critical time step which is approximately defined be the ratio of the smallest element length to the wave propagation speed in the finite element model. This will always be sufficient to capture unstable, transient, nonlinear hull responses due to operational/accidental moving loads on commercial hull structures, and the calculation efficiency per time-step generally results in efficient model run times.

The remainder of this discussion focuses on the application of explicit time-integration finite element techniques to the modelling of moving loads on commercial ship and offshore structure hulls. These guidelines are broadly applicable to any brand of explicit finite element solver.

Mesh requirements and element type: Structural instabilities often occur at much lower load magnitudes for moving loads, than for stationary loads (Quinton 2008; 2015), and capturing these localized deformations often requires a high mesh density. It is common and practical to model hull structures using shell elements, and a higher mesh density increases ratio of element thickness to length and width, implying that the shell elements may require "thick shell" or Reissner-Mindlin plate theory. Further, reduced integration shell elements with warping stiffness and (at least) five through-thickness integration points are recommended. Beam elements are not recommended in areas achieving highly nonlinear material and geometric behavior, as their inability to change their cross-sectional shape limits their usefulness in this respect.

Boundary Conditions: Should be sufficiently distant from the area of application of the moving load, so that the local boundary conditions of loaded structural components are not artificially stiff. Further, plasticity at the applied boundary conditions should be avoided.

Material Model: A bilinear kinematic elastic-plastic material model is sufficient for thick plates. Thinner plates exhibiting plastic membrane stretching, and frames in general, may require a

multi-linear elastic-plastic model. Special consideration for repeated/cyclic loads should be reflected by appropriate implementation of isotropic/kinematic hardening. Strain-rate effects may be included.

Contact: A standard penalty formulation is recommended for steel-rigid contact. A modified penalty formulation may be required if the compliance of the impacting objects is significantly different.

Load: Application of ice loads is a tedious and complex subject. Some guidance is given below.

Nonlinear Finite Element Numerical Ice Models

Ice-structure interaction is a highly non-linear transient dynamic problem. Ice exhibits a myriad of failure mechanisms, including: creep, elasticity, plasticity, crushing, fracture (spalling), extrusion/comminution of crushed/spalled material, melting/re-freezing, and cohesion. To date, it has not been possible, to capture all these mechanisms in a single omnibus numerical ice model. It is possible to accurately model the creep, elasticity and plasticity behaviours of ice, using either implicit or explicit finite element codes, however these behaviours are only dominant at very low to low rates of strain. Melting/refreezing and cohesion are difficult to model numerically, but again these behaviours generally do not dominate the interaction of ice with ship hull structures. The remaining failure mechanisms - i.e. crushing, spalling, and extrusion/comminution - generally do dominate for typical ship and offshore structure ice-structure interactions, and are difficult to model numerically. These mechanisms are highly non-linear transient dynamic processes which are not suited for simulation in an implicit finite element simulation environment. Furthermore, ice-structure interactions often occur over very short periods of time (e.g. bow-shoulder impacts). Such scenarios are better suited to explicit finite element codes.

Flexural Failure

Cohesive Element Method: Separate solid elements are connected using zero-volume cohesive elements (various authors), and the ice is modelled as elasto-plastic material. This bulk material behaves like a solid until the failure criteria in the cohesive elements are met. When this happens, the cohesive elements fail, thereby freeing the bond between adjacent box elements and effectively modelling flexural failure.

Erosion Method: Another way to model flexural failure is to model ice cover with solid elements that are far smaller than would normally be practical, and then set a failure strain for them. Therefore, when the failure strain in a very small cube element is exceeded, it erodes (i.e. disappears), instigating crack propagation. The elements need to be small so that the mass loss due to the disappearing elements is negligible. A major downside is the time it takes to solve the model as the timestep in an explicit simulation is directly proportional to the size of the smallest elements.

Pressure (non-contact) Modelling

The "4D Pressure Method" (Quinton, Daley, and Gagnon 2013) uses a sophisticated algorithm to model the ice as a time series of spatially changing pressures, applied directly to individual structural elements. It has been used to apply discretised natural (i.e. from 1980s field trials of the USCGC Polar Sea) temporally/spatially changing pressure distributions to hull structures.

Hail Impacts

Carney et al. (2006) developed a novel, calibrated, material model for modelling hail impacting a space shuttle. This material model was successfully used in an arbitrary Lagrangian-Eulerian formulation to capture small-scale, high velocity ice-structure interaction; including fracture/spalling behaviours.

A.2 SIMULATORS

Aalto Ice Mechanics DEM

The Aalto Ice Mechanics DEM code is an in-house development, which is currently used for research purposes by the Aalto University Ice Mechanics group. The simulation tool is based on techniques, which are well reported in scientific literature by the group. The simulation-based analysis by the group has provided new insight on ice mechanics and phenomena behind ice loads. Namely, the studies have focused on ice-structure interaction process, on understanding ice rubble behaviour and resistance, and on ice rubble material modelling. Part of the code development in Aalto is rigorous validation, which, in laboratory scale, is partly enabled by the Aalto University Ice Tank. Aalto invites researchers in the ice mechanics community to use and further develop the code, but does not provide technical support or open access to the code.

CARD Stationkeeping Simulation Model

To simulate the complex dynamics of the broken ice field and to assess the sensitivity of different scenarios on loads experienced by the station-keeping system, an interactive dynamic discrete element model (DEM) is developed. For simplicity, the model approximates the shape of managed sea ice floes by circular discs of random diameters (to be updated to polygons in next iteration). The mechanics of the broken ice field is driven by the contact forces between individual floes. A viscoelastic contact model is used with boundary conditions and environmental forcings that vary both in time and space. Once a certain contact force between floes or between a floe and the structure is exceeded, the interaction mechanics switches to ice crushing model. The influence on loads of (1) floe size distribution and concentration; (2) stiffness of the station-keeping system; and (3) changes (including rate) in ice drift direction can be examined. The ability to correctly model these factors is critical for effective ice management operations. The model is used to study and highlight the relative importance of those factors for evaluating operational ice management strategies and for defining operating envelopes.

MUN GPU Event Mechanics (GEM)

MUN's GEM software is a novel simulation tool that simulates ice-structure and ice-ice interaction in hyper-real-time, for multiple ships and/or offshore structures operating in pack ice. These interactions are modelled by strategically solving numerous analytical and semi-empirical equations appropriate to each interaction. For each body in the simulation, ice impact forces are based on a modified Popov method. Each impact is treated as an 'event'. Other physical 'events' such as floe bending fracture and rafting are also included. Each ice body has equations of motion with additional inputs of wind and current drag. Vessels have additional forces from rudders, thrusters, moorings. The software is presently limited to convex bodies. All motions are solved in two-dimensions (2D), though certain aspects are treated in three-dimensions (e.g. Popov collision loads assumes 3D, as does ice floe flexure, and mooring mechanics). While GEM resembles other discrete multi-body simulations, GEM is focused more on operational decision support than on scientific analysis.

NTNU Simulator for Arctic Marine Structures

A high-fidelity numerical simulator for precise load calculations used for design and engineering of ships and structures to be operated in realistic ice conditions is developed at NTNU. The simulator, Simulator for Arctic Marine Structures (SAMS), comprises a module to generate realistic ice and environmental conditions, a multi-body dynamics module with realistic generalized contact compliance based on contact crushing assumptions. In addition, SAMS enables ice failure in bending, splitting and crushing, as well as more advanced hydrodynamics such as added mass and modelling of wave dispersion in ice and ice breakup in waves. SAMS does also consider ships on DP, mooring or sailing. The simulator applies for designing ice-going ships and offshore floaters both for intact sea ice (level ice and ridges) and broken ice conditions.

TUHH simulator for ice-breaking and ice-going ships

A numerical model for simulation of viscous flow ship-ice interaction in level ice conditions is being developed at TUHH. Unlike most existing interaction models, TUHH's model features realistic modelling of the icebreaking pattern, i.e., allowing the bow shape design to influence the results, as well as a rigid-body dynamics approach. Rigid-body dynamics approach takes into account all non-hydrodynamic influences (gravitational, buoyancy, damping and contact forces) on the bodies in the domain. The coupling of the rigid-body system with a Lattice Boltzmann based free surface flow solver supplements the hydrodynamic forces to update the positions of the floating objects in the simulation. Two main direct outcomes of the simulation model are local ice loads that act on the ship hull, and the level ice resistance force, calculated as a sum of the instantaneous ice forces in longitudinal direction. A wide range of applications include level ice resistance predictions, bow shape design based on contact and load distribution, as well as ship performance and transit simulations in ice.

Proceedings of the 20th International Ship and Offshore Structures Congress (ISSC 2018) Volume II – M.L. Kaminski and P. Rigo (Eds.)

doi:10.3233/978-1-61499-864-8-391

COMMITTEE V.7

STRUCTURAL LONGEVITY

COMMITTEE MANDATE

Concern for the structural longevity of ship, offshore and other marine structures. This shall include diagnosis and prognosis of structural health, prevention of structural failures such as corrosion and fatigue, and structural rehabilitation. The focus shall be on methodologies translating monitoring data into operational and life-cycle management advice. The research and development in passive, latent and active systems including their sensors and actuators shall be addressed.

AUTHORS/COMMITTEE MEMBERS

Chairman: P. Hess
S. Aksu
M. Vaz
G. Feng
L. Li
P. Jurisic
M. R. Andersen
P. Caridis
D. Boote
H. Murayama
N. Amila
B. Leira
M. Tammer
J. Blake
N. Chen
A. Egorov

KEYWORDS

Ship structures, fatigue, service life, corrosion, structural health monitoring, digital twin, structural longevity, structural inspection, structural repair, structural maintenance, structural damage detection, fatigue life, crack detection, structural life-cycle assessment, structural life-cycle management, structural sensing, acoustic emission

CONTENTS

1. INTRODUCTION 394
1.1 Background & Mandate 394

1.2 STRUCTURAL LONGEVITY CONSIDERATIONS 394
1.3 Report Content 395

2. LIFE-CYCLE ASSESSMENT & MANAGEMENT FOR STRUCTURAL LONGEVITY 395
2.1 Introduction 395
2.2 Life-cycle Assessment & Integrity Management 396
2.2.1 Classification Societies 396
2.2.2 Offshore platform - API and ISO Rules 397
2.3 Lifetime Extension 399
2.4 Challenges and Opportunities 399
2.5 Conclusions 402

3. INSPECTION AND MONITORING 402
3.1 Introduction 402
3.2 Inspection 402
3.3 Monitoring techniques 405
3.4 Hull monitoring systems 406
3.5 Data acquisitions, transfer, processing, and management 410
3.6 Conclusions 413
3.7 Recommendations 413

4. OFFSHORE STRUCTURAL LONGEVITY METHODS AND EXAMPLES 414
4.1 Introduction 414
4.2 Prediction of Longevity 414
4.3 Main factors influencing longevity 415
4.3.1 Corrosion 416
4.3.2 CP/Anode depletion / Coating deterioration 416
4.3.3 Wear & tear 417
4.3.4 Fatigue 417
4.3.5 Buckling 419
4.4 Methods ensuring safe operation 420
4.4.1 General 420
4.4.2 Structural Integrity Management (SIM) 420
4.4.3 Codes and guidelines covering structural integrity management 421
4.4.4 Survey and inspection methods 422
4.4.5 Repair/mitigation 423
4.4.6 Lifetime extension 424
4.5 Special items 425
4.5.1 Risers / pipelines 425
4.5.2 Mooring lines 425
4.5.3 Caisson 426
4.5.4 Conductors 426
4.5.5 Wind turbines 427
4.6 Offshore Platform Longevity Processes 428
4.7 Conclusions and Recommendations 429

5. SHIP STRUCTURAL LONGEVITY METHODS AND EXAMPLES 429

5.1 Introduction 429
5.2 Prediction of longevity 429
5.2.1 Models for prediction of longevity 429
5.2.2 Failure Modes Contributing to Longevity Assessment 431
5.3 Main factors influencing longevity 436
5.3.1 Role of Life Extension Programs 438
5.4 Methods for ensuring safe operation 440
5.4.1 Current practice and future directions 440
5.4.2 Structure Monitoring, Inspection, Maintenance, and Repairs 440
5.4.3 At-sea damage response: measurement, analysis, repair, and/or change in operation 441
5.4.4 Remaining Service Life 442
5.5 Notional Examples of Longevity and Life Extension Decisions 442
5.5.1 Naval Ship 442
5.5.2 Bulk carrier / Tanker/Container 443
5.5.3 Inland Vessels 444
5.6 Discussion and Conclusions 446

6. CONCLUSIONS & RECOMMENDATIONS 447
6.1 Conclusions 447
6.2 Recommendations 448

REFERENCES 449

1. INTRODUCTION

1.1 Background & Mandate

The structural longevity of ships, offshore, and other marine platform structures is a function of design, operation, and life-cycle management. Each of these aspects together determines the ability of a structure to endure safely and effectively without risk of significant failures, significant need for repair, or early retirement. This committee was formed to explore these aspects and encompasses technical domains across the ISSC technical community. Care was taken in the development of this report to investigate recent research and practice that determine, evaluate, and affect longevity of ship and offshore structures in accordance with the mandate, beyond that contained in the ISSC 2015 report of this committee (Hess et al, 2015).

Concern for structural longevity requires assessment of the technology reviewed by all of the committees of ISSC 2018 from loading to design to fabrication, but with an emphasis on maintenance of the structure to ensure a successful life. The design process requires development of conservative estimates of loading (including environmental and seaway), fabrication methods and tolerances, material performance, operation, and maintenance (e.g. inspection, monitoring, corrosion-prevention). Assumptions are made during design regarding construction methods, loading, environment, design criteria, material performance, operation, maintenance, and service life. However, if any design assumption proves incorrect then this could result in a risk and cost to the owner and operator.

The mandate of this committee overlaps that of committees IV.2, Design Methods, which calls for "integration [of design] with production, maintenance and repair" and V.2, Experimental Methods, which calls for "…advances in…in-service monitoring and their role in the design, construction, inspection and maintenance of ship and offshore structures". Efforts have been made to avoid repetition of overlapping material in the reports of the three committees.

1.2 Structural Longevity Considerations

The heart of current practice for assessment of the structural condition of a ship or offshore structure is the periodic survey where the condition of the structure is compared to the standards of a classification society or other standards. The ideal of structural management for longevity is that assessment be carried forward to a prediction of future deterioration over the planned lifetime, that appropriate maintenance activities be performed, and that a monitoring and inspection plan be developed and instituted to ensure that the goals for continued operation are met. In forecasting future conditions of the structure, assumptions of operational effects are made. These, in general, are not as conservative as the assumptions made in design, where the worst operational conditions are assumed. For a structural longevity assessment, an estimate of future operating conditions is made. If possible, the loading history from hull monitoring and operational records is used to make that forecast. With a structural health monitoring system, the actual operational conditions are used to regularly update that forecast and modify it on the basis of detected changes in the integrity of the structure. The actual condition, use, and performance of the platform structure changes over time. This requires updated maintenance requirements for scheduling and budgeting, decisions on limiting or expanding the operational use, and predicting remaining useful service life.

Life-cycle management can evoke risk-based inspection, which rather than using a preset timetable for inspection and structural assessment, establishes inspection intervals on the basis of the probability of deterioration or fatigue fracture and the consequences of such failures. Structural health monitoring is an important part of that process, providing updates based on actual operation and indications of changes in the structure.

Establishment of a digital twin of the structure is a new concept that exploits the capability for structural computations and management of data. A mathematical model of the structure is constructed through finite element modeling, and that model is constantly updated as information from condition assessments, structural hull monitoring, and other sources such as modification and repairs to the structure is received. This digital twin can then be used for "what-if" studies of different scenarios of operation, inspection, maintenance, and repair for management of the structure over its lifetime.

There are great challenges in ensuring today's complex ships, offshore, and other marine structures have an affordable and adequate service life, which, ideally, should not be limited by structural considerations such as deterioration from corrosion, fatigue cracking or structural overload (buckling, collapse, or fracture). Developing technology for diagnosis and prognosis of structural health enhances prediction and planning of future structural maintenance costs. Classification societies are providing guidance and additional class notation for the installation of onboard structural monitoring systems, and research continues into means of translating the data collected from those systems into operational advice and life-cycle management. Making new designs more resilient by going beyond the safety-based requirements specified by the cognizant authority such as a classification society involves a greater initial cost, which can be justified by incorporating life-cycle maintenance considerations into the initial design cycle. Allowance for condition-based maintenance strategies might be made in the design process to reduce conservatism in design assumptions and support a more sophisticated and economical life-cycle management scheme.

1.3 Report Content

Chapter 2 describes the need to assess the structural lifetime of ships/vessels and offshore structures and the subsequent management for structural longevity. It also provides an overview of how structural longevity is handled using existing rule-sets and processes that result from governing requirements such as Class rules and the International Maritime Organization (IMO).

Chapter 3 focuses on inspection and structural hull and health monitoring technologies including relative costs and effectiveness, data acquisition systems, existing guidelines/rules. This chapter builds upon the reports of ISSC 2003 V.3, Inspection and Monitoring, and ISSC 2015 V.7, Structural Longevity.

Chapter 4 describes offshore structure specific aspects of longevity, including secondary load-carrying structure (risers, conductors, etc.), lifetime extension, and decommissioning.

Chapter 5 describes ship structure specific aspects of longevity, including failure modes of ship structure, lifetime extension, and conversion. Methods for ensuring safe operation are discussed, including monitoring, inspection, maintenance and repairs as well as assessment of damage. Examples on a naval ship, tanker, and inland vessel are provided.

2. LIFE-CYCLE ASSESSMENT & MANAGEMENT FOR STRUCTURAL LONGEVITY

2.1 Introduction

This chapter will provide an overview of how structural longevity for ship and offshore structures is handled using existing rule-sets and processes that result from governing requirements such as Class rules. Additionally, this chapter reflects upon advances in analytical methods that can be directed for structural assessment and current practice across other industry sectors concerned with maintaining and extending the life of high value, safety critical assets.

Following the definition in ISSC 2015, life-cycle assessment is defined as that which monitors structural health and extrapolates, or predicts, the expected structural life of the asset allowing informed but complex decisions by the owner/operator on the asset's future, including the facility for life extension (Hess et al., 2015). As such the "cycle" is defined from the point that assessment of the structure in the as-built/as-fabricated condition is made to the final end of life, including where the asset has been life extended. During this time, information on the asset's condition is utilized for life assessment.

2.2 Life-cycle Assessment & Integrity Management

Whether a ship or offshore structure, an asset's current structural condition is determined by periodic survey whereby all the present characteristics of the structure are described in detail, recording all service history including routes and loading conditions, damage incurred, subsequent repairs, refitting, and any modifications from the original as-built condition. To complete a picture of structural health, a comprehensive thickness measurement of all the structural components should be carried out. This information is recorded in a database which can be continuously updated and integrated with subsequent surveys and made available to the technical office in charge of evaluating the residual structural capacity of the asset.

An increasingly common practice to facilitate the residual capacity is to have a mathematical model, a "digital twin", of the asset as-built and by this approach it is possible to continually update it and get a "real-time" life prediction. These digital twins will become increasingly powerful as inverse finite element methods (iFEM) develop. Classification societies are encouraging the installation of structural hull monitoring systems which produce a large volume of live on-board strain data. This spatially discrete data can be input to FE models which then infers the asset's global shape. From the strain-displacement relationship, the full field strains are produced which, with the material properties of the structure, allow the full field stresses to be calculated that would elicit these strains (Kefal and Oterkus, 2016).

Preliminary hull girder and local strength assessment are carried out on the basis of the as-built scantlings and compared with respect to the Rules currently enforced for new builds. A detailed fatigue analysis of structural details is carried out by calculating the fatigue damage originated by the fluctuating stresses induced in the critical areas as identified in the initial analyses by the hull girder and local wave loads, combined with the ballast and full load cargo conditions. The fatigue life of the detail, in years, is calculated from the fatigue damage index. In the case where there is little data on the actual sea loads an asset experiences, this information must be supplemented by design code information or modelling, using seakeeping models and spectral fatigue analysis. Bayesian updating could be used to combine any initially assumed wave-load information with actual observed data (see, for example, Zhu & Frangopol, 2013).

Classification, certification, and verification ensure compliance of an asset's structural and equipment safety with internationally recognized industrial standards (for example, API or ISO) and IMO codes and regulations. The process of classification, certification, and verification covers all stages of design, construction, installation, operation, life extension and decommissioning and is undertaken by the classification societies.

2.2.1 Classification Societies

Most classification societies have guidelines for evaluating the structural condition of assets of different typologies. The aim of these guides is to provide criteria to carry out an objective condition assessment in order to assign a rating based on the condition of an asset, independently of its classification. The asset's condition assessment is based on the evaluation of (hull) structures, coating rating, machinery, and most importantly outfit components.

At the end of the evaluation procedure a rating is assigned to the ship. This rating consists typically of four levels:

1. Very good: Items examined and measured, found to have deficiencies of a superficial nature not requiring correction or repairs and/or found to have thicknesses significantly above class limits.
2. Good: Items examined and measured, found to have deficiencies of a minor nature not requiring correction or repairs and/or found to have thicknesses significantly above class limits.
3. Satisfactory: Items examined and measured either found to have deficiencies which do not require immediate corrective actions, or found to have thicknesses which, although generally above class renewal levels, have areas of substantial corrosion.
4. Poor: Items examined and measured either found to have deficiencies which may affect the ship's potential to remain in class, or found in some areas to have thicknesses that are at or below the class renewal levels.

Each classification society has their own procedures and a few examples are given here. A number of classification societies, including the US' American Bureau of Shipping (ABS), the Italian classification society, RINA S.p.A, France's Bureau Veritas (BV) and UK's Lloyds Register (LR) have what they term a condition assessment program or procedure (CAP) (e.g. RINA S.p.A, 2008; BV, 2015). Initially, the asset's operational records are examined and any information from, say, ultrasonic thickness measurements, are included in preliminary analyses. These include a re-assessment of the asset using its as-built scantlings measured against the latest rules and, generally, a fatigue assessment of identified critical areas. These analyses would provide an inspection protocol for the CAP survey, allowing close visual inspection of critical "hot spot" locations.

ABS rules have 3 groups to which they apply fatigue assessment: ships (ABS, 2017a), ship-shaped (e.g. FPSO) (ABS, 2017b–d) and non-ship-shaped offshore structures (e.g. Mobile Offshore Units, MOU) (ABS, 2017e). In any of the cases, the simplified treatment of the structures with 2-D analyses or 3-D FEA can be advanced to include a spectral-based fatigue assessment (ABS, 2017f; ABS, 2014a&b) where the loads are obtained through seakeeping analysis and a full asset FEA model deployed. For the offshore units (ship or non-ship-shaped), the analyses incorporate Environmental Severity Factors, previous damage and the consideration of the loading/unloading profile, which is significantly different from the loading profiles for more conventional ships. The significant outfitting and equipment mounted on the hull topsides and the interaction of this with the hull is evaluated using the Offshore rules. Offshore non-ship-like assets are treated under MOU rules. If a more advanced rating is required, then spectral based fatigue methods are deployed.

DNV GL determine the remaining strength of an aged ship using their Hull Life Cycle Programme (HLP) (DNV GL, 2017a). This captures the current condition of the ship for 3D FEA, including detailed thickness measurements, from which residual life is calculated (Wilken et al., 2013; DNV GL, 2015). As thicknesses change, the FEA analysis updates to re-evaluate remaining life constrained by an acceptable level of steel diminution through corrosion (DNV GL, 2016a). DNV GL provides a class notation, HMON (DNV GL, 2017a), to recognize assets incorporating live hull monitoring and stress warning alarms to inform immediate action and future maintenance and repair strategies.

2.2.2 Offshore platform - API and ISO Rules

An effective survey of rules development on this subject has been outlined in Copello et al. (2015). During the early 1990's the American Petroleum Institute (API) developed a new sec-

tion (Section 17—Assessment of Existing Platforms), to provide guidance for evaluating the fitness-for-purpose of old existing fixed offshore platforms.

Further updating to that guidance was provided by API in the mid 2000's by either revision of that Section 17 (by issue of a "supplement" to API RP 2A in October 2005) or development of a new recommended practice (RP), initially called RP 2SIM, as described in API (2005), which covers the management of existing platforms.

In the mid-1990's the International Standard Organization (ISO) developed the 19900 suite of guidelines to address design requirements and assessment of all types of offshore structures, including fixed steel structures (ISO, 1995). The rules were subsequently updated in 2007, becoming ISO 19902 (ISO, 2007).

According to both mentioned API and ISO rules, the actual structural performance is revised by introducing the present conditions of the structure, which means a reassessment process carried out by a procedure which can be summarized in five main steps:

1. *Data gathering*: before starting the reassessment process, a complete set of information about the platform is collected, including original design data, date and site of installation, construction and fabrication data, and platform history. This last one series of data consists of environmental loading history, changes in topside layout and weight, accidental events and relative damages, survey and maintenance records, repairs etc.
2. *Current platform survey*: to complete the previous data collection, the present condition of the platform is described with specific field inspections and on-site measurements, relative to the above water (deck, layout of wells, conductors) and underwater structures (jacket pipes members and nodal joints, anodes, marine growth measurements).
3. *Updating of the platform model*: by the gathered information the structural scheme and the FE model is updated for subsequent verifications.
4. *Review of the loads*: the new design loads, (relative to those used at the construction age) are defined according to updated design codes and rules. The data upon which predictions of environmental extremes were made at the design stage might no longer be appropriate for the reassessment.
5. *Strength assessment of the existing platform structure*: the structural updated model of the platform is verified with respect to both operational and extreme storm loading conditions, as normally done in the design of the new platform, by checking that prescribed limit state verification for the structural components are compliant. Present fatigue and corrosion conditions of each component are analyzed and verified according to the original design safety margin. According to the philosophy suggested by Copello et al. (2015) and ISO (2007), in the verification procedure it is permissible to have limited individual component failures provided that the remaining parts of the structure have sufficient reserve strength to redistribute the loads.

According to the described methodology, the existing structure can be considered adequate when, introducing the specific site conditions and given operational requirements (such as the desired life extension) the risk of structural failure leading to unacceptable consequences is adequately low. Thus, the required safety target can be related to the actual system capacity of the platform, measured by the residual strength reserve of the whole jacket evaluated by a push-over analysis, and then introduced in a reliability assessment system capable of determining the actual residual life of the structure and maximum return period of the extreme environmental loading that the platform is still capable of withstanding.

2.3 Lifetime Extension

The design life of any marine asset depends on the load type and return periods of the highest considered load. In the case of ships and offshore platforms this period is typically in the range of 20 – 25 years. On the other hand, due to changes in worldwide economic conditions, in particular the current low price of oil, it is more cost effective for operators to continue exploiting assets beyond their 20–25-year designed life instead of investing in a new asset. Experience shows that for many assets at the end of this period, they appear to have the structural capacity to continue their operative life. The challenge then is to quantify and qualify the true residual capability of the asset: to continue to safely use ships and offshore platforms that have reached the end of their designed lifetime and have an extended use approved by statutory authorities.

The lifetime extension of the asset should be undertaken on the basis of the present design load rules. By verifying the model with the current design loads as imposed by the most recent Rules, it is possible to assign a theoretical remaining lifetime. This is crucial as with the case most clearly seen with offshore assets, API RP2A has evolved to consider a 25-year return period as insufficient and in fact the asset should be designed now for 100-year return period. This, Potty and Mohd Akram (2009) write, increases the loading on offshore assets from 2–4 times the recommendations from early editions of the same guidance. Aeran et al. (2017) propose a new framework for the life-cycle assessment of structural integrity for offshore jacket platforms, specifically with the view to life extension. Guidance for operation of assets beyond their original design requirements can be found in e.g. NORSOK N-006, "Assessment of Structural Integrity for Existing Offshore Load-Bearing Structures (NORSOK, 2015)." Further, in the ISO community, a new guideline on structural integrity management is under preparation.

2.4 Challenges and Opportunities

Recently Ibrahim (2015a–d; 2016a–b) undertook an extensive six-part review of the current state-of-the-art in ship and offshore structural life assessment based on over 1,800 references: "Overview of Structural Life Assessment and Reliability Parts I–VI." Ibrahim (2016b) concluded that despite the volume of research invested in structural life assessment and structural health monitoring, in nearly all instances these two areas had not been integrated. Current approaches for mapping motions and loads into stress responses can be advanced (using for example coupled fluid structure interaction hydroelasticity) to include the research advances in the areas of fracture mechanics and probabilistic design, providing an integrated solution for ship and offshore structure design. In particular, there is a need to develop probability and reliability methods for extreme values where Monte Carlo simulations combined with the path integral approach benefit computational speed with accuracy (see for example, Kougioumtzoglou & Spanos, 2013).

Similarly, Caines et al. (2013) in looking at the treatment of corrosion under insulation noted that while risk-based inspection (RBI) is well documented and becoming standard practice in industry, the methods are based on simplified probability and consequence modelling. More long-term testing of materials and laboratory standards as well as better probability models are required if RBI is going to be accurate. New inspection techniques to determine corrosion rates from on-line monitoring need to be developed.

Shafiee and Animah (2017) conducted an extensive review of the literature published between 1986 and 2015 on the mechanisms of life extension of assets across a wide range of sectors. The breadth of this review is captured in their figure reproduced in Figure 1.

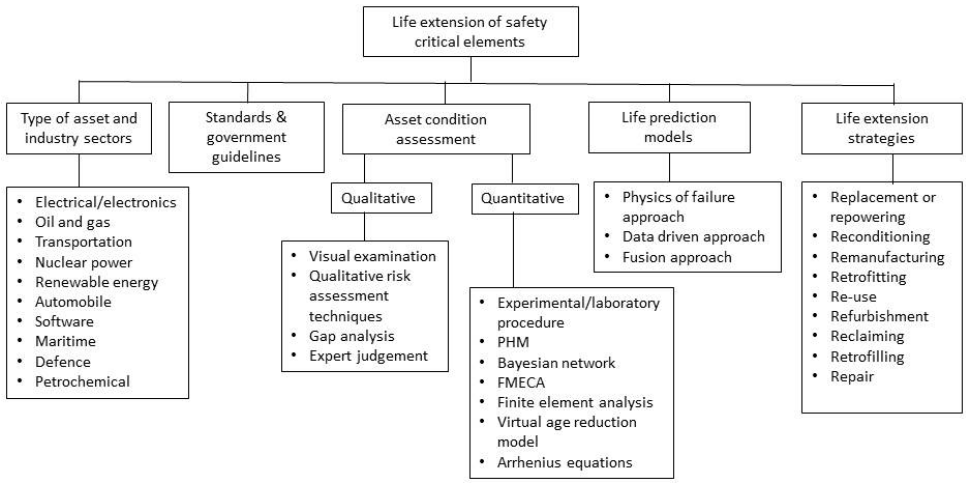

Figure 1. A framework to classify the literature on life extension of safety critical assets (Shafiee & Animah, 2017).

While their review concentrated on life extension, the decision supporting framework by necessity incorporates condition assessment strategies and life prediction models for life-cycle structural assessment. They identified that while there was a sizeable amount of research on life extension of safety critical assets there were many unresolved issues for future study, namely:

1. A lack of integration of life extension considerations within the more studied areas of design, installation, operation and maintenance; this could be used to improve life-cycle decision making. Furthermore, life-cycle management should include the combination of techno-economic and social effects on decision making.
2. A need to better understand alternative strategies to prolong and manage structural health in "reconditioning," "remanufacturing," and "use-up."
3. Much research has focused on the development of condition assessment tools. However, there is a need to understand their limitations, the constraints under which they should be deployed, and how these tools change their effectiveness for different applications.
4. Accurate lifetime prediction models capable of determining residual life are still lacking.
5. Despite life extension being deemed as economically attractive, little research has focused on how a life-extended asset's maintenance strategy may change.
6. Asset obsolescence management is a challenge. As the asset is operated beyond the end of its life, integrating state of the art control and automation systems to support safe operation may not be achievable or economically viable.
7. Quality of data supporting life-cycle assessment and management must be improved by the investment in platforms, policies, and procedures to store and manage the data acquired during the asset's life-cycle.
8. Little attention has been paid to the study of human and organizational challenges such as an ageing workforce and loss of expertise and the retention of historical information and knowledge about an asset's past. In preserving such knowledge there is a primary question as to how to "capture tacit knowledge and transfer it to successors" (IAEA, 2006).

9. As already available in the electrical/electronic, offshore oil and gas, and nuclear power industries, more case studies and analysis of best practice on successful life-cycle and life extensions examples should be centered on offshore renewables and shipping.

Shafiee and Animah's conclusions are echoed by Aeran et al. (2017), who add that where issues related to technological, knowledge-base and operational ageing are concerned, the incorporation of these elements in decision-making is most important for future research.

Ibrahim (2015a-d, 2016a-b) identified key areas for future research in life-cycle assessment and management for ship and offshore structures in each of his six studies.

- Given the importance of initial flaws or cracks, fatigue life assessment should be based upon fracture or crack propagation approaches.
- Designers and builders should revise rules for tankers based on climate changes and extreme weather conditions.
- IACS characteristic wave bending moment should be revised (following Bitner-Gregersen et al., 2011).
- Pierson-Moskowitz spectrum should be revised to accommodate extreme weather conditions.
- Consider corrosion and hydrogen embrittlement in life assessment of ocean structures.
- The dynamic progressive failure of marine structures under extreme loads (slamming, sloshing, grounding, collisions, etc.) needs more attention to account for the random response and nonlinear processes.
- Extend the quasi-static analyses to impact analyses.
- Application of structural reliability methods to consider the extreme tail events with the additional influence of corrosion, hydrogen embrittlement, joints and welds.
- Phenomenological models of preload fasteners and joints should be integrated with the probabilistic description of failure.
- For composites, delamination under impact should be included in reliability analyses.
- Conduct sinusoidal and random excitation tests to monitor and measure the evolution of structural joint's dynamic characteristics under preload.
- Continue development of methods for analysis of multiaxial fatigue on ship structural details as the current tools are insufficiently validated or developed: what is the fatigue response of complex welded details under loading conditions with variable time-dependent principal stress?

Despite these major reviewers' comments on the sparsity of publicly accessible integrated research into fatigue life assessment and lifecycle management, a joint industry project (VALID) between the U.S. Coast Guard and MARIN provides an example of such a holistic treatment whereby the state of the art practice in fatigue assessment and implications on vessel lifetime management has been tested against reality (Stambaugh et al., 2014). This case study showed the importance of capturing and quantifying the operating wave environment. It was recommended that future fatigue damage modelling should include impact loading and whipping responses; that FEA analyses could be used to monitor fatigue damage accumulation in key areas for operator benefit and route planning (e.g. Frangopol & Decò, 2015); and that small investments in fatigue life predictions lead to large improvements in reducing total operating costs and greater returns on investment when spectral fatigue analysis is included early in the design stage. Additionally, Soliman et al. (2016) suggested a probabilistic approach for integrating inspection, maintenance, and repair actions for a fatiguing ship's side shell detail,

optimizing the action against minimal life cycle cost and maximizing service life. They showed how sensitive optimal decisions were on accurate costs for structural failure and cost and time for inspection techniques.

2.5 Conclusions

Since ISSC 2015, there has been increasing research on the incorporation of structural life-cycle assessment practice for ship and offshore structures and a transfer of knowledge across industry sectors. Much of this is driven by the advantages in capital expenses and operating expenses, advances in sensing technology and condition monitoring practices, better material knowledge and construction practices and increasingly attractive life extension opportunities for ageing assets.

Class societies and standards are evolving and starting to embrace technological advancements that can better capture operational profiles, structural response and statistical methods for material- through to asset's structural-life prediction.

Two major reviews have identified current limitations, challenges and opportunities in issues related to life-cycle assessment of an asset's structure, but it is clear that the need for an integrated approach of measuring, modelling, monitoring, analyzing, and forecasting is recognized as being critical for short term actions, long term strategic decision making, and reduced operational costs and that this approach should be incorporated as early as possible in future designs.

Comparing the ship and the offshore communities, it seems that life cycle management and the ability to predict the remaining life of a structure is more matured in the offshore industry which now uses some of the latest methods for model updating including cloud computing on a commercial level.

3. INSPECTION AND MONITORING

3.1 Introduction

This chapter builds upon the ISSC 2003 V.3 "Inspection and Monitoring" (Bruce et al., 2003) and the ISSC 2015 V.7 (Hess et al., 2015) reports and describes current practices and trends in structural inspection and monitoring techniques to optimize maintenance, repair, and operation (MRO) practices.

From the perspective of classification, legal requirements and proper asset integrity management, structural inspections are a necessity to safeguard structural longevity. A leading paradigm is that inspections should be carried out as a result of the intersection between the economic principle of reasonableness and the fact that unnecessary, disruptive and costly inspection and maintenance could result in unintended and expensive downtime, subsequent damage, and inherent risks.

3.2 Inspection

At this moment, (empirical) inspection practices are deployed as the key instrument to identify and mitigate system anomalies and unanticipated defects. In general, the outcome of periodical and event-driven asset inspections provide input for repairs and the future determination of the components' (compiled) probability of failure. Subsequently, the latter can be combined with the consequences of failure to provide a risk profile and future inspection scheme to prevent incidents, maintain a specific safety level, and to enhance design and operational practices (such as future inspections) through feedback. Although this structured method is a step forward from overall inspection with some specific focus on hot-spots, inherently, it is still a reactive measure.

The advances in sensing and monitoring technologies and inspection methodologies (e.g. risk-based inspection) are now being combined in state-of-the-art methodologies, such as advisory hull monitoring systems (AHMS). The expectation is that this will trigger a paradigm-shift into a more holistic and pro-active system approach. This is nicely captured in the model of drivers for predictive maintenance by Adams (2007). Figure 2 shows these perceived benefits of structural health monitoring (SHM) as a methodology for pro-actively managing the structural and functional integrity during the useful life of physical assets. These benefits consist of:

1. Reduction of initial risk after fabrication;
2. Optimization of the system performance;
3. Extend asset life;
4. Reduce the logistics burden without introducing risk;
5. Manage risk as wear accumulates;
6. Impact design to reduce risk and conservatism;
7. More ambitious design.

In addition, the highly stochastic nature of the aging process has provided a multitude of models and inherent uncertainties, which emphasize a probabilistic foundation. Despite considerable developments in both structural reliability theory and computational methods, the probabilistic approach has gained little ground on the deterministic practices (Van den Berg et al., 2014). The lack of acceptance of probabilistic methods for the assessment of aging may be assigned to the complexity and computational effort concerned with the approach, and the long absence of research into practical applications.

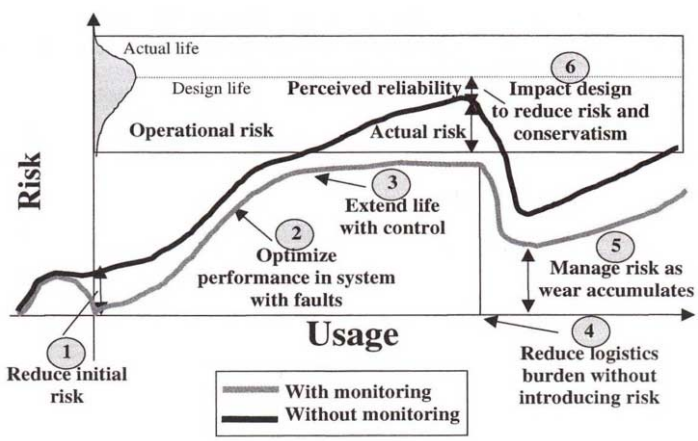

Figure 2. Potential Impact of Structural Health Monitoring (Adams, 2007).

Consequently, most operators of ship and offshore structures base decisions regarding Inspection, Repair, and Maintenance (IMR) efforts primarily on empirical procedures (ergo: inspection). Hence, structural inspection practices are deployed as the key instrument to assess the actual asset integrity by identification and mitigation of system anomalies and unanticipated defects to ensure structural longevity and an adequate level of safety to comply with statuary rules and company policy. The general perspective of inspections is still (and logically) based on empirical findings. Current practices therefore consist of the a-priori determination of technical and organizational measures to ensure future economic system effectiveness and safety. Measure optimization is generally done by posteriori analysis on correlation and cau-

sality of usage, external influences, and costs to improve the knowledge of physical system degradation, predict the future behavior, and further refine the measures accordingly.

However, by integrating this understanding of degradation propagation with the classification of the inherent risks of this process and the consequences of failure and the addition of (hot-spot) monitoring, a far more specific inspection plan can be made as an alternative for prescriptive practices - which could be unsuitable for a specific asset design and/or operational context (over- or under stringent). In essence, this is the foundation upon which practices such as risk-based inspection (RBI) are based (Tammer and Kaminski, 2013).

It is clear that the application of such (integrated) methodologies asks for sound inspection and monitoring techniques and proper data acquisition, transfer, processing, and management, which are outlined in the following paragraphs.

The offshore industry has been aware of the importance of Inspection, Maintenance and Repair (IMR) to the long-term structural integrity management (SIM) of marine and offshore structures. The aim of an inspection is to detect defects and their sizing. In structural integrity assessment such as engineering critical assessment (ECA), the results are generally evaluated in terms of acceptable assessment criteria (BS 7910, 2013). However, inspections on offshore structures are costly, and can be hazardous and often difficult because of the access limitations. In order to obtain optimized inspection schemes, risk and reliability techniques, generally referred to as risk-based inspection (RBI) schemes, have been used. Among a variety of RBI strategies available, quantitative approaches are preferred in engineering practice for the rationality in direct assessment of the probability and consequences of failure. A state-of-the-art example is the inspection planning approach for fatigue cracks which couples fracture mechanics with Bayesian updating (Chen et al., 2011). The detected crack size is also an important input parameter in this RBI approach.

For the capability of accurately identifying damage and irregularities in materials, non-destructive testing (NDT) has been introduced into a wide range of industries for structure inspection and health monitoring. There are many NDT techniques, each with their specific capabilities and limitations. The particular choice of a NDT technique is application specific, dependent not only on the structure and material of the component to be examined, but also on the nature of the defects (crack, corrosion, erosion, etc.). The studies initiated by the offshore industry and academia to apply and improve NDT techniques for various ships and offshore structures are fruitful. Ibrahim (2015) made a review on the NDT technologies of marine composite structures. Raišutis et al. (2016) performed a comprehensive overview of NDT for defects in wind turbine blades. Constantinis et al. (2016) proposed a new approach for underwater hull inspection of floating offshore assets. Feng et al. (2016) reviewed NDT techniques applied to in-line inspection for defects in pipeline girth welding.

NDT techniques for general applications include visual inspection, magnetic testing (MT), liquid (or dye) penetrant inspection, radiography (X-rays or gamma-rays), ultrasonic testing (UT), eddy current (EC), acoustic emission (AE), thermography and so on. Among those NDT techniques, time of flight diffraction (TOFD), alternating current potential drop (ACPD), and alternating current field measurement (ACFM) are often used for assessing fatigue and weld defects. Magnetic flux leakage (MFL) is a magnetic method for detecting corrosion, and pitting in metallic structures, most commonly pipelines and storage tanks. Some methods are only able to measure the length of a defect, while others also have the capability to measure the height of a defect. The methods also vary in their capacity to characterize a defect, i.e. to determine if a defect is voluminous, planar, sharp etc. Different physical principals cause differences in performance on which the methods depend and in conditions of application. To inspect a structure fully, the use of more than one method is often required. For example, the UT helps in the detection of internal defects while the EC examination is more appropriately applied in the detection of surface breaking defects. However, information from

different NDT systems can be conflicted, incomplete, or vague. The concept of data fusion can be used to combine information from multiple NDT techniques and help in decision making to reduce human errors associated with interpretation.

NDT rules and guidelines can be found in the NDT yearbook by British Institute of Non-Destructive Testing (BINDT, 2017), NDT handbook by the American Society for NDT (ASNDT, 2012), and ASM Handbook by American Society for Metals (ASM, 1989). ABS also published guidelines for NDT Inspection of Hull Welds (ABS, 2014c) in which radiographic, ultrasonic, liquid penetrant, magnetic particle, ACFM, as well as eddy current NDT techniques are included. The American Petroleum Institute (API) published a Recommended Practice RP 580 (API, 2009) for risk-based inspection of pressure containment systems, pipelines, storage tanks, and other process equipment. NDT is also mentioned in BS 7910 (2013) and API 579 (2016) for engineering critical assessments (ECA).

The outcome of NDT-inspections and the quality of the information gained is limited by the Probability of Detection (PoD) and Probability of Sizing (PoS), which are highly influenced by these constraints:

1. The deployed methodology and technology. References that denote specific PoD/PoS-curves for different inspection methods and -scenarios are quite limited;
2. Inspector competency. Often the framework for both competency/qualification and execution is limited.
3. If qualified, intrinsic human limitations in observation and interpretation (still) play a significant role;
4. Circumstances during inspection execution, such as non-ideal conditions due to limited visibility, weather etc.
5. The inspectability of details due to accessibility limitations.

Stringent codes and the deployment of complementary techniques are used to limit the first constraint. More focused (such as RBI) and automated inspection and monitoring techniques are gaining more and more interest to rule out constraints 2 to 5.

3.3 Monitoring techniques

While inspection supplies discrete measurement at points in time, the monitoring system gives actual time histories of measurands in terms of conditions on structures, equipment/machinery, cargo, ballast, metocean, and so on. Maritime and offshore industries are developing a strong interest in on-board and real-time monitoring systems in line with a noticeably growing trend in the Internet of Things (IoT), Big Data, machine learning, SHM, and digital twin. The monitoring system is supposed to provide essential or useful information for optimizing Maintenance, Repair, and Operation (MRO).

Also, the latent need to integrate (or enhance) the functionality of inspection techniques with condition monitoring activities and pro-active management strategies (e.g. RBI) was emphasized upon in the conclusion of the ISSC Fatigue and Fracture Committee III.2 (Horn et al, 2009).

"*The re-assessment of fatigue loading is important and fatigue hotspots need to be re-evaluated, in order to ensure a safe operation. The (class) societies today are working in order to peruse guidelines and recommendations, however there are still several uncertain questions that have to be fulfilled, like to judge if an old unit has operated within the design conditions specified. The fast development of monitoring technology opens new possibilities for continuous recording and new platforms today can be monitored in order to ensure that the unit operates within design conditions specified. However, monitoring of platforms will*

create tremendous information and one main challenge would be how to analyze the data and draw meaningful conclusions." Section 0 will focus on the data paradigm.

The ISSC 2015 V.7 report recommended that SHM systems need to be expanded to address real structures. The strong trend toward using monitoring data in various aspects is a driving force to apply the monitoring system to operating ships and structures. Promising examples are found in:

- The Monitas (Monitoring Advisory System) Joint Industry Project, which has concluded and delivered an automated measurement system and data analysis procedure to monitor the fatigue lifetime consumption of FPSO hulls. The background of the Monitas system is described by Kaminski (2007) and the Monitas methodology and -application are discussed in more detail by Aalberts et al. (2010), L'Hostis et al. (2013), and Van der Meulen and Hageman (2013).
- The CrackGuard Joint Industry Project hinges on the principle of Quantitative Non-Destructive Evaluation (QNDE) for automated in-service inspection and monitoring. Current practices after anomaly detection consist of ultrasonic testing, magnetic and/or radiographic testing and sometimes strain monitoring on critical locations. The CrackGuard project goal consists of precompetitive research and the development of an affordable system for (wireless) monitoring of detected fatigue cracks (Van der Horst et al, 2014).
- The Japanese Joint Industry Project, i-Shipping, supported by Japanese government between 2016 and 2020, is aiming to apply the digital twin concept for estimating vessel performance in actual service condition (Yonezawa et al., 2017). In this project, SHM for container ships, in which data obtained from hull and metocean monitoring are shared, is addressed to enable safer maneuvering with consideration for hull strength and rational design.
- VALID I and II Joint Industry Projects led by MARIN have employed structural hull and metocean monitoring to determine fatigue life predictions on a range of U.S. Coast Guard ships and vessels, to inform remaining service life estimates and maintenance needs (Stambaugh et al., 2014 and Drummen et al., 2017). The project includes hull structure monitoring on two U.S. Coast Guard cutters, one of which has been instrumented for strains and ship motions as part of an ongoing hull structure monitoring effort of long-term monitoring to support life-cycle decisions and improve supporting technologies. Other aspects of the project include development of the technology of the ship as a wave buoy to measure the actual sea states encountered, better understanding of fatigue, and structural reliability assessment.

With the development of state-of-the-art technologies in terms of the monitoring system, the classification societies' standards and guidelines on conventional hull monitoring system have been formatted well for ship structures. On the other hand, SHM systems for offshore structures are currently being more and more mature. These are described in the following subsections.

3.4 Hull monitoring systems

Hull monitoring systems are intended to close the gap between design and operation, i.e. in design the vessel is designed to withstand still water loads and wave loads, while in operation the hull monitoring system should work as a dynamic loading computer and verify the static loading computer on board when installed. The hull monitoring system can include sensors for several purposes, e.g., global structural response of the hull, local structural response of the hull, motions and accelerations, pressures, sloshing and slamming, ice response monitoring, environmental monitoring, comfort and vibration.

The measured signals are typically split into given time intervals for data processing and the results from the data processing for each time interval are stored. The filters are initiated at the start-up of the hull monitoring system, and are continuously active as long as the system is running during normal operation. The following statistical parameters may be calculated for each of the selected response parameters: maximum value, minimum value, mean value, standard deviation, skewness, kurtosis, mean zero crossing period (or mean crossing up count), maximum peak to peak values, and number of observations used to calculate statistical parameters.

The hull girder stress monitor may warn a vessel's operating personnel that the hull girder stresses, resulting from still water loads and wave loads, are approaching a level at which corrective action is advisable. To reduce the risk of local bow damage due to slamming, the whipping response from the global strain sensors may be considered and an alert would be provided to the operators if the levels exceed some predetermined damage threshold value. The accumulated fatigue damage may be estimated based on the stress response histogram, a relevant stress concentration factor (K factor) and the S-N curve. Miner's cumulative damage techniques, in conjunction with rain-flow counting, are typically used for fatigue life estimation. Alarm settings refer to warning values for global strain sensors, motions (roll and pitch), and accelerometers.

The results from the calculations for each time interval may be arranged in such way that a sequence of the latest data from each individual sensor can be displayed as a trend. The sequence should at least include data from the last few hours for displacement ships and 30 minutes for high-speed light craft. One approach is to use a four-hour data sequence from each individual sensor to form the basis for a forecast trend prediction of the expected response from each individual sensor for at least the half or the next hour. When the signal from an individual sensor exceeds a certain fraction of a specified threshold value (e.g., 80%) for that sensor, the expected time to reach the threshold value can be predicted based on trend analyses. If a critical limit level will be expected to be reached, then changes to the vessel's operation may be advisable. This decision process may be enhanced through the use of an artificial intelligence algorithm or an expert system.

The specific requirements for a hull monitoring system by different classification societies are listed in Table 1 (ABS, 2015; ABS, 2011; BV, 2017; CCS, 2015; DNVGL, 2017a; KR, 2017; LR, 2012; NK, 2017).

The use of structural hull/health monitoring (SHM) systems is thereby becoming a key discipline for re-assessing of offshore structures due to the fact that SHM systems have the potential for extensive increase in the lifetime of ageing platforms, reduction of maintenance costs, and at the same time reducing uncertainties and increase of safety. While used rather interchangeably, "Hull" monitoring involves acquiring data about the hull through sensors while "Health" monitoring includes the use of the collected data to determine meaning and thus insight into the "health" of the structure. For the purposes of this report, SHM will denote "Structural Health Monitoring" according to the preceding definition.

Today, the SHM systems range from "simple" updates of FE models based on measurements to advanced models, which incorporate the newest analysis methods of today including nonlinear system identification, expansion processes, probabilistic FEM updating, wave load calibration, quantification of uncertainties (Bias and CoV), and re-assessment analysis with input to Risk- and reliability Based Inspection planning (RBI). The more advanced components of the SHM systems combine the latest developments from a number of other related disciplines such as from Electrical Systems, Control Systems, Machine Learning, Data mining, etc. An overview of some of the features forming part of the current state of SHM systems (marked by heavy dashed lines in the lower right quadrant) and future/less matured features is given in Figure 3.

Table 1. Requirements for hull monitoring system by classification societies.

Year	ABS 2015	ABS(ice) 2011	BV 2017	CCS 2015	DNVGL 2017	KR 2017	LR 2012	NK 2017
Notation	HM1 (motion) HM2 (stress) HM3 (Voy. Data)	ILM	MON-HULL	HMS	HMON	HMS	SEA(HSS) SEA(ICE)	HMS
Strain Range Acc range	x x	x x	±2000μ ±2G	x ±2G	±2000μ ±2G	x ±1G	x ±2G	x ±2G
Angle range	x	x	x	-90º~+90º(roll) -45º~+45º(pitch) -180º~+180º(yaw)	-90º~+90º(roll) -45º~+45º(pitch) -180º~+180º(yaw)	x	-30º~+30º(roll) -10º~+10º(pitch)	
Frequency Range (Strain/Acc)	0-5Hz/0-5Hz	0-150Hz	0-1Hz/ 0.2Hz-1Hz	0.01-3Hz(motion) 5-100Hz(slamming) 30-1200Hz(sloshing)	0.01-5Hz(motion) 5-100Hz(slamming) 30-1000Hz(sloshing)	0-5Hz/ 0-5Hz	0-5Hz/ 0-5Hz	0-5Hz/ 0.5HZ (fw.0~100Hz)
Sampling Rate	3 times the maximum F.R.	More than 150Hz	20 times the low-pass filtering freq.	20Hz(motion) 500Hz(slamming) 3000Hz(sloshing)	20Hz(motion) 300Hz(slamming) 2000Hz(sloshing)	3 times max F.R.	4 times max F.R.	x
Accuracy St./Acc/ang. Setting/ Calibration	5μ/±0.01G in a known LC/ annually	1μ/x in a known LC/annually	20μ/x in a known LC/-	x/0.01G/0.5º in a known LC/-	5μ/±0.01G/0.5º in a known LC/annually	20μ/1% in a known LC/annually	5μ/0.02G in a known LC/annually	10μ/0.01G in a known LC/-
UPS	4h	30 min	30 min	10 min	10 min	10min	x	x
VDR	IMO Res.A.861(20)	x	IEC61162	IEC61162	IMO Res.A.861(20) IEC61162	x	IEC61162	x

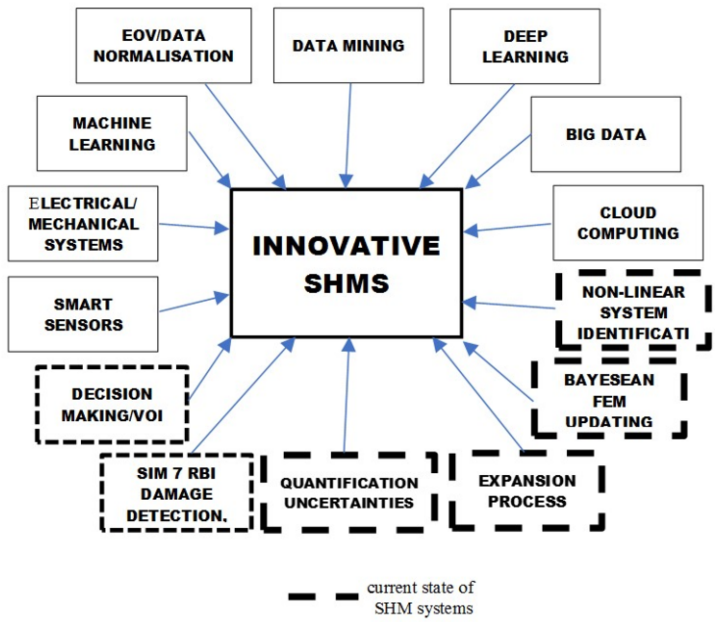

Figure 3. Innovative SHM systems reproduced from overview by Tygesen et al. (2016).

One issue with field measurements is that they normally generate large amounts of data that have to be processed. However, the analysis of huge data sets from the SHM systems can now be accomplished using the latest development within Big Data processing by cloud computing solutions, i.e. now available computational power enables extracting of information from measured data, which was not possible just a few years ago.

When designing SHM systems, one has to distinguish between platforms which are "born" with measuring devices installed and platforms where measuring devices are post-installed. This section presents some examples of how field and laboratory measurement can feed into the SHM system models of today allowing for increased accuracy in areas such as fatigue life estimations. The focus is on systems, which are based on post installed devices allowing for evaluation of existing platforms including their possible lifetime extension.

The accumulated fatigue damage is known to be one of the main factors, which dominates the "structural health" of a ship or offshore platform exposed to significant wave loading. Hence, when trying to extend the life of an existing platform beyond the design fatigue life, an accurate determination of the accumulated fatigue life is of major importance.

One of the simpler and oftentimes efficient methods of increasing the predicted fatigue life of a structure, is to reduce some of the conservatisms inherited in the existing fatigue analyses. Rosen et al. (2016) used data from accelerometers mounted on the topsides of a wellhead platform and a mono-tower platform. The two platforms were positioned at 100 m and 52 m of water depth, respectively. Based on measured data covering years for both platforms, the natural period and damping of the platforms were determined. Relative to the 2% structural damping prescribed by the code (API), significant increases of damping could be justified by the measurements and predicted fatigue lives could be increased correspondingly.

When determining the fatigue lives using standard "code-based assessments" there will often be significant conservatisms on the action side. A direct measuring of the actual loading is usually not feasible due to sensor/data limitations. To overcome that problem, Perišić and Tygesen (2014) presented an evaluation of two methods for load calibration based on a lim-

ited number of measurements of dynamic responses, i.e. modal expansion or Kalman filter-based methods. Both methods were found to provide relatively accurate estimations of loading allowing for wave load calibration using the single measuring points positioned on the topsides. The advantages and disadvantages of the load estimation methods are summarized in Table 2. Further, it is noted that the use of calibrated loading reduces the uncertainty in the load modelling significantly, which is a significant input to the RBI models.

Table 2. Pros and cons using Kalman filter or Modal expansion methods, Perišić and Tygesen (2014).

Property	Kalman filter-based method	Modal expansion method
Computational complexity	Low	High
Stochastic model	Yes	No
Number of estimations	Operational	All
Operational in real time	Yes	Near-real time
Structural model complexity	Low	High

Skafte et al. (2017) have worked on a more direct methodology for full field strain estimations using a limited number of vibration sensors. These sensors can be post installed on existing platforms above water minimizing the cost for field measurements. The main idea is that the measured response of an offshore structure exposed to wave loading can be split into two parts using complementary filters, i.e. a low frequency response imposed by quasi-static action from the waves and a high frequency response given by the modal properties of the structure. The low frequency part of the signal is decomposed and expanded using Ritz-vectors that represent the displacement of the structure imposed by wave loading while the high frequency part of the signal is decomposed using experimentally obtained mode shapes and expanded using the analytical mode shapes. The expanded signals from the two frequency domains are added together to the full strain history. Skafte et al. (2017) performed physical tests on a 1:50 scale version of a typical tripod jacket platform. The test model was equipped with 12 accelerometers which were positioned on the topsides and top of the center column (i.e. above water). The analytical Ritz vectors were determined by adding a static load to an FE model of the test setup. The theoretical/experimental work shows promising results regarding estimation of the strain history in the full structure using a limited number of measuring points. However, for full scale structures, the wave force will be acting at frequencies lower than 0.05 Hz requiring that the accelerometers have a very good signal-to-noise ratio in the frequency region. One way to overcome this issue can be to combine accelerometers with GPS sensors as these often are superior to accelerometers in the very low frequency region.

An overview of the current state-of-the-art for predictive modelling using machine learning for maintenance is given in Tygesen et al. (2018). The focus of the paper is the creation of a validated model of the jacket structure, including an estimate of the wave loading, updated with information from the measured sea state. Measurements from a jacket installed in the North Sea is used for validation and good agreement is found. One of the main experiences gained from working with SHM is that the uncertainties in the prediction models are reduced. Any reduction in uncertainties results in cost reductions for maintenance.

3.5 Data acquisitions, transfer, processing, and management

Diagnosis of structural integrity is implemented based on NDT inspection and/or structural hull monitoring. Future behavior of damage/degradation and the remaining useful life of an in-service system are predicted based on the diagnosis result and prognostics methods. Inspection and sensor data also facilitate the prognostics which use data-driven and physics-based approaches. Data-driven approaches use information from previously collected data (training data) to identify the characteristics of the currently measured damage state and to predict the

future trend. The data-driven approaches are divided into two categories: (1) artificial intelligence approaches that include neural network and fuzzy logic and (2) statistical approaches that include gamma process, the hidden Markov model, and a regression-based model. Physics-based approaches assume that a physical model describing the behavior of damage is available and can be combined with measured data to identify model parameters and predict the future behavior. Model parameter identification is performed with an estimation algorithm, such as the Kalman filter and Bayesian method (An et al., 2013).

The capabilities of inspection tools collecting precise defect data and sensing devices monitoring actual conditions are vital to diagnosis/prognosis. The higher the data precision is, the narrower the safety redundancy, meaning a lower cost for structural construction and maintenance. Accuracy and reliability are two essential aspects of inspection and monitoring data.

Accuracy in inspection is established by determining if all the defects above a certain size are detected and reported, as well as the precision of the detected defect size measurement of depth and length. Thus, the PoD and PoS are required. The reported dimensions of a defect may be increased by sizing errors. Risk is related to both the consequences and probability of failure. The required inspection reliability and the rigor with which it is determined should be agreed between the interested parties and documented: see ASME Boiler and Pressure Vessel Code, Section V (ASME, 2010) and ENIQ Report NR 31 (European Commission, 2007). Provisions for NDT detection precision are given, for example, in DNV-OS-C101 (DNV, 2012), NASA-STD-5009 (NASA, 2008), ECSS-E-ST-32-01C (ECSS, 2009), and ASME Boiler and Pressure Vessel Code, Section XI, Mandatory Appendix VIII (ASME, 2010). Precision of NDT inspection can usually be improved if complementary techniques or repeated inspections are conducted.

Installation, calibration, and the usage environment of sensors should be carefully taken into account, since accuracy in monitoring with the sensors is influenced by them. The installation and calibration procedures of sensors in a hull monitoring system can be submitted to a certification society for approval. For fiber-optic sensors that have been commonly used in a hull monitoring system, standards or reports are helpful to understand their capabilities or limitations (e.g., IEC 61757-1-1, 2016 and SAE AIR 6258, 2015). Sensor faults substantially affect sensor data and compromise the reliability and accuracy of SHM. The integrity of the sensor data needs to be preserved to enhance the reliability and accuracy of SHM system outputs as well as the robustness of algorithms implemented for SHM (Smarsly et al., 2016).

Represented by IoT technologies such as cloud computing, big data analytics, wireless intelligence and robotics, the current trend of automation and data exchange (called “industry 4.0”) has brought great changes to traditional NDT inspection. The inspection tool can be made “smarter” invoking state-of-the-art machine leaning techniques based on big data acquired, or more specifically by re-designing the software to incorporate efficient machine-learning algorithms. For example, it is very practical to train and test magnetic flux leakage (MFL) tools to accurately interpret a feature (such as its dimensions: length, width, and depth) indicated by reflected signals, using a known collection of measured defects. Extensive testing/learning can be performed before the MFL tool undertakes an inspection task. Knowing the actual dimensions of a feature makes it relatively easy to make simple correlations of signals to actual anomalies found in the material. When signals in an actual inspection have similar characteristics to the signals found during testing it is logical to assume that the features would be similar. Specific algorithms should be devised for calculating the dimensions of a defect feature. A carefully designed artificial intelligence network then selects defect candidates and reduces the number of indications to be manually checked. The display of the data, using at-times proprietary software, will allow the analyst to quickly access the relevant portions of the data and enter conclusions. With the anomaly reported in a simplified fashion as a cubic feature of estimated length, width and depth, the effective area of metal loss can be calculated easily (Rao and Jayakumar, 2012).

Recent advances in NDT inspection also include signal digitizing and image processing techniques, and model-based optimization. There is a trend of combining multiple tasks and NDT techniques (Karuppasamy et al., 2016). For example, the pig for in-line inspection of subsea pipelines (Figure 4) uses array sensors, image fusion, inversion approaches, and model-based investigations to significantly enhance the application of the NDT techniques for material evaluation. Miniaturization of sensors, wireless sensor networks, and multi-sensor fusion techniques extracting different data from different regions by different sensors are expected to further enhance the capability of the tool. In order to optimize the capability of corrosion inspection and wall thickness measurement, the compound NDT techniques such as MFL and UT, each enhancing and extending the capability of detection and sizing of the tool, have led to increased values regarding the PoD and confidence levels for sizing and feature identification.

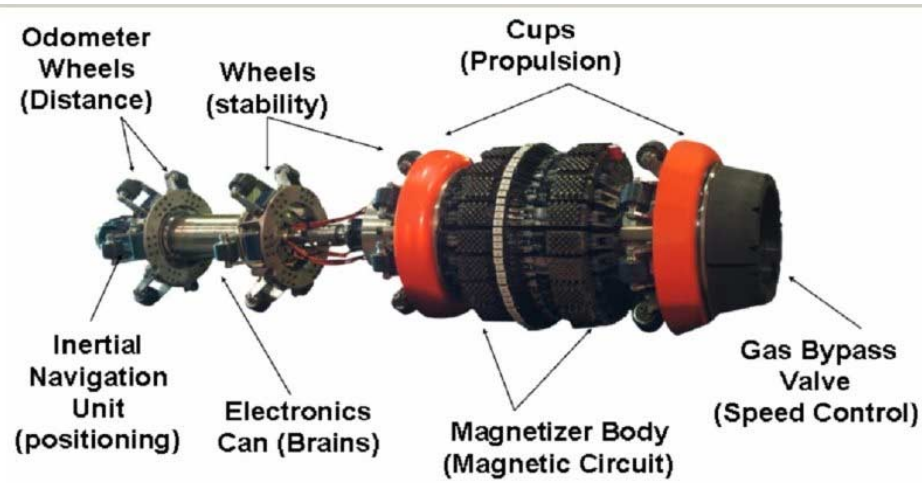

Figure 4. Pig used for in-line inspection for pipelines (Orabi, 2016).

The field feedback can contribute to the new NDT system's maturity as well. Since it is impossible to replicate all the defects that exist in all cases in the field in the shop, good communication between the inspection operators and the R&D staff as to what was reported and what was visually observed in the field is even helpful to the new inspection system's redevelopment. As electronics and software become more and more powerful, one trend we may expect is a new generation of "smart robotic" NDT inspection system (Figure 5) which will offer automated efficient inspection with optimized tool performance and precise defect identification (Shukla and Karki, 2016).

Ships and offshore plants are increasingly using systems that rely on digitization, integration, and automation, which requires paying more attention to data management and cyber risk management on board as well as on shore. Two international standards for collecting shipboard data are under development. One is ISO/DIS 19847 (ISO, 2017a) whose scope is to specify requirements for a shipboard data server that is used to collect data from other onboard equipment or systems and further share the collected data in a safe and efficient manner. Another is ISO/DIS 19848 (ISO, 2017b) which is intended for implementers of software used for capture and processing of sensor data from the structure of the ship and onboard machinery and equipment. IMO has developed guidelines that provide high-level recommendations on maritime cyber risk management to safeguard shipping from current and emerging cyber threats and vulnerabilities (IMO, 2017). A joint industry project is offering guidelines

(Fitzsimons, 2018)

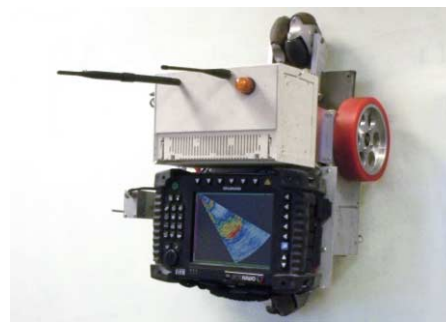

(AWI, 2018)

Figure 5. Robotic ultrasonic inspection systems

on cyber security onboard ships which are aligned with the IMO guidelines and provide practical recommendations on maritime cyber risk management (BIMCO et al., 2017).

In addition, services on data transfer and data platform are being enhanced to handle large amounts of data from inspection and monitoring. Inmarsat is operating the Fleet Xpress which offers high-speed broadband maritime satellite communication. Some certification societies and maritime companies are providing data platform services, such as Veracity (DNV GL), ShipDC (Class NK), and kognify (Kongsberg).

3.6 Conclusions

Inspection and the monitoring systems are still based on empirical findings and conventional schemes (i.e., HMS), respectively. However, the fusion between multiple inspection data or between inspection and monitoring data helps in mitigation of the limitation, such as low PoD, uncertainty, difficult accessibility, and human error, with each inspection/monitoring technique. IoT technologies and digital twin concepts promote data-driven and physics-based approaches in RBI and the diagnosis/prognosis of structural integrity. Furthermore, maritime and offshore industries are developing an interest in automated inspection and measurement techniques that can not only rule out the existing constraints, but also realize labor-saving or unmanned operations. Standards, guidelines, or services on data acquisition/transfer/platform/security have been recently developed for such a highly digitized system.

One of the main experiences gained from working with SHM is that the uncertainties in the prediction models are reduced. Any reduction in uncertainties results in cost reductions for maintenance.

3.7 Recommendations

- Automated inspection and measurement techniques should be developed to mitigate the existing constraints.
- The applicability of data-driven and physics-based approaches with inspection and measurement data should be investigated and compared in both laboratory and full-field testing to enhance the implementation of the RBI, SHM, or digital twin.
- Efforts to improve the accuracy and reliability of existing inspection and monitoring techniques should be continued, since these are essential for the subsequent processes.
- Reference should be made to standards and guidelines and then feedback provided to the governing bodies to support the safety and reliability activities in the industries.

4. OFFSHORE STRUCTURAL LONGEVITY METHODS AND EXAMPLES

4.1 Introduction

In this chapter, a critical review of the literature has been conducted in relation to application of the principles discussed in Chapters 2 and 3 to offshore structures. This chapter deals with bottom-fixed as well as compliant and floating offshore structures. This implies that structures such as Tension-Leg Platforms (TLPs), Spar buoys, and semi-submersibles are also addressed. As compared to ships, offshore structures are generally more difficult both to inspect and to repair. While ships regularly visit harbor areas with the possibility of dry-docking, offshore structures are typically located in areas far from shore and are only occasionally taken away from their sites.

In the following, the main focus is on steel structures while concrete structures are only briefly addressed.

4.2 Prediction of Longevity

Prediction of longevity and integrity assessments of critical structures and marine systems normally require numerical analyses which simulate the effect of actions on structures and marine systems. In order to cover all hazard scenarios (storm, fatigue, impact, etc.), a comprehensive set of analyses may be required for each structural and marine system.

These analyses must be updated if their assessment premises are significantly altered by surveillance findings. The following basic Key Performance Indicators (KPIs) are therefore typically appropriate for the integrity assessment analyses, NORSOK N-005 (2016): existence of analysis models covering all relevant action scenarios, status of anomalies which have been registered and status of as-is assurance analyses.

A concept which is becoming more and more widespread in connection with asset integrity management (ISO, 2014a and ISO, 2014b) in relation to ships and offshore structures is the so-called “digital twin.” The term “device shadow” is also used for the concept of a digital twin. This concept refers to computerized companions of physical assets that can be used for various purposes. Digital twins use data from sensors installed on physical objects to represent their near real-time status, their working condition, and/or their position.

One example of digital twins can be the use of 3-D modeling to create a digital companion for the physical object. It can be used to view the status of the actual physical object, which provides a way to project physical objects into the digital world. As an example, when sensors collect data from a connected device, the sensor data can be used to update a “digital twin” copy of the device's state in real time. The digital twin is meant to be an up-to-date and accurate copy of the physical object's properties and states, including shape, position, gesture, status, and motion.

In another context, a digital twin can be also used for monitoring, diagnostics, and prognostics. In this field, sensory data is sufficient for building digital twins. These models help to improve the outcome of prognostics by using and archiving historical information of physical assets and perform comparison between a fleet of geographically distributed machines. Therefore, complex prognostics and intelligent maintenance system platforms can leverage the use of digital twins in finding the root cause of issues and possibly improve productivity.

Engineering, procurement, construction, and installation (EPCI) contractors, shipyards, and classification societies already routinely build finite element models of offshore plants and use them to assess initial design strength and suitability and to inform maintenance and life extension decisions. However, these models take time to build and have to be adapted for each purpose.

The digital transformation comes from the speed at which the model can now be built, and the need to build only one complete model that can be used for everything and kept up to date easily. The basic idea is to build a complete digital twin model of the actual asset and a systematic procedure that will keep it updated automatically so that it continuously reflects the actual condition of the asset and equipment.

Within the domain of offshore structures, the main computational engine for the digital twin seems to be based on the Reduced Basis Finite Element Analysis (RB-FEA) model which was developed at the Massachusetts Institute of Technology (see e.g. Grepl and Patera, 2005). This is now commercially available in the form of computer software. This computational engine enables very fast fully 3D structural analysis to be performed. This approach routinely produces structural models faster than FEA by orders of magnitude for industrial-scale simulations, and it also delivers models that are orders of magnitude larger. This speedup and level of detail is a key enabler for the digital twin technology and holds the promise to allow true condition-based modeling of large and critical assets. The relevant structural details can be included in the model, along with inspection-based condition data in relation to crack defects, corrosion, and damage due to impact or collision.

On the input side, the digital twin can interface with connected surveyors and inspection and testing data, and with live data from sensors on the equipment. On the output side, the digital twin will interface directly with structural calculation tools and with risk-based inspection (RBI) planning tools that will enable continual refinement and focusing of inspection effort. An interface with the operator's display panels can also be established.

Cleary, the usefulness of a digital twin depends heavily on the feature that it really is a twin and not an incomplete or inadequate representation of the physical component, structure, or system.

4.3 Main factors influencing longevity

In the North Sea, offshore jacket structures have served the oil & gas industry conventionally under shallow waters with an average life expectancy of 20 years. Some offshore structures have also extended their uses beyond their life expectancy through proper servicing and maintenance to enable oil recovery under feasible economic conditions while emphasizing the importance of safety.

Structural longevity is most commonly concluded through specifications and safety practices of a specific design by the owner (Ersdal, 2005) and (Guedes Soares and Garbatov, 2015). Besides, a thorough safety inspection should be conducted if a structure is expected to be used exceeding its life expectancy. The process will include factors which contribute to structural deterioration such as fatigue, environmental conditions, and loading patterns affected by subsidence.

In Hess et al. (2015) it is stated that the essence of fatigue is confined and collective and it should be included when defining the longevity of an offshore structure. Therefore, the statement explains that the life span of an offshore structure at a particular point will be shortened through exposure to a given load. On the other hand, the longevity of an offshore structure does not necessarily mean the fatigue life of a specific point since local fatigue failure in a redundant structure does not constitute a threat to survival. Considering all factors which affect the longevity of a structure, a universal design and fatigue life larger than fatigue limit for specific points is produced. Nonetheless, in Hess et al. (2015) it is mentioned that "…a survey provided by May (2014), request for more guidance by the codes for managing short fatigue lives and handling corrosion and material degradation." (p. 830).

4.3.1 Corrosion

A number of offshore installations worldwide are approaching or have already exceeded their original design life. Therefore, it is essential to check the feasibility of life extension by estimation of the remaining life and residual capacities. To address the above need, several degradation mechanisms and life extension issues are identified (Aeran et al., 2016). Corrosion is a major cause of structural deterioration in marine and offshore structures. It affects the life of process equipment and pipelines, and can result in structural failure, leakage, product loss, environmental pollution, and the loss of life.

Aeran et al. (2016) present various corrosion wastage models. A modal flexibility-based damage index is introduced to identify the damage state of the offshore jacket structures. Finally, the effect of ageing issues on life extension and significance of introduced damage index is highlighted through a case study.

Corrosion and fatigue are the main mechanisms of deterioration of wind power structures (OWS). The use of corrosion protection systems is essential to reach the expected service life for which a structure was designed. Different protection systems can be used to delay and mitigate corrosion initiation and its related consequences such as safety, structural integrity and service life. A passive approach to corrosion protection involves depositing a barrier layer that prevents contact of a material with the corrosive environment. Active approaches reduce the corrosion rate when the protective barrier is already damaged and corrosive agents come into contact with the metal substrate. Only the combination of both approaches can provide reliable protection against corrosion of metallic structures in harsh environments for the entire design life (Seth et al., 2017).

The application of coating systems is the most common method used to control corrosion. The coating process involves the application of organic coatings, metallic coatings, or the combination of these two types (generally named as a duplex system) on the steel surface. Coating offshore is more expensive than onshore due to several factors including the logistics of transporting manpower and materials to the job site and limited access to the offshore structures due to weather conditions. Expert judgment is of primary importance when coating systems are applied in very specific conditions such as the harsh offshore environment (Seth et al., 2017). Several studies have shown that bird droppings degrade the coating systems via chemical mechanisms (Rafiei et al., 2016; Ramezanzadeh et al., 2011, 2009). In order for offshore structure to maintain structural integrity over their design lives, the use of adequate and cost-effective coating systems will need to be employed in combination with adequate health monitoring and in-service inspection plans.

The paper by Lomasney et al. (2015) is focused on test results from applications of nano-laminated materials (Modumetal) for coating purposes. The aim is to improve the longevity of assets and support increased efficiency over the extended life. Applications for offshore rig maintenance and downhole production lift systems are described. Due to its low-cost, low-capex manufacturing process, this material can possibly provide improvements at comparable or lower cost to conventional metals.

Future work should involve an in-depth scientific study of the corrosion mechanism. Adequate engineering predictive models are recommended in order to assess failure, and thereby attempt to increase the remaining life of offshore assets. The present status of existing models is discussed in (Melchers, 2016), where also examples of developed models for corrosion of steel, aluminum, and copper-nickels are presented.

4.3.2 CP/Anode depletion / Coating deterioration

Fundamental corrosion protection measures for offshore wind power structures (OWS) include protective coatings and/or cathodic protection (CP), corrosion allowance, inspec-

tion/monitoring systems, material and weld design decisions, and control of environment for internal zones DNV-OS-J101 (DNV, 2014) and DNV-OS-C101 (DNV, 2017b). Corrosion protection of an OWS, typically consists of two or three epoxy-based coatings with a polyurethane top coat. However, this can vary according to exposure and location (Momber et al., 2008, 2015). CP is commonly used in submerged and tidal areas.

CP by sacrificial galvanic anodes for OWS is generally the preferential CP system used in industry nowadays. Impressed current cathodic protection (ICCP) is an alternative CP system option; however, it is uncommon today because it is more susceptible to environmental damage and third-party mechanical damage than galvanic anodes systems (DNV-OS-J101, 2014). ICCP typically requires more maintenance and inspection which is costly to provide for unmanned OWSs. Also, there are currently no industry design standards detailing requirements for impressed current systems as there currently are for the galvanic anode systems. Design considerations for impressed current systems were deleted from the scope of DNV-RP-B401 for the 2004 revision. (Seth et al., 2017)

Table 3 shows corrosion zones, methods for corrosion control and forms of corrosion in OWSs.

Undercoats are generally used to increase the overall thickness of the coating system. The top coat protects the layers below it from environmental agents such as UV light from the sun and provides primary abrasion resistance and decoration when necessary (Sahoo et al., 2017).

The two most common deterioration processes for coating are corrosion and fatigue. The most common non-destructive method (NDM) applied to old and new structures is visual inspection (Seth et al., 2017).

For corrosion protection coating systems, the research focus is on new environmentally friendly coatings systems with the ability to behave and adapt in response to environmental demands (Azemar et al., 2015; Carteau et al., 2014). The coatings should be effective in corrosion control for long service lives in a wide range of environments (Figueira, 2016). According to Gibson and Arun (2016) further improvements in the field of deep water construction using composite materials is necessary in order to improve the performance of the offshore industry.

4.3.3 Wear & tear

Assessment of aged offshore structures based on current and historical data is a critical issue for the life extension of offshore structures. The leak-before-break (LBB) approach can also be applied as a robust and cost-effective tool for structural integrity management of offshore structures that are either partly submerged (jackets, semi-submersible, ships), or contain fluids (pipes, pressure vessels). The core idea of LBB consists of guaranteeing that enough time is available between the moment a crack breaks through the hull or wall, causing a detectable leakage, and the moment when the crack becomes unstable, causing a structural failure. Ren et al. (2015) presents a case study of applying the LBB concept for a tether string that is part of the mooring system of an offshore structure.

4.3.4 Fatigue

Life extension of ageing assets is becoming increasingly important for the offshore oil and gas industry. Many pressure vessels in service have reached or are about to reach the end of their design lives, but their continued operation is required until the economic field life is exhausted. Many vessels in-service were designed over 30 years ago, when fatigue assessment was not required by the design standards. Therefore, fatigue reassessment is a critical part of the life extension process. Hutchison et al. (2015) presents reassessment of a benchmark vessel as a case study for life extension of other similar vessels. By determining the commonality

between a vessel and the benchmark vessel, it may be possible with suitable on-going in-service inspection to justify life extension of the vessel without the need for a full fatigue life extension reassessment in every case.

Table 3. Corrosion zones, methods for corrosion control, and forms of corrosion in OWSs (from DNV-OS-J101, 2014)

Corrosion Zones	Corrosion Control	Form of corrosion
Atmospheric Zone		
External and internal areas of steel structures	Coating systems	Uniform and erosion-corrosion, stress corrosion cracking (SCC)
Internal surfaces without control of humidity	Corrosion allowance	Uniform and pitting corrosion, SCC
Internal surfaces of structural parts such as girders and columns	Corrosion allowance should be based on a corrosion rate ≥ 0.10 mm/year	
Critical components (e.g. bolting and other fastening devices)	Corrosion resistant materials are applicable such as stainless steel	Crevice, pitting and galvanic corrosion, SCC
Splash and Tidal Zones		
External and internal surfaces of steel structures	Coating systems	Uniform, crevice and pitting corrosion, microbial-induced corrosion (MIC)
Critical structures and components	Coating systems combined with corrosion allowance	
Internal surfaces of critical structures	Corrosion allowance and the use of coating systems is optional	Uniform, crevice and pitting corrosion
Structures and components below mean water level (MWL)	CP	
Structures and components below 1.0 m of the MWL	Coating systems	Uniform corrosion, MIC
External surfaces in the splash zone below MWL	CP	
Submerged zone		
External surfaces of steel structures	CP, the use of coating systems is optional and these should be compatible with the CP	Uniform corrosion and erosion-corrosion, MIC
Internal surfaces of steel structures	CP or corrosion allowance (with or without coating systems in combination)	Uniform, crevice and pitting corrosion, MIC
Critical structures and components	Corrosion allowance should be based on a corrosion rate ≥ 0.10 mm/year. Marine growth (bacteria) may cause a mean corrosion rate ≥ 0.10 mm/year, and the application of a coating system should be considered.	Uniform and/or pitting corrosion, MIC, SCC

Considering that offshore structures should stay fit for service during the remainder of the design and extended operating life of the field, a comprehensive methodology for the survey and inspection of the unit during this period was developed. Nezamian and Clarke (2014) provides an overall view in using the inspection and site specific characteristic data for calibrations/validations of the original design values to maintain the safety level by means of a maintenance and inspection program balancing the ageing mechanisms and improving the reliability of the collected platform conditions. Beganovic and Söffker (2016) introduce an approach to use operating conditions to control and extend a system's lifetime for larger wind turbine systems. The safety and reliability control engineering concept (SRCE), first discussed in Söffker and Raikowski (1997), introduces the idea of using knowledge about the current State-of-Health to predict remaining lifetime and integrate related information into the control loop targeting to adapt the control strategy to the current State-of-Health. The implementation leads to reliability-based (or health-state-based) system usage.

Reinforcement and repair of components using composite patches can be used for piping to reduce the stress intensity factors at the crack-front of a corrosion fatigue crack. For this purpose, an offshore pipe made of low-strength steel containing an initial fatigue corrosion crack repaired by glass/epoxy composite patch was considered. A parametric study was performed by numerical methods in order to find the effects of patch thickness on fatigue crack growth life extension and crack-front shape of the repaired pipes, (Ghaffari and Hosseini-Toudeshky, 2013). It was shown that repair of cracked pipes with glass/epoxy composite leads to significant life extension for both restarting crack growth and crack propagation period; even a repair with two layers of composite leads to a 65% life extension for restarting crack growth. It was also shown that the crack-front shape curvatures of the repaired pipes are more bent for increasing number of patch layers, but the crack-front shape changes are not significant for more than eight patch layers.

Haagensen et al. (2015) describe the original repair and strengthening program of a floating platform with extensive fatigue cracking, and the types of subsequent fatigue damage that necessitated new repairs. The recent life extension program has resulted in safe operation of the platform for an estimated additional period of 20 years.

The most common methods to improve fatigue life for offshore welded structures are grinding and peening.

4.3.5 Buckling

Buckling failures of offshore structures or sub-components of these structures are usually associated with extreme loading events. There are numerous different types of buckling, e.g. column buckling, plate buckling, local beam buckling, and stiffened plate buckling. Clearly, reduction of cross-sectional area caused by corrosion or local damage due to impact loading will generally tend to lower the buckling resistance.

Non-linear finite element approaches are now applied in the assessment of buckling resistance of complicated details. For such assessments it is very important that effect of local imperfections and residual stresses are included in the assessments. Guidance for how to carry out non-linear FE analyses can be found in DNV GL guideline “Determination of Structural Capacity by Non-Linear Finite Element Analysis Methods,” DNV GL-RP-C208 (2016b).

Regarding very localized buckling, the effects of anti-symmetric buckling on the fracture and fatigue behavior of tension cracked plates was studied experimentally. Results showed that these effects can reduce the fracture capacity and the fatigue life by 35% and 59% respectively. (Seif and Kabir, 2017).

4.4 Methods ensuring safe operation

4.4.1 General

The aim of integrity management is in general to ensure management and continuous follow up for structures and marine systems from the safety, environmental, operational, maintenance, and quality management viewpoints. The process needs to include handling and understanding the effect of degradation, damage, changes in e.g. actions, organization, procedures and use, accidental overloading, and the development in offshore design and operational practices.

The objective of integrity management of structures and marine systems is further to document an acceptable level of safety and suitability of the relevant assets for their intended purposes during all phases of their life. This includes: implementation of integrity management activities that cover all aspects of the safety of the structures and marine systems, surveillance of parameters to detect changes which may affect as-is integrity assessment results, and initiation of timely and relevant responses to detected changes, which also includes assessments and compensating measures as necessary.

4.4.2 Structural Integrity Management (SIM)

The operator is required to manage integrity of the structures and marine systems in a systematic manner in order to determine with a reasonable level of confidence, the existence, extent, and consequence of changes affecting safety and performance.

Per NORSOK-N005 (NORSOK, 2016), structural integrity management will typically include the following:

- Definition of performance requirements for the structures and marine systems;
- Identification of performance limitations based on as-is condition and definition of operating limitations if found necessary (e.g. operating manual);
- Management and execution of the surveillance process;
- Contingency plans for emergency response;
- Mitigations, repairs, and other mitigating actions if systems, elements, components exceed their performance limitations;
- Requirements to personnel qualifications, competence, organization and availability;
- A strategy for acquiring and implementing best practices;
- New knowledge and techniques for improved surveillance and in-service structural and marine system integrity management;
- Continuous updating of the in-service integrity management process for structures and marine systems.

Interfaces between disciplines responsible for structures, penetrations in structures and supports (e.g. for piping, cables, ventilation ducts, riser, caissons, conductor, and equipment) also need to be defined.

Integrity management may provide a framework for:

- Understanding the hazards to and failure modes of structures and marine systems and their components;
- Understanding how the structures and marine systems are intended to withstand and be protected against these hazards;

- Understanding the context under which the evaluations are valid;
- Forming an integrity strategy and specific performance criteria for operation of the structures and marine systems;
- Operating in accordance with operational limitations, design basis, surveillance strategy, and performance criteria as formalized in operating procedures;
- Surveillance of the condition of structural and the marine systems, the metrological and oceanographic conditions, the actions and hazards, modifications and other changes in condition or use, including inspection planning and maintenance, data management and storage (including reports);
- Acting upon undesired conditions and changes to the basis for integrity assessment e.g. by defect evaluation/anomaly assessment and if necessary integrity analyses, emergency response preparedness, implementing repairs and mitigations;
- Measuring and verifying the performance of the structure and marine systems;
- Improving the structure and marine systems when deemed necessary;
- Quality assurance and verification of the integrity management work;
- Exception analysis.

4.4.3 Codes and guidelines covering structural integrity management

Codes and guidelines covering structural integrity management typically introduce a classification of structures and structural components. Such a classification makes it possible to establish the basis for risk screening and determination of what types of inspection and what methods to use.

The classification of structural components will typically consider the following issues: likelihood of corrosion, likelihood of overload, likelihood of fatigue cracks, consequence of component failure (the remaining structure's ability to withstand actions e.g. by damage tolerance or redundancy), possibility of progressive failure, deficiencies, misalignments and non-conformances reported in the design, fabrication, and installation (DFI) résumé, inspection history, presence of stress concentrations and critical load transfer connections, access and preparations to facilitate access for inspection, maintenance and repair, extent of monitoring for the structural component, and inspection method suitability (i.e. deployment, reliability, accuracy).

Classification of structural components according to design class is based on the complexity of the relevant joint, the consequences of failure, and the stress level. However, such classification may not be directly applicable for use in the classification of structural parts for in-service integrity management. This is due to the design classification society's classification not taking into account the exposure to deterioration, changes to the structure, and its variable loads. More comprehensive evaluation of likelihood and consequences of failure are frequently required.

Re-classification from classification society rule-based design to risk-based classification of members and components primarily used for fabrication, transport and installation phases may accordingly be necessary, see e.g. NORSOK N-005 (NORSOK, 2016).

With respect to the task of assessing residual fatigue lifetime, recent updates of the DNV GL rules are described in Lotsberg et. al. (2016). The recommended practice DNV GL-RP-C203 on fatigue design of offshore steel structures has been revised a number of times since it was first issued in 2001. The 2016 revision includes additional information on a number of items

such as: residual stresses in tubular sections made from cold forming, S-N data for subsea application, change in validity of S-N curve in seawater with cathodic protection, relation between surface roughness and requirements for roughness for coating, S-N curves and stress concentration factors for fatigue assessment of pipelines, relation between fabrication tolerances and S-N curves in different types of structural details, and hot spot stress analysis for rainflow counting. The background for this is explained in the paper. In addition, the paper includes some information on recommendations for fatigue design of single-sided tubular joints that was included in the 2014 revision of the Recommended Practice.

4.4.4 Survey and inspection methods

Depending on how and where the execution is performed, several campaigns may be required that can be executed independently of one another, for example: onshore documentation surveillance, as-built weights and documentation (project surveillance), operational changes surveillance, offshore physical surveillance, condition above water/above cellar deck or freeboard deck (not wave dependent), condition above water/below cellar deck or freeboard deck (wave dependent), condition in wave zone (special access equipment), condition below water, ROV (executed by a marine contractor), condition below water, diver (executed by a diving contractor), as-is weight and layout control, level, distance, and freeboard surveys.

Campaign work packages

Planning the execution of surveillance tasks (i.e. structural monitoring and inspection) is facilitated by grouping similar tasks into Work packages. The organization of work packages is typically decided by a surveillance campaign planner.

The following are examples of criteria which may be used to sort tasks into work packages: facility ID (if there are several facilities), facility area (if the facility is divided into areas), method of inspection (if the campaign contains special inspections), types of structure (e.g. major structures, inventory structures).

Surveillance task execution description

The format of the task descriptions is inspection planning system dependent. Typically, a task description will refer to a general execution procedure, and in addition provide the following information: campaign name and ID, work package name and ID, task ID, surveillance type (planned inspection type and deployment method), location details, locations drawings/plots, task description, and special requirements.

Surveillance task reporting requirements

Predefined formats may be provided for the purpose of standardizing reporting of surveillance findings. These will typically contain the following reporting fields: inspection execution date, inspector name and company, inspection problems (yes/no), description of any inspection problems, inspection type(s) and deployment method used, inspection findings (yes/no), finding description and data, probable cause and possible consequence, corrective actions taken, recommended further action, and reference to separate reports/images/videos.

In the following, a summary of different inspection methods is given. Further details are found in the ISSC2015 V.7 report (Hess et al., 2015).

General visual inspection

General visual inspection (GVI) is the most commonly applied inspection method used to confirm general configurations and to detect large scale anomalies. GVI requires a satisfactory light level and visibility. Used subsea, GVI is normally performed without removal of marine growth.

Close visual inspection

Close visual inspection (CVI) is used for detailed examination of structural components or to provide further information on suspected anomalies. Used subsea, CVI requires removal of marine growth. When light color paint is used, small fatigue cracks may be detected by CVI due to paint cracking or rust staining. Close visual inspection should always be carried out before NDE work is started.

Non-destructive examination (NDE)

Thickness measurements are carried out by UT. Thickness measurements need not be carried out as long as the corrosion protection systems are maintained. Surface breaking defects for magnetic materials may be detected by means of dye penetration, ACFM, MPE, EC, or in some cases by UT. For non-magnetic materials, surface breaking defects may be detected by dye penetration, EC, or in some cases UT.

Pressure testing and tightness testing

Hydrostatic pressure testing may be used to verify structural integrity and water tightness of decks and bulkheads between adjacent tanks and compartments. Aerostatic pressure testing combined with soap water may be used for tightness testing of penetration closures and through thickness cracks in welds and base materials. The overpressure should not exceed the design pressure of the tank, and should be controlled by means of a water-tube. For personnel risk reasons the overpressure should not exceed 2,000 mm water column.

Flooded member detection

Flooded member detection can be used to detect through thickness cracks of air-filled submerged hollow members. The method should be used at the lower end to detect water in vertical and inclined members, and used vertically to detect water filling in horizontal members.

At the moment, there are ongoing efforts within the offshore industry related to development of fully autonomous subsea inspection systems based on application of AUVs and ROVs, see e.g. Offshore Energy Today (2017). This may comprise acoustic and laser sensor technology as well as artificial intelligence-based navigation software. The data from inspections can be uploaded into a platform that may include robust data ingestion, automatic defect recognition, predictive analytics, and a visualization portal for the operators and other users. Laser scanning can be repeated numerous times per second to generate coordinate values for millions of points on a surface. These points will provide highly accurate and intricate 3D models of subsea infrastructure. This may serve to expand capabilities for inspections of FPSO as well as ship hulls, underwater production fields, subsea pipelines and cables, and offshore wind farm assets.

4.4.5 Repair/mitigation

The type of repair method will typically depend on the type of offshore structure which is being considered, NORSOK-N005 (NORSOK, 2016):

For jackets:

Due to the long history of jacket structures there is considerable world-wide experience with respect to remedial measures. This comprises actions such as load reduction (marine growth removal, topside weight reduction, spider deck walkway removal), strengthening/repair/replacement (clamps, grouting, additional braces), application of insert piles and "piggy back" piles, conductor and caisson guide gap reduction, changes related to operational mode and procedures (operational restrictions), weld profiling, crack grinding, crack arrestor holes, repair welding, and intensified surveillance.

In Zhang et. al. (2016) and Zhu et. al. (2017), application of an expansive grouted clamp has been outlined with focus on verification of slip capacity and bolt prying. A typical jacket platform is employed for illustration of the analysis. A method to simulate the clamp on the FE model of the platform using line elements is proposed. The influence of bolt prestress load is also considered. Reference is also made to Li and Shi (2014) for a description of this method.

For concrete structures:

Corrective maintenance should be implemented on concrete structures to prevent escalation of minor damage into major damage. It is especially important to maintain steel reinforcements, pre-tension, and embedded pipes to secure their structural functionality during the whole lifetime of the structure.

Column stabilized unit hull structures (CSU), Ship shaped units, and Tension Leg Platforms

Temporary measures may include drilling of crack arrestors, temporary strengthening, temporary load reductions, operational limitations and changes (draft, trim, ballast, mooring pretension, etc.), increased inspection activities, and use of specific monitoring equipment. It is important that all temporary measures are subjected to a criticality and consequence evaluation.

4.4.6 Lifetime extension

Damaged structures and marine systems that, following as-is assurance assessments, cannot be shown to meet in-service integrity requirements must be corrected by appropriate permanent measures. These may involve the following: strengthening/repair/replace, physical modifications that reduce permanent and/or variable actions, modified operating procedures that reduce variable actions, modified operating procedures that reduce consequences of potential further escalation, and modified operating mode to meet the minimum facility requirements.

Activities leading to and concluding long-term compensating measures can include:

- Further detailed damage survey and evaluation;
- Full damaged integrity analysis of the structure or marine system;
- If necessary, the design of repairs, reinforcements, and/or other compensating measures;
- Revision of the defined safe operating sea-states, draft, trim, cog, pre-tension, etc.;
- Update of the as-is analysis model such as with a digital twin.

Integrity assessments of critical structures and marine systems normally require extensive numerical analyses, which simulate the effects of relevant actions. These analyses must be updated if their assessment premises are found to be significantly altered during the operation phase. Key Performance Indices (KPIs) also must be specified.

In Tang et. al. (2015) structural monitoring and early warning conditions of aging jacket platforms are considered. Characteristics of aging jacket offshore platforms are established, including the monitoring and early warning conditions in relation to displacements, pile end bearing loads, and platform subsidence. On the basis of pushover analysis, the curves of base shear force versus deck displacement are developed. Furthermore, the anticipated risks are classified into three levels due to different deformations in the collapse process. A set of three level early warning conditions are established accordingly. A method for monitoring the bearing loads of the pile end is proposed, based on calculation of the load transmission function. The early warning condition that the bearing loads of the pile end should not exceed half of the ultimate pile capacity based on API RP2A-WSD is provided. A long-term monitoring method of the platform subsidence is presented based on calculation of the difference between the elevations for any two pile tops. Early warning conditions considering the stress and tilt requirements are also established. The monitoring method has been applied to a jacket off-

shore platform located in the South China Sea, and the results illustrate the feasibility of the proposed method.

Andrews and Fecarotti (2017) address system design and maintenance modelling for safety in extended life operations in more general terms. The condition and performance of existing systems, which are operated beyond their originally intended design life, are typically controlled through maintenance. For new systems there is the option to simultaneously develop the design and the maintenance processes for best effect when a longer life expectancy is planned. The paper considers application of a combined Petri net and Bayesian network approach to investigate the effects of design and maintenance features on the system performance. For the assessment of aging systems, the method avoids the need to assume a constant failure rate over the lifetime duration. In addition, the assumption of independence between component failure events is relaxed. In comparison with the commonly applied system modelling techniques, this methodology is claimed to have the capability to represent the maintenance process in some detail. Accordingly, options for inspection and testing, servicing, reactive repair, and component replacement based on system condition, age or use are represented in the analysis. In considering system design options, levels of redundancy and diversity along with the component types selected can be investigated. The model has the possibility to evaluate different system failure modes. Application of the approach is demonstrated through assessment of a remote un-manned wellhead platform from the oil and gas industry.

4.5 Special items

4.5.1 Risers / pipelines

Timely detection of damage in deepwater risers is important to keep the consequence and economic loss due to damage to a minimum. Hence, continuous monitoring is needed. Vibration based monitoring is the most widely used method used in offshore structures.

Huang et. al. (2013) address time-frequency methods for structural health monitoring (SHM) of deepwater risers subjected to vortex induced vibrations (VIV). An approach based on a new damage index, distributed force change (WDFC) for monitoring the structural health of risers used for production in deepwater floating platforms, is presented. Experiments with a scaled pipe are carried out to validate the vibration-based damage identification method. The influences of multiple cracks on the WDFC damage index are studied. Furthermore, this paper illustrates the utility of wave propagation based structural health monitoring (SHM) strategies within the pipe model. This is realized based on the results of numerical investigation obtained by the use of the finite element method (FEM) together with application of a Time-of-Flight damage identification method. The damage severity is indicated by the root mean square of the damage-reflected wave. The influence of crack(s) in the riser/pipe on the wave propagation is studied by the authors. The results from the experiments and numerical analysis indicate that the investigated identification methods can provide information about the estimated crack location(s) and the possible crack extent. Hence the methods are believed to be suitable both for global and local monitoring of the structural health of deepwater risers.

4.5.2 Mooring lines

Life extension and asset integrity of floating production unit (FPU) moorings are issues of increasing importance for operators due to changing production requirements, the requirement to extend service life, and circumstances where the metocean basis of design (BOD) has increased significantly over the life of the field. Reliability methods are gaining wider acceptance as enhanced computing power allows large numbers of simulations to be undertaken using realistic fully coupled models that are validated against prior experiments. When applied to the re-qualification and life extension of FPU moorings, particularly with regard to

requalification and life extension of in-place moorings, reliability analysis may offer considerable advantages over conventional deterministic return period design.

Life extension and asset integrity of mooring systems for FPUs are addressed in Rosen et. al. (2016). In Rosen et.al. (2016), application of a reliability approach is used for re-qualification and life extension of a turret-moored FPU for which design metocean conditions have increased significantly over the life of the field. The results of this study illustrate the significant advantages to the industry conferred by adopting reliability methods in the re-certification and life extension of existing FPU moorings. In particular, the study highlights that conventional mooring code deterministic design methods, while adequate for original design purposes, lack sufficient fidelity to address the multi-faceted issue of re-assessment of notionally marginal legacy systems. For a degraded existing mooring, an application of these methods can demonstrate that the level of reliability of the system is still acceptable, whereas a conventional approach may produce an overly conservative indication that the mooring is non-compliant.

4.5.3 Caisson

Caissons are an important part of offshore installations. The major design consideration for the hydrocarbon riser caisson is to protect the risers against external impact from vessels, hydrodynamic loading, and corrosion. However, this makes the inspection of the riser external wall and caisson internal wall very difficult (Schmidt, 2013).

A hydrocarbon riser caisson represents a safety critical item of an offshore platform installation. Loss of the riser caisson integrity compromised by corrosion can have a devastating impact on production capability. Corrosion can affect the riser external surface and the caisson internal surface if the caisson annulus is not well managed. The corrosion process will gradually reduce the wall thickness of the riser until failure resulting from pressure build-up of hydrocarbon within the caisson annulus. The likelihood of caisson failure is increased if the caisson itself has suffered from internal or external corrosion (Anunobi, 2010).

Hall (2012), describes the integrity management of caissons using a retrofit cathodic protection (CP) system. On the other hand, Schmidt (2013) reports on an alternative approach to managing corrosion problems in a caisson using composite materials for repair.

4.5.4 Conductors

Well integrity is typically understood as the required actions which imply reduction of the risks of release of formation fluids into the environment during the operating lifespan of the well. Frequently, a minimum requirement of a two-barrier well construction is applied in order to prevent any leaks to the environment. The conductor and casings fall into the category of the well structural barrier, along with the annuli cement. Typical wells are designed for 25 years of service life, and operators worldwide are beginning to encounter wells operating beyond 30 years and even up to 40 years in some areas.

Continued services are usually expected of these older wells for several reasons. The primary reason is due to the availability of a significant amount of reserves remaining in the reservoir, accompanied by excessive cost in replacement/abandonment activities. This implies that the integrity of the wells must be continuously assured if extended service life is expected. It is common for operators to carry out scheduled site inspections and surveys to monitor the integrity of their wells (Abdalla and Fahim, 2013). However, it is very likely that these data are not used or are misinterpreted in evaluating the integrity of ageing wells. This may potentially result in catastrophic failures such as casing collapse and wellhead and surface tree settlement.

In an ageing well, the heavy external corrosion on the conductor and outer side of the casing will result in loss in overall stiffness to resist the topside weights and environmental loads. In areas with large pits and holes, seawater ingress will cause internal corrosion on the inner side

of the conductor, and to some extent also the surface of the casing. Continued corrosion of the inner surface of the conductor can result in rust flakes formation (Talabani et al., 2000). This will in turn diminish the annular cement capacity to bond with the pipes inside the annulus effectively. Over time, this may cause cement shortfall, i.e. the cementation losing its shear bond capacity and dropping further downhole.

As described by Balmer (2012), under potentially high loading from the well topsides equipment (axial) and the environment (bending), and from the reduced stiffness from the heavy wall loss and cement shortfall, possible collapse of the conductor/casing pipes can occur, resulting in the wellhead and tree dropping vertically (settlement).

4.5.5 Wind turbines

Research activities related to lifecycle design and monitoring of wind turbines (WT) are proliferating. In recent years, structural health monitoring of WT systems is significantly improved through automated on-line fault detection and health or condition monitoring (CM) system integration

Beganovic and Söffker (2016) consider Structural Health Monitoring (SHM) systems applied to WTs. Challenges resulting from contradictions between requirements related to efficient operation with respect to energy production costs and those related to lifetime and maintenance are discussed. Especially pronounced in larger WT systems, structural loads contribute to lifetime shortening due to damage accumulation and damage-caused effects influencing subsystems of the wind turbine. Continuous monitoring of the WT system concerning State-of-Health is necessitated to provide information about the condition of the system guaranteeing reliable and efficient operation, as well as efficient energy extraction. The focus is given to hardware components (mainly sensor technologies) and methods used for change evaluation, damage detection, and damage accumulation estimation. The paper comprises recent knowledge about methods and approaches of handling structural loads with emphasis on offshore wind turbine systems and applied sensing technologies (especially with respect to wind turbine blades, gearboxes, and bearings). A key idea of the introduced approach is to use the operating conditions to control and especially to extend system's lifetime. An actual state-of-the-art analysis and overview related to the use and application of SHM-related technologies and methods are presented.

In Ziegler, L. and Muskulus, M. (2016), fatigue reassessment in order to decide about lifetime extension of aging offshore wind farms is addressed. A methodology to identify important parameters to monitor during the operational phase of offshore wind turbines is presented. An elementary effects method is applied to analyze the global sensitivity of residual fatigue lifetimes to environmental, structural, and operational parameters. Renewed lifetime simulations are performed for a case study which consists of a 5 MW turbine with a monopile substructure in 20 m water depth. Results show that corrosion, turbine availability, and turbulence intensity are the most influential parameters. It is cautioned that this can vary strongly for other settings (water depth, turbine size, etc.) making case-specific assessments necessary.

Vera-Tudela, L. and Kühn, M. (2017) address lifetime evaluation with fatigue loads for wind turbines. This is usually done during the design phase, but rarely during operation due to the cost of extra measurements. Fatigue load prediction with neural networks, using existing supervisory control and data acquisition (SCADA) signals, is a potential cost-effective alternative to continuously monitoring lifetime consumption. The evaluations were limited to single cases and the implication for the design of a monitoring system was not discussed. Hence, metrics to evaluate prediction quality were proposed. Using one year of measurements at two wind turbines, predictions in six different flow conditions were evaluated. The quality of fatigue load predictions was assessed for bending moments of two blades, in edgewise and flapwise directions. Results based on 48 analyses demonstrated that prediction quality varies

marginally with varying flow conditions. Predictions were accurate in all cases and had an average error below 1.5%, but their precision slightly deteriorated in wake flow conditions. In general, results demonstrated that a reasonable monitoring system can be based on a neural network model without the need to distinguish between inflow conditions.

4.6 Offshore Platform Longevity Processes

Many would define the longevity of a platform as the operational phase. However, the longevity of an offshore platform includes several phases, which all more or less affect the total lifetime of the platform. In offshore engineering, it is common to distinguish between seven main phases as outlined in Table 4 (definitions by Vugts, 2013). Included in the table are 1) main tasks involved in each phase, 2) main factors effecting the longevity, 3) tools required to obtain/maintain the desired longevity and 4) parties involved.

Table 4 Generic phase defining the full life cycle of a platform (based on definitions outlined by Vugts 2013).

Phases					
Planning (P)	Design (D)	Fabrication (F)	Transport (T) & installation (I)	Operation (O) (incl. lifetime extension)	Decommissioning / abandonment (A)
Main Tasks					
Design and operational philosophy is defined. Design specifications are made.	Preliminary design (FEED). Detailed design.	Procurement. Fabrication.	Load out & offshore tow. Lifting or Launching operations. Foundation.	Monitoring. Inspection. Maintenance. Repair. Lifetime extension.	
Main factors with effect on longevity					
Redundancy is defined in form of DFF* (minimum DFF* is code defined).	Platform is designed to meet the desired operational life time including desired contingency.	Quality of fabrication and NDT	Loads induced by tow and installation, e.g. driving of piles.	Quality of maintenance and repair. Correct response to survey findings. Modification of platforms, e.g. increased topsides weight. Lifetime extensions.	
Tools					
	Detailed fatigue life calculations using global/local FE models. Good environmental models/statistics Fatigue "friendly" designs.	Surveys at fabrication yard ensuring quality.	Sea transportation analyses. Pile driving analyses.	Inspections (can be Risk Based Inspection, RBI). Possible monitoring (e.g. online SHM Systems). Details SIM systems / digital twins.	Crane vessels, dive support vessels, ROVs.
Parties involved					
Consultants. Authorities. Intended owner.	Consultants. Certifying agencies. Contractors (EPC). Owners/possible future owners.	Contractors.	Contractors.	Owners. Consultants. Contractors.	Owners. Consultants. Contractors. Authorities.

* DFF: Design Fatigue Factor

4.7 Conclusions and Recommendations

Ongoing developments represent a trend towards integration of an extensive number of sensors with increasingly refined processing algorithms and decision support systems. Furthermore, robotic systems are entering the scene. These features pose challenges with respect to a good understanding of the structural behavior and also require that proper guidelines for operation of increasingly complex health monitoring systems are developed. Accordingly, it is also recommended that the multi-disciplinary nature of teams involved in design of such systems is properly acknowledged such that an adequate communication between different experts can be achieved.

5. SHIP STRUCTURAL LONGEVITY METHODS AND EXAMPLES

5.1 Introduction

In this chapter, a critical review of the literature has been conducted in relation to application of the principles discussed in Chapters 2 and 3 to ships.

5.2 Prediction of longevity

Due to increased competition and demanding economic conditions, owners and operators often want to continue exploiting ships and offshore platforms beyond their designed life instead of investing in a new asset.

The challenge in extending the life of an asset is to maintain adequate safety while continuing to operate cost effectively. In doing so, a level of technical assurance is required through approval by national and international statutory authorities. In Chapter 2, the approaches taken by classification societies to carry out a comprehensive re-appraisal of conditions of assets is discussed, which takes into account its past history and present condition of the structure. In this chapter, models for prediction of longevity based on first principles are discussed.

5.2.1 Models for prediction of longevity

Prediction of longevity is carried out using a combination of numerical, experimental, and full-scale measurement approaches. These predictions can either be deterministic or probabilistic.

Magoga et al. (2014; 2017) performed full scale measurements on board the Australian navy *Armidale* class patrol boats that were fitted with sensors used to predict slamming in a variety of ways. It was found that the most successful criterion for slam detection is based on whipping stress rate. Although the authors suggested a robust threshold value of whipping stress ratio for the class of vessel studies, they concluded that for individual ship types it is necessary to verify the appropriate criterion and sensor locations. Vincent et al. (2015) presented a program of work incorporating the design, installation, and performance of an integrated set of sensors capable of monitoring global as well as local structural response of an aluminum patrol craft of the Australian navy. Practical conclusions concerning their design, installation, and performance are discussed in the paper.

Clauss and Klein (2016) described an experimental study of the effect of freak waves on the total loading of the hull girder and in particular the relation of loading to the geometry of the forward structure of three types of ships. Sea conditions corresponding to the Draupner wave were generated in a test tank and the responses of a bulk carrier, a ro-ro, and a container ship were monitored. In general, it was found that the geometry of the bow structure on total loading is significant. Specifically, it was found that in the case of the containership, the addition of a freeboard extension in way of the bow area resulted in an increase in VBM amidships of around 20 percent.

A wireless system of sensors was developed in order to measure structural and motion response of free-running models or ships at full scale (Figure 6) as described in Bennet et al. (2014). The system can capture rigid body motions and three axis accelerations using a 9 d.o.f. sensor node while the structural deformation of the hull girder is obtained from three nodes in parallel. The output consists of time-synchronized inertial and magnetic data for ship models at an accuracy that is comparable to that of optical wired systems.

Shen et al. (2015) investigated the suitability of two types of fiber Bragg grating (FBG) strain gauges for use in long term hull health monitoring under conditions of corrosion and fatigue. Both gauge types were checked for signal linearity and stability in laboratory conditions simulating real conditions and also using finite element analysis.

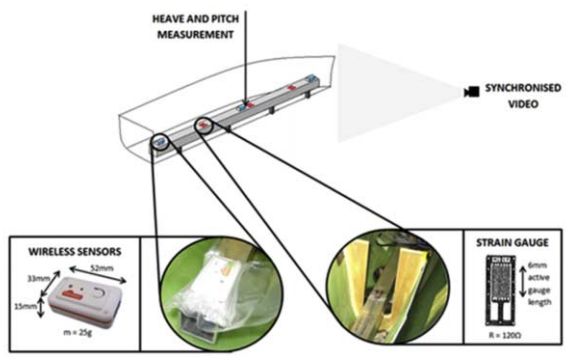

Figure 6. Locations of wireless sensors for structural and motion response (Bennett et al., 2014).

A computationally accurate, robust, and rapid algorithm named the inverse Finite Element Method (iFEM) was recently developed and applied to aerospace structures by Tessler and Spangler (2003, 2005). It was based on a three-node inverse shell element (iMIN3) using lowest order anisoparametric co-continuous functions and thus models in-plane displacements and bending rotations in a linear manner, introducing a quadratic constrained-type deflection. The iFEM methodology possesses a general applicability to complex structures subjected to complicated boundary conditions in real-time, and works on the principle that discrete strain data (shape and stress sensing) obtained from on board sensors are used to re-construct the displacement, strain, and stress fields using algorithms minimizing the weighted-least-squares functions. Kefal and Oterkus (2016) applied the iFEM methodology for the first time in the field of naval architecture for shape and stress sensing of a chemical tanker, and introduced a four-node inverse quadrilateral shell (iQS4) element, based on Mindlin's first-order plate theory. The steps followed in this study were: (a) Hydrodynamic analysis of the vessel to determine hydrodynamic forces; (b) FE analysis of the vessel using as input the hydrodynamic forces to determine the strain data to be used as input for the iFEM analysis; and (c) iFEM analysis using the strain data. Results are shown in Figure 7. The method appears to offer potential benefits in the sense that a very limited strain data obtained from several strain rosettes located at a deck stiffener, the centerline longitudinal bulkhead, and the centerline girder can be sufficient to reconstruct a precise global deformed shape and stress field in the entire structure. It is seen that the results are excellent although the practical challenge is to obtain robust and reliable results using a limited number of sensors.

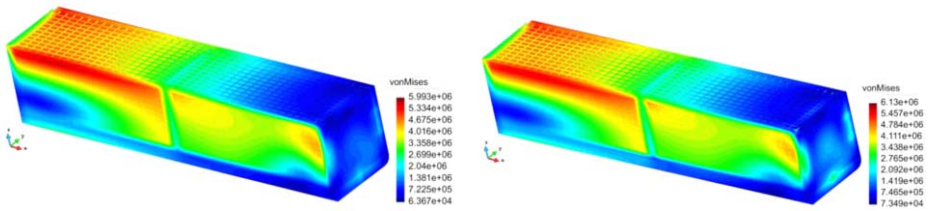

(a) iFEM for one-to-one strain data *(b) Direct finite element stress distribution*

Figure 7. Von Mises stress distributions (Kefal and Oterkus, 2016).

A structural reliability assessment procedure is presented and its operation is illustrated for the case of a Capesize bulk carrier (Michala et al., 2017). The aim of the procedure is to identify weak points in the structure from the fatigue point of view and to assist in decision-making processes (planning of future repairs). It relies on hydrodynamic analysis, a finite element representation of the structure amidships, and structural reliability theory.

A series of extensive review papers were published by Ibrahim (2015a–d, 2016a–b) that deal with the application of structural reliability theory to structural longevity-related issues for naval ship structures. Consideration is given to fracture mechanics theory, corrosion, hydrogen embrittlement, impacts, and crack growth in joints. A detailed exposition of the theory is given in each case and recent developments are presented.

Lynch et al. (2012) proposed a strategy for the estimation of the remaining fatigue life of a naval structure. The strategy makes use of onboard sensors that provide raw data that is processed so that the current state of the hull girder can be assessed. The method is based on fatigue theory in conjunction with a statistical approach called the Dirlik procedure. The purpose of this is to use a limited number of parameters from the power spectrum thus avoiding the continuous processing that is necessary in rainflow counting. The method was validated by comparison with test data.

Zhu and Collette (2015) used Dynamic Bayesian Networks (DBNs) to model system behavior and update reliability and uncertainty analysis with data such as fatigue cracking. A fundamental difficulty arises when considering low probability failure events and the authors have presented an algorithm which dynamically partitions the discretization intervals at each iteration. The algorithm was validated using two crack growth models and it was concluded that it can achieve the same degree of accuracy as static discretization with less than half the number of intervals. Furthermore, it avoids the need to manually iterate through different static discretization methods and resolution levels to achieve convergence.

Das et al. (2015) performed reliability analyses of aluminum unstiffened and stiffened plates that resulted in the determination of partial safety factors for use in strength design. In the case of stiffened plates, use was made of Paik's two analytical formulations (Paik et al., 2008) that apply to T-bar and flatbar stiffened plates respectively. Sensitivity analyses were performed for model uncertainty, plate thickness, loading, breadth, material yield stresses, elasticity modulus, and corresponding partial safety factors with respect to ultimate strength obtained.

Akpan et al. (2014) illustrated application of structural assessment methodology incorporating advanced computational methods, damage models, probabilistic tools, and optimization techniques for redesign of a tanker structure for optimal performance and reliability.

5.2.2 Failure Modes Contributing to Longevity Assessment

Lifetime assessment of a vessel is typically based on particular failure modes at the component and system levels. The primary failure modes are: failure of the hull girder by reaching

its ultimate strength capacity, failure of a stiffened panel by material yielding or instability, fatigue failure of structural details due to cyclic loading, fracture due to overload, and combinations of these. Consideration of deterioration due to corrosion should also be given in all the failure modes (for example in Ayyub et al., 2015).

Panel Yielding/Collapse Strength Buckling

The overall failure of ship structures is evaluated based on the buckling and elastic- plastic collapse of the plates and stiffened panels in the deck, bottom, and sometimes side shell. Therefore, the accurate assessment of the collapse strength of plates and stiffened panels is an important task in the structural design and safety assessment of ship. Application of the common structural rules (CSR) of the International Association of Classification Societies (IACS, 2014) for collapse strength of plates and stiffened panels can be used. Yielding on the other hand affects serviceability such as in connection with plate permanent set resulting from lateral pressure loading.

For the collapse strength of stiffened panels, the procedure proposed in CSR assumes that the ultimate compressive strength is the lowest of the three different buckling modes: beam column flexural buckling, stiffener torsional buckling, and local buckling of the stiffener web. More details of the procedure employed, including the comparison of the CSR procedure with the non-linear FE method is provided in Corak et al. (2010).

The increase of the deck stress due to the loss of hull girder section modulus (HGSM) was analyzed by Jurisic and Parunov (2015) and at the same time the reduction of the collapse strength of plates and stiffened panels of the main deck due to what the authors claim is a reduction in elastic modulus and yield strength due to corrosion was determined. This simple method shows the point in time as illustrated in Figure 8 when it is expected that the applied stress will exceed the strength of stiffened panels of the main deck. The solution is to replace the corroded plating with a new one to avoid an unsafe zone for the aging ships.

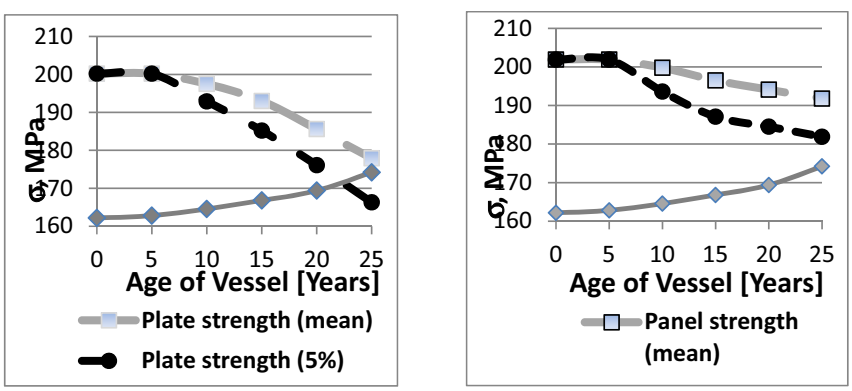

Figure 8. Safety margin of plates (left) and stiffener panels (right), cargo oil tanks of sample tanker (Jurisic and Parunov, 2015).

Ultimate Hull Girder Strength

Ship's structure in operation is exposed to the various loads such as hydrostatic pressure, static and dynamic pressure of cargo carried, the wave loads, and vibration loads such as whipping. During navigation the ship hull is deformed (sagging and hogging), and in these conditions the maximum stresses affect structural elements that are farthest from the neutral axis of the cross section of the ship (deck and bottom). Therefore, there is a danger that when the stress exceeds the strength in these elements, they are no longer able to carry all of the applied loads. Overstressed structural elements then collapse and may further cause global collapse of

the main deck or the bottom. This could result in a loss of overall hull girder strength of the ship's hull. Therefore, the problem of the ultimate capacity of the cross section, also known as the ultimate strength of the ship hull, becomes an essential segment in the calculation of the ship strength (Harmonized Common Structural Rules for Bulk Carriers and Double Bottom Tankers, IACS, 2014).

Recently, based on some major ship accidents, numerous research studies, and public pressure, the approach for longitudinal strength assessment through hull girder section modulus (HGSM) of new-built ships started to be complemented by the hull girder ultimate strength (HGUS) assessment, as a more effective criterion by which to judge the capacity of the ship hull.

Fatigue

Fatigue is one of the main deterioration mechanisms that affect the longevity of ship structures. Fatigue cracks can appear at various locations along the ship structure and may occur at early stages in the service life of a ship. Large fatigue cracks may influence ship structural safety in two ways. Firstly, if a stress intensity factor at a fatigue-induced crack tip exceeds its critical value, then unstable crack propagation may take place. Secondly, even during stable crack propagation, the load-carrying area is reduced because of the presence of the crack, and consequently, the structural capacity of plates and stiffened panels is reduced (Paik et al., 2005).

Experimental studies are performed to analyze fatigue life of welded specimens corroded in real seawater conditions. Unexpectedly, it was found that cracks initiate at local pits, rather than at weld toes. Fatigue life of such specimens with pitting corrosion is much lower compared to uncorroded specimens (Garbatov et al., 2014a). Garbatov (2016) performed fatigue strength and reliability assessment of a complex double hull tanker structure, utilizing local structural finite element models, accounting for the uncertainties originating from the loads, nominal stresses, hot spot stress calculations, weld quality estimations and misalignments, and fatigue S-N parameters including the correlation between load cases and the coating life and corrosion degradation. Fatigue reliability during the service life was modelled as a system of correlated events. The analysis showed that the uncertainty in the fatigue stress estimation and fatigue damage were the most important variables.

Significant efforts have been spent to investigate the reliability of ship structures. However, there has been a lack of research that focuses on risk-based performance assessment of ship structures. The importance of risk as a performance indicator was emphasized by Dong and Frangopol (2015). Based on a probabilistic approach, optimum inspection and repair planning was solved as a multi-objective optimization problem for a VLCC structure considering corrosion and fatigue. The key findings of the research were that corrosion and fatigue have significant impact on the risk of structural failure of ships; the risk of structural failure increases rapidly with time due to corrosion and fatigue; and the risk of ship failure can be reduced significantly by optimum inspection and repair planning.

Degradation of hull structure due to loss of coating protection and corrosion

The marine environment is generally the most aggressive naturally occurring environment. The hull being constantly exposed to the seawater environment experiences general corrosion, which reduces the plate thickness, but it is also likely to experience pitting, galvanic corrosion, and others. The mechanism of corrosion wastage in marine environments on ship's structures is dependent on many different factors, such as: the type of cathodic protection, humidity, type of cargo and cargo operations, fluid flow, dissolved oxygen, temperature, and salinity (Ibrahim, 2015d; Jurisic and Parunov, 2015). Therefore, the corrosion wastage for different ship structural elements is defined based on the type of element and its location, and varies as a function of the corrosion environmental conditions.

Corrosion degradation needs to be modelled as a function of time in order to predict hull structural deterioration during the service life. In that way, the effect of corrosion degradation during its service life may be taken into account in the ship structural design and in repair planning. While such a model will allow changes in the environmental factors to be reflected in the corrosion rates, the historical data available do not contain that information.

Corrosion can interfere with the operation of ships and impose increasing stresses, accelerate deterioration of ship structures, and increase the hydrodynamic drag. Furthermore, it can cause degradation of coatings as shown by tests carried out under laboratory conditions. It was found that aging of marine organic coatings (due to raised temperature, in air or immersed in sea-water) has a negative impact on the coatings' mechanical properties and in particular the fracture strain can be reduced substantially.

Typical histograms of corrosion thickness measurements, based on which the mean value is calculated, are presented in Figure 9, where the corrosion wastage of the main deck plates in cargo tanks for a ship after 15 and 20 years in service are shown.

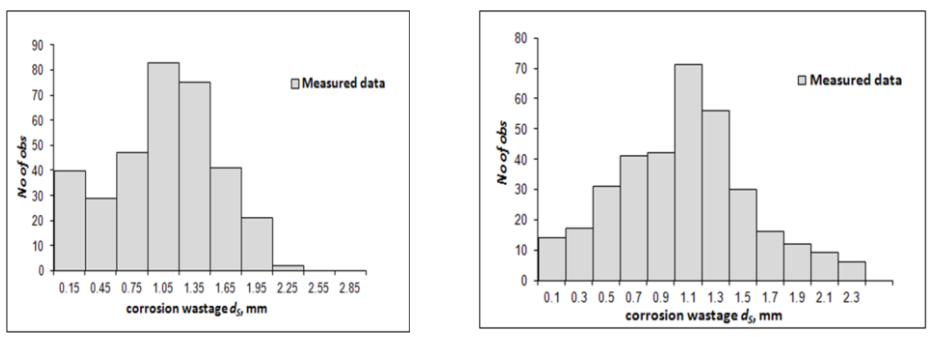

Figure 9. Corrosion wastage of main deck plates in the cargo tanks of sample oil tanker after 15 years (left) and 20 years (right) (Jurasic et al., 2014)

Corrosion progression models are used by classification societies and ship owners in order to predict long-term behavior of hull structure and to decide if the renewal of the hull structure is necessary and the optimal time for the repair. A typical model of the corrosion process consists of at least two phases: a phase without corrosion because of the durability or life of the protective coating and a phase of corrosion progression. Three widely used models for corrosion progression in ship structures are those originally developed by Melchers (2008), Yamamoto and Ikagaki (1998), and Guedes Soares and Garbatov (Garbatov et al., 2007). The model of corrosion degradation GS&G was proposed by Garbatov et al. (2007). The corrosion wastage model G&A was originally defined by Yamamoto and Ikagaki (1998) and later applied in the analysis by Guo et al. (2008). Comparison of these two prediction models with thickness measurements on three oil tankers is presented in Figure 10.

In order to quantify the uncertainty of the corrosion degradation models used, the complete results for the predicted and measured mean corrosion thicknesses are presented in Figure 10 and are statistically analyzed. It can be concluded that corrosion wastage in cargo tanks is larger than in ballast tanks, while deck stiffeners in cargo tanks experienced the largest corrosion wastage of all ship structural components analyzed (Jurisic and Parunov, 2015). This trend is well predicted by both methods. The phenomenon has already been observed in Garbatov et al. (2007) and was explained to be caused by sulphur from oil gases in combination with surface rust to the back face of an oil tanker deck. In such cases, corrosion mechanisms can create more damage in a cargo tank than from the sea water in the ballast tank.

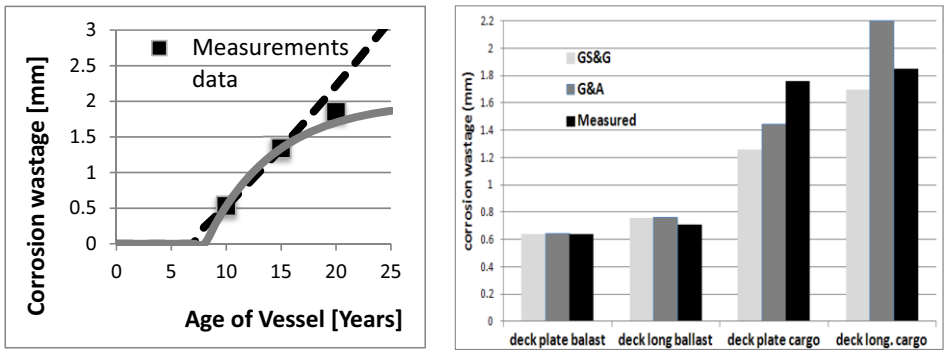

Figure 10. Measured and predicted mean annual corrosion wastage for main deck stiffeners in cargo oil tanks (COT) and complete corrosion wastage after 20 years of example tanker (Jurisic et al., 2014).

Combined factors e.g. strength, fatigue, and corrosion

For the assessment of structural longevity at the middle or near the end of the designed life of a vessel, long term prediction of corrosion effects on fatigue and ultimate strength becomes very important (Garbatov et al., 2014a; Garbatov et al., 2014b; Guo et al., 2008).

Corrosion wastage and fatigue cracks are recognized as the two most important long-term degradation mechanisms of ship structures. The consequences of age related damages can be catastrophic in some circumstances, requiring that experts in the maritime industry take into consideration degradation factors on ship structural safety. Aging effects need to be appropriately addressed (Jurisic et al., 2017). Due to these reasons, much research effort has been spent in the past few decades aiming to understand and model the degradation phenomena and to develop practically applicable models for long-term prediction of both these phenomena. The nature of corrosion and fatigue crack progression is extremely complex and unpredictable, and consequently large uncertainties are associated with computational models for their prediction, as both phenomena often occur at the same time and are mutually dependent.

Recently a comprehensive experimental work was performed in identifying the effect of corrosion on the mechanical properties of ageing marine structures. Corroded box girders have been tested for ultimate strength, showing an important reduction of mechanical properties. Further analyses have been performed using the tensile test specimens that have been cut from corroded box girders. The analysis of the results from specimens confirmed changes in mechanical properties of the corroded steel. It was shown that the modulus of elasticity and yield strength of corroded shipbuilding steel reduces with time. The phenomenon is quite unexpected and still unexplained, as the grain size and chemical composition of the steel are not expected to change due to corrosion (Garbatov et al., 2014b). To cause such corrosion degradation, accelerated anodic polarization of the metal surface was used. Anodic electric current was supplied by an external source. The highly accelerated test was done in 90 days as opposed to a more natural corrosion evolution and it is unclear if this aggressive technique was or was not the cause of the change in mechanical properties.

Further studies have been undertaken to investigate the consequence of corrosion-induced mechanical degradation on the local collapse strength of plates and stiffeners, and on the ultimate strength of an 88,000-t tanker structure. The losses in hull girder section modulus (HGSM) and hull girder ultimate strength (HGUS) for a corroded ship with and without degradation of mechanical properties of hull structure are obtained using single step method calculations proposed by CSR DH OT (Jurisic et al., 2017). These are shown in Figure 12.

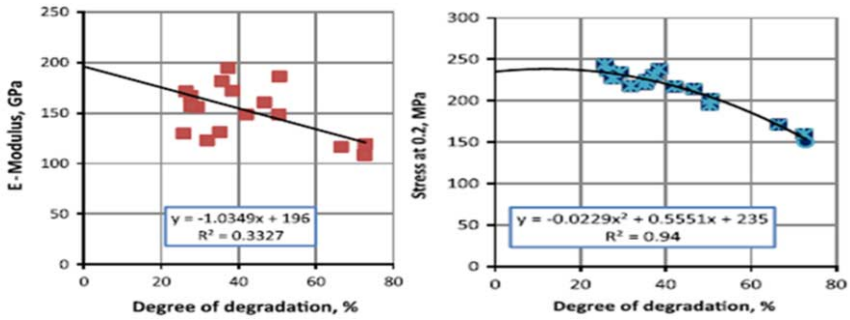

Figure 11. E-modulus, GPa (left) and yield strength 0.2 MPa (right) decreasing (Garbatov, 2016)

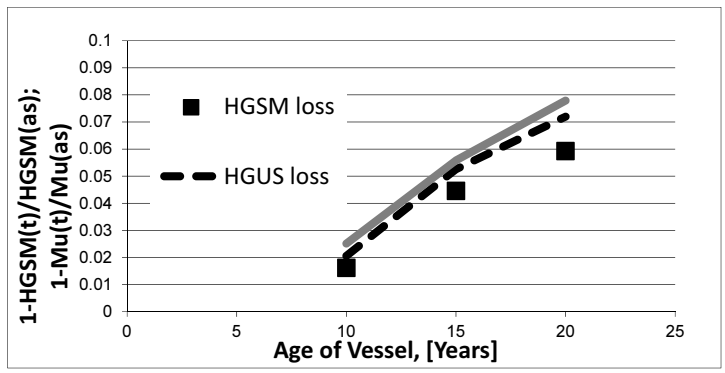

Figure 12. Measured HGSM losses and calculated HGUS losses for example oil tanker (Jurisic et al., 2017).

It can be seen from Figure 12 that the degradation of mechanical properties has a minor effect on the HGUS. The maximum difference in the reduction of hull girder ultimate strength by taking into account degradation of mechanical properties is about 1% of the initial HGUS. However, similar studies performed on plates and stiffened panels indicate that the influence of degradation on local collapse strength may be significant in certain cases (Jurisic and Parunov, 2015).

5.3 Main factors influencing longevity

The failure modes affecting longevity of surface ships, namely yielding, fatigue, and corrosion, have been discussed in section 5.2 of this chapter. In this section consideration will be given to related aspects and how they affect longevity.

Classification societies recognize that no ceiling ought to be imposed on a ship's lifetime, and thus periodical surveys are planned to ensure that with advancement in ship's age, a more thorough evaluation of condition is carried out and stricter requirements and related tests are in place prior to issuance of class certificates. Commercial pressures dictate that for many of the world's merchant ships, insufficient time is devoted to periodical surveys and related repairs. This is a situation that is much more serious in the case of larger ships (Figure 13).

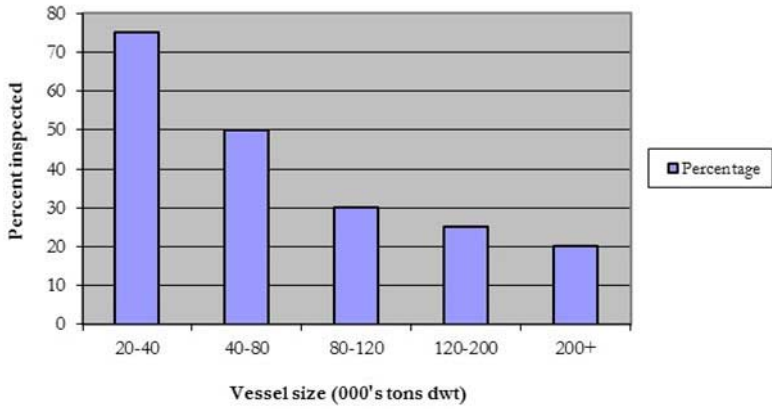

Figure 13. Proportion of hull structure inspected based on vessel size (Bell et al., 1989).

There are other types of ships that operate under much stricter regimes (LNG carriers, chemical carriers) so that this problem does not arise to the same extent. In addition to classification society requirements, there exist other bodies that perform ship surveys (OCIMF, the Oil Companies International Marine Forum, and vetting of oil tankers on behalf of the major oil companies). During vetting, emphasis is placed on safety and pollution prevention during cargo handling operations, although structural issues are also addressed (OCIMF, 2016).

Clearly, a well-designed and well-built ship will outlast a poorly designed and/or poorly built one and it is necessary to point out what characterizes good design and good practice. It is also necessary to point out that there exist different regimes that govern ship structural adequacy, depending on whether the vessels are merchant or naval ships, on the type of ship, and on their individual operating regimes. It may therefore not be possible to speak in terms of requirements to be imposed throughout the world fleet, although techniques developed may by universally applicable. For example, adequate design at the structural detail level is necessary to ensure the requisite fatigue life and the avoidance of yielding.

Although most commercial ship owners have a non-technical understanding of good construction quality they are nevertheless prepared to invest in it, the reason being that experience has shown that a high-quality ship will operate more efficiently from the investment point of view (shorter off-hire periods) and during later stages of its life it will be easier and less costly to maintain. Yard practice varies throughout the world's shipyards, with certain yards having a superior reputation to others. Owners are aware of this, and this knowledge is important when investment decisions are being made. Concomitant to yard practice is quality control, and this figures largely in quality of construction. It has to be understood that the vast majority of individual owners do not have the time or resources to perform in-depth studies of shipyard quality, and thus their decisions are based on past experience and knowledge.

Finally, it is important to distinguish between technical and economic obsolescence. The former has been discussed throughout this report. Of equal importance however is economic obsolescence, whose presence has indirect effects on technical obsolescence. We understand economic obsolescence to be the withdrawal of a ship from active trading despite the fact that it is not technically obsolete. This may arise as a result of market conditions, that is, very low freight rates over a long period of time. When a ship is likely to become economically obsolete, the owner will understandably be reluctant to invest in repairs that are costly and lengthy. In such a situation, repairs will be reduced to the minimum necessary to ensure that the ship can continue trading in the short term.

5.3.1 Role of Life Extension Programs

Aging of water transport represents a serious problem, with the cost of maintaining the safe state of vessels increasing while the vessels' operational qualities and competitiveness are steadily decreased. Certainly, new shipbuilding is the best cure of such problems, but the leading shipping companies that built many vessels in the past are reluctant or unable to build in a crisis market. Therefore, it is necessary to pay close attention to the compromised technical solutions for the prolongation of life of existing vessels. The types of approaches adopted for river-sea vessels are general modernization, renovation, overhaul, and conversion (vessel's construction with use of donor vessel's elements), as described in Egorov and Avtutov (2016):

1. Modernization of hulls: Existing hatch coamings / trunks are the most loaded elements and hence were critical for fatigue life. Use of highly continuous longitudinal hatch coamings or trunks would allow for significant section modulus increases to enhance the general strength of vessel's hull, cargo holds' / tanks' capacity, and deadweight in accordance with requirements of International Load Lines Convention.
2. Renovation: Renovation of a vessel's hull is the most known and widely used scheme for prolonging the vessel's life that is applied in commercial shipping. The main drawback of this procedure is that renovation concerns only an assessment of hull reliability. Engines, mechanisms, devices and systems remain without changes. As a general rule, this scheme does not allow a decrease in insurance rates and influences vessel's economy by little, since in general the risk of the vessel's operation depends not only on hull condition, but also on condition of the other vessel's elements.
3. Overhaul: Overhaul combines structural renovation with repair of the engines, mechanisms, devices, and systems. Average overhaul cost of a 5,000-t tanker is about 3.0 million U.S. dollars which is estimated to be around 20-24% of the new built cost.
4. Conversion: Conversion occupies a special place among different variants of essential modernizations; it means considerable, as a rule, dimensional modernization of the vessel with survey of all her parts as if new, i.e. in compliance with requirements of the international conventions and rules of the classification society for date of survey. Conversion allows remediating problems important to life extension and increasing the safety with less time and cost than that of new construction.

Conversion requires the accounting of the following defects which were accumulated during operation of the vessel pre-conversion:

- Corrosion and mechanical wear of hull constructions and welded joints, especially local thinning which are badly documented and not considered at the traditional strength calculations;
- Deformations of the inner bottom and inner side as a result of contact with cargo and cargo handling gauges in ports;
- Deformation of the outer shell as a result of contact with ground at shallow water, with walls of locks or channels, with berthing facilities or ice;
- Accumulated fatigue damage at the zone of stress concentration, especially microcrack and violations of crystal structure of material which cannot be found at surveys;
- Possible alternation of physical-mechanical properties of material of the hull (ageing).

Conversion is based on the following basic principles:

- The scientific-based approach to determine the need for new elements or use the old ones;

- The full compliance with the international and national requirements for the building date of the new vessel;
- Ensuring reliability for the set operational term of the vessel;
- Has the same quality as a new build from the point of view of the primary use;
- Uses modern calculation methods and technologies.

The most striking example of a vessel's building with usage of elements of the existing donor vessels is creation of a series of river-sea dry-cargo vessels with a deadweight about 6,000 tons of "Chelsea" type (Egorov and Avtutov, 2016).

River dry-cargo "Volga-Don" type vessels that were built in the 1960s, were used as donors. The scheme of vessel's construction with pointing the new (marked) elements is shown in Figure 14. The vessels construction consisted of keeping part of the existing structure (about 650 tons), adding about 650 tons of new construction (new coamings, second deck, forecastle and poop, new deck-house and hatch covers) and replacing about 550 tons of existing hull elements. Total cost for converting a single "Chelsea" type vessel was about 5.5-6.0 million U.S. dollars. In comparison, construction cost of a similar new build vessel is about 11-14 million U.S. dollars.

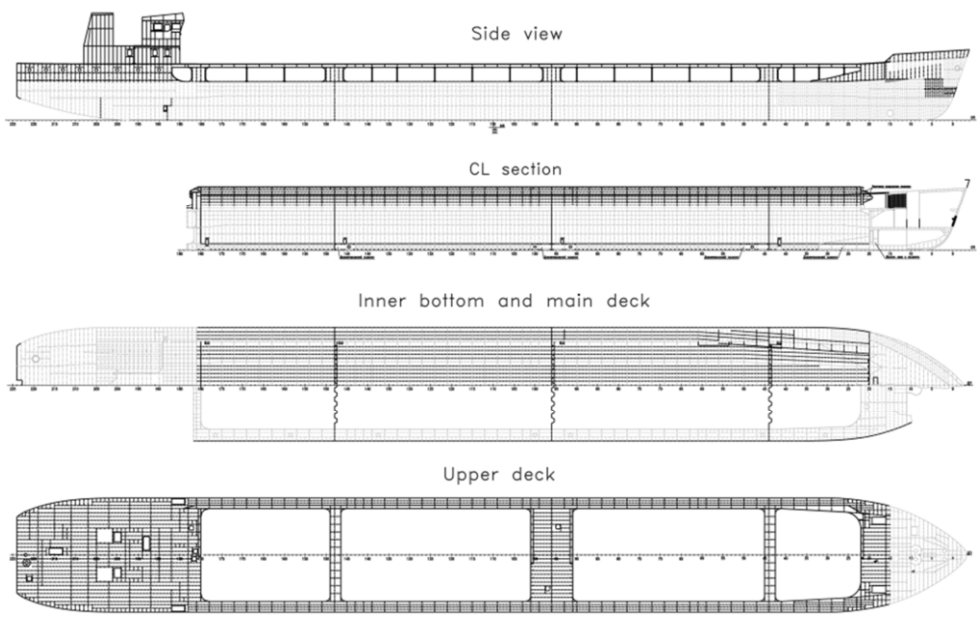

Figure 14. Scheme of construction of dry-cargo vessel of "Chelsea" type (Egorov and Avtutov, 2016).

It is necessary to understand clearly that a vessel's life prolongation schemes are not an alternative to new shipbuilding. These schemes allow provision of necessary transport needs during the next 10-15 years; offering a compromise solution between lowering fleet transportation rates and the rising demands of the economy while financial and industrial resourced are limited.

5.4 Methods for ensuring safe operation

5.4.1 Current practice and future directions

Chapter 3 of the previous committee report (Hess, et al., 2015) provided current practice three years ago. It was observed in preparing the current ISSC2018 Committee V.7 report that little has changed in practice in three years. The recent literature relevant to ensuring safe operation of ships has been presented in the following sub-sections.

5.4.2 Structure Monitoring, Inspection, Maintenance, and Repairs

Sanchez-Silva et al. (2016) discuss the main conceptual and theoretical principles involved in the maintenance and operation of infrastructure under uncertainty. The concepts discussed form the basis to build models that can be used for making better decisions for maintaining and operating infrastructure systems.

Structural health monitoring systems constitute effective tools for measuring the structural response and assessing the structural performance under actual operational conditions. Inspection, monitoring, and/or repair actions are applied to prevent sudden failures of structural components due to fatigue and their associated consequences. However, these actions increase the operational cost of the ship and should be optimally planned during its service life.

Magoga et al. (2015) reviewed the benefits and challenges of utilizing hull monitoring data with respect to naval high-speed light craft (HSLC). While full-scale data is obtained in the actual operational environment in real-time with non-linear loads taken into account implicitly, the measurements must be high-quality to be reliable, and it is relatively costly and time-consuming. Aksu et al. (2015) discussed the utilization of data collected from a hull monitoring system (HMS) onboard an aluminum patrol boat, to support sustainment of the fleet.

Soliman et al. (2016) argued that the planning of inspection, monitoring, and/or repair actions of a maritime asset should be performed probabilistically, given the presence of significant uncertainties associated with crack initiation and propagation, and proposed a probabilistic approach for inspection, monitoring, and maintenance optimization for ship details under fatigue effects. Based on the stress distribution and the crack geometry at the damaged location, a multi objective optimization problem, with the objective functions being the minimization of the life-cycle cost and maximizing the expected service life, was solved to determine intervention times and types.

An accurate, quantifiable means of assessing a structural damage condition are paramount for maintaining the structural integrity of ship hull forms. A non-contact approach to identifying and characterizing imperfections within the submerged bow section of a representative ship hull was developed (Reed and Earls, 2015) using simulated sonar pulses. The pressure field local to the acoustically excited hull section was monitored. It is shown that the resulting data can be used to identify the parameters describing the structural damage field. A Bayesian, reversible jump Markov chain Monte Carlo approach is then used to generate the imperfection parameter estimates and quantify the uncertainty in those estimates.

The idea of leak-before-break (LBB) is based principally on guaranteeing that enough time is available between the moment a crack breaks through the hull or wall, and the moment when the crack becomes unstable, causing a structural failure. The concept was originally developed and applied in the nuclear power industry and has recently been applied to the structural safety of a tether string that is part of the mooring system of an offshore structure (Ren et al., 2015). Application of the LBT concept to ship structural safety should be investigated.

Fatigue damage is proportional to the third power of stress range (Drummen, et al., 2017) and influenced by the operator avoiding heavy weather when possible. Furthermore, it is beneficial to monitor the fatigue damage accumulation. Drummen, et al. (2017) argued that this can

be done with a simple system, calibrated to key locations using FEA. Such a simple system can enable long term cost effective monitoring approach for reducing uncertainties and risk in life-cycle and end of service life decisions.

Stambaugh et al. (2014) discussed a reliability-based fatigue life prediction approach, in relation to the U.S. Coast Guard's Fatigue Life Assessment Project (FLAP), along with how it may be used to evaluate options for life cycle management of fatigue and the return on investment (ROI) for considering fatigue early in the design. With the knowledge of the time varying structural fatigue reliability, it is possible to evaluate the cost of alternative design and maintenance strategies and the ROI of these alternatives. Example ROI estimates showing the benefits of considering structural fatigue analysis (SFA) early in the design process, prior to construction, during construction, and in the ship's service life is given in Table 5 (Stambaugh et al., 2014). In this example, ROI is defined as net cost savings (cost avoidance) divided by the cost invested by considering fatigue in preliminary design shown as base option in Table 5.

Various approaches have been adopted by researchers to determine the remaining useful life of structures: noisy gamma deterioration process by Le Son et al. (2016); and monitoring of corrosion damage using high frequency guided waves (Chew and Fromme, 2014).

Table 5. Example return on investment (ROI) of SFA in preliminary design as compared to incurred repair costs in service (after Stambaugh et al., 2104).

Life Phase	Relative Cost/Cutter	ROI of fatigue design	Lost Operation Days	Comments
Preliminary design	0.5	Base option	0	Essentially the cost of added steel
Detail design	1.0	1.5:1	85+	Including design rework
Construction	4	7:1	170	One-year delay in delivery
After delivery	20	39:1	85	Half year dry dock
Repair through 30-year service life	10-30	>19.5:1	340+	6 – 2-week EDS+ 2 – 1-month EDD

EDD: Emergency Dry Dock; EDS: Emergency Dock Side

5.4.3 At-sea damage response: measurement, analysis, repair, and/or change in operation

Incorporating life-cycle concepts in structural design and assessment codes is gaining momentum in recent years (Frangopol and Soliman, 2016). The main principles, concepts, methods, and strategies are discussed by Biondini and Frangopol (2014). The concepts of life-cycle performance assessment and maintenance planning are used to formulate the life-cycle reliability-based design problem in an optimization context.

Dong et al. (2016) presented a decision support system for mission-based ship routing considering multiple performance criteria. The generalized decision-making framework developed performs a variety of tasks such as the flexural and fatigue performance evaluation of ship structures and employs multi-attribute utility theory to evaluate ship mission performance. The expected repair cost, cumulative fatigue damage, total travel time, and carbon dioxide emissions associated with ship routing are considered as consequences within the risk assessment procedure.

Frangopol and Soliman (2016) presented aspects of life cycle management decisions such as the performance prediction under uncertainty and optimization of life-cycle cost and interven-

tion activities, the role of structural health monitoring and non-destructive testing techniques as well as integration of risk, resilience, sustainability, and their integration into the life-cycle management.

Decò and Frangopol (2015) calculated the risk of a vessel integrating structural health monitoring data. Optimal short-range routing of ships was accomplished by solving two- and three-objective optimization problems with objectives being the estimated time of arrival, mean total risk, and fuel cost. It was found that optimizing three objectives provided a comprehensive set of optimal solutions.

Knowledge of the current structural state can be used to predict structural integrity at a future time and allows actions to be taken to improve safety, minimize ownership costs, and/or increase the operating envelope. Nichols et al. (2014) described a structured decision making (SDM) process for taking available information (loading data, model output, etc.) and producing a plan of action for maintaining the structure. It was demonstrated that SDM produced the optimal trip plan by minimizing transit time and probability of failure.

A self-powered, wireless system offers a versatile and powerful SHM tool to enhance the reliability and safety of avionics platforms, jet fighters, helicopters, and commercial aircraft that use lightweight composite material structures (Mendoza et al., 2012).

Saad-Eldeen et al. (2014) compared the behavior of three corroded box girders experimentally tested with respect to collapse modes, strain measurements, residual stresses, load-displacement relationship, moment-curvature relationship and the effect of different corrosion levels on structural integrity.

5.4.4 Remaining Service Life

The Structural Life Assessment of Ship Hulls (SLASH) methodology for the structural reliability analysis of marine vessels based on failure modes of their hull girders, stiffened panels including buckling, fatigue, and fracture and corresponding life predictions at the component and system levels was presented by Ayyub et al. (2015). It employs time-dependent reliability functions for hull girders, stiffened panels, fatigue details, and fracture at the component and system levels, but only considers time to first failure and does not consider additional failures or repair. The methodology was implemented as a web-enabled, cloud-computing-based tool with a database for managing vessels analyzed.

Soliman et al. (2015) quantified the accumulated fatigue damage and the fatigue reliability based on structural health monitoring data acquired from an aluminum naval vessel operating under different operational conditions (speed, sea states, and heading angles). The hot spot structural stress approach was used for the fatigue assessment. Estimates of target fatigue life for different operational profiles were performed for the reliability index, β, target values of 2.0 and 3.0.

5.5 Notional Examples of Longevity and Life Extension Decisions

5.5.1 Naval Ship

The navies are increasingly forced to extend the service life of aging ships due to budgetary and political constraints. In making such service life extension decisions, maintaining the seaworthiness of the platform is critical. On these grounds, interest in the utilization of in-service loads and strain data for through-life structural management of naval ships has recently grown. In the case of aluminum lightweight high speed naval craft, additional challenges are posed in extreme environments when sustaining significant wave induced impacts and slamming, resulting in a higher incidence of fatigue-related cracks (Magoga et al., 2014).

Modern high strength and ductile steels are a key element of U.S. Navy ship structural technology. Matic et al. (2015) reviewed the analytical and computational tools, driving simulation methods and experimental techniques that were developed to provide ongoing insights into the material, damage, and fracture characteristics of these alloys. Knowledge gained about fracture resistance was used to meet minimum fracture initiation, crack growth, and crack arrest characteristics as part of overall structural integrity considerations.

However, the emphasis of fatigue analysis research has tended to be on increasing the accuracy of numerical approaches by considering more parameters of influence and higher fidelity modelling. The approaches also tend to be validated via other numerical methods and experimental data. In comparison, use of in-service load and response data combined with survey reports to establish practicable methodologies and to update service life predictions has been limited (Soliman et al., 2015). A typical procedure for life of type assessment of a naval vessel covers the following steps:

- Determination of operational history;
- Areas of operation, speed profile, sea state information, loading changes (displacement increase due to mid-life upgrade and weapon and combat systems upgrades;
- Determination of long term loads;
- Using seakeeping codes or hull monitoring data;
- FE modelling and analysis for critical locations;
- Identification of critical joints for fatigue assessment;
- Incorporation of degradation (corrosion) into FEA;
- Determination of stress range histograms at critical locations;
- Fatigue damage estimation.

Magoga et al. (2016) applied the aforementioned methodology for Life of Type assessment of a generic patrol boat. Drummen et al. (2017) conducted structural fatigue life assessment and maintenance needs for a new class of U.S. Coast Guard Cutters using a very similar procedure.

5.5.2 Bulk carrier / Tanker/Container

The current trends in the global marine marketplace is that new building orders for bulk carriers, oil tankers, and container ships have significantly reduced, resulting in a more important need for life extension. (for example, Parunov et al., 2010).

Before purchase of existing ships, it is necessary to perform condition assessment of a vessel including determination of corrosion damage based on the hull thickness measurements (Jurisic et al. 2011). classification societies are currently developing software packages for ships in service that have an integrated corroded structure module within the finite element method (FEM) model allowing incorporation of hull inspection survey reports.

The nonlinear finite element method (NLFEM) is an important tool in the analysis of structures with the significant influence of geometric and material nonlinearities. Today NLFEM can be considered sufficiently developed for the use in the design of ship structures and in the assessment of the ultimate compressive strength of plates and stiffened panels. In the ultimate strength analysis of unstiffened plate and stiffened panel both types of nonlinearity appear: geometrical nonlinearity due to large deflection and material nonlinearity due to the nonlinear behavior of material in the plastic region.

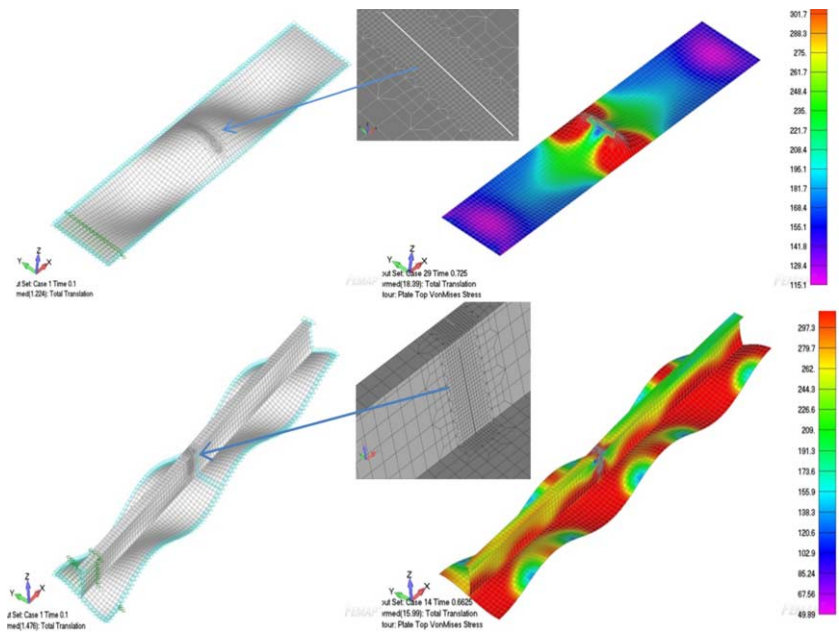

Figure 15. NFEM model of cracks of deck plate and stiffener panel for example oil tanker (Jurisic et al., 2017).

As an illustrative example, the model of the plate with a simulated fatigue crack has been shown on the upper left side of Figure 15. Cracks quite often appear in an aged structure after many years of ship in service, as shown in the lower left side of Figure 15. The resulting von Mises stresses at the plate collapse are presented on the upper right side, and for the stiffener panel on the lower right side of Figure 15. It can be noticed that the stress increases in the area of the crack, reaching limit condition values of 315 MPa, corresponding to steel AH 32 yield strength.

5.5.3 Inland Vessels

Reliability and failure analysis of river passenger vessels (RPV) hulls was made in (Egorov and Egorov, 2015). It was observed that RPVs operational conditions are less severe than for cargo vessels; they are operated with permanent qualified personnel, they have smaller draughts and correspondingly less probability for grounding, they have almost constant load conditions, they have seasonal operations which practically excludes ice damage risk, they include sideshell protection by crinolines so the level of side damage is lower than for cargo vessels despite large numbers of mooring locking through operations, and they have no aggressive cargoes and grab cargo-handling operations (Egorov and Egorov, 2015).

Corrosion damage accumulation for a RPV is 2–4 times smaller than that of cargo vessels. Investigations (Egorov and Egorov, 2015) showed that corrosion was, as follows: 2.4% for bottom shell, 2.1% for side shell, 6.3% for main deck shell, 2.1% for tank top shell, 2.8% for transverse bulkhead plating, 2.1% for bottom elements, 2.4% for side elements, 2.3% for deck elements. Increased corrosion damage was found on decks where the crew and passenger compartments are located (places of bilge waters) and at the sewage tanks.

Description of river and river-sea passenger vessel new construction was given by (Egorov and Kalugin, 2015). Analysis of inland vessels was made for Danube river barges. Typical non-propelled vessels are dry-cargo and tanker river sectional barges of “Europe-2B” type with cargo capacity of 1,600–2,000 t. Analysis of the operation of such vessels was conducted

to identify the factors that make the greatest impact on the risk during the whole lifetime (Egorov and Egorova, 2016).

Due to the nature of the operations of inland vessels passing through locks, contacts with walls of the locks and canals are common, leading to the additional scuffing of sheer-strake and bilge strake of shell plating and strake stiffeners' deformation.

Analysis of repair documents, cargo operation books, and logbooks for 140 vessels was conducted to identify the typical defects and damages to their hulls after having undergone a long period of operation. The typical hull's damages are shown in Figure 16 and corresponding causes are shown in Figure 17. Most hull breakages occur during cargo loading and unloading.

The overwhelming majority of the inland vessel's hull failures (especially on the Rhine–Main–Danube Canal system, where there are no significant waves) are associated with buckling failure of the elements of the compressed strake of the hull girder which could be the result of widespread use of transverse framing system in European river shipbuilding.

Longitudinal strength improvements can be provided by the following measures (Egorov and Egorova, 2016):

- Increasing of thickness and sizes of hull members;
- Better estimation of loads due to longitudinal bending;
- Changing of the method of longitudinal strength calculation due to safety factor increase; checking hull strength while taking into account life-cycle degradation and damage;
- Changing of the transverse framing system of the hull girder extreme strakes to longitudinal stiffening;
- Increasing of buckling strength of longitudinal members of longitudinal framing system by reducing frame spacing and increasing the cross-sectional moment of inertia.

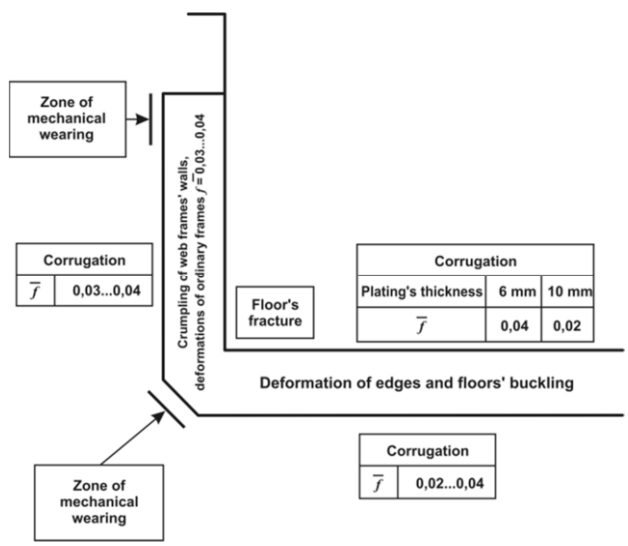

Figure 16. Hull damage in barge of "Europe-2B" type – relative deflection (Egorov and Egorova, 2016).

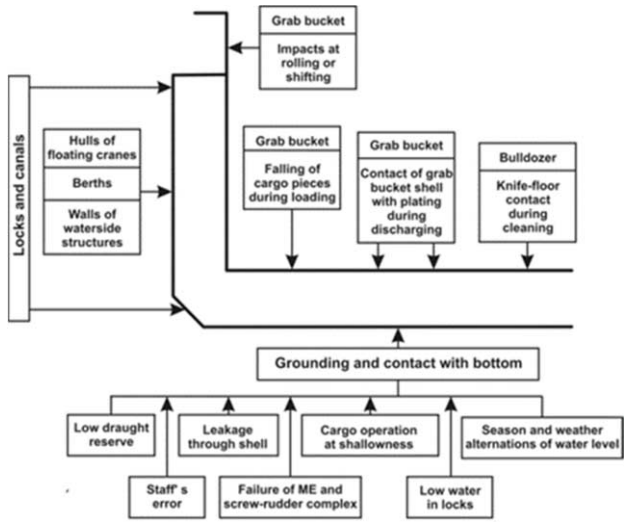

Figure 17. Sources of damage in sectional barge hulls (Egorov and Egorova, 2016).

5.6 Discussion and Conclusions

- First-principles based prediction of longevity is carried out using experimental, numerical, full scale measurements approaches. The current literature is reviewed in relation to the application of dominant longevity factors (yielding, ultimate strength, fatigue and corrosion) to ship structures.
- Wireless sensors and fiber Bragg grating strain gauges represent new technology that is applied to obtain hull response data for use in experimental predictions.
- The inverse finite element method is one of the methods used to analyze experimental sensor data to determine displacements, strains and stresses throughout the structure.
- Dynamic Bayesian Networks are being used to model system behavior and update reliability and uncertainty analysis with data such as fatigue cracking.
- The primary failure modes that affect structural longevity are: failure of the hull girder by reaching its ultimate strength capacity; failure of a stiffened panel by material yielding or instability; fatigue failure of structural details due to cyclic loading; fracture due to overload; and combinations of these. The dominant longevity factors for different types of vessels are presented in Table 6.
- Structural health monitoring systems constitute effective tools for measuring the structural response and assessing the structural performance under actual operational conditions. The planning of inspection, monitoring and/or repair actions of a maritime asset should be performed probabilistically to minimize life-cycle cost and maximize the expected service life.
- A reliability-based fatigue life prediction approach can be used to evaluate options for life cycle management of fatigue and the return on investment for considering fatigue early in design.

Table 6. Dominant longevity factors vs. ship/vessel type

Ship Type	Yielding	Ultimate Strength	Fatigue	Corrosion	General Comments
Naval Vessels	High		High	High	Extended operational life
Aluminium high-speed craft	High		High		High dynamic loading
Tanker		High	High	High	Relative importance of these depends on vessel size
Bulk Carrier		High	High	High	Relative importance of these depends on vessel size
Container ship		High	High	High	Open deck, reduced capacity, overloading above safe limits
Passenger ship			High		Large openings, extensive deckhouse
Inland ship			High		Accounting of local loadings (mooring operations, canal and locks passages, shallow water) on design stage
River-sea ship		High	High	High	Accounting of local loadings, flex hull as the result of metal consumption optimization, wave height restrictions

6. CONCLUSIONS & RECOMMENDATIONS

6.1 Conclusions

The high level mandate for this committee was to develop an understanding of structural longevity and the factors that shape this topic, both in importance and how it is managed or maintained. Chapters 2, and 3 describe the importance of structural longevity from different perspectives, as well as describe some of the methods used in life-cycle management such as monitoring and inspection. Chapters 4 and 5 describe the application of the methods of structural longevity to offshore structures and to ships.

It is clear that there is a growing concern for the structural longevity of ship, offshore and other marine structures, with systemized methods developed or under development to provide the owners with information to make a decision on the future of their assets, the lifetime assessment that is balanced by economic, structural, maintenance, systems, and resilience considerations. However, the development and approaches to life extension of assets for the marine industry has been driven by regulatory bodies, with little reporting in the literature by ship and offshore owners and operators of current or planned practice. Significant work has been done on life-cycle fatigue analysis, but there is little indication that the results of such studies have been integrated into life-cycle management plans or structural health monitoring systems other than identifying problem areas for inspections. For many owners, the concept of structural longevity is limited to following the requirements of classification societies and only performing the structural repairs and modifications that are necessary to last until the next five-year inspection. Specific conclusions are as follows:

- Since ISSC 2015 there has been increasing research on the incorporation of structural lifetime assessment of ship and offshore structures and a transfer of knowledge across industry sectors.
- Classification societies and other standards provide guidance for the assessment of the current state of an asset, but not for assessment of future conditions.
- There is a need to integrate structural hull/health monitoring with structural assessment to manage the structural longevity over the remaining life of ships' structures as has been increasingly done for offshore structures.
- Integrating an understanding of degradation propagation with the classification of inherent risks in inspection and the consequences of failure can be used to develop specific inspection plans (risk-based-inspection).
- Many non-destructive testing techniques are being used across a wide range of industries to identify damage and irregularities in materials.
- The probability of detection and probability of sizing defects are being improved through stringent codes, the use of complementary techniques, and the use of more focused and automated inspection and monitoring techniques.
- Non-destructive inspection techniques are being improved through methods such as signal digitizing, image processing, and machine-learning techniques.
- Increasing use of digitization, integration, and automation of inspection and monitoring data requires more attention to data management and cyber-risk management.
- The increase in the number of offshore wind turbines has led to research in the life-cycle design and monitoring to ensure the longevity of these structures.
- Structural integrity management systems are being developed to provide a framework for ensuring the longevity of marine structures.
- Advances continue to be made in the assessment of the current condition of ships' structure and the evaluation of the probability of future fatigue damage.

6.2 Recommendations

This committee report describes elements important to structural longevity, building upon past ISSC committee efforts. The following recommendations should be considered by the industry, regulatory bodies, and researchers.

- Develop structural prediction models capable of incorporating structural condition data (from sensors or inspection) that are able to predict remaining life, and continue support management of the asset over that life.
- Develop guidance for the use of digital twins to manage the structure of a marine asset over its entire life-cycle.
- Develop better corrosion rates from on-line monitoring.
- Conduct research to verify that corroded steel mechanical properties of steel either change or stay the same to ensure proper accounting in failure analyses and longevity assessments.
- Conduct research into practical applications of probabilistic methods for the assessment of aging, including risk-based inspection and risk-based maintenance.
- Industry design standards are needed for the impressed current systems used to reduce corrosion of offshore structures.

REFERENCES

Aalberts, P.J., Cammen, Van der, J. and Kaminski, M.L. (2010) The Monitas System for the Glas Dowr FPSO, Proceedings of the Offshore Technology Conference, 3-6 May, Houston, Texas, USA.

Abdalla, D. and Fahim, M. (2013) Casing Corrosion Measurement to Extend Asset Life, Oilfield Review, 3, 25.

ABS (2011) Guide for Ice Load Monitoring Systems, American Bureau of Shipping (ABS), Houston, Texas, USA[online] Available from: https://www.eagle.org/eagleExternalPortalWEB/ShowProperty/BEA%20Repository/Rules&Guides/Current/178_iceloadsmon/icloadsmon_guide.

ABS (2014 a) Rules for Survey After Construction, American Bureau of Shipping, Houston, Texas, USA.

ABS (2014 b) Spectral-based Fatigue Analysis for Floating Production, Storage and Offloading (FPSO) Installations, American Bureau of Shipping, Houston, Texas, USA.

ABS (2014 c) Guide for Non-destructive Inspection of Hull Welds, American Bureau of Shipping, Houston, Texas, USA.

ABS (2015) Guide for Hull Condition Monitoring Systems, American Bureau of Shipping, Houston, Texas, USA.

ABS (2017 a) Rules for Building and Classing Steel Vessels - Part 5C1 and 5C2, Specific Vessel Types, American Bureau of Shipping, Houston, Texas, USA.

ABS (2017 b) Rules for Building and Classing Floating Production Installations, Part 5A, Chapter 3, Structural Design Requirements American Bureau of Shipping, Houston, Texas, USA.

ABS (2017 c) Guide for Building and Classing Floating Offshore Liquefied Gas Terminals, Chapter 3, Structural Design Requirements, Appendix 1, Guide for Fatigue Strength Assessment, American Bureau of Shipping, Houston, Texas, USA.

ABS (2017 d) Guide for Building and Classing Drillships - Hull Structural Design and Analysis, Appendix 2, Fatigue Strength Assessment of Drillships, American Bureau of Shipping, Houston, Texas, USA.

ABS (2017 e) Guide for Building and Classing Mobile Offshore Units, American Bureau of Shipping, Houston, Texas, USA.

ABS (2017 f) Guide for Spectral-Based Fatigue Analysis for Vessels, American Bureau of Shipping, Houston, Texas, USA.

Adams, D.E. (2007) Health Monitoring of Structural Materials and Components, John Wiley and Sons Ltd., Chichester, West Sussex, UK. ISBN: 978-0-470-3313-5.

Aeran, A., Siriwardane, S.C., and Mikkelsen, O. (2016) Life Extension of Ageing Offshore Structures: Time Dependent Corrosion Degradation and Health Monitoring, Proceedings of the 26th International Ocean and Polar Engineering Conference, Rhodes, Greece, June 26–July 1 2016, International Society of Offshore and Polar Engineers, Cupertino, California, USA.

Aeran, A., Siriwardane, S.C., Mikkelsen, O., and Langan, I. (2017) A Framework to Assess Structural Integrity of Ageing Offshore Jacket Structures for Life Extension, Marine Structures, 56, pp. 237–259.

Akpan, U.O., Ayyub, B.M., Koko, T.S. and Rushton, P.A. (2014) Development of Reliability-Based Damage-Tolerant Optimal Design of Ship Structures, ASCE-ASME Journal of Risk and Uncertainty in Engineering Systems, Part A: Civil Engineering, 1, 4.

Aksu, S., Magoga, T. and Riding B. (2015) Analysis of HMAS GLENELG's Onboard Structural Monitoring Data, Proceedings of the International Maritime Conference 2015, Sydney, Australia, 6–8 October.

An, D., Kim, N.H., and Choi, J-H. (2013) Options for Prognostics Methods: A Review of Data-Driven and Physics Based Prognostics, Annual Conference of the Prognostic and Health

Management Society, 14–17 October, New Orleans, Louisiana, USA, Prognostics and Health Management Society, Rochester, New York, USA.

Andrews, J. and Fecarotti, C. (2017) System Design and Maintenance Modelling for Safety in Extended Life Operation, Reliability Engineering and System Safety, 163, pp. 95–108.

Anunobi, K. U. (2010) Integrity Management of Hydrocarbon Riser Caisson System, Society of Petroleum Engineers International Conference on Oilfield Corrosion, 24-25 May 2010, Aberdeen, Scotland, UK, Society of Petroleum Engineers, Richardson, Texas, USA, doi:10.2118/130193-MS.

API (2005) API RP2A-WSD, Recommended Practice for Planning, Designing and Constructing Fixed Offshore, 21st edition, October, American Petroleum Institute, Washington, D.C.

API (2009) API R.P. 580, Recommended Practice for Risk-Based Inspection, American Petroleum Institute, Washington, D.C.

API (2016) API R.P. 579-1/ASME FFS-1, Fitness-For-Service, American Petroleum Institute, Washington, D.C.

ASM (1989) ASM Handbook, Volume 17, Non-destructive Evaluation and Quality Control, 9th Edition, American Society for Metals, ISBN 10: 0-87170-023-9.

ASNDT (2012) NDT Handbook, 3rd Edition (Volume 10), American Society for Non-destructive Testing, Columbus, Ohio, USA.

ASME (2010) Boiler and Pressure Vessel Code, Section XI — Rules for In-service Inspection of Nuclear Power Plant Components, Mandatory Appendix VIII — Performance Demonstration for Ultrasonic Examination Systems, American Society of Mechanical Engineers, New York, ISBN 9780791832561.

AWI (2018) AWI - developing autonomous mobile robots to inspect weld lines on ships, London South Bank University, http://www.lsbu.ac.uk/case-studies/awi-developing-autonomous-mobile-robots-inspect-weld-lines, accessed 27 Feb 2018.

Ayyub, B.M., Stambaugh, K. A., McAllister, T. A., de Souza, G. F. and Webb, D. (2015) Structural Life Expectancy of Marine Vessels: Ultimate Strength, Corrosion, Fatigue, Fracture, and Systems, Journal of Risk and Uncertainty in Engineering Systems, Part B: Mechanical Engineering, 1, 1, pp. 1–13.

Azemar, F., Faÿ, F., Réhel, K., and Linossier, I. (2015) Development of Hybrid Antifouling Paints, Progress in Organic Coatings, 87, pp. 10–19.

Balmer, B. (2012) ADMA OPCO, Development of Asset Replacement Plans for 20 Years for Zakum, Umm Shaif and Das Island, Society of Petroleum Engineers, doi:10.2118/161249-MS.

Beganovic, N. and Söffker, D. (2016) Structural Health Management Utilization for Lifetime Prognosis and Advanced Control Strategy Deployment of Wind Turbines: An Overview and Outlook Concerning Actual Methods, Tools, and Obtained Results, Renewable and Sustainable Energy Reviews, 64, pp. 68–83.

Bell H.H. et al. (1989) Report of the Tanker Safety Study Group, U.S. Department of Transportation, U.S. Coast Guard, Washington, D.C., October.

Bennett, S.S., Brooks, C.J., Winden, B., Taunton, D.J., Forrester, A.I.J., Turnock, S.R. and Hudson, D.A. (2014) Measurement of Ship Hydroelastic Response Using Multiple Wireless Sensor Nodes, Ocean Engineering, 79, pp. 67–80.

BIMCO, CLIA, ICS, INTERCARGO, INTERTANKO, OCIMF and IUMI (2017) The Guidelines on Cyber Security Onboard Ships, Intertanko, Available online at http:// www.intertanko.com/Documents/Industry_guidelines_cyber_security_July_2017.pdf, (last accessed 28 February 2018.

BINDT (2017) NDT Yearbook, British Institute of Non-destructive Testing, ISSN 0952 2395.

Biondini, F. and Frangopol, D.M. (2014) Time-Variant Robustness of Aging Structures, Chapter 6 in Maintenance and Safety of Aging Infrastructure, Frangopol, D.M. and

Tsompanakis, Y. (Eds), CRC Press / Balkema, Taylor and Francis Group, London, pp. 163-200, doi:10.1201/b17073-7.

Bitner-Gregersen, E.M., Horte, T., and Skjong, R. (2011) Potential Impact of Climate Change on Tanker Design, ASME 30th International Conference on Ocean, Offshore and Arctic Engineering, Rotterdam, 19–24 June, The Netherlands.

BS (2013) British Standard BS 7910, Guide to Methods for Assessing the Acceptability of Flaws in Metallic Structures, British Standards Institution, London.

Bruce, G., et al. (2003) International Ship and Offshore Structures Congress (ISSC), Specialist Committee V.2, Inspection and Monitoring, 15th ISSC Congress, 11–15 August, San Diego, California, USA.

BV (2015) Condition Assessment Programme (CAP), Bureau Veritas, Neuilly sur Seine Cedex, France, 2015.

BV (2017) Rules for the Classification of Steel Ships, Bureau Veritas, Neuilly sur Seine Cedex, France, 2015.

Caines, S., Khan, F., and Shirokoff, J. (2013) Analysis of Pitting Corrosion on Steel Under Insulation in Marine Environments, Journal of Loss Prevention in the Process Industries, 26, pp. 1466–1483.

Carteau, D., Vallée-Réhel, K., Linossier, I., Quiniou, F., Davy, R., Compère, C., Delbury, M., and Faÿ, F. (2014) Development of Environmentally Friendly Antifouling Paints Using Biodegradable Polymer and Lower Toxic Substances, Progress in Organic Coatings, 77, pp. 485–493.

CCS (2015) Rules for Classification of Sea-Going Steel Ships, Ch. 21, Pt. 8, China Classification Society, Beijing, China.

Chen, N.Z., Wang, G.N., and Soares, C.G. (2011) Palmgren-Miner's Rule and Fracture Mechanics-Based Inspection Planning, Engineering Fracture Mechanics, 78, 1, pp. 3166–3182.

Chew, D. and Fromme, P. (2014) Monitoring of Corrosion Damage using High-Frequency Guided Ultrasonic Waves, Proceedings of The International Society for Optical Engineering, 9064, 90642F (8 pp.) and Proceedings of Health Monitoring of Structural and Biological Systems, 2014. San Diego, California, USA.

Clauss, G.F. and Klein, M. (2016) Experimental Investigation on the Vertical Bending Moment in Extreme Sea States for Different Hulls, Ocean Engineering, 119, pp. 181–192.

Constantinis, A.D., Forsyth, J., and Botta, H. (2016) A New Approach for Effective Underwater Hull Inspection of Floating Offshore Assets, Offshore Technology Conference, 2–5 May, Houston, Texas, USA.

Copello, S., Petrillo, F., and Gaugenrieder, S. (2015) A System Approach for Evaluating Residual Life of Existing Fixed Offshore Platform, 12th Offshore Mediterranean Conference and Exhibition, Ravenna, Italy, 25–27 March.

Corak, M., Parunov, J., Teixeira, A.P., and Guedes Soares, C. (2010) Performance of the Common Structural Rules Design Formulations for the Ultimate Strength of Uniaxially Loaded Plates and Stiffened Panels, in Advanced Ship Design for Pollution Prevention, Guedes Soares, C. and Parunov, J. (Eds.), Taylor and Francis Group, London, UK, pp. 113–120.

Das, P., Dodds, B., Paik, J., Aksu, S., and Peschmann, J. (2015) Reliability Analysis of Stiffened and Unstiffened Aluminium Plated Structures, Proceedings of International Conference on Light Weight Design of Marine Structures, LIMAS, 9–11 November, Glasgow, Scotland, UK.

Decò, A. and Frangopol, D.M. (2015) Real-Time Risk of Ship Structures Integrating Structural Health Monitoring Data: Application to Multi-Objective Optimal Ship Routing, Ocean Engineering, 96, pp. 312–329.

DNV (2012) Offshore Standard: Submarine Pipeline Systems, DNV-OS-F101, Det Norske Veritas.

DNV (2014) Design of Offshore Wind Turbine Structures, DNV-OS-J101, DNV GL-Energy, Arnhem, The Netherlands.

DNV GL (2015) Class Guideline 0129, Fatigue Assessment of Ship Structures, October.

DNV GL (2016 a) Class Guideline 0182, Allowable Thickness Diminution for Hull Structure, February.

DNV GL (2016 b) Determination of Structural Capacity by Non-Linear Finite Element Analysis Methods, DNV GL-RP-C208.

DNV GL (2017 a) Ships, Part 6 Additional Class Notations, Chapter 9 Survey Arrangements, pp. 17–42.

DNV GL (2017 b) Design of Offshore Steel Structures, General (LRFD Method), DNV-OS-C101, DNV GL-Energy, Arnhem, The Netherlands.

Dong, Y. and Frangopol, D.M. (2015) Risk-Informed Life-Cycle Optimum Inspection and Maintenance of Ship Structures Considering Corrosion and Fatigue, Ocean Engineering, 101, 3072, pp. 161–171.

Dong, Y., Frangopol, D.M., and Sabatino, S. (2016) A Decision Support System for Mission-Based Ship Routing Considering Multiple Performance Criteria, Reliability Engineering and System Safety, 150, pp. 190–201.

Drummen, I. et al. (2014) Full Scale Trials, Monitoring and Model Testing Conducted to Assess the Structural Fatigue Life of a New U.S. Coast Guard Cutter, presented at the Ship Structure Committee Symposium, 18–20 May, Linthicum Heights, Maryland, USA.

Drummen, I., Hageman, R., and Stambaugh, K. (2017) Structural Fatigue Life Assessment and Maintenance Needs for a New Class of U.S. Coast Guard Cutters, Life-Cycle of Engineering Systems: Emphasis on Sustainable Civil Infrastructure, Bakker, Frangopol, and van Breugel (Eds.), CRC Press Book, Delft, The Netherlands.

ECSS (2009) Fracture Control, ECSS Engineering Standard ECSS-E-ST-32-01C Rev. 1, European Space Agency, Noordwijk, The Netherlands.

Egorov, G.V. and Avtutov, N.V. (2016) Grounding of New Hull Structures Designed with Elements of Vessels-Donors, Proceedings of the Thirteenth International Conference on Marine Sciences and Technologies, Black Sea, 2016, Varna, Bulgaria, pp. 24–30.

Egorov, G.V. and Egorov, A.G. (2015) Research of Reliability and Risk of Operation of Native River Cruise Passenger Vessels, ONMU Reporter, Odessa, Ukraine, 1, 43, pp. 5–31.

Egorov, G.V. and Egorova, O.G. (2016) Dry-Cargo Barges of "Europe-2B" type of 1635OY, 1635OMDL, 1635OMDL-S, RDB06 and RDB11 Design for Operation in Danube-Main-Rhein Water System, Proceedings of the Thirteenth International Conference on Marine Sciences and Technologies, 12–14 October, Black Sea, Varna, Bulgaria, pp. 90–97.

Egorov, G.V. and Kalugin, Ya.V. (2015) Line-up of New Generation River-Sea Navigation Cruise Passenger Vessels for Russian Inland Waterways, Proceedings of the 29th Asian Technical Exchange and Advisory Meeting on Marine Structures (TEAM 2015), 12–15 October, Vladivostok, Russia, pp. 87–94.

Ersdal, G. (2005) Assessment of Existing Offshore Structures for Life Extension, Department of Mechanical and Structural Engineering and Material Sciences, University of Stavanger, Norway.

European Commission (2007) European Methodology for Qualification of Non Destructive Testing - Third Issue, ENIQ Report NR. 31, European Network for Inspection and Qualification, Westerduinweg, The Netherlands.

Feng, Q., Li, R., Nie, B., Liu, S., Zhao, L., and Zhang, H. (2016) Literature Review: Theory and Application of In-Line Inspection Technologies for Oil and Gas Pipeline Girth Weld Defection, Sensors, 17, 1.

Figueira R.B., Fontinha, I.R., Silva, C.J.R., and Pereira, E.V. (2016) Hybrid Sol-Gel Coatings: Smart and Green Materials for Corrosion Mitigation, Coatings, 6, 12.

Fitzsimons, B. (2018) Sounds ultra advanced, http://www.aerospacetestinginternational.com/articles.php?ArticleID=1185, accessed 27 Feb 2018

Frangopol, D.M. and Decò, A. (2015) Real-Time Risk of Ship Structures Integrating Structural Health Monitoring Data: Application to Multi-Objective Optimal Ship Routing, Ocean Engineering, 96, pp. 312–329.

Frangopol, D.M. and Soliman, M. (2016) Life-Cycle of Structural Systems: Recent Achievements and Future Directions, Structure and Infrastructure Engineering, 12, 1, pp. 1–20. Also in Proceedings of the 4th International Symposium on Life-Cycle Civil Engineering, IALCCE, Tokyo, 16–19 November.

Garbatov, Y. (2016) Fatigue Strength Assessment of Ship Structures Accounting for a Coating Life and Corrosion Degradation, International Journal of Structural Integrity, 7, 2, pp. 305–322.

Garbatov, Y., Guedes Soares, C., and Parunov, J. (2014 a) Fatigue Strength Experiments of Corroded Small-Scale Steel Specimens, International Journal of Fatigue, 59, pp. 137–144.

Garbatov, Y., Guedes Soares, C., Parunov, J., and Kodvanj, J. (2014 b) Tensile Strength Assessment of Corroded Small Scale Specimens, Corrosion Science, 85, pp. 296–303.

Garbatov, Y., Parunov, J., Kodvanj, J., Saad-Eldeen, S., and Guedes Soares, C. (2016) Experimental Assessment of Tensile Strength of Corroded Steel Specimens Subjected to Sandblast and Sandpaper Cleaning, Marine Structures, 49, pp. 18–30.

Garbatov, Y., Guedes Soares, C., and Wang, G. (2007) Nonlinear Corrosion Wastage of Deck Plates of Ballast and Cargo Holds of Tankers, Journal of Offshore Mechanics and Arctic Engineering, 129, 1, pp. 48–55.

Ghaffari, M. A. and Hosseini-Toudeshky, H. (2013) Fatigue Crack Propagation Analysis of Repaired Pipes With Composite Patch Under Cyclic Pressure, Journal of Pressure Vessel Technology, Transactions of the ASME, 135, 3, American Society of Mechanical Engineers, New York.

Gibson A.G and Arun S. (2016) Composite Materials in the Offshore Industry, In Module in Materials Science and Materials Engineering, Elsevier, Amsterdam, The Netherlands.

Grepl, M.A. and Patera, A.T. (2005) A-Posteriori Error Bounds for Reduced-Basis Approximations of Parametrized Parabolic Partial Differential Equations, Mathematical Modelling and Numerical Analysis, 39, 1, pp. 157–181.

Guedes Soares, C. G. and Garbatov, Y. (Eds.) (2015) Ships and Offshore Structures XIX, CRC Press, Boca Raton, Florida, USA.

Guo, J., Wang, G., Ivanov, L., and Perakis, A. (2008) Time-Varying Ultimate Strength of Aging Tanker Deck Plate Considering Corrosion Effect, Marine Structures, 21, pp. 402–419.

Haagensen P. J., Larsen J. E., and Vårdal, O. T. (2015) Long Term Effectiveness of Life Extension Methodologies Applied to Offshore Structures, Engineering Failure Analysis, 58, pp. 499–513.

Hall, S. (2012) Retrofit CP System Designed to Restore Caisson Integrity, Offshore, 72, 12, pp. 68.

Hess, P., et al. (2015) Structural Longevity, Specialist Committee V.7, 19th International Ship and Offshore Structures Congress, 6-10 September, Cascais, Portugal.

Horn, A.M., et al. (2009) Fatigue and Fracture, Committee III.2, 17th International Ship and Offshore Structures Congress, 16–21 August, Seoul, Korea.

Huang, C., Suna P., Nagarajaiahb, S., and Gopalakrishnan, S. (2013) Time-Frequency Methods for Structural Health Monitoring of Deepwater Risers Subjected to Vortex Induced Vibrations, In Sensors and Smart Structures Technologies for Civil, Mechanical, and Aerospace Systems 2013, Lynch, J. P., Yun, C.-B., Wang, K.-W. (Eds), Proceedings of SPIE, 8692, 86923E-1, SPIE CCC code: 0277-786X/13/$18 · doi: 10.1117/12.2010592, International Society for Optics and Photonics, Bellingham, Washington, USA.

Hutchison, E., Wintle, J., O'Connor, A., Buennagel, E., and Buhr, C. (2015) Fatigue Reassessment to Modern Standards for Life Extension of Offshore Pressure Vessels, American Society of Mechanical Engineers, Pressure Vessels and Piping Division

Publication PVP, 7, ASME 2015 Pressure Vessels and Piping Conference, July 19–23, 2015, Boston, Massachusetts, USA.

IACS (2014) Harmonized Common Structural Rules for Bulk Carriers and Double Bottom Tankers., International Association of Classification Societies, London, UK.

Ibrahim, M. (2015) Non-Destructive Testing and Structural Health Monitoring of Marine Composite Structures, Graham-Jones, J. and Summerscales, J. (Eds.), Marine Applications of Advanced Fibre-Reinforced Composites, Chapter 7, Woodhead Publishing, Sawston, Cambridge, UK.

Ibrahim, R.A. (2015 a) Overview of Structural Life Assessment and Reliability, Part I: Basic Ingredients of Fracture Mechanics, Journal of Ship Production and Design, 31, 1, February, pp. 1–42.

Ibrahim, R.A. (2015 b) Overview of Structural Life Assessment and Reliability, Part II: Fatigue Life and Reliability Assessment of Naval Ship Structures, Journal of Ship Production and Design, 31, 2, May, pp. 100–128.

Ibrahim, R.A. (2015 c) Overview of Structural Life Assessment and Reliability, Part III: Impact, Grounding, and Reliability of Ships under Extreme Loading, Journal of Ship Production and Design, 31, 3, pp. 137–169.

Ibrahim, R.A. (2015 d) Overview of Structural Life Assessment and Reliability, Part IV: Corrosion and Hydrogen Embrittlement of Naval Ship Structures, Journal of Ship Production and Design, 31, 4, pp. 241–263.

Ibrahim, R.A. (2016 a) Overview of Structural Life Assessment and Reliability, Part V: Joints and Weldments, Journal of Ship Production and Design, 32, 1, February, pp. 1–20.

Ibrahim, R.A. (2016 b) Overview of Structural Life Assessment and Reliability, Part VI: Crack Arrestors, Journal of Ship Production and Design, 32, 2, May, pp. 71–98.

IEC (2016) Fibre Optic Sensors — Part 1-1: Strain Measurement — Strain Sensors Based on Fibre Bragg Grating, IEC 61757-1-1, International Electrotechnical Commission, Geneva, Switzerland.

IMO (2017) MSC-FAL.1/Circ. 3 on Guidelines on Maritime Cyber Risk Management, International Maritime Organization, London, UK.

ISO (1995) Petroleum and Natural Gas Industries — Offshore Structures — Part 1: General Requirements, ISO 13819-1, January, International Organization for Standardization, Geneva, Switzerland.

ISO (2007) Petroleum and Natural Gas Industries — Fixed Steel Offshore Structures, ISO 19902. December, International Organization for Standardization, Geneva, Switzerland.

ISO (2014 a) Asset Management — Overview, Principles and Terminology, ISO 55000, International Organization for Standardization, Geneva, Switzerland.

ISO (2014 b) Asset Management - Management Systems — Requirements, ISO 55001, International Organization for Standardization, Geneva, Switzerland.

ISO (2017 a) Ships and Marine Technology — Shipboard Data Servers to Share Field Data at Sea, ISO/DIS 19847:2017(E), International Organization for Standardization, Geneva, Switzerland.

ISO (2017 b) Ships and Marine Technology — Standard Data for Shipboard Machinery and Equipment, ISO/DIS 19848:2017(E). International Organization for Standardization, Geneva, Switzerland.

Jurisic, P. and Parunov, J. (2015) Influence of Corrosion-Related Degradation of Mechanical Properties of Shipbuilding Steel on Collapse Strength of Plates and Stiffened Panels. Towards Green Marine Technology and Transport, Guedes Soares, C.; Dejhalla, R.; Pavletić, D. (Eds.), Taylor and Francis Group, London, UK, pp. 427-432.

Jurisic, P., Parunov, J. and Ziha, K. (2011) Uncertainty in Corrosion Wastage Prediction of Oil Tankers, Proceedings of the 14th International Congress of the International Maritime Association of the Mediterranean IMAM 2011, Guedes Soares, C. and Rizzuto, E. (Eds.) London: Taylor and Francis Group, London, UK, pp. 395-401.

Jurisic, P., Parunov, J., and Garbatov, Y. (2014) Comparative Analysis Based on Two Nonlinear Corrosion Models Commonly Used for Prediction of Structural Degradation of Oil Tankers, Transactions of Faculty of Mechanical Engineering and Naval Architecture, University of Zagreb, Croatia, 38, 2, 21–30.

Jurisic, P., Parunov, J., and Garbatov, Y. (2017) Aging Effects on Ship Structural Integrity, Shipbuilding, 68, 2, pp. 15–28.

Jurisic, P., Parunov, J., and Garbatov, Y. (2014) Comparative Analysis Based on Two Nonlinear Corrosion Models Commonly Used for Prediction of Structural Degradation of Oil Tankers, Transactions of Faculty of Mechanical Engineering and Naval Architecture, University of Zagreb, Croatia, 38, 2, pp. 21–30.

Jurisic, P., Parunov, J., and Ziha, K. (2011) Uncertainty in Corrosion Wastage Prediction of Oil Tankers, Proceedings of the 14th International Congress of the International Maritime Association of the Mediterranean (IMAM 2011), Guedes Soares, C. and Rizzuto E (Eds.) London: Taylor and Francis Group, pp. 395–401.

Kaminski, M.L. (2007) Sensing and Understanding Fatigue Lifetime of New and Converted FPSOs, Proceedings of the 2007 Offshore Technology Conference, 30 April–3 May, Houston, Texas, USA.

Karuppasamy, P., Abudhahir, A., Prabhakaran, M., Thirunavukkarasu, S., Rao, B.P.C., and Jayakumar, T. (2016) Model-Based Optimization of MFL Testing of Ferromagnetic Steam Generator Tubes, Journal of Non-destructive Evaluation, 35, 1, pp. 1–9.

Kefal, A. and Oterkus, E. (2016) Displacement and Stress Monitoring of a Chemical Tanker Based on Inverse Finite Element Method, Ocean Engineering, 112, pp. 33–46.

Kougioumtzoglou, I.A. and Spanos, P.D. (2013) A Wiener Path Integral Technique for Determining the Response of a Bending Beam with Random Material Properties, in Safety, Reliability, Risk and Life-Cycle Performance of Structures and Infrastructures, Deodatis, G., Ellingwood, B., and Frangopol, D. (Eds.), CRC, Taylor and Francis Group, London, ISBN 978-1-138-00086-5, 2013.

KR (2017) Rules and Guidance for the Classification of Steel Ships, Part 9, Chapter 6, pp. 129–133, Korean Register of Shipping, Busan, South Korea.

L'Hostis, D., Cammen, Van der, J., Hageman, R.B., and Aalberts, P.J. (2013) Overview of the Monitas II Project, Proceedings of the 23rd International Offshore and Polar Engineering Conference, 1–5 July, Anchorage, Alaska, USA.

Le Son, K., Fouladirad, M., and Barros, A. (2016) Remaining Useful Lifetime Estimation and Noisy Gamma Deterioration Process, Journal of Reliability Engineering and System Safety, 149, 76–87.

Li, C. and Shi, X. (2014) Design Method of a New Type of Expansive Stressed Grouted Clamp, Advanced Materials Research, 838–841, pp. 586–592.

Lomasney, C., Collinson, L., and Burnett, T. (2015) Developments in Nanolaminated Materials to Enhance the Performance and Longevity of Metal Components in Offshore Applications, Offshore Technology Conference, doi:10.4043/25830-MS.

Lotsberg, I., Fjeldstad, A., and Ronold, K.O. (2016) Background for Revision of DNVGL-RP-C203, Fatigue Design of Offshore Steel Structures, in 2016, Paper No. OMAE2016-54939, Proceedings of International Conference on Ocean, Offshore and Arctic Engineering (OMAE 2016), Busan, South Korea.

LR (2012) Ship Event Analysis, Lloyds Register, London.

Lynch, J.P., Law, K.H., and O'Connor, S. (2012) Probabilistic and Reliability-based Health Monitoring Strategies for High-Speed Naval Vessels, Office of Naval Research Report, January, Arlington, Virginia, USA.

Magoga, T., Aksu, S., Thomas, G., Ojeda, R., and Cannon, S. (2014) Identification of Slam Events Experienced by a High-Speed Craft, ASRANET Conference: International Conference on Safety and Reliability of Ship, Offshore and Subsea Structures, 18–19 August, Glasgow, UK.

Magoga, T., Aksu, S., Cannon, S., Ojeda, R. and Thomas, G. (2015) The Need for Fatigue Life Prediction Methods Tailored to High-Speed Craft, Proceedings of the International Maritime Conference 2015, 6–8 October, Sydney, Australia.

Magoga, T., Aksu, S., Cannon, S., Ojeda, R., and Thomas, G. (2016) Comparison Between Fatigue Life Values Calculated Using Standardised and Measured Stress Spectra of a Naval High-Speed Light Craft, 13th International Symposium on Practical Design of Ships and Other Floating Structures, 4–8 September, Copenhagen, Denmark.

Magoga, T., Aksu, S., Cannon, S., Ojeda, R., and Thomas, G. (2017) Identification of Slam Events Experienced by a High-Speed Craft, Ocean Engineering, 140, pp. 309–321.

Matic, P., Geltmacher, A., and Rath, B. (2015) Computational Aspects of Steel Fracturing Pertinent to Naval Requirements, Philosophical Transactions A, 373, 2038, 20140127 (22 pp.).

May, P. (2014) Gaps and Issues Regarding Codes and Standards for SIM, Structural Integrity Management Conference, 6–7 November, Aberdeen, UK.

Melchers, R.E. (2008) Development of New Applied Models for Steel Corrosion in Marine Applications Including Shipping, Ships and Offshore Structures, 3, 2, pp. 135–144.

Melchers, R.E. (2016) Developing Realistic Deterioration Models, Keynote lecture in Life-Cycle of Engineering Systems: Emphasis on Sustainable Civil Infrastructure, Proceedings of the Fifth International Symposium on Life-Cycle Civil Engineering (IALCCE 2016). Jaap and Bakker. (Eds.), Delft, The Netherlands.

Mendoza, Edgar, John Prohaska, Connie Kempen, Yan Esterkin, Sunjian Sun, and Sridhar Krishnaswam (2012) Distributed Fiber Optic Acoustic Emission Sensor (FAESense™) System for Condition Based Maintenance of Advanced Structures, 6th European Workshop on Structural Health Monitoring, 3–6 July 2012, Bremen, Germany..

Michala, A.L., Barltrop, N., Amirafshari, P., Lazakis, I., and Theotokatos, G. (2017) An Intelligent System for Vessels' Structural Reliability Evaluation, in Life-Cycle of Engineering Systems: Emphasis on Sustainable Civil Infrastructure, Bakker, Frangopol and van Breugel (Eds.), Taylor and Francis Group, London.

Momber, A.W., Plagemann, P., Stenzel, V., and Schneider, M. (2008) Investigating Corrosion Protection of Offshore Wind Towers: Part 1: Background and Test Program, Journal of Protective Coatings and Linings, 30, pp. 1–14.

Momber, A.W., Plagemann P. and Stenzel, V. (2015) Performance and Integrity of Protective Coating Systems for Offshore Wind Power Structures After Three Years Under Offshore Site Conditions, Renewable Energy, 74, pp. 606–617.

NASA (2008) Non-destructive Evaluation Requirements for Fracture-Critical Metallic Components, NASA Technical Standard NASA-STD-5009, National Aeronautics and Space Administration, Washington, D.C., USA.

Nezamian A. and Clarke E. (2014) Optimised Fatigue and Reliability RBI Program for Requalification, Life Extension, and Integrity Management of Offshore Structure, Offshore Technology Conference Asia: Meeting the Challenges for Asia's Growth, Offshore Technology Conference ASIA 2014, 25–28 March, Kuala Lumpur, Malaysia.

Nichols, J.M., Fackler, P.L., Pacifici, K., Murphy, K.D., and Nichols, J.D. (2014) Reducing Fatigue Damage for Ships in Transit Through Structured Decision Making, Marine Structures, 38, pp. 18–43.

NK (2017) Rules for Hull Monitoring Systems, Nippon Kaiji KyokaI (Class NK) Tokyo.

NORSOK (2015) Assessment of Structural Integrity for Existing Offshore Load-Bearing Structures, NORSOK-N-006, Standards Norway [online], Available from: www.standard.no/petroleum.

NORSOK (2016) In-service Integrity Management of Structures and Maritime Systems, NORSOK-N-005, Standards Norway, [online], Available from: www.standard.no/petroleum.

OCIMF (2016) Ship Inspection Report (SIRE) Programme, Vessel Inspection Questionnaires for Oil Tankers, Combination Carriers, Shuttle Tankers. Chemical Tankers, and Gas Tankers, Oil Companies International Marine Forum, London, February.

Offshore Energy Today (2017) Avitas, Kraken Team Up for Robotic Subsea Inspection. October 27.

Orabi, A.R. (2016) Intelligent Pigging VS ROV for the offshore pipeline inspection, https://www.linkedin.com/pulse/intelligent-pigging-vs-rov-offshore-pipeline-ahmed-raafat-orabi, published 1 June, accessed 27 Feb 2018.

Paik, J.K., Satish Kumar, Y.V., and Lee, J.M. (2005) Ultimate Strength of Cracked Plate Elements Under Axial Compression or Tension, Thin-Walled Structures, 43, pp. 237–272.

Paik, J., Balli, A., Ryu, J., Jang., Seo, J. Park, S., Soe, S., Renaud, C., and Kim, N. (2008) Mechanical Collapse Testing on Aluminium Stiffened Panels for Marine Applications, Ship Structure Committee Report SSC-451, U.S. Coast Guard, Washington, D.C.

Parunov, J., Žiha, K., Mage, P., and Jurišić, P. (2010) Hull Girder Fatigue Strength of Corroding Oil Tanker, in Advanced Ship Design for Pollution Prevention, ed. Guedes Soares and Parunov, Taylor and Francis Group, London, pp. 149–154.

Perišić, N. and Tygesen, U.T. (2014) Cost-Effective Load Monitoring Methods for Fatigue Life Estimation of Offshore Platform, in ASME 2014 33rd International Conference on Ocean, Offshore and Arctic Engineering, American Society of Mechanical Engineers, pp. V04BT02A005–V04BT02A005.

Potty, N.S. and Mohd Akram, M.K.B. (2009) Structural Integrity Management for Fixed Offshore Platforms in Malaysia, WASET, International Journal of Civil, Environmental, Structural, Construction and Architectural Engineering, 3, 10.

Rafiei, R., Mohseni, M., Yari, H., and Mahdavi, M. (2016) Evaluation of Degradability of Two Polyurethane Refinish Coatings Against Biological Materials: A Case Study, Progress in Organic Coatings, 93, pp. 1–10.

Raišutis, R., Jasiūnienė, E., Šliteris, R., and Vladišauskas, A. (2016) The Review of Non-Destructive Testing Techniques Suitable for Inspection of the Wind Turbine Blades, Ultragarsas, Ultrasound, 63, 2, pp. 49–52.

Ramezanzadeh, B., Mohseni, M., Yari, H., and Sabbaghian, S. (2009) An Evaluation of an Automotive Clear Coat Performance Exposed to Bird Droppings Under Different Testing Approaches, Progress in Organic Coatings, 66, pp. 149–160.

Ramezanzadeh, B., Mohseni, M., and Yari, H. (2011) On the Electrochemical and Structural Behaviour of Biologically Degraded Automotive Coatings; Part 1: Effect of Natural and Simulated Bird Droppings, Progress in Organic Coatings, 71, pp. 19–31.

Rao, B.P.C. and Jayakumar, T. (2012) Recent Trends in Electromagnetic NDE Techniques and Future Directions, in 18th World Conference on Non-Destructive Testing, Durban, South Africa, 16–20 April.

Reed, H.M. and Earls, C.J. (2015) Stochastic Identification of the Structural Damage Condition of a Ship Bow Section Under Model Uncertainty, Ocean Engineering, 103, pp. 123–143.

Ren, X. B., Nyhus, B., Lange, H.L., and Hague, M. (2015) Leak-Before-Break Analysis of a Pipe Containing Circumferential Defects, Engineering Failure Analysis, 58, pp. 369–379.

RINA S.p.A. (2008) GUI-7, Guide for Ship Condition Assessment Program (CAP), Registro Italiano Navale, Genova, Italy, January.

Rosen, J., Johnstone, D., Sincock, P., Potts A.E., and Hourigan, D. (2016) Application of Reliability Analysis to Re-Qualification and Life Extension of Floating Production Unit Moorings, Paper No. OMAE 2016-54677, Proceedings of International Conference on Ocean, Offshore and Arctic Engineering (OMAE 2016), Busan, South Korea.

SAE AIR6258 (2015) Fiber Optic Sensors for Aerospace Applications, SAE Standard AIR 6256, SAE International, Warrendale, Pennsylvania, USA.

Saad-Eldeen, S., Garbatov, Y., and Guedes Soares, C. (2014) Experimental Assessment of Corroded Steel Box Girders Subjected to Uniform Bending, Ships and Offshore Structures, 9.

Sahoo, P., Das, S.K., and Paulo, D.J. (2017) Surface Finish Coatings A2, In Comprehensive Materials Finishing, Hashmi, M.S.J., Ed., Elsevier, Oxford, UK, pp. 38–55.

Sánchez-Silva, M., Frangopol, D.M., Padgett, J. and Soliman, M. (2016) Maintenance and Operation of Infrastructure Systems: Review, Journal of Structural Engineering, 142, 9.

Schmidt, V. (2013) Corrosion Problems Solved with Composite Materials, Offshore Engineers, 1 June.

Seif, A.E. and Kabir, M. Z. (2017) Experimental Study on the Fracture Capacity and Fatigue Life Reduction of the Tensioned Cracked Plate Due to the Local Buckling, Engineering Fracture Mechanics, 15, April, pp. 168–183.

Seth, J., Pric, R., and Figueira, B. (2017) Corrosion Protection Systems and Fatigue Corrosion in Offshore Wind Structures: Current Status and Future Perspectives, Coatings 7, 25, pp. 1–51.

Shafiee, M. and Animah, I. (2017) Life Extension Decision Making of Safety Critical Systems: An Overview, Journal of Loss Prevention in the Process Industries, 47, pp. 174–188.

Shen, W., Yan, R., Xu, L., Tang, G., and Chen, X. (2015) Application Study on FBG Sensor Applied to Hull Structural Health Monitoring, Optik—International Journal for Light and Electron Optics, 126, pp. 1499–1504.

Shukla, A. and Karki, H. (2016) Application of Robotics in Offshore Oil and Gas Industry—A Review Part II, Robotics and Autonomous Systems, 75, pp. 508–524.

Skafte, A., Kristoffersen, J., Vestermark, J., Tygesen, U.T., and Brincker, R. (2017) Experimental Study of Strain Prediction on Wave Induced Structures Using Modal Decomposition and Quasi Static Ritz Vectors, Engineering Structures, 136, pp. 261–276.

Smarsly, K., Dragos, K., and Wiggenbrock, J. (2016) Machine Learning Techniques for Structural Health Monitoring, presented at the 8th European Workshop on Structural Health Monitoring (EWSHM 2016), 5–8 July, Bilbao, Spain.

Söffker, D. and Rakowsky, U.K. (1997) Perspectives of Monitoring and Control of Vibrating Structures by Combining New Methods of Fault Detection with New Approaches of Reliability Engineering, Proceedings of the 12th ASME Conference on Reliability, Stress Analysis, and Failure Prevention, Virginia Beach, Virginia, USA, April, Pusey, H.C. (Ed.), A Critical Link: Diagnosis to Prognosis, A Publication of the Society for Machinery Failure Prevention Technology, pp. 671–82.

Soliman, M., Barone, G., and Frangopol, D.M. (2015) Fatigue Reliability and Service Life Prediction of Aluminum Naval Ship Details Based on Monitoring Data, Structural Health Monitoring 14, 1, pp. 3–19.

Soliman, M., Frangopol, D.M., and Mondoro, A. (2016) A Probabilistic Approach for Optimizing Inspection, Monitoring, and Maintenance Actions Against Fatigue of Critical Ship Details, Structural Safety, 60, pp. 91–101.

Stambaugh, K., Drummen, I., Cleary, C., Sheinberg, R., and Kaminski, M. L. (2014) Structural Fatigue Life Assessment and Sustainment Implications for a new class of U.S. Coast Guard Cutters, Ship Structure Committee Ship Structures Symposium, Linthicum Heights, Maryland, USA, 18–20 May.

Talabani, S., Atlas, B., Al-Khatiri, M.B., and Islam, M.R. (2000) An Alternate Approach to Downhole Corrosion Mitigation, Journal of Petroleum Science and Engineering, 26, 41–48.

Tammer, M.D. and Kaminski, M.L. (2013) Fatigue Oriented Risk Based Inspection and Structural Health Monitoring of FPSOs, Proceedings of the 23rd International Offshore and Polar Engineering Conference (ISOPE), Anchorage, Alaska, USA. pp. 438–449.

Tang, Y., Qing, Z., Zhu, L., and Zhang, R. (2015) Study on the Structural Monitoring and Early Warning Conditions of Aging Jacket Platforms, Ocean Engineering, 101, pp. 152–160.

Tessler, A. and Spangler, J.L. (2003) A Variational Principle for Reconstruction of Elastic Deformation of Shear Deformable Plates and Shells, National Aeronautics and Space Administration TM-2003–212445, Washington, D.C., USA.

Tessler, A. and Spangler, J.L. (2005) A Least-Squares Variational Method for Full-Field Reconstruction of Elastic Deformations in Shear-Deformable Plates and Shells, Computer Methods in Applied Mechanics and Engineering, 194, 2, pp. 327–339.

Tygesen U. (2016) Structural Integrity New Challenges—New Technologies, Presented at the Offshore North Sea: ONS 2016 Exhibition Conference Festival, Stavanger, Norway.

Tygesen., U.T., Worden, K., Rogers, T., Manson, G., and Cross, E.J. (2018) State-of-the-Art and Future Directions for Predictive Modelling of Offshore Structure Dynamics using Machine Learning, Presented at IMAC-XXXVI Conference and Exposition on Structural Dynamics, 12–15 February, Orlando, Florida, USA.

Van den Berg, D., Tammer, M.D., and Kaminski, M.L. (2014) Updating Fatigue Reliability of Uninspectable Joints using Structurally Correlated Inspection Data, Proceedings of the 24th International Ocean and Polar Engineering Conference, 15–20 June, Busan, Korea, ISSN 1098-6189.

Van der Horst, M.P., Kaminski, M.L., Puki, E., and Lepelaars, E. (2014) Testing and Numerical Simulation of Magnetic Fields Affected by Presence of Fatigue Cracks, presented at the 24th International Offshore and Polar Engineering Conference, 15–20 June, Busan, South Korea.

Van der Meulen, F.H. and Hageman, R.B. (2013) Fatigue Predictions using Statistical Inference within the Monitas II JIP, Proceedings of the 23rd International Offshore and Polar Engineering Conference, 1–5 July, Anchorage, Alaska, USA.

Vera-Tudela, L. and Kühn, M. (2017) Analysing Wind Turbine Fatigue Load Prediction: The Impact of Wind Farm Flow Conditions, Renewable Energy, 107, pp. 352–360.

Vincent, P., Wilson, A., Brincat, M., and Yiannakopoulos, G. (2015) Design, Installation and Repair of Hull Sensors for the Measurement of Hull Slamming Pressure Loads on Armidale Class Patrol Boats, Proceedings of International Maritime Conference, Pacific 2015, 6–8 October, Sydney, Australia.

Vugts, J.H. (2013) Handbook of Bottom Founded Offshore Structures—Part 1: General Features of Offshore Structures and Theoretical Background, Eburon Delft 2013, ISBN: 978-90-5972-796-0.

Wilken, M., Langhecker, U., and Moldenhauer, M. (2013) An Advanced Solution for Recording, Visualization, and Assessment of Thickness Measurements of Ships, Proceedings of the 13th International Conference on Computer Applications in Shipbuilding, ICCAS, 24–26 September, Busan, Korea.

Yamamoto, N. and Ikagaki, K. (1998) A Study on the Degradation of Coating and Corrosion on Ship´s Hull Based on the Probabilistic Approach, Journal of Offshore Mechanics and Arctic Engineering, 120, pp. 121–128.

Yonezawa, T., Ando, H., and Kakuta, R. (2017) Vessel Performance Model and its Utilization in Shipping Company, Hull Performance and Insight Conference (HullPIC) 2017, 27–29 March, Castle Ulrichshusen, Germany.

Zhang, C.J., Zhang, H.H., Shi, X., Chen, J.R., and Zhou, L. (2016) Design Method of an Expansive Stressed Grouted Clamp on a Joint of a Jacket Platform, ISOPE 2016, 26 June–2 July, Rhodes (Rodos), Greece.

Zhu, B. and Frangopol, D.M. (2013) Reliability Assessment of Ship Structures Using Bayesian Updating, Engineering Structure, 56, pp. 1836–1847.

Zhu, J. and Collette, M. (2015) A Dynamic Discretization Method for Reliability Inference in Dynamic Bayesian Networks, Reliability Engineering and System Safety, 138, pp. 242–252.

Zhu, W.L., Shi, X., Chen, J.R., Zhou, L., and Zhang, C.J. (2017) Analysis on Design Method of Expansive Stressed Grouted Clamp for Platforms Assessing the Modified Stiffness and the Increased Environmental Loads, ISOPE 2017, 25–30 June, San Francisco, California, USA.

Ziegler, L. and Muskulus, M. (2016) Fatigue Reassessment for Lifetime Extension of Offshore Wind Monopile Substructures, Journal of Physics: Conference Series, 753 092010.

Proceedings of the 20th International Ship and Offshore Structures Congress (ISSC 2018) Volume II – M.L. Kaminski and P. Rigo (Eds.)

doi:10.3233/978-1-61499-864-8-461

COMMITTEE V.8

REPORT FOR SUBSEA TECHNOLOGY

COMMITTEE MANDATE

Concern for the safety and reliability of subsea production systems for oil and gas offshore. This shall include subsea equipment for production and processing, flowlines and risers, with emphasis to design, fabrication, qualification, installation, inspection, maintenance, repair and decommissioning. Structural design for flow assurance and safe underwater operations shall be considered.

AUTHORS/COMMITTEE MEMBERS

Chairman: Menglan Duan, *China*
Shuhong Chai, *Australia*
Ilson Paranhos Pasqualino, *Brazil*
Liping Sun, *China*
Claus Myllerup, *Denmark*
Spyros Mavrakos, *Greece*
Asokendu Samanta, *India*
Kieran Kavanagh, *Ireland*
Masahiko Ozaki, *Japan*
Svein Sævik, *Norway*
Angelo Teixeira, *Portugal*
Ying Min Low, *Singapore*
Jung Kwan Seo, *South Korea*
Sebastian Schreier, *The Netherlands*
Pieter Swart, *The Netherlands*
Hao Song, *USA*

KEYWORDS

Subsea Production System, Subsea Processing, Flow Assurance, Fabrication, Testing for Qualification, Deepwater Installation, Subsea Operations, Inspection, Maintenance and Decommissioning, Hydrates, Pipelines, Risers and Umbilicals, Reliability and Safety

CONTENTS

1. INTRODUCTION 464

2. SUBSEA PROCESSING EQUIPMENT AND FABRICATION 465
2.1 Introduction 465
2.2 Separators 466
2.2.1 Subsea Gas-Liquid Separation 466
2.2.2 Subsea Multiphase Separation 467
2.2.3 Recent Studies 467
2.3 Pumps 468
2.4 Compressors 468
2.5 Electrical Systems 469
2.6 Material for Fabrication of Key Components 469

3. FLOW ASSURANCE OF SUBSEA PRODUCTION ENGINEERING 470
3.1 Thermal management 470
3.2 Chemical injection 472
3.3 Operation and equipment 472
3.4 Software technology 473
3.5 Prospective approach 474
3.6 Conclusions 474

4. TESTING FOR QUALIFICATION OF SUBSEA PRODUCTION SYSTEM 475
4.1 Qualification 475
4.2 Advanced Testing for Qualification of All-Electric Subsea Production 476
4.3 Advanced Testing for Qualification of Multiphase Pumping 478
4.3.1 Worn Balance Piston Test 479
4.3.2 Slug Test 479
4.4 Advanced Testing for Qualification of Subsea Wet Gas Compressor 480
4.5 Advanced Testing for Qualification of Subsea Transformer 481

5. INSTALLATION AND OPERATIONS FOR EMERGENCIES 482
5.1 Installation for Subsea Hardware 482
5.1.1 Lifting Method 482
5.1.2 Drilling Riser Method 483
5.1.3 Sheave Method 483
5.1.4 Pencil Buoy Method 484
5.1.5 Subsea 7 Method 484
5.1.6 Pendulous Installation Method 485
5.2 Oil Spill in Gulf of Mexico and Measures Taken against The Accident 486
5.3 Responses to Oil Spill 487
5.3.1 Dispersants 487
5.3.2 In-suit burning of oil 488
5.3.3 Spill surveillance, monitoring and visualization 488
5.3.4 Deepwater subsea waterjet 489
5.3.5 Subsea emergency response system 489
5.4 Responses to Pipeline Emergency 490
5.4.1 Temporary by-pass 490
5.4.2 Installation of a bolted clamp 490
5.4.3 Lift up and repair/Above water repair 490
5.4.4 Remote welding system 490

6. INSPECTION, MAINTENANCE AND DECOMMISSIONING OF SUBSEA SYSTEMS 491
6.1 Technology Developments of Subsea Systems Inspection 491
6.1.1 Robotics in Deep Water 491
6.1.2 3D Laser Imaging Systems 492
6.1.3 Non-Destructive Examination of Flexible Risers 492
6.2 Advances in Maintenance of Subsea Systems 492
6.2.1 Risk Based Asset Management (RBAM) 492
6.2.2 Pipeline Maintenance Plan 492
6.2.3 Well Maintenance Plan 492
6.3 Advance in Decommissioning of Subsea Systems 493
6.3.1 Subsea Cutting Technology 493
6.3.2 Sub Bottom Cutter 493
6.3.3 Pipe Cutting Tool 494
6.3.4 Plugging and De-oiling 494
6.3.5 External Latch Mechanical for Well Decommissioning 495
6.4 Conclusion 495

7. TECHNOLOGIES FOR HYDRATES AND OTHER SUBSEA RESOURCES 496
7.1 Depressurization 496
7.2 Thermal Stimulation 497
7.3 Chemical Inhibitor 497
7.4 CO_2-CH_4 Replacement 498

8. PIPELINES, RISERS AND UMBILICALS 499
8.1 Soil-Structure Interaction 499
8.1.1 Industry Standards 499
8.1.2 Steel Catenary Risers 499
8.1.3 Top Tensioned Risers 500
8.1.4 Hybrid Riser Systems 500
8.1.5 Pipelines 501
8.2 Local/Global Buckling and Propagation 501
8.3 Vortex Induced Vibration of Cylindrical Structure 503
8.4 Dynamic Behavior and Fatigue 504
8.5 Special Issues for Flexible Pipes and Umbilicals 505

9. RELIABILITY AND SAFETY IN SUBSEA SYSTEM 508
9.1 Introduction 508
9.2 Reliability and Safety Engineering Standards 508
9.2.1 Standards and Codes for Safety and Reliability of Subsea System 508
9.2.2 Update in the Newer Version of API RP 17N 508
9.3 New progress on reliability and safety evaluation of subsea systems 509

10. CONCLUSIONS AND RECOMMENDATIONS 511

ACKNOWLEDGEMENTS 512

REFERENCES 512

1. INTRODUCTION

With rapid development of industry, the world's energy consumption has increased steadily since the 1950s, and the fossil fuels (oil, natural gas and coal) still amount to 80% of the world's energy consumption. Since the 1960s, the increasing demand for oil and the depletion of onshore and offshore shallow-water reserves, fasten the exploration and production of oil in deep waters, and challenge the offshore industries. As an efficient and cost-effective plan for the development of deep-water oil and gas fields, subsea production systems have become more and more important for the exploitation of offshore oil and gas. Due to its huge potential, more and more operators and owners have been attracted by subsea production systems.

A subsea production system consists of a subsea completed well, seabed wellhead, subsea production X-tree, subsea tie-in to flowline system, and subsea equipment and control facilities to operate the well, as shown in Figure 1.1. It can range in complexity from a single satellite well with a flowline linked to a fixed platform, FPSO (Floating Production, Storage and Offloading), or onshore facilities, to several wells on a template or clustered around a manifold that transfer to a fixed or floating facility or directly to onshore facilities. As the oil and gas fields move further offshore into deeper water and deeper geological formations in the quest for reserves, the technology of drilling and production has advanced dramatically. The latest subsea technologies have been proven and formed into an engineering system, namely, the subsea production system, which is associated with the overall process and all the equipment involved in drilling, field development, and field operation. The subsea production system consists of the following components:

- Subsea drilling systems;
- Subsea wellhead and Christmas trees;
- Subsea processing and boosting systems;
- Subsea injecting system;
- Subsea manifolds and jumper systems;
- Tie-in and flowline systems;
- Umbilical and riser systems;
- Subsea power and control systems;
- Subsea installation and decommissioning.

Figure 1.1: Subsea production system (courtesy Petrobras)

Most subsea structures are built onshore and transported to the offshore installation site. The process of moving subsea hardware to the installation site involves three operations: load-out, transportation, and installation. A typical subsea installation also includes three phases: lowering, landing, and locking. After the production system has been installed, numerous opera-

tions are in place to ensure safe and pollution-free operations and support the continued flow of hydrocarbons. The following are typical of post installation operations:

- Commissioning and start-up (start-up could be “cold” or “hot”);
- Normal operations;
- Production processing;
- Chemical injection;
- Routine testing;
- Maintenance and repair (remotely operated vehicle - ROV, routine surface);
- Emergency shutdown;
- Securing facilities (e.g., from extreme weather events);
- Intervention.

The complex mixture of hydrocarbon compounds or components can exist as a single-phase liquid, a single-phase gas, or as a multiphase mixture, depending on its pressure, temperature, and the composition of the mixture. The hydraulic theory underlying single-phase flow is well understood and analytical models may be used with confidence. Multiphase flow is significantly more complex than single-phase flow. However, the technology to predict multiphase-flow behavior has improved dramatically in the past decades. It is now possible to select pipeline size, predict pressure drop, and calculate flow rate in the flowline with an acceptable engineering accuracy.

The exploration and production of oil and gas resources entail a variety of risks, which, if not adequately managed, have the potential to result in a major incident. All subsea field development procedures involved in designing, manufacturing, installing, and operating subsea equipment are vulnerable to a financial impact if poor reliability is related to the procedure. Equipment reliability during exploration and production is one of the control factors on safety, production availability, and maintenance costs. In the early design phases, the target levels of reliability and production availability can be controlled through application of a systematic and strict reliability management program.

This report presents recent advances and possible future trends in subsea production system. Papers published since the ISSC 2015 Congress are mainly discussed here, but older publications of 2014 are also included if they are considered to present fundamental and important findings in line with the mandate of the present Committee.

2. SUBSEA PROCESSING EQUIPMENT AND FABRICATION

2.1 Introduction

Subsea processing has been applied in all the four major global offshore oil and gas clusters: the North Sea, Gulf of Mexico, West Africa deepwater and Brazilian Pre-Salt. Major oil and gas companies are active in the campaign for developing new technologies on subsea processing. The operators and their partners have developed different processing systems based on specific project requirements, either to enable economic development of deeper green fields, or to extend production life of brown fields and to enhance oil recovery. Under the former situation, subsea gas-liquid two phase separation combined with subsea boosting of liquids is the common solution, while for the latter, subsea gas/oil/water/sand multiphase separation with water reinjection is used.

As part of the corporate technology strategy Statoil has launched a technology plan for the Subsea Factory concept. The plan describes how to combine subsea production and processing technology elements with key business cases and define enabling and cost-efficient development concepts. Statoil has successfully deployed subsea pumps and subsea separators (Troll Pilot and Tordis) (Radicioni et al., 2016) including the world’s first subsea compressors at both Åsgard and Gullfaks fields. It has also launched an All-Electric Subsea (AES) initia-

tive to prove the feasibility of new flexible, cost efficient subsea production system to meet future demands. And on 4 August 2016, the world's first fully all-electric well of subsea industry, K5F3, has been open to production. The all-electric subsea well consist of an electric subsea Christmas tree, electric downhole safety valve, and associated subsea control modules. (Winther-Larssen *et al.*, 2016; Schwerdtfeger *et al.*, 2017; Abicht *et al.*, 2017; Rubio *et al.*, 2017).

Also, some developments are reported on production optimization in the BC-10 field in Brazil and in Girassol oil field in Angola. Some advanced subsea processing system is empoyed. (Sleight *et al.*, 2015, Delescen *et al.*, 2015).

The fast development of the SPS shall be based on the advances in the fabrication of the components and assembling of the complex subsea hardware, which influence the reliability of the system and the service life of the key components in the HTHP environment of strong corrosion. However, little references have been presented from the academic cycle and the product suppliers do not publish their results due to the confidentiality of their technologies.

2.2 Separators

Although a single multiphase pumping can be considered a subsea processing, many of the related equipment installed up to now provide any type of separation or pre-processing.

2.2.1 Subsea Gas-Liquid Separation

The Pazflor project locates approximately 93 miles offshore Luanda, Angola, at water depth between 600 m and 1,200 m. The Pazflor development involves four fields, Perpetua, Acacia, Zinia and Hortensia. Approximately two-thirds of the oil is heavy oil from the Miocene reservoirs of Hortensia, Perpetua and Zinia fields. The heavy Miocene oil is very viscous and reservoir pressure is relatively low, which requires adequate artificial lift methods. Also, to assure fluid flow in an environment prone to generate gas hydrates, subsea separation units are installed near the initial production well at each field. The subsea separation module consists of a vertical separator for gas/liquid separation and two hybrid pumps for lifting the separated liquids (Figure 2.1).

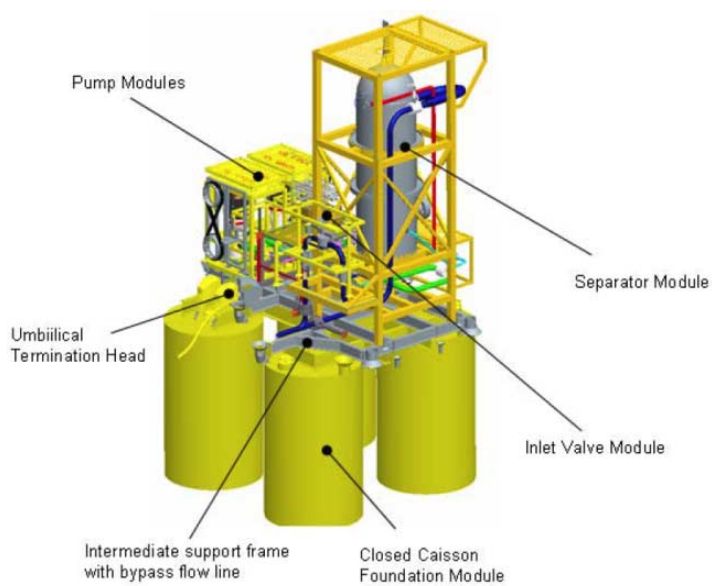

Figure 2.1: Principle overview of subsea separation unit used in Pazflor

2.2.2 Subsea Multiphase Separation

The Marlim field has produced its first oil in 1991 and is located at the northeastern part of Campos Basin, Brazil, at a water ranging from 650 to 1,050m. As it approaches the end of production life, extensive water production restricts further development. To debottleneck water processing capacity at production unit, a pilot subsea separation station with 29m length, 10.8m width, 8.4m height and overall assembly weight of 392 ton was installed at water depth of 870m for the pilot well MRL-141 in 2011.

The subsea processing station performs gas/oil/water/sand separation and water reinjection (Figure 2.2). The production stream firstly goes through an inline multiphase sand remover responsible to remove the bulk part of produced solids. Downstream the multiphase sand remover, gas is separated from liquid through a set of vertically arranged pipes, named as "harp". Right downstream of it, there is a long pipe separator of 60m to perform oil-water separation. At the very end of the pipe separator loop, oil is recombined with separated gas and flows free in a multiphase stream to the topside stationary production unit, while separated water with oil content above limits for reservoir reinjection is routed to a polishment system, which comprises another inline sand remover and two stages of hydro cyclones. It reduces the amount of oil in water to acceptable levels for reinjection through a centrifugal pump.

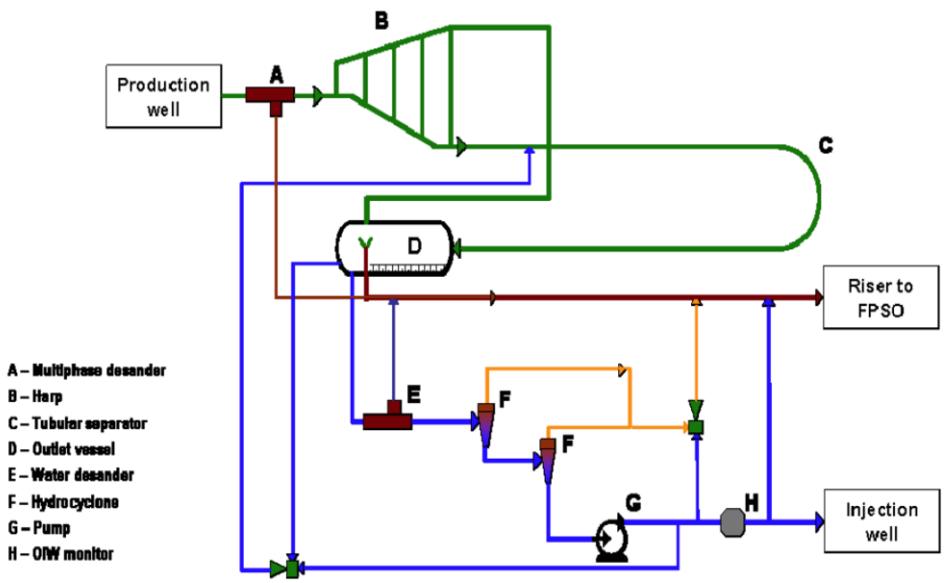

Figure 2.2: Flow diagram of the subsea separation unit at Marlim

2.2.3 Recent Studies

Prescott *et al*. (2016) have studied linear pipe separators to propose less expensive solutions that can provide satisfactory phase separation. Two types of separators were studied, gas-liquid and gas-liquid-solid separators under CFD simulations. The results have proved their effectiveness and also showed that pipe separators can be made with standard pipes with cost reduction of up to 500%.

Tamal *et al*. (2017) developed a simplified 6-state model for gravity separator (often used as a first stage separator in subsea separation systems) with lumped fluid properties. The model is used in an Extended Kalman Filter estimator using measurements of levels and densities of fluids inside the separator in order to estimate unmeasured disturbances, namely inlet total

flow rate, inlet oil cut and inlet droplet diameter. Results show that the estimated disturbances converge to their true values when process changes.

2.3 Pumps

Homstvedt *et al.* (2015) proposed a new type of electrical submerged pump (ESP) that is different from the vertical concept of BC-10 and Perdido, considering that the concept in vertical caisson is too expensive for installation and maintenance. Instead, they proposed horizontal ESP inside flowline jumpers provided of a system to separate gas before pumping and return it to stream after pumping. Beside the low cost, the proposed new concept can be arranged in serial or parallel configurations.

In order to reduce the cost of umbilical power cable, Margarida *et al.* (2017) have worked in a higher voltage subsea pump (3,2MW), to operate at 13,6kV (before from 4.16 to 6.6kV) and reduce cable amperage. The ongoing project can reduce significantly the cable diameter and consequently the associated cost.

Hjelmeland *et al.* (2017) have developed and qualified the world's first high pressure subsea pump. Three units were installed at water depths around 2,100m to sustain production pressure from the ultra-deep reservoirs Jack and St. Malo to Walker Ridge Regional semi-submersible, the largest in displacement in the world. The 3MW pumps provide a differential pressure up to 4,000psi to a minimum inlet pressure of 1,200psi.

2.4 Compressors

The subsea boosting allows the reduction of the well backpressure and consequently increases the flow rate, improving the total reservoir recovery. In addition, it improves flow assurance issues by increasing velocities in pipeline, increasing temperature and stabilizing production.

The Åsgard compression system was set up in 2015 to deliver the world´s first subsea compression station and provide an additional production of 306 million barrels of oil equivalent up to 2032 (Storstenvik, 2016). The system was installed in a water depth of 270m and comprises two parallel 11.5 MW compressor trains with total weight of 5100 tons that are among the biggest structures in the subsea world (74x45x26m). The system requires a pre-processing of the hydrocarbons stream from manifolds using a gas-liquid vertical separator. The gas is compressed with the aid of a centrifugal compressor while the liquid is pumped by a centrifugal pump and both are recombined in a single multiphase stream to a semi-submersible platform Åsgard B located 40km from compression station. It is controlled by an all-electric control system with chemicals (MEG and N2) from Åsgard B while the power supply is provided from a FPSO of Åsgard A. Time and Torpe (2016) reports the commissioning and Dahle et al. (2016) the installation and intervention procedures of the Åsgard compression system.

In 2015 the world´s first subsea multiphase compression system (gas volume fraction between 95 and 100%) was installed at the Gullfaks field. It is comprised of two 5MW wet gas compressors operating in a water depth around 200m that can deliver 32bar of differential pressure (Hjelmeland and Torkildsen, 2016a). The technology is based in a helico-axial impeller and the gas recovery is foreseen to increase from 62 to 74% (22 million barrels of oil equivalent) by using combined multiphase compression with low pressure production. Different from the Åsgard compression system, no pre-processing is required in this case. The system operation can be changed to a parallel configuration to facilitate high flow rate, as well as a lower flow rate and higher differential pressure provided through serial compressor configuration. The qualification and implementation of Gullfaks compression system was presented by Hjelmeland and Torkildsen (2016b) while the commissioning aspects was presented by Birkeland et al. (2016).

2.5 Electrical Systems

Electrical systems are of increasing application to subsea processing, as the need for large power supply together with reduced infra-structure and extended reach of an all-electric control system.

Hasan *et al.* (2015) compared the conventional electro-hydraulic control system with all-electric options showing the benefits of the new technology. Beside the advantages related to HSE, there were significant CAPEX and OPEX reduction due to the reduced infra-structure needed to the all-electric control system. The comparison was based on new valve actuators, subsea control modules (SCMs) and subsea distribution units (SDUs), where electrical units replaced the hydraulic components. Following similar premise, Dobson and Deighton (2017) stated that both all-electric control system and subsea power supply were needed to decrease production cost in view of reduced oil price and to provide the necessary technology to subsea processing development. All-electric control system provided several applications like heated pipelines that are important to flow assurance in many cases, subsea separators, single or multiphase boosting, seawater treatment to reinjection or disposal, electrical power transmission and subsea chemical storage. The future to control and power supply at long distances will be a combination of DC umbilical (low loss) and fiber optics that can provide data rates of 10Gb/s instead of 10Mb/s of copper cables.

Bugge and Ingebrigtsen (2017) report a JIP for subsea power that has the aim to provide 100MW of power transmission along 600km at 3000m water depth. They are working on qualification of components, sub-assemblies and equipment to achieve the reliability of the developed technology which is comprised of subsea medium voltage switchgear and variable speed drivers with associated controls and low voltage distribution. These new products will provide large amounts of power for applications such as subsea compression and boosting.

The first all-electric subsea Christmas tree was installed in 2016 as repoted by Schwerdtfeger *et al.*, 2017, who showed the development and qualification tests of the all-electric subsea Christmas tree components and stated that not only the costs were reduced but also the environmental impacts were reduced and the safety at topside increased.

2.6 Material for Fabrication of Key Components

Subsea Christmas tree, as an example of SPS, is under the complex conditions of deep water, high temperature, high pressure and strong corrosion. The research is focused on design and type-selection of base material, anticorrosion material and sealing material of key parts of subsea trees. The subsea Christmas tree plant is constructed by a series of production and control channels with high temperature, high pressure and high corrosion resistance of crude oil, including tree body, tubing hanging, hydraulic control valve body, double-hole connector, pipe connector and production cross-pipe and other major components of the key components. In view of the low temperature environment, the external environmental load and the internal high pressure bearing conditions, the key components of the subsea tree are required to have low temperature toughness and thermal resistance and fatigue performance. The key components shall present good overall mechanical properties.

Based on the above-mentioned requirements, several low-alloy steel materials (including 4130, 4140, 4340 and F22) commonly used in subsea equipment were compared. In the design, low-alloy high strength steel material F22 (ASTM A182) was chosen as basic material for key components (Norsok M-001 Materials Selection, 2014).

In order to resist the strong corrosion of crude oil and seawater, taking into account the relevant standard requirements, subsea tree material design shall consider the following anti-corrosion measures:

- Inconel 625 of surfacing layer is selected for fluid infiltration surface of production and sealing surface corrosion layer.
- Inconel 718 for the metal seal material of valve seat, stem and valve plate, the annulus and the center hole of the hydraulic control valve.
- duplex stainless steel is used for spiral cross - tube and chemical injection of pipe materials.
- The Christmas tree is equipped with underwater surface fitting parts and fasteners surface with ultra-thin composite PTFE coating material for surface spraying.

For subsea pipeline systems a total corrosion allowance of 10 mm is recommended as a general upper limit for use of carbon steel. Carbon steel can be used in pipelines where calculated inhibited annual corrosion rate is less than 10 mm divided by design life. Otherwise corrosion resistant alloys, solid or clad or alternatively flexible pipe, should be used. For pipelines with dry gas or dry oil, no corrosion allowance is required. Corrosion during installation and testing prior to start-up shall be considered.

The external atmospheric environment shall be considered wet with the condensed liquid saturated with chloride salts. Material selection and surface protection shall be such that general corrosion is cost effectively prevented and chloride stress corrosion cracking, pitting and crevice corrosion are prevented.

Corrosion allowance sizing for carbon steel in the splash zone should follow the below guidelines (Norsok M-001 Materials Selection, 2014):

- Structures with thin film coating: Min. 5 mm. For design lives > 17.5 years. Corrosion allowance = (Design life - 5 years) x 0.4 mm/year.
- Risers: Min. 2 mm in combination with min. 12 mm vulcanized chloroprene rubber. At elevated temperature the corrosion allowance should be increased by 1 mm pr. 10 degrees C increase in temperature above 20 °C.

3. FLOW ASSURANCE OF SUBSEA PRODUCTION ENGINEERING

Flow assurance technologies could be categorized into different solution types: Thermal management, Chemical injection, Operation and Equipment, and Software and control system.

3.1 Thermal management

Cherkaoui et al. (2016) presented an electrically heat traced flowline that is a pipe-in-pipe enclosing in its annulus high performance thermal insulation and specifically designed electrical heating wires. Powering one of these wires is done with a combined system of electrical subsea connectors and penetrators to access inside the sealed pipe-in-pipe annulus.

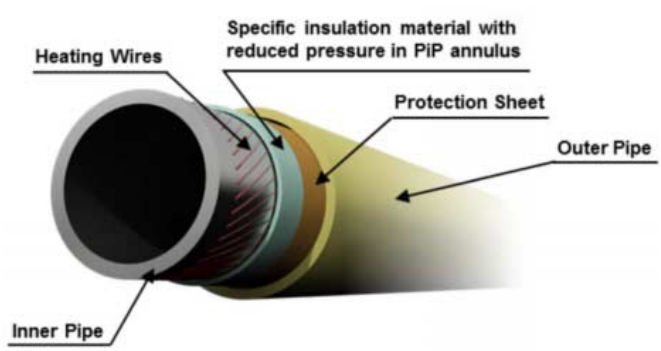

Figure 3.1: Electrically heat traced flowline schematics (Cherkaoui et al., 2016)

The Laboratory of subsea technology (LTS) in UFRJ, Brazil developed a new concept of sandwich pipe, which consist of three layers (Estefen et al., 2016). The mid layer consists of a material with good strength and thermal properties (SHCC), while the external pipe and internal pipe are both carbon steel, to provide the support. As shown in Figure 3.2.

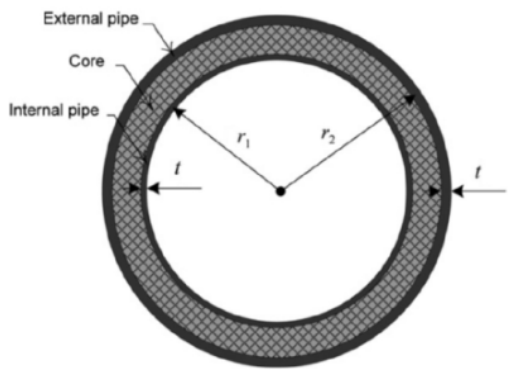

Figure 3.2: Typical section of a Sandwich Pipe (Estefen et al., 2016)

The sandwich pipe could also be applied with thermal insulation layers. Under this condition, the pipe and the insulation layer form multilayer configuration, and the thermal calculation is very important to the insulation design and flow assurance modeling. An and Su (2015) provided improved lumped parameter models for transient thermal analysis of multilayered composite pipeline with active heating, which became an effective analytical tool for the thermal design and analysis of composite pipelines for oil and gas production in deepwater conditions.

The active heating mentioned above is an important way of keeping the flow temperature. Electrically heated flow line systems work on the basis of utilizing the heat generated by the electrical resistance of a conducting material when using an alternating current. There are mainly two types of solutions: Direct electrical heating (DEH) and Trace heated pipe-in-pipe.

In DEH systems the pipe wall is used as the conductor of electric current which directly heats the pipeline (Louvet et al., 2016), as shown in the Figure 3.3.

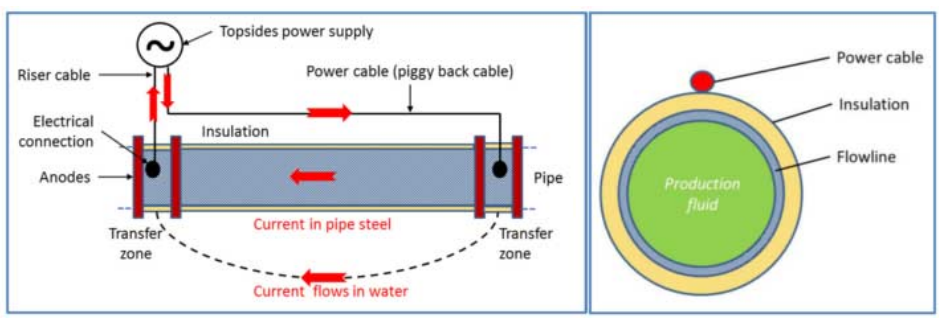

Figure 3.3: DEH system (Louvet et al., 2016)

Tzotzi et al. (2016) discussed the application of electrical trace heated pipe-in-pipe (ETH-PIP) in flow assurance. The ETH-PIP is an improvement of standard Pipe-in-Pipe by adding 4 heat trace cables, and 2 distributed temperature sensing (DTS) optical fibers spiralled against the inner pipe and covered by a high performance thermal insulation, as shown in Figure 3.4.

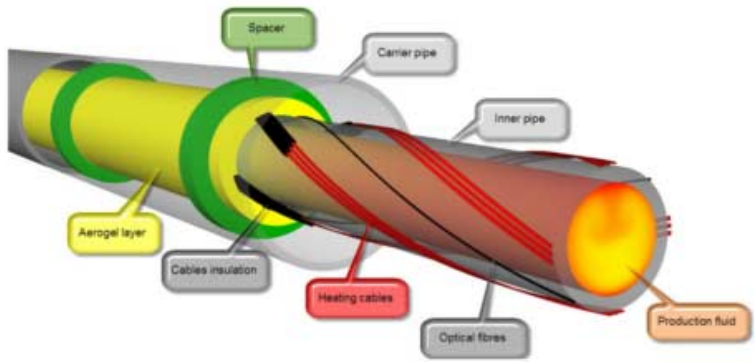

Figure 3.4: Configuration of ETH-PIP (Tzotzi et al., 2016)

Until recently, low voltage (below 1000V) heating elements and low power heating cables have been the typical solutions for down hole and subsea electric heating applications. Wilson (2016), Molnar & Riley (2016) discusses the feasibility and benefits of using medium voltage technology for flow assurance and hydrate prevention applications. This kind of technology could bring reduction of cost, power consumption and line loss.

Subsea components such as X-tree and manifold also need insulation and the thermal dynamic calculation is very important to design and monitor the insulation performance. Gharaibah et al. (2016) combined the experimental and numerical results and recommended a robust thermal modelling procedure for subsea components that allows a favorable balance between conservatism and accuracy. Janoff et al., (2014) introduced a non-destructive evaluation technique used for dielectric materials can be used to detect cracking, voids, and other defects in the installed insulation systems that may cause a degradation in performance.

3.2 Chemical injection

Chemicals are injected to the subsea system or directly to the well bottom to change the property of fluid, thus prevent the formation of wax, hydrate and other type of solids that may block the pipeline or wellbore. Commonly used chemicals could be categorized into nine types based on the function thermodynamic hydrate inhibitors (TDI), Low dosage hydrate inhibitors (LDHI), Defoamers, Asphaltene inhibitiors, Paraffin inhibitors, Scale inhibitors, H2S scavengers, chemical demulsifiers and Drag reducing agents. Actually, chemical injection is relatively a mature technology, and many works focus on the property of chemical and the injection process (Alharooni et al., 2017; Vershinin et al., 2017).

3.3 Operation and equipment

Some subsea equipment could be applied to help ensure the flow assurance through designed operation process. For example, subsea separator could separate oil, water and gas, thus helping prevent the formation of hydrate slug flow and erosion, and the amount of injected chemical could be reduced (Kondapi et al., 2017; Prescott et al., 2016).

Pigging is the practice of using devices known as "pigs" to perform various maintenance operations, including cleaning the pipe due to blockage. Carvalho and Rotava (2017) evaluate the simulation effectiveness to estimate pig total travel time and pig speed profile for a gas pipe line, and Wan et al. (2017) summarized the pigging solution of subsea wet gas pipeline, providing method of calculating pigging period, and scheme of reduce instantaneous slug.

Subsea Cooler technology is usually used for subsea gas dehydration, anti-surge cooling, cold flow and so on. It is getting increased attention primarily due to cost benefits realized by reducing or controlling temperatures. The simplest and most matured cooling device would be a long un-insulated flow line, as shown below.

Figure 3.5: Subsea passive cooler, from NOV: subsea cooler systems

Carrejo et al. (2015) presents a kind of high-strength dissolvable metal (HSDM), to operate as a fluid-loss barrier that can be run-in on the liner. The HSDM dissolves, acts as a screen equal in filtration performance but better than current sand control alternatives in its erosion resistance, and is good to sand and erosion management. An application of this kind of material is shown in Figure 3.6.

Figure 3.6: Gas lift valve with HSDM (Carrejo et al., 2015)

3.4 Software technology

Software technology does not immediately contribute to flow assurance, but it helps monitoring and decision making, which is very important during operation.

A Flow Assurance System (FAS) is installed on Ormen Lange in order to give information about the multiphase flow through the entire subsea production and pipeline system and onshore slug catchers to support the operation of the field (Dianita et al., 2015)

Osokogwu et al., 2014, Wilfred and Appah, 2015, presented a quick and easy tool, PROSYS, which helps in the preliminary screening of asphaltene, to determine if the operator will experience severe or mild problems arising from deposition of asphaltene and also estimates the dissociation temperature of hydrate in a pipeline during depressurization and the thickness of the melted ice in the pipeline.

Brower et al. (2014) introduced a post installed subsea monitoring system for flow assurance evaluation, providing real time operation data, thus helping decision making for flow assurance.

Zhang et al. (2014) discussed an application of integrated management strategy of flow assurance for digital field. An innovative rating system covering all types of flow assurance problems by design of experiments (DoE) and Fuzzy Logic methods was presented firstly. And then this system was combined with the digital field technologies, helping address various flow assurance issues.

3.5 Prospective approach

There are some newly proposed approaches dealing with the flow assurance of subsea production system. For example, the phase change material is a kind of potential alternative for the insulation layer. It can effectively regulate fluid temperature during production fluctuations or increase the cool-down time during production shutdown. Parsazadeh and Duan (2015) introduced a nano-enhanced phase change materials that allow thermal energy storage in the pipeline system.

Wax deposition begins from the pipe wall and generally form a wax layer. If the inner pipe wall is oleophobic, the wax molecule is hard to absorb into the pipe wall. Therefore, it becomes one way of assuring fluid flow. Liang et al. (2015) developed a bio-inspired composite coating with excellent wax prevention and anti-corrosion properties. The prepared coating is composed of three films, including an electrodeposited Zn film for improving corrosion resistance, a phosphating film for constructing fish-scale morphology and a silicon dioxide film modified by simply spin coating method for endowing surface with superhydrophilicity.

As for hydrate formation, a kind of technologies using nano-scale membrane to dehydrate the natural gas attract many attentions. Shirazian and Ashrafizadeh (2015) obtained high-quality nanoporous inorganic membranes applicable to dehydration of natural gas through synthesized and three stage modified process of LTA zeolite mem-branes.

Although these approaches have not been applied to subsea production system yet, the concepts and the performance inside the laboratory indicate large potential for the flow assurance of subsea production system.

3.6 Conclusions

In this section, methods about flow assurance in subsea production system were briefly discussed. Practically, these methods are usually applied together for a subsea system, which is an integrated work (Bouamra et al., 2017; Jain et al., 2015). Besides, the uncertainty and risk should also be analyzed carefully (Morgan and Zakarian, 2015; Twerda and Omrani, 2015).

Flow assurance attracts more and more attention due to the harsh environment of subsea. It is a combination of better material, proper facilities, and scientific management. There is still a long way to go, to overcome the flow assurance problems we are facing during the development of offshore field, especially in deep water.

4. TESTING FOR QUALIFICATION OF SUBSEA PRODUCTION SYSTEM

4.1 Qualification

API RP 17Q (2nd Edition, 2017) recommends that all subsea equipment are subjected to qualification to ensure they meet defined reliability, integrity, and operational requirements. A proper technology maturity assessment should be carried out to assess the need for executing a technology qualification.

The purpose of a qualification program is to provide evidence that a selected technology or equipment will meet functional and performance requirements, within specified operational limits, with an acceptable level of confidence. There are ten steps of a qualification program as defined in API RP 17Q 2nd Edition.

- Requirements planning
- Technology Maturity Assessment
- Select Qualification Program
- Qualification FMECA (Q-FMECA)
- Qualification Plan
- Qualification Execution
- Results Evaluation
- Improvements and Modifications
- Qualification Assurance
- End Users Qualification Program

API RP 17N defined eight Technology Readiness Levels (TRL) and Technical Risk Categorization (TRC) to assess technology maturity and technical risk respectively. Eight TRLs range from minimum of 0, corresponding to an unproven idea, to a maximum of 7, corresponding to proven technology as follows.

- Unproven Concept (basic R&D, paper concept)
- Proven Concept (proof of concept as a paper study or R&D experiments)
- Validated Concept (experimental proof of concept using physical model tests)
- Prototype Tested (system function, performance and reliability tested)
- Environment Tested (pre-production system environment tested)
- System Tested (production system interface tested)
- System Installed (production system installed and tested)
- Field Proven (production system field proven)

TRCs are a means of assessing technical risk across a set of change categories. Five change risk factors are defined including reliability, technology, architecture/configuration, environment and organization that are assessed against four different levels of risk (very high, high, medium, low) based on the perceived deviation from previous experience. The TRL and TRC are combined into a matrix to guide the user to the appropriate qualification activities for that specific phase of development.

The technology maturity assessment uses TRL and TRC to evaluate the technical risk and maturity of a concept in line with specified goals and requirements. Four paths are available for qualification based on the technology maturity assessment:

- Research & Development Program (for TRL < 1);
- Technology Qualification Program (TQP, for $1 \leq$ TRL < 4);
- Standard Qualification Program (SQP, for $1 \leq$ TRL < 4);
- Proven Technology (for $4 \leq$ TRL < 7);

Selection of a TQP or SQP is mainly based on the assessed TRC and project requirements. TQP uses Q-FMECA to identify necessary qualification activities for technology qualification. TQPs are typically for novel or less mature technology, where the application is new or environment is not well understood, and/or where no existing standard is applicable to that technology. TQPs usually require more efforts and are more complex than comparable SQPs as a result of increased uncertainty in technology or environment.

SQP uses predefined qualification activities in existing applicable standards to qualify technology. Usually SQPs are for components, sub-assemblies, and assemblies using existing technologies that are modified to satisfy an incrementally more stringent requirement.

The TQP and SQP are normally carried out by a technology developer or equipment supplier. As soon as equipment achieves TRL 4, the technology is ready to be applied by an end user, then an appropriate End Users Qualification Program (including testing and monitoring) is to be established to progress the equipment TRL through TRLs 5, 6 and 7.

With the development of the subsea production technology, a lot of advanced testing processes of qualification are employed in the subsea production system.

4.2 Advanced Testing for Qualification of All-Electric Subsea Production

ABB Oil & Gas is running a Joint Industry Project (JIP) together with Statoil, Total and Chevron to develop technologies for subsea power transmission, distribution and conversion at greater distances, in deeper waters, and in harsher environments (Bugge, 2017). The project started up in 2013 and is targeting a 3000-hour shallow-water system test in 2018, including the qualification of pressure tolerant medium voltage switchgear, medium voltage drives, as well as supporting controls and auxiliary supplies.

The project follows the TRL development stages for technology qualification applied to components, sub-assemblies and equipment. For the JIP, this first required a breakdown of the overall subsea power system into separate manageable technology parts, the further to classify these with respect to novelty. Other important aspects of the DNV recommended practice is to be able to identify required design changes at an early stage and also to improve confidence in the new technology by close interactions and traceable documentation, see e.g. documentation process in Figure 4.1.

Since the test matrix is extremely large and difficult to handle considering several hundred unique critical components and various stress conditions, it was necessary to find a pragmatic way to structure the test such as to maximize the risk mitigation before pre-qualifying for full-scale prototypes. The key test philosophies are listed below:

- Test derived from a common understanding of realistic component/equipment specific stresses throughout design life (life-cycle mission profile)
- Comprehensive confirmation of the desired function as well as reliability testing primarily conducted at the level of the component, where a functional failure can be defined, and accelerated conditions applied
- Sub-assemble level testing geared toward confirmation of the overall function, design margins, and the thermal and high-current aspects. Special attention to novel aspects in subsea power, where the use of customized versions of existing standards may be required
- Seek the simplest of conceivable tests for verifying the investigated function, rather than strictly following a standard developed for entirely different reasons or conditions
- Utilize standardized tests for subsea electronics located in 1 atm chambers, unless the impact of meeting these standards introduce a negative impact on the design
- Hypothesis-based testing, with knowledge of how to interpret different possible outcomes of a test, supported by numerical simulations where possible

- Use well-established failure modes and design rules unless theoretical or experimental evidence suggest new adverse effect in subsea environment
- Focus on learning the behavior and limits of design, rather than just “passing tests”.

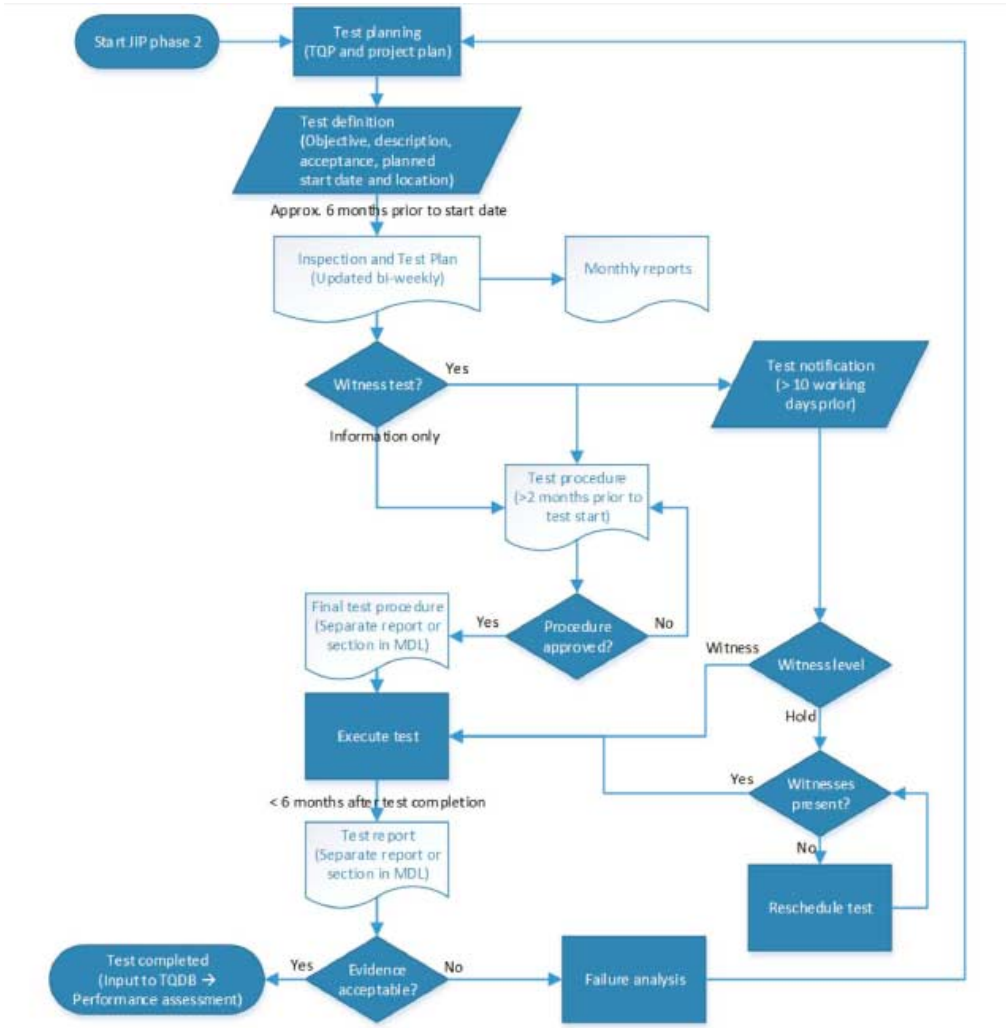

Figure 4.1: Qualification test execution flow-chart (Bugge *et al.*, 2017)

One of the key sub-assemblies is the medium voltage drive cell. This has been pressure tested at 300 bar in Statoil R&D facility in Trodheim as shown in Figure 4.2 below. The first test was performed in 2016, and a second 3000 hours cell test planned for the same year.

Formal qualification of key components and sub-assemblies was also planned for 2017. Key sub-assemblies will also be tested for 162/3 Hz supply in order to demonstrate that developed technology can be used in subsea drive system with LFAC power transmission and distribution. Based on the pre-qualified components, full-scale prototypes will be assembled in 2018 for a 3000hours shallow-water system demonstration.

Figure 4.2: Medium voltage drive cell pressure test at Statoil R&D facility Rotvoll (Bugge *et al.*, 2017)

4.3 Advanced Testing for Qualification of Multiphase Pumping

The Girassol Resources Initiatives (GirRI) is a major brownfield deepwater project, which seeks to optimize the Girassol FPSO production (Bibet, 2016). It is also the third subsea boosting project developed offshore Angola by Total, the operator, and OneSubsea, the contractor. High boost multiphase pumps (MPPs), with an operating ΔP of 110 bar at 53% GVF are deployed subsea on two exiting deepwater oil production loops to enhance the Rosa field reserves and production, a world's first for the oil and gas industry.

The pump system implemented includes two MPP stations on the sea floor (Figure 4.3), one on the production loop P70, and one on the production loop P80. On P70, the MPP station is located near the riser tower while on P80 the MPP station is located 17 km away from the FPSO. Each MPP station holds two MPPs, in a segregated scheme of one MPP per production branch.

Figure 4.3: View of a high boost MPP station (Bibet *et al.*, 2016)

For all subsea equipment, it is standard practice for both the operator and the contractor to validate the pump through a comprehensive pump factory test (FAT). It is also standard to validate the overall pumping system from topside to subsea through a comprehensive system integration test (SIT), with the pump running in shallow water. The standard contractor pump FAT covers performance mapping with a full range of flow/AP/speed in water + nitrogen, then in viscous oil + nitrogen (Exxcol D80 oil used for GirRI), and a 24-hour endurance test under a full load and at full speed.

The philosophy is also to mitigate, through testing, any new risk caused by conditions specified for the application. For this first high boost MPP application, two new major risks were

anticipated: the behavior of the pump with a worn balance piston and the proper sizing of the flow mixer. To address these potential risks, dedicated tests were run with one MPP.

4.3.1 Worn Balance Piston Test

The overall objective of this test was to demonstrate the stability of the pump when operating with a worn balance piston, and in so doing ensure acceptable hydraulic, rotor-dynamic, and mechanical performance of the pump.

Conducting tests on the pump involved seven steps:

- Pump performance tests with a new balance piston. The goal of these tests was to map the performance and compare some test results with the ones obtained later with a worn-out liner.
- Dismantling of the pump to install a worn-out balance piston line: inspection of the pump internals during disassembling to detect any marks, wear, etc.
- Reassembly of the pump with a worn-out, bronze piston liner.
- Performance test with the worn-out balance piston.
- Dismantling of the pump to re-install the new balance piston liner. Inspection of the pump internals during disassembling to detect any marks, water, etc.
- Reassembly of the pump to new conditions.
- Standard OneSubsea MPP factory acceptance test program (performance and endurance tests, 24 hours accumulated testing).

Vibration levels for the worn liner design remain in the same order of magnitude to what was observed for the nominal design, in spite of the wear introduction for the balance piston (double clearance and removal of swirl breaks). Post-test pump disassembly and inspection revealed that all parts were in good condition.

4.3.2 Slug Test

For all MPPs a flow mixer is installed at the pump inlet to homogenize the process fluid and to smooth the gas/liquid transients, which in turn provide optimal inlet condition for the first pump impeller. The design and sizing of the flow mixer depends on the hydrodynamic slug size, GVF, pressure, and flow rate. The slug test was conducted to verify that the GirRI MPP would work well with the slug regime predicted by the flow assurance studies. The expected slug regime was therefore reproduced on the test loop. A slug loop was built in the OneSubsea test facilities, with a length of approximately 130m to enable a fully developed hydrodynamic slug flow at the pump station inlet (Figure 4.4 and Figure 4.5).

Figure 4.4: Slug test loop arrangement (Bibet *et al.*, 2016)

Through the slug test, the Project Team was able to demonstrate that the flow mixer was working well with a slug regime identical to an actual one used on site.

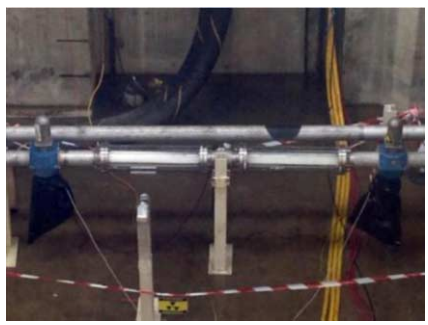

a. "See-through" pipe

b. MPP under slug test

Figure 4.5: "See-through" pipe and MPP under slug test (Bibet *et al.*, 2016)

After all the qualification tests (green boxes on Figure 4.6), the pump was deemed ready for development and made available to the project teams for immediate application: GirRI.

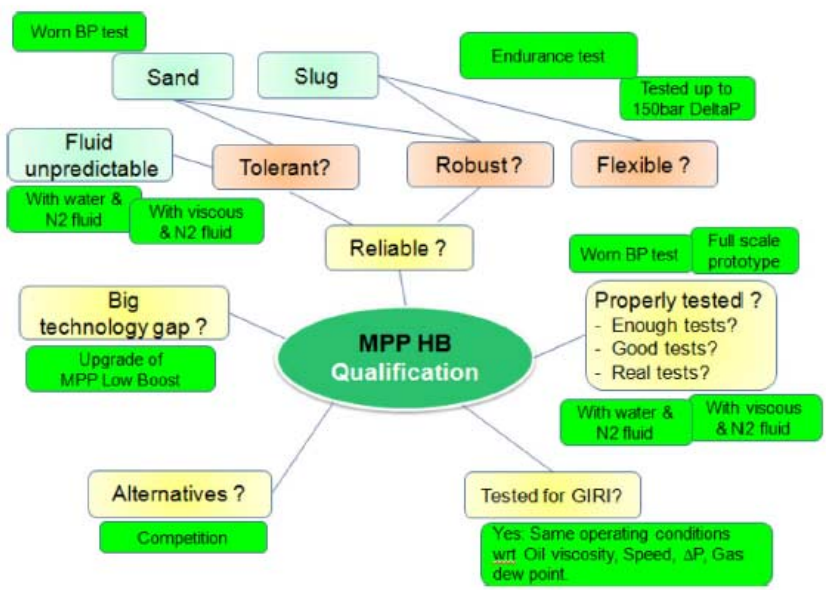

Figure 4.6: High boost MPP qualification process. In the green boxes, all tests done to address the identified risks (Bibet *et al.*, 2016)

4.4 Advanced Testing for Qualification of Subsea Wet Gas Compressor

In May 2009, a two-year contract was awarded for the execution of a TQP for the Gullfaks 2030 Subsea Compression project, to mature the concept of subsea compression, as well as the key building blocks of the system (Hjelmeland, 2016).

The qualification program included engineering, procurement, construction and testing activities of the subsea multiphase compressor, based on the WGC400 compression technology. The first compressor, defined as WG4000 Series 0, was built to fall subsea specification. Other parts of the qualification program comprised a representative cooler bundle element, electrical monitoring system, vibration monitoring, as well as control system interface. For quali-

fication testing of the compressor, a novel high pressure live hydrocarbon flow loop was engineered and built in OneSubsea's facility in Fusa (shown in Figure 4.7), outside of Bergen, Norway. The work was conducted efficiently and successfully, and in close collaboration with the expertise and personal of Statoil's K-Lab.

Figure 4.7: High pressure hydrocarbon test loop (Hjelmeland *et al.*, 2016)

Testing of the compressor post manufacturing was performed at the new hydrocarbon test loop in the period from August 2010 to April 2011.

The test program that formed basis for the machine qualification was as follows:

Test Campaign #1 – Ideal Fluid Performance Test (Nitrogen/Exxol D80)

- Mechanical run test
- Assembled compressor gas leakage test
- Hydraulic performance mapping at 24 bara suction pressure
- Mechanical design verification on ideal fluids

Test Campaign #2 – Hydrocarbon Fluids Performance Test

- Hydraulic performance mapping at 72, 65.3, 36, 24 and 12 bara suction pressure and hydrocarbon fluids
- Acceptance test of hydraulic performance
- Mechanical design verification on hydrocarbon fluids

Test Campaign #3 – Ideal Fluids Endurance Test

- Mechanical Integrity Tests, including minimum flow and no-surge tolerance verification, liquid start-up and operation
- Endurance testing (3000 running hours)
- Machine inspection and verification of mechanical design for acceptance

4.5 Advanced Testing for Qualification of Subsea Transformer

The Jack and St. Malo fields were developed in a deepwater Gulf of Mexico (GoM) setting by Chevron and co-owners and commenced production in 2014, the reservoirs are located roughly 40km apart, about 400km southwest of New Orleans, Louisiana. Water depths in both fields are around 2333m, and the reservoirs are approximately 9km below the water surface (Hjelmeland, 2017). The Jack and St. Malo fields were developed with subsea completions flowing back to the Walker Ridge Regional Platform, the largest, by displacement, semi-submersible floating production unit (FPU) in the GoM.

The power system topology for Jack and St. Malo fields was based on elevated transmission voltage in the umbilical, utilizing step-up transformers on the FPU and step-down transformers on the seabed. A TQP was initiated to qualify the subsea step-down transformer which

would reduce the voltage. Transmission at elevated voltage levels results in lower power losses and increased overall efficiency for the power system.

Qualification for the subsea step-down transformer modules (Figure 4.8) was based on testing and qualification of sub-components prior to assembly and qualification of the finished transformer unit. A number of test and qualification efforts were initiated as part of the TQP:

- Qualification of wet mate high power connectors;
- Stress tests of wet mate connector components;
- Vibration test of wet mate connectors;
- Test of high resistance ground;
- Transformer current test;
- Test of instrumentation;
- Test of oil filled transformer core;
- Test of internal components;
- Qualification test of subsea step-down transformer.

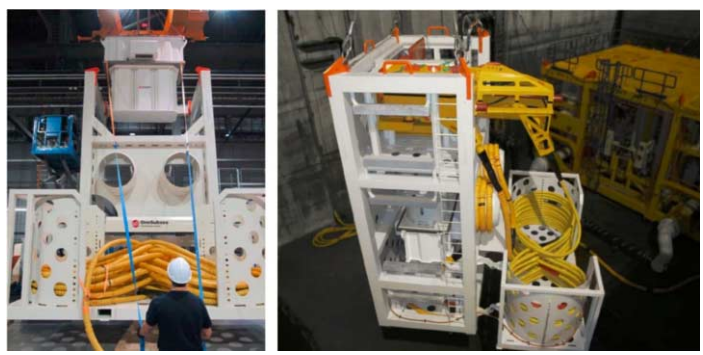

Figure 4.8: Subsea step-down transformer modules with electrical flying leads during assembly (left) and during system testing (right) (Hjelmeland *et al.*, 2017)

5. INSTALLATION AND OPERATIONS FOR EMERGENCIES

5.1 Installation for Subsea Hardware

Offshore oil and gas production relies on the subsea systems, and the underwater installation is the foundation for construction of the systems. The combination of deeper offshore field developments and larger, more complex subsea structures results in new requirements and challenges for installation vessels and related deployment systems. The conventional vertical deployment systems are struggling to meet the industries requirement of installing heavy subsea structures in deep water.

5.1.1 Lifting Method

Currently, several techniques are used to carry out the full installation activities. The traditional one is lifting method. The object can be transported on the deck of the barge and then lowered down with a crane installed on the barge or a heavy-lift crane vessel. Such type of transportation is considered to be relatively fast, but at the same time this method is sensitive to weather conditions like wind and wave forces, slamming and current forces. This method is limited by water depth. The self-weight of steel wire increases and axial resonance occurs due to very long length. The requirements of lifting capability, positioning, heave compensating and deck areas also get limited. What is worse, the costs is getting more expensive in deeper waters. Figure 5.1 shows the lifting method.

Figure 5.1: Lifting method

5.1.2 Drilling Riser Method

In 2001 Petrobras installed a 241 ton manifold in 940m water depth with drilling riser method. The manifold is connected to the end of riser and lowered by a semi-submersible. The disadvantages are the high costs, time consuming and high requirements for the vessel. The MODU or drilling vessel also needs the heavy lifting capability, DP system and heave compensating system. Figure 5.2 illustrates the drilling riser method.

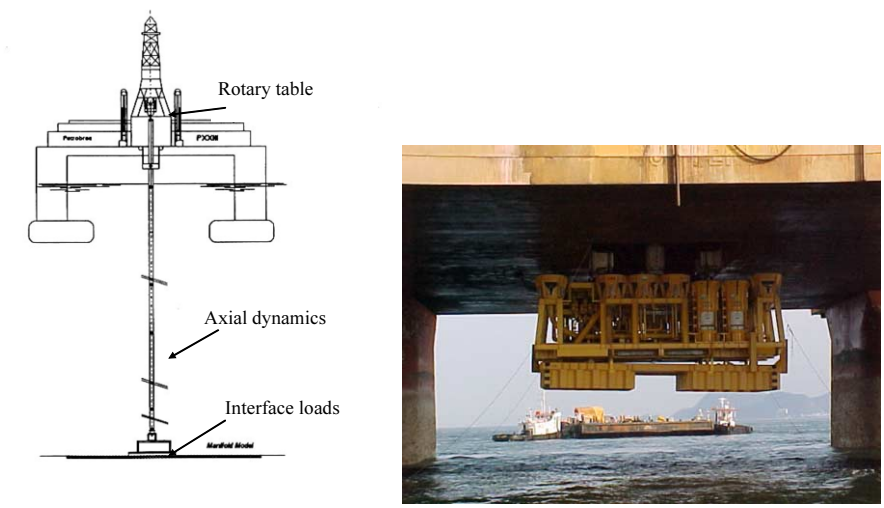

Figure 5.2: Drilling riser method

5.1.3 Sheave Method

The first application of sheave method was in 2002 by Petrobras. A manifold weighted 175ton was installed in 1885m water depth. The manifold is lowered by multi vessels and a sheave was connected to it. A steel wire around the sheave is the main installing line. One end is connected to a drilling platform and the other to an AHTS. When the equipment is lowered to 90m depth the sling is cut and the manifold is lowered to seabed with the steel wire. The other AHTS helps to prevent the wire from damage due to twisting. The dominant disadvantage is the complexity, which makes it difficult to numerical simulation and scheme design. Besides, it needs more vessels and DP and heave compensating. Figure 5.3 shows the sheave method.

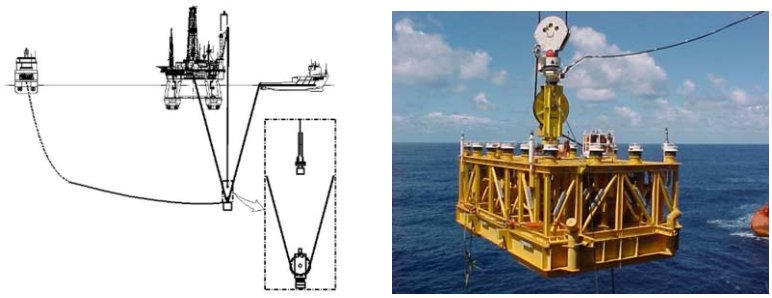

Figure 5.3: Sheave method

5.1.4 Pencil Buoy Method

The pencil buoy method is a subsurface transportation and installation method developed by the company Aker Marine Contractors. The pencil buoy method reduces the offshore installation sequence from a lifting and lowering operation to a pure lowering operation. This is done by wet towing the structure from an inshore load out site to the desired offshore location.

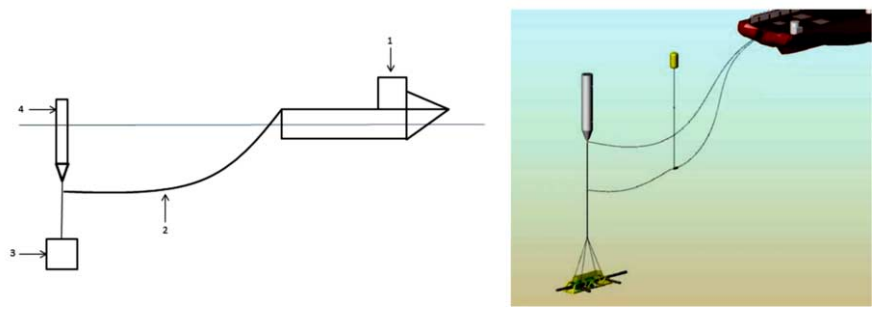

Figure 5.4: Pencil buoy method

This method has several advantages:

- There is no risk of cargo pendulum motions in the air.
- Slamming/uplift loads during lowering through splash zone are excluded.
- Large deck space for transportation is not needed.
- Less crane capacity is required.

5.1.5 Subsea 7 Method

The Subsea 7 method is developed for installation of massive subsea structures in harsh environmental conditions. It enlists the service of a small monohull construction vessel and allows carrying out the installation in a single operation. Subsea 7 promotes this method as more reliable and cost efficient compared to the traditional transportation on the barge.

Towing is done through the moon pool of the vessel, which enables towing of heavy weighted cargos and improves the towing criteria. The hang-off point of the cargo should be as close to the vessels motion centre as possible in order to decrease the effects of the vessels motions, what results in good performance in severe weather conditions. For that purposes, the hang-off tower is installed over the moon pool of the installation vessel. Some operational stages are depicted in Figure 5.5.

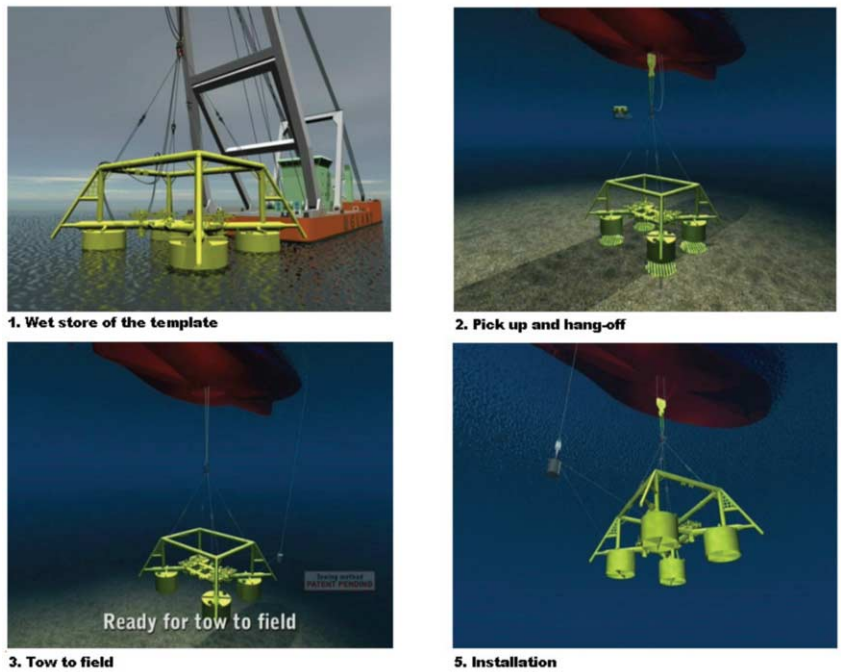

Figure 5.5: Illustration of four operation stages: wet-store, pick up and hang-off, tow to field and installation

The Company reported that installation expenses were significantly lower than the cost of using a heavy lift vessel, and all operations were held in a safe manner because of the limited use of "sophisticated" cranes and crane modes subject to higher risk of technical/software failures and all heavy lifts are performed inshore in sheltered waters. Tow speed can be increased at lower sea states.

5.1.6 Pendulous Installation Method

The Pendulous Installation Method (PIM) was developed by Petrobras to install large manifolds in water depth of 1900m. PIM is a non-conventional technique involving small conventional deepwater construction or offshore support vessels, without drilling platforms. PIM is capable to deploy heavy manifolds or other equipment in water depth up to 3000m.

Numerical simulations by OrcaFlex and model tests were conducted by Fernandes to assess the fundamental aspects and study the feasibility and parameters. Sensitivity studies were carried out by Roveri for pendulous method, where the comparison of numerical analysis and tests were made. The hydrodynamic performance and parameters, including added mass and drag coefficients, were estimated by Fernandes via experimental and numerical methods. Full scale model tests were carried on and finally two subsea manifolds were successfully installed in 1845m and 1900m water depth, respectively.

The PIM is a cost effective solution in comparison with conventional installation methods, for instance, installation with drilling rigs. The resonant motion during deepwater installation can be avoided. However, due to the complex geometry of the manifold, hydrodynamic instability may occur during installation. Therefore, to prevent rotation of the cargo, an anti-rotation system such as counter weights should be installed. Installation process is shown in Figure 5.6.

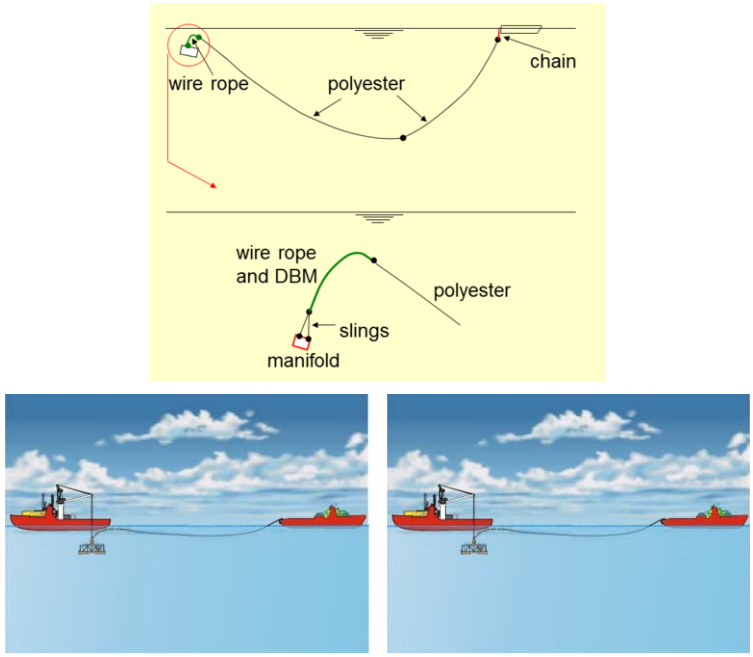

Figure 5.6: Pendulous installation method

5.2 Oil Spill in Gulf of Mexico and Measures Taken against The Accident

Subsea oil and gas exploration and production face many challenges such as harsh weather and working conditions, remote location and lack of infrastructure. These can lead to emergency accidents and present difficulties for handling and rescue. The major accidents are listed in the Table 5.1.

Table 5.1: Major accidents (Basharat *et al*., 2014)

No	Accident	No	Accident
1	Non-ignited hydrocarbon leaks	7	Drifting object
2	Ignited hydrocarbon leaks	8	Structural damage to platform/stability/anchoring/ positioning failure
3	Well kicks/loss of well control	9	Fire/explosion in other areas
4	Leaking from subsea production systems/pipelines/risers/flow lines/loading buoys/loading hoses	10	Damage to subsea production equipment/pipeline systems/diving equipment caused by fishing gear
5	Vessel on collision course	11	Evacuation
6	Collision with field-related vessel/installation/shuttle tanker	12	Helicopter crash/emergency landing on/near installation

On April 20th 2010, the semi-submersible drilling platform "Deepwater Horizon" located in the Gulf of Mexico rented by BP exploded. Thirty six hours after the explosion, the drilling platform sank, and eleven crew died in the accident. From 24th, the oil continued to spill from the oil wellhead, causing a large-scale crude oil pollution.

From April 24th to July 8th, American experts evaluated that 300 thousand tons oil had leaked. On July 15th, BP announced that the newly installed "control cover" had successfully

suppressed the underwater oil wells. Eventually, the disaster of the Gulf of Mexico oil spill was put to an end 85 days later.

Preliminary survey results showed that the accident caused nearly a thousand kilometers of coastline to be contaminated, and the polluted area covers more than 20,000 square kilometers. The oil spill caused a severe natural disaster in the ecological environment of the Gulf of Mexico.

Since April 20th after the explosion, the accident developed to become more and more serious. Initially, BP took three measures: the first is to send a ROV to examine and repair the safety valve which was out of service; the second is to send vessels to absorb oil; and the last is to reduce the pressure of oil wellheads by drilling two new wells, in order to reduce the leakage rate. To prevent the disaster from becoming even worse, BP worked with the US government, engaged more than twenty four thousand people, and 1400 vessels in the rescue. Furthermore, more than 610 kilometers water gate was involved, in the manner of "ring oil" to besiege and intercept the oil floating in the sea. In addition, the "capping", "top kill", "hair oil absorption" and other means have been adopted, yet all the means were ineffective or failed at last.

Top kill is one of the method through the assistance of the ROV, the main technical index of the ROV is as follows: four horizontal vector directions and a vertical thruster, five cameras, a LED lamp, a seven functions manipulator and function of automatic directional. A large number of high-density liquid, metal debris *etc*. play a blocking role on the material in oil wells, balancing the pressure in wells, and with the cement injected into the wells, the entrance can be sealed, achieving the effect of plug.

Capping is a method that cuts off the oil spill above the blowout preventer by closing the valves to control the oil spill, and installing an oil drain pipe above the valve to drain and transporting the spilt oil to the waiting vessel.

Faced with this unprecedented environment catastrophe, the US government made considerable efforts in terms of manpower, material resources, and financial resources to clean up pollution. The measures include spraying oil dispersing agent at the surface and under the water, laying out of oil fence and oil absorption railing, using oil recovery machine, burning the spilled oil, *etc*.

5.3 Responses to Oil Spill

After the catastrophic incident in the Gulf of Mexico, the entire oil and gas industry gave much attention to drilling safety and emergency response. The need for safer operations led the industries to promote adequate Emergency Response (ER) System as well as investments in advanced techniques and methodologies to prepare for and efficiently respond to any possible accidental scenarios arising from operations.

The International Oil and Gas Producers Association (IOGP) learned from this and similar accidents, established a program to enhance future prevention and preparedness. They set up an Oil Spill Preparedness Framework, including: risk based plan scenarios, response strategies using NEBA, oil spill response resources, incident management system, and stakeholder engagement. Many new tools and techniques are used in handling oil spill (Flynn, 2016; Coolbaugh, 2017).

5.3.1 Dispersants

Dispersants can be rapidly deployed and are one of the most effective tools in a majority of scenarios (Flynn, 2016). They work just like soap and shampoos, and contain many of the same ingredients. They break the oil into very tiny droplets, which are rapidly diluted and biodegraded by naturally occurring microorganisms in the marine environment. They can

avoid floating oil from impacting sensitive near-shore areas and accelerates the natural bio-degradation process.

In particular, the application of subsea dispersants for response to well release in deeper water has significantly developed. This technique aims to prevent oil reaching the surface by dispersing the oil close to the point of release. A greater proportion of the released oil breaks into smaller oil droplets that can be dispersed, diluted and biodegraded in the water column, unlike the larger oil droplets will float up to the sea surface.

5.3.2 In-suit burning of oil

In-suit burning is a response technique which involves the controlled burning of oil. Prior to the Macondo spill, the technique had not been used in such an operationally complex scenario. In the case of the Macondo response, more than 400 successful individual burns were completed, a number for hours at a time. Now controlled burns of up to 10 hours were routinely used, demonstrating the importance of the new technique for combatting offshore spill.

5.3.3 Spill surveillance, monitoring and visualization

Oil Spill Contingency and Response model (OSCAR) is a modelling tool developed by SINTEF to simulate the oil spill behavior; it is a multi-component 3-dimensional oil spill modeling tool to predict the movement of oil both on the water surface and in the water column. The oil spill model is developed for objective analysis of spill response strategies according to the predicted movement of the oil on the water surface and in the environment (Iazeolla, 2016). Two main model methods are used with OSCAR to evaluate the effects of oil spill scenarios.

a). Stochastic modeling

Stochastic simulations predict the probable behavior of potential oil spills under typical historical meteorological and oceanographic conditions, such as database of wind and marine currents speed and direction. Their outputs indicate the probability of where the spill may spread and give statistical information on the possible consequences. They do not indicate volumes of oil. It provides an estimation of the contamination probability and of oil stranding times, stochastic simulation outputs support the selection of the most appropriate response equipment and strategies. Stochastic modeling is used in the ER planning phase, to evaluate the most probable outcomes of a spill and to set up the most appropriate response options.

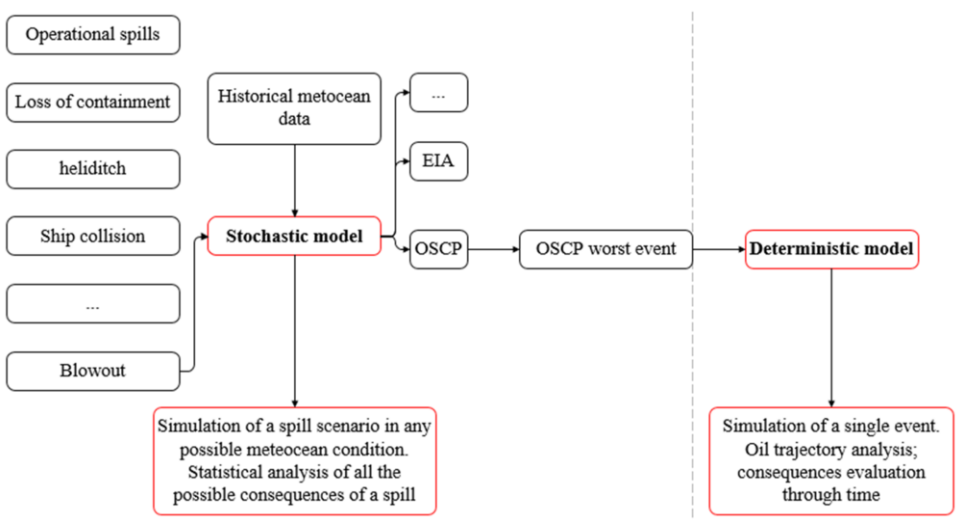

Figure 5.7: Oil spill modeling along Oil Spill Risk Assessment progress (Iazeolla *et al*., 2016)

b). Deterministic modeling

Deterministic modeling is used to predict the route of a hydrocarbon slick over time, and to estimate the oil weathering profile, under a single set of meteorological and oceanographic conditions. It investigates potential beaching or intersection of maritime boundaries under specific (worst case) wind and marine current speed and direction. Result can be integrated into GIS-based systems that enable the crossing of consequence data and response means equipment location and availability. Deterministic modeling is employed during emergencies to predict the development of the spill in the first days after the spill.

5.3.4 Deepwater subsea waterjet

Deepwater subsea waterjet is applied in subsea emergency response situations, and provides an opportunity to prepare for tier 2 and tier 3 oil spill emergencies without depth limitation in the world's deepest water exploration and production sites (Bruce Kivisto, 2014). It can also minimize the risk to the environment during common offshore exploration and production. Waterjet cutting is a cold cutting process and does not generate enough energy to ignite most confined gases, so it is safe and efficient to conduct cutting and repair operations in the presence of hydrocarbons and other combustible gases. Meanwhile, it does not introduce a heat affected zone (HAZ) into the material being cut, this reduces the possibility of introducing stress fractures and other physical deformities to the work piece. A waterjet stream is a soft tool that cannot bind in the cut and can start the cut at any point on the work surface, which allows the waterjet muzzle to place inside the pipe or other hollow subject work piece, and to cut from the inside to the outside. An intensifier-style pump is used to pressurize a stream of water to ultra-high pressure (3,900 bar), and several streams are formed and rotated to produce a uniform application of energy on the subject work piece, which have sufficient energy to remove even the most difficult coatings (epoxy, concrete, marine growth, rust scale,) with minimal risk of cutting into or through. With the addition of abrasive, it is effective at cutting steel up to 250mm thick. It can successfully operate at 1,430m seawater, which allows for cutting of steel and other materials, as well as for hydrate remediation and isolation of valves, ports, caps, boils and weld seams in the deep water subsea space.

Subsea waterjet system is used in emergency response, because of its unique cold-soft tool characteristic, which can rapidly produce a clean cut on the wellhead to make it ready to accept a cap or diversion device.

5.3.5 Subsea emergency response system

Total created the Subsea Emergency Response System Project (SERS), in order to develop and supply tools for use if an intervention was required in response to an uncontrolled hydrocarbon leak (Bourguignon, et al., 2014). This set of tools can be split into two systems: a dynamic killing system and a diverter system.

The dynamic killing system is capable of injecting fluids into a leaking Christmas tree, either directly into the flowing well or through an adjacent well, in the case of the flowing well being damaged or not being accessible. The system can handle an injection flow rate of up to 3,000 lt/mn, aimed to neutralize a leak and bullhead the effluent back into the reservoir. The advantage of this system is that it is reasonably simple and quick to deploy and operate from any available drill ship or light well intervention vessel.

The diverter system can be connected on the top of each subsea Christmas tree for capping shut-in or diverting the fluid to a containment system. It can be used for capping on subsea blowout preventers (BOPs) or subsea wellheads in the case of a blowout. The diverter system can be run from a dynamically positioned drilling rig using an existing installation workover control system with its lower riser package, emergency disconnect package and landing string.

5.4 Responses to Pipeline Emergency

Offshore oil and gas pipeline are important assets for maintaining stable energy supply. Some critical pipeline damages need emergency repairs, these defects include rupture, sabotage, vandalism, material failure, anchor drag damage on any of the operator's critical pipeline.

5.4.1 Temporary by-pass

This method is usually employed as a temporary measure to maintain flow around a damaged pipeline section whilst a more permanent repair method is planned. It is mostly recommended for pipeline defects of significant size by installing the temporary bypass section to allow the pipeline to be put back to service quickly.

5.4.2 Installation of a bolted clamp

Bolted clamps are designed to contain the full pipeline pressures and are generally thick and heavy as a result of the large bolts required to provide the required clamping force. To better contain the pressure for leaking pipelines, these clamps are designed with elastomeric seal. Usually, they are recommended for repairs of minor pipeline defects such as pin-hole leaks, localized corrosion and weld defects.

5.4.3 Lift up and repair/Above water repair

This method is recommended for offshore pipelines installed in shallow waters region in the water depth less than 40m. This method requires the deployment of pipe lay vessel with side mounted davits. The main advantages of this methods are that it minimizes the use of subsea connectors and number of such connectors installed on the pipeline, hence reducing the potential leak points along the pipeline and investment.

5.4.4 Remote welding system

The new remote welding system consist of three main modules: a habitat proving a dry gas filled work location at the tie-in location, a power and control unit launched separately providing all essential services needed for the job and the remote welding tool performing the welding operation itself (Berge, 2015). This new technology uses hyperbaric welding to repair large diameter subsea pipelines in water depth down to 1,300m. The first operational step is to install the remote welding habitat by means of the vessel crane. After landing the habitat on the seabed, the pipe ends are lifted into the habitat and secured by the pipe claws the pipe doors are closed. Then the habitat closure is filled with Argon gas and the atmosphere dehumidified in order to establish acceptable conditions for welding progress. The second stage is to launch the remote welding POCO, using an A-frame launch and recovery system over the vessel side or by means of a module-handling tower through the vessel moon-pool. The POCO will be landed on the habitat side platform and engaged on the connection interface. After verifying the interface seals are tight, the connection system is dewatered and opened to allow

Figure 5.8: Remote welding system in operation (Berge *et al*., 2015)

the remote welding tool to be moved sideways and engaged around the pipe. At last, the pre-heat system then heat the pipe to a specified temperature and the welding path is learnt and logged by the welding tool, the welding is performed under supervision and control by welding operator and a welding engineer.

6. INSPECTION, MAINTENANCE AND DECOMMISSIONING OF SUBSEA SYSTEMS

6.1 Technology Developments of Subsea Systems Inspection

6.1.1 Robotics in Deep Water

Unmanned underwater vehicles (UUVs) and its associated tooling are the most widely used equipment completing different missions under different working conditions and exchange information and data with the ship or station, as they are unoccupied, reliable and highly maneuverable. They have been widely applied to scientific research, acquiring information of oceans and life-forms, and are being increasingly utilized in subsea installation and maintenance operations (Shukla and Karki, 2016). The present UUVs are mainly classified as three types, remote operated underwater vehicles (ROVs), autonomous underwater vehicles (AUVs) and autonomous underwater gliders (AUGs), as shown in Figure 6.1.

Figure 6.1: Different kinds of ROVs and AUVs (Shukla and Karki, 2016)

Recently, to response to the lessons from The Deepwater Horizon oil spill accident off Louisiana in the Gulf of Mexico in 2010, an autonomous underwater robot (SOTAB-I) was proposed and tested for early detection and monitoring system as one technological measure around offshore oil and gas production systems (Kato *et al.*, 2017). The mission of this robot

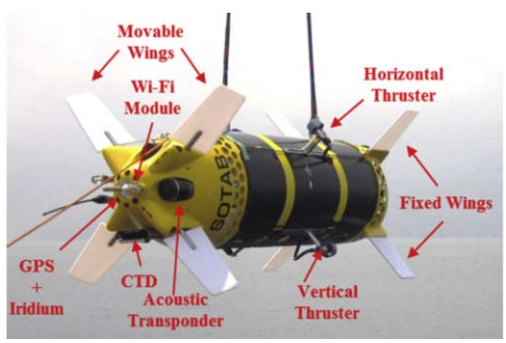

Figure 6.2: SOTAB-I (Kato *et al*., 2017)

is to monitor not only detailed structure of oil and gas plumes in the water columns, but also time-varying structure of transportation of oil droplets in 3-D space. Technologies of control, communication, navigation and power supply are still the main difficulties in developing UUVs for better subsea inspection and other operations.

6.1.2 3D Laser Imaging Systems

Lockheed Martin has developed the capability to conduct AUV-based structural survey and post-hurricane platform inspection using 3D mapping and change detection with a 3D sonar. The company is now extending its revolutionary 3D modeling and change detection to employ a 3D laser sensor, thereby improving model resolution and accuracy from centimeter scale to millimeter scale. The system about AUV outfitted with 3D laser imaging systems will provide new, high accuracy tools for inspection of flowlines, risers, and other subsea infrastructure.

6.1.3 Non-Destructive Examination of Flexible Risers

There is a significant requirement from operators to have a reliable, high quality method of identifying damage and quantifying the remaining life of aging operating flexible risers. The DRIFT (Digital Radiographic Inspection of Flexible Risers Tool) has been proven to detect the defects of concern in fine detail, including corrosion, cracks, carcass collapse and loss of interlock (Crane, 2016). This technology has significant potential for extension to SCRs, as well as other subsea hardware and for use in greater water depths.

6.2 Advances in Maintenance of Subsea Systems

6.2.1 Risk Based Asset Management (RBAM)

According to Risk Based Inspection (RBI) and Reliability Centered Maintenance (RCM) methodologies, a risk-based inspection methodology for asset management offering an organized analysis with knowledge sharing for collaborative possibilities in a multidisciplinary context is investigated (Kamsu-Foguem, 2016). The RCM process aims to create a precise, targeted and optimized maintenance program in order to achieve optimum reliability from the facility. Compared with RCM, the RBAM approach optimizes the cost of preventive maintenance and the corresponding expected cost of failures. The RBAM focuses on implementing a maintenance and inspection plan which focuses in the possibility of continuous improvement.

6.2.2 Pipeline Maintenance Plan

It is not an easy task to provide timely response and effective maintenance in challenging operating environments for subsea pipelines with the challenges of ultra-deep water, high pressure, corrosive products, and unstable soil conditions. Integrity management programs are used to prevent, detect and mitigate threats in lifecycle of subsea pipelines. The Pipeline Integrity Management (PIM) system includes design, operation, QA/QC, corrosion management, and management of other risks (Liu *et al.*, 2017). The PIM plan has the following responses: preventive response — removes the threat or mitigates the consequence; predictive response — detects and confirms the threat likelihood, its location and characteristics; and corrective response — address the detected threat prior to failure either by non-intrusive means or intrusive repair.

To deal with the emergency and reduce the downtime, an Emergency Pipeline Repair System (EPRS) is introduced. It can put the right material, equipment, resources and construction spreads into place before an emergency occur (Sun *et al.*, 2017), and can make full preparation before the failure and reduce the bad consequence.

6.2.3 Well Maintenance Plan

It is necessary to perform maintenance interventions to avoid leaks and keep safe during well operation. A quantitative and dynamic risk assessment (QDRA) is developed to evaluate the

safety of well maintenance activities (Villa *et al.*, 2016). It is an easy method to quantify the available IBS (integrity barriers set) by proper software before operations. The QDRA approach with database containing entire mapped information about barrier components, barriers, IBS, operations and their relationships can be automated to make safety assessment of the well construction or maintenance plan.

6.3 Advance in Decommissioning of Subsea Systems

New technological developments are necessary for the safe and cost effective execution of the project in decommissioning of subsea systems.

6.3.1 Subsea Cutting Technology

Cutting techniques are numerous low-energy solutions including shears, diamond wire, and water-jet cutting. Higher energy solutions include gas cutting and other burning methods. Solutions are chosen on the basis of best-for-task, equipment, safety assessments, and overall energy balance.

6.3.2 Sub Bottom Cutter

The idea of the Sub Bottom Cutter (SBC) has been originated by exploiting diamond wire cutting technology and designing underwater cutting equipment autonomously operating under remote supervision, in response to legislative requirements for the safe and efficient removal of offshore structures such as jacket piles and wellheads below the seabed soil (Buch *et al.*, 2015). The development of the SBC prototype has been sponsored by four oil companies: BP Amoco, Total, Amerada Hess and Shell. The project brings forth:

- A reliably tailored set-up: The robotic platform;
- A low-impact duty-scheme: The dig-and-saw process;
- A new technology: The diamond wire cutting;
- A safe work-cycle: remote monitoring and control of the system functions.

This approach in the unique task of cutting underwater structures below the seabed soil is aimed at reducing the excavation volume to less than 10 cubic meters, enabling the safe disposal of the excavation refuse without disturbance of the surrounding environment.

The SBC (Figure 6.3) leading by Cutting Underwater Technologies Ltd is principally composed of the following parts: The support platform (including bridles, 3 suction anchors, hydraulic/electric junction box); The Main Frame (with tilting rams and frame, sledge guides and rack); The Excavation System (Twin Guide Tubes, sledge frame and feeding system); The Cutting Assembly (the Twin Guide Tubes with the relevant actuation, monitoring and diamond wire cleaning systems).

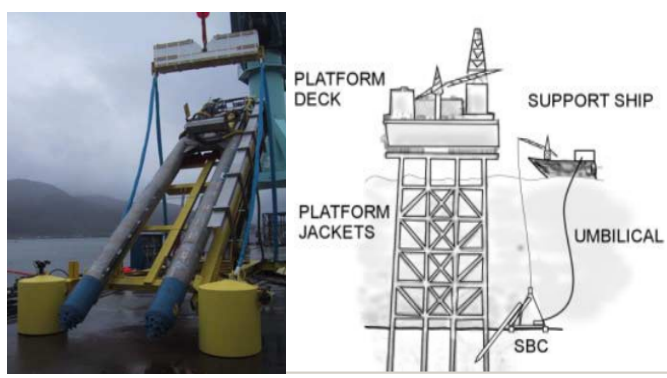

Figure 6.3: The prototype SBC robotic platform (left) and Operating Configuration (right)

The robotic platform developed within the SBC project provides reliable and effective means for underwater oil plants decommissioning, thus giving a positive answer to the market request for new technology.

The operating sequence of the SBC systems (Figure 6.4) is as follows:

- Stand-by, the reference state after deployment on the sea-bed;
- Emergency, if a failure arises, the alarm state is enabled, specifying the originating site;
- Positioning (anchorage), the robotic platform is located and its altitude set to start cutting operation;
- Tilt, the platform cradle is bent up to the selected engagement slope;
- Drilling, the twin pipe drill-and-dig heads perform the required digging beneath the sea-bed soil;
- Cutting, the diamond wire equipment accomplishes the planned task.

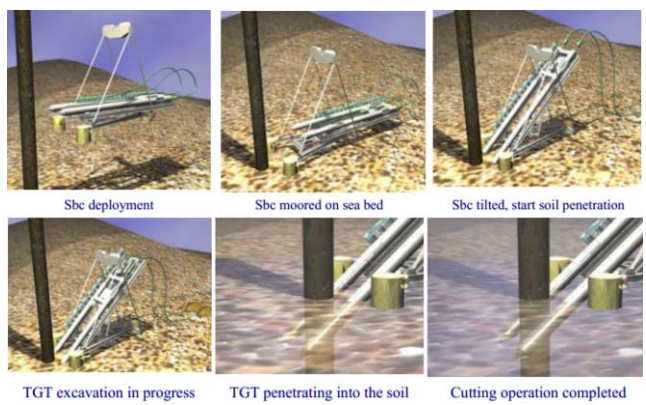

Figure 6.4: Operating Sequences

6.3.3 Pipe Cutting Tool

In order to reduce rig time during work-over operations, a new electric line mechanical pipe cutting tool invented by Welltec was designed and tested. This particular mechanical cutter was chosen for its non-explosive design, where a rotating crown removes pipe wall by grinding creating a smooth beveled surface without shavings. This approach made the ability to cut the tubing in compression, without the requirement for the pipe to be put in neutral weight or tension.

A key benefit of mechanical pipe cutters is that they eliminate the use of explosives and chemicals which can pose HSE and operational risks, especially when simultaneous operations are being conducted. In addition, this mechanical solution eliminates the need for dress runs, and tubing recovery is optimized from a rig time perspective. Typically, more than 80% of the pipe wall at the cut must be removed or the rig may be unable to pull the tubing apart, or the pull will prematurely release a packer or other equipment.

The new cutting tools have been operated for the field testing in the Middle East. A series of field testing indicates the tools perform as designed, cutting the pipe on each application with no tool sticking, e-line over-pulls other mechanical problems.

6.3.4 Plugging and De-oiling

Conventional methods of decommissioning subsea pipeline infrastructure are inherently very expensive with the mobilization and operation of DSV (Dive Support Vessel), equipment and

personnel. In this case the only other viable option was to mobilize a DSV to hot tap the flowlines and circulate fluid from the platform before filling the line with cement. This operation would have incurred considerable expenditure so the operator sought a more cost effective solution (Mackenzie and Jones, 2015).

The solution from Paradigm Flow Services utilized an ultra lightweight, miniaturized coiled tubing system, which was deployable from the platform lower decks with minimal lay-down area required. The system had the ability of traverse multiple bends (360° total), de-oil the line and deliver an expandable cement to plug the pipeline by means of a single operation.

The system had been previously been deployed to remove a 470m sand blockage within a riser and pipeline system from an FPSO in West Africa.

Compared to conventional solutions, the innovative and more cost effective method approach provides an alternative solution for operators to consider when planning pipeline decommissioning. The result of the operation has been outlined as well as the future of this new technology within the decommissioning sector.

6.3.5 External Latch Mechanical for Well Decommissioning

Subsea wells are wells in which the subsea wellhead, Christmas tree and production control equipment are located on the sea bed. At the end of its life cycle, a subsea well and its supporting infrastructure must be carefully dismantled to ensure they pose no safety or environment threats and to salvage useable components. Plug and abandonment (P&A) operation are carried out to close a well either temporarily or permanently. The challenge is to retrieve the wellhead without damage so that it can be used again, minimizing or eliminating damage not only to the wellhead but also to personnel and environment.

There are different methods of severing and removing subsea wellheads. For casing severing, there are explosives severance methods, jet cutting method, and mechanical cutting methods. One such advanced technology system for subsea well abandonment and well suspension, is the external latch mechanical outside single trip (MOST) system which can reduce rig time by cutting and retrieving multiple cemented or uncemented strings in a single trip.

The distinct advantage of the external latch is that it eliminates damage to the internal seal surface of the high-pressure wellhead housing and that it also provides good lateral support for the wellhead assembly thus eliminating any lateral whipping that might impede cutting. Preventing a swarf build-up provides more room for cutting to flow out.

In the Gulf of Mexico, the job was performed in a shallow area (313 ft) with a smaller, inexpensive semi-submersible rig; the well did not require BOP or risers. The production string cuts were done using mud motors since this rig had limited top driver capabilities. The tension cut system offers additional benefits such as where the ocean floor is at an inclination and the wellhead is top-heavy, or the wellhead sticks up higher than normal above the mud-line which could cause the wellhead to list and start the partially cut-section to close in on the knives before the cut is fully severed, a potential additional run can be eliminated by using the tension cut system. The system is currently being used not only in Gulf of Mexico and offshore Australia, but also in other regions such as North Sea, Asia-Pacific region, offshore West Africa, offshore Canada, *etc*.

6.4 Conclusion

The technical evaluation of this field shows that a number of issues require further study such as solid ballast removal techniques, the sealing of conductor penetrations and data delivery in inspection. Such issues would receive the necessary attention during the engineering planning leading up to the inspection, maintenance and decommissioning operation.

The objective of all the technical developments is to reduce the costs in the process of inspection, maintenance and decommissioning of subsea systems. But during subsea structure design for a new project, there is an opportunity to reduce the cost of the operating mentioned above. If the methodology for inspection, maintenance and decommissioning is developed during design, then the design can be amended to ensure that the cost and time for inspection, maintenance and decommissioning is minimized.

7. TECHNOLOGIES FOR HYDRATES AND OTHER SUBSEA RESOURCES

Natural gas hydrate (NGH), ice-like compounds containing methane, which extensively exist in sea-floor, will become an important energy in the future for the fossil fuels owing to the increasing energy consumption. The NGH exists stably in reservoir for the phase equilibrium condition of high pressure and low temperature. The key point of NGH exploitation technology is how to break the phase equilibrium condition destroying the structure of the hydrate and releasing the methane. There are 4 main NGH exploitation technologies widely accepted: depressurization, thermal stimulation, chemical inhibitor and CO_2-CH_4 replacement.

7.1 Depressurization

The technique of depressurization seeks for gas production from NGH reservoirs by lowering the pressure below to the NGH equilibrium pressure at the local temperature. The sustainability of gas production by depressurization depends on the diffusion of pressure, the NGH saturation and effective permeability in the NGHs reservoirs. The latest progress of the technique of depressurization is focused on the numerical simulation aspect.

Konno *et al.* (2016) proposed the cyclic depressurization method. Numerical simulations were conducted and the results shown that gas production rate was high during preliminary stage after primary depressurization; however, the production rate drastically decreased because the sensible heat of the reservoir was exhausted owing to hydrate dissociation.

Yu *et al.* (2017) utilized a one-dimensional mathematical model for methane hydrates decomposition by depressurization in porous media, as shown in Figure 7.1. Ice generation occurred along with the hydrates decomposition process.

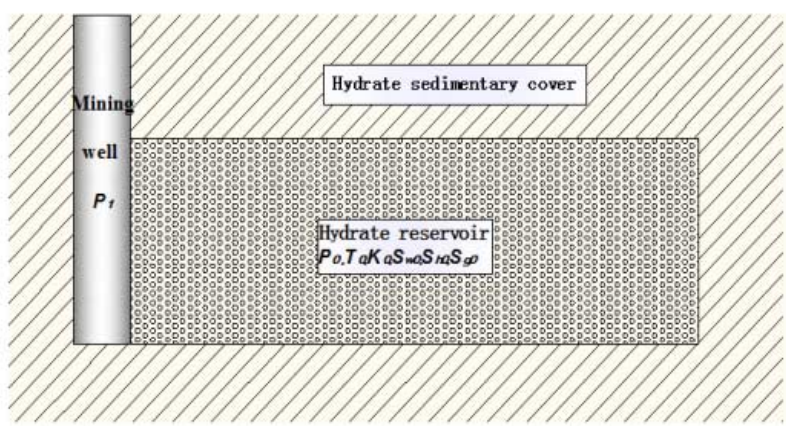

Figure 7.1: Schematic of gas hydrate decomposition by depressurization (Yu *et al.*, 2017)

Zhao *et al.* (2015) analyzed the process of gas production for natural gas hydrate. The methane gas production process can be divided into three main stages: free gas liberation, hydrate dissociation sustained by the sensible heat of the reservoir, and hydrate dissociation

driven by ambient heat transfer, as shown in Figure 7.2. Hydrate reformation and ice generation always occur in the reservoir interior due to insufficient heat transfer. The paper found that the sensible heat of the reservoir and ambient heat transfer played a dominant role in hydrate dissociation, and that both were dependent on production pressures.

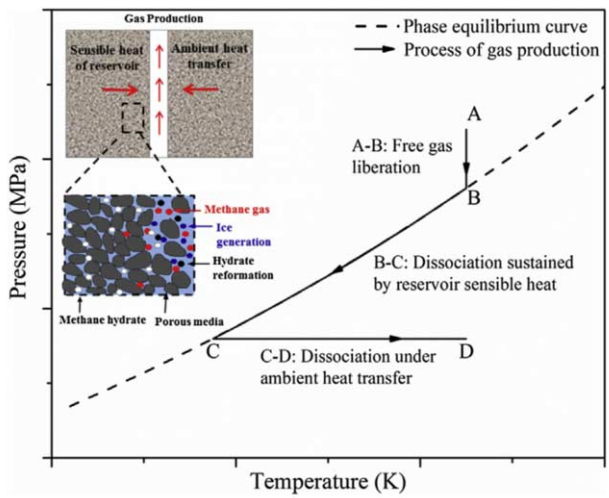

Figure 7.2: Pressure-temperature relationship (Zhao *et al.*, 2015)

Han *et al.* (2017) took siltstone, sand and clay reservoirs in Shenhu area of South China Sea as examples to investigate the effects of the magnitude and anisotropy of reservoir permeability on NGH production process. They found that permeability anisotropy could impede advective interaction of fluids in vertical direction, significantly changing temperature and pressure evolution during NGH dissociation.

7.2 Thermal Stimulation

The local temperature turns to above the phase equilibrium temperature at the local pressure by thermal stimulation, resulting in local NGHs dissociating and natural gases releasing along with water.

Zhao *et al.* (2015) investigated the influence of heat transfer on methane gas production by thermal stimulation. The results showed that during hydrate decomposition, increasing the specific heat capacity of porous media containing hydrate inhibited the gas generation rate.

7.3 Chemical Inhibitor

Chemical inhibitor injection works by shifting the NGH phase equilibrium curve to higher pressure and lower temperature, leaving the NGHs unstable in the local condition of temperature and pressure.

Walker *et al.* (2015) found antifreeze proteins (AFPs) could be effective against structure II (sII) hydrates formed from the liquid tetrahydrofuran, sI and sII gas hydrates formed from single gases, as well as sII natural gas hydrates, as shown in Figure 7.3. For the most part, AFPs were more effective than the commercial kinetic hydrate inhibitor (KHI) polyvinylpyrolidone, even under field conditions where saline and liquid hydrocarbons are present and efforts to overcome the difficulties of recombinant protein production were ongoing.

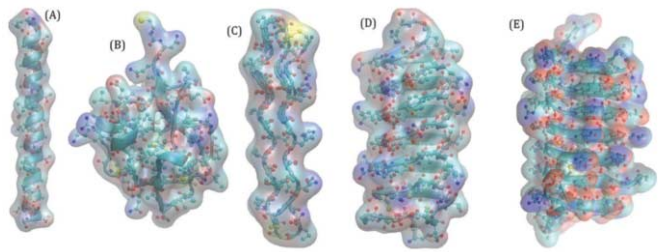

Figure 7.3: AFPs modeled structures, Walker et al. (2015)

Mohamed *et al.* (2017) found new biocompatible gas hydrate inhibitors and tested the gas hydrate inhibition properties of choline acetate (ChOAc), choline bistriflamide (ChNtf2) and choline chloride (ChCl) for methane and a multicomponent Qatari natural gas type mixture (QNG-S1).

Lee et al. (2016) conducted experiments investigating synergetic effect of ionic liquids on the kinetic inhibition performance of poly (N-vinylcaprolactam) (PVCap) for natural gas hydrate formation. The experimental results revealed PVCap and 1-hexyl-1-methylpyrrolidinium tetrafluoroborate (HMP-BF4) showed the best hydrate inhibition effectiveness even under higher pressures, and the combination of 1.0 wt % PVCap and 0.5 wt % HMP-BF4 was found to provide the longest induction time.

7.4 CO_2-CH_4 Replacement

By the CO_2 replacement method, a mutual complementation can be gained between the heat adsorption during the CH_4 hydrate decomposition and the heat release during the generation of CO_2 hydrate. CO_2 hydrate is generated after NGH hydrate decomposition by heat compensation and the secondary hydrate generation can maintain the hydrate reservoir stability.

Khlebnikov *et al.* (2016) proposed a new method combining CO_2 replacement method with thermodynamic hydrate inhibitor technology to accelerate the decomposition of CH_4 hydrate, as shown in Figure 7.4. As a kind of thermodynamic inhibitor for CH_4 hydrate, alcohol showed a more efficient performance than electrolyte.

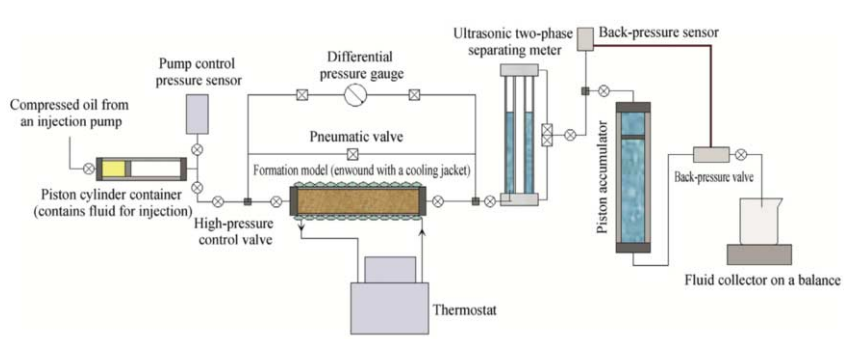

Figure 7.4: Schematic diagram of the experimental apparatus (Khlebnikov *et al.*, 2016)

A novel natural gas hydrate production method combined with methane steam reforming and CO_2/H_2 replacement was proposed to improve the replacement effect and reduce the cost of later gas separation, as shown in Figure 7.5. The experimental results showed H_2 could de-

crease the partial pressure of methane in gas phase and help to break the methane hydrate stability (Wang *et al.*, 2017).

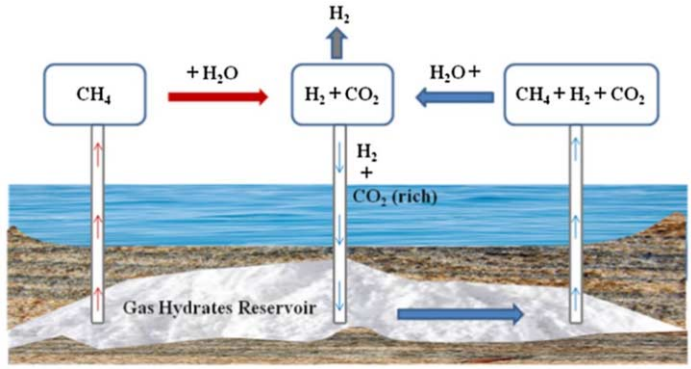

Figure 7.5: Schematic diagram of cyclic hydrogen production from hydrates reservoir (Wang *et al.*, 2017)

8. PIPELINES, RISERS AND UMBILICALS

8.1 Soil-Structure Interaction

8.1.1 Industry Standards

The Addendum 1 of API RP 2GEO 1st Edition (modified from ISO 19901-4:2003) "Geotechnical and Foundation Design Considerations" added a new Section 9 on soil-structure interaction for risers, flowlines and auxiliary subsea structures in October 2014. This section details the recommendations on geotechnical investigation, riser-soil interaction including steel catenary riser (SCR), top tension riser (TTR), riser tower and pipeline-soil interaction.

API RP 17P (identical to ISO 13628-15:2011) "Design and Operation of Subsea Production Systems-Subsea Structures and Manifolds" provides detailed requirements on foundation design for subsea structures, including suction piles, driven piles, skirted structures and non-skirted structures.

8.1.2 Steel Catenary Risers

Riser-soil interaction is one of the major concerns for SCRs design and integrity management as it affects riser strength due to excessive bending and tensile stresses in the riser wall as well as riser fatigue due to cumulative damage to the riser from motion-induced changes in bending stress in the region of the touchdown point.

Clukey and Zakeri (2016) proposed a new non-linear model that considered the soil response for fully-degraded soil based on Zakeri *et al.* (2015) and C-CORE centrifuge results. Yuan et al. (2017) observed the effects of water entrainment and large amplitude cyclic loading in experimental studies.

Model testing for SCR-soil interaction has primary two modules: segment tests and sectional tests. Segment tests are carried out by measuring the response of a moving short pipe section in the soil, such as Aubeny *et al.* (2015) and Yuan *et al.* (2017). Segment tests observe the fundamental soil behavior which is the base of a soil model development. Sectional test simulates the actual SCR configuration by starting a pipe from a point above the seabed to the touchdown zone, for instance the centrifuge tests at C-CORE. The C-CORE test results have been used to validate a fully degraded secant stiffness values based non-linear soil model proposed by Clukey and Zakeri (2016). Three non-linear curves which had slightly higher stiffness values than the curve derived from the segment data provided a very good fit to the

measured fatigue data. These curves were then averaged to provide the best overall fit to the results (Clukey *et al.*, 2017).

Consolidation effects have been studied by a number of model tests (Clukey *et al.*, 2017; Yuan *et al.*, 2017). The vertical cyclic motions of a SCR in the touchdown zone (TDZ) induce shearing of the surrounding soil (or soft clays), leading to excess pore pressure building up. The impact of long term consolidation has not been fully resolved, however, it is found that larger numbers of cycles did produce larger initial stiffness values (Clukey *et al.*, 2017).

Field data on SCRs have been collected from a number of real projects, unfortunately none of them are in the public domain. The recent launched STREAM (STeel Riser Enhanced Analytics using Measurements) JIP will use full-scale field data from six deepwater SCR systems to benchmark design, identify gaps and derive calibrated modeling parameters. It is expected that STREAM JIP will provide a measurement-based foundation for SCR modelling to allow for accurate fatigue assessment, especially in TDZ.

Studies were carried out on the trench effect on SCR fatigue damages, such as Clukey and Zakeri (2016), and Wang and Low (2016).However, other recent simulations using different numerical approaches for trench formation for two different SCR systems in different loading conditions showed mixed results. 23 of the 29 cases showed a positive impact on the SCR fatigue lives while only 6 cases showed a negative impact. In addition, centrifuge testing results have shown no impact for a trench to SCR fatigue lives (Clukey *et al.*, 2017).

During the STRIDE JIP, remotely operated vehicle (ROV) surveys of the SCR TDZ in the Gulf of Mexico (GoM) showed the shape and extent of the trench. Consequently, efforts were made to collect other SCR trench videos in GoM and offshore Brazil. The observations showed that the overall trench was shaped like a ladle, with maximum width at the touchdown point typically 5-10 pipe diameters.

8.1.3 Top Tensioned Risers

Top tensioned riser (conductor) design should consider both ultimate and fatigue limit states. Generally, TTR-soil interaction is analogous to that of a laterally loaded pile. Therefore, lateral soil springs provided for offshore piles have often been used for TTR-soil interaction (API RP 2GEO 2014).

However, the soil springs for piles were originally developed for steel jackets subjected to large storm loads. It focuses on the characteristics of the soil near yield, not the soil response at smaller displacement, therefore it is not suitable for TTR-soil interaction.

Procedures in Templeton for developing p-y curves through FEA are recommended by API RP 2GEO. It is also suggested by API RP 2GEO that if the critical bending moments are below the mudline, the curves given by API 2A-WSD, can be initially used. If the critical fatigue point is above the mudline, the p-y curves given by API 2A-WSD, can be non-conservative. For a drilling riser with heavier lower stacks (LMRP, BOP), using stiffer soil (or fixed at mudline) does not guarantee the results to be in the conservative side even if the critical fatigue point is above the mudline (API RP 2GEO).

8.1.4 Hybrid Riser Systems

There are a number of possible foundation options for the subsea hybrid riser system (HRS): gravity base, suction caissons and driven piles. The selection of the HRS foundation is normally based on technical and economic criteria, soil properties, installation methods, as well as the in-place performance of HRS.

The design guidance of driven piles and gravity base is given in API RP 2T (2015) and the design guidance of suction caissons is provided in API RP 2SK (2015) with the considerations of the following aspects:

- penetration and retrieval
- holding capacity including long-term uplift capacity
- long-term displacement
- soil reactions to be used for the structural design

ABS Guidance Notes on Subsea Hybrid Riser Systems also provides detailed guidance on the design and analysis of foundation piles for HRS based on industry common practices (ABS, 2017).

8.1.5 Pipelines

More complex pipeline-soil models are developed in the recent years, especially in SAFEBUCK JIP. Either upper or lower bound values of the pipe-soil interaction forces can be critical for a limit state, therefore each bound should be assessed as recommended in API RP 2GEO.

SAFEBUCK GEO is a JIP dedicated to pipe-soil interaction during lateral buckling, running alongside SAFEBUCK III. The numerical pipe-soil interaction model developed in SAFEBUCK GEO considers pipe embedment, axial pipe-soil interaction, and lateral pipe-soil interaction. Centrifuge tests were conducted at the University of Western Australia to calibrate the numerical results. FEA were also carried out to supplement the centrifuge data and provide the relationship between forces on the pipe and pipe movement (Atkins, 2015 and Rismanchian, 2015).

COFS-MERIWA JIP focuses on the simulation of slide runout and the assessment of the resulting loading and deformation of seabed pipelines. The JIP worked on slide-pipeline interaction with regard to the following aspects (White *et al.*, 2016):

- characterization of soils at the solid-fluid transition
- computational modelling of slide runout – via depth-averaged and continuum finite element methods
- physical and numerical modelling of slide runout and pipeline impact
- analytical studies of pipeline response during slide loading.

He summarized the recent advances in the pipeline-soil interaction from late 1990s to 2017. The review covers submarine slide, pipeline embedment, axial and lateral pipe-soil interaction, scour and self-burial et al. (White *et al.*, 2017).

8.2 Local/Global Buckling and Propagation

Subsea pipelines buckle globally because of their movement relative to surrounding soil. Global buckling is often triggered by high operational temperature of the oil in pipelines, initial imperfections in the pipeline, and/or a combination of both. Global buckling is increasingly difficult to control due to the increase in temperature and pressure. Therefore, location prediction and buckling control are critical to pipeline design.

Liu *et al.* (2014) proposed four numerical simulation methods based on finite element method (FEM) program ABAQUS to simulate pipeline global buckling under different temperatures. An analysis method based on modal analysis that introduces initial pipeline imperfection is also presented to analyze thermal buckling in an initially imperfect pipeline.

Liu *et al.* (2014) introduced energy method to get the analytical solution suitable for the global buckling modes of idealized subsea pipeline and analyze the relationship between the critical buckling temperature, buckling length and amplitude under different high-order global lateral buckling modes. To obtain consistent formulation of the problem, the principles of virtual displacements and the variation calculus for variable matching points are applied.

Experimental and finite element results for buckle interaction in subsea pipelines are presented by Hassan and Albermani (2014). The effect of linear and clad materials on the effective

axial force has been determined by analytical deduction. It was concluded that it is important to include the effects of the linear or clad materials in the effective axial force.

Wang *et al.* (2015) studied static and dynamic analysis on upheaval buckling of unburied subsea pipelines. Two analysis procedures are proposed for different stages in buckling. Procedure 1 links Newton- Raphson and arc-length method. Procedure 2 links static and dynamic nonlinear analysis seamlessly which effectively solves the convergence problem when dealing with snap buckling.

Using a preheating method combined with constraints from two segmented ditching constructions which are scheduled before and after preheating, Zhao and Feng (2015) proposed an upheaval buckling solution for high temperature subsea pipelines. In this solution, some selected pipe segments along the route were curve-laid and preserved resting on the seabed in the first ditching construction, while other straight segments were trenched. The subsequent hot water flushing operation induced the curve-laid segments to buckle on the seabed, and then these pre-buckles were laterally constrained by the second ditching operation carried out during preheating. After preheating, the cooling rebound of these pre-buckles was constrained by the new trenches, and axial pretension was induced in the pipe wall to offset the axial compression in service and upgrade the thermal stability of the entire pipeline.

Zhao and Duan (2017) proposed an upheaval buckling prediction approach for high-temperature Cased Insulated Flowlines (CIFs). Based on the tensile cracking and compression crushing analyses of the CIF concrete-weighted coats, the curvature-related nonlinear bending stiffnesses of CIF systems are discussed firstly and a changeable stiffness is included in this buckling prediction approach developed using a transfer matrix method. Using the approach developed, the field-joint stress of a CIF carrier pipe and the interlayer shear forces of the CIF pipe coats can be obtained along the buckling path of the CIF systems by plotting the relationship curves between the carrier pipe axial forces and the CIF buckle lengths.

Zeng *et al.* (2014) noticed that the upheaval buckling pipelines have some different approximation formulas for the critical buckling axial forces. However, these formulas did not take into account of the imperfection out-of-straightness (OOS) as a whole. Based on dimensional analysis and finite element (FE) analysis some brand new formulas were presented for the critical upheaval buckling forces for three typical imperfections, which could be used to estimate the critical forces of the imperfect pipelines quickly. Meanwhile, Zeng and Duan (2014) investigated the laterally buckling behavior of partially embedded submarine high pressure and high temperature (HP/HT) pipelines. They modeled the lateral buckling pipeline by an axial compressive beam supported by lateral distributing nonlinear springs. It is found that the model is governed by a time-independent Swift–Hohenberg equation and that the equation's localized solutions are corresponding to the different buckling modes of the pipelines. Based on numerical results the range of the possible critical axial forces was found out and two critical axial force formulas corresponding to the range boundaries were presented..

Zhang and Duan (2015) studied the upheaval buckling behaviors of eight groups of pipeline segments with different imperfection shapes and different out-of-straightness using the finite element method. A new parameter is defined to express the differences of imperfection shapes. An approximation and universal formula is proposed to calculate the critical axial force which covers the new parameter and the out-of-straightness of pipeline.

Wang *et al.* (2017) proposed a new nonlinear pipe-soil interaction model and deduced the governing differential equation of an imperfect pipeline on soft foundation. The solution to the governing differential equation is proposed based on nonlinear perturbation expansions. The effect of soil conditions, burial depth and initial imperfections on critical force as well as localization pattern of upheaval buckling are discussed.

Zhang *et al.* (2017) proposed a new lateral pipe-soil interaction model. Three dimensional Finite Element Models are built to simulate the lateral buckling and post-buckling. The effects of pipe-soil interaction parameters, initial imperfection shape and out-of-straightness of pipe on critical buckling force and localization patterns of lateral buckling are discussed.

8.3 Vortex Induced Vibration of Cylindrical Structure

Novel model tests on the riser dynamic response under vessel motion have been performed for the steel catenary riser (SCR) by Wang et al. (2015), the water intake riser (WIR) by Wang et al. (2016), the steel lazy wave riser (SLWR) by Cheng et al. (2016) and the free-hanging drilling riser (FHR) by (Wang et al., 2017) recently. A representative experimental setup is demonstrated in Figure 8.1, concerning a large-scale SCR model test under vessel motion. The top end of the SCR is connected to the forced motion system, which simulates the vessel motion time histories. The riser dynamic response is measured by a large amount of Fiber Bragg Gratting (FBG) strain sensors and several underwater cameras. The main contribution of these work is the discovery of out-of-plane VIVs induced by purely in-plane vessel motions, termed as vessel motion-induced VIVs. Vessel motion-induced VIVs were recognized to have greatly amplified the riser fatigue damages compared with the global dynamic response under vessel motion, and would lead to more fatigue damage than steady ocean flow induced VIVs (Wang et al., 2014). These new findings indicated the necessities of including vessel motion-induced VIVs during the riser deign, which is yet to be implemented into the design standards (DNV, 2014). With further experimental investigations, they found some more novel phenomena of VIV under oscillatory flows: unsteady VIV with three developing stages steps of "building up - locking in - dying out", hysteresis of motion trajectories, and VIV could occur even when the KC number is down to 20 (Fu et al., 2014).

Shur and Strelets (2015) used SRANS method to simulate incompressible flow past a circular cylinder, with a simple and generic geometry. They found by introducing Vortex Generators (VG), flow separations of smooth bluff bodies were significantly delayed together with a substantial decrease of the pressure drag force (up to 60%) of the bodies in the transcritical flow regime. Chen and Gao (2015) also used the RANS method to simulate the VIV of an inclined cable under wind with varying velocity profiles, and found the cable undergoing single-vibration mode with small velocity changes, and multi-vibration modes with large velocity changes.

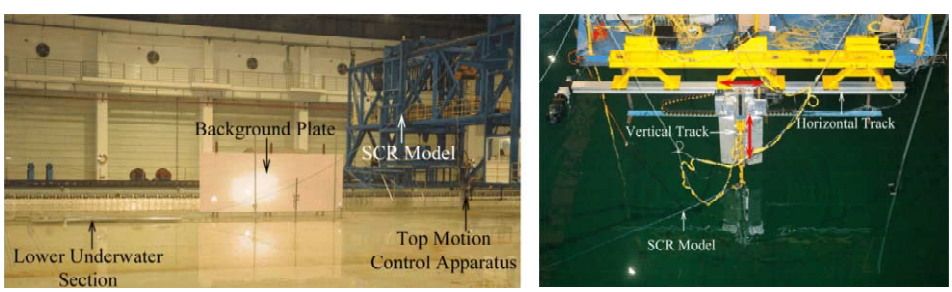

(a) (b)

Figure 8.1: Vessel motion-induced VIV modet test of a SCR at SJTU (Wang et.al., 2015) (a: overview of the experimental setup in air; b: overview of the top motion apparatus)

Quadrante and Nishi (2014) studied the effect of tripping wires on the vibration of a circular cylinder subject to flows. They placed a pair of tripping wires on to the surface of a circular cylinder symmetrically about the stagnation point, and submerged the cylinder clamped or elastically mounted. They determined the angular positions giving the maximum and minimum of the hydrodynamic force. The experiments on the cylinder demonstrate that the pres-

ence of tripping wires remarkably alters the response of VIV. In particular, for β=120 degrees, the VIV is completely suppressed throughout the reduced velocity range tested.

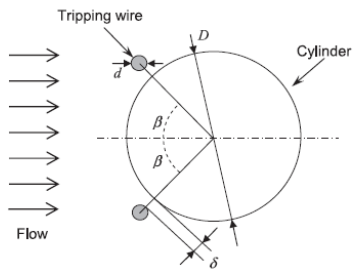

Figure 8.2: Cross section of cylinder and tripping wire (Quadrante and Nishi, 2014)

Chen and Gao (2015) designed four perforated pipes with different numbers of suction/jet holes, as shown in Figure 8.3.

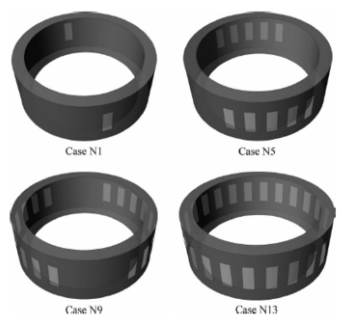

Figure 8.3: Schematic drawing of the passive jet control pipe units (Chen and Gao, 2015)

N represents the number of suction/jet holes on each side of the pipe, the pipes were put around a circular cylinder suffered from incoming air flow. It was found that the passive jet control method is very effective in manipulating the wake vortex shedding process from the circular cylinder. The perforated pipe designs with more suction/jet holes were found to be more effective in reducing drag and suppressing fluctuating amplitude of the dynamic wind loads acting on the test model. The periodicity of the vortex shedding was also observed to be diminished and eventually disappeared with the number increase in the suction/jet holes.

8.4 Dynamic Behavior and Fatigue

Very recently, there have been some studies on the development of fast and reasonably accurate methods for long-term fatigue analysis of risers, spurred by its practical importance.

Song *et al.* (2016) attempted to systematize the blocking method by proposing an approach to determine the equivalent wave height, wave period and probability of occurrence for each block. Giraldo *et al.* (2015) investigated the asymptotic approach for a riser suspended and moored by chains, using time domain analysis. The highly efficient asymptotic approach is found to be generally quite accurate for this application. Giraldo *et al.* (2016) proposed to use the univariate dimension reduction technique, testing it on a steel lazy wave riser (SLWR). This approach requires only 21 stochastic dynamic simulations, and appears to give a reasonable estimation of the long-term fatigue damage. One of its main advantage is that the integration points are pre-determined, and the results are applicable to any stress location. Gao and Cheung (2015) proposed a response surface approach for fatigue analysis of a flexible riser in

the time domain. Five environmental parameters were considered, namely the significant wave height, wave period, wave direction, wind velocity, and current.

Methods have also been proposed to improve the efficiency of Monte Carlo simulation. Such methods have the advantage of producing an unbiased estimate of the fatigue damage, and allowing an error estimate. Gao and Low (2016) developed an efficient simulation method based on importance sampling, applying the method on unbonded flexible risers. Low (2016) proposed a variance reduction technique based on control variables. This method has the advantage of being a post-processing scheme, allowing the fatigue damage to be evaluated at multiple stress locations using the same set of simulation results.

Wang and Duan (2017) proposed a 2D nonlinear dynamic model for steel lazy wave riser (SLWR) based on Euler-Bernoulli beam theory with initial conditions and boundary conditions under top excitations considering the effect of ocean current and internal flow. Keller Box finite difference scheme was adopted to solve the partial differential equations and numerical analysis is conducted to investigate the influences of tangential and normal excitations on the dynamic response of SLWR.

Researchers have also explored the use of artificial neural networks (ANN) to reduce the amount of nonlinear time domain simulations required for a full fatigue analysis of moorings and risers. Christiansen (2015) proposed an algorithm to optimize the training procedure, and applied it on mooring lines; however the approach is equally appropriate for risers. Aguiar *et al.* (2015) implemented ANN for fatigue analysis of a buoy support riser, while Chaves *et al.* (2015) used ANN to analyze the bending stiffener of a flexible pipe. In the above mentioned studies, ANN is found to be a promising approach for substantially reducing the computational effort while maintaining an acceptable accuracy. However, further studies are still required to determine whether ANN is sufficiently robust to be used in a wide range of riser systems, for example the highly nonlinear touchdown region of a steel catenary riser.

8.5 Special Issues for Flexible Pipes and Umbilicals

Installation of flexible pipes and cables is normally carried out in the J-lay mode. The wave induced vessel motions give rise to dynamic tension and curvature at the touch down zone (TDZ) limiting the weather window within witch the installation operation can take places. Commonly used acceptance criteria during global installation analysis are the minimum radius of curvature and (API 2014) and the common practice of not allowing compression to occur. An important question for the industry in later years has been whether effective axial compression can be allowed at TDP during installation of umbilicals and power cables. If this can be allowed, the current practice of not allowing compression can be relaxed which will have a direct economic benefit with respect to the installation costs. However, there are several issues that relates to the interaction between local instability of individual helix element and global torsion instability modes, which are not yet fully understood and need to be resolved.

As flexible pipes are normally installed in empty condition, a high external pressure in combination with the empty bore will introduce a large compressive end cap force. This means that the load condition that might lead to kink formation is fundamental different between flexible pipes and umbilicals. For the flexible pipe, local instability can occur even if the cross-section is in effective tension. The global configuration is stable; however, due to local buckling effects resulting from true wall compression, a condition of torsion unbalance occurs gradually by cyclic curvature until severe torsion deformation forces a kink to be formed. This requires either full scale testing or coupled numerical models that are capable of describing the coupling between local lateral transverse helix buckling and global behavior, (Sævik, 2014) and (Zhou *et al.*, 2014), to determine the capacity.

For the umbilical case, due to the lack of an empty bore, local instability cannot occur unless the effective axial force is in compression, which means that the global configuration already

might not be stable. The structural analysis model can then in first instance be assumed uncoupled and governed by the global behavior. This is then followed by component capacity checks, which for the case of axial compression also must include the local helix instability modes that include both lateral transverse helix buckling and bird-caging as for the flexible pipe case.

Kink formation might, however, occur even if the effective tension is positive, depending on the amount of torque in the catenary. This will again be influenced by a range of parameters such as the catenary length (water depth), cross-section torsion balance, seabed routing, vessel heading and motions, seabed friction and built-in torque from the manufacturing and installation procedures. If kink formation occurs, permanent deformations in terms of residual curvature will occur due to the friction between the layers, i.e. the friction moment effect. Then any attempt of straightening the kink may result in severe curvatures that may destroy the cross-section components. Neto and Martins developed an FE model based on a geometric exact beam element formulation and addressed the issue of kinking of an elastic cross-section during deep water installation (Neto, *et al.*, 2014). They investigated the effect of the tension distribution and seabed friction on the critical torsion moment with reference to the Greenhill equation for a straight beam. On the basis of the same installation parameters, Koloshkin (2016) addressed the effect of the friction moment and vessel motion, concluding that this significantly influenced the critical torsion moment. A standard Euler-Bernoulli co-rotated beam elements was successfully applied to address the torsion stability problem. The concept of a critical curvature parameter associated to kink formation was also proposed to address the issue during installation analyses. Then Neto *et al.* (2015) developed a finite element procedure describing self-contact as a result of extreme torsion deformation. Good correlation with test data was obtained.

More focus is, however, needed to address the amount of torque that actually occurs during an installation scenario as this governs the amount of tension (or compression) that can be allowed for a given installation scenario.

For deep-water flexible pipes, bird-caging is a limiting factor in addition to lateral transverse helix buckling and associated global instability. Ebrahimi *et al.* (2016), addressed radial buckling of tensile armour wires numerically by developing a 3D FE model in ABAQUS and used this to study the effect of external/internal pressure and pipe damage. Then, Rabelo *et al.* (2015) investigated the role of local shell buckling in the external polymer layer and established a simple criterion for bird-caging, based on the yield stress of the external polymer layer. The criterion was assessed analytically, numerically and experimentally, and compared well with previous experimental observations. Sævik and Thorsen (2017) proposed a simple analytical model considering the interaction between yield stress, elastic buckling and tape/polymer layer yield failure where good correlation with test data was found.

Collapse of flexible pipes is a complex phenomenon that is influenced by the support from all cross-section members. Normally, the pessimistic approach is taken that the external polymer layer is broken such that the carcass is exposed to the full external pressure. Then the pressure spiral layers will act as an additional support leading to a constrained instability mode. Chen *et al.* (2015) proposed an analytical approach for assessing the collapse strength of an unbonded flexible pipe, taking the pressure armour support into account. The results were compared with FEM and experiments proving the analytical model to give conservative results when the radius/thickness ratio was large. Bai *et al.* (2016), studied confined collapse of an unbonded multi-layer pipe subjected to external pressure including the contact/support effect from surrounding layers. They proposed an analytical model where the support effect was included in terms of springs and applied both FEM and experiments to validate the model.

Wang and Duan (2014a, 2014b, 2015a, 2015b, 2015c) have done comprehensive researchers on the mechanic performance and installation analysis on the steel lazy wave riser (SLWR).

The governing equations which consist of conventional small deformation beam theory for the portion of pipeline lying on the seabed, coupled with a large deformation beam theory for the suspended section are established. The deepwater steel lazy-wave riser configuration with ocean current and internal flow in the process of abandonment, recovery and transfer during installation are researched. These are all based on the static analysis. And in the dynamic analysis, a 2D nonlinear dynamic model for SLWR based on Euler-Bernoulli beam theory with initial conditions and boundary conditions under top excitations considering the effect of ocean current and internal flow are proposed. Keller Box finite difference scheme was adopted to solve the partial differential equations. It is an alternative solution for the SLWR dynamic response besides the FEM.

Kang *et al*. (2017) investigated the sealing design of connector at the end of the flexible jumper pipes. The theoretical relationship between the sealing contact load and the amount of compression was obtained from the contact model among the lenticular gasket ring and hubs on the basis of Hertz contact theory. Taking the requirements for sealing and strength into consideration, a design principle for the lenticular gasket structure is proposed to determine the limits of the amount of compression. Finally, an analytical equation for calculating compression limits is developed. The contact model is verified by utilizing the finite element method.

Drumond *et al*. (2018) presented a literature review on failure events experienced by the industry concerning pipelines, risers, and umbilical cables, describing their causes, consequences, and severity. With regard to floating risers, approximately 85% of them are of flexible type. Although flexible risers may fail in different ways, collapse due to external pressure is reported as the most frequent failure mode. For umbilical cables, the major failure modes are found to occur under tension or compression, torsion, fatigue, wear and sheaving.

Gao and Duan *et al.* (2018) designed a test setup to study the structural deformation and resulting performance degradation of photoelectric composite cable impacted by dropped anchors. The nonlinear dynamic finite element model was developed and verified by the tests.

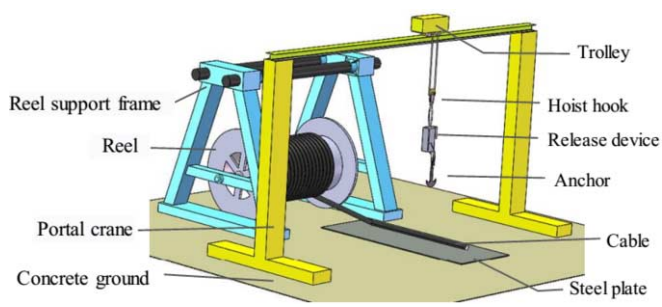

(a) Schematic diagram of test setup

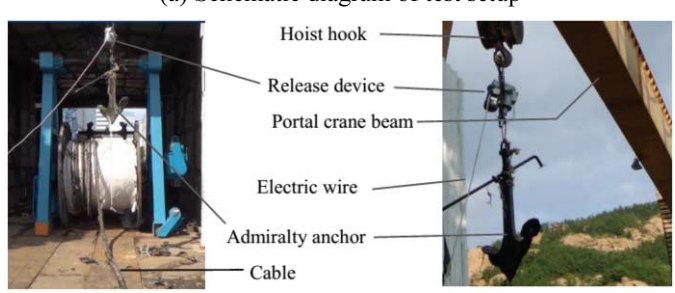

(b) Real photos of test setup

Figure 8.5: Impact test setup (Gao and Duan *et al.*, 2018)

They presented a parametric analysis of different impact directions and impact velocities. The permanent indentation of armor layer increases with falling height, obviously with increase tendency slowing down. From the initial collision contact, the indentation grew with time to its maximum, until the anchor stopped. The anchor began to bounce back under the action of contact reaction force. And the armor layer also partially restored and vibrated with decreasing magnitude, because of energy dissipation by interface friction, leaving some permanent indentation. As falling heights increase, the differences between maximum indentations diminished gradually. And the cable sooner ceased vibrating, especially at higher collision speed.

Zhang et al. (2017a) investigated the sealing design of connector at the end of the flexible jumper pipes. The theoretical relationship between the sealing contact load and the amount of compression was obtained from the contact model among the lenticular gasket ring and hubs on the basis of Hertz contact theory. Taking the requirements for sealing and strength into consideration, a design principle for the lenticular gasket structure is proposed to determine the limits of the amount of compression. Finally, an analytical equation for calculating compression limits is developed. The contact model is verified by utilizing the finite element method.

9. RELIABILITY AND SAFETY IN SUBSEA SYSTEM

9.1 Introduction

The exploration and production of oil and gas resources entail a variety of risks, which, if not adequately managed, have the potential of resulting in a major incident. A recent accident is the Deepwater Horizon drilling rig explosion and oil spill of 2010, which indicate the importance of improving the reliability and safety of the subsea system. This report presents the advances and developing of reliability and safety in subsea system, including the standard, methodology, database and software, which may be referenced by the researchers and engineers related.

9.2 Reliability and Safety Engineering Standards

9.2.1 Standards and Codes for Safety and Reliability of Subsea System

Throughout the 1900s and the early 2000s, there are a number of standards and codes concerning the reliability and safety of subsea system, as presented in Figure 9.1. Along with the development of new technologies and the increase of the occurrence frequency of accidents, particular concerns are raised regarding the reliability and safety of subsea systems achieved by targeted reliability and integrity strategy for large, high risk subsea development projects. These standards and codes aim to provide a common language and approach to the management of safety, reliability and integrity, that subsea projects could accept as recommended practice and guiding documents which would be used to achieve higher levels of safety and reliability performance. In response to these demands, a number of well-known organizations and institutes such as API, DNV and ISO have released a range of standards and codes related to the reliability and safety of subsea system.

The main standards and codes and the timeline are given in Figure 9.1. From the timeline, there are two versions of API RP 17N, three versions of DNV RP A203, and the DNVGL RP 0002 was released in November 2014 after DNV and GL merged into DNVGL. Hence, it is attempted to reflect the advancement of standards and codes through comparison.

9.2.2 Update in the Newer Version of API RP 17N

The first edition of API RP 17N mainly focuses on production reliability and availability and the management of risks to reliable production performance but very little about integrity, and the guidance related to the operation stage was very limited. In consideration of these

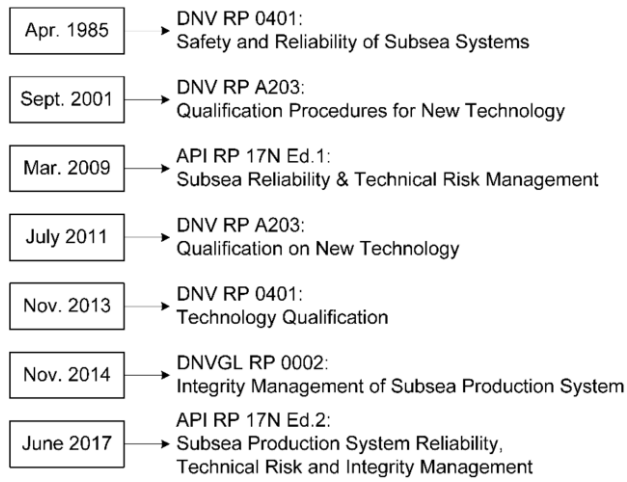

Figure. 9.1: Main standards and codes for subsea system

limitations of the 2009 edition, the updated edition of API RP 17N include the incorporation of integrity management, the inclusion of human factors, the subdivision of life cycle and the extension of the reliability assurance cycle, and these changes make the API RP 17N to has a wider industry implication.

9.3 New progress on reliability and safety evaluation of subsea systems

Several new progresses on reliability and safety evaluation of subsea systems have been reported recently. Various methodologies were developed to analyze and evaluate the reliability and safety of subsea system. The following parts address some cases.

A fatigue reliability analysis of dented pipeline subjected to internal pressure load has conducted by Garbatov (2017). Based on limited experimental data, different failure criteria considering the dent size and applied load are analyzed and reliability as a function of number of load cycles is defined.

Rowland (2014) studied the effects of systematic faults in the development phase of a safety instrumented system, especially the relation between systematic faults and operational common cause failures.

Failure Elimination and Prevention Strategy (FEPS) was designed to prevent failures and improve the reliability of valves and the overall reliability of Wet Christmas tree. Ellen *et al.* (2014) presented and discussed analytical approaches that can be used to quantify the PDF_{avg} of a specific HIPPS implementation, and to study how the various input parameters influence the value of the PFDavg.

Pearse (2014) focused on the financial impacts of subsea equipment failure and how real time data improves subsea equipment availability.

Anietie *et al.* (2014) focused on subsea tree-mounted electro-hydraulic (E-H) SCM responsible for the underwater control of oil and gas production.

Bailey (2014) utilized some of recent extensions of standard Cox formulation to analyze components of ESP systems where multiple competing risks from individual components exist (intra-component correlations, intra-installation correlation and time-dependent explanatory variables). These model extensions utilize a more involved analysis undertaking and demand some careful preliminary data treatment. The work illustrates the concept of time-dependent competing risks with an example of an individual component, a specific motor, from its first

deployment and subsequent re-deployments in different ESP system in a systematic and unbiased manner.

Liu *et al*. (2015) published a monograph related to reliability modeling and evaluation methodologies of subsea blowout preventer systems. For improving the accuracy of reliability evaluation, some important factors and actions, such as common cause failure, imperfect coverage, imperfect repair and preventive maintenance were considered.

Blount (2015) described the optical fiber "health" monitoring program, reviewed case histories, emphasized the importance of this diagnostic information, and monitoring program, review case histories, emphasized the importance of this diagnostic information, and summarizes developments to improve FO system reliability.

Cai *et al.* (2015) proposed a real-time reliability evaluation methodology by combining root cause diagnosis phase based on Bayesian networks and reliability evaluation phase based on dynamic Bayesian networks. The application of the proposed methodology was demonstrated using a case of a subsea pipe ram blowout preventer system. A novel fault diagnosis methodology of non-permanent faults including transient faults and intermittent faults for the control system of subsea blowout preventers were also developed by the same authors (Cai *et al*. 2017), increasing the reliability of subsea system greatly.

Okaro *et al*. (2016) proposed an enhanced Weibull-Corrosion Covariate model for reliability assessment of a system facing operational stresses. The newly developed model was applied to a Subsea Gas Compression System planned for offshore West Africa to predict its reliability index.

Choi *et al*. (2016) proposed the concept of subsea production systems with a seabed storage tank to provide an alternative to conventional floating facilities and performs the reliability, maintainability and availability study for the seabed storage tank. The reliability assessment of the seabed storage tank performs a four-step procedure by using fault tree analysis. The four-step procedure is to define the system boundary, collect the reliability data, construct a fault tree and estimate the reliability. Reliability of the seabed storage tank was estimated with a consideration of critical events.

Low *et al.* (2016) developed a joint probability density function of the variables based on experimental data. A new fast reliability approach is proposed for the VIV fatigue reliability analysis, while Monte Carlo simulations are performed for comparisons. Case studies of a vertical riser in a uniform flow show that the proposed method compares favorably with Monte Carlo in terms of predicting the failure probability as well as safety factors conforming to prescribed reliability levels. Moreover, this study reveals that the randomness of wake coefficients leads to large variability in the riser fatigue damage. The correlation between the coefficients should be properly incorporated as it affects the fatigue reliability of risers experiencing VIV.

Dave (2015) presented an overview of the development and implementation of a Topsides safety and control system to mitigate the risk of a downhole caprock breach in the BC-10 Phase 2 waterflood development.

Cai *et al.* (2016) developed a novel safety integrity levels (SILs) determination methodology based on multiphase dynamic Bayesian networks for safety instrumented systems of subsea systems. Proof test interval phase and proof test phase are modeled separately using dynamic Bayesian networks, and integrated together to form the multiphase dynamic Bayesian networks. The proposed model solves the problems of binary variable constraint and state space explosion of traditional methods, is considered to be important supplements to the calculation methods of international standard IEC61508. The target failure measures, that is, probability of failure on demand, average probability of failure on demand, probability of

failing safely, average probability of failing safely, and SIL of safety instrumented systems operating in a low demand mode, are evaluated using the proposed multiphase dynamic Bayesian networks.

Akyuz (2016) performed a comprehensive human reliability assessment during cargo operations of a mooring unit to enhance maritime safety in off-shore units. The paper prompts a methodological extension of human error assessment and reduction technique by incorporating interval type-2 fuzzy sets which overcome more of the uncertainty of experts' judgement and expression in decision-making. In 2014, United States Department published NTL to authorize the use of the Barrier Concept as the basis for using alternate procedures or equipment in the safety systems for subsea production operations and to clarify the differences between topsides and subsea production operation.

Zhang et al. (2017b) presented the possibilities of success or failure in the installation process of subsea collet connector. Risk matrix method is adopted to analyze the risk of installation failure event of subsea collet connectors. Accurate values of occurrence probabilities and impact levels of risk factors must be provided in traditional risk matrix analysis, while risk factors in the installation process of subsea connector are lack of these data. To solve this problem, the authors introduced expert evaluation and fuzzy theory into risk matrix analysis. And finally, a fuzzy risk matrix analysis method is put forward. Based on the fuzzy risk matrix method, the offshore installation trial of a subsea connector is guided and conducted successfully.

Li *et al*. (2018) proposed a computational framework to calculate the reliability of subsea pipelines subjected to a random earthquake by using subsea simulation, which is an advanced Monte Carlo simulation approach. This framework takes full account of the physical features of pipelines and the earthquake, and also retains high computing precision and efficiency.

10. CONCLUSIONS AND RECOMMENDATIONS

Subsea production system is a relatively new concept developed from difficulties and cost effective strategies in moving to deeper waters for oil and gas. The emerging problems quite different from shallower waters have been challenging the industry to improve both the reliability of the SPS and the service life of all the hardware, and to reduce the CAPEX/OPEX by managing the risk and safety of the system. The technological progresses are characterized by requirements for severe service, multiphase processing, high reliability and low-maintenance solutions. This report reviews the recent advances of the past years in subsea technology area including subsea processing equipment, flow assurance, key components fabrication, qualification testing, installation and operations for emergencies, inspection and maintenance, hydrate exploitation, flowlines and umbilicals, reliability and safety.

The following recommendations are made for future work in the area of innovative technology in the subsea industry.

•It is confirmed that All-Electric Subsea complies with or even exceeds current safety and reliability requirements. CAPEX and OPEX savings have been identified for application of the All-Electric subsea production system while more efforts shall be made to improve the maturity of the AES.

•Efforts are recommended to develop new multiphase compressor system which enables gas compression directly from the well stream without upstream separation, and will be an attractive technology to increase the recovery factor for remote gas field to make gas fields development more profitable.

•New strategies are necessary to simplify the system design, installation and intervention to reduce weight and cost of subsea boosting systems, which is promising for brownfield application.

•Innovative material technologies have cost-efficient potential to be utilized to deal with the flow assurance issues such as remediation of wax deposits or hydrate inhibition in deep-water and long subsea tiebacks.

•Condition and performance monitoring offers critical real-time data to the operator which can avoid unplanned shutdowns saving expenses in lost production and ensuring system integrity. More efforts should be conducted to develop monitoring system to gain feedback on the mechanical fitness, electrical condition and operating performance of subsea rotating machinery such as subsea pumps, boosting and compression systems.

ACKNOWLEDGEMENTS

This report was critically read by Prof. Segen Estefen whose comments and suggestions improved its quality. Prof. Chen An was invited to act as the secretary of the committee, who has been involved in all discussions of committee meetings and proposed the draft of the report. His excellent job of the past three years for the committee is a garrantee of the report.

Prof. Baoping Cai from China University of Petroleum and Prof. Shixiao Fu from Shanghai Jiaotong University made their contributions to the report of their interest. The PhD candidates of Prof. Duan and Prof. Segen are the contributors of the draft report, who are Liu Bingqi, Hong Cheng, Yi Huanggao, Li Fangqiu, Yuan Ye, Zhang Yulong, Zhang Peng, Li Tongtong and Feng Junkai.

The committee is also pleased to acknowledge the strong support of China National Key Research and Development Plan (Grant No. 2016YFC0303700).

Finally, Prof. Duan is greatly grateful to all members of the committee for their active participation in all committee activities and their contributions to this report. Special thanks go to Prof. Yingqiu Chen for his encouragement and support from ISSC China.

REFERENCES

ABS (2017). Guidance Notes on Subsea Hybrid Riser Systems. Houston, USA, 2017.

Akyuz, E. and Celik, E. (2016). A modified human reliability analysis for cargo operation in single point mooring (SPM) off-shore units, Applied Ocean Research, 2016, 58: pp. 11-20.

Anders, S. (2016). Subsea Compression - Designing and Building a Subsea Compressor Station, In Proceeding of the Offshore Technology Conference, Houston, Texas, USA, 2-5 May, 2016. (OTC-27197-MS)

ANSYS CFX 11.0, Computer software. Canonsburg, PA, Ansys.

API RP 1111 (2015). Recommended Practice for the Design, Construction, Operation, and Maintenance of Offshore Hydrocarbon Pipelines (Limit State Design), 5th Edition, Washington, DC.

API RP 17B (2014). Recommended Practice for Flexible Pipe, 5th Edition, Washington, DC.

API RP 17H (2013). Remotely Operated Tools and Interfaces on Subsea Production Systems, 2nd Edition, Washington, DC.

API RP 17N (2017). Recommended Practice Subsea Production System Reliability, Technical Risk and Integrity Management, 2nd Edition, Washington, DC.

API RP 17P (2013). Design and Operation of Subsea Production Systems - Subsea Structures and Manifolds, 1st Edition, Washington, DC.

API RP 17Q (2017). Recommended Practice on Subsea Equipment Qualification, 2nd Edition, Washington, DC.

API RP 17R (2015). Recommended Practice for Flowline Connectors and Jumpers, 1st Edition, Washington, DC.

API RP 17S (2015). Recommended Practice for the Design, Testing, and Operation of Subsea Multiphase Flow Meters, 1st Edition, Washington, DC.
API RP 17U (2015). Recommended Practice for Wet and Dry Thermal Insulation of Subsea Flowlines and Equipment, 1st Edition, Washington, DC.
API RP 17V (2015). Recommended Practice for Analysis, Design, Installation, and Testing of Safety Systems for Subsea Applications, 1st Edition with Errata, Washington, DC.
API RP 17 (2014). Recommended Practice for Subsea Capping Stacks, 1st Edition, Washington, DC.
API RP 17X (2017). Recommended Practice for Subsea Pumps, 1st Edition, Washington, DC.
API RP 17Y (2018). Recommended Practice for Design, Testing & Operations of Subsea Chemical Injection System, 1st Edition, Washington, DC.
API RP 17Z (2018). Bonded Composite Pipe, 1st Edition, Washington, DC.
API RP 2GEO (2014). Geotechnical and Foundation Design Considerations, 1st Edition with Addendum 1 and Errata, Washington, DC.
API RP 2SK (2015). Design and Analysis of Stationkeeping Systems for Floating Structures. 3rd Edition with Addendum 1, Reaffirmed 2015, Washington, DC, 2015.
API RP 2T (2015). Recommended Practice for Planning, Designing and Constructing Tension Leg Platforms. 3rd Edition, Reaffirmed 2015, Washington, DC, 2015.
API RP 17P (2013). Design and Operation of Subsea Production Systems - Subsea Structures and Manifolds. 1st Edition, Washington, DC, 2013.
API SPEC 17D (2015). Design and Operation of Subsea Production Systems—Subsea Wellhead and Tree Equipment, 2nd Edition with Addendum 1 and Errata 7, Washington, DC.
API SPEC 17J (2017). Specification for Unbonded Flexible Pipe, 4th Edition with Errata 1 and Errata 2, Washington, DC.
API SPEC 5L (2015). Specification for Line Pipe, 45th Edition with Errata, Washington, DC.
API SPEC 5LC (2015). CRA line Pipe, 4th Edition with Errata, Washington, DC.
API STD 17F (2014). Standard for Subsea Production Control Systems, 3rd Edition, Washington, DC.
API STD 17O (2014). Standard for Subsea High Integrity Pressure Protection Systems (HIPPS), 2nd Edition, Washington, DC.
API STD 2RD (2013). Dynamic Risers for Floating Production Systems, 2nd Edition, Washington, DC.
API TR 17TR7 (2017). Verification and Validation of Subsea Connectors, 1st Edition, Washington, DC.
Atkins (2015). SAFEBUCK JIP - Safe Design of Pipelines with Lateral Buckling: Design Guideline, Report No. 5087471 / 01 / C.
Aubeny, C. P., White, T. A., Langford, T., Meyer, V., and Clukey, E. C. (2015). Seabed Stiffness Model for Steel Catenary Risers, Proc. International Symposium on Foundations and Offshore Geotechnics (ISFOF), Oslo, Norway. 2015.
Bai, X., Huang, W., Vaz, M. A., Yang, C., and Duan, M. L. (2015). Riser-Soil Interaction Model Effects On The Dynamic Behavior Of A Steel Catenary Riser, Marine Structures, Vol, 41, pp. 53-76, 2015.
Bai, Y., Yuan, S., Cheng, P., Han, P., Ruan, W., and Tang, G. (2016). Confined collapse of unbonded multi-layer pipe subjected to external pressure, Composite Structures, Vol 158, pp 1-10, 15 December, 2016.
Bailey, W. J., Couet, B., and Weir, I. S. (2014). Component Analysis with Competing Risks: How Re-Use of Individual Components of an ESP Impacts Reliability, In Proceeding of the SPE Artificial Lift Conference & Exhibition-North America, Houston, Texas, USA, 6-8 October, 2014. (SPE-171368-MS)
Bibet, P.J., Huet, N., and Âsmul, V. (2016). The World's First Deepwater Multiphase Pumping Application above 100bar ΔP, Technological Risks and Mitigations, In Proceeding of the

Offshore Technology Conference, Houston, Texas, USA, 2-5 May, 2016. (OTC-27236-MS)

Birkeland, B., Bøe, C., and Jensen, R.O. (2016). Gullfaks Subsea Compression – Subsea Commissioning, Start-Up and Operational Experiences. In Proceeding of the Offshore Technology Conference, Houston, Texas, USA, 2-5 May, 2016. (OTC-27159-MS).

Blount, C. G., Friehauf, K. E., Smith, B. E., Smith, D. P., Jaaskelainen, M., and Baldwin, C. S. (2015). Improving Fiber-Optic System Reliability in Permanent Installations, In Proceeding of the SPE Annual Technical Conference and Exhibition, Houston, Texas, USA, 28-30 September, 2015. (SPE-174928-MS)

Borges, F. C. L., Roitman, N., Magluta, C., Castello, D. A., and Franciss, R. (2014). A concept to reduce vibrations in steel catenary risers by the use of viscoelastic materials, Ocean Engineering, Vol 77, pp 1-11, 1 February, 2014,.

Bouamra, R., Vielliard, C., Spilling, K.E., and Nilsen, F.P. (2017). Integrated Production Management Solution for Maximized Flow Assurance and Reservoir Recovery, In Proceeding of the Offshore Technology Conference Brasil, Rio de Janeiro, Brazil, 24-26 October, 2017. (OTC-28042-MS)

Brower, D.V., Brower, A.D., Hedengren, J.D., and Shishiavan, R.A. (2014). A Post-Installed Subsea Monitoring System for Structural and Flow Assurance Evaluation, In Proceeding of the Offshore Technology Conference, Houston, Texas, USA, 5-8 May, 2014. (OTC-25368-MS)

Bruce, K. and Chukar W. (2014). Deepwater Subsea Waterjet Impact on HSE, In Proceeding of the Offshore Technology Conference-Asia, Kuala Lumpur, Malaysia, 25-28 March, 2014. (OTC-24783-MS)

Buch J., Skeie, T., and Eikeland, T. (2015). New Mechanical Pipe Cutting Capabilities on Electric Line - A Compilation of Case Stories from Norway, In Proceeding of SPE Bergen One Day Seminar, Bergen, Norway, 22 April, 2015. (SPE-173833-MS)

Bugge, J.Ø. and Ingebrigtsen, S. (2017). Subsea Power JIP-As Enabler for All-Electric Subsea Production, In Proceeding of the Offshore Technology Conference, Houston, Texas, USA, 1-4 May, 2017. (OTC-27684-MS)

Cai, B., Liu, Y., and Fan, Q. (2016). A multiphase dynamic Bayesian networks methodology for the determination of safety integrity levels. Reliability Engineering & System Safety, vol. 150, pp. 105-115, 2016.

Cai, B., Liu, Y., Ma, Y., Liu, Z., Zhou, Y., and Sun, J. (2015). Real-time reliability evaluation methodology based on dynamic Bayesian networks: A case study of a subsea pipe ram BOP system. ISA Transactions, vol. 58, pp. 595-604, 2015.

Cai, B., Liu, Y., and Xie, M. (2017). A dynamic-Bayesian-network-based fault diagnosis methodology considering transient and intermittent faults. IEEE Transactions on Automation Science and Engineering, 14(1): 276-285, 2017.

Carrejo, N., Espinoza, O.R., Wibowo, H., and Gaudette, S.L., (2015). Developing A New High-Strength, Lightweight Material Using Nano-Coated Smart Materials for Oilfield Applications, In Proceeding of the Offshore Technology Conference Brasil, Rio de Janeiro, Brazil, 27-29 October, 2015. (OTC-26282-MS)

Carvalho, M.H.P. and Rotava, E. (2017). Planning and Execution of Pigging Procedure for Gas Pipeline, In Proceeding of the Offshore Technology Conference Brasil, Rio de Janeiro, Brazil, 24-26 October, 2017. (OTC-28063-MS)

Chaves, V., Sagrilo, L. V. S., and Vignoles, M. A. (2015). Artificial neural networks applied to flexible pipes fatigue calculations, In Proceedings of the 34th international conference on ocean, offshore and arctic engineering, 2015.

Chen, Y. G., Liu, J., Zhu, L. F., Tan, Z. M., and Karabelas, G. (2015). An analytical approach for assessing the collapse strength of an unbonded flexible pipe, Journal of Marine Science and Application, 14(2): 196-201, 2015.

Chen, W. L., Gao, D. L., Yuan, W. Y., Li, H., and Hu, H. (2015). Passive jet control of flow around a circular cylinder, Experiments in Fluids, vol. 56, article 201, 2015.

Cheng, J., Cao, P., Fu, S., Constantinides, Y., 2016. Experimental and Numerical Study of Steel Lazy Wave Riser Response in Extreme Environment. ASME 2016 35th International Conference on Ocean, Offshore and Arctic Engineering, Volume 5, Pipelines, Risers, and Subsea Systems, Busan, South Korea, June 19–24, 2016.

Choi, I. H. and Chang, D. (2016). Reliability and availability assessment of seabed storage tanks using fault tree analysis. Ocean Engineering, vol. 120, pp. 1-14, 2016.

Chris, C. (2016). Subsea Production Optimizationin Field BC-10 Offshore Brazil, Journal of Petroleum Technology, Vol 68, Issue 15. May, 2016. (SPE-0516-0067-JPT)

Christiansen, N. H., Voie, P. E. T., Winther, O., and Høgsberg, J. (2015). Optimization of neural networks for time-domain simulation of mooring lines. In Proceedings of the Institution of Mechanical Engineers, Part M: Journal of Engineering for the Maritime Environment, 1475090215573090, 2015.

Clukey, E.C. and Zakeri, A. (2016). Recent Advances in Nonlinear Soil Models for Fatigue Evaluation of Steel Catenary Risers (SRCs). In Proceeding of the Offshore Technology Conference, Houston, Texas, USA, 2-5 May, 2016. (OTC-27627-MS)

Clukey, E.C., Zakeri, A., and Aubeny, C. et al. (2017). A Perspective on the State of Knowledge Regarding Soil-Pipe Interaction for SCR Fatigue Assessment, In Proceeding of the Offshore Technology Conference, Houston, Texas, USA, 1-4 May, 2017. (OTC-27564-MS)

Crane, R. (2016). Radiographic Inspection of Composite Materials, Reference Module in Materials Science and Materials Engineering. December 2016.

Dahle, M., Meignan, L., Rossi, R. and Ludvigsen, A. (2016). Large Module Installation and Intervention System at Åsgard, In Proceeding of the Offshore Technology Conference, Houston, Texas, USA, 2-5 May, 2016. (OTC-27078-MS).

Dai, H. L., Abdelkefi, A., Wang, L., and Liu, W. B. (2015). Time-delay feedback controller for amplitude reduction in vortex-induced vibrations, Nonlinear Dynamics, vol. 80, no. 1-2, pp. 59-70, 2015.

Daniel, A. and Rune, M. R. (2017). Subsea All Electric, In Proceeding of the Offshore Technology Conference, Houston, Texas, USA, 1-4 May, 2017. (OTC-27896-MS)

Dave, H., and Murat, K. (2015). Water Injection Pressure Protection System (WIPPS) in Deep-Water Development Offshore Brazil, In Proceeding of the Offshore Technology Conference, Houston, Texas, USA, 4-7 May, 2015. (OTC-25815-MS)

Dianita, S. and Gandi, R.S. (2015). Full Field Integrated Modelling Throughout Life-Cycle Phases of Field Development: A Subsea Processing Case Study, In Proceeding of SPE/IATMI Asia Pacific Oil & Gas Conference and Exhibition. Nusa Dua, Bali, Indonesia, 22 October, 2015. (SPE-176232-MS)

Delescen, K., Nicholson, M., Olijnik, L., et al., (2015). BC-10 Subsea Production System Integrated Approach, In Proceeding of the Offshore Technology Conference Brasil, Rio de Janeiro, Brazil, 27-29 October, 2015. (OTC-26131-MS)

DNV, G., 2014. DNV-RP-C205: Enviromental Conditions and Enviromental Loads. Det Norske Veritas AS, Oslo.

Dobson, A. and Deighton, A. (2017). Design Challenges for Power & All Electric Control Umbilicals, In Proceeding of the Offshore Technology Conference, Houston, Texas, USA, 1-4 May, 2017. (OTC-27670-MS).

Drumond, G. P. , Pasqualino, I. P. , Pinheiro B. S. and Stefen, S. F. (2018), Pipelines, Risers and Umbilicals Failures: A Literature Review, Ocean Engineering, Vol. 148(2018) 412-425

Ebrahimi, A., Kenny, S., and Hussein, A. (2016). Radial Buckling of Tensile Armour Wires in Subsea Flexible Pipe—Numerical Assessment of Key Factors, Journal of Offshore Mechanics and Arctic Engineering, 138(3): 031701-031701-031708, 2016.

Efemena, I. and Mobolaji, A. (2014). Developing a Robust Emergency Pipeline Repair System in Nigeria, In Proceeding of the SPE Nigeria Annual International Conference and Exhibition, Lagos, Nigeria, 5-7 August, 2014. (SPE-172394-MS)

Ellen, M. S. (2014). Reliability Assessment of a Subsea Hipps, Norwegian University of Science and Technology, 2014.

Estefen, S.F., Lourenço, M.I., Feng, J., MouraPaz, C., and Lima Jr., D.B. (2016). Sandwich pipe for long distance pipelines: Flow assurance and cost, In Proceeding of the International Conference on Ocean, Offshore and Arctic Engineering. Busan, South Korea, 19–24 June, 2016. (OMAE2016-54950).

Flynn, S. A. (2016). Applying the Learning from the Gulf of Mexico Response to Enhance Emergency and Oil Spill Preparedness, In Proceeding of the International Petroleum Technology Conference, Bangkok, Thailand, 14-16 November, 2016. (IPTC-18681-MS)

Gao, Y. and Cheung, S.H. (2015). Long-term fatigue analysis of risers with multiple environmental random variables in time domain, In Proceedings of the 25th International ocean and polar engineering conference, pp. 228-233, 2015.

Gao, Y. and Low, Y. M. (2016). An efficient importance sampling method for long-term fatigue assessment of deepwater risers with time domain analysis, Probabilistic Engineering Mechanics, vol. 45, pp. 102-114, 2016.

Garbatov, Y. and Soares, C. G. (2017). Fatigue reliability of dented pipeline based on limited experimental data. International Journal of Pressure Vessels & Piping, 155, 2017.

Gay Neto, A., Pimenta, P. M. and Wriggers, P. (2015). Self-contact modeling on beams experiencing loop formation, Computational Mechanics, 55(1): 193-208, 2015.

Geovana, P. D., Ilson, P. P., Bianca, C. P., and Segen, F. E. (2018). Pipelines, risers and umbilicals failures: A literature review, Ocean Engineering, Vol. 148, pp: 412-425, 2018.

Gharaibah, E., Antel, B., Sreenivasulu, K., and Barri, M. (2016). Thermal and Cooldown Modelling of Subsea Components and Validation, In Proceedings of Offshore Technology Conference. Kuala Lumpur, Malaysia. 22-25 March, 2016. (OTC-26846-MS)

Giraldo, J. S. M., Sagrilo, L. V. S., and Dantas, C. M.S. (2015). Efficient probabilistic fatigue analysis of a riser suspended and moored by chains, In Proceedings of the 34th international conference on ocean, offshore and arctic engineering, 2015.

Giraldo, J. S. M., Dantas, C. M. S and Sagrilo, J. V.S. (2016). Probabilistic fatigue analysis of marine structures using the univariate dimension-reduction method, Marine Structures, vol. 50, pp. 189-204, 2016.

Giuliana, I., Maurizio, M., Luca, C., Michele, M., Juan, M. D., and Melania, B. (2016). Advanced Oil Spill Modelling in the Offshore Oil & Gas Industry: Improving the Emergency Response Management along the Project Life-Cycle, In Proceeding of the SPE International Conference and Exhibition on Health, Safety, Security, Environment, and Social Responsibility, Stavanger, Norway, 11-13 April, 2016. (SPE-179365-MS)

Gu, Y., Ju, P., Qin, J., Wang, C., and Wei, H. (2014). Challenge and Solution of PanYu35-2 Subsea Manifold Design Fabrication and Testing, In Proceeding of the International Ocean and Polar Engineering Conference, Busan, Korea. 15-20 June, 2014. (ISOPE-I-14-146)

Han, D., Wang, Z., Song, Y., Zhao, J., and Wang, D. (2017). Numerical analysis of depressurization production of natural gas hydrate from different lithology oceanic reservoirs with isotropic and anisotropic permeability, Journal of Natural Gas Science & Engineering. Volume 46, pp 575-591, October 2017.

Hasan, Z., Kapetanic, N., Vaughan, J. and Robinson, G.M. (2015). Subsea Field Development Optimization Using All Electric Controls as an Alternative to Conventional Electro-Hydraulic, In Proceeding of the Asia Pacific Oil & Gas Conference, Nusa Dua, Bali, Indonesia, 20-22 October, 2015. (SPE-176403-MS).

Hawlader, B., Dutta, S., Fouzder, A., and Zakeri, A. (2015). Penetration of Steel Catenary Riser in Soft Clay Seabed - Finite Element and Finite Volume Methods. ASCE Journal of International Journal of Geomechanics, Vol. 15, 2015.

Hjelmeland, M. and Torkildsen, B.H. (2016a). The Deployment of the World´s First Subsea Multiphase Compression System – Enabling Increased Recovery. In Proceeding of the Offshore Technology Conference, Kuala Lumpur, Malaysia, 22-25 March, 2016. (OTC-26815-MS).

Hjelmeland, M. and Torkildsen, B.H. (2016b). Qualification and Implementation of a Subsea Wet Gas Compressor Solution. In Proceeding of the Offshore Technology Conference, Houston, Texas, USA, 2-5 May, 2016. (OTC-27224-MS).

Hjelmeland, M., Reimers, O., Hey, C., and Broussard, D. (2017). Qualification and Development of the World's First High Pressure Subsea Boosting System for the Jack and St. Malo Field Development, In Proceeding of the Offshore Technology Conference, Houston, Texas, USA, 1-4 May, 2017. (OTC-27800-MS).

Homstvedt, G., Pessoa, R., Portman, L., Wang, S., Gonzalez, J., Maldaner, M., and Margulis, J. (2015). Step-Change Seabed ESP Boosting, In Proceeding of the Offshore Technology Conference, Houston, Texas, USA, 27-29 October, 2015. (OTC-26141-MS).

Jain, A.K., Sharma, K., Negi, D.S., Sarkar, A., and Tewari, D.C. (2015). Flow assurance study in deep waters- a case study from Eastern offshore field, India, In Proceeding of the SPE Oil & Gas India Conference and Exhibition, Mumbai, India, 24-26 November, 2015. (SPE-178118-MS)

Jan, O. B., Mike, A., and Neil, W. (2015). Welding Robot Repairing Subsea Pipelines, In Proceeding of the Offshore Technology Conference, Houston, Texas, USA, 4-7 May, 2015. (OTC-25969-MS)

Janoff, D., Venkateswaran, S.P., and McNicol, D. (2014). Non-Destructive Evaluation of Subsea Thermal Insulation Using Microwave Imaging, In Proceeding of NACE International, San Antonio, Texas, USA, 9-13 March,2014. (NACE-2014-3823)

Jean-Claude, B., Michael, R., and Michael, B. (2014). Subsea Emergency Response System (SERS): Optimised Response for Subsea Production Well Incidents in the Gulf of Guinea, In Proceeding of the International Petroleum Technology Conference, Kuala Lumpur, Malaysia, 10-12 December, 2014. (IPTC-18222-MS)

Kamsu-Foguem B. (2016). Information structuring and risk-based inspection for the marine oil pipelines, Applied Ocean Research, Volume 56, pp. 132-142, March 2016.

Karampour, H. and Albermani, F. (2014). Experimental and numerical investigations of buckle interaction in subsea pipelines, Engineering Structures, Vol. 66, pp. 81-88, 2014.

Kato, N., Choyekh, M., Dewantara, R., et al. (2017). An autonomous underwater robot for tracking and monitoring of subsea plumes after oil spills and gas leaks from seafloor, Journal of Loss Prevention in the Process Industries, Vol 50, Part B, pp. 386-396, November 2017.

Khlebnikov, V., Antonov, S., Mishin, A., et al., (2016). A new method for the replacement of CH4 with CO2 in natural gas hydrate production, Natural Gas Industry B, Vol 3, Issue 5, pp 445-451, November 2016.

Koloshkin, E. (2016). Torsion Bucklking of Dynamic Flexible Risers, Norwegian University of Scence and Technology, 2016.

Kondapi, P.B., Chin, D., Srivastava, A., and Yang, Z.F. (2017). How Will Subsea Processing and Pumping Technologies Enable Future Deepwater Field Developments?, In Proceeding of the Offshore Technology Conference, Houston, Texas, USA, 1-4 May, 2017. (OTC-27661-MS)

Konno, Y., Masuda, Y., Akamine, K., Naiki, M. and Nagao, J. (2016). Sustainable gas production from methane hydrate reservoirs by the cyclic depressurization method, Energy Conversion & Management, Vol 108, pp 439-445, 15 January, 2016.

Lee, W., Shin, J.Y., Kim, K.S. and Kang, S.P. (2016). Synergetic Effect of Ionic Liquids on the Kinetic Inhibition Performance of Poly (N-vinylcaprolactam) for Natural Gas Hydrate Formation, Energy & Fuels, 30(11), October 2016.

Li, Y., Zhang, Y., and Kennedy, D. (2018). Reliability analysis of subsea pipelines under spatially varying ground motions by using subset simulation. Reliability Engineering & System Safety, vol. 172, pp. 74-83, 2018.

Liang, W., Zhu, L., Li, W., Yang, X., Xu, C., and Liu, H., (2015). Bioinspired Composite Coating with Extreme Underwater Superoleophobicity and Good Stability for Wax Prevention in the Petroleum Industry. Langmuir, Vol. 31, pp. 11058–11066, 2015.

Liu, H., Khan, F., and Thodi, P. (2017). Revised burst model for pipeline integrity assessment. Engineering Failure Analysis, Volume 80, pp. 24-38, October 2017.

Liu, R., Xiong, H., Wu, X. L., and Yan, S. W. (2014). Numerical studies on global buckling of subsea pipeline, Ocean Engineering, Vol. 78, pp 62-72, 2014.

Liu, R., Liu, W. B., WU X. L., and Yan, S. W. (2014). Global lateral buckling analysis of idealized subsea pipelines, Journal of Central South University, Vol 21, pp 416-427, 2014.

Liu, Y., Cai, B., Ji, R., Liu, Z., Zhang, Y. (2015) Reliability modeling and evaluation of subsea blowout preventer system. Beijing: Science Press, ISBN 978-7-03-044005-1.

Lockheed Martin Homepage. <http://www.lockheedmartin.com/us.html> (last accessed 13.10.2017).

Louvet, E., Giraudbit, S., Seguin, B., and Sathananthan, R. (2016). Active Heated Pipe Technologies for Field Development Optimisation, In Proceeding of the Offshore Technology Conference Asia, Kuala Lumpur, Malaysia, 22-25 March, 2016. (OTC-26578-MS)

Low, Y. M. and Narakorn S. (2016). VIV fatigue reliability analysis of marine risers with uncertainties in the wake oscillator model, Engineering Structures, Vol 106, pp 96-108, 2016.

Low, Y. M. (2016). A variance reduction technique for long-term fatigue analysis of offshore structures using Monte Carlo simulation, Engineering Structures. vol. 128, pp. 283–295, 2016.

Mackenzie, H. and Jones, C. (2015). Cost Reducing Pipeline Decommissioning Technology, In Proceeding of the SPE Offshore Europe Conference and Exhibition, Aberdeen, Scotland, UK, 8-11 September, 2015. (SPE-175487-MS)

Margarida, A., Pimental, J., Thibaut, E. and Cardoso, E. (2017). High Voltage Subsea Pump - A Low Cost Subsea Boosting Enabler. In Proceeding of the Offshore Technology Conference, Houston, Texas, USA, 1-4 May, 2017. (OTC-27929-MS).

Mcdermott, P., Sathananthan, R. (2014). Active Heating for Life of Field Flow Assurance, In Proceeding of the Offshore Technology Conference, Houston, Texas, USA, 5-8 May, 2014. (OTC-25107-MS)

Molnar, C. and Riley, M. (2016). Flow Assurance and Hydrate Prevention Methods Enabled by Medium Voltage Electric Heating Technology, In Proceeding of the Offshore Technology Conference Asia, Kuala Lumpur, Malaysia, 22-25 March, 2016. (OTC-26389-MS)

Morgan, J.E.P. and Zakarian, E. (2015). Development of a Quantitative Approach to Risk Based Flow Assurance, In Proceeding of the Offshore Technology Conference, Houston, Texas, USA, 4-7 May, 2015. (OTC-25786-MS)

Mohamed, N. A., Tariq, M., Atilhan, M., Khraisheh, M., Rooney, D., and Garcia, G., et al. (2017). Investigation of the Performance of Biocompatible Gas Hydrate Inhibitors via Combined Experimental and DFT Methods. The Journal of Chemical Thermodynamics, 111, March 2017.

Neto, A. G., Martins, C., Vis, A., and Pimenta, P. M. (2014). Static analysis of offshore risers with a geometrically-exact 3D beam model subjected to unilateral contact, Computational Mechanics 53(1): 125-145, 2014.

Norsok M-001 (2014). Materials Selection, 2014.

Okaro, I. A. and Tao, L. (2016). Reliability analysis and optimisation of subsea compression system facing operational covariate stresses. Reliability Engineering & System Safety, vol. 156, pp. 159-174, 2016.

Olayemi, S., Cano, M., Sanchez, S., Shea, C.O., Letendre, F., Solc, P., Verney, M., Maru, M. (2014). Hydrocarbon Flow Assurance : Low Rate and Pressure Gas Field Case study asset description, In Proceeding of the SPE Latin American and Caribbean Petroleum Engineering Conference. Maracaibo, Venezuela, 21-23 May, 2014. (SPE-169240-MS)

Ole, Ø. and Rune, M. R. (2015). Subsea Factory–Standardization of the Brownfield Factory, In Proceeding of the Offshore Technology Conference, Houston, Texas, USA, 04-07 May, 2015. (OTC-25903-MS)

Osokogwu, U., Emuchay, D., Ottah, D.G., Aliu, S. and Ajienka, J.A. (2014). Improved Method of Predicting and Monitoring Flow Assurance Problems in the Niger Delta Using PROSYS, In Proceeding of the SPE Nigeria Annual International Conference and Exhibition. Lagos, Nigeri, 5-7 August, 2014. (SPE-172443-MS)

Parsazadeh, M. and Duan, X., (2015). Thermal insulation with latent energy storage for flow assurance in subsea pipelines, In Proceeding of the International Conference on Ocean, Offshore and Arctic Engineering. St. John's, Newfoundland and Labrador, Canada, 31 May - 05 June, 2015. (OMAE-2015-41285)

Per A. N. (2015). Subsea Technology Enabling Cost Effective Developments – Subsea History and Perspective of the Subsea Future, In Proceeding of the SPE Annual Caspian Technical Conference & Exhibition, Baku, Azerbaijan, 4-6 November, 2015. (SPE-177365-MS)

Pearse, J. A., and Botto, A. (2014). Optimizing Response Strategies to Improve Subsea Equipment Availability, In Proceeding of the Offshore Technology Conference, Houston, Texas, USA, 5-8 May, 2014. (OTC-25199-MS)

Prescott, N., Mantha, A., Kundu, T. and Swenson, J. (2016). Subsea Separation - Advanced Subsea Processing with Linear Pipe Separators, In Proceeding of the Offshore Technology Conference, Houston, Texas, USA, 2-5 May, 2016. (OTC-27136-MS).

Quadrante, L. A. R. and Nishi, Y. (2014). Amplification/suppression of flow-induced motions of an elastically mounted circular cylinder by attaching tripping wires, Journal of Fluids and Structures, Vol. 48, pp. 93-102, 2014.

Rabelo, M. A., Pesce, C. P., Santos, C. C. P., Ramos J, R., Franzini, G. R. and Gay Neto, A. (2015). An investigation on flexible pipes birdcaging triggering, Marine Structures 40: 159-182, 2015.

Radicioni A. and Fontolan M. (2016). Open Source Architectures Development for Subsea Factory, In Proceeding of the Offshore Technology Conference Asia, Kuala Lumpur, Malaysia, 22-25 March, 2016. (OTC-26628-MS)

Rismanchian, A. (2015). Pipe-Soil Interaction During Lateral Buckling of Marine Pipelines, The University of Western Australia, 2015.

Rowland M. (2014). Using reliability growth testing to reveal systematic faults in safety-instrumented systems, Norwegian University of Science and Technology, 2014.

Rubio A., Zeid H A., and Meyer J.H. (2017). Benefits of Using an Electric Choke for Subsea Applications, In Proceeding of the Offshore Technology Conference Brasil, Rio de Janeiro, Brazil, 24-26 October, 2017. (OTC-28138-MS)

Ruiz, A.J.C., Plazas, J.J.I., Ramirez, E.A.L. (2014). New Technology for Flow Assurance in an Extra Heavy Oil Field : Case Study in the Akacias Field, In Proceeding of the SPE Heavy and Extra Heavy Oil Conference - Latin America. Medellin, Colombia, 24-26 September, 2014. (SPE-171080-MS)

Salma, B. and K. Øien. (2014). Accidents and Emergency Response in the Arctic Sea, In Proceeding of the Offshore Technology Conference Arctic Technology Conference, Houston, Texas, USA, 10-12 February, 2014. (OTC-24609-MS)

Sarra, A. Di, Viadana, G., Scaramellini, S., Bianco, A., Masi, S. (2014). A Real Case of Integrated Multiphase Gathering System Optimization through a Flow Assurance

Workflow, In Proceeding of the International Petroleum Technology Conference. Kuala Lumpur, Malaysia, 10-12 December, 2014. (IPTC-17968-MS)

Schwerdtfeger, T., Scott, B., and Akker, J.V.D. (2017). World-First All-Electric Subsea Well, In Proceeding of the Offshore Technology Conference, Houston, Texas, USA, 1-4 May, 2017. (OTC-27701-MS).

Shirazian, S. and Ashrafizadeh, S.N., (2015). Synthesis of substrate-modified LTA zeolite membranes for dehydration of natural gas. Fuel, Vol. 148, pp. 112–119, 2015.

Shiri, H. (2014). Influence of Seabed Trench Formation on Fatigue Performance of Steel Catenary Risers in Touchdown Zone, Marine Structures, Vol. 36, pp. 1-20, 2014.

Shukla A. and Karki H. (2016). Application of robotics in offshore oil and gas industry- A review Part II. Robotics and Autonomous Systems, Vol 75, Part B, pp. 508-524, January 2016.

Shur, M. L., Strelets, M. K., Travin, A. K. and Spalart, P. R. (2015). Evaluation of vortex generators for separation control in a transcritical cylinder flow, AIAA Journal, vol. 53, no. 10, pp. 2967-2977, 2015.

Sleight, N. C. and Oliveira, N. (2015). BC-10-Optimizing Subsea Production, In Proceeding of the Offshore Technology Conference Brasil, Rio de Janeiro, Brazil, 27-29 October, 2015. (OTC-26220-MS)

Song X., Du J., Wang S., Li. H., and Chang A. (2016). An innovative block partition and equivalence method of the wave scatter diagram for offshore structural fatigue assessment, Applied Ocean Research, vol. 60, pp. 12-28, 2016.

Storstenvik, A. (2016). Subsea Compression – Designing and Building a Subsea Compressor Station, In Proceeding of the Offshore Technology Conference, Houston, Texas, USA, 2-5 May, 2016. (OTC-27197-MS)

Sun, C., Mao, D., Zhao, T., Shang, X., and Wang, Y., et al. (2015). Investigate Deepwater Pipeline Oil Spill Emergency Repair Methods, Aquatic Procedia, Volume 3, pp. 191-196, March 2015.

Sævik, S. and Thorsen, M. J. (2017). An Analytical Treatment of Buckling and Instability of Tensile Armours in Flexible Pipes, Journal of Offshore Mechanics and Arctic Engineering 139(4), March 2017.

Sævik, S. (2014). Differential equation for evaluating transverse buckling behaviour of tensile armour wires, In Proceeding of the 33rd International Conference on Ocean, Offshore and Arctic Engineering. San Francisco, USA, 8-13 June, 2014.

Tamal, D., Christoph, J. B., and Johannes, J. (2017). A model for subsea oil-water gravity separator to estimate unmeasured disturbances, Computer Aided Chemical Engineering, Vol.40, pp.1489-1494, 2017.

Thomas, S. and Bruce, S., (2017). World-First All-Electric Subsea Well, In Proceeding of the Offshore Technology Conference, Houston, Texas, USA, 1-4 May, 2017. (OTC-27701-MS)

Thomas, S., Bruce, S., and Joseph, C. (2016). World First All Electric Subsea Well, In Proceeding of the SPE Offshore Europe Conference & Exhibition, Aberdeen, United Kingdom, 5-8 September, 2016. (SPE-186150-MS)

Time, N.P. and Torpe, H. (2016). Subsea Compression – Åsgard Subsea Commissioning, Start-Up and Operational Experiences, In Proceeding of the Offshore Technology Conference, Houston, Texas, USA, 2-5 May, 2016. (OTC-27163-MS).

Twerda, A. and Omrani, P.S. (2015). Parametric Analysis and Uncertainty Quantification for Flow Assurance, In Proceeding of the International Petroleum Technology Conference. Doha, Qatar. 6-9 December, 2015. (IPTC-18376-MS)

Tzotzi, C., Parenteau, T., Kaye, D., Turner, D.J., Bass, R., Morgan, J.E.P., Zakarian, E., Rolland, J., and Decrin, M. K. (2016). Safe Hydrate Plug Dissociation in Active Heating Flowlines and Risers - Full Scale Test, In Proceeding of the Offshore Technology Conference, Houston, Texas, USA, 2-5 May, 2016. (OTC-27051-MS)

Vershinin, V., Fedorov, K., and Gankin, Y., (2017). Control Methods of Propellant Fracturing for Production Stimulation, In Proceeding of SPE Russian Petroleum Technology Conference. Moscow, Russia, 16-18 October, 2017. (SPE-187691-MS)

Villa, V., Paltrinieri, N., Khan, F., and Cozzani, V. (2016). Towards dynamic risk analysis: A review of the risk assessment approach and its limitations in the chemical process industry, Safety Science, Vol 89, pp. 77-93, November 2016.

Wan, Y., Liu, R., Wang, W., Du, X., Qu, Z., Liu, C., and Qian, X. (2017). Study on Pigging Solution of Subsea Wet-Gas Pipeline, In Proceeding of the 27th International Ocean and Polar Engineering Conference, San Francisco, California, USA, 25-30 June, 2017. (ISOPE-I-17-428)

Wang, J., Duan, M., He, T., and Cao, J. (2014). Numerical solutions for nonlinear large deformation behaviour of deepwater steel lazy-wave riser, Ships and Offshore Structures, Vol 9, Number 6, pp.655-668, 2 November 2014.

Wang, J. and Duan, M. (2015). A nonlinear model for deepwater steel lazy-wave riser configuration with ocean current and internal flow, Ocean Engineer. Vol 94, pp. 155-162, 15 January 2015.

Wang, J., Duan, M., and Luo, J. (2015). Mathematical model of steel lazy-wave riser abandonment and recovery in deepwater, Marine Structures. Volume 41, pp. 127-153, April 2015.

Wang, J., Duan, M., Wang, Y., Li, X., and Luo, J. (2015). A nonlinear mechanical model for deepwater steel lazy-wave riser transfer process during installation, Applied Ocean Research. Vol 50, pp. 217-226, March 2015.

Wang, J., Duan, M., and He, R. (2017). A nonlinear dynamic model for 2D deepwater steel lazy-wave riser subjected to top–end imposed excitations, Ships and Offshore Structures, Vol 13, Issue 4, pp.1-13, October 2017.

Wang, J., Fu, S., Baarholm, R., Wu, J., Larsen, C.M., 2014. Fatigue damage of a steel catenary riser from vortex-induced vibration caused by vessel motions. Marine Structures 39, 131-156.

Wang, J., Fu, S., Baarholm, R., Wu, J., Larsen, C.M., 2015. Out-of-plane vortex-induced vibration of a steel catenary riser caused by vessel motions. Ocean Engineering 109, 389-400.

Wang, J., Fu, S., Wang, J., Li, H., Ong, M.C., 2017. Experimental Investigation on Vortex-Induced Vibration of a Free-Hanging Riser Under Vessel Motion and Uniform Current. Journal of Offshore Mechanics and Arctic Engineering 139(4), 041703.

Wang, J., Xiang, S., Fu, S., Cao, P., Yang, J., He, J., 2016. Experimental investigation on the dynamic responses of a free-hanging water intake riser under vessel motion. Marine Structures 50, 1-19.

Wang, K. and Low, Y.M. (2016). Study of Seabed Trench Induced by Steel Catenary Riser and Seabed Interaction, In Proceeding of the 35th International Conference on Ocean, Offshore and Arctic Engineering, Busan, South Korea, 19-24 June, 2016. (OMAE2016-54236,)

Wang, X., Sun, Y., Wang, Y., et al., (2017). Gas production from hydrates by CH_4-CO_2/H_2 replacement, Applied Energy, Vol 188, pp 305-314, 15 February, 2017.

Wang, Y., Zhang, X., Zhao, Y., Chen, H., Duan, M., and Estefen, S. F. (2017). Perturbation analysis for upheaval buckling of imperfect buried pipelines based on nonlinear pipe-soil interaction, Ocean Engineering, Vol 132, pp. 92-100, 1 March, 2017.

Wang, Z., Zhi, H. C., Liu, H. B. and Bu, Y. D. (2015). Static and Dynamic analysis on upheaval buckling of unburied subsea pipelines, Ocean Engineering, Vol. 104, pp 249-256, 2015.

Walker, V., Zeng, H., Ohno, H., et al., (2015). Antifreeze proteins as gas hydrate inhibitors, Canadian Journal of Chemistry 93(8):150203143345006, February 2015.

White, D. J., Clukey, E. C., Randolph, M. F., Boylan, N. P., Bransby, M. F., Zakeri A., Hill, A. J. and Jaeck, C. (2017). The State of Knowledge of Pipe-Soil Interaction for On-Bottom

Pipeline Design, In Proceeding of the Offshore Technology Conference, Houston, Texas, USA, 1-4 May, 2017. (OTC-27623-MS)

White, D. J., Randolph, M. F., Gaudin, C., Boylan, N. P., Wang, D., Boukpeti, N., Zhu, H., and Sahdi, F. (2016). The Impact of Submarine Slides on Pipelines: Outcomes from the COFS-MERIWA JIP, In Proceeding of the Offshore Technology Conference, Houston, Texas, USA, 2-5 May, 2016. (OTC-27034-MS)

Wilfred, O. and Appah, D., (2015). Analyzing Thermal Insulation for Effective Hydrate Prevention in Conceptual Subsea Pipeline Design. International Journal of Current Engineering and Technology, Vol. 5, pp. 2492–2499, 2015.

Wilson, A. (2016). Flow-Assurance Methods Enabled by Medium-Voltage Heating Technology, Journal of Petroleum Technology, Vol 68, Issue 11. November, 2016. (SPE-1116-0080-JPT)

Winther-Larssen, E., Massle, D. and Eriksson, K.G. (2016). Subsea All Electric Technology: Enabling Next Generation Field Developments, In Proceeding of the Offshore Technology Conference, Houston, Texas, USA, 2-5 May, 2016. (OTC-27243-MS)

Yuan, F., White, D. W., and O'Loughlin, S. D. (2017). The evolution of Seabed Stiffness During Cyclic Movement in a Riser Touchdown Zone on Soft Clay, Géotechnique, Vol. 67, pp. 127-137, 2017.

Yu, M., Li, W., Yang, M., et al., (2017). Numerical Studies of Methane Gas Production from Hydrate Decomposition by Depressurization in Porous Media. Energy Procedia, Volume 105, Pages 250-255, May 2017.

Zakeri, A., Clukey, E., Kebadze, B., Jeanjean, P., Piercey, G., Templeton, J., Connelly, L., and Aubeny, C. (2015). Recent Advances in Soil Response Modelling for Well Conductor Fatigue Analysis and Development of New Approaches, In Proceeding of the Offshore Technology Conference, Houston, Texas, USA, 4-7 May, 2015. (OTC-25795-MS)

Zeng X. and Duan M. (2014). Mode localization in lateral buckling of partially embedded submarine pipelines, International Journal of Solids and Structures. Vol. 51, pp. 1991-1999, 2014.

Zeng X., Duan M., and Che X. (2014). Critical upheaval buckling forces of imperfect pipelines, Applied Ocean Research. Vol. 45, pp. 33-39, 2014.

Zhang, H., Company, R.S., Li, J., and Khor, S.H. (2014). Integrated Management Strategy of Flow Assurance for Digital Field, In Proceeding of the SPE Annual Technical Conference and Exhibition. Amsterdam, The Netherlands, 27-29 October, 2014. (SPE-170968-MS)

Zhang, K., Huang, H., Duan, M., Hong, Y., Segen, F. E., (2017a). Theoretical investigation of the compression limits of sealing structures in complex load transferring between subsea connector components, Journal of Natural Gas Science and Engineering. Vol. 44, pp. 147-159, 2017.

Zhang, K., Duan, M., Luo, X., Hou, G., (2017b) A Fuzzy Risk Matrix Method and its Application to the Installation operation of the Subsea Collet Connector, Journal of Loss Prevention in the Process Industries. Vol. 45, pp. 147-159, 2017.

Zhang, X. and Duan, M. (2015). Prediction of the upheaval buckling critical force for imperfect submarine pipelines, Ocean Engineering. Vol 109, pp. 330-343, 15 November 2015.

Zhang, X., An, C., Duan, M., and Guedes Soares, C. (2017). Lateral buckling and post-buckling response based on a modified nonlinear pipe-soil interaction model, In Proceedings of the 6th International Conference On Marine Structures (Marstruct 2017), April 2017.

Zhao, J., Wang, J., Liu, W., and Song, Y., (2015). Analysis of heat transfer effects on gas production from methane hydrate by thermal stimulation, International Journal of Heat & Mass Transfer, Volume 87, Pages 145-150, August 2015.

Zhao, J., Zhu, Z., Song, Y., et al., (2015). Analyzing the process of gas production for natural gas hydrate using depressurization, Applied Energy, Volume 142, Pages 125-134, 15 March 2015.

Zhao T. and Duan M. (2017). Upheaval buckling of in-service cased insulated flowline, Ships & Offshore Structures, vol.12(5), pp.706-714, 2017.

Zhao T. and Feng X. (2015). Upheaval buckling solution for submarine pipelines by segmented ditching and hot water flushing, Ocean Engineering, vol.102, pp.129–135, 2015.

Zhou, C., Ye, N. and Sævik, S. (2014). Effect of Anti-Wear Tape on Behavior of Flexible Risers, In Proceeding of the 33rd International Conference on Ocean, Offshore and Arctic Engineering, San Francisco, California, USA, 8–13 June, 2014.

This page intentionally left blank

Subject Index

3D Structural Printing 279
abnormal environmental event 1
accidental situations limit states 1
acoustic emission 391
adhesive 143
approval 143
arctic 143
Arctic Sea transportation 347
Arctic Ships 347
autonomous vessel 279
benchmark on grounding simulation 1
big-data 73
collision 1
composites 143
correlation 73
corrosion 391
crack detection 391
deepwater installation 461
design 193
digital twin 391
distortions 143
emergency response service 1
experimentation 73
explosion fires 1
fabrication 461
fatigue 143, 391
fatigue life 391
field measurement 193
floating wind turbine 193
flow assurance 461
free-fall lifeboat 279
full-scale test 73
grounding 1
heavy lift ship 279
helideck design 279
high frequency mechanical impact (HFMI) 143
HSC Rules 279
hybrid testing method 193
hydrates 461
ice mechanics 347
iceberg 347
icebreaker 279
IMO 347
inspection 461
integrated dynamic analysis 193
laboratory testing 73
lightweight 143
limit states design 347
maintenance and decommissioning 461
marine operations 193
mission-based design 347
model test 193
moonpools 279
motor yachts 279
naval craft 279
naval standards 279
North West Passage 347
Northern Sea Route 347
ocean current turbine 193
offshore operation vessels 279
offshore wind turbine 193
pipelines 461
Polar Class 347
Polar Ship 279
Polaris 347
probabilistic design 347
qualification 143
reliability and safety 461
residual stress 143
risers and umbilicals 461
sailing yachts 279
sea ice 347
sensors 73
service life 391
ship structures 391
similarity laws 73
small and large scale 73
special craft 279
special hull structures 279
steels 143
structural damage detection 391
structural health monitoring 391
structural inspection 391
structural life-cycle assessment 391

structural life-cycle management 391
structural longevity 391
structural maintenance 391
structural repair 391
structural sensing 391
structural testing 73
structures 279
subsea operations 461
subsea processing 461
subsea production system 461
SWATH 279
testing for qualification 461
tidal turbine 193
total cost of ownership 279
wave energy converter 193
wave-piercing catamaran 279
welding 143
yachts 279

Author Index

Adam, F. 193
Aksu, S. 391
Amila, N. 391
Andersen, M.R. 391
Begovic, E. 279
Bingham, H.B. 193
Blake, J. 391
Boote, D. 391
Brennan, F. 73
Brubak, L. 1
Caridis, P. 391
Catipovic, I. 193
Chai, S. 461
Chen, N. 391
Colicchio, G. 193
Czaban, Z. 279
de Carvalho Pinheiro, B. 143
Dessi, D. 73
Duan, M. 461
Egorov, A. 391
Ehlers, S. 347
Fang, C. 193
Feng, G. 391
Fukui, T. 347
Gaiotti, M. 143
Gao, Z. 193
Hess, P. 391
Holtmann, M. 279
Hoogeland, M. 73
Horn, A.M. 143
Hu, Z. 1
Ingram, D. 193
Ji, C. 193
Josefson, L. 143
Jurisic, P. 391
Kaminski, M. v
Karmakar, D. 193
Karr, D.G. 193
Kavanagh, K. 461
Kim, E. 347
Kim, G.S. 1
Kim, M.H. 143
Kolios, A. 193
Kõrgesaar, M. 1
Kuehnlein, W. 347
Leira, B. 391
Li, L. 391
Li, XB. 73
Liu, P. 193
Low, Y.M. 461
Luo, H. 279
Mavrakos, S. 461
Michailides, C. 73
Mishra, B. 143
Moslet, P.O. 347
Murayama, H. 391
Myllerup, C. 461
Nahshon, K. 1
Nicholls-Lee, R. 279
Nilva, A. 1
Osawa, N. 143
Oterkus, E. 279
Ozaki, M. 461
Pasqualino, I.P. 461
Pearson, D. 73
Polojärvi, A. 347
Quinton, B. 347
Ralph, F. 347
Remes, H. 143
Rigo, P. v
Rizzuto, E. 1
Rodrigues, J.M. 193
Roland, F. 143
Romanoff, J. 73
Sævik, S. 461
Samanta, A. 461
Schipperen, I. 1
Schreier, S. 461
Sensharma, P. 279
Seo, J.K. 461
Sheng, W. 193
Shi, XH. 73
Shin, H.-K. 193
Sirkar, J. 347
Slätte, J. 193
Song, H. 461

Stadie-Frohboes, G. 1
Stoev, L. 193
Sugimura, T. 73
Sun, L. 461
Suzuki, K. 1
Swart, P. 461
Tabri, K. 1
Tammer, M. 391
Teixeira, A. 461
Truelock, D. 279
Utsunomiya, T. 193
van Duin, S. 143
Vaz, M. 391
Ventura, M. 279
Vredeveldt, A. 347
Wægter, J. 1
Wan, Z. 347
Wang, G. 73
Wang, X. 279
Yang, N. 143
Yasuda, A. 279
Yu, L. 143
Zamarin, A. 143

This page intentionally left blank

This page intentionally left blank

The International Ship and Offshore Structures Congress (ISSC) is a forum for the exchange of information by experts undertaking and applying marine structural research. The aim of the ISSC is to facilitate the evaluation and dissemination of results from recent investigations, to make recommendations for standard design procedures and criteria, to discuss research in progress and planned, to identify areas requiring future research and to encourage international collaboration in furthering these aims. Ships and other marine structures used for transportation, exploration and exploitation of resources in and under the oceans are in the scope of the ISSC.

This publication contains the 8 Specialist Committee reports presented and discussed at the 20th International Ship and Offshore Structures Congress (ISSC 2018) held in Liège (Belgium) and Amsterdam (The Netherlands), 9–14 September 2018.

The reports of the 8 Technical Committees are published in volume 1 of the Progress in Maritime Science and Technology book series. The Official discusser's reports, all floor discussions together with the replies by the committees, will be published after the congress in electronic form.

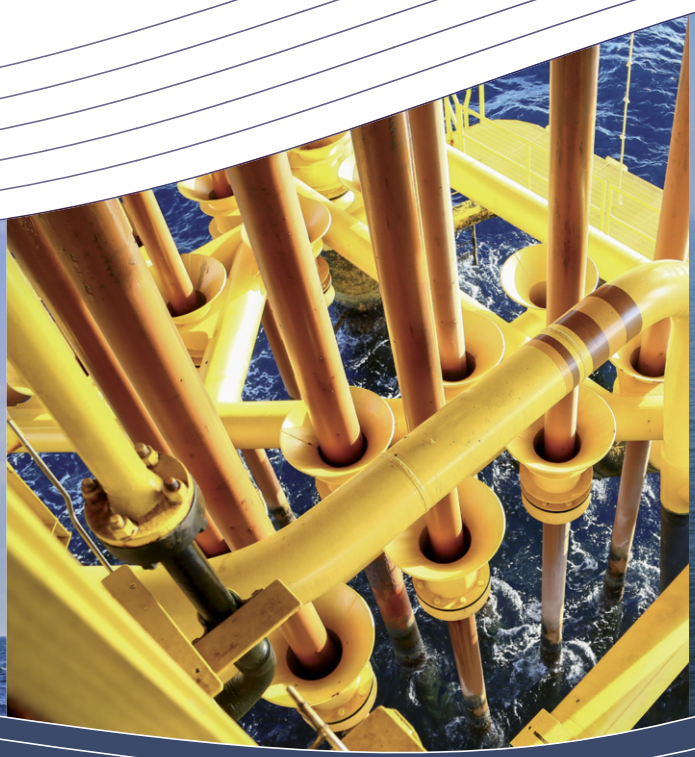

ISBN 978-1-61499-863-1

ISBN 978-1-61499-863-1 (print)
ISBN 978-1-61499-864-8 (online)
ISSN 2543-0955 (print)
ISSN 2543-0963 (online)

IOS Press